

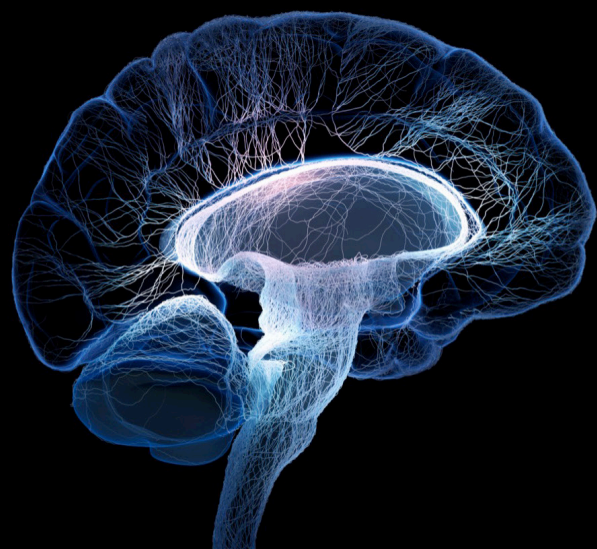
Cell adhesion molecules in neural development and disease

Edited by

Zsolt Lele and Robert Hindges

Published in

Frontiers in Neuroscience



FRONTIERS EBOOK COPYRIGHT STATEMENT

The copyright in the text of individual articles in this ebook is the property of their respective authors or their respective institutions or funders. The copyright in graphics and images within each article may be subject to copyright of other parties. In both cases this is subject to a license granted to Frontiers.

The compilation of articles constituting this ebook is the property of Frontiers.

Each article within this ebook, and the ebook itself, are published under the most recent version of the Creative Commons CC-BY licence. The version current at the date of publication of this ebook is CC-BY 4.0. If the CC-BY licence is updated, the licence granted by Frontiers is automatically updated to the new version.

When exercising any right under the CC-BY licence, Frontiers must be attributed as the original publisher of the article or ebook, as applicable.

Authors have the responsibility of ensuring that any graphics or other materials which are the property of others may be included in the CC-BY licence, but this should be checked before relying on the CC-BY licence to reproduce those materials. Any copyright notices relating to those materials must be complied with.

Copyright and source acknowledgement notices may not be removed and must be displayed in any copy, derivative work or partial copy which includes the elements in question.

All copyright, and all rights therein, are protected by national and international copyright laws. The above represents a summary only. For further information please read Frontiers' Conditions for Website Use and Copyright Statement, and the applicable CC-BY licence.

ISSN 1664-8714
ISBN 978-2-83251-421-4
DOI 10.3389/978-2-83251-421-4

About Frontiers

Frontiers is more than just an open access publisher of scholarly articles: it is a pioneering approach to the world of academia, radically improving the way scholarly research is managed. The grand vision of Frontiers is a world where all people have an equal opportunity to seek, share and generate knowledge. Frontiers provides immediate and permanent online open access to all its publications, but this alone is not enough to realize our grand goals.

Frontiers journal series

The Frontiers journal series is a multi-tier and interdisciplinary set of open-access, online journals, promising a paradigm shift from the current review, selection and dissemination processes in academic publishing. All Frontiers journals are driven by researchers for researchers; therefore, they constitute a service to the scholarly community. At the same time, the *Frontiers journal series* operates on a revolutionary invention, the tiered publishing system, initially addressing specific communities of scholars, and gradually climbing up to broader public understanding, thus serving the interests of the lay society, too.

Dedication to quality

Each Frontiers article is a landmark of the highest quality, thanks to genuinely collaborative interactions between authors and review editors, who include some of the world's best academicians. Research must be certified by peers before entering a stream of knowledge that may eventually reach the public - and shape society; therefore, Frontiers only applies the most rigorous and unbiased reviews. Frontiers revolutionizes research publishing by freely delivering the most outstanding research, evaluated with no bias from both the academic and social point of view. By applying the most advanced information technologies, Frontiers is catapulting scholarly publishing into a new generation.

What are Frontiers Research Topics?

Frontiers Research Topics are very popular trademarks of the *Frontiers journals series*: they are collections of at least ten articles, all centered on a particular subject. With their unique mix of varied contributions from Original Research to Review Articles, Frontiers Research Topics unify the most influential researchers, the latest key findings and historical advances in a hot research area.

Find out more on how to host your own Frontiers Research Topic or contribute to one as an author by contacting the Frontiers editorial office: frontiersin.org/about/contact

Cell adhesion molecules in neural development and disease

Topic editors

Zsolt Lele — Laboratory of Molecular Neurobiology, Institute of Experimental Medicine, Hungary

Robert Hindges — King's College London, United Kingdom

Citation

Lele, Z., Hindges, R., eds. (2023). *Cell adhesion molecules in neural development and disease*. Lausanne: Frontiers Media SA. doi: 10.3389/978-2-83251-421-4

Table of contents

04	Editorial: Cell adhesion molecules in neural development and disease Robert Hindges and Zsolt Lele
06	Synapse Formation and Function Across Species: Ancient Roles for CCP, CUB, and TSP-1 Structural Domains Inés González-Calvo, Mélissa Cizeron, Jean-Louis Bessereau and Fekrije Selimi
21	To Stick or Not to Stick: The Multiple Roles of Cell Adhesion Molecules in Neural Circuit Assembly Trevor Moreland and Fabienne E. Poulain
37	Role of Teneurin C-Terminal Associated Peptides (TCAP) on Intercellular Adhesion and Communication Thomas L. Dodsworth and David A. Lovejoy
44	Spatiotemporal Control of Neuronal Remodeling by Cell Adhesion Molecules: Insights From <i>Drosophila</i> Hagar Meltzer and Oren Schuldiner
53	Endoglycan Regulates Purkinje Cell Migration by Balancing Cell-Cell Adhesion Thomas Baeriswyl, Martina Schaettin, Simone Leoni, Alexandre Dumoulin and Esther T. Stoeckli
63	<i>Pcdh11x</i> controls target specification of mossy fiber sprouting Wenshu Luo, Natalia Andrea Cruz-Ochoa, Charlotte Seng, Matteo Egger, David Lukacsovich, Tamás Lukacsovich and Csaba Földy
81	Flying under the radar: CDH2 (N-cadherin), an important hub molecule in neurodevelopmental and neurodegenerative diseases Zsófia I. László and Zsolt Lele
102	Modifying PCDH19 levels affects cortical interneuron migration Anna Pancho, Manuela D. Mitsogiannis, Tania Aerts, Marco Dalla Vecchia, Lena K. Ebert, Lieve Geenen, Lut Noterdaeme, Ria Vanlaer, Anne Stulens, Paco Hulpiau, Katrien Staes, Frans Van Roy, Peter Dedeker, Bernhard Schermer and Eve Seuntjens
126	Teneurin paralogues are able to localise synaptic sites driven by the intracellular domain and have the potential to form <i>cis</i>-heterodimers Angela Cheung, Greta Schachermayer, Aude Biehler, Amber Wallis, Mégane Missaire and Robert Hindges



OPEN ACCESS

EDITED AND REVIEWED BY

Jaewon Ko,
Daegu Gyeongbuk Institute of Science
and Technology (DGIST), Republic
of Korea

*CORRESPONDENCE

Robert Hindges
✉ robert.hindges@kcl.ac.uk
Zsolt Lele
✉ lele.zsolt@koki.hu

SPECIALTY SECTION

This article was submitted to
Neurodevelopment,
a section of the journal
Frontiers in Neuroscience

RECEIVED 30 November 2022

ACCEPTED 20 December 2022

PUBLISHED 10 January 2023

CITATION

Hindges R and Lele Z (2023) Editorial:
Cell adhesion molecules in neural
development and disease.
Front. Neurosci. 16:1112300.
doi: 10.3389/fnins.2022.1112300

COPYRIGHT

© 2023 Hindges and Lele. This is an
open-access article distributed under
the terms of the [Creative Commons
Attribution License \(CC BY\)](#). The use,
distribution or reproduction in other
forums is permitted, provided the
original author(s) and the copyright
owner(s) are credited and that the
original publication in this journal is
cited, in accordance with accepted
academic practice. No use, distribution
or reproduction is permitted which
does not comply with these terms.

Editorial: Cell adhesion molecules in neural development and disease

Robert Hindges^{1,2*} and Zsolt Lele^{3*}

¹Centre for Developmental Neurobiology, King's College London, London, United Kingdom, ²MRC Centre for Neurodevelopmental Disorders, King's College London, London, United Kingdom,

³Laboratory of Molecular Neurobiology, Institute of Experimental Medicine, Budapest, Hungary

KEYWORDS

cell adhesion molecules, protocadherin, teneurin, N-cadherin, circuit assembly

Editorial on the Research Topic

Cell adhesion molecules in neural development and disease

Cell-to cell adhesion is a defining, hence essential condition of being a multicellular organism. It has been more than 60 years that Weiss published the first in a series of pioneering papers detailing various aspects of cellular adhesion (Weiss, 1959). Since then, a large number of papers has been published on this fascinating Research Topic describing all the studies that contributed to the state-of-the-art knowledge of today. In this Research Topic of Frontiers in Neuroscience, we collected a series of papers, both original research articles and reviews to emphasize the importance of cell adhesion molecules in neural development and disease. Two of the original research papers presents novel data involving protocadherins. Members belonging to this family have previously been demonstrated to be responsible for dendritic self-avoidance (Kostadinov and Sanes, 2015; Lefebvre et al., 2015; Ing-Estevés, 2018), axon sorting of olfactory sensory (Mountoufaris, 2017), and serotonergic neurons (Chen, 2017; Katori, 2017). In this Research Topic, Pancho et al. demonstrates the importance of PCDH19 in interneuron migration while Luo et al. propose the involvement of PCDH11x in target specification of hippocampal mossy fibers. An excellent overview provided by Moreland and Poulain outlining the role various cell adhesion molecules play in neural circuit assembly. As a perfect continuation of this Research Topic, another review by Meltzer and Schuldiner discusses the involvement of CAMs in neuronal remodeling. As a sharp contrast to these broad reviews, and as a reflection of recent surprising developments, László and Lele tell everything you wanted to know about N-cadherin in neural development and disease. An important general issue is the fine balancing of activities controlled by adhesion molecules. This includes not only the positive regulation of cell-cell contacts, but can also involve negative activities. Here, Baeriswyl et al. characterize such balance between positive and negative action in the context of Purkinje cell migration. Two reports focus on the teneurin family of cell adhesion molecules. A review by Dodsworth and Lovejoy focuses on the teneurin C-terminal associated peptides (TCAP), which are encoded by the last

exon of teneurins. Interestingly, despite a general transsynaptic interaction of full-length teneurins with latrophilins, evidence suggests that released TCAP molecules have an additional binding capacity to these partners and might elicit distinct cellular process. The presence of teneurins at synapses and their ability of heterocomplexes in cis is described in an article by Cheung et al. The results suggest that the diversity of molecular complexes at synaptic localizations is bigger than previously thought, which thus would increase the combinatoric power to control synaptic specificity. Finally, the process of how synapse formation is controlled through structural domains of different proteins across species is presented in an article by González-Calvo et al. therefore enabling us to recognize the evolutionary conservation of these fundamental processes.

It is evident that many open questions about the structure and roles of cell adhesion molecules still exist. However, the recent progresses made are encouraging and point toward a better understanding not only in biochemical and cell biological terms, but importantly also in the context of disorders, where there is a clear need for the development of novel therapeutic strategies.

Author contributions

RH and ZL wrote the summary. Both authors contributed to the article and approved the submitted version.

References

- Chen, W. V, Nwakeze, C. L, Denny, C. A, O'Keeffe, S, Rieger, M. A, Mountoufaris, G, et al. (2017). Pcdh α 2 is required for axonal tiling and assembly of serotonergic circuitries in mice. *Science* 356, 406–411. doi: 10.1126/science.aal3231
- Ing-Esteves, S, Kostadinov, D, Marocha, J, Sing, A. D, Joseph, K. S, Laboulaye, M. A, et al. (2018). Combinatorial effects of alpha- and gamma-protocadherins on neuronal survival and dendritic self-avoidance. *J. Neurosci.* 38, 2713–2729. doi: 10.1523/JNEUROSCI.3035-17.2018
- Katori, S, Noguchi-Katori, Y, Okayama, A, Kawamura, Y, Luo, W, Sakimura, K, et al. (2017). Protocadherin- α 2 is required for diffuse projections of serotonergic axons. *Sci. Rep.* 7, 15908. doi: 10.1038/s41598-017-16120-y
- Kostadinov, D., and Sanes, J. R. (2015). Protocadherin-dependent dendritic self-avoidance regulates neural connectivity and circuit function. *Elife* 4, 22. doi: 10.7554/eLife.08964.022
- Lefebvre, J. L., Sanes, J. R., and Kay, J. N. (2015). Development of dendritic form and function. *Annu. Rev. Cell Dev. Biol.* 31, 741–777. doi: 10.1146/annurev-cellbio-100913-013020
- Mountoufaris, G, Chen, W. V, Hirabayashi, Y, O'Keeffe, S, Chevee, M, Nwakeze, C. L, et al. (2017). Multiclust Pcdh diversity is required for mouse olfactory neural circuit assembly. *Science* 356, 411–414. doi: 10.1126/science.aai8801
- Weiss, L. (1959). Studies on cellular adhesion in tissue culture. I. The effect of serum. *Exp. Cell Res.* 17, 499–507. doi: 10.1016/0014-4827(59)90070-9

Funding

Support to RH has been provided by the Leverhulme Trust (RPG-2021-385) and the Medical Research Council (MR/W006251/1). Support to ZL has been provided by the National Research, Development and Innovation Fund of Hungary under the 'Frontline' - Research Excellence Program KKP_19 (KKP 129961) and the National Program in Brain Sciences (2017-1.2.1-NKP-2017-00002) funding scheme.

Conflict of interest

The authors declare that the research was conducted in the absence of any commercial or financial relationships that could be construed as a potential conflict of interest.

Publisher's note

All claims expressed in this article are solely those of the authors and do not necessarily represent those of their affiliated organizations, or those of the publisher, the editors and the reviewers. Any product that may be evaluated in this article, or claim that may be made by its manufacturer, is not guaranteed or endorsed by the publisher.



Synapse Formation and Function Across Species: Ancient Roles for CCP, CUB, and TSP-1 Structural Domains

Inés González-Calvo^{1†‡}, Mélissa Cizeron^{2‡}, Jean-Louis Bessereau² and Fekrije Selimi^{1*}

¹ Center for Interdisciplinary Research in Biology (CIRB), Collège de France, CNRS, INSERM, PSL Research University, Paris, France, ² Univ Lyon, Université Claude Bernard Lyon 1, CNRS UMR-5284, INSERM U-1314, MeLiS, Institut NeuroMyoGène, Lyon, France

OPEN ACCESS

Edited by:

Zsolt Lele,
Institute of Experimental Medicine,
Hungary

Reviewed by:

Lorenzo A. Cingolani,
Italian Institute of Technology (IIT), Italy
Corette J. Wierenga,
Utrecht University, Netherlands

*Correspondence:

Fekrije Selimi
fekrije.selimi@college-de-france.fr

† Present address:

Inés González-Calvo,
Instituto de Biomedicina de Sevilla
(IBiS) HUVR/CSIC/Universidad de
Sevilla, Departamento de Fisiología
Médica y Biofísica and CIBERNED,
Seville, Spain

‡ These authors have contributed
equally to this work

Specialty section:

This article was submitted to
Neurodevelopment,
a section of the journal
Frontiers in Neuroscience

Received: 31 January 2022

Accepted: 28 March 2022

Published: 25 April 2022

Citation:

González-Calvo I, Cizeron M,
Bessereau J-L and Selimi F (2022)
Synapse Formation and Function
Across Species: Ancient Roles
for CCP, CUB, and TSP-1 Structural
Domains.
Front. Neurosci. 16:866444.
doi: 10.3389/fnins.2022.866444

The appearance of synapses was a crucial step in the creation of the variety of nervous systems that are found in the animal kingdom. With increased complexity of the organisms came a greater number of synaptic proteins. In this review we describe synaptic proteins that contain the structural domains CUB, CCP, or TSP-1. These domains are found in invertebrates and vertebrates, and CUB and CCP domains were initially described in proteins belonging to the complement system of innate immunity. Interestingly, they are found in synapses of the nematode *C. elegans*, which does not have a complement system, suggesting an ancient function. Comparison of the roles of CUB-, CCP-, and TSP-1 containing synaptic proteins in various species shows that in more complex nervous systems, these structural domains are combined with other domains and that there is partial conservation of their function. These three domains are thus basic building blocks of the synaptic architecture. Further studies of structural domains characteristic of synaptic proteins in invertebrates such as *C. elegans* and comparison of their role in mammals will help identify other conserved synaptic molecular building blocks. Furthermore, this type of functional comparison across species will also identify structural domains added during evolution in correlation with increased complexity, shedding light on mechanisms underlying cognition and brain diseases.

Keywords: synapse, molecular conservation, CCP, CUB, TSP-1, invertebrates, vertebrates

INTRODUCTION

The emergence of synapses is an ancient process which is not fully elucidated (Arendt, 2020). Much of our knowledge comes from comparing synaptic proteins in different animal species. The ancestor of chemical synapses, the Ursynapse, appeared in the common ancestor of cnidarians and bilaterians and some synaptic proteins, named protosynaptic proteins, existed before the emergence of the Ursynapse (Ryan and Grant, 2009). Since many synaptic proteins are shared by all bilaterians, studies carried in invertebrate animal models have proven very useful to identify and characterize key synaptic proteins. For instance, historical genetic screens conducted in *Caenorhabditis elegans* by Sydney Brenner identified many genes required for synaptic function, such as *unc-13*, which encodes a protein essential for synaptic vesicle exocytosis (Brenner, 1974).

The early identification of *unc-13* enabled the identification of several vertebrate orthologues with functional conservation and involvement in genetic diseases. Conversely, studies in vertebrates, in particular using proteomics, have revealed a considerable diversity of synaptic proteins (Bayés et al., 2011). This diversity arises at least in part from the two rounds of whole-genome duplication events that occurred at the base of the chordate lineage (Van de Peer et al., 2009). Some paralogs, such as members of the DLG (disk large homolog) family that are localized at the postsynaptic density, acquired specific functions (Nithianantharajah et al., 2013) and specific spatiotemporal expression patterns (Zhu et al., 2018; Cizeron et al., 2020). Other synaptic proteins, such as the GABAergic postsynaptic scaffolds Gephyrin and Collybistin, are present in vertebrates but are absent in *Caenorhabditis elegans* (Arendt, 2020). Comparing the synaptic machineries across species is thus a powerful approach to understand the molecular basis of synaptic complexity in vertebrates.

Certain synaptic proteins were initially characterized for their function outside the central nervous system (CNS). The seminal work of the laboratory of Dr. Carla Shatz, followed by others, showed that proteins of the immune system are also expressed by neurons, are regulated by activity and contribute to synapse development and function (for a review cf. (Boulanger, 2009)). One particular category of immune-related proteins with neuronal function are the proteins of the complement system implicated in innate immunity or their regulators: the complement proteins C1q and C3 contribute to synaptic pruning in the developing brain (Stephan et al., 2012) and the complement inhibitor SUSD4 (Sushi domain-containing protein 4) regulates synaptic plasticity (González-Calvo et al., 2021). Invertebrates do not have a complement system or an adaptative immune system. Yet they express proteins with domains typically found in proteins of these systems, such as the immunoglobulin (Ig) domain or the Complement Control Protein domain (Figure 1). During evolution these structural domains may have been used for establishing neuronal synapses before being used to build the complement or adaptative immune systems. Thus, rather than thinking about entire proteins, identifying the presence of specific structural domains and the function of the corresponding proteins at neuronal synapses across species might provide an insight into the mechanisms that control core aspects of the development and function of neuronal synapses. In particular, it might help understand how the high diversity of synapse types needed to produce large neuronal networks in vertebrates was attained.

In line with this idea, Vogel and Chothia studied 38 eukaryotic genomes, ranging from unicellular organisms to mammals, and tested the correlation between the number of proteins in superfamilies characterized by specific structural domains and the complexity of the organisms as defined by the number of cell types (Vogel and Chothia, 2006). They identified 194 superfamilies with a correlation ≥ 0.80 (Vogel and Chothia, 2006): these included the Ig domain containing superfamily (correlation: 0.97), but also several other superfamilies of proteins with immune-related roles such as the CCP (Complement Control Protein, also known as Sushi or

the short consensus repeats (SCR) domain), CUB (complement C1r/C1s, Uegf, Bmp1), and TSP-1 (thrombospondin type-1) domains (correlation 0.94, 0.84, 0.91, respectively). Like the Ig domain, these three domains possess a structure characterized by sandwich like folds that might favor protein-protein and protein-glycan interactions (Zinn and Özkan, 2017) (Figure 1). The CCP, CUB, and TSP-1 domains have been previously identified in synaptic proteins in *C. elegans* prompting us to review the role of these three superfamilies in different species. The role of the Ig superfamily in the nervous system has been addressed in several reviews recently (Sytnyk et al., 2017; Zinn and Özkan, 2017; Cameron and McAllister, 2018; Sanes and Zipursky, 2020).

KEY SYNAPTIC ROLES FOR THE TSP-1, CCP, AND CUB STRUCTURAL DOMAINS IDENTIFIED IN INVERTEBRATES

Genetic screens in *Caenorhabditis elegans* were instrumental for the identification of new synaptic proteins and their function at the neuromuscular junction (NMJ). In particular, screens using the anthelmintic drug levamisole identified two genes, *lev-9* and *lev-10*, coding for synaptic proteins required for the aggregation of levamisole-sensitive cholinergic receptors (L-AChRs) on muscle cells (Gendrel et al., 2009). The LEV-9 and LEV-10 proteins are characterized by a specific structural domain: CCP (Complement Control Protein, also known as Sushi or the short consensus repeats (SCR) domain) and CUB (complement C1r/C1s, Uegf, Bmp1) domains (Figure 1), respectively. Later, *madd-4* was identified as a gene encoding a protein composed of up to 10 thrombospondin type-1 (TSP-1) domains (Figure 1), and necessary for the correct localization of LEV-9/LEV-10/L-AChR complexes. Thus, CCP, CUB, and TSP-1 domains have important roles at *C. elegans* NMJs.

The TSP-1 domain (approximately 60 amino acids in length, also known as TSR-1 repeat domain or TSR) was first described in thrombospondins, multimeric glycoproteins present at the cell surface and in the extracellular matrix. It is composed of an antiparallel, three-stranded fold with a positively charged groove (Tan et al., 2002). The CCP domain was first described in the human complement component factor B. It is also found in several complement-related proteins like the complement receptor C1R, the complement protein C2 and the serine proteases MASP1-3 to list a few (cf. Annex 1 for the list of CCP containing proteins expressed in the human brain). The CCP consensus sequence spans ~60 residues and contains hydrophobic residues forming a β -sheet core held together *via* disulphide bridges between four cysteine residues that are conserved in 80% of the sequences (Figure 1; Reid and Day, 1989). The CUB domain was first identified in the complement subcomponent C1r/C1s, sea urchin protein Uegf, and BMP-1 proteins. It spans about 100-110 residues (Bork and Beckmann, 1993). The consensus sequence (Figure 1) often comprises four conserved cysteines that can form two disulfide bounds, as well as conserved hydrophobic and aromatic positions that organize into a compact ellipsoidal β -sandwich (Bork and Beckmann, 1993; Varela et al., 1997).

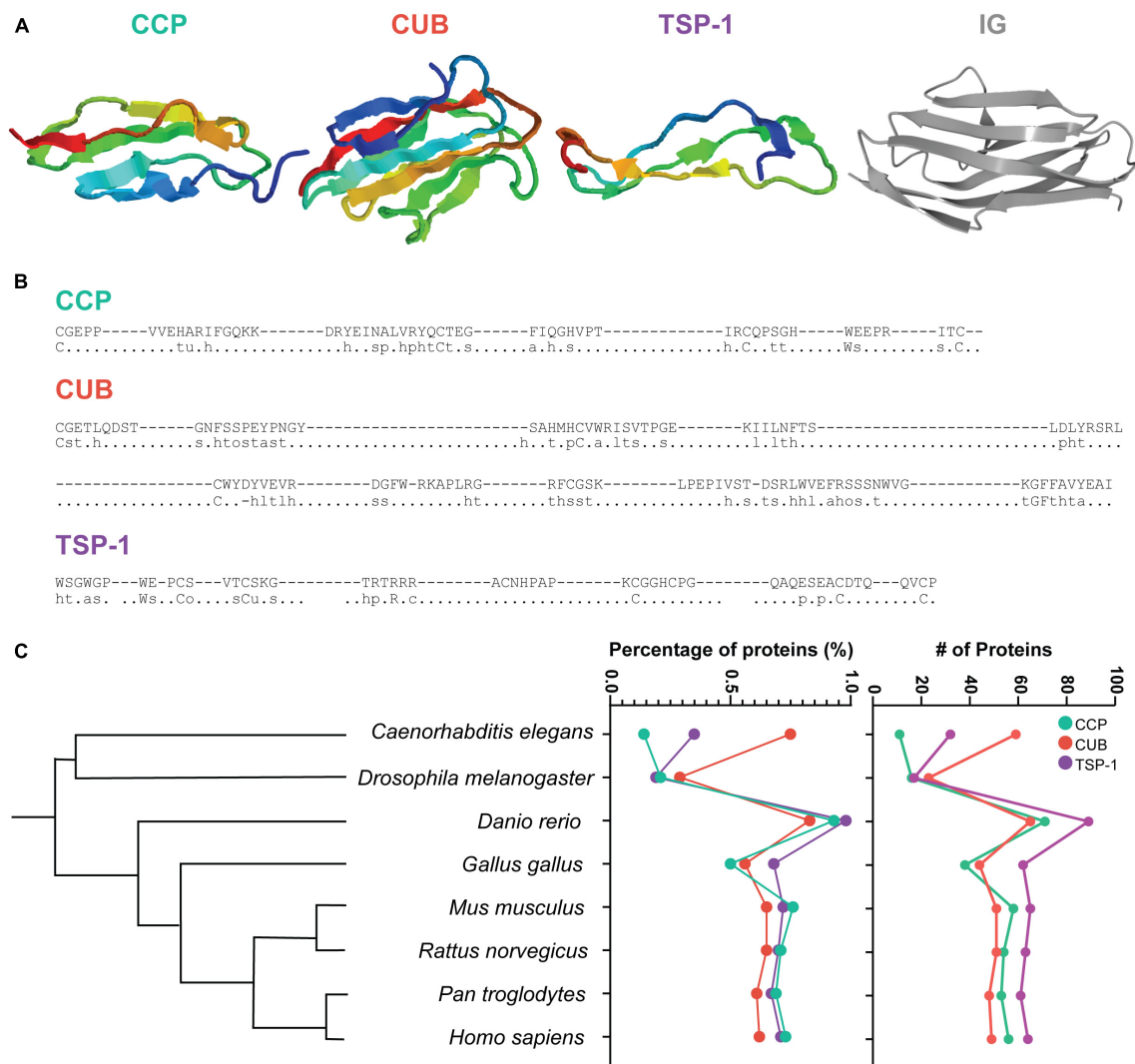


FIGURE 1 | CCP, CUB, and TSP-1 domains. **(A)** Three-dimensional structure of a CCP domain (from rat GABA B Receptor 1a (Blein et al., 2004), PDB id: 1srz), a CUB domain (from human tumor necrosis factor-inducible gene 6 protein (Briggs et al., 2015), PDB id: 2wno), a TSP-1 domain (from rat F-spondin (Pääkkönen et al., 2006), PDB id: 1szl) and a IG domain (from mouse NCAM (Jensen et al., 1999), PDB id: 3ncm). Adapted from ebi.ac.uk/pdbsum **(B)** For each domain, an example is given (top sequence: β -2-glycoprotein 1 from Bos Taurus (PGCA_BOVIN/1-5) for the CCP domain; bone morphogenetic protein 1 from Homo sapiens (BMP1_HUMAN/1-1) for the CUB domain and Properdin from Homo sapiens (PROP_HUMAN/2-0) for the TSP-1 domain), as well as the consensus terms (80%, bottom sequence). Adapted from smart.embl.de. **(C)** Number and percentage of proteins containing CCP, CUB, or TSP-1 domains (green, red and purple, respectively, right) for different species ordered via a phylogenetic tree (left). Data from SMART genomic mode domain evolution (smart.embl.de) and the interactive Tree of Life (itol.embl.de).

All three domains were present in the last common ancestor of eumetazoans, as shown by their presence in bilaterians (described in this review) and in cnidarians (SMART website). Proteins containing these structural domains can thus be expected to play ancient and key roles in the building and function of neuronal circuits.

The TSP-1 Domain Containing Protein MADD-4 and Synapse Type Specification

In *C. elegans*, the NMJ has been used as a model to study synapse specificity on body-wall muscle cells, which receive both

excitatory (ACh) and inhibitory (GABAergic) inputs. MADD-4, a TSP-1 domain containing protein, is secreted presynaptically by motoneurons and defines the identity of postsynaptic domains by controlling the clustering of cholinergic receptors (AChRs) and GABAergic A receptors (GABA_ARs) in front of the corresponding neurotransmitter release sites (Pinan-Lucarré et al., 2014; Zhou et al., 2020). The *madd-4* locus generates three MADD-4 isoforms through the use of alternative promoters and alternative splicing. The two long MADD-4L isoforms (MADD-4A and MADD-4C) differ by 2 amino acids and are composed of 10 TSP-1 repeats, an ADAMTS (a disintegrin and metalloproteinase with thrombospondin motifs) cysteine-rich

module, an ADAMTS spacer module, an Ig-like C2-type domain and a PLAC (Protease and LACunin) domain (Figure 2). The MADD-4S isoform is identical to the C-terminal moiety of MADD-4L and contains only 7 TSP-1 repeats, an Ig-like C2-type

domain and a PLAC domain (Figure 2). MADD-4L is exclusively expressed by cholinergic motoneurons and triggers the clustering of AChRs. MADD-4S is expressed by both cholinergic and GABAergic motoneurons. At GABAergic NMJs, it promotes

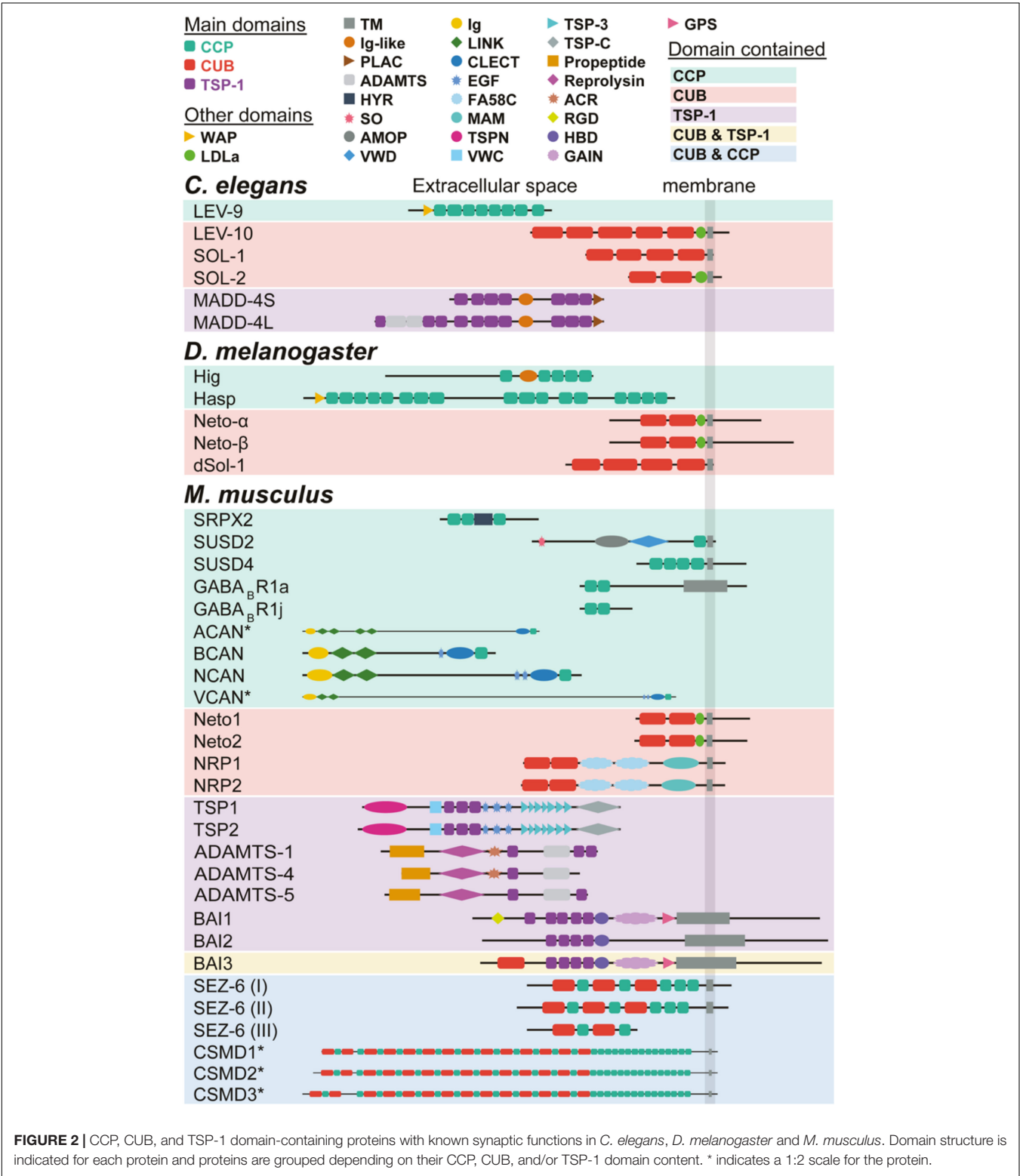


FIGURE 2 | CCP, CUB, and TSP-1 domain-containing proteins with known synaptic functions in *C. elegans*, *D. melanogaster* and *M. musculus*. Domain structure is indicated for each protein and proteins are grouped depending on their CCP, CUB, and/or TSP-1 domain content. * indicates a 1:2 scale for the protein.

the recruitment of GABA_ARs. At cholinergic NMJs, it prevents the inappropriate recruitment of GABA_ARs. In the absence of MADD-4 protein, both AChR and GABA_AR clusters relocate to extrasynaptic areas (Pinan-Lucarré et al., 2014). Hence, the repertoire of isoforms expressed by specific MNs controls post-synaptic identity (Pinan-Lucarré et al., 2014). Recently, a study of *madd-4* null mutants showed that MADD-4 also controls the timing of synapse remodeling during development (Chen et al., 2021).

The control of synapse specification by MADD4 isoforms requires the control of distinct molecular pathways for each type of receptors. MADD-4L allows the correct positioning of LEV-9/LEV-10/L-AChRs complexes (cf. below) in front of cholinergic boutons (Pinan-Lucarré et al., 2014). MADD-4S positions GABA_ARs by two parallel pathways. First, it localizes Neuroligin-1 (NLG-1) at GABA postsynaptic sites through direct interactions (Maro et al., 2015; Tu et al., 2015). Second, it activates the netrin receptor UNC-40/DCC (Tu et al., 2015), which triggers the formation of an intracellular scaffold involving LIN-2/CASK and FRM-3/FARP (Zhou et al., 2020). This intracellular scaffold promotes the recruitment of GABA_ARs onto NLG-1 clusters. In addition, the mechanism allowing the dual function of MADD-4S at cholinergic versus GABAergic synapses remains to be understood, but probably involves dimerization with the long isoform MADD-4L. Finally, both MADD-4 isoforms promote the synaptic localization of the heparan sulfate glycoprotein syndecan/SDN-1, a key-component of cholinergic NMJs (Zhou et al., 2021). The specific role of the TSP-1 domains in these various molecular interactions remains to be determined.

CCP Containing Proteins and Neurotransmitter Receptor Clustering

LEV-9 (*Caenorhabditis elegans*)

LEV-9 is a secreted protein composed of eight CCP domains and one WAP (whey acidic protein) domain (Figure 2). L-AChRs are undetectable at NMJs of *lev-9* mutants, while ACh presynaptic boutons and postsynaptic GABA_ARs are normally distributed (Gendrel et al., 2009). Surprisingly, biochemical and electrophysiological experiments demonstrated that L-AChRs are expressed at normal levels in *lev-9* mutants, highlighting that it is dispensable for correct expression and surface targeting of functional L-AChRs (Gendrel et al., 2009). However, the evoked response after stimulation of AChRs was reduced and presented an increased time to peak and decay time in *lev-9* mutants (Gendrel et al., 2009). These data supported the presence of declustered L-AChRs in the absence of LEV-9. LEV-9 is expressed by muscles, where it functions cell-autonomously, and localizes to cholinergic NMJs (Gendrel et al., 2009). LEV-9 activation by C-terminal cleavage is required for proper L-AChR clustering but not for LEV-9 secretion (Briseño-Roa and Bessereau, 2014). The WAP domain from LEV-9 is dispensable for its role in L-AChR clustering (Gendrel et al., 2009), indicating that the CCP domains are the main actors of LEV-9 clustering function.

Hig and Hasp (*Drosophila melanogaster*)

Two CCP domain-containing proteins with similar function in invertebrates have been studied in *Drosophila melanogaster*:

Hikaru genki (Hig) and Hasp (Hig-anchoring scaffold protein). The Hig protein contains five CCP domains and one immunoglobulin (Ig)-like domain, while Hasp contains one WAP domain followed by up to seventeen CCP domains (Figure 2). Like LEV-9, Hig and Hasp are processed, but the identity of the functionally important fragment is unknown (Nakayama et al., 2016). Both *hig* and *hasp* mutants have reduced locomotion and longevity (Hoshino et al., 1993; Nakayama et al., 2016). In the adult brain, Hig and Hasp mostly localize to the synaptic cleft of cholinergic synapses, where they occupy distinct, overlapping areas (Nakayama et al., 2014, 2016). When expressed ectopically, Hig is able to diffuse in the extracellular space and is trapped at cholinergic synaptic clefts (Nakayama et al., 2014, 2016). Analysis of loss of function mutants (Nakayama et al., 2014, 2016) shows that Hasp interacts with Hig to anchor it at the synaptic cleft of cholinergic synapses, and that the localization of Hig at synapses is reciprocally dependent on AChRs (Nakayama et al., 2016). Thus, Hig is functionally similar to LEV-9 and controls AChR clustering at synapses in *D. melanogaster*.

CUB Containing Proteins and Regulation of Neurotransmitter Receptor Clustering and Properties

LEV-10 (*Caenorhabditis elegans*)

The first discovery of the involvement of the CUB domain in the regulation of ionotropic receptors came from the identification of *lev-10* (Gally et al., 2004). LEV-10 is a type 1 transmembrane protein composed of an extracellular LDLa (low-density lipoprotein receptor domain class A) domain and five extracellular CUB domains (Figure 2). *Lev-10* mutants present similar phenotypes to *lev-9* mutants: *lev-10* is dispensable for expression and membrane targeting of L-AChRs, but its absence leads to declustering and redistribution of the receptors to extrasynaptic areas (Gally et al., 2004). Like LEV-9, LEV-10 is expressed in muscles, distributes to cholinergic NMJs and functions cell-autonomously (Gally et al., 2004). In the absence of LEV-9, LEV-10 or L-AChRs, the other proteins fail to localize to cholinergic NMJs, showing that they form a tripartite complex necessary for their mutual clustering (Gally et al., 2004; Gendrel et al., 2009). An additional partner contributes to this extracellular scaffold: OIG-4 contains a single immunoglobulin domain and stabilizes the interaction between L-AChRs and LEV-10 (Rapti et al., 2011). The extracellular part of LEV-10 is sufficient to rescue L-AChR clustering in *lev-10* mutants and the LDLa domain is dispensable (Gally et al., 2004; Rapti et al., 2011), highlighting the role of LEV-10 CUB domains in L-AChR clustering.

SOL-1 and SOL-2 (*Caenorhabditis elegans*)

In *C. elegans*, two other CUB domain-containing proteins have known synaptic functions: SOL-1 and SOL-2. Both proteins regulate the channel properties of the glutamate receptor GLR-1, an ortholog of AMPA receptors (Walker et al., 2006; Zheng et al., 2006, 2004; Wang et al., 2012). SOL-1 and SOL-2 are both type 1 transmembrane proteins that differ by their extracellular domain: SOL-1 contains four extracellular CUB domains and SOL-2

one LDLa and two CUB domains (**Figure 2**). These proteins were both discovered in genetic screens looking for suppressors of the *lurcher* phenotype, a hyperreversal behavior caused by hyperactive AMPA receptors in a specific *glr-1* mutant. *sol-1* and *sol-2* mutants, like *glr-1* mutants, present defects in tactile avoidance, duration of forward movement and show delayed response to a drop of hyperosmotic solution (Zheng et al., 2004; Wang et al., 2012). These behavioral phenotypes are accompanied by defects in synaptic transmission: glutamate and kainate-evoked currents are reduced while NMDA-evoked currents are unchanged (Zheng et al., 2004; Wang et al., 2012). SOL-1 and SOL-2 function cell autonomously in AVA neurons (Zheng et al., 2004; Wang et al., 2012). The third CUB domain is critical for SOL-1 function as shown by rescue experiments using different mutant constructs (Zheng et al., 2006). Synaptic defects are not due to changes in expression levels or surface expression of GLR-1 complexes (Zheng et al., 2004; Walker et al., 2006; Wang et al., 2012). Rather, SOL-1 increases glutamate currents by slowing GLR-1 desensitization kinetics and by increasing its recovery from desensitization (Walker et al., 2006). This role in the control of receptor properties is further supported by experiments in *Xenopus* oocytes showing that the minimal composition for a functional GLR-1 complex is constituted by the GLR-1 subunit, one TARP (Transmembrane AMPA receptor Regulatory Protein) homolog (STG-1 or STG-2) and SOL-1 (Walker et al., 2006; Wang et al., 2012). Indeed, GLR-1, SOL-1 and SOL-2 colocalize in puncta that distribute along the processes of AVA neurons (Wang et al., 2012). While a soluble version of SOL-1 (s-SOL-1), containing only its extracellular part (i.e., 4 CUB domains), is sufficient to partially rescue the behavioral and physiological defects in *sol-1* mutants (Zheng et al., 2006), it requires the presence of SOL-2 to function, indicating that SOL-2 may be involved in linking SOL-1 to the GLR-1 complex (Wang et al., 2012). Rescue experiments in *sol-2* mutants showed an additional SOL-1-independent role of SOL-2 in modulating GLR-1 gating (Wang et al., 2012). Thus, SOL-1 and SOL-2 are two auxiliary subunits of GLR-1 that differentially regulate its gating and SOL-2 has an additional structural role in bridging the GLR-1 receptor to SOL-1.

Neto (*Drosophila melanogaster*)

The *D. melanogaster* Neto has a domain composition similar to *C. elegans* SOL-2: it contains a type I transmembrane domain, two extracellular CUB domains and a LDLa motif (**Figure 2**). Alternative splicing generates two different isoforms, Neto- α and - β , which differ by their intracellular domains (Han et al., 2015; Ramos et al., 2015). In *D. melanogaster*, *neto* is an essential gene, as null mutations result in paralyzed embryos that never hatch into larval stages, while hypomorphic alleles cause severe locomotor defects (Kim et al., 2012). Although Neto- β is the predominant isoform at glutamatergic NMJs (Ramos et al., 2015; Han et al., 2020), expression of either Neto isoform in muscles rescues locomotion and allows the development of viable and fertile adults (Kim et al., 2012; Ramos et al., 2015). The importance of the extracellular CUB and LDLa domains is highlighted by the fact that muscle expression of a chimera, in which the intracellular part is

replaced by GFP, can rescue lethality and paralysis in *neto* mutants (Ramos et al., 2015). Neto mostly localizes at type I (glutamatergic) neuromuscular junctions, where it colocalizes with ionotropic glutamate receptors (iGluRs) at postsynaptic densities (Kim et al., 2012). Neto is dispensable for normal levels and surface expression of iGluRs (Kim et al., 2012, 2015). In the absence of Neto, synapses form normally at the prepattern stage but iGluRs fail to cluster at postsynaptic densities and maintenance of the postsynaptic site is altered (Kim et al., 2012). This is accompanied by electrophysiological defects in miniature and evoked excitatory junctional potentials (Kim et al., 2012). In contrast, when *neto* is over-expressed, it accumulates at extrajunctional sites and results in synapse defects, probably due to extrajunctional trapping of iGluRs (Kim et al., 2015). In iGluR mutants, Neto clusters do not form, indicating a codependency of iGluRs and Neto (Kim et al., 2012), which is reminiscent of the dependent clustering of LEV-10 with L-AChRs in *C. elegans* and Hig/Hasp with AChRs in *D. melanogaster*. Co-expression of Neto- α or Neto- β with iGluR subunits in *Xenopus* oocytes greatly enhances receptor currents, suggesting that the clustering mechanism may enhance receptor function (Han et al., 2015). The two isoforms have distinct roles. Neto- β , via its intracellular domain, regulates the composition of the postsynaptic side at NMJs, by promoting a preferential recruitment of GLURIIA over GLURIIIB (Ramos et al., 2015). Neto- β is also involved in regulating the postsynaptic structure by promoting the formation of subsynaptic reticulum (Ramos et al., 2015). On the postsynaptic side, Neto- α limits the size of the receptor fields. On the presynaptic side, the extracellular domains of Neto- α are sufficient for the modulation of basal neurotransmission and its intracellular domain regulates presynaptic homeostasis (Han et al., 2020). Thus, the common extracellular domains, including the CUB domains, of the two Neto isoforms modulate channel properties while the divergent intracellular domains control specific functions of Neto proteins in regulating synapse composition and homeostasis.

dSol-1 (*Drosophila melanogaster*)

dSol-1 is another CUB domain-containing protein recently identified in a screen looking for genes regulating presynaptic homeostasis at the *drosophila* NMJs (Kiragasi et al., 2020). It has a structure very close to *C. elegans* SOL-1 with four extracellular CUB domains and a transmembrane domain (**Figure 2**). Interestingly, both dSol-1 or *C. elegans* SOL-1 are able to enhance GLR-1 receptor function in heterologous cells (Walker et al., 2006), highlighting the functional conservation of the two proteins. *dSol-1* is expressed in the nervous system and excluded from postsynaptic muscles (Kiragasi et al., 2020). At *drosophila* NMJs, proper baseline transmission and presynaptic homeostatic potentiation requires the presynaptic Kainate-type ionotropic glutamate receptor subunit 1D KaiR1D (Kiragasi et al., 2020). Loss of function and rescue experiments showed the presynaptic requirement of dSol-1 for these two aspects (Kiragasi et al., 2020), and in addition, suggest that *dSol-1* may directly modulate the function of KaiR1D to enhance basal neurotransmitter release (Kiragasi et al., 2020).

CONSERVATION AND EXTENSION OF ANCIENT FUNCTIONS IN CENTRAL SYNAPSES OF MAMMALS

The percentage and absolute numbers of proteins containing CCP and TSP-1 domains increases in vertebrates compared to invertebrates (**Figure 1** and smart.embl.de). For example, the number of proteins containing at least one CCP domain in *C. elegans* is 11, representing 0.14% of the total pool of proteins, while in *Rattus norvegicus*, 54 CCP-containing proteins are found, representing 0.71% of the total pool of proteins. This suggests a correlation between the number of proteins containing these domains and organism complexity. This relationship is true for the CUB domain when numbers are compared with *D. melanogaster*, but not with *C. elegans* where a large number of CUB domain-containing proteins are found, suggesting a specific evolution in this organism (**Figure 1**)¹. Many of these proteins have yet to be studied functionally and only a few have been identified to play roles at neuronal synapses in mammals.

TSP-1 Domain-Containing Proteins and Synaptogenesis Thrombospondins

The Thrombospondin family is composed of five different members (TSP1-5), which are large secreted extracellular matrix (ECM) proteins that mediate cell–cell and cell–ECM interactions (reviewed in (Ferrer-Ferrer and Dityatev, 2018)). Amongst them, TSP1 and TSP2 are characterized by the presence of three TSP-1 domains, in addition to the Type 2 and Type 3 repeats common to all thrombospondins (Adams and Tucker, 2000; **Figure 2**). They are secreted by astrocytes and promote synapse formation in various neuronal types and networks (Christopherson et al., 2005). All TSPs have a synaptogenic effect in cultured retinal ganglion cells, indicating that this function is independent of the TSP-1 domain (Eroglu et al., 2009). *Tsp1* and *Tsp2* double knockout mice present a reduction of 50% of excitatory synapse numbers in the cortex at postnatal day P8 and a reduction of around 30% is still found by P21 (Christopherson et al., 2005). Both TSP1 and TSP2 can increase synapse numbers in cultured retinal ganglion cells. While those TSP-induced synapses are ultrastructurally normal and presynaptically active, they are postsynaptically silent (Christopherson et al., 2005). In the mouse inner ear, TSP1 and TSP2 are also required for afferent synaptogenesis and synapse function and they are only partially functionally redundant (Mendus et al., 2014).

TSPs have many interacting partners (reviewed in (Risher and Eroglu, 2012)), including synaptic proteins. TSP1 can bind to beta1-integrins *via* its TSP-1 domains (Calzada et al., 2004). Beta-integrins control the accumulation of GlyRs at inhibitory synapses in cultured spinal cord neurons and TSP1 can reduce their mobility and increase their accumulation at synapses as well (Charrier et al., 2010). TSP1 also reduces the accumulation of AMPA receptors at synapses in spinal cord neurons (Hennekinne et al., 2013). Furthermore, TSP1 can inhibit the accumulation of

AMPA-type glutamate receptors at synapses induced by PTX-3 (Fossati et al., 2019), independently of the synaptogenic domain identified by Eroglu et al. These results suggest a dual function of TSP1, on one hand in promoting synapse formation, independent of its TSP-1 domains, and on the other hand in putting a brake on receptor accumulation at synapses *via* its TSP-1 domain.

The Adhesion Receptors BAI1, BAI2, and BAI3

The three brain-specific angiogenesis inhibitor receptors (BAI1-3, **Figure 2**) are a subgroup of the adhesion-GPCR family of receptors (Sigoillot et al., 2016; Scholz et al., 2019). They all share the same organization: an intracellular domain with a PDZ binding domain, a seven transmembrane domain, a proteolytic cleavage site, a hormone binding domain and a long extracellular domain with four TSP-1 domains for BAI2 and BAI3 and five for BAI1. Particularities are the presence of a CUB domain at the N-terminus of BAI3 and an RGD domain at the N-terminus of BAI1, indicating that these receptors might not be completely functionally redundant.

BAI1 is enriched in biochemical preparations of postsynaptic densities (Duman et al., 2013; Stephenson et al., 2013), and besides interacting with proteins regulating the cytoskeleton, can interact with several synaptic proteins such as PSD95 intracellularly (Stephenson et al., 2013) and Neuroligin-1 extracellularly (Tu et al., 2018). Knockdown of BAI1 in hippocampal neurons leads to reduced spine density and immature spine morphogenesis both in primary cultures and *in vivo* (Duman et al., 2013; Tu et al., 2018). BAI1 can induce the clustering of the VGlut1 presynaptic vesicle protein in a co-culture assay through its extracellular domain, and both this function and its synaptogenic ability in cultured hippocampal neurons necessitate the N-terminal TSP-1 containing domain (Tu et al., 2018). No deficits in spinogenesis were found in hippocampal neurons of BAI1 knockout mice (Zhu et al., 2015), suggesting a potential non-cell autonomous compensation. However, knockout of BAI1 in mice leads to a decrease in PSD95 protein levels and PSD thickness and a deficient long-term synaptic plasticity in CA1 hippocampal neurons (Zhu et al., 2015).

The first role described for the BAI3 receptor in neurons was the regulation of dendritogenesis in cerebellar Purkinje cells (Lanoue et al., 2013). BAI3 was further shown to promote spinogenesis and synaptogenesis in cerebellar Purkinje cells (Sigoillot et al., 2015), and in the olfactory bulb (Wang et al., 2020). BAI3 binds to the globular domain (gC1q) of the C1QL subfamily of C1q-related proteins *via* both the TSP-1 domains and the CUB domain (Bolliger et al., 2011; Kakegawa et al., 2015). Loss-of-function studies have shown that C1QL proteins are required for proper synaptogenesis in the cerebellum (Kakegawa et al., 2015; Sigoillot et al., 2015), amygdala and cortex (Martinelli et al., 2016) and olfactory bulb (Wang et al., 2020). The CUB domain of BAI3 is indeed essential for BAI3 synaptic function in cerebellar Purkinje cells, since a mutant lacking this domain cannot rescue the BAI3 loss-of-function phenotype (Kakegawa et al., 2015). Since C1QL proteins are secreted, it is probable that C1QL proteins form a bridge between BAI3 receptors postsynaptically and a membrane

¹smart.embl.de

protein presynaptically, in a manner similar to the neurexin-CBLN-GluD2 tripartite complex. Indeed, C1QL2 and C1QL3 can bind to neurexin 3 (Matsuda et al., 2016) and a very recent study suggests the formation of a tripartite complex between neuronal pentraxin-1, C1QL3 and BAI3 (Sticco et al., 2021). Very recently, BAI1 and BAI3 receptors were shown to promote synapse formation via transsynaptic binding of RTN4 receptors (Wang et al., 2021). One of the TSP-1 domains in BAI receptors, and its glycosylation, is essential for this binding (Wang et al., 2021), highlighting the importance of TSP-1 domains for synapse formation.

CCP Domain: From Receptor Trafficking to Synaptic Plasticity

GABA_B Receptors

Metabotropic GABA_B receptors mediate slow inhibitory transmission in the central nervous system. These receptors are heterodimers composed of GABA_BR1 and GABA_BR2 subunits. There are two major R1 splice variants, R1a and R1b, that differ by the presence of two CCP domains in the N terminus of R1a (**Figure 2**). Several other R1 splice variants contain CCP domains but no transmembrane domain, indicating that they are secreted (Lee et al., 2010). The CCP domains of R1a are sufficient to target an otherwise diffuse protein to axons, suggesting that the CCP domains of R1a function as an axon targeting signal (Biermann et al., 2010). Furthermore, these CCP domains confer greater surface stabilization to R1a/R2 GABA_B receptors compared to R1b/R2 and are sufficient when fused to mGluR2 receptors to increase their surface stability (Hannan et al., 2012). The isoforms R1a and R1b also differ in their probability to diffuse laterally at postsynaptic sites: R1a/R2 are more mobile than R1b/R2 (Hannan et al., 2016). The R1j isoform encodes the signal peptide and the two CCP domains of R1a (**Figure 2**). A recombinant protein mimicking this isoform can bind to neuronal membranes and impairs the inhibitory effect of GABA_B receptors on glutamate release but does not affect the activity of the GABA_B receptors (Tiao et al., 2008). CCP domains can thus regulate the axonal trafficking and surface stabilization of GABA_B receptors as well as their function at excitatory synapses. These functions involve the interaction of the first CCP domain of GABA_BR1a with APP, AJAP-1 and PIANP (Schwenk et al., 2016; Dinamarca et al., 2019), further highlighting the functional importance of CCP domains in the regulation of synaptic protein localization and synapse function.

SRPX2

SRPX2 (Sushi-repeat protein X-linked 2) was identified as the causal gene for Rolandic (also known as Sylvian) epilepsy (Roll et al., 2006) and encodes a 465 amino acid secreted protein containing three CCP domains and one hyaline repeat (**Figure 2**). The hyaline repeat domain folds similarly to the IG-like domain found in the protein Hig from *Drosophila*. The Y72S mutation identified in patients with Rolandic epilepsy is in the immediate vicinity of a cysteine residue that is predicted to participate in the disulfide bond of the SRPX2 CCP domain (Roll et al., 2006), showing the importance of CCP domains for the brain function of SRPX2.

In rodents, *SrpX2* is expressed during the development of the cortex (Salmi et al., 2013). In utero *SrpX2* gene silencing in rats leads to impaired neuronal migration, altered positioning of projection neurons and altered dendritogenesis, together with a dramatic increase in glutamatergic and GABAergic spontaneous burst-type activities (Salmi et al., 2013), in line with seizures in humans with *SRPX2* mutations. However, other studies in the mouse, using knockdown or knockout models, and dissociated cultured neurons, support a role for *SRPX2* in promoting excitatory synapse formation and function in various regions of the cortex (Sia et al., 2013; Cong et al., 2020). Indeed, mice lacking *SRPX2* expression have decreased spine density and synapse numbers in the retinogeniculate pathway and in the somatosensory cortex and a decreased maximum AMPA receptor current at retinogeniculate synapses (Cong et al., 2020). Cong et al. (2020) also showed that *SRPX2* can interact with the complement protein C1Q, and that it inhibits complement C3 accumulation and microglial-mediated synapse elimination (Cong et al., 2020). These data show that *SRPX2* promotes excitatory synapse formation at least in part by inhibiting synapse elimination. Thus, the exact role of *SRPX2* and the mechanism leading to epilepsies remains to be determined. A yeast two-hybrid screen identified several other *SRPX2* interactors: a GPI-anchored plasminogen activator receptor named uPAR, the cysteine protease cathepsin B and the metalloproteinase ADAMTS4 (Royer-Zemmour et al., 2008). Notably, all these proteins are components of the extracellular proteolysis machinery, suggesting that, in addition to its regulation of the complement, the role of *SRPX2* in synaptogenesis could involve remodeling of the extracellular matrix, thereby regulating the clustering of glutamate receptors.

SUSD2 and SUSD4

The Sushi domain-containing protein (SUSD) family is composed of six proteins, which all contain one or more CCP domains (**Figure 2**), and, except *SUSD1*, a transmembrane domain. The *Susd2* and *Susd3* genes also encode a shorter secreted isoform. *SUSD2* was the first member with a described function at neuronal synapses (Nadjar et al., 2015) and localizes in somata and dendrites of cultured hippocampal neurons. Knockdown of *Susd2* results in increased dendritic length, reduced axon length and branching and reduced excitatory synapse numbers (Nadjar et al., 2015). Loss-of-function of *Susd4* in mice leads to motor coordination adaptation and learning impairments (Zhu et al., 2020; González-Calvo et al., 2021) and misregulation of synaptic plasticity in cerebellar Purkinje cells with decreased long-term depression (González-Calvo et al., 2021). *SUSD4* interacts *via* its cytoplasmic domain with several HECT ubiquitin ligases of the NEDD4 subfamily (González-Calvo et al., 2021). These ubiquitin ligases promote the ubiquitination and degradation of a large number of cellular substrates, including AMPA Receptors (Schwarz et al., 2010; Zhu et al., 2017). Loss-of-function of *Susd4* prevents activity-dependent degradation of GluA2 AMPA receptor subunits after chemical LTD induction (González-Calvo et al., 2021). Thus interaction of *SUSD4* with GluA2 and NEDD4 ubiquitin ligases could promote the targeting of AMPA receptors to the

degradation compartment and long-term synaptic depression (González-Calvo et al., 2021). Interestingly, the extracellular domain of SUSD4, containing the CCP domains, interacts strongly with the GluA2-containing AMPA receptors (González-Calvo et al., 2021): given the existence of potential cleavage sites that could release the extracellular domain, further work should aim at testing whether this domain alone regulates the localization and/or function of GluA2 subunits. Besides *SUSD4*, *SUSD1*, *SUSD5* and *SUSD6* are expressed in the human primary motor cortex with the highest expression level found in excitatory neurons (Annex 1), suggesting a role for these other SUSD members in brain development and/or function.

Proteins of the Extracellular Matrix

The extracellular matrix plays an active role in synapse function and plasticity (reviewed in (Frischknecht et al., 2014)) and contains several CCP domain-containing proteins: Aggrecan (ACAN), Brevican (BCAN), Neurocan (NCAN, also known as CSPG3) and Versican (VCAN). All four proteins contain a single CCP domain at their C-terminus (**Figure 2**) and are found in perineuronal nets, a specialized structure of the extracellular matrix around various types of neurons (Fawcett et al., 2019). In the absence of BCAN, perineuronal nets around neurons of the hippocampus are disorganized and sparse (Brakebusch et al., 2002). Synapses between the Schaffer collaterals and the CA1 pyramidal neurons in *Bcan* knockout mice are dramatically impaired for the maintenance of synaptic long-term potentiation (LTP), while the basic properties of excitatory and inhibitory synapses as well as LTP induction are normal (Brakebusch et al., 2002). In the *Ncan* knockout mice, maintenance of synaptic LTP in the CA1 region is impaired while the perineuronal nets appear largely normal (Zhou et al., 2001). Experiments in cultured neurons indicate that these proteins might also contribute to the regulation of synapse numbers (Geissler et al., 2013; Gottschling et al., 2019). CCP domain-containing proteins in the extracellular matrix are thus essential for the formation of perineuronal nets and the formation and function of synapses, but the role of the CCP domain in these proteins remains to be deciphered.

CUB-Domain Containing Proteins: From Auxiliary Subunits to Synapse Formation

NETO1 and NETO2

NETO1 and NETO2 are brain-specific proteins with a domain organization resembling the one of CUB-domain containing proteins in invertebrates (LEV-10, SOL-2 and *Drosophila* Neto). They are both type 1 transmembrane proteins with a large ectodomain composed of one LDLa domain and two CUB domains (Stohr et al., 2002; Michishita et al., 2003, 2004). The C-terminal region of NETO1 and NETO2 contains a class I- and class II- PDZ binding motif, respectively (Ng et al., 2009; Tang et al., 2012; **Figure 2**). The CUB domains of NETO proteins are required for their interaction with NMDARs (Ng et al., 2009), kainate receptors KARs (Tang et al., 2011) and the K⁺-Cl⁻ cotransporter KCC2 (Ivakine et al., 2013). NETO2 interacts with GRIP through its C-terminal PDZ binding motif (Tang et al., 2012) while NETO1 interacts with the scaffolding protein PSD-95 (Ng et al., 2009). Both NETO1 and NETO2 are enriched

in biochemical fractions enriched in postsynaptic densities (Ng et al., 2009; Zhang et al., 2009).

In vertebrates, NETO1 and NETO2 have been primarily studied for their role as auxiliary subunits of kainate receptors (Zhang et al., 2009; Copits et al., 2011; Straub, 2011; Fisher and Mott, 2013). Coexpression of Neto1 or Neto2 with kainate receptors in heterologous cells greatly enhances glutamate-evoked currents (Zhang et al., 2009). More specifically, Neto1 increases KAR affinity for kainate and glutamate (Straub, 2011; Fisher and Mott, 2013), increases KAR EPSC amplitude (Straub, 2011; Tang et al., 2011), and regulates KAR desensitization properties (Copits et al., 2011; Straub, 2011; Fisher and Mott, 2013; Sheng et al., 2015). However, exactly how NETO proteins regulate KARs may vary depending on the subunit composition and on the synapse. NETO1 and NETO2 have a different pattern of expression in the brain. NETO2 is very abundant in the cerebellum, while NETO1 is highly expressed in the hippocampus, particularly in the CA3 field (Michishita et al., 2003, 2004; Ng et al., 2009; Straub, 2011; Tang et al., 2011, 2012). Indeed, KAR mediated currents are reduced at the mossy fiber/CA3 synapse of *Neto1*^{-/-} mice but not *Neto2*^{-/-} mice (Tang et al., 2011). Moreover, NETO1, but not NETO2, regulates KAR currents in hippocampal interneurons (Wyeth et al., 2017). In addition to the defects in kainate mediated currents, *Neto1*^{-/-} mice present NMDAR defects at specific synapses: NMDAR mediated currents are reduced at CA1/Schaffer collateral synapses and at associational/commissural CA3 synapses but not at mossy fiber CA3 synapses (Ng et al., 2009; Straub, 2011; Tang et al., 2011). No defects in AMPAR mediated currents have been detected in the absence of *Neto1* or *Neto2* (Ng et al., 2009; Zhang et al., 2009).

Besides their role in regulating glutamate receptor function, NETO proteins could also regulate receptor localization, although the evidence for this role is contradictory. While some studies did not detect any changes in KAR abundance at synapses in the absence of NETO proteins (Zhang et al., 2009; Straub, 2011), others suggest that NETO proteins may be involved in the recruitment and/or stabilization of KARs at synapses (Tang et al., 2011, 2012; Wyeth et al., 2014; Mennesson et al., 2019). In *Neto1* knockout mice, GluN2A levels are reduced in PSD fractions but not in whole brain extract, and surface GluN2A are unchanged (Ng et al., 2009). This suggests that NETO1 could have a role in clustering of GluN2A at glutamatergic synapses, reminiscent of the role of CUB-domain containing proteins in invertebrates. Furthermore, the absence of *Neto1* leads to loss of presynaptic kainate receptors at immature CA3-CA1 synapses and a deficit in synaptogenesis (Orav et al., 2017). Thus, besides their role as auxiliary subunits of glutamate receptors, NETO proteins could also contribute to the regulation of synapse formation and molecular composition.

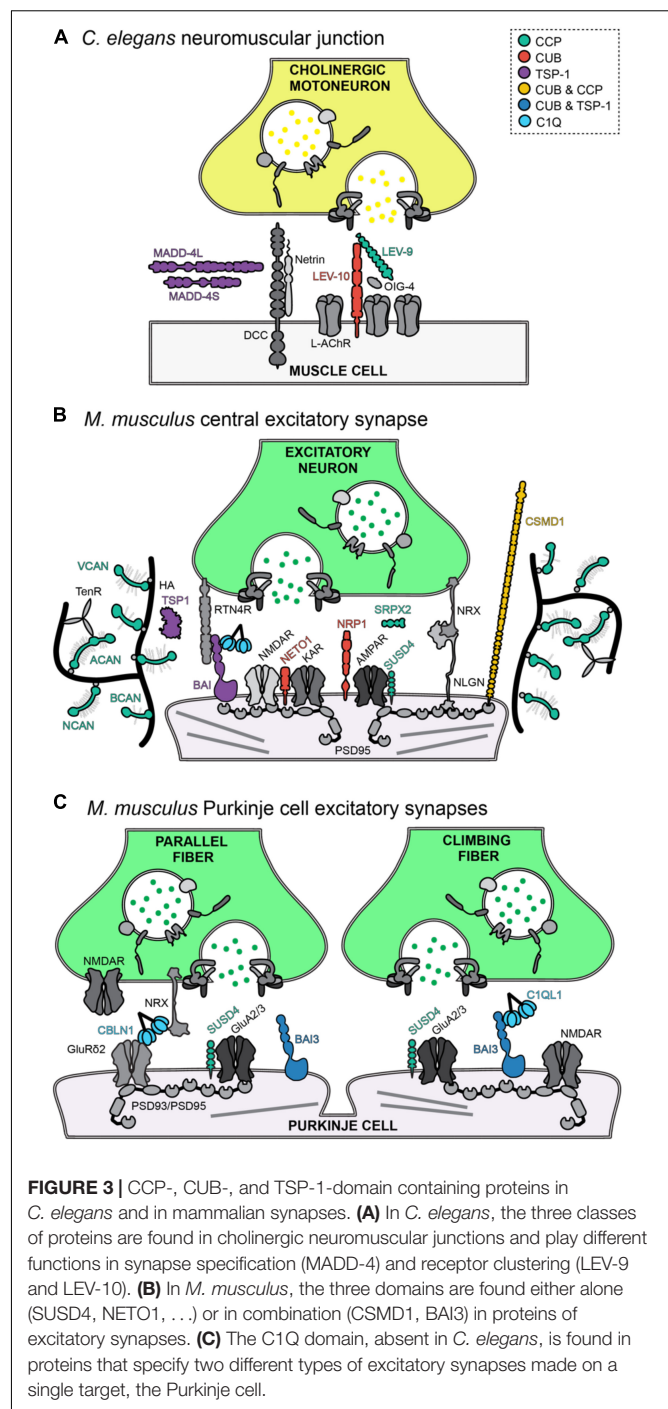
Neuropilin-1 and 2

The Neuropilin family is composed of two members, neuropilin-1 and neuropilin-2 (NRP-1 and NRP-2, respectively, **Figure 2**). Both neuropilins are transmembrane glycoproteins with one short cytosolic domain, a MAM domain (for meprin, A-5 protein and receptor protein tyrosine phosphatase mu), a

discoidin domain and two N-terminal CUB domains (Kolodkin et al., 1997). Neuropilins are the receptors for class 3 secreted semaphorins: NRP-1 binds with high affinity to semaphorin 3A (SEMA3A) and NRP-2 binds to SEMA3F. While they were first described as receptors for axon guidance cues (Kolodkin et al., 1997), both are enriched in synaptosomal and PSD preparations from the adult hippocampus and have been shown to play synaptic roles. In the cerebellum, Basket cells express NRP-1 and Purkinje cells express its ligand SEMA3A (Telley et al., 2016). Proper contact and synapse development between Purkinje cells and basket cell axons require the interaction of NRP-1 with the adhesion protein NF186. This interaction is facilitated by SEMA3A secretion in Purkinje cells (Telley et al., 2016). While the CUB domain of NRP-1 is involved in the interaction with its ligand SEMA3A, whether it is involved in additional aspect of NRP-1 function at synapses remain to be determined. Knockout for *Nrp2* in mice leads to increased epileptogenicity (Eisenberg et al., 2021). Increased spine densities and changes in spine morphogenesis are found in both mouse knockout for *Nrp-2* and *Sema3F*, a ligand of NRP2 (Tran et al., 2009). In the *Nrp-2* knockout mice, patch-clamp recordings found increased mEPSC frequency in cortical and hippocampal neurons in the absence of changes in the paired-pulse ratio (Tran et al., 2009) and decreased mIPSCs in CA1 neurons accompanying a reduction in interneuron numbers (Eisenberg et al., 2021), indicating an effect on the number of synapses. In addition, loss-of-function of NRP-2 prevents homeostatic plasticity since it prevents bicuculline-induced reduction in surface AMPA receptors and in synaptic strength in cortical neurons. NRP-2 is found in spines of cultured cortical neurons where it colocalizes with the GluA1 subunit of AMPA receptors (Wang et al., 2017). NRP-2 interacts with GluA1-containing AMPA receptors through its CUB domains, and this interaction is modulated by neuronal activity and SEMA3F (Wang et al., 2017). These results show that the CUB domains of NRP-2 are key for homeostatic plasticity at excitatory synapses by enabling interaction with GluA1 AMPA receptor subunits.

ADDITION AND COMBINATION OF STRUCTURAL DOMAINS IN VERTEBRATE SYNAPTIC PROTEINS ACCOMPANIES THE COMPLEXIFICATION OF SYNAPSES

Comparing the structure of CCP, CUB, and TSP-1-containing proteins across species shows that invertebrates contain synaptic proteins with stretches of a single domain type whereas mammalian synaptic proteins are composed of combinations of CCP, CUB, and TSP-1 domains, together with a large diversity of other domains (Figure 2). This suggests that multiple functions have been combined in vertebrates in single proteins and that the function of a particular domain could be partially inferred by the function of invertebrate proteins. CCP containing proteins in invertebrates such as LEV9 (Figure 3), Hig and Hasp play a major role in the clustering of synaptic proteins, in particular



neurotransmitter receptors. CUB domain containing proteins in invertebrates, such as SOL1 (Figure 3) or dSOL1, function as auxiliary subunit and/or control receptor gating. The phenotype of mouse mutants for CCP or CUB domain-containing proteins indicate that their function might be indeed conserved: CCP proteins such as SRPX2 and SUSD4 play roles in controlling receptor numbers at synapses while CUB containing NETO proteins control kainate receptor gating. The studies of MADD-4 in *C. elegans* suggest a role for TSP-1 containing proteins in

synapse specification on a given target cell (**Figure 3**) and the Thrombospondins and BAI proteins in mammals play a role in synaptogenesis and receptor localization. Conversely, studies in mammals can reveal the importance of structural domains that are not found in invertebrates. For example the C1q globular domain defines a large family of proteins that includes proteins with known synaptic functions: the innate immunity protein C1Q that also regulates synapse elimination in the nervous system, the cerebellins and C1QL proteins (Bolliger et al., 2011; Yuzaki, 2011; Sigoillot et al., 2015). C1QL1 is specifically secreted by one type of excitatory input of the cerebellar Purkinje cells, the climbing fibers, and is essential, together with its receptor BAI3, for excitatory synapse specification in cerebellar Purkinje cells (**Figure 3**). The C1q globular domain is not found in *C. elegans*, suggesting that the appearance of this structural domain might have contributed to the increased diversity of synapse types in vertebrates. Interestingly, while CCP, CUB, and C1Q domain containing proteins were identified first in the immune system, the presence of CCP and CUB domain proteins in *C. elegans* suggest an ancient role for these structural domains in forming and regulating signaling complexes, in particular with neurotransmitter receptors, a role that could have been then tethered to various biological systems during evolution.

CCP and CUB domains are combined in neuronal proteins such as SEZ6 isoforms (Shimizu-Nishikawa et al., 1995; Osaki et al., 2011) and CSMD1-3 (CUB and Sushi multiple domains family of proteins; **Figure 2**). Neurons lacking SEZ-6 present fewer spines, PSD95 puncta and reduced EPSPs (Gunnarsen et al., 2007), suggesting a yet to be understood synaptic function. All three CSMD proteins have fourteen CUB domains and twenty-six to twenty-eight CCP domains (**Figure 2**). CSMD1 and CSMD2 are both synaptic (Loh et al., 2016; Gutierrez et al., 2019). CSMD2 directly interacts with the scaffold PSD-95 through its PDZ-binding domain and knockdown of CSMD2 reduces spine density in cultured hippocampal neurons (Gutierrez et al., 2019). Thus, both for SEZ-6 and CSMD proteins, their precise synaptic function, and in particular, whether the functions of CUB and CCP domains in clustering and gating receptors are conserved, remains to be demonstrated. Interestingly, TSP-1 domains in synaptic proteins are not associated to CUB or CCP domains, except for BAI3 that contains a single CUB domain at its N-terminus (**Figure 2**). Thus, synapse specification on one hand and receptor clustering and gating on the other hand might be two synaptic aspects controlled independently by proteins containing TSP-1 and CUB/CCP domains, respectively. To demonstrate this hypothetical division of labor, further studies of the precise roles of independent domains in mammalian synaptic proteins using mutagenesis are warranted.

The percentage of proteins containing CCP, CUB, and TSP-1 domains is increased in vertebrates compared to invertebrates

(**Figure 1**). Many families of such proteins are highly expressed in the human brain (Annex 1), but their role remains to be determined. In addition, while the role of proteins containing CCP, CUB, and TSP-1 domains at excitatory synapses in mammals starts to be better understood, their role at inhibitory synapses remains largely unknown and deserves further study. In many cases, mutations in genes coding CCP, CUB, or TSP-1 containing proteins in humans have been associated with brain diseases highlighting their importance for brain development and function. In *Homo sapiens*, the *SUSD4* gene is located in the chromosome deletion linked with Fryns syndrome, which is an autosomal recessive multiple congenital neurodevelopmental disorder associated with intellectual disability (Shaffer et al., 2007) and *SUSD4* variants have also been associated with autism spectrum disorders (Cuscó et al., 2009; Coe et al., 2019). *ADGRB1-3* genes have been associated with disorders such as autism spectrum disorders (Michaelson et al., 2012), schizophrenia (DeRosse et al., 2008), bipolar disorder (McCarthy et al., 2012), intellectual disability (Scuderi et al., 2019) and addiction (Liu et al., 2006). Variants in *ADAMTSL3*, the human orthologue of *C. elegans* MADD-4, and all three *CSMD* genes have been associated with schizophrenia (Need et al., 2009; Dow et al., 2011; Schizophrenia Psychiatric Genome-Wide Association Study (GWAS) Consortium, 2011; Luo et al., 2018). Understanding the specific functions of the CCP, CUB, or TSP-1 containing proteins is thus an emerging field with direct relevance for the treatment of brain diseases.

AUTHOR CONTRIBUTIONS

IG-C, MC, J-LB, and FS contributed to conception of the manuscript. IG-C, MC, and FS wrote sections of the manuscript. All authors contributed to manuscript revision, read, and approved the submitted version.

FUNDING

This work was supported by the European Research Council SynID grant 724601 to FS and ERC_Adg C.NAPSE #695295 (within the framework of the LABEX CORTEX (ANR-11-LABX-0042 of Université de Lyon) to J-LB and MC.

SUPPLEMENTARY MATERIAL

The Supplementary Material for this article can be found online at: <https://www.frontiersin.org/articles/10.3389/fnins.2022.866444/full#supplementary-material>

REFERENCES

- Adams, J. C., and Tucker, R. P. (2000). The thrombospondin type 1 repeat (TSR) superfamily: diverse proteins with related roles in neuronal development. *Dev. Dyn.* 218, 280–299.
- Arendt, D. (2020). The evolutionary assembly of neuronal machinery. *Curr. Biol.* 30, R603–R616. doi: 10.1016/j.cub.2020.04.008
- Bayés, À, van de Lagemaat, L. N., Collins, M. O., Croning, M. D. R., Whittle, I. R., Choudhary, J. S., et al. (2011). Characterization of the proteome, diseases

- and evolution of the human postsynaptic density. *Nat. Neurosci.* 14, 19–21. doi: 10.1038/nn.2719
- Biermann, B., Ivankova-Susankova, K., Bradaia, A., Abdel Aziz, S., Besseyrias, V., Kapfhammer, J. P., et al. (2010). The sushi domains of GABAB receptors function as axonal targeting signals. *J. Neurosci. Off. J. Soc. Neurosci.* 30, 1385–1394. doi: 10.1523/JNEUROSCI.3172-09.2010
- Blein, S., Gingham, R., Uhrin, D., Smith, B. O., Soares, D. C., Veltel, S., et al. (2004). Structural analysis of the complement control protein (CCP) modules of GABAB receptor 1a only one of the two CCP modules is compactly folded. *J. Biol. Chem.* 279, 48292–48306. doi: 10.1074/jbc.M406540200
- Bolliger, M. F., Martinelli, D. C., and Südhof, T. C. (2011). The cell-adhesion G protein-coupled receptor BAI3 is a high-affinity receptor for C1q-like proteins. *Proc. Natl. Acad. Sci. U.S.A.* 108, 2534–2539. doi: 10.1073/pnas.1019577108
- Bork, P., and Beckmann, G. (1993). The CUB domain, a widespread module in developmentally regulated proteins. *J. Mol. Biol.* 231, 539–545. doi: 10.1006/jmbi.1993.1305
- Boulanger, L. M. (2009). Immune proteins in brain development and synaptic plasticity. *Neuron* 64, 93–109. doi: 10.1016/j.neuron.2009.09.001
- Brakebusch, C., Seidenbecher, C. I., Asztely, F., Rauch, U., Matthies, H., Meyer, H., et al. (2002). Brevican-deficient mice display impaired hippocampal CA1 long-term potentiation but show no obvious deficits in learning and memory. *Mol. Cell. Biol.* 22, 7417–7427. doi: 10.1128/mcb.22.21.7417-7427.2002
- Briggs, D. C., Birchenough, H. L., Ali, T., Rugg, M. S., Waltho, J. P., Ievoli, E., et al. (2015). Metal ion-dependent heavy chain transfer activity of TSG-6 mediates assembly of the cumulus-oocyte matrix. *J. Biol. Chem.* 290, 28708–28723. doi: 10.1074/jbc.M115.669838
- Brenner, S. (1974). The genetics of *Caenorhabditis elegans*. *Genetics* 77, 71–94. doi: 10.1093/genetics/77.1.71
- Briseno-Roa, L., and Bessereau, J.-L. (2014). Proteolytic processing of the extracellular scaffolding protein LEV-9 is required for clustering acetylcholine receptors. *J. Biol. Chem.* 289, 10967–10974. doi: 10.1074/jbc.C113.534677
- Calzada, M. J., Annis, D. S., Zeng, B., Marcinkiewicz, C., Banas, B., Lawler, J., et al. (2004). Identification of novel $\beta 1$ integrin binding sites in the type 1 and type 2 repeats of thrombospondin-1. *J. Biol. Chem.* 279, 41734–41743. doi: 10.1074/jbc.M406267200
- Cameron, S., and McAllister, A. K. (2018). Immunoglobulin-like receptors and their impact on wiring of brain synapses. *Annu. Rev. Genet.* 52, 567–590. doi: 10.1146/annurev-genet-120417-031513
- Charrier, C., Machado, P., Tweedie-Cullen, R. Y., Rutishauser, D., Mansuy, I. M., and Triller, A. (2010). A crosstalk between $\beta 1$ and $\beta 3$ integrins controls glycine receptor and gephyrin trafficking at synapses. *Nat. Neurosci.* 13, 1388–1395. doi: 10.1038/nn.2645
- Chen, C., Fu, H., He, P., Yang, P., and Tu, H. (2021). Extracellular matrix muscle arm development defective protein cooperates with the one immunoglobulin domain protein to suppress precocious synaptic remodeling. *ACS Chem. Neurosci.* 12, 2045–2056. doi: 10.1021/acscchemneuro.1c00194
- Christopherson, K. S., Ullian, E. M., Stokes, C. C. A., Mallowney, C. E., Hell, J. W., Agah, A., et al. (2005). Thrombospondins are astrocyte-secreted proteins that promote CNS synaptogenesis. *Cell* 120, 421–433. doi: 10.1016/j.cell.2004.12.020
- Cizeron, M., Qiu, Z., Koniaris, B., Gokhale, R., Komiyama, N. H., Fransén, E., et al. (2020). A brain-wide atlas of synapses across the mouse lifespan. *Science* 369, 270–275. doi: 10.1126/science.aba3163
- Coe, B. P., Stessman, H. A. F., Sulovari, A., Geisheker, M. R., Bakken, T. E., Lake, A. M., et al. (2019). Neurodevelopmental disease genes implicated by de novo mutation and copy number variation morbidity. *Nat. Genet.* 51, 106–116. doi: 10.1038/s41588-018-0288-4
- Cong, Q., Soteros, B. M., Wollet, M., Kim, J. H., and Sia, G.-M. (2020). The endogenous neuronal complement inhibitor SRPX2 protects against complement-mediated synapse elimination during development. *Nat. Neurosci.* 23, 1067–1078. doi: 10.1038/s41593-020-0672-0
- Copits, B. A., Robbins, J. S., Frausto, S., and Swanson, G. T. (2011). Synaptic targeting and functional modulation of GluK1 kainate receptors by the auxiliary neuropilin and toll-like (NETO) proteins. *J. Neurosci.* 31, 7334–7340. doi: 10.1523/JNEUROSCI.0100-11.2011
- Cuscó, I., Medrano, A., Gener, B., Vilardell, M., Gallastegui, F., Villa, O., et al. (2009). Autism-specific copy number variants further implicate the phosphatidylinositol signaling pathway and the glutamatergic synapse in the etiology of the disorder. *Hum. Mol. Genet.* 18, 1795–1804. doi: 10.1093/hmg/ddp092
- DeRosse, P., Lencz, T., Burdick, K. E., Siris, S. G., Kane, J. M., and Malhotra, A. K. (2008). The genetics of symptom-based phenotypes: toward a molecular classification of schizophrenia. *Schizophr. Bull.* 34, 1047–1053. doi: 10.1093/schbul/sbn076
- Dinamarca, M. C., Raveh, A., Schneider, A., Fritzius, T., Früh, S., Rem, P. D., et al. (2019). Complex formation of APP with GABAB receptors links axonal trafficking to amyloidogenic processing. *Nat. Commun.* 10:1331. doi: 10.1038/s41467-019-09164-3
- Dow, D. J., Huxley-Jones, J., Hall, J. M., Francks, C., Maycox, P. R., Kew, J. N. C., et al. (2011). ADAMTSL3 as a candidate gene for schizophrenia: gene sequencing and ultra-high density association analysis by imputation. *Schizophr. Res.* 127, 28–34. doi: 10.1016/j.schres.2010.12.009
- Duman, J. G., Tzeng, C. P., Tu, Y.-K., Munjal, T., Schwechter, B., Ho, T. S.-Y., et al. (2013). The adhesion-GPCR BAI1 regulates synaptogenesis by controlling the recruitment of the Par3/Tiam1 polarity complex to synaptic sites. *J. Neurosci. Off. J. Soc. Neurosci.* 33, 6964–6978. doi: 10.1523/JNEUROSCI.3978-12.2013
- Eisenberg, C., Subramanian, D., Afrasiabi, M., Ziobro, P., DeLucia, J., Hirschberg, P. R., et al. (2021). Reduced hippocampal inhibition and enhanced autism-epilepsy comorbidity in mice lacking neuropilin 2. *Transl. Psychiatry* 11:537. doi: 10.1038/s41398-021-01655-6
- Eroglu, Ç., Allen, N. J., Susman, M. W., O'Rourke, N. A., Park, C. Y., Özkan, E., et al. (2009). Gabapentin receptor $\alpha 2\delta$ -1 is a neuronal thrombospondin receptor responsible for excitatory CNS synaptogenesis. *Cell* 139, 380–392. doi: 10.1016/j.cell.2009.09.025
- Fawcett, J. W., Ohashi, T., and Pizzorusso, T. (2019). The roles of perineuronal nets and the perinodal extracellular matrix in neuronal function. *Nat. Rev. Neurosci.* 20, 451–465. doi: 10.1038/s41583-019-0196-3
- Ferrer-Ferrer, M., and Dityatev, A. (2018). Shaping synapses by the neural extracellular matrix. *Front. Neuroanat.* 12:40. doi: 10.3389/fnana.2018.00040
- Fisher, J. L., and Mott, D. D. (2013). Modulation of homomeric and heteromeric kainate receptors by the auxiliary subunit neto1: neto1 modulation of kainate receptors. *J. Physiol.* 591, 4711–4724. doi: 10.1113/jphysiol.2013.256776
- Fossati, G., Pozzi, D., Canzi, A., Mirabella, F., Valentino, S., Morini, R., et al. (2019). Pentraxin 3 regulates synaptic function by inducing AMPA receptor clustering via ECM remodeling and $\beta 1$ -integrin. *EMBO J.* 38:e99529. doi: 10.15252/embj.201899529
- Frischknecht, R., Chang, K.-J., Rasband, M. N., and Seidenbecher, C. I. (2014). “Neural ECM molecules in axonal and synaptic homeostatic plasticity,” in *Progress in Brain Research*, eds S. Waxman, D. G. Stein, D. Swaab, and H. Fields (Amsterdam: Elsevier), 81–100. doi: 10.1016/B978-0-444-63486-3.00004-9
- Gally, C., Eimer, S., Richmond, J. E., and Bessereau, J.-L. (2004). A transmembrane protein required for acetylcholine receptor clustering in *Caenorhabditis elegans*. *Nature* 431, 578–582. doi: 10.1038/nature02893
- Geissler, M., Gottschling, C., Aguado, A., Rauch, U., Wetzel, C. H., Hatt, H., et al. (2013). Primary hippocampal neurons, which lack four crucial extracellular matrix molecules, display abnormalities of synaptic structure and function and severe deficits in perineuronal net formation. *J. Neurosci.* 33, 7742–7755. doi: 10.1523/JNEUROSCI.3275-12.2013
- Gendrel, M., Rapti, G., Richmond, J. E., and Bessereau, J.-L. (2009). A secreted complement-control-related protein ensures acetylcholine receptor clustering. *Nature* 461, 992–996. doi: 10.1038/nature08430
- González-Calvo, I., Iyer, K., Carquin, M., Khayachi, A., Giuliani, F. A., Sigoillot, S. M., et al. (2021). Sushi domain-containing protein 4 controls synaptic plasticity and motor learning. *Elife* 10:e65712. doi: 10.7554/eLife.65712
- Gottschling, C., Wegryn, D., Denecke, B., and Faissner, A. (2019). Elimination of the four extracellular matrix molecules tenascin-C, tenascin-R, brevican and neurocan alters the ratio of excitatory and inhibitory synapses. *Sci. Rep.* 9:13939. doi: 10.1038/s41598-019-50404-9
- Gunnersen, J. M., Kim, M. H., Fuller, S. J., De Silva, M., Britto, J. M., Hammond, V. E., et al. (2007). Seiz-6 proteins affect dendritic arborization patterns and excitability of cortical pyramidal neurons. *Neuron* 56, 621–639. doi: 10.1016/j.neuron.2007.09.018
- Gutierrez, M. A., Dwyer, B. E., and Franco, S. J. (2019). Csm2 is a synaptic transmembrane protein that interacts with PSD-95 and is required for neuronal maturation. *eNeuro* 6, ENEURO.434–ENEURO.418. doi: 10.1523/ENEURO.0434-18.2019

- Han, T. H., Dharkar, P., Mayer, M. L., and Serpe, M. (2015). Functional reconstitution of *Drosophila melanogaster* NMJ glutamate receptors. *Proc. Natl. Acad. Sci. U.S.A.* 112, 6182–6187. doi: 10.1073/pnas.1500458112
- Han, T. H., Vicidomini, R., Ramos, C. I., Wang, Q., Nguyen, P., Jarnik, M., et al. (2020). Neto- α Controls synapse organization and homeostasis at the *Drosophila* neuromuscular junction. *Cell Rep.* 32:107866. doi: 10.1016/j.celrep.2020.107866
- Hannan, S., Gerrow, K., Triller, A., and Smart, T. G. (2016). Phospho-dependent accumulation of GABABRs at presynaptic terminals after NMDAR activation. *Cell Rep.* 16, 1962–1973. doi: 10.1016/j.celrep.2016.07.021
- Hannan, S., Wilkins, M. E., and Smart, T. G. (2012). Sushi domains confer distinct trafficking profiles on GABAB receptors. *Proc. Natl. Acad. Sci. U.S.A.* 109, 12171–12176. doi: 10.1073/pnas.1201660109
- Hennekinne, L., Colasse, S., Triller, A., and Renner, M. (2013). Differential control of thrombospondin over synaptic glycine and AMPA receptors in spinal cord neurons. *J. Neurosci.* 33, 11432–11439. doi: 10.1523/JNEUROSCI.5247-12.2013
- Hoshino, M., Matsuzaki, F., Nabeshima, Y., and Hama, C. (1993). hikaru genki, a CNS-specific gene identified by abnormal locomotion in *Drosophila*, encodes a novel type of protein. *Neuron* 10, 395–407.
- Ivakine, E. A., Acton, B. A., Mahadevan, V., Ormond, J., Tang, M., Pressey, J. C., et al. (2013). Neto2 is a KCC2 interacting protein required for neuronal Cl⁻ regulation in hippocampal neurons. *Proc. Natl. Acad. Sci. U.S.A.* 110, 3561–3566. doi: 10.1073/pnas.1212907110
- Jensen, P., Soroka, V., Thomsen, N., Ralets, I., Berezin, V., Bock, E., et al. (1999). Structure and interactions of NCAM modules 1 and 2, basic elements in neural cell adhesion. *Nat. Struct. Mol. Biol.* 6, 486–493. doi: 10.1038/8292
- Kakegawa, W., Mitakidis, N., Miura, E., Abe, M., Matsuda, K., Takeo, Y. H., et al. (2015). Anterograde Clq1 signaling is required in order to determine and maintain a single-winner climbing fiber in the mouse cerebellum. *Neuron* 85, 316–329. doi: 10.1016/j.neuron.2014.12.020
- Kim, Y.-J., Bao, H., Bonanno, L., Zhang, B., and Serpe, M. (2012). *Drosophila* neto is essential for clustering glutamate receptors at the neuromuscular junction. *Genes Dev.* 26, 974–987. doi: 10.1101/gad.185165.111
- Kim, Y.-J., Igiesuorobo, O., Ramos, C. I., Bao, H., Zhang, B., and Serpe, M. (2015). Prodomain removal enables neto to stabilize glutamate receptors at the *Drosophila* neuromuscular junction. *PLoS Genet.* 11:e1004988. doi: 10.1371/journal.pgen.1004988
- Kiragasi, B., Goel, P., Perry, S., Han, Y., Li, X., and Dickman, D. (2020). The auxiliary glutamate receptor subunit dSol-1 promotes presynaptic neurotransmitter release and homeostatic potentiation. *Proc. Natl. Acad. Sci. U.S.A.* 117, 25830–25839. doi: 10.1073/pnas.1915464117
- Kolodkin, A. L., Levengood, D. V., Rowe, E. G., Tai, Y. T., Giger, R. J., and Ginty, D. D. (1997). Neurophilin is a semaphorin III receptor. *Cell* 90, 753–762. doi: 10.1016/S0092-8674(00)80535-8
- Lanoue, V., Usardi, A., Sigoillot, S. M., Talleur, M., Iyer, K., Mariani, J., et al. (2013). The adhesion-GPCR BAI3, a gene linked to psychiatric disorders, regulates dendrite morphogenesis in neurons. *Mol. Psychiatry* 18, 943–950. doi: 10.1038/mp.2013.46
- Lee, C., Mayfield, R. D., and Harris, R. A. (2010). Intron 4 containing novel GABAB1 isoforms impair GABAB receptor function. *PLoS One* 5:e14044. doi: 10.1371/journal.pone.0014044
- Liu, Q.-R., Drgon, T., Johnson, C., Walther, D., Hess, J., and Uhl, G. R. (2006). Addition molecular genetics: 639,401 SNP whole genome association identifies many “cell adhesion” genes. *Am. J. Med. Genet. B Neuropsychiatr. Genet.* 141B, 918–925. doi: 10.1002/ajmg.b.30436
- Loh, K. H., Stawski, P. S., Draycott, A. S., Udeshi, N. D., Lehrman, E. K., Wilton, D. K., et al. (2016). Proteomic analysis of unbounded cellular compartments: synaptic clefts. *Cell* 166, 1295.e–1307.e. doi: 10.1016/j.cell.2016.07.041
- Luo, N., Sui, J., Chen, J., Zhang, F., Tian, L., Lin, D., et al. (2018). A schizophrenia-related genetic-brain-cognition pathway revealed in a large Chinese population. *EBioMedicine* 37, 471–482. doi: 10.1016/j.ebiom.2018.10.009
- Maro, G. S., Gao, S., Olechwiec, A. M., Hung, W. L., Liu, M., Özkan, E., et al. (2015). MADD-4/punctin and neurexin organize C. elegans GABAergic postsynapses through neuroligin. *Neuron* 86, 1420–1432. doi: 10.1016/j.neuron.2015.05.015
- Martinelli, D. C., Chew, K. S., Rohlmann, A., Lum, M. Y., Ressler, S., Hattar, S., et al. (2016). Expression of Clq3 in discrete neuronal populations controls efferent synapse numbers and diverse behaviors. *Neuron* 91, 1034–1051. doi: 10.1016/j.neuron.2016.07.002
- Matsuda, K., Budisantoso, T., Mitakidis, N., Sugaya, Y., Miura, E., Kakegawa, W., et al. (2016). Transsynaptic modulation of kainate receptor functions by Clq-like proteins. *Neuron* 90, 752–767. doi: 10.1016/j.neuron.2016.04.001
- McCarthy, M. J., Nievergelt, C. M., Kelsoe, J. R., and Welsh, D. K. (2012). A survey of genomic studies supports association of circadian clock genes with bipolar disorder spectrum illnesses and lithium response. *PLoS One* 7:e32091. doi: 10.1371/journal.pone.0032091
- Mendus, D., Sundaresan, S., Grillet, N., Wangsawihardja, F., Leu, R., Müller, U., et al. (2014). Thrombospondins 1 and 2 are important for afferent synapse formation and function in the inner ear. *Eur. J. Neurosci.* 39, 1256–1267. doi: 10.1111/ejn.12486
- Mennesson, M., Rydgren, E., Lipina, T., Sokolowska, E., Kuleskaya, N., Morello, F., et al. (2019). Kainate receptor auxiliary subunit NETO2 is required for normal fear expression and extinction. *Neuropsychopharmacology* 44, 1855–1866. doi: 10.1038/s41386-019-0344-5
- Michaelson, J. J., Shi, Y., Gujral, M., Zheng, H., Malhotra, D., Jin, X., et al. (2012). Whole-genome sequencing in autism identifies hot spots for de novo germline mutation. *Cell* 151, 1431–1442. doi: 10.1016/j.cell.2012.11.019
- Michishita, M., Ikeda, T., Nakashiba, T., Ogawa, M., Tashiro, K., Honjo, T., et al. (2004). Expression of Btcl2, a novel member of Btcl gene family, during development of the central nervous system. *Dev. Brain Res.* 153, 135–142. doi: 10.1016/j.devbrainres.2004.06.012
- Michishita, M., Ikeda, T., Nakashiba, T., Ogawa, M., Tashiro, K., Honjo, T., et al. (2003). A novel gene, Btcl1, encoding CUB and LDLA domains is expressed in restricted areas of mouse brain. *Biochem. Biophys. Res. Commun.* 306, 680–686. doi: 10.1016/S0006-291X(03)01035-0
- Nadjar, Y., Triller, A., Bessereau, J.-L., and Dumoulin, A. (2015). The Susd2 protein regulates neurite growth and excitatory synaptic density in hippocampal cultures. *Mol. Cell. Neurosci.* 65, 82–91. doi: 10.1016/j.mcn.2015.02.007
- Nakayama, M., Matsushita, F., and Hama, C. (2014). The matrix protein hikaru genki localizes to cholinergic synaptic clefts and regulates postsynaptic organization in the *Drosophila* brain. *J. Neurosci.* 34, 13872–13877. doi: 10.1523/JNEUROSCI.1585-14.2014
- Nakayama, M., Suzuki, E., Tsunoda, S., and Hama, C. (2016). The matrix proteins hasp and hig exhibit segregated distribution within synaptic clefts and play distinct roles in synaptogenesis. *J. Neurosci. Off. J. Soc. Neurosci.* 36, 590–606. doi: 10.1523/JNEUROSCI.2300-15.2016
- Need, A. C., Ge, D., Weale, M. E., Maia, J., Feng, S., Heinzen, E. L., et al. (2009). A genome-wide investigation of SNPs and CNVs in schizophrenia. *PLoS Genet.* 5:e1000373. doi: 10.1371/journal.pgen.1000373
- Ng, D., Pitcher, G. M., Szilard, R. K., Sertié, A., Kanisek, M., Clapcote, S. J., et al. (2009). Neto1 is a novel CUB-domain NMDA receptor-interacting protein required for synaptic plasticity and learning. *PLoS Biol.* 7:e1000041. doi: 10.1371/journal.pbio.1000041
- Nithianantharajah, J., Komiyama, N. H., McKechanie, A., Johnstone, M., Blackwood, D. H., Clair, D. S., et al. (2013). Synaptic scaffold evolution generated components of vertebrate cognitive complexity. *Nat. Neurosci.* 16, 16–24. doi: 10.1038/nn.3276
- Orav, E., Atanasova, T., Shintyapina, A., Kesaf, S., Kokko, M., Partanen, J., et al. (2017). NETO1 guides development of glutamatergic connectivity in the hippocampus by regulating axonal kainate receptors. *eNeuro* 4, ENEURO.48–ENEURO.17. doi: 10.1523/ENEURO.0048-17.2017
- Osaki, G., Mitsui, S., and Yuri, K. (2011). The distribution of the seizure-related gene 6 (Sez-6) protein during postnatal development of the mouse forebrain suggests multiple functions for this protein: an analysis using a new antibody. *Brain Res.* 1386, 58–69. doi: 10.1016/j.brainres.2011.02.025
- Pääkkönen, K., Tossavainen, H., Permi, P., Rakkolainen, H., Rauvala, H., Raulo, E., et al. (2006). Solution structures of the first and fourth TSR domains of F-spondin. *Proteins* 64, 665–672. doi: 10.1002/prot.21030
- Pinan-Lucarré, B., Tu, H., Pierron, M., Cruceyra, P. I., Zhan, H., Stigloher, C., et al. (2014). C. elegans punctin specifies cholinergic versus GABAergic identity of postsynaptic domains. *Nature* 511, 466–470. doi: 10.1038/nature13313
- Ramos, C. I., Igiesuorobo, O., Wang, Q., and Serpe, M. (2015). Neto-mediated intracellular interactions shape postsynaptic composition at the *Drosophila* neuromuscular junction. *PLoS Genet.* 11:e1005191. doi: 10.1371/journal.pgen.1005191
- Rapti, G., Richmond, J., and Bessereau, J.-L. (2011). A single immunoglobulin-domain protein required for clustering acetylcholine receptors in C. elegans:

- role of *C. elegans* OIG-4 in AChR clustering. *EMBO J.* 30, 706–718. doi: 10.1038/emboj.2010.355
- Reid, K. B., and Day, A. J. (1989). Structure-function relationships of the complement components. *Immunol. Today* 10, 177–180. doi: 10.1016/0167-5699(89)90317-4
- Risher, W. C., and Eroglu, C. (2012). Thrombospondins as key regulators of synaptogenesis in the central nervous system. *Matrix Biol.* 31, 170–177. doi: 10.1016/j.matbio.2012.01.004
- Roll, P., Rudolf, G., Pereira, S., Royer, B., Scheffer, I. E., Massacrier, A., et al. (2006). SRPX2 mutations in disorders of language cortex and cognition. *Hum. Mol. Genet.* 15, 1195–1207. doi: 10.1093/hmg/ddl035
- Royer-Zemmour, B., Ponsolle-Lenfant, M., Gara, H., Roll, P., Lévêque, C., Massacrier, A., et al. (2008). Epileptic and developmental disorders of the speech cortex: ligand/receptor interaction of wild-type and mutant SRPX2 with the plasminogen activator receptor uPAR. *Hum. Mol. Genet.* 17, 3617–3630. doi: 10.1093/hmg/ddn256
- Ryan, T. J., and Grant, S. G. N. (2009). The origin and evolution of synapses. *Nat. Rev. Neurosci.* 10, 701–712. doi: 10.1038/nrn2717
- Salmi, M., Bruneau, N., Cillario, J., Lozovaya, N., Massacrier, A., Buhler, E., et al. (2013). Tubacin prevents neuronal migration defects and epileptic activity caused by rat *SrpX2* silencing in utero. *Brain J. Neurol.* 136, 2457–2473. doi: 10.1093/brain/awt161
- Sanes, J. R., and Zipursky, S. L. (2020). Synaptic specificity: recognition molecules, and assembly of neural circuits. *Cell* 181, 536–556. doi: 10.1016/j.cell.2020.04.008
- Schizophrenia Psychiatric Genome-Wide Association Study (GWAS) Consortium (2011). Genome-wide association study identifies five new schizophrenia loci. *Nat. Genet.* 43, 969–976. doi: 10.1038/ng.940
- Scholz, N., Langenhan, T., and Schöneberg, T. (2019). Revisiting the classification of adhesion GPCRs. *Ann. N. Y. Acad. Sci. U.S.A* 1456, 80–95. doi: 10.1111/nyas.14192
- Schwarz, L. A., Hall, B. J., and Patrick, G. N. (2010). Activity-dependent ubiquitination of GluA1 mediates a distinct AMPA receptor endocytosis and sorting pathway. *J. Neurosci. Off. J. Soc. Neurosci.* 30, 16718–16729. doi: 10.1523/JNEUROSCI.3686-10.2010
- Schwenk, J., Pérez-García, E., Schneider, A., Kollwe, A., Gauthier-Kemper, A., Fritzius, T., et al. (2016). Modular composition and dynamics of native GABAB receptors identified by high-resolution proteomics. *Nat. Neurosci.* 19, 233–242. doi: 10.1038/nn.4198
- Scuderi, C., Saccuzzo, L., Vinci, M., Castiglia, L., Galesi, O., Salemi, M., et al. (2019). Biallelic intragenic duplication in ADGRB3 (BAI3) gene associated with intellectual disability, cerebellar atrophy, and behavioral disorder. *Eur. J. Hum. Genet.* 27, 594–602. doi: 10.1038/s41431-018-0321-1
- Shaffer, L. G., Theisen, A., Bejjani, B. A., Ballif, B. C., Aylsworth, A. S., Lim, C., et al. (2007). The discovery of microdeletion syndromes in the post-genomic era: review of the methodology and characterization of a new 1q41q42 microdeletion syndrome. *Genet. Med. Off. J. Am. Coll. Med. Genet.* 9, 607–616.
- Sheng, N., Shi, Y. S., Lomash, R. M., Roche, K. W., and Nicoll, R. A. (2015). Neto auxiliary proteins control both the trafficking and biophysical properties of the kainate receptor GluK1. *Elife* 4:e11682. doi: 10.7554/eLife.11682
- Shimizu-Nishikawa, K., Kajiwar, K., and Sugaya, E. (1995). Cloning and characterization of seizure-related gene, SEZ-6. *Biochem. Biophys. Res. Commun.* 216, 382–389.
- Sia, G. M., Clem, R. L., and Haganir, R. L. (2013). The human language-associated gene SRPX2 regulates synapse formation and vocalization in mice. *Science* 342, 987–991. doi: 10.1126/science.1245079
- Sigoillot, S. M., Iyer, K., Binda, F., González-Calvo, I., Talleur, M., Vodjdani, G., et al. (2015). The secreted protein C1QL1 and its receptor BAI3 control the synaptic connectivity of excitatory inputs converging on cerebellar purkinje cells. *Cell Rep.* 10, 820–832. doi: 10.1016/j.celrep.2015.01.034
- Sigoillot, S. M., Monk, K. R., Piao, X., Selimi, F., and Harty, B. L. (2016). Adhesion GPCRs as novel actors in neural and glial cell functions: from synaptogenesis to myelination. *Handb. Exp. Pharmacol.* 234, 275–298. doi: 10.1007/978-3-319-41523-9_12
- Stephan, A. H., Barres, B. A., and Stevens, B. (2012). The complement system: an unexpected role in synaptic pruning during development and disease. *Annu. Rev. Neurosci.* 35, 369–389. doi: 10.1146/annurev-neuro-061010-113810
- Stephenson, J. R., Paavola, K. J., Schaefer, S. A., Kaur, B., Van Meir, E. G., and Hall, R. A. (2013). Brain-specific angiogenesis inhibitor-1 signaling, regulation, and enrichment in the postsynaptic density. *J. Biol. Chem.* 288, 22248–22256. doi: 10.1074/jbc.M113.489757
- Sticco, M. J., Peña Palomino, P. A., Lukacovich, D., Thompson, B. L., Földy, C., Ressler, S., et al. (2021). C1QL3 promotes cell-cell adhesion by mediating complex formation between ADGRB3/BAI3 and neuronal pentraxins. *FASEB J.* 35:e21194. doi: 10.1096/fj.202000351RR
- Stohr, H., Berger, C., Frohlich, S., and Weber, B. H. F. (2002). A novel gene encoding a putative transmembrane protein with two extracellular CUB domains and a low-density lipoprotein class A module: isolation of alternatively spliced isoforms in retina and brain. *Gene* 286, 223–231.
- Straub, C. (2011). Distinct functions of kainate receptors in the brain are determined by the auxiliary subunit Neto1. *Nat. Neurosci.* 14:10.
- Sytnyk, V., Leshchynska, I., and Schachner, M. (2017). Neural cell adhesion molecules of the immunoglobulin superfamily regulate synapse formation, maintenance, and function. *Trends Neurosci.* 40, 295–308. doi: 10.1016/j.tins.2017.03.003
- Tan, K., Duquette, M., Liu, J., Dong, Y., Zhang, R., Joachimiak, A., et al. (2002). Crystal structure of the TSP-1 type 1 repeats. *J. Cell Biol.* 159, 373–382. doi: 10.1083/jcb.200206062
- Tang, M., Ivakine, E., Mahadevan, V., Salter, M. W., and McInnes, R. R. (2012). Neto2 interacts with the scaffolding protein GRIP and regulates synaptic abundance of kainate receptors. *PLoS One* 7:e51433. doi: 10.1371/journal.pone.0051433
- Tang, M., Pelkey, K. A., Ng, D., Ivakine, E., McBain, C. J., Salter, M. W., et al. (2011). Neto1 is an auxiliary subunit of native synaptic kainate receptors. *J. Neurosci.* 31, 10009–10018. doi: 10.1523/JNEUROSCI.6617-10.2011
- Telley, L., Cadilhac, C., Cioni, J.-M., Saywell, V., Jahnault-Talignani, C., Huettl, R. E., et al. (2016). Dual function of NRP1 in axon guidance and subcellular target recognition in cerebellum. *Neuron* 91, 1276–1291. doi: 10.1016/j.neuron.2016.08.015
- Tiao, J. Y., Bradaia, A., Biermann, B., Kaupmann, K., Metz, M., Haller, C., et al. (2008). The sushi domains of secreted GABA(B) isoforms selectively impair GABA(B) heteroreceptor function. *J. Biol. Chem.* 283, 31005–31011. doi: 10.1074/jbc.M804464200
- Tran, T. S., Rubio, M. E., Clem, R. L., Johnson, D., Case, L., Tessier-Lavigne, M., et al. (2009). Secreted semaphorins control spine distribution and morphogenesis in the postnatal CNS. *Nature* 462, 1065–1069. doi: 10.1038/nature08628
- Tu, H., Pinan-Lucarré, B., Ji, T., Jospin, M., and Bessereau, J.-L. (2015). C. elegans punctin clusters GABAA receptors via neuroligin binding and UNC-40/DCC recruitment. *Neuron* 86, 1407–1419. doi: 10.1016/j.neuron.2015.05.013
- Tu, Y.-K., Duman, J. G., and Tolias, K. F. (2018). The adhesion-PCR BAI1 promotes excitatory synaptogenesis by coordinating bidirectional trans-synaptic signaling. *J. Soc. Neurosci.* 38, 8388–8406. doi: 10.1523/JNEUROSCI.3461-17.2018
- Van de Peer, Y., Maere, S., and Meyer, A. (2009). The evolutionary significance of ancient genome duplications. *Nat. Rev. Genet.* 10, 725–732. doi: 10.1038/nrg2600
- Varela, P. F., Romero, A., Sanz, L., Romão, M. J., Töpfer-Petersen, E., and Calvete, J. J. (1997). The 2.4 Å resolution crystal structure of boar seminal plasma PSP-I/PSP-II: a zona pellucida-binding glycoprotein heterodimer of the spermadhesin family built by a CUB domain architecture. *J. Mol. Biol.* 274, 635–649. doi: 10.1006/jmbi.1997.1424
- Vogel, C., and Chothia, C. (2006). Protein family expansions and biological complexity. *PLoS Comput. Biol.* 2:e48. doi: 10.1371/journal.pcbi.0020048
- Walker, C. S., Francis, M. M., Brockie, P. J., Madsen, D. M., Zheng, Y., and Maricq, A. V. (2006). Conserved SOL-1 proteins regulate ionotropic glutamate receptor desensitization. *Proc. Natl. Acad. Sci. U.S.A* 103, 10787–10792. doi: 10.1073/pnas.0604520103
- Wang, C. Y., Liu, Z., Ng, Y. H., and Südhof, T. C. (2020). A synaptic circuit required for acquisition but not recall of social transmission of food preference. *Neuron* 107, 144.e–157.e. doi: 10.1016/j.neuron.2020.04.004
- Wang, J., Miao, Y., Wicklein, R., Sun, Z., Wang, J., Jude, K. M., et al. (2021). RTN4/NoGo-receptor binding to BAI adhesion-GPCRs regulates neuronal development. *Cell* 184, 5869.e–5885.e. doi: 10.1016/j.cell.2021.10.016

- Wang, Q., Chiu, S.-L., Koropouli, E., Hong, I., Mitchell, S., Easwaran, T. P., et al. (2017). Neuropilin-2/PlexinA3 receptors associate with GluA1 and mediate Sema3F-dependent homeostatic scaling in cortical neurons. *Neuron* 96, 1084.e–1098.e. doi: 10.1016/j.neuron.2017.10.029
- Wang, R., Mellem, J. E., Jensen, M., Brockie, P. J., Walker, C. S., Hoerndli, F. J., et al. (2012). The SOL-2/Neto auxiliary protein modulates the function of AMPA-subtype ionotropic glutamate receptors. *Neuron* 75, 838–850. doi: 10.1016/j.neuron.2012.06.038
- Wyeth, M. S., Pelkey, K. A., Petralia, R. S., Salter, M. W., McInnes, R. R., and McBain, C. J. (2014). Neto auxiliary protein interactions regulate kainate and NMDA receptor subunit localization at mossy fiber-CA3 pyramidal cell synapses. *J. Neurosci.* 34, 622–628. doi: 10.1523/JNEUROSCI.3098-13.2014
- Wyeth, M. S., Pelkey, K. A., Yuan, X., Vargish, G., Johnston, A. D., Hunt, S., et al. (2017). Neto auxiliary subunits regulate interneuron somatodendritic and presynaptic kainate receptors to control network inhibition. *Cell Rep.* 20, 2156–2168. doi: 10.1016/j.celrep.2017.08.017
- Yuzaki, M. (2011). Cbln1 and its family proteins in synapse formation and maintenance. *Curr. Opin. Neurobiol.* 21, 215–220. doi: 10.1016/j.conb.2011.01.010
- Zhang, W., St-Gelais, F., Grabner, C. P., Trinidad, J. C., Sumioka, A., Morimoto-Tomita, M., et al. (2009). A transmembrane accessory subunit that modulates kainate-type glutamate receptors. *Neuron* 61, 385–396. doi: 10.1016/j.neuron.2008.12.014
- Zheng, Y., Brockie, P. J., Mellem, J. E., Madsen, D. M., Walker, C. S., Francis, M. M., et al. (2006). SOL-1 is an auxiliary subunit that modulates the gating of GLR-1 glutamate receptors in *Caenorhabditis elegans*. *Proc. Natl. Acad. Sci. U.S.A.* 103, 1100–1105. doi: 10.1073/pnas.0504612103
- Zheng, Y., Mellem, J. E., Brockie, P. J., Madsen, D. M., and Maricq, A. V. (2004). SOL-1 is a CUB-domain protein required for GLR-1 glutamate receptor function in *C. elegans*. *Nature* 427, 451–457. doi: 10.1038/nature02244
- Zhou, X., Gueydan, M., Jospin, M., Ji, T., Valfort, A., Pinan-Lucarré, B., et al. (2020). The netrin receptor UNC-40/DCC assembles a postsynaptic scaffold and sets the synaptic content of GABAA receptors. *Nat. Commun.* 11:2674. doi: 10.1038/s41467-020-16473-5
- Zhou, X., Vachon, C., Cizeron, M., Romatiff, O., Bülow, H. E., Jospin, M., et al. (2021). The HSPG syndecan is a core organizer of cholinergic synapses. *J. Cell Biol.* 220:e202011144. doi: 10.1083/jcb.202011144
- Zhou, X. H., Brakebusch, C., Matthies, H., Ohashi, T., Hirsch, E., Moser, M., et al. (2001). Neurocan is dispensable for brain development. *Mol. Cell. Biol.* 21, 5970–5978. doi: 10.1128/mcb.21.17.5970-5978.2001
- Zhu, D., Li, C., Swanson, A. M., Villalba, R. M., Guo, J., Zhang, Z., et al. (2015). BAI1 regulates spatial learning and synaptic plasticity in the hippocampus. *J. Clin. Invest.* 125, 1497–1508. doi: 10.1172/JCI74603
- Zhu, F., Cizeron, M., Qiu, Z., Benavides-Piccione, R., Kopanitsa, M. V., Skene, N. G., et al. (2018). Architecture of the mouse brain synaptome. *Neuron* 99, 781.e–799.e. doi: 10.1016/j.neuron.2018.07.007
- Zhu, H., Meissner, L. E., Byrnes, C., Tuymetova, G., Tiffit, C. J., and Proia, R. L. (2020). The complement regulator Susd4 influences nervous-system function and neuronal morphology in mice. *iScience* 23:100957. doi: 10.1016/j.isci.2020.100957
- Zhu, J., Lee, K. Y., Jewett, K. A., Man, H.-Y., Chung, H. J., and Tsai, N.-P. (2017). Epilepsy-associated gene Nedd4-2 mediates neuronal activity and seizure susceptibility through AMPA receptors. *PLoS Genet.* 13:e1006634. doi: 10.1371/journal.pgen.1006634
- Zinn, K., and Özkan, E. (2017). Neural immunoglobulin superfamily interaction networks. *Curr. Opin. Neurobiol.* 45, 99–105. doi: 10.1016/j.conb.2017.05.010

Conflict of Interest: The authors declare that the research was conducted in the absence of any commercial or financial relationships that could be construed as a potential conflict of interest.

Publisher's Note: All claims expressed in this article are solely those of the authors and do not necessarily represent those of their affiliated organizations, or those of the publisher, the editors and the reviewers. Any product that may be evaluated in this article, or claim that may be made by its manufacturer, is not guaranteed or endorsed by the publisher.

Copyright © 2022 González-Calvo, Cizeron, Bessereau and Selimi. This is an open-access article distributed under the terms of the Creative Commons Attribution License (CC BY). The use, distribution or reproduction in other forums is permitted, provided the original author(s) and the copyright owner(s) are credited and that the original publication in this journal is cited, in accordance with accepted academic practice. No use, distribution or reproduction is permitted which does not comply with these terms.



To Stick or Not to Stick: The Multiple Roles of Cell Adhesion Molecules in Neural Circuit Assembly

Trevor Moreland and Fabienne E. Poulain*

Department of Biological Sciences, University of South Carolina, Columbia, SC, United States

OPEN ACCESS

Edited by:

Robert Hindges,
King's College London,
United Kingdom

Reviewed by:

Esther Stoeckli,
University of Zurich, Switzerland
Eloisa Herrera,
Institute of Neurosciences (CSIC),
Spain

*Correspondence:

Fabienne E. Poulain
fpoulain@mailbox.sc.edu

Specialty section:

This article was submitted to
Neurodevelopment,
a section of the journal
Frontiers in Neuroscience

Received: 03 March 2022

Accepted: 28 March 2022

Published: 28 April 2022

Citation:

Moreland T and Poulain FE (2022)
To Stick or Not to Stick: The Multiple
Roles of Cell Adhesion Molecules
in Neural Circuit Assembly.
Front. Neurosci. 16:889155.
doi: 10.3389/fnins.2022.889155

Precise wiring of neural circuits is essential for brain connectivity and function. During development, axons respond to diverse cues present in the extracellular matrix or at the surface of other cells to navigate to specific targets, where they establish precise connections with post-synaptic partners. Cell adhesion molecules (CAMs) represent a large group of structurally diverse proteins well known to mediate adhesion for neural circuit assembly. Through their adhesive properties, CAMs act as major regulators of axon navigation, fasciculation, and synapse formation. While the adhesive functions of CAMs have been known for decades, more recent studies have unraveled essential, non-adhesive functions as well. CAMs notably act as guidance cues and modulate guidance signaling pathways for axon pathfinding, initiate contact-mediated repulsion for spatial organization of axonal arbors, and refine neuronal projections during circuit maturation. In this review, we summarize the classical adhesive functions of CAMs in axonal development and further discuss the increasing number of other non-adhesive functions CAMs play in neural circuit assembly.

Keywords: growth cone, axon targeting, pathfinding, synaptic specificity, signaling, contact

INTRODUCTION

Forming precise neural circuits is critical for nervous system function. Defects in neuronal connectivity have notably been observed in multiple neurodevelopmental disorders including fragile X syndrome (Swanson et al., 2018), autism spectrum disorders (McFadden and Minshew, 2013; Di Martino et al., 2014; Avital et al., 2015), tuberous sclerosis complex (Widjaja et al., 2010; Baumer et al., 2015; Im et al., 2016) and others, making the wiring of axonal connections a subject of intense research.

Developing axons navigate along precise paths toward their target by responding to attractive and repulsive guidance cues present in their environment. Navigation is ensured by highly motile structures at the leading end of axons, the growth cones, which harbor a unique repertoire of receptors at their surface that allow them to interpret the various extracellular signals they encounter. Many secreted and membrane-anchored factors including cell adhesion molecules (CAMs) (Tessier-Lavigne and Goodman, 1996), the canonical guidance cues Ephrins, Netrins, Semaphorins, and Slits (Dickson, 2002), neurotrophic and growth factors (Charoy et al., 2012), and morphogens (Sánchez-Camacho and Bovolenta, 2009; Yam and Charron, 2013), provide long-range or contact-mediated signals. Growth cones integrate the guidance information they receive from these signals and in turn, transduce the mechanical forces required for axon extension and turning (Kerstein et al., 2015). After reaching their final destination, axons stop elongating, branch

extensively to form a terminal arbor and establish specific synaptic connections with appropriate partners. Patterns of connectivity are subsequently remodeled and refined in an activity-dependent manner, leading to the establishment of precise local circuits for an efficient transfer of information (Kutsarova et al., 2017). Axon pathfinding, selective target innervation and specificity of synapse formation are central aspects of circuit wiring that all critically rely on long-range as well as contact-mediated signaling between axons and their substrate or surrounding cells.

CAMs form a very large group of transmembrane or glycosylphosphatidylinositol (GPI)-anchored proteins that mediate contacts between cells or cells and a substrate *via* homophilic or heterophilic interactions. First identified in the mid-70s as molecules mediating cell-cell adhesion (Rutishauser et al., 1976), CAMs have historically been classified into four main families including integrins, CAMs of the immunoglobulin superfamily (IgSF), cadherins, and selectins based on the structural composition of their extracellular domain (Bock, 1991). However, this classification omits molecules discovered afterward that also act as cell adhesion proteins such as neuroligins, neurexins, teneurins, and synaptic proteins containing extracellular leucine-rich repeats (LRRs) (Figure 1). Thanks to their diverse extracellular domains conferring distinct adhesion modalities and engaging in unique protein interactions, CAMs regulate many aspects of neural development ranging from neurogenesis (Homan et al., 2018; Huang et al., 2020) and neuronal migration (Schmid and Maness, 2008; Solecki, 2012; Chen et al., 2018) to neurite development (Pollerberg et al., 2013; Missaire and Hindges, 2015), synaptogenesis (Gerrow and El-Husseini, 2006; Yogev and Shen, 2014) and myelination (Rasband and Peles, 2021). Not surprisingly, many mutations in CAMs have been linked to neurodevelopmental and psychiatric disorders (Sakurai, 2017; Cuttler et al., 2021; Jaudon et al., 2021). Interestingly, whereas CAMs have long been known to regulate axonal development and synaptogenesis through their adhesive properties, other non-adhesive and perhaps counterintuitive functions of CAMs have more recently emerged. In this review, we summarize the classical adhesive functions of CAMs in axonal and synaptic development and further discuss the increasing number of other non-adhesive roles CAMs play in neural circuit assembly and maturation.

ADHESIVE FUNCTIONS OF CAMS IN CIRCUIT WIRING

Through their adhesive properties, CAMs mediate stabilizing contacts and attachment between axons and their surrounding environment that are critical for axon navigation, fasciculation, target selection, and synaptogenesis.

Interactions With the Extracellular Matrix and Glial Cells for Axon Navigation

Proper axon pathfinding requires a tightly controlled adhesion of growth cones to their substrate. The assembly and detachment of adhesions to the extracellular matrix (ECM) is especially

critical for the advance of pioneer axons that are the first to extend in a particular region. Like non-neuronal cells that form integrin-mediated focal adhesions at their leading edge during migration (Mishra and Manavathi, 2021), growth cones assemble similar integrin-dependent adhesions named point contacts with the ECM (Gomez et al., 1996; Woo and Gomez, 2006). Point contacts form after integrins at the surface of growth cones bind ECM ligands, leading to the clustering of integrins and subsequent recruitment of adaptor proteins linking integrins to the actin cytoskeleton (Figure 2A). By stabilizing filopodial protrusions and restraining the retrograde flow of actin at the growth cone periphery, point contacts promote the advance of the growth cone and axon extension (Woo and Gomez, 2006; Myers and Gomez, 2011; Nichol et al., 2016; Kershner and Welshhans, 2017). Interestingly, many extracellular factors regulate axon elongation and cell migration by modulating integrin-mediated adhesions (Nakamoto et al., 2004; Bechara et al., 2008). Substrates or guidance cues that promote or inhibit the localized assembly and turnover of point contacts lead to growth cone turning *in vitro* (Hines et al., 2010; Myers and Gomez, 2011; Nichol et al., 2016; Kerstein et al., 2017), further suggesting a direct role for integrin-mediated attachment in axon pathfinding. In mammals, 18 α and 8 β integrins can assemble into 24 heterodimers that bind with different affinities to a large diversity of ECM ligands (Hynes, 2002). Inhibiting integrin β 1 that forms the majority of integrin heterodimers reduces retinal axon elongation in zebrafish (Lilienbaum et al., 1995). It also prevents ipsilateral retinal projections from innervating a specific sublamina of the superior colliculus that expresses the ECM glycoprotein Nephronectin in mouse (Su et al., 2021; Figure 2B). Thus, integrin-mediated interactions between growth cones and the ECM not only regulate the rate of axon elongation but also directly specify target selection for circuit wiring. To what extent a cell-specific integrin code generated by the different combinations of α and β integrins contributes to the specificity of network assembly remains to be elucidated.

In addition to adhering to the ECM, pioneer growth cones directly interact with surrounding glial cells such as neuroepithelial cells, radial glial cells, and astrocytes during their navigation (Rigby et al., 2020). Glial cells often localize at intermediate choice points along migratory routes where they act as guideposts providing contact-mediated spatial information or acting as a permissive substrate for growth. For instance, radial glia create a palisade at the optic chiasm where they directly contact and guide retinal axons (Marcus et al., 1995). More recently, neural stem cells residing in the ventricular zone of the forebrain medial ganglionic eminence have been shown to use their radial fiber scaffold to direct corticospinal axons at the junction between the striatum and globus pallidus (Kaur et al., 2020). Most adhesive contacts between navigating growth cones and glial cells appear to be mediated by CAMs of the Immunoglobulin and Cadherin superfamilies. N-cadherin and NCAM, for instance, promote retinal axon outgrowth over astrocytes *in vitro* (Neugebauer et al., 1988). They also mediate strong interactions between growth cones of olfactory axons and ensheathing cells *in vivo*, enabling olfactory axons to ride along ensheathing cell bodies as they pioneer the path toward the

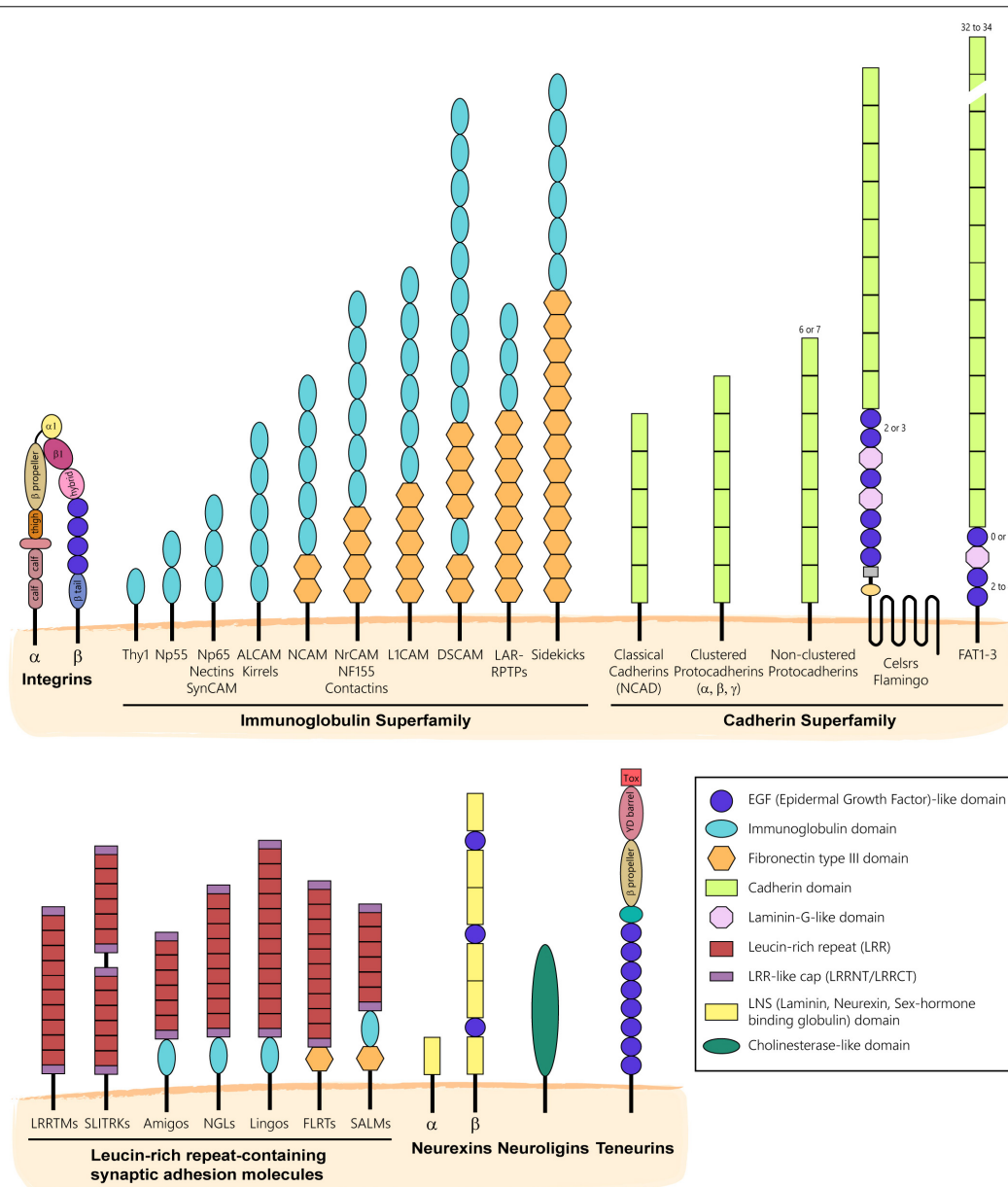


FIGURE 1 | Main families of CAMs expressed in the nervous system. CAMs have historically been classified into families based on the structural composition of their extracellular domain. Integrins form obligate heterodimers composed of α and β integrin subunits that cluster at the plasma membrane to mediate adhesion to the extracellular matrix. CAMs of the Immunoglobulin Superfamily (IgSF) are characterized by the presence of one or more Ig-like domains that can be followed by Fibronectin type III domain (Fn3) repeats. IgSF CAMs mediate adhesion by engaging in homophilic or heterophilic interactions. Most of them include a transmembrane and intracellular domains, but some like Contactins are GPI-anchored. CAMs of the Cadherin Superfamily mostly engage in homophilic interactions and are characterized by the presence of one or more calcium-binding cadherin repeats. The Leucine-rich repeat (LRR) Superfamily includes adhesion molecules that are characterized by the presence of LRRs and can include Ig or Fn3 domains in their extracellular domain. LRR CAMs are often found at synapses and engage in both homophilic or heterophilic *trans*-interactions. Neurexins and Neuroligins engage in heterophilic interactions in *trans* at nascent synapses to promote synaptic differentiation and stabilization. Teneurins are type II single-pass transmembrane proteins that interact homophilically or engage in *trans*-interactions with Latrophilins, a class of adhesion G-protein coupled receptors (not shown).

olfactory bulb (Su and He, 2010). In the spinal cord, NrCAM expressed by floor plate cells guides commissural axons across the midline by, in part, interacting with Contactin-2 (Cntn2, also known as TAG-1 or axonin-1) at the axonal surface (Stoeckli et al., 1997; Fitzli et al., 2000). NrCAM is also expressed by radial

glia at the optic chiasm and promotes the crossing of NrCAM-positive retinal axons projecting contralaterally (Williams et al., 2006; Kuwajima et al., 2012). Along the optic tract, NF-protocadherin, a member of the Cadherin superfamily, mediates interactions between retinal axons and their neuroepithelial

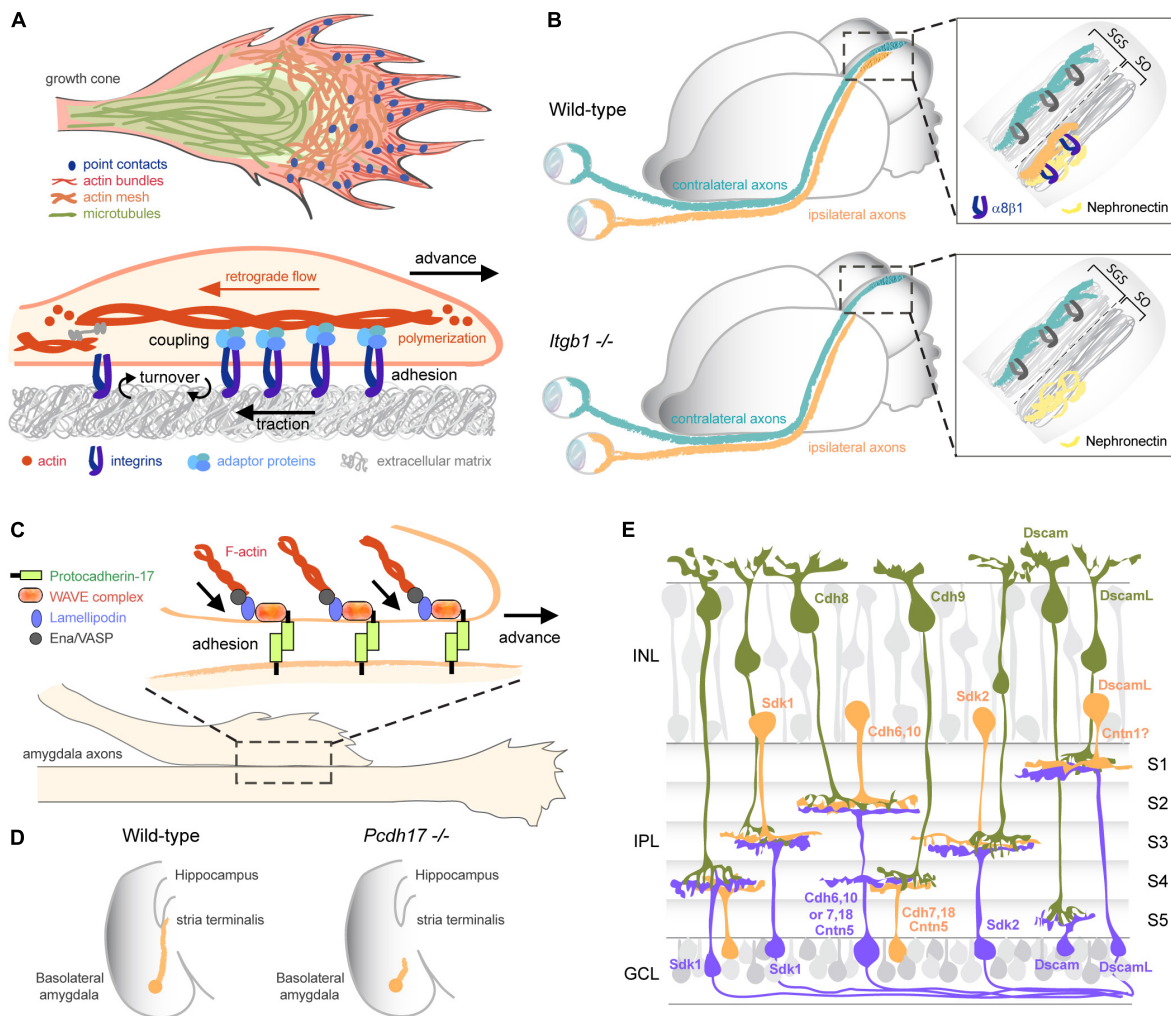


FIGURE 2 | Adhesive functions of CAMs in circuit wiring. **(A)** Integrins mediate adhesion to the ECM for growth cone advance. Binding of integrins to ECM ligands leads to the clustering of integrins and the recruitment of adaptor proteins linking integrins to the actin cytoskeleton. The point contacts hence formed promote growth cone advance by stabilizing filopodial protrusions and restraining the retrograde flow of actin at the growth cone periphery. **(B)** Integrins mediate adhesion to the ECM for target selection. In the visual system, integrin $\alpha 8 \beta 1$ is selectively expressed by retinal ganglion cells projecting ipsilaterally. Its ligand, the ECM glycoprotein Nephronectin, is restricted to a sublamina at the target. Interaction between integrin $\alpha 8 \beta 1$ and Nephronectin is necessary for the laminar targeting of ipsilateral axons to the rostral stratum opticum (SO). Deleting integrin $\alpha 8 \beta 1$ or Nephronectin causes a dramatic loss of ipsilateral projections while contralateral projections remain unaffected in the stratum griseum superficial (SGS). Adapted from Su et al. (2021). **(C,D)** Protocadherin-17 (Pcdh17) mediates *trans*-axonal interactions for proper tract formation. **(C)** Pcdh17 accumulates at homotypic contacts between growth cones and axons from amygdala neurons, where it recruits the WAVE complex, Lamellipodin, and Ena/VASP proteins that remodel the actin cytoskeleton and promote membrane protrusion. Pcdh17-mediated adhesion enhances growth cone motility and enable growth cone advance along homotypic axons. **(D)** Pcdh17 is required for the extension of amygdala axons through the stria terminalis toward the hypothalamus. Adapted from Hayashi et al. (2014). **(E)** A CAM code specifies laminar targeting and synaptic specificity in the retina. Sdk1, Sdk2, Dscam, DscamL, and Cntns (not all a represented here) are expressed in non-overlapping subsets of bipolar (green), amacrine (orange), and retinal ganglion cells (purple) and engage in homophilic *trans*-interactions to direct synapse formation between matching partners in specific laminae (S1–S5) of the inner plexiform layer (IPL). Classical cadherins (Cdh) also contribute to the molecular code specifying connections. INL, inner nuclear layer; GCL, ganglion cell layer. Adapted from Sanes and Zipursky (2020).

substrate for proper pathfinding (Leung et al., 2013). Retinal axons expressing L1CAM are then guided in the superior colliculus by collicular cells expressing ALCAM (also called BEN, DM-GRASP, SC1, or Neurolin) (Buhusi et al., 2009). In the absence of ALCAM, axonal branches fail to extend mediolaterally, leading to defects in retinotopic map formation. Outside the visual system, recent work has revealed that Celsr3, a

member of the Flamingo group within the Cadherin superfamily, is present at the surface of commissural growth cones and promotes axon pathfinding across the floor plate by binding in *trans* to Dystroglycan, a transmembrane protein at the surface of neuroepithelial cells (Lindenmaier et al., 2019). Interestingly, other families of CAMs such as teneurins and neuroligins have been found to accumulate in growth cones during axon elongation

(Suzuki et al., 2014; Gutford et al., 2021). Determining whether they also mediate adhesion between pioneer growth cones and glial cells will be important to gain a more comprehensive view of the inter-cellular interactions that govern neural circuit assembly during early development.

Axon Fasciculation for Tract Formation

Pioneer axons play a critical role in neural circuit assembly, not only by defining first itineraries toward appropriate targets, but also by acting as guides and providing a scaffold for later-born axons that follow them (Pike et al., 1992; Hidalgo and Brand, 1997; Rash and Richards, 2001). In the olfactory and retinotectal systems, for instance, ablation of early-born pioneer neurons causes follower axons to misroute and fail to build proper connections (Whitlock and Westerfield, 1998; Pittman et al., 2008; Okumura et al., 2016). The formation of axon tracts en route to a target involves homotypic or heterotypic fasciculation between axons, which are usually initiated after a growth cone contacts the shaft of a neighboring axon and moves along it. Alternatively, axon shafts can dynamically interact, leading to a zippering behavior triggering their fasciculation (Šmít et al., 2017). Extensive literature has demonstrated a major role for IgSF CAMs in regulating homotypic axon-axon interactions (Spead and Poulain, 2021). CAMs engaged in homophilic (between same CAMs) or heterophilic (between different CAMs) *trans*-interactions mediate the selective recognition between elongating growth cones and pre-existing axon shafts, thereby dictating the specificity of axonal bundling for tract formation. They also provide the adhesive force required for growth cone advance through their coupling to the actin cytoskeleton (Pollerberg et al., 2013; Abe et al., 2018). Not surprisingly, the loss of specific CAMs leads to disorganized tracts in many circuits. Blocking L1CAM in the chick hindlimb, for instance, causes a defasciculation of both motor and sensory axons that fail to project to their respective targets (Landmesser et al., 1988; Honig and Rutishauser, 1996; Honig et al., 2002). L1CAM is also required for the fasciculation between axons innervating the peduncle of the mushroom bodies in *Drosophila* (Siegenthaler et al., 2015). Likewise, ALCAM and DSCAM both regulate the fasciculation of retinal axons in the visual system (Pollerberg and Mack, 1994; Ott et al., 1998; Weiner et al., 2004; Bruce et al., 2017). Continuous synthesis of ALCAM in growth cones is notably required for the preferential growth of retinal axons on ALCAM substrates and maintained by local mRNA translation (Thelen et al., 2012). In the mouse motor system, Cntn2 accumulates in the distal segment of motor axons extending in the periphery and controls their fasciculation (Suter et al., 2020). Conversely in the peripheral system, SynCAM2 and SynCAM3 were found to regulate contacts between sensory afferents as they enter the dorsal root entry zone of the spinal cord (Frei et al., 2014). Similarly to IgSF CAMs, members of the Cadherin superfamily have also emerged as important regulators of tract organization. Tectofugal projections innervating different parts of the brain elongate along pre-existing axonal pathways expressing the same cadherin, demonstrating that cadherins mediate selective axon fasciculation through homotypic *trans*-interactions (Treubert-Zimmermann et al., 2002). As such, cadherins organize axonal tracts depending on their selective

expression in the nervous system. N-cadherin and Cadherin-8, for instance, are both required for the fasciculation of mossy fibers in the hippocampus (Bekirov et al., 2008), while Cadherin-11 promotes the bundling of motor axons (Marthiens et al., 2005). More recently, Protocadherin-17 (Pcdh17) has been found to regulate the formation of homotypic contacts between amygdala axons elongating toward the hypothalamus and ventral striatum (Hayashi et al., 2014; **Figures 2C,D**). Growth cones lacking Pcdh17 no longer migrate along Pcdh17-positive axons, whereas axons ectopically expressing Pcdh17 intermingle with axons expressing endogenous Pcdh17.

Guidance cues can regulate axon fasciculation and pathfinding by modulating the levels of CAMs at the axonal surface. Semaphorin3D, for instance, promotes the bundling of medial longitudinal fascicle axons in zebrafish by increasing L1CAM protein levels (Wolman et al., 2007). In *Drosophila*, Semaphorin-1a reverse signaling promotes the fasciculation of photoreceptor axons by inhibiting Rho1, a small GTPase known to mediate the degradation of the NCAM ortholog Fasciclin 2 (Hsieh et al., 2014). Conversely in the *Xenopus* visual system, Semaphorin-3A (Sema3A) prevents retinal axons from exiting their normal trajectories by inducing the local translation of NF-protocadherin in retinal growth cones (Leung et al., 2013). Alternatively, extracellular factors can regulate the strength of growth cone adhesion by modulating the coupling of CAMs to the actin cytoskeleton. Netrin-1, for instance, promotes traction force for growth cone migration by enhancing the coupling of L1CAM to F-actin *via* the adaptor Shootin1a (Kubo et al., 2015; Baba et al., 2018). Whether other guidance cues such as Ephrins (Luxey et al., 2013) or Slits (Jaworski and Tessier-Lavigne, 2012) regulate axon fasciculation by modulating CAMs and their adhesive properties remains to be determined.

Trans-Interactions for Synaptic Specificity

CAMs not only regulate axon growth, fasciculation and guidance toward a main target but also dictate the specificity of synapse formed between axons and dendrites. After reaching their main target area, axons must establish synapses with appropriate partners while avoiding unsuitable ones. Synaptic specificity is achieved by both laminar targeting, during which axon terminals and dendrites of post-synaptic neurons sharing similar functional properties assemble into local layers within the main target, and specific cellular and sub-cellular synapse assembly.

Studies on the mechanisms governing laminar targeting in the visual system have demonstrated critical roles for IgSF CAMs and cadherins in mediating *trans*-cellular recognition between correct synaptic partners (Huberman et al., 2010; Sanes and Zipursky, 2020). In the chick retina, Sidekick 1 (Sdk1), Sdk2, Dscam, DscamL, and Cntns were found to be uniquely expressed in non-overlapping subsets of two classes of interneurons, the bipolar and amacrine cells, as well as in their post-synaptic partners, the retinal ganglion cells (RGCs) (**Figure 2E**). Interestingly, RGCs and interneurons with matching expression of these IgSF CAMs form synapses in specific sublaminae of the inner plexiform

layer (Yamagata et al., 2002; Yamagata and Sanes, 2008, 2012). Modifying the “CAM code” a neuron expresses by depleting or overexpressing any of these CAMs diverts axonal arbors to sublaminae expressing the matching set of CAMs, indicating an essential role for homophilic *trans*-interactions in laminar targeting. Similar laminar targeting defects were observed in mice lacking Sdks, DSCAM, or Cntn5, suggesting conserved roles for these CAMs across vertebrates (Fuerst et al., 2010; Krishnaswamy et al., 2015; Peng et al., 2017; Yamagata and Sanes, 2019). However, whereas Sdks and Cntn5 regulate laminar targeting by homophilic interactions in both mouse and chick, DSCAM appears to exert its function differently in mouse by masking signaling from cadherins (Simmons et al., 2017; Garrett et al., 2018). Indeed, cadherins also contribute significantly to the coding of laminar targeting through their homophilic interactions. Among the 15 different classical cadherins detected in the direction-selective circuits in the retina, six are expressed in combination or individually in populations of functionally distinct interneurons and RGCs and control their laminar connectivity (Duan et al., 2014, 2018). Cadherin-8 (Cdh8) and Cdh9, for instance, direct axons of a subset of bipolar cells to RGCs responding to bright or dark moving objects, whereas Cdh7 and Cdh18 specify synapses formed between amacrine cells and RGCs responding to nasal motion. Cdh6, on the other hand, targets not only amacrine cell axons to RGCs responding to ventral motion in the retina, but also RGC axons to their specific visual targets in the brain (Osterhout et al., 2011). A similar coding principle for axon-target matching has been observed in other circuits. In the hippocampus, for instance, Cdh9 specifically regulates the formation of mossy fiber synapses between dentate gyrus and CA3 neurons (Williams et al., 2011). Likewise in the cerebellum, Cdh7 mediates synapse formation between pontine axons and granule neurons (Kuwako et al., 2014). More recently, IgSF11 has been identified as the homophilic adhesion molecule controlling synapse formation between inhibitory chandelier cells and pyramidal neurons in the cortex (Hayano et al., 2021).

Other CAMs besides IgSF CAMs and cadherins regulate synaptic specificity. Teneurins, for instance, are expressed in several inter-connected regions in the nervous system and form *trans*-synaptic interactions by binding homophilically or heterophilically to Latrophilins, a class of adhesion G-protein coupled receptors (Boucard et al., 2014; Araç and Li, 2019). The role of teneurins in synaptic partner matching was first established in *Drosophila*, in which Ten-a and Ten-m instruct target selection in the motor and olfactory systems (Hong et al., 2012; Mosca et al., 2012). Teneurins were found afterward to also specify connectivity in the hippocampus and the visual system of vertebrates. Teneurin-2 (Tenm2) promotes synapse formation between CA3 Schaffer collaterals and CA1 pyramidal hippocampal neurons by forming a *trans*-synaptic complex with Latrophilin-3 (Lphn3) and FLRT3 (Sando et al., 2019). In contrast, Tenm3 homophilic interactions are required for the precise targeting of proximal CA1 axons to the distal subiculum (Berns et al., 2018). Tenm3 also regulates the connectivity of orientation-selective RGCs in the zebrafish retina and optic tectum (Antinucci et al., 2013, 2016).

Thus, homophilic and heterophilic *trans*-interactions between specific CAMs generate a combinatorial recognition code for synaptic matching in addition to signaling for axon growth termination and synapse formation. This code not only specifies connectivity between distinct sets of neurons but can also direct synaptic specificity at a sub-cellular level through the accumulation of CAMs at defined sites. In the cerebellum, for instance, the IgSF CAM Neurofascin-185 accumulates in the axon initial segment (AIS) of Purkinje cells and directs the formation of pinceau synapses by basket interneurons (Ango et al., 2004). Similarly in the cortex, anchoring of L1CAM to the AIS of pyramidal neurons is required for selective innervation by Chandelier cells (Tai et al., 2019). The code specifying cellular or sub-cellular synaptic interactions is most often generated by the differential expression of CAMs among neurons but can also be achieved by the temporal regulation of CAM expression. In *Drosophila*, for instance, N-Cadherin is expressed by both R7 and R8 photoreceptors, albeit at different levels and moments. N-Cadherin expression peaks in R8 cells at the time R8 axons arrive at their target layer in the medulla, leading to axonal innervation of that layer. In contrast, R7 axons that express high levels of N-cadherin at a later timepoint bypass the R8 target and terminate in a more distant layer (Petrovic and Hummel, 2008). Alternatively, CAM *trans*-interactions can be modulated by alternative splicing. Splicing of Tenm2, for instance, changes the structure of Tenm2's extracellular β -propeller domain and determines which *trans*-synaptic partner Tenm2 interacts with (Li et al., 2018, 2020). Tenm2 lacking the splice insert interacts with Latrophilins to promote excitatory synapse formation, whereas Tenm2 containing the insert cannot and specifies inhibitory synapses instead. Contact-mediated signaling between matching *trans*-synaptic partners eventually initiates synapse formation and stabilization by recruiting additional CAMs such as neuroligins, neuroligins and LRR-containing adhesion molecules. As for synaptic matching, the assembly of synapses with specific properties is governed by the type of *trans*-synaptic molecules engaged. This vast field of research falls outside the scope of this review, but we refer interested readers to excellent recent articles on that topic (Schroeder and de Wit, 2018; Gomez et al., 2021; Südhof, 2021).

BEYOND GLUE: THE NON-ADHESIVE FUNCTIONS OF CAMS IN CIRCUIT WIRING

Although the adhesive properties of CAMs play critical roles at all stages of circuit wiring, CAM functions go far beyond adhesion and mechanical stabilization. Through their intracellular domains and interactions with other receptors at the plasma membrane, CAMs can activate or modulate a panoply of intracellular signaling pathways leading to morphological or transcriptional changes. They can also be cleaved from the plasma membrane and act as bona fide signaling ligands in the extracellular environment. CAMs have thus emerged as major signaling orchestrators of nervous system assembly.

Transcriptional Regulation of Axon Growth

Axons elongating over long distances require the synthesis of new raw materials to sustain the assembly of cytoskeletal structures and membrane components. While local mRNA translation can be activated in growth cones to induce rapid changes in response to local cues (Dalla Costa et al., 2020; Agrawal and Welshhans, 2021), a constant communication between the growth cone and the nucleus regulates nuclear transcription to adjust gene expression to axonal needs. An increasing body of evidence indicates that CAMs regulate transcription in developing neurons, both indirectly by regulating the activation or trafficking of transcription factors, and directly, by acting in the nucleus themselves.

Several CAMs stimulate gene transcription by activating intracellular signaling pathways, either through the activity of their intracellular domain or by interacting with signaling receptors (**Figure 3A**). L1CAM and NCAM, for instance, were both reported to activate mitogen-activated protein kinase (MAPK) pathways to promote neurite outgrowth (Kolkova et al., 2000; Schmid et al., 2000; Poplawski et al., 2012). NCAM interacts with the fibroblast growth factor receptor (FGFR) to activate MAPK and, in turn, the transcription factors CREB and c-Fos (Jessen et al., 2001; Niethammer et al., 2002). Activation of MAPK by L1CAM, on the other hand, requires L1CAM internalization (Schaefer et al., 1999; Schmid et al., 2000). Alternatively, CAMs might regulate transcription by directly modulating the nuclear trafficking of proteins with transcriptional activity. The intracellular domain of NF-protocadherin, for instance, directly binds TAF1, a component of the basal transcription factor complex TFIID (Heggem and Bradley, 2003). Inhibiting either NF-protocadherin or TAF1 severely impairs retinal axon initiation and elongation, suggesting that NF-protocadherin might regulate TAF1-dependent transcriptional programs to promote axonal growth (Piper et al., 2008). Conversely, classical cadherins constitutively retain the transcriptional coactivators β -catenin and p120 at the plasma membrane, thereby preventing them from translocating to the nucleus (Nelson and Nusse, 2004). Whether such a sequestration contributes to the transcriptional regulation of axonal development remains, however, unclear.

In addition to activating transcriptional pathways from the plasma membrane, a number of CAMs have recently emerged as transcriptional activators or repressors acting directly in the nucleus for controlling axon elongation (**Figure 3A**). Indeed, several proteases including caspases, matrix metalloproteases, and members of the ADAM family, can cleave the intracellular domains of transmembrane CAMs, which then translocate to the nucleus to regulate transcription. Activation of NCAM, for instance, leads to its cleavage by a serine protease and the subsequent nuclear import of a C-terminal fragment that is necessary for NCAM-induced axon growth (Kleene et al., 2010; Homrich et al., 2018). Interestingly, the fragment generated after cleavage includes not only the intracellular domain of NCAM but also its transmembrane domain and a stub of its extracellular domain, indicating that NCAM is proteolytic processed by an extracellular enzyme. Modification of the extracellular stub by

polysialic acid, a glycan known to modulate NCAM function, does not prevent its nuclear import but leads to the transcription of a distinct set of genes, demonstrating a unique role for NCAM glycosylation in transcriptional regulation (Westphal et al., 2016, 2017a,b). L1CAM, DSCAM and DSCAML1 also regulate transcription after cleavage. Like NCAM, activated L1CAM undergoes a serine protease-dependent cleavage at the plasma membrane that generates a fragment containing the intracellular, transmembrane and part of the extracellular domains (Lutz et al., 2012, 2014). The sumoylated L1CAM fragment hence generated traffics to endosomes and the cytoplasm before translocating in a sumoylation-dependent manner to the nucleus where it interacts with multiple nuclear proteins (Girbes Minguez et al., 2020). Interaction with heterochromatin protein 1 is notably required for L1CAM-mediated neurite outgrowth in cultured cortical neurons (Kleene et al., 2022). Conversely, the intracellular domains generated after cleavage of DSCAM and DSCAML1 by γ -secretase alter the transcription of genes regulating circuit formation and inhibit axon growth when overexpressed in cortical neurons (Sachse et al., 2019). Other CAMs besides IgSF CAMs appear to directly regulate transcription in the nucleus. The intracellular domain of Tenm2, for instance, is released after homophilic interaction and represses the activity of Zic1, a transcription factor known to regulate the targeting of mossy fibers in the cerebellum (Bagutti et al., 2003; Dipietrantonio and Dymecki, 2009). Conversely, Tenm3's intracellular domain interacts with Zic2, another member of the Zic family that specifies binocular vision by regulating the guidance of retinal axons projecting ipsilaterally in the visual system (Herrera et al., 2003; Glendinning et al., 2017). Both Zic2 and its transcriptional target EphB1 are upregulated in Tenm3 mutants, which likely explains the strong ipsilateral targeting defects observed in these mice (Leamey et al., 2007; Dharmaratne et al., 2012). As for Tenm1, its intracellular domain has been shown to regulate transcription by binding to the transcriptional repressors MBD1 and HINT1 (Nunes et al., 2005; Schöler et al., 2015). Defining the mechanisms controlling the release and transport of CAM intracellular domains, and identifying the cell-specific nuclear partners they interact with, remain important questions to address for better understanding how long distance communication between axons and soma modulate axon guidance at choice points and target innervation.

Repulsive Signaling for Axon Pathfinding

Although CAMs were first shown to promote axon growth through their adhesive properties, many of them have since emerged as signaling receptors or ligands instructing growth cone guidance independently of adhesion. Perhaps unexpectedly, CAMs were found to actively participate in the control of axon repulsion by dictating the axon's sensitivity to repulsive signals. Many IgSF CAMs, for instance, form signaling complexes with receptors to repulsive guidance cues. L1CAM directly binds in *cis* to Neuropilin-1 (Nrp1), the receptor to Sema3A, and is required for Sema3A-induced growth cone collapse (Castellani et al., 2000, 2002). L1CAM mediates both signaling downstream of Nrp1 and Nrp1 internalization upon Sema3A binding, thus coordinating signaling cascades instructing growth cone collapse

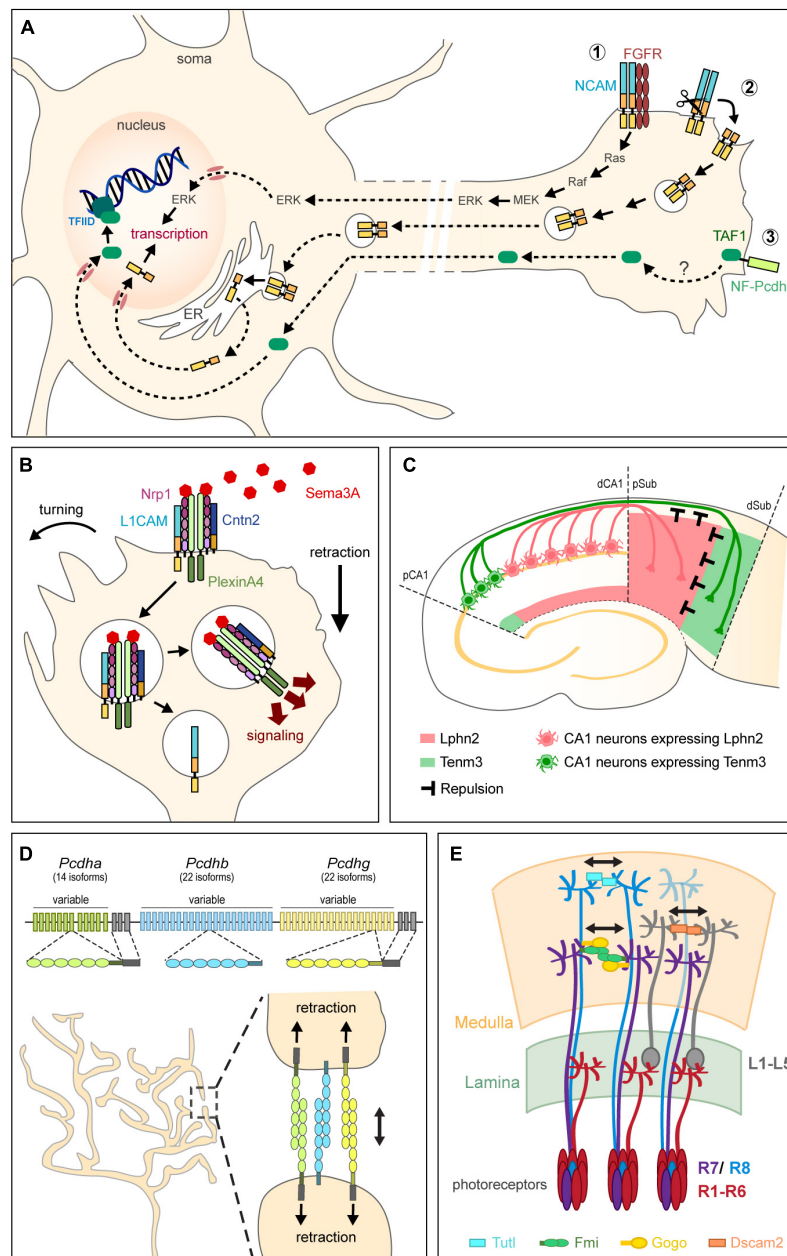


FIGURE 3 | Non-adhesive functions of CAMs in circuit assembly. **(A)** CAMs regulate transcription for axon growth by activating intracellular signaling pathways from the plasma membrane (1), acting directly in the nucleus after proteolytic cleavage (2), or regulating the transport of molecules with transcriptional activity (3). NCAM, for instance, interacts with FGFR to activate the MAPK pathway and in turn, transcription (1). Alternatively, proteolytic processing of NCAM releases a fragment that is trafficked through endosomes and the endoplasmic reticulum (ER), released in the cytoplasm, and finally translocated into the nucleus where it regulates transcription (2). NF-protocadherin (NF-Pcdh) directly interacts with TAF1, a component of the basal transcription factor complex TFIID, suggesting that NF-Pcdh might regulate axon elongation through TAF1-mediated transcriptional control. **(B)** CAMs instruct axon repulsion by modulating signaling pathways. Both L1CAM and Cntn2 form a complex with Nrp1, the receptor to the repulsive guidance cue Sema3A, at the plasma membrane. Cntn2 modulates axon response to Sema3A by regulating the endocytosis of the Nrp1/L1CAM/Sema3A complex. After internalization, L1CAM and Nrp1 become segregated by Cntn2 into two distinct trafficking pathways. Nrp1 is routed to endocytic compartments where its increased association with PlexinA4 signals for collapse. Adapted from Law et al. (2008) and Dang et al. (2012). **(C)** CAMs instruct repulsion by acting as guidance cues. In the hippocampus, reciprocal repulsions mediated by Tenm3 and Lphn2 ensure proper target selection. Axons originating from proximal CA1 (pCA1) neurons (green) express Tenm3 and project to the distal subiculum (dSub) after being repelled by Lphn2 (pink) present in the proximal subiculum (pSub). Conversely, distal CA1 (dCA1) axons expressing Lphn2 (pink) are repelled by Tenm3 in dSub (green) and project to pSub. Adapted from Pederick et al. (2021). **(D)** Clustered Pcdhs regulate self-avoidance. Pcdh genes are organized into three adjacent clusters that include several variable exons. Each variable exon codes for an extracellular and transmembrane domains and is preceded by a promoter randomly activated in individual neurons to drive transcription. Stochastic promoter choice leads to the production of different Pcdh isoforms from each of the three clusters in a

(Continued)

FIGURE 3 | cell-specific manner, thereby generating a unique combination of Pcdh α , β , and γ expression in each neuron. Sister branches from the same terminal arbor express the same code of Pcdhs at their surface and repel each other after Pcdhs interact homophilically in *trans*. **(E)** CAMs ensure tiling of terminal arbors. In the *Drosophila* visual system, DSCAM2, Turtle (Tutl), and Flamingo (Fmi) together with Gogo engage in homophilic *trans*-interactions to activate repulsion, thereby control the proper spacing of L1-L5, R8, and R7 terminal arbors, respectively, in the medulla. Adapted from Spead and Poulain (2021).

with a decreased adhesiveness (Castellani et al., 2004; Bechara et al., 2008). Interestingly, Cntn2 also forms a complex with Nrp1 and L1CAM at the plasma membrane and regulates axon response to Sema3A by modulating the endocytosis of the Nrp1/L1CAM/Sema3A complex (Law et al., 2008; **Figure 3B**). L1CAM and Nrp1 are endocytosed together but become segregated by Cntn2 into two distinct trafficking pathways (Dang et al., 2012). Nrp1 is notably routed to endocytic compartments where it increases its association with PlexinA4, which in turn signals for collapse. In the absence of Cntn2, Nrp1, and L1CAM are no longer separated intracellularly and signaling is reduced. Similarly to L1CAM that associates with Nrp1, NrCAM forms a complex with Nrp2 and PlexinA3 (Falk et al., 2005; Demyanenko et al., 2011). In response to Sema3F, NrCAM clusters Nrp2 and PlexinA3 at the plasma membrane, which activates signaling for growth cone collapse. Thalamocortical axons lacking NrCAM are no longer sensitive to Sema3F *in vivo* and misproject caudally in the ventral telencephalon (Demyanenko et al., 2011). Other guidance pathways besides Semaphorin signaling are controlled by IgSF CAMs. NCAM, for instance, clusters and activates EphA3 in response to ephrin-A5, thereby eliciting RhoA-dependent growth cone collapse in GABAergic interneurons (Sullivan et al., 2016). Similarly, DSCAM interacts with Unc5 to trigger the repulsion of cerebellar axons away from Netrin-1 (Purohit et al., 2012). More recently, the LRR-containing adhesion molecule FLRT3 was shown to directly interact with Robo1, a receptor to Slits (Leyva-Díaz et al., 2014). FLRT3 not only modulates the repulsion of rostral thalamocortical axons in response to Slit1 *in vitro*, but also their attraction toward Netrin-1 in a Robo1-dependent manner *in vivo*.

In addition to forming signaling complexes with guidance receptors, CAMs can act directly as instructive cues for axon repulsion. In *Drosophila*, for instance, Integrins $\alpha 1$ and $\alpha 2$ mediate *trans*-axonal repulsive signaling between motor axons to induce their defasciculation and target them to proper targets (Huang et al., 2007). Mutants lacking either of these integrins have increased axon fasciculation that causes a lack of muscle innervation. Likewise *in vitro*, the close homolog of L1CAM, Chl1, engages in homophilic interactions to repel ventral midbrain dopaminergic axons (Alsanie et al., 2017). Very recently, repulsive interactions between Tenm3 and Lphn2 were shown to topographically direct CA1 axons to the subiculum in the hippocampus (Pederick et al., 2021; **Figure 3C**). CAMs can instruct axon repulsion not only locally by signaling from the surface of cells or others axons, but also distally by acting as a gradient after shedding of their extracellular domain. The ectodomains of FLRT2 and FLRT3, for instance, are released after cleavage by metalloproteases and act as repulsive guidance cues for hippocampal axons expressing Unc5 (Yamagishi et al., 2011). While many CAMs are processed by metalloproteases (Safitig and Lichtenthaler, 2015), the functions

of their ectodomains in circuit assembly remain surprisingly unknown. We can anticipate, though, that ectodomain release would increase the functional diversity of CAMs and provide an additional level of spatiotemporal regulation for signaling. The ectodomain of Tenm2, for instance, is proteolytically cleaved during development and was recently shown to attract hippocampal axons *in vitro* by binding to Lphn1 (Vysokov et al., 2016, 2018).

Contact-Mediated Self-Avoidance and Tiling

Neuronal connectivity and function rely on the precise innervation of targets by axons. After reaching their final destination, axons branch extensively to form elaborate terminal arbors within specific territories. Branching patterns form dynamically and become spatially organized to maximize the coverage of an area while minimizing redundancy of targeting. Optimal coverage is achieved through two main mechanisms (Grueber and Sagasti, 2010). Isoneural spacing or self-avoidance refers to the repulsion between axonal branches of a same neuron, so that branches avoid overlapping with each other. Likewise, arbors from distinct neurons that share the same function do not overlap, a phenomenon referred to as heteroneural avoidance or tiling. Both self-avoidance and tiling pertain to axons as well as dendrites and are achieved by contact-mediated repulsion (Sagasti et al., 2005).

First described in studies analyzing the receptor fields of sensory neurons in the leech (Nicholls and Baylor, 1968), self-avoidance relies on the ability of sister branches from the same terminal arbor to discriminate “self” from “non-self” before repelling each other. This selective recognition is achieved by the expression of a cell-surface molecular code that is common to sister branches but distinct among branches from different neurons. In *Drosophila*, DSCAM1 generates such a code. Alternative splicing of DSCAM1 pre-mRNA produces 38,016 distinct isoforms that differ in their ectodomain and are expressed in a probabilistic way (Schmucker et al., 2000). Consequently, each isoform gives an individual neuron a unique molecular identity. As only identical ectodomains can engage in homophilic *trans*-interactions due to conformational constraints, only sister branches sharing the same isoform will recognize each other (Wojtowicz et al., 2004, 2007). DSCAM1-mediated homophilic interactions initiate repulsion rather than adhesion in this context, which contrasts with the known function of DSCAM in promoting axon fasciculation (Bruce et al., 2017). DSCAM1-mediated self-avoidance enables the proper spatial organization of both axonal and dendritic arbors in diverse neuronal populations (Wang J. et al., 2002; Zhan et al., 2004; Hattori et al., 2007; Matthews et al., 2007; Soba et al., 2007). In the absence of DSCAM1, branches fail to separate and overlap or fasciculate

instead. Interestingly, although the vertebrate ortholog DSCAM and its homolog DSCAML mediate self-avoidance in the mouse retina (Fuerst et al., 2008, 2009), they are not highly spliced and thus do not generate a molecular code like DSCAM1. Instead, DSCAM appears to mask adhesion-promoting signaling from other CAMs like cadherins (Garrett et al., 2018). If not DSCAM, which cell-surface molecules generate a recognition code in vertebrates? Like DSCAM1, clustered Protocadherins (Pcdhs) exist in a multitude of isoforms and as such, represent the largest subgroup in the Cadherin superfamily. About 60 Pcdh genes are organized into three adjacent clusters designed as Pcdh α , β , and γ (Wu and Maniatis, 1999; **Figure 3D**). Each cluster includes several variable exons that each codes for an extracellular and transmembrane domains. Each variable exon is further preceded by a promoter that is randomly activated in individual neurons to drive transcription (Tasic et al., 2002; Wang X. et al., 2002). Thus, stochastic promoter choice leads to the production of different Pcdh isoforms from each of the three clusters in a cell-specific manner, thereby generating a unique combination of Pcdh α , β , and γ expression in each neuron (Esumi et al., 2005; Kaneko et al., 2006; Thu et al., 2014; Mountoufaris et al., 2017). Clusters α and γ further include constant exons coding for a common intracellular domain that are combined to each variable exon by alternative splicing. Like DSCAM1, Pcdhs engage in strict homophilic *trans*-interactions and as such, provide a recognition code for sister branches of the same neuron (Hasegawa et al., 2012; Thu et al., 2014; Mountoufaris et al., 2017). They also form multimers in *cis* at the plasma membrane and signal through the intracellular domain of Pcdhs α and γ to initiate repulsion. Thanks to their diversity, Pcdhs have emerged as the main mediators of axonal and dendritic self-avoidance in vertebrates (Lefebvre et al., 2012). Deleting all three Pcdh clusters in mice, for instance, causes a loss of self-avoidance and severe arborization defects in olfactory axons (Mountoufaris et al., 2017). Conversely, “erasing” the Pcdh code by overexpressing a single-triclustere gene repertoire prevents olfactory axons from converging into stereotypically positioned glomeruli in the olfactory bulb.

Protocadherins also appear to regulate axonal tiling in addition to self-avoidance. In the basal ganglia and hippocampus, for instance, serotonergic axon terminals are evenly spaced in their target fields but become clumped together in mice lacking Pcdh α 2, the only Pcdh α isoform expressed in serotonergic neurons (Chen et al., 2017). Whether tiling of other axonal populations is similarly regulated by the expression of unique Pcdhs remains to be determined. Other CAMs, however, have been identified as tiling regulators. DSCAM is notably required for proper axonal and dendritic tiling of bipolar cells in the retina (Simmons et al., 2017). Likewise in the *Drosophila* visual system, DSCAM2, the atypical cadherin Flamingo (Fmi), and the IgSF CAM Turtle (Tutl) enable proper spacing of distinct classes of axons in spatially restricted columns in the medulla (Millard et al., 2007; Tomasi et al., 2008; Ferguson et al., 2009; Hakeda-Suzuki et al., 2011; **Figure 3E**). Tutl engages in homophilic *trans*-interactions to prevent adjacent R7 photoreceptor cell terminals from overlapping (Ferguson et al., 2009). Similarly, Fmi mediates repulsive *trans*-interactions between R8 photoreceptors axons. Fmi interacts in *cis* with

Gogo, another transmembrane receptor eliciting repulsive axon-axon interactions, suggesting that both proteins might act as a complex at the surface of branches to ensure tiling (Tomasi et al., 2008; Hakeda-Suzuki et al., 2011). Lastly, DSCAM2 ensures proper spacing of L1 axonal arbors, thereby restricting them to specific columns. In *dscam2* mutants, L1 axons still innervate the correct layer of the medulla but are no longer restricted to a single column (Millard et al., 2007). Altogether, these studies indicate that the selective expression of individual or combined CAMs generates a cell-surface recognition code that ensures the segregation of terminal arbors into non-overlapping domains while instructing laminar targeting and synaptic specificity.

CONCLUSION AND PERSPECTIVES

In conclusion, a large body of literature now demonstrates that CAMs orchestrate a striking number of developmental processes that are critical for neural circuit wiring. By engaging in homophilic and heterophilic *trans*-interactions, CAMs not only provide the adhesion and mechanical stabilization required for proper axon guidance and fasciculation, but also generate a cell-surface recognition code essential for synaptic specificity and contact-mediated self-avoidance and tiling. CAMs further act as bona fide signaling factors instructing growth cone behavior, modulating the activities of guidance receptors, and controlling transcriptional programs for axonal development.

Surprisingly, whether CAMs also contribute to the regressive events that refine neural circuits remains poorly known. Selective axon degeneration, for instance, is used to remodel axonal projections during metamorphosis in insects or prune exuberant axons or axonal branches in vertebrates (Riccomagno and Kolodkin, 2015; Schuldiner and Yaron, 2015). In the visual system, retinal axons that mis-sort along the optic tract selectively degenerate, leading to proper pre-target topographic ordering of retinal projections (Poulain and Chien, 2013). Refinement of terminal retinal arbors also occurs at the target in an activity-dependent manner, leading to the sharpening of retinotopic maps and the segregation of ipsi- and contralateral axons into eye-specific territories in animals with binocular vision (Stellwagen and Shatz, 2002; Chandrasekaran et al., 2005; Ben Fredj et al., 2010). Interestingly, Cntn2 was recently identified as a key regulator of retinotectal map sharpening in zebrafish (Spead et al., 2021). Nasal retinal axons progressively refine their projection domain to the posterior tectum in wild-type but not in the absence of Cntn2, causing a lack of retinotopic map refinement along the antero-posterior axis. How Cntn2 remodels axon terminal arbors remains to be determined but might involve an interplay between Cntn2 signaling and neuronal activity. Indeed, neuronal activity might modulate the targeting of Cntn2 to the plasma membrane, just as it regulates that of Cntn1 in hypothalamic axons (Pierre et al., 2001). Conversely, Cntn2 could modulate neuronal activity by regulating sodium or potassium channels. Cntn1, for instance, interacts with several voltage-gated sodium channels and increases their density at the plasma membrane (Kazarinova-Noyes et al., 2001; Liu et al., 2001).

Dissecting the cross-talk between CAMs and other signaling pathways will be critical to fully comprehend the multiple roles CAMs play at various stages of circuit assembly. It might also provide new strategies for correcting mechanisms that get dysregulated in the context of neurodevelopmental disorders.

AUTHOR CONTRIBUTIONS

Both authors listed have made a substantial, direct, and intellectual contribution to the work, and approved it for publication.

REFERENCES

- Abe, K., Katsuno, H., Toriyama, M., Baba, K., Mori, T., Hakoshima, T., et al. (2018). Grip and slip of L1-CAM on adhesive substrates direct growth cone haptotaxis. *Proc. Natl. Acad. Sci. USA* 115, 2764–2769. doi: 10.1073/pnas.1711667115
- Agrawal, M., and Welshhans, K. (2021). Local translation across neural development: a focus on radial glial cells, axons, and synaptogenesis. *Front. Mol. Neurosci.* 14:717170. doi: 10.3389/fnmol.2021.717170
- Alsanie, W. F., Penna, V., Schachner, M., Thompson, L. H., and Parish, C. L. (2017). Homophilic binding of the neural cell adhesion molecule CHL1 regulates development of ventral midbrain dopaminergic pathways. *Sci. Rep.* 7:9368. doi: 10.1038/s41598-017-09599-y
- Ange, F., di Cristo, G., Higashiyama, H., Bennett, V., Wu, P., and Huang, Z. J. (2004). Ankyrin-based subcellular gradient of neurofascin, an immunoglobulin family protein, directs GABAergic innervation at purkinje axon initial segment. *Cell* 119, 257–272. doi: 10.1016/j.cell.2004.10.004
- Antinucci, P., Nikolaou, N., Meyer, M. P., and Hindges, R. (2013). Teneurin-3 specifies morphological and functional connectivity of retinal ganglion cells in the vertebrate visual system. *Cell Rep.* 5, 582–592. doi: 10.1016/j.celrep.2013.09.045
- Antinucci, P., Suleyman, O., Monfries, C., and Hindges, R. (2016). Neural mechanisms generating orientation selectivity in the retina. *Curr. Biol.* 26, 1802–1815. doi: 10.1016/j.cub.2016.05.035
- Araç, D., and Li, J. (2019). Teneurins and latrophilins: two giants meet at the synapse. *Curr. Opin. Struct. Biol.* 54, 141–151. doi: 10.1016/j.sbi.2019.01.028
- Avital, H., Behrman, M., and Malach, R. (2015). The idiosyncratic brain: distortion of spontaneous connectivity patterns in autism spectrum disorder. *Nat. Neurosci.* 18, 302–309. doi: 10.1038/nn.3919
- Baba, K., Yoshida, W., Toriyama, M., Shimada, T., Manning, C. F., Saito, M., et al. (2018). Gradient-reading and mechano-effector machinery for netrin-1-induced axon guidance. *Elife* 7:e34593. doi: 10.7554/eLife.34593
- Bagutti, C., Forro, G., Ferralli, J., Rubin, B., and Chiquet-Ehrismann, R. (2003). The intracellular domain of teneurin-2 has a nuclear function and represses zic-1-mediated transcription. *J. Cell. Sci.* 116, 2957–2966. doi: 10.1242/jcs.00603
- Baumer, F. M., Song, J. W., Mitchell, P. D., Pienaar, R., Sahin, M., Grant, P. E., et al. (2015). Longitudinal changes in diffusion properties in white matter pathways of children with tuberous sclerosis complex. *Pediatr. Neurol.* 52, 615–623. doi: 10.1016/j.pediatrneurol.2015.02.004
- Bechara, A., Nawabi, H., Moret, F., Yaron, A., Weaver, E., Bozon, M., et al. (2008). FAK-MAPK-dependent adhesion disassembly downstream of L1 contributes to semaphorin3A-induced collapse. *EMBO. J.* 27, 1549–1562. doi: 10.1038/emboj.2008.86
- Bekirov, I. H., Nagy, V., Svoronos, A., Huntley, G. W., and Benson, D. L. (2008). Cadherin-8 and N-cadherin differentially regulate pre- and postsynaptic development of the hippocampal mossy fiber pathway. *Hippocampus* 18, 349–363. doi: 10.1002/hipo.20395
- Ben Fredj, N., Hammond, S., Otsuna, H., Chien, C. B., Burrone, J., and Meyer, M. P. (2010). Synaptic activity and activity-dependent competition regulates axon arbor maturation, growth arrest, and territory in the retinotectal projection. *J. Neurosci.* 30, 10939–10951. doi: 10.1523/JNEUROSCI.1556-10.2010

FUNDING

This study was supported by the National Institutes of Health/National Institute of Neurological Disorders and Stroke (R01NS109197 and R21NS124542 to FP).

ACKNOWLEDGMENTS

We thank all referees for their constructive feedback and apologize for omitting any references owing to space restrictions.

- Berns, D. S., DeNardo, L. A., Pederick, D. T., and Luo, L. (2018). Teneurin-3 controls topographic circuit assembly in the hippocampus. *Nature* 554, 328–333. doi: 10.1038/nature25463
- Bock, E. (1991). Cell-cell adhesion molecules. *Biochem. Soc. Trans.* 19, 1076–1080. doi: 10.1042/bst0191076
- Boucard, A. A., Maxeiner, S., and Südhof, T. C. (2014). Latrophilins function as heterophilic cell-adhesion molecules by binding to teneurins: regulation by alternative splicing. *J. Biol. Chem.* 289, 387–402. doi: 10.1074/jbc.M113.504779
- Bruce, F. M., Brown, S., Smith, J. N., Fuerst, P. G., and Erskine, L. (2017). DSCAM promotes axon fasciculation and growth in the developing optic pathway. *Proc. Natl. Acad. Sci. USA* 114, 1702–1707. doi: 10.1073/pnas.1618606114
- Buhusi, M., Demyanenko, G. P., Jannie, K. M., Dalal, J., Darnell, E. P., Weiner, J. A., et al. (2009). ALCAM regulates mediolateral retinotopic mapping in the superior colliculus. *J. Neurosci.* 50, 15630–15641. doi: 10.1523/JNEUROSCI.2215-09.2009
- Castellani, V., Chédotal, A., Schachner, M., Faivre-Sarrailh, C., and Rougon, G. (2000). Analysis of the L1-deficient mouse phenotype reveals cross-talk between Sema3A and L1 signaling pathways in axonal guidance. *Neuron* 27, 237–249. doi: 10.1016/s0896-6273(00)00033-7
- Castellani, V., De Angelis, E., Kenwrick, S., and Rougon, G. (2002). Cis and trans interactions of L1 with neuropilin-1 control axonal responses to semaphorin 3A. *EMBO. J.* 23, 6348–6357. doi: 10.1093/emboj/cdf645
- Castellani, V., Falk, J., and Rougon, G. (2004). Semaphorin3A-induced receptor endocytosis during axon guidance responses is mediated by L1 CAM. *Mol. Cell Neurosci.* 26, 89–100. doi: 10.1016/j.mcn.2004.01.010
- Chandrasekaran, A. R., Plas, D. T., Gonzalez, E., and Crair, M. C. (2005). Evidence for an instructive role of retinal activity in retinotopic map refinement in the superior colliculus of the mouse. *J. Neurosci.* 25, 6929–6938. doi: 10.1523/JNEUROSCI.1470-05.2005
- Charoy, C., Nawabi, H., Reynaud, F., Derrington, E., Bozon, M., Wright, K., et al. (2012). gdnf activates midline repulsion by Semaphorin3B via NCAM during commissural axon guidance. *Neuron* 75, 1051–1066. doi: 10.1016/j.neuron.2012.08.02
- Chen, W. V., Nwaeze, C. L., Denny, C. A., O'Keefe, S., Rieger, M. A., Mountoufaris, G., et al. (2017). Pcdhac2 is required for axonal tiling and assembly of serotonergic circuitries in mice. *Science* 356, 406–411. doi: 10.1126/science.aal3231
- Chen, Y. A., Lu, I. L., and Tsai, J. W. (2018). Contactin-1/F3 regulates neuronal migration and morphogenesis through modulating RhoA Activity. *Front. Mol. Neurosci.* 11:422. doi: 10.3389/fnmol.2018.00422
- Cutler, K., Hassan, M., Carr, J., Cloete, R., and Barden, S. (2021). Emerging evidence implicating a role for neurexins in neurodegenerative and neuropsychiatric disorders. *Open Biol.* 11:210091. doi: 10.1098/rsob.210091
- Dalla Costa, I., Buchanan, C. N., Zdradzinski, M. D., Sahoo, P. K., Smith, T. P., et al. (2020). The functional organization of axonal mRNA transport and translation. *Nat. Rev. Neurosci.* 22, 77–91. doi: 10.1038/s41583-020-00407-7
- Dang, P., Smythe, E., and Furley, A. J. (2012). TAG1 regulates the endocytic trafficking and signaling of the semaphorin3A receptor complex. *J. Neurosci.* 32, 10370–10382. doi: 10.1523/JNEUROSCI.5874-11.2012
- Demyanenko, G. P., Riday, T. T., Tran, T. S., Dalal, J., Darnell, E. P., Brennaman, L. H., et al. (2011). NrCAM deletion causes topographic mistargeting of

- thalamocortical axons to the visual cortex and disrupts visual acuity. *J. Neurosci.* 31, 1545–1558. doi: 10.1523/JNEUROSCI.4467-10.2011
- Dharmaratne, N., Glendinning, K. A., Young, T. R., Tran, H., Sawatari, A., and Leamey, C. A. (2012). Ten-m3 is required for the development of topography in the ipsilateral retinocollicular pathway. *PLoS One* 7:e43083. doi: 10.1371/journal.pone.0043083
- Di Martino, A., Yan, C. G., Li, Q., Denio, E., Castellanos, F. X., and Alaerts, K. (2014). The autism brain imaging data exchange: towards a large-scale evaluation of the intrinsic brain architecture in autism. *Mol. Psychiatry* 19, 659–667. doi: 10.1038/mp.2013.78
- Dickson, B. J. (2002). Molecular mechanisms of axon guidance. *Science* 298, 1959–1964. doi: 10.1126/science.1072165
- Dipietrantonio, H. J., and Dymecki, S. M. (2009). Zic1 levels regulate mossy fiber neuron position and axon laterality choice in the ventral brain stem. *Neuroscience* 162, 560–573. doi: 10.1016/j.neuroscience.2009.02.082
- Duan, X., Krishnaswamy, A., De la Huerta, I., and Sanes, J. R. (2014). Type II cadherins guide assembly of a direction-selective retinal circuit. *Cell* 158, 793–807. doi: 10.1016/j.cell.2014.06.047
- Duan, X., Krishnaswamy, A., Laboulaye, M. A., Liu, J., Peng, Y. R., Yamagata, M., et al. (2018). Cadherin combinations recruit dendrites of distinct retinal neurons to a shared interneuronal scaffold. *Neuron* 99, 1145–1154. doi: 10.1016/j.neuron.2018.08.019
- Esumi, S., Kakazu, N., Taguchi, Y., Hirayama, T., Sasaki, A., Hirabayashi, T., et al. (2005). Monoallelic yet combinatorial expression of variable exons of the protocadherin- α gene cluster in single neurons. *Nat. Genet.* 37, 171–176. doi: 10.1038/ng1500
- Falk, J., Bechara, A., Fiore, R., Nawabi, H., Zhou, H., Hoyo-Becerra, C., et al. (2005). Dual functional activity of semaphorin 3B is required for positioning the anterior commissure. *Neuron* 48, 63–75. doi: 10.1016/j.neuron.2005.08.033
- Ferguson, K., Long, H., Cameron, S., Chang, W. T., and Rao, Y. (2009). The conserved Ig superfamily member Turtle mediates axonal tiling in *Drosophila*. *J. Neurosci.* 29, 14151–14159. doi: 10.1523/JNEUROSCI.2497-09.2009
- Fitzli, D., Stoeckli, E. T., Kunz, S., Siribour, K., Rader, C., Kunz, B., et al. (2000). A direct interaction of axonin-1 with NgCAM-related cell adhesion molecule (NrCAM) results in guidance, but not growth of commissural axons. *J. Cell Biol.* 149, 951–968. doi: 10.1083/jcb.149.4.951
- Frei, J. A., Andermatt, I., Gesemann, M., and Stoeckli, E. T. (2014). The SynCAM synaptic cell adhesion molecules are involved in sensory axon pathfinding by regulating axon-axon contacts. *J. Cell Sci.* 127, 5288–5302. doi: 10.1242/jcs.157032
- Fuerst, P. G., Bruce, F., Tian, M., Wei, W., Elstrott, J., Feller, M. B., et al. (2009). DSCAM and DSCAML1 function in self-avoidance in multiple cell types in the developing mouse retina. *Neuron* 64, 484–497. doi: 10.1016/j.neuron.2009.09.027
- Fuerst, P. G., Harris, B. S., Johnson, K. R., and Burgess, R. W. (2010). A novel null allele of mouse DSCAM survives to adulthood on an inbred C3H background with reduced phenotypic variability. *Genesis* 48, 578–584. doi: 10.1002/dvg.20662
- Fuerst, P. G., Koizumi, A., Masland, R. H., and Burgess, R. W. (2008). Neurite arborization and mosaic spacing in the mouse retina require DSCAM. *Nature* 460, 470–474. doi: 10.1038/nature06514
- Garrett, A. M., Khalil, A., Walton, D. O., and Burgess, R. W. (2018). DSCAM promotes self-avoidance in the developing mouse retina by masking the functions of cadherin superfamily members. *Proc. Natl. Acad. Sci. USA* 115, E10216–E10224. doi: 10.1073/pnas.1809430115
- Gatford, N. J. F., Deans, P. J. M., Duarte, R. R. R., Chennell, G., Sellers, K. J., et al. (2021). Neuroligin-3 and Neuroligin-4X form Nanoscopic clusters and regulate growth cone organization and size. *Hum. Mol. Genet.* 20:ddab277. doi: 10.1093/hmg/ddab277
- Gerrow, K., and El-Husseini, A. (2006). Cell adhesion molecules at the synapse. *Front. Biosci.* 11:2400–2419. doi: 10.2741/1978
- Girbes Mínguez, M., Wolters-Eisfeld, G., Lutz, D., Buck, F., Schachner, M., and Kleene, R. (2020). The cell adhesion molecule L1 interacts with nuclear proteins via its intracellular domain. *FASEB. J.* 34, 9869–9883. doi: 10.1096/fj.201902242R
- Glendinning, K. A., Liu, S. C., Nguyen, M., Dharmaratne, N., Nagarajah, R., Iglesias, M. A., et al. (2017). Downstream mediators of Ten-m3 signalling in the developing visual pathway. *BMC Neurosci.* 18:78. doi: 10.1186/s12868-017-0397-5
- Gomez, A. M., Traunmüller, L., and Scheiffele, P. (2021). Neurexins: molecular codes for shaping neuronal synapses. *Nat. Rev. Neurosci.* 22, 137–151. doi: 10.1038/s41583-020-00415-7
- Gomez, T. M., Roche, F. K., and Letourneau, P. C. (1996). Chick sensory neuronal growth cones distinguish fibronectin from laminin by making substratum contacts that resemble focal contacts. *J. Neurobiol.* 29, 18–34. doi: 10.1002/(SICI)1097-4695(199601)29:1<18::AID-NEU2>3.0.CO;2-A
- Grueber, W., and Sagasti, A. (2010). Self-avoidance and tiling: Mechanisms of dendrite and axon spacing. *Cold Spring Harb. Perspect. Biol.* 2:a001750. doi: 10.1101/cshperspect.a001750
- Hakeda-Suzuki, S., Berger-Müller, S., Tomasi, T., Usui, T., Horiuchi, S. Y., Uemura, T., et al. (2011). Golden Goal collaborates with Flamingo in conferring synaptic-layer specificity in the visual system. *Nat. Neurosci.* 14, 314–323. doi: 10.1038/nn.2756
- Hasegawa, S., Hirabayashi, T., Kondo, T., Inoue, K., Esumi, S., Okayama, A., et al. (2012). Constitutively expressed Protocadherin- α regulates the coalescence and elimination of homotypic olfactory axons through its cytoplasmic region. *Front. Mol. Neurosci.* 5:97. doi: 10.3389/fnmol.2012.00097
- Hattori, D., Demir, E., Kim, H. W., Virag, E., Zipursky, S. L., and Dickson, B. J. (2007). Dscam diversity is essential for neuronal wiring and self-recognition. *Nature* 449, 223–227. doi: 10.1038/nature06099
- Hayano, Y., Ishino, Y., Hyun, J. H., Orozco, C. G., Steinecke, A., Potts, E., et al. (2021). IgSF11 homophilic adhesion proteins promote layer-specific synaptic assembly of the cortical interneuron subtype. *Sci. Adv.* 7:eabf1600. doi: 10.1126/sciadv.abf1600
- Hayashi, S., Inoue, Y., Kiyonari, H., Abe, T., Misaki, K., Moriguchi, H., et al. (2014). Protocadherin-17 mediates collective axon extension by recruiting actin regulator complexes to interaxonal contacts. *Dev. Cell* 30, 673–687. doi: 10.1016/j.devcel.2014.07.015
- Heggem, M. A., and Bradley, R. S. (2003). The cytoplasmic domain of *Xenopus* NF-protocadherin interacts with TAF1/set. *Dev. Cell* 2003, 419–429. doi: 10.1016/s1534-5807(03)00036-4
- Herrera, E., Brown, L., Aruga, J., Rachel, R. A., Dolen, G., Mikoshiba, K., et al. (2003). Zic2 patterns binocular vision by specifying the uncrossed retinal projection. *Cell* 114, 545–557. doi: 10.1016/s0092-8674(03)00684-6
- Hidalgo, A., and Brand, A. H. (1997). Targeted neuronal ablation: The role of pioneer neurons in guidance and fasciculation in the CNS of *Drosophila*. *Development* 124, 3253–3262. doi: 10.1242/dev.124.17.3253
- Hines, J. H., Abu-Rub, M., and Henley, J. R. (2010). Asymmetric endocytosis and remodeling of β 1-integrin adhesions during growth cone chemorepulsion by MAG. *Nat. Neurosci.* 13, 829–837. doi: 10.1038/nn.2554
- Homan, C. C., Pederson, S., To, T. H., Tan, C., Piltz, S., Corbett, M. A., et al. (2018). PCDH19 regulation of neural progenitor cell differentiation suggests asynchrony of neurogenesis as a mechanism contributing to PCDH19 Girls Clustering Epilepsy. *Neurobiol. Dis.* 116, 106–119. doi: 10.1016/j.nbd.2018.05.004
- Homrich, M., Es-Saddiki, F., Gotthard, I., Laurini, C., Stein, E., Wobst, H., et al. (2018). NCAM140 is translocated into the nucleus by an importin- β 1-dependent mechanism. *Exp. Cell Res.* 371, 372–378.
- Hong, W., Mosca, T. J., and Luo, L. (2012). Teneurin instruct synaptic partner matching in an olfactory map. *Nature* 484, 201–207. doi: 10.1038/nature10926
- Honig, M. G., and Rutishauser, U. S. (1996). Changes in the segmental pattern of sensory neuron projections in the chick hindlimb under conditions of altered cell adhesion molecule function. *Dev. Biol.* 175, 325–337. doi: 10.1006/dbio.1996.0118
- Honig, M. G., Camilli, S. J., and Xue, Q. S. (2002). Effects of L1 blockade on sensory axon outgrowth and pathfinding in the chick hindlimb. *Dev. Biol.* 243, 137–154. doi: 10.1006/dbio.2001.0556
- Hsieh, H. H., Chang, W. T., Yu, L., and Rao, Y. (2014). Control of axon-axon attraction by Semaphorin reverse signaling. *Proc. Natl. Acad. Sci. USA* 111, 11383–11388. doi: 10.1073/pnas.1321433111
- Huang, R., Yuan, D. J., Li, S., Liang, X. S., Gao, Y., et al. (2020). NCAM regulates temporal specification of neural progenitor cells via profilin2 during corticogenesis. *J. Cell Biol.* 219:e201902164. doi: 10.1083/jcb.201902164
- Huang, Z., Yazdani, U., Thompson-Peer, K. L., Kolodkin, A. L., and Terman, J. R. (2007). Crk-associated substrate (Cas) signaling protein functions with

- integrins to specify axon guidance during development. *Development* 134, 2337–2347. doi: 10.1242/dev.004242
- Huberman, A. D., Clandinin, T. R., and Baier, H. (2010). Molecular and cellular mechanisms of lamina-specific axon targeting. *Cold Spring Harb. Perspect. Biol.* 2:a001743. doi: 10.1101/cshperspect.a001743
- Hynes, R. O. (2002). Integrins: bidirectional, allosteric signaling machines. *Cell* 110, 673–687. doi: 10.1016/s0092-8674(02)00971-6
- Im, K., Ahtam, B., Haehn, D., Peters, J. M., Warfield, S. K., Sahin, M., et al. (2016). Altered structural brain networks in tuberous sclerosis complex. *Cereb. Cortex* 26, 2046–2058. doi: 10.1093/cercor/bhv026
- Jaudon, F., Thalhammer, A., and Cingolani, L. A. (2021). Integrin adhesion in brain assembly: from molecular structure to neuropsychiatric disorders. *Eur. J. Neurosci.* 53, 3831–3850. doi: 10.1111/ejn.14859
- Jaworski, A., and Tessier-Lavigne, M. (2012). Autocrine/juxtacrine regulation of axon fasciculation by Slit-Robo signaling. *Nat. Neurosci.* 15, 367–369. doi: 10.1038/nn.3037
- Jessen, U., Novitskaya, V., Pedersen, N., Serup, P., Berezin, V., and Bock, E. (2001). The transcription factors CREB and c-Fos play key roles in NCAM-mediated neurite outgrowth in PC12-E2 cells. *J. Neurochem.* 79, 1149–1160. doi: 10.1046/j.1471-4159.2001.00636.x
- Kaneko, R., Kato, H., Kawamura, Y., Esumi, S., Hirayama, T., Hirabayashi, T., et al. (2006). Allelic gene regulation of Pcdh-alpha and Pcdh-gamma clusters involving both monoallelic and biallelic expression in single Purkinje cells. *J. Biol. Chem.* 281, 30551–30560. doi: 10.1074/jbc.M605677200
- Kaur, N., Han, W., Li, Z., Madrigal, M. P., Shim, S., Pochareddy, S., et al. (2020). Neural stem cells direct axon guidance via their radial fiber scaffold. *Neuron* 107, 1197–1211. doi: 10.1016/j.neuron.2020.06.035
- Kazarinova-Noyes, K., Malhotra, J. D., McEwen, D. P., Mattei, L. N., Berglund, E. O., Ranscht, B., et al. (2001). Contactin associates with Na⁺ channels and increases their functional expression. *J. Neurosci.* 21, 7517–7525. doi: 10.1523/JNEUROSCI.21-19-07517.2001
- Kershner, L., and Welshhans, K. (2017). RACK1 is necessary for the formation of point contacts and regulates axon growth. *Dev. Neurobiol.* 77, 1038–1056. doi: 10.1002/dneu.22491
- Kerstein, P. C., Nichol, R. H. I. V., and Gomez, T. M. (2015). Mechanochemical regulation of growth cone motility. *Front. Cell Neurosci.* 9:244. doi: 10.3389/fncel.2015.00244
- Kerstein, P. C., Patel, K. M., and Gomez, T. M. (2017). Calpain-mediated proteolysis of talin and FAK regulates adhesion dynamics necessary for axon guidance. *J. Neurosci.* 6, 1568–1580. doi: 10.1523/JNEUROSCI.2769-16.2016
- Kleene, R., Loers, G., Castillo, G., and Schachner, M. (2022). Cell adhesion molecule L1 interacts with the chromo shadow domain of heterochromatin protein 1 isoforms α , β , and γ via its intracellular domain. *FASEB J.* 36:e22074. doi: 10.1096/fj.202100816R
- Kleene, R., Mzoughi, M., Joshi, G., Kalus, I., Bormann, U., Schulze, C., et al. (2010). NCAM-induced neurite outgrowth depends on binding of calmodulin to NCAM and on nuclear import of NCAM and fak fragments. *J. Neurosci.* 30, 10784–10798. doi: 10.1523/JNEUROSCI.0297-10.2010
- Kolkova, K., Novitskaya, V., Pedersen, N., Berezin, V., and Bock, E. (2000). Neural cell adhesion molecule-stimulated neurite outgrowth depends on activation of protein kinase C and the Ras-mitogen-activated protein kinase pathway. *J. Neurosci.* 20, 2238–2246. doi: 10.1523/JNEUROSCI.20-06-02238.2000
- Krishnaswamy, A., Yamagata, M., Duan, X., Hong, Y. K., and Sanes, J. R. (2015). Sidekick 2 directs formation of a retinal circuit that detects differential motion. *Nature* 524, 466–470. doi: 10.1038/nature14682
- Kubo, Y., Baba, K., Toriyama, M., Minegishi, T., Sugiura, T., Kozawa, S., et al. (2015). Shootin1-cortactin interaction mediates signal-force transduction for axon outgrowth. *J. Cell. Biol.* 210, 663–676. doi: 10.1083/jcb.201505011
- Kutsarova, E., Munz, M., and Ruthazer, E. S. (2017). Rules for Shaping Neural Connections in the Developing Brain. *Front. Neural. Circuits.* 10:111. doi: 10.3389/fncir.2016.00111
- Kuwajima, T., Yoshida, Y., Takegahara, N., Petros, T. J., Kumanogoh, A., Jessell, T. M., et al. (2012). Optic chiasm presentation of Semaphorin6D in the context of Plexin-A1 and Nr-CAM promotes retinal axon midline crossing. *Neuron* 74, 676–690. doi: 10.1016/j.neuron.2012.03.025
- Kuwako, K. I., Nishimoto, Y., Kawase, S., Okano, H. J., and Okano, H. (2014). Cadherin-7 regulates mossy fiber connectivity in the cerebellum. *Cell Rep.* 9, 311–323. doi: 10.1016/j.celrep.2014.08.063
- Landmesser, L., Dahm, L., Schultz, K., and Rutishauser, U. (1988). Distinct roles for adhesion molecules during innervation of embryonic chick muscle. *Dev. Biol.* 130, 645–670. doi: 10.1016/0012-1606(88)90358-2
- Law, C. O., Kirby, R. J., Aghamohammadzadeh, S., and Furley, A. J. W. (2008). The neural adhesion molecule TAG-1 modulates responses of sensory axons to diffusible guidance signals. *Development* 135, 2361–2371. doi: 10.1242/dev.009019
- Leamey, C. A., Merlin, S., Lattouf, P., Sawatari, A., Zhou, X., Demel, N., et al. (2007). Ten_m3 regulates eye-specific patterning in the mammalian visual pathway and is required for binocular vision. *PLoS Biol.* 5:e241. doi: 10.1371/journal.pbio.0050241
- Lefebvre, J. L., Kostadinov, D., Chen, W. V., Maniatis, T., and Sanes, J. R. (2012). Protocadherins mediate dendritic self-avoidance in the mammalian nervous system. *Nature* 488, 517–521. doi: 10.1038/nature11305
- Leung, L. C., Urbančič, V., Baudet, M. L., Dwivedy, A., Bayley, T. G., Lee, A. C., et al. (2013). Coupling of NF-protocadherin signaling to axon guidance by cue-induced translation. *Nat. Neurosci.* 16, 166–173. doi: 10.1038/nn.3290
- Leyva-Díaz, E., del Toro, D., Menal, M. J., Cambray, S., Susín, R., Tessier-Lavigne, M., et al. (2014). FLRT3 is a Robo1-interacting protein that determines Netrin-1 attraction in developing axons. *Curr. Biol.* 24, 494–508. doi: 10.1016/j.cub.2014.01.042
- Li, J., Shalev-Benami, M., Sando, R., Jiang, X., Kibrom, A., Wang, J., et al. (2018). Structural basis for teneurin function in circuit-wiring: a toxin motif at the synapse. *Cell* 173, 735–748. doi: 10.1016/j.cell.2018.03.036
- Li, J., Xie, Y., Cornelius, S., Jiang, X., Sando, R., Kordon, S. P., et al. (2020). Alternative splicing controls teneurin-latrophilin interaction and synapse specificity by a shape-shifting mechanism. *Nat. Commun.* 11:2140. doi: 10.1038/s41467-020-16029-7
- Lilienbaum, A., Reszka, A. A., Horwitz, A. F., and Holt, C. E. (1995). Chimeric integrins expressed in retinal ganglion cells impair process outgrowth in vivo. *Mol. Cell. Neurosci.* 6, 139–152. doi: 10.1006/mcne.1995.1013
- Lindenmaier, L. B., Parmentier, N., Guo, C., Tissir, F., and Wright, K. M. (2019). Dystroglycan is a scaffold for extracellular axon guidance decisions. *Elife* 8:e42143. doi: 10.7554/eLife.42143
- Liu, C. J., Dib-Hajj, S. D., Black, J. A., Greenwood, J., Lian, Z., and Waxman, S. G. (2001). Direct interaction with contactin targets voltage-gated sodium channel Na(v)1.9/NaN to the cell membrane. *J. Biol. Chem.* 276, 46553–46561. doi: 10.1074/jbc.M108699200
- Lutz, D., Wolters-Eisfeld, G., Joshi, G., Djogo, N., Jakovcevski, I., Schachner, M., et al. (2012). Generation and nuclear translocation of sumoylated transmembrane fragment of cell adhesion molecule L1. *J. Biol. Chem.* 287, 17161–17175. doi: 10.1074/jbc.M112.346759
- Lutz, D., Wolters-Eisfeld, G., Schachner, M., and Kleene, R. (2014). Cathepsin E generates a sumoylated intracellular fragment of the cell adhesion molecule L1 to promote neuronal and Schwann cell migration as well as myelination. *J. Neurochem.* 128, 713–724. doi: 10.1111/jnc.12473
- Luxey, M., Jungas, T., Laussu, J., Audouard, C., Garces, A., and Davy, A. (2013). Ephrephrin-B1 forward signaling controls fasciculation of sensory and motor axons. *Dev. Biol.* 383, 264–274. doi: 10.1016/j.ydbio.2013.09.010
- Marcus, R. C., Blazeski, R., Godement, P., and Mason, C. A. (1995). Retinal axon divergence in the optic chiasm: uncrossed axons diverge from crossed axons within a midline glial specialization. *J. Neurosci.* 5, 3716–3729. doi: 10.1523/JNEUROSCI.15-05-03716.1995
- Marthiens, V., Gavard, J., Padilla, F., Monnet, C., Castellani, V., Lambert, M., et al. (2005). A novel function for cadherin-11 in the regulation of motor axon elongation and fasciculation. *Mol. Cell. Neurosci.* 28, 715–726. doi: 10.1016/j.mcn.2004.12.001
- Matthews, B. J., Kim, M. E., Flanagan, J. J., Hattori, D., Clemens, J. C., Zipursky, S. L., et al. (2007). Dendrite self-avoidance is controlled by Dscam. *Cell* 129, 593–604. doi: 10.1016/j.cell.2007.04.013
- McFadden, K., and Minshew, N. J. (2013). Evidence for dysregulation of axonal growth and guidance in the etiology of ASD. *Front. Hum. Neurosci.* 7:671. doi: 10.3389/fnhum.2013.00671
- Millard, S. S., Flanagan, J. J., Pappu, K. S., Wu, W., and Zipursky, S. L. (2007). Dscam2 mediates axonal tiling in the Drosophila visual system. *Nature* 447, 720–724. doi: 10.1038/nature05855
- Mishra, Y. G., and Manavathi, B. (2021). Focal adhesion dynamics in cellular function and disease. *Cell Signal.* 85:110046. doi: 10.1016/j.celsig.2021.110046

- Missaire, M., and Hindges, R. (2015). The role of cell adhesion molecules in visual circuit formation: from neurite outgrowth to maps and synaptic specificity. *Dev. Neurobiol.* 75, 569–583. doi: 10.1002/dneu.22267
- Mosca, T. J., Hong, W., Dani, V. S., Favaloro, V., and Luo, L. (2012). Trans-synaptic Teneurin signalling in neuromuscular synapse organization and target choice. *Nature* 484, 237–241. doi: 10.1038/nature10923
- Mountoufaris, G., Chen, W. V., Hirabayashi, Y., O'Keeffe, S., Chevee, M., Nwakeze, C. L., et al. (2017). Multicenter Pcdh diversity is required for mouse olfactory neural circuit assembly. *Science* 356, 411–414. doi: 10.1126/science.aai8801
- Myers, J. P., and Gomez, T. M. (2011). Focal adhesion kinase promotes integrin adhesion dynamics necessary for chemotropic turning of nerve growth cones. *J. Neurosci.* 31, 13585–13595. doi: 10.1523/JNEUROSCI.2381-11.2011
- Nakamoto, T., Kain, K. H., and Ginsberg, M. H. (2004). Neurobiology: New connections between integrins and axon guidance. *Curr. Biol.* 14, R121–R123. doi: 10.1016/j.cub.2004.01.020
- Nelson, W. J., and Nusse, R. (2004). Convergence of Wnt, beta-catenin, and cadherin pathways. *Science* 303, 1483–1487. doi: 10.1126/science.1094291
- Neugebauer, K. M., Tomaselli, K. J., Lilien, J., and Reichardt, L. F. (1988). N-cadherin, NCAM, and integrins promote retinal neurite outgrowth on astrocytes in vitro. *J. Cell Biol.* 107, 1177–1187. doi: 10.1083/jcb.107.3.1177
- Nichol, R. H., Hagen, K. M., Lumbard, D. C., Dent, E. W., and Gómez, T. M. (2016). Guidance of axons by local coupling of retrograde flow to point contact adhesions. *J. Neurosci.* 36, 2267–2282. doi: 10.1523/JNEUROSCI.2645-15.2016
- Nicholls, J. G., and Baylor, D. A. (1968). Specific modalities and receptive fields of sensory neurons in CNS of the leech. *J. Neurophysiol.* 31, 740–756. doi: 10.1152/jn.1968.31.5.740
- Niethammer, P., Dellling, M., Sytnyk, V., Dityatev, A., Fukami, K., and Schachner, M. (2002). Cosignaling of NCAM via lipid rafts and the FGF receptor is required for neurite outgrowth. *J. Cell Biol.* 157, 521–532. doi: 10.1083/jcb.200109059
- Nunes, S. M., Ferralli, J., Choi, K., Brown-Luedi, M., Minet, A. D., and Chiquet-Ehrismann, R. (2005). The intracellular domain of teneurin-1 interacts with MBD1 and CAP/ponsin resulting in subcellular codistribution and translocation to the nuclear matrix. *Exp. Cell Res.* 305, 122–132. doi: 10.1016/j.yexcr.2004.12.020
- Okumura, M., Kato, T., Miura, M., and Chihara, T. (2016). Hierarchical axon targeting of Drosophila olfactory receptor neurons specified by the proneural transcription factors Atonal and Amos. *Genes Cell. Devot. Mol. Cell Mech.* 21, 53–64. doi: 10.1111/gtc.12321
- Osterhout, J. A., Josten, N., Yamada, J., Pan, F., Wu, S. W., Nguyen, P. L., et al. (2011). Cadherin-6 mediates axon-target matching in a non-image-forming visual circuit. *Neuron* 71, 632–639. doi: 10.1016/j.neuron.2011.07.006
- Ott, H., Bastmeyer, M., and Stuermer, C. A. (1998). Neurolin, the goldfish homolog of DM-GRASP, is involved in retinal axon pathfinding to the optic disk. *J. Neurosci.* 18, 3363–3372. doi: 10.1523/jneurosci.18-09-03363.1998
- Pederick, D. T., Lui, J. H., Gingrich, E. C., Xu, C., Wagner, M. J., Liu, Y., et al. (2021). Reciprocal repulsions instruct the precise assembly of parallel hippocampal networks. *Science* 372, 1068–1073. doi: 10.1126/science.abg1774
- Peng, Y. R., Tran, N. M., Krishnaswamy, A., Kostadinov, D., Martersteck, E. M., and Sanes, J. R. (2017). Satb1 regulates contactin 5 to pattern dendrites of a mammalian retinal ganglion cell. *Neuron* 95, 869–883. doi: 10.1016/j.neuron.2017.07.019
- Petrovic, M., and Hummel, T. (2008). Temporal identity in axonal target layer recognition. *Nature* 456, 800–803. doi: 10.1038/nature07407
- Pierre, K., Dupouy, B., Allard, M., Poulain, D. A., and Theodosis, D. T. (2001). Mobilization of the cell adhesion glycoprotein F3/contactin to axonal surfaces is activity dependent. *Eur. J. Neurosci.* 14, 645–656. doi: 10.1046/j.0953-816x.2001.01682.x
- Pike, S. H., Melancon, E. F., and Eisen, J. S. (1992). Pathfinding by zebrafish motoneurons in the absence of normal pioneer axons. *Development* 114, 825–831. doi: 10.1242/dev.114.4.825
- Piper, M., Dwivedy, A., Leung, L., Bradley, R. S., and Holt, C. E. (2008). NF-protocadherin and TAF1 regulate retinal axon initiation and elongation in vivo. *J. Neurosci.* 28, 100–105. doi: 10.1523/JNEUROSCI.4490-07.2008
- Pittman, A. J., Law, M. Y., and Chien, C. B. (2008). Pathfinding in a large vertebrate axon tract: Isotypic interactions guide retinotectal axons at multiple choice points. *Development* 135, 2865–2871. doi: 10.1242/dev.025049
- Pollerberg, G. E., and Mack, T. G. (1994). Cell adhesion molecule SC1/DMGRASP is expressed on growing axons of retina ganglion cells and is involved in mediating their extension on axons. *Dev. Biol.* 165, 670–687. doi: 10.1006/dbio.1994.1284
- Pollerberg, G. E., Thelen, K., Theiss, M. O., and Hochlehnert, B. C. (2013). The role of cell adhesion molecules for navigating axons: density matters. *Mech. Dev.* 130, 359–372. doi: 10.1016/j.mod.2012.11.002
- Poplawski, G. H., Tranziska, A. K., Leshchynska, I., Meier, I. D., Streichert, T., et al. (2012). L1CAM increases MAP2 expression via the MAPK pathway to promote neurite outgrowth. *Mol. Cell Neurosci.* 50, 169–178. doi: 10.1016/j.mcn.2012.03.010
- Poulain, F. E., and Chien, C. B. (2013). Proteoglycan-mediated axon degeneration corrects pretarget topographic sorting errors. *Neuron* 78, 49–56. doi: 10.1016/j.neuron.2013.02.005
- Purohit, A. A., Li, W., Qu, C., Dwyer, T., Shao, Q., Guan, K. L., et al. (2012). Down syndrome cell adhesion molecule (DSCAM) associates with uncoordinated-5C (UNC5C) in netrin-1-mediated growth cone collapse. *J. Biol. Chem.* 287, 27126–27138. doi: 10.1074/jbc.M112.340174
- Rasband, M. N., and Peles, E. (2021). Mechanisms of node of Ranvier assembly. *Nat. Rev. Neurosci.* 22, 7–20. doi: 10.1038/s41583-020-00406-8
- Rash, B. G., and Richards, L. J. (2001). A role for cingulate pioneering axons in the development of the corpus callosum. *J. Comp. Neurol.* 434, 147–157. doi: 10.1002/cne.1170
- Riccomagno, M. M., and Kolodkin, A. L. (2015). Sculpting neural circuits by axon and dendrite pruning. *Annu. Rev. Cell Dev. Biol.* 31, 779–805. doi: 10.1146/annurev-cellbio-100913-013038
- Rigby, M. J., Gomez, T. M., and Puglielli, L. (2020). Glial cell-axonal growth cone interactions in neurodevelopment and regeneration. *Front. Neurosci.* 14:203. doi: 10.3389/fnins.2020.00203
- Rutishauser, U., Thiery, J. P., Brackenbury, R., Sela, B. A., and Edelman, G. M. (1976). Mechanisms of adhesion among cells from neural tissues of the chick embryo. *Proc. Natl. Acad. Sci. USA* 73, 577–581. doi: 10.1073/pnas.73.2.577
- Sachse, S. M., Lievens, S., Ribeiro, L. F., Dascenco, D., Masschaele, D., et al. (2019). Nuclear import of the DSCAM-cytoplasmic domain drives signaling capable of inhibiting synapse formation. *EMBO J.* 38:e99669. doi: 10.15252/emboj.201899669
- Saftig, P., and Lichtenhaler, S. F. (2015). The alpha secretase ADAM10: A metalloprotease with multiple functions in the brain. *Prog. Neurobiol.* 135, 1–20. doi: 10.1016/j.pneurobio.2015.10.003
- Sagasti, A., Guido, M. R., Raible, D. W., and Schier, A. F. (2005). Repulsive interactions shape the morphologies and functional arrangement of zebrafish peripheral sensory arbors. *Curr. Biol.* 15, 804–814. doi: 10.1016/j.cub.2005.03.048
- Sakurai, T. (2017). The role of cell adhesion molecules in brain wiring and neuropsychiatric disorders. *Mol. Cell Neurosci.* 81, 4–11. doi: 10.1016/j.mcn.2016.08.005
- Sánchez-Camacho, C., and Bovolenta, P. (2009). Emerging mechanisms in morphogen-mediated axon guidance. *Bioessays* 31, 1013–1025. doi: 10.1002/bies.200900063
- Sando, R., Jiang, X., and Südhof, T. C. (2019). Latrophilin GPCRs direct synapse specificity by coincident binding of FLRTs and teneurins. *Science* 363:eaav7969. doi: 10.1126/science.aav7969
- Sanes, J. R., and Zipursky, S. L. (2020). Synaptic specificity, recognition molecules, and assembly of neural circuits. *Cell* 181, 536–556. doi: 10.1016/j.cell.2020.04.008
- Schaefer, A. W., Kamiguchi, H., Wong, E. V., Beach, C. M., Landreth, G., and Lemmon, V. (1999). Activation of the MAPK signal cascade by the neural cell adhesion molecule L1 requires L1 internalization. *J. Biol. Chem.* 274, 37965–37973. doi: 10.1074/jbc.274.53.37965
- Schmid, R. S., and Maness, P. F. (2008). L1 and NCAM adhesion molecules as signaling coreceptors in neuronal migration and process outgrowth. *Curr. Opin. Neurobiol.* 18, 245–250. doi: 10.1016/j.conb.2008.07.015
- Schmid, R. S., Pruitt, W. M., and Maness, P. F. (2000). A MAP kinase-signaling pathway mediates neurite outgrowth on L1 and requires Src-dependent endocytosis. *J. Neurosci.* 20, 4177–4188. doi: 10.1523/JNEUROSCI.20-11-04177.2000

- Schmucker, D., Clemens, J. C., Shu, H., Worby, C. A., Xiao, J., Muda, M., et al. (2000). Drosophila Dscam is an axon guidance receptor exhibiting extraordinary molecular diversity. *Cell* 101, 671–684. doi: 10.1016/s0092-8674(00)80878-8
- Schöler, J., Ferralli, J., Thiry, S., and Chiquet-Ehrismann, R. (2015). The intracellular domain of teneurin-1 induces the activity of microphthalmia-associated transcription factor (MITF) by binding to transcriptional repressor HINT1. *J. Biol. Chem.* 290, 8154–8165. doi: 10.1074/jbc.M114.615922
- Schroeder, A., and de Wit, J. (2018). Leucine-rich repeat-containing synaptic adhesion molecules as organizers of synaptic specificity and diversity. *Exp. Mol. Med.* 50, 1–9. doi: 10.1038/s12276-017-0023-8
- Schuldiner, O., and Yaron, A. (2015). Mechanisms of developmental neurite pruning. *Cell Mol. Life Sci.* 72, 101–119. doi: 10.1007/s00018-014-1729-6
- Siegenthaler, D., Enneking, E. M., Moreno, E., and Pielage, J. (2015). L1CAM/Neuroglian controls the axon-axon interactions establishing layered and lobular mushroom body architecture. *J. Cell Biol.* 208, 1003–1018.
- Simmons, A. B., Bloomsburg, S. J., Sukeena, J. M., Miller, C. J., Ortega-Burgos, Y., Borghuis, B. G., et al. (2017). DSCAM-mediated control of dendritic and axonal arbor outgrowth enforces tiling and inhibits synaptic plasticity. *Proc. Natl. Acad. Sci. USA* 114, E10224–E10233. doi: 10.1073/pnas.1713548114
- Šmit, D., Fouquet, C., Pincet, F., Zapotocky, M., and Trembleau, A. (2017). Axon tension regulates fasciculation/defasciculation through the control of axon shaft zippering. *Elife* 6:e19907. doi: 10.7554/eLife.19907
- Soba, P., Zhu, S., Emoto, K., Younger, S., Yang, S. J., Yu, H. H., et al. (2007). Drosophila sensory neurons require Dscam for dendritic self-avoidance and proper dendritic field organization. *Neuron* 54, 403–416. doi: 10.1016/j.neuron.2007.03.029
- Solecki, D. J. (2012). Sticky situations: recent advances in control of cell adhesion during neuronal migration. *Curr. Opin. Neurobiol.* 5, 791–798. doi: 10.1016/j.conb.2012.04.010
- Spead, O., and Poulain, F. E. (2021). Trans-axonal signaling in neural circuit wiring. *Int. J. Mol. Sci.* 21:5170. doi: 10.3390/ijms21145170
- Spead, O., Weaver, C. J., Moreland, T., and Poulain, F. E. (2021). Live imaging of retinotectal mapping reveals topographic map dynamics and a previously undescribed role for Contactin 2 in map sharpening. *Development* 148:dev199584. doi: 10.1242/dev.199584
- Stellwagen, D., and Shatz, C. J. (2002). An instructive role for retinal waves in the development of retinogeniculate connectivity. *Neuron* 33, 357–367. doi: 10.1016/s0896-6273(02)00577-9
- Stoeckli, E. T., Sonderegger, P., Pollerberg, G. E., and Landmesser, L. T. (1997). Interference with axonin-1 and NrCAM interactions unmasks a floor-plate activity inhibitory for commissural axons. *Neuron* 18, 209–221. doi: 10.1016/s0896-6273(00)80262-7
- Su, J., Sabbagh, U., Liang, Y., Olejníková, L., Dixon, K. G., Russell, A. L., et al. (2021). A cell-ECM mechanism for connecting the ipsilateral eye to the brain. *Proc. Natl. Acad. Sci. USA* 118:e2104343118. doi: 10.1073/pnas.2104343118
- Su, Z., and He, C. (2010). Olfactory ensheathing cells: biology in neural development and regeneration. *Prog. Neurobiol.* 9, 517–532. doi: 10.1016/j.pneurobio.2010.08.008
- Südhof, T. C. (2021). The cell biology of synapse formation. *J. Cell Biol.* 220:e202103052. doi: 10.1083/jcb.202103052
- Sullivan, C. S., Kümper, M., Temple, B. S., and Maness, P. F. (2016). The neural cell adhesion molecule (NCAM) promotes clustering and activation of EphA3 Receptors in GABAergic interneurons to induce ras homolog gene family, member A (RhoA)/Rho-associated protein kinase (ROCK)-mediated Growth Cone Collapse. *J. Biol. Chem.* 291, 26262–26272. doi: 10.1074/jbc.M116.760017
- Suter, T., Blagburn, S. V., Fisher, S. E., Anderson-Keightley, H. M., D'Elia, K. P., and Jaworski, A. (2020). TAG-1 multifunctionality coordinates neuronal migration, axon guidance, and fasciculation. *Cell Rep.* 30, 1164–1177. doi: 10.1016/j.celrep.2019.12.085
- Suzuki, N., Numakawa, T., Chou, J., de Vega, S., Mizuniwa, C., and Sekimoto, K. (2014). Teneurin-4 promotes cellular protrusion formation and neurite outgrowth through focal adhesion kinase signaling. *FASEB J.* 28, 1386–1397. doi: 10.1096/fj.13-241034
- Swanson, M. R., Wolff, J. J., Shen, M. D., Styner, M., Estes, A., Gerig, G., et al. (2018). Development of white matter circuitry in infants with fragile X Syndrome. *JAMA Psychiatry* 75, 505–513. doi: 10.1001/jamapsychiatry.2018.0180
- Tai, Y., Gallo, N. B., Wang, M., Yu, J. R., and Van Aelst, L. (2019). Axo-axonic innervation of neocortical pyramidal neurons by GABAergic chandelier cells requires ankyrin-associated L1CAM. *Neuron* 102, 358–372. doi: 10.1016/j.neuron.2019.02.009
- Tasic, B., Nabholz, C. E., Baldwin, K. K., Kim, Y., Rueckert, E. H., Ribich, S. A., et al. (2002). Promoter choice determines splice site selection in protocadherin alpha and gamma pre-mRNA splicing. *Mol. Cell.* 10, 21–33. doi: 10.1016/s1097-2765(02)00578-6
- Tessier-Lavigne, M., and Goodman, C. S. (1996). The molecular biology of axon guidance. *Science* 274, 1123–1133. doi: 10.1126/science.274.5290.1123
- Thelen, K., Maier, B., Faber, M., Albrecht, C., Fischer, P., and Pollerberg, G. E. (2012). Translation of the cell adhesion molecule ALCAM in axonal growth cones-Regulation and functional importance. *J. Cell Sci.* 125, 1003–1014. doi: 10.1242/jcs.096149
- Thu, C. A., Chen, W. V., Rubinstein, R., Chevee, M., Wolcott, H. N., Felsovalyi, K. O., et al. (2014). Single-cell identity generated by combinatorial homophilic interactions between α , β , and γ protocadherins. *Cell* 158, 1045–1059. doi: 10.1016/j.cell.2014.07.012
- Tomasi, T., Hakeda-Suzuki, S., Ohler, S., Schleiffer, A., and Suzuki, T. (2008). The transmembrane protein Golden goal regulates R8 photoreceptor axon-axon and axon-target interactions. *Neuron* 57, 691–704. doi: 10.1016/j.neuron.2008.01.012
- Treubert-Zimmermann, U., Heyers, D., and Redies, C. (2002). Targeting axons to specific fiber tracts in vivo by altering cadherin expression. *J. Neurosci.* 22, 7617–7626. doi: 10.1523/JNEUROSCI.22-17-07617.2002
- Vysokov, N. V., Silva, J. P., Leliana, V. G., Ho, C., Djamgoz, M. B., Tonevitsky, A. G., et al. (2016). The mechanism of regulated release of Lasso/Teneurin-2. *Front. Mol. Neurosci.* 9:59. doi: 10.3389/fnmol.2016.00059
- Vysokov, N. V., Silva, J. P., Leliana, V. G., Suckling, J., Cassidy, J., Blackburn, J. K., et al. (2018). Proteolytically released Lasso/teneurin-2 induces axonal attraction by interacting with latrophilin-1 on axonal growth cones. *Elife* 7:e37935. doi: 10.7554/eLife.37935
- Wang, J., Zugates, C. T., Liang, I. H., Lee, C. H., and Lee, T. (2002). Drosophila Dscam is required for divergent segregation of sister branches and suppresses ectopic bifurcation of axons. *Neuron* 33, 559–571. doi: 10.1016/s0896-6273(02)00570-6
- Wang, X., Su, H., and Bradley, A. (2002). Molecular mechanisms governing Pcdh-gamma gene expression: evidence for a multiple promoter and cis-alternative splicing model. *Genes Dev.* 16, 1890–1905. doi: 10.1101/gad.1004802
- Weiner, J. A., Koo, S. J., Nicolas, S., Fraboulet, S., Pfaff, S. L., Pourquie, O., et al. (2004). Axon fasciculation defects and retinal dysplasias in mice lacking the immunoglobulin superfamily adhesion molecule BEN/ALCAM/SC1. *Mol. Cell. Neurosci.* 27, 59–69. doi: 10.1016/j.mcn.2004.06.005
- Westphal, N., Kleene, R., Lutz, D., Theis, T., and Schachner, M. (2016). Polysialic acid enters the cell nucleus attached to a fragment of the neural cell adhesion molecule NCAM to regulate the circadian rhythm in mouse brain. *Mol. Cell Neurosci.* 74, 114–127. doi: 10.1016/j.mcn.2016.05.003
- Westphal, N., Loers, G., Lutz, D., Theis, T., Kleene, R., and Schachner, M. (2017a). Generation and intracellular trafficking of a polysialic acid-carrying fragment of the neural cell adhesion molecule NCAM to the cell nucleus. *Sci. Rep.* 7:8622. doi: 10.1038/s41598-017-09468-8
- Westphal, N., Theis, T., Loers, G., Schachner, M., and Kleene, R. (2017b). Nuclear fragments of the neural cell adhesion molecule NCAM with or without polysialic acid differentially regulate gene expression. *Sci. Rep.* 7:13631. doi: 10.1038/s41598-017-14056-x
- Whitlock, K. E., and Westerfield, M. A. (1998). transient population of neurons pioneers the olfactory pathway in the zebrafish. *J. Neurosci.* 18, 8919–8927. doi: 10.1523/jneurosci.18-21-08919.1998
- Widjaja, E., Simao, G., Mahmoodabadi, S. Z., Ochi, A., Snead, O. C., Rutka, J., et al. (2010). Diffusion tensor imaging identifies changes in normal-appearing white matter within the epileptogenic zone in tuberous sclerosis complex. *Epilepsy Res.* 89, 246–253. doi: 10.1016/j.epilepsyres.2010.01.008
- Williams, M. E., Wilke, S. A., Daggett, A., Davis, E., Otto, S., Ravi, D., et al. (2011). Cadherin-9 regulates synapse-specific differentiation in the developing hippocampus. *Neuron* 71, 640–655. doi: 10.1016/j.neuron.2011.06.019

- Williams, S. E., Grumet, M., Colman, D. R., Henkemeyer, M., Mason, C. A., and Sakurai, T. (2006). A role for Nr-CAM in the patterning of binocular visual pathways. *Neuron* 50, 535–547. doi: 10.1016/j.neuron.2006.03.037
- Wojtowicz, W. M., Flanagan, J. J., Millard, S. S., Zipursky, S. L., and Clemens, J. C. (2004). Alternative splicing of *Drosophila* Dscam generates axon guidance receptors that exhibit isoform-specific homophilic binding. *Cell* 118, 619–633. doi: 10.1016/j.cell.2004.08.021
- Wojtowicz, W. M., Wu, W., Andre, I., Qian, B., Baker, D., and Zipursky, S. L. (2007). A vast repertoire of Dscam binding specificities arises from modular interactions of variable Ig domains. *Cell* 130, 1134–1145. doi: 10.1016/j.cell.2007.08.026
- Wolman, M. A., Regnery, A. M., Becker, T., Becker, C. G., and Halloran, M. C. (2007). Semaphorin3D regulates axon axon interactions by modulating levels of L1 cell adhesion molecule. *J. Neurosci.* 27, 9653–9663. doi: 10.1523/jneurosci.1741-07.2007
- Woo, S., and Gomez, T. M. (2006). Rac1 and RhoA promote neurite outgrowth through formation and stabilization of growth cone point contacts. *J. Neurosci.* 26, 1418–1428. doi: 10.1523/JNEUROSCI.4209-05.2006
- Wu, Q., and Maniatis, T. (1999). A striking organization of a large family of human neural cadherin-like cell adhesion genes. *Cell* 97, 779–790. doi: 10.1016/s0092-8674(00)80789-8
- Yam, P. T., and Charron, F. (2013). Signaling mechanisms of non-conventional axon guidance cues: the Shh, BMP and Wnt morphogens. *Curr. Opin. Neurobiol.* 23, 965–973. doi: 10.1016/j.conb.2013.09.002
- Yamagata, M., and Sanes, J. R. (2008). Dscam and Sidekick proteins direct lamina-specific synaptic connections in vertebrate retina. *Nature* 451, 465–469. doi: 10.1038/nature06469
- Yamagata, M., and Sanes, J. R. (2012). Expanding the Ig superfamily code for laminar specificity in retina: expression and role of contactins. *J. Neurosci.* 32, 14402–14414. doi: 10.1523/JNEUROSCI.3193-12.2012
- Yamagata, M., and Sanes, J. R. (2019). Expression and roles of the immunoglobulin superfamily recognition molecule sidekick1 in mouse retina. *Front. Mol. Neurosci.* 11:485. doi: 10.3389/fnmol.2018.00485
- Yamagata, M., Weiner, J. A., and Sanes, J. R. (2002). Sidekicks: synaptic adhesion molecules that promote lamina-specific connectivity in the retina. *Cell* 110, 649–660. doi: 10.1016/s0092-8674(02)00910-8
- Yamagishi, S., Hampel, F., Hata, K., Del Toro, D., Schwark, M., Kvachnina, E., et al. (2011). FLRT2 and FLRT3 act as repulsive guidance cues for Unc5-positive neurons. *EMBO J.* 30, 2920–2933. doi: 10.1038/emboj.2011.189
- Yogev, S., and Shen, K. (2014). Cellular and molecular mechanisms of synaptic specificity. *Annu. Rev. Cell. Dev. Biol.* 30, 417–437. doi: 10.1146/annurev-cellbio-100913-012953
- Zhan, X. L., Clemens, J. C., Neves, G., Hattori, D., Flanagan, J. J., Hummel, T., et al. (2004). Analysis of Dscam diversity in regulating axon guidance in *Drosophila* mushroom bodies. *Neuron* 43, 673–686. doi: 10.1016/j.neuron.2004.07.020

Conflict of Interest: The authors declare that the research was conducted in the absence of any commercial or financial relationships that could be construed as a potential conflict of interest.

Publisher's Note: All claims expressed in this article are solely those of the authors and do not necessarily represent those of their affiliated organizations, or those of the publisher, the editors and the reviewers. Any product that may be evaluated in this article, or claim that may be made by its manufacturer, is not guaranteed or endorsed by the publisher.

Copyright © 2022 Moreland and Poulain. This is an open-access article distributed under the terms of the Creative Commons Attribution License (CC BY). The use, distribution or reproduction in other forums is permitted, provided the original author(s) and the copyright owner(s) are credited and that the original publication in this journal is cited, in accordance with accepted academic practice. No use, distribution or reproduction is permitted which does not comply with these terms.



Role of Teneurin C-Terminal Associated Peptides (TCAP) on Intercellular Adhesion and Communication

Thomas L. Dodsworth and David A. Lovejoy*

Department of Cell and Systems Biology, University of Toronto, Toronto, ON, Canada

OPEN ACCESS

Edited by:

Robert Hindges,
King's College London,
United Kingdom

Reviewed by:

Richard P. Tucker,
University of California, Davis,
United States
Uwe Drescher,
King's College London,
United Kingdom

*Correspondence:

David A. Lovejoy
david.lovejoy@utoronto.ca

Specialty section:

This article was submitted to
Neurodevelopment,
a section of the journal
Frontiers in Neuroscience

Received: 02 February 2022

Accepted: 17 March 2022

Published: 02 May 2022

Citation:

Dodsworth TL and Lovejoy DA
(2022) Role of Teneurin C-Terminal
Associated Peptides (TCAP) on
Intercellular Adhesion
and Communication.
Front. Neurosci. 16:868541.
doi: 10.3389/fnins.2022.868541

The teneurin C-terminal associated peptides (TCAP) are encoded by the terminal exon of all metazoan teneurin genes. Evidence supports the liberation of a soluble TCAP peptide either by proteolytic cleavage from the mature transmembrane teneurin protein or by a separately transcribed mRNA. Synthetic versions of TCAP, based on its genomic structure, are efficacious at regulating intercellular communication by promoting neurite outgrowth and increasing dendritic spine density *in vitro* and *in vivo* in rodent models. This is achieved through cytoskeletal re-arrangement and metabolic upregulation. The putative receptors for TCAPs are the latrophilin (LPHN) family of adhesion G-protein coupled receptors, which facilitate TCAP's actions through G-proteins associated with cAMP and calcium-regulating signalling pathways. The teneurin/TCAP and latrophilin genes are phylogenetically ancient, likely serving primitive functions in cell adhesion and energy regulation which have been since adapted for a more complex role in synaptogenesis in vertebrate nervous systems.

Keywords: peptides, GPCR, energy, latrophilin, evolution, calcium, cytoskeleton, brain

INTRODUCTION TO THE TENEURIN C-TERMINAL ASSOCIATED PEPTIDES (TCAPs)

The teneurin C-terminal associated peptides (TCAPs) were initially discovered in a screen of a rainbow trout hypothalamic cDNA library for genes related to the corticotropin releasing factor (CRF) family. In this study, Qian et al. (2004) used a hamster urocortin cDNA probe to identify a neuropeptide-like region representing the C-terminal 40 amino acids of rainbow trout teneurin-3, named in accordance with its placement in this gene. Vertebrates have four paralogous forms of this 40–41 amino acid peptide, with each paralogue found at the C-terminus of one of the teneurin genes, hence their nomenclature as TCAPs 1–4. The teneurins were initially identified in a screen for proteins related to the tenascins and were named based on their high expression in the central nervous system (CNS; Baumgartner et al., 1994; review: Baumgartner and Wides, 2019). Teneurins possess a functional importance in development and maintenance of the nervous system. Homophilic and heterophilic teneurin interactions mediate process outgrowth, cell adhesion and synaptic organization in both vertebrates and invertebrates (reviews: Mosca, 2015; Tucker, 2018).

Some paralogues have specific functions: for example, teneurin-3 is important for neuronal wiring in the developing visual system and hippocampus (Young and Leamey, 2009; Berns et al., 2018). The teneurins possess many functional domains within their extracellular C-terminal region which will not be discussed in detail here, as we will primarily focus on the function on the TCAP region and its ability to modulate neuronal connectivity.

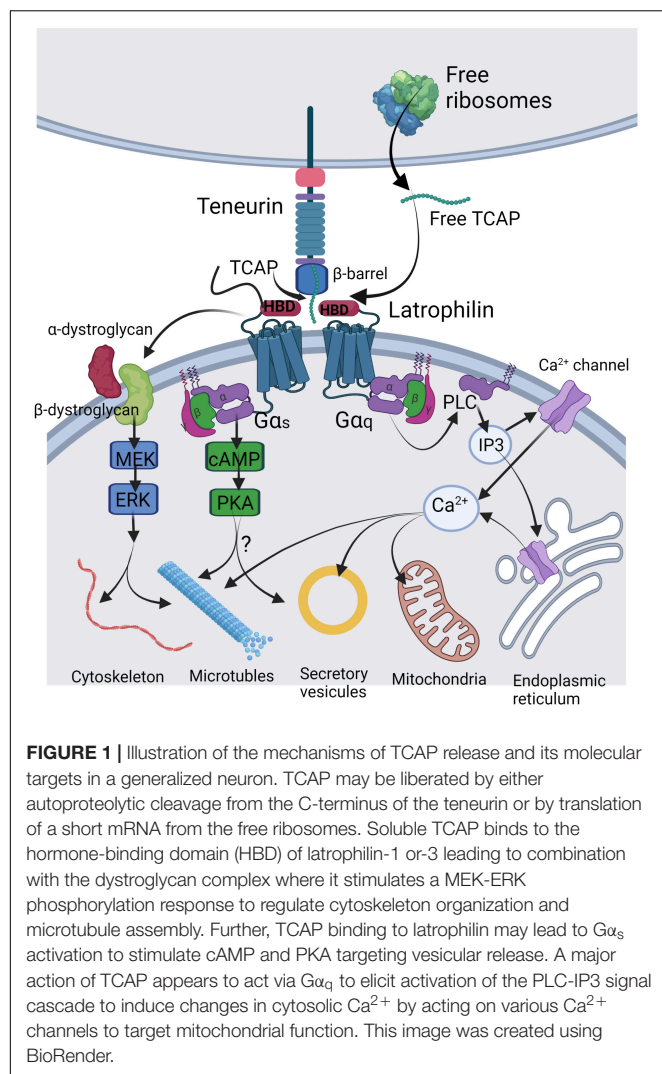
The TCAP sequence is located within the terminal exon of the teneurin mRNA and is flanked by a prohormone convertase (PC)-like cleavage signal at the 5' end and a glycine-lysine-arginine (GKR) amidation motif at the 3' end which precedes the stop codon and subsequent 3' untranslated region (Qian et al., 2004; Wang et al., 2005). Additional basic/dibasic cleavage sites are located further upstream of TCAP, but only some are conserved (Chand et al., 2013). These conserved cleavage sites indicate that TCAPs may be cleaved from teneurin and act on receptors in an autocrine or paracrine manner (Chand et al., 2013). Based on the criteria outlined by Seidah and Chrétien (1997), the translated portion of the terminal exon of mouse teneurin-1 possesses five potential sites for cleavage by prohormone convertases, where three of these sites are conserved across all teneurins (Chand et al., 2013). TCAP is exteriorly oriented when teneurin is folded, and therefore the exposed helix at the N-terminus of TCAP could be accessed by proteases (Jackson et al., 2018; Li et al., 2018). There is also evidence that some TCAP paralogues may be functionally processed as an individual peptide through separate transcription and translation (Chand et al., 2013). *In situ* hybridization experiments have revealed some differences between the expression of TCAP-1 and teneurin-1 in the rodent brain; specifically, TCAP-1 has high expression in the diencephalon and limbic system, whereas teneurin-1 does not (Zhou et al., 2003; Wang et al., 2005). Similarly, immunocytochemical labelling has shown distinct cellular localization of teneurin-1 and TCAP-1 in mouse hippocampal E14 cells, where both co-localize on the plasma membrane, but TCAP-1 labelling alone is detected diffusely in the cytosol (Chand et al., 2013). Northern blot studies suggest that the terminal exons of teneurin-1 and 3, which contain TCAP-1 and 3, can be transcribed independently from their full-length teneurin genes (Chand et al., 2013). Using 5' rapid amplification of cDNA ends polymerase chain reaction (5'RACE PCR), a 485-base pair transcript that contains TCAP-1 was isolated from whole mouse brain RNA. The separate TCAP-1 mRNA produces a 13-kDa propeptide when hypothetically translated from the first ATG signal. In fact, Chand et al. (2013) did identify a 13-kDa TCAP-1-immunoreactive band by Western blot, but it is unclear if this band is the product of TCAP-1 mRNA translation or the product of teneurin cleavage at one of the prohormone convertase motifs. Regardless, the putative translation product of the TCAP-1 mRNA does not code for a signal peptide, which could explain the diffuse immunoreactivity of TCAP-1 in E14 cells as the propeptide would be translated by free ribosomes and remain in the cytosol. This contrasts with the teneurin-derived form, which enters the secretory pathway and becomes associated with the extracellular face of the plasma membrane due to the type II orientation of the teneurin protein. Given the distinction in cellular localizations, a separately transcribed form

of TCAP-1 may have physiological functions that are distinct from the teneurin-1-derived form.

The three-dimensional structure of human (Li et al., 2018) and chicken (Jackson et al., 2018), teneurin-2 reveals that the extracellular region of teneurin possesses a unique bacteria "Tc" toxin-like organization. Bacterial Tc toxins are comprised of three proteins (A, B, C) where the "A" protein allows binding to target cells and the "B" and "C" proteins form a shell that protects the carboxy-terminal toxic component from the host (Busby et al., 2013). In typical fashion for such toxins, the teneurin extracellular domain contains prokaryotic-like YD repeats that form a spiralling "Barrel" domain made of up β -hairpins which act as a shell for a hydrophobic core (Jackson et al., 2018; Li et al., 2018). Unlike Tc toxins, where the toxin payload is protected in this shell, the C-terminal 120 amino acids of teneurin exit through a gap in the wall of the Barrel domain; this exposed "toxin-like" or "Tox-GHH" domain is therefore accessible for protein-protein interactions. Structurally, TCAP appears to be part of the toxin-like domain, occupying the distal part of an α -helical DNA-binding region at its N-terminus and forming a β -hairpin loop structure at its C-terminus, where unwinding of the helix could allow proteases to access and release soluble forms of TCAP (Jackson et al., 2018; Li et al., 2018; **Figure 1**).

CELLULAR- AND ORGANISMAL-LEVEL ACTIONS OF TENEURIN C-TERMINAL ASSOCIATED PEPTIDES IN THE NERVOUS SYSTEM

Given evidence that the teneurin C-terminal region may be processed as a soluble peptide, synthetic forms of TCAP have been thoroughly probed for bioactivity at the cellular and organismal levels. Synthetic TCAP-1 has been shown to regulate cytoskeletal architecture in both immortalized and primary neuronal cell culture models. In N38 mouse immortalized hypothalamic cells, TCAP-1 treatment elicited increased process length but fewer processes per cell as well as increased β -actin and β -tubulin protein expression (Al Chawaf et al., 2007a). Similar increases in actin polymerization, expression of α -tubulin and β -tubulin, and process formation and length were observed in hippocampal E14 cells (Chand et al., 2012). TCAP-1 co-localizes with β -dystroglycan on the cell surface of E14 cells and may induce cytoskeletal rearrangement through the dystroglycan-associated mitogen-activated protein kinase-extracellular signal-regulated kinase 1/2 (MEK-ERK 1/2) pathway, leading to phosphorylation of stathmin at serine-25 and filamin A at serine-2152 to modulate microtubule formation and actin polymerization, respectively (Chand et al., 2012; **Figure 1**). *In vivo*, TCAP-1 treatment increased dendritic spine density in the CA1 and CA3 regions of the rat hippocampus (Tan et al., 2011). Together, these results indicate that TCAP-1 regulates neuronal function in a manner that modulates contacts between neurons through rearrangement of cytoskeletal elements. TCAP-1 also possesses neuroprotective actions, as it reduced alkalosis-associated necrotic cell death in N38 cells



by upregulating expression of Cu-Zn superoxide dismutase 1 (SOD1) and catalase enzymes (Trubiani et al., 2007).

Teneurin C-terminal associated peptides provides sufficient cellular energy for actin and tubulin rearrangement in neurons through actions on metabolism (Hogg et al., 2018). *In vivo* studies in rats showed that TCAP-1 increased uptake of ^{18}F -deoxyglucose in the frontal cortex and subcortical regions of the brain, which coincided with a decrease in serum glucose levels. Increased glucose uptake was also observed *in vitro* in TCAP-1-treated N38 cells, along with increased translocation of GLUT3 (the primary glucose transporter in the brain) to the plasma membrane, likely through activation of the phosphoinositide-3 kinase-protein kinase B (AKT) pathway and/or the MEK-ERK 1/2 pathway. TCAP-1 also increased intracellular ATP concentrations and decreased intracellular pyruvate and lactate concentrations in N38 cells, indicating that glucose metabolism through aerobic pathways was also upregulated.

These cellular-level changes offer a possible mechanistic explanation for the ability of TCAP-1 to modulate stress- and anxiety-related behaviours in rodents. TCAP-1-treated rats with

high baseline emotionality (i.e., stress-sensitive) experienced a decrease in their acoustic startle response, a measure of their innate anxiety, whereas rats with low baseline emotionality (i.e., stress-insensitive) showed an increase, suggesting that TCAP-1 has a normalizing effect on anxiety (Wang et al., 2005). In elevated plus-maze experiments, another behavioural test for anxiety, TCAP-1-treated rats spent less time in the open arms, whereas rats treated with TCAP-1 and the stress-inducing hormone, corticotropin-releasing factor (CRF), showed a decrease in stretch-attend posture compared to those treated with CRF alone (Al Chawaf et al., 2007b; Tan et al., 2011) indicating again that TCAP treatment regulated anxiety in rodents. Similarly, TCAP-1 treatment significantly reduced CRF-induced expression of *c-Fos* in rat brain regions associated with anxiety (Tan et al., 2009). These results indicate that TCAP-1 may attenuate stress through functional antagonism of CRF actions.

INVOLVEMENT OF TENEURIN C-TERMINAL ASSOCIATED PEPTIDES IN INTERCELLULAR ADHESION VIA THE TENEURIN-LATROPHILIN TRANS-SYNAPTIC COMPLEX

Given its homology to CRF, TCAP was initially hypothesized to act as an antagonist on one or both of the CRF receptors (CRF-Rs) or another member of the Secretin family of G-protein coupled receptors (GPCRs) (see Qian et al., 2004; Wang et al., 2005). However, no such interactions have been reported to date. Although TCAP-1 co-localizes with β -dystroglycan, there is no direct evidence of a ligand-receptor interaction between the two molecules, indicating their co-localization may be part of a larger complex (Chand et al., 2012). More recently, the latrophilin (LPHN) family of Adhesion GPCRs, which are known *trans*-synaptic binding partners with the teneurins, have been identified as putative receptors for the TCAPs based on molecular evidence of their interaction. We therefore posit that soluble TCAP's ability to modulate neuronal connectivity via cytoskeletal modulation occurs at least in part through latrophilin-associated G-protein signalling.

The latrophilins are members of the Adhesion family of GPCRs – a relatively unexplored class of GPCRs with unusually large extracellular domains that possess adhesive properties (review: Bjarnadóttir et al., 2007). Latrophilins were initially discovered as proteins with high affinity for α -latrotoxin, which is the main vertebrate-affecting neurotoxin in black widow spider (*Latrodectus tredecimguttatus*) venom (Frontali et al., 1976). The structure of latrophilin is typical of Adhesion GPCRs: they are type I-oriented with 7 looping transmembrane regions, a long N-terminal extracellular domain, and a shorter C-terminal cytoplasmic tail. In vertebrates, the extracellular region possesses several domains functional in cell adhesion, including a lectin-like domain (LEC) and an olfactomedin-like domain (OLF), which are involved in binding ligands such as the neurexins and fibronectin-like domain-containing leucine-rich transmembrane proteins (FLRTs; reviews:

Silva and Ushkaryov, 2010; Meza-Aguilar and Boucard, 2014). Proximal to the cell membrane, the latrophilins possess a hormone-binding domain (HBD) which shares homology with CRF receptors and other Secretin family GPCRs, and is among several domains required for binding of α -latrotoxin (Holz and Habener, 1998; Krasnoperov et al., 1997, 1999; Ushkaryov et al., 2008). Intracellularly, the latrophilins interact with a variety of heterotrimeric G-proteins. Using α -latrotoxin affinity chromatography, LPHN-1 co-purified with G_{α_o} and G_{α_q} subunits *in vitro* (Rahman et al., 1999). Stimulation of LPHN-1-over-expressing cells with α -latrotoxin led to increased cAMP and inositol 1,4,5-triphosphate (IP_3) production, where treatment with a phospholipase C (PLC) inhibitor eliminated α -latrotoxin-induced vesicular exocytosis (Lelianova et al., 1997; Davletov et al., 1998). Similarly, simian COS-7 cells overexpressing mouse LPHN-2 and certain splice variants of LPHN-3 experienced increases in IP_1 , the terminal metabolite of IP_3 , when stimulated with its self-derived “*Stachel*” peptide (Röthe et al., 2019). This indicates a functional role for the $G_{q/11}$ -protein signalling system, where intracellular calcium release from the endoplasmic reticulum evokes vesicular exocytosis characteristic of α -latrotoxin bioactivity (Lelianova et al., 1997). The $G_{i/o}$, G_s and $G_{12/13}$ families may also be involved in some contexts, as functional associations have been shown between human LPHN-1 and G_i or $G_{12/13}$, between *C. elegans* LPHN-1 and G_{α_s} , and between a pancreas-specific splice variant of LPHN-3 and G_i (Müller et al., 2015; Nazarko et al., 2018; Röthe et al., 2019).

The first evidence for the existence of a teneurin-latrophilin ligand-receptor interaction was established by Silva et al. (2011), where teneurin-2 expressed on post-synaptic dendritic branches bound to LPHN-1 expressed on pre-synaptic nerve terminals to form a *trans*-synaptic complex. Similar *trans*-cellular interactions were observed between teneurins-2 and 4 and all three latrophilins (Boucard et al., 2014) and between teneurin-1 and LPHN-3 (O’Sullivan et al., 2014). The LEC domain alone is sufficient for latrophilins to bind teneurins, but the interaction is strengthened by the OLF domain, and an alternative splice site between the LEC and OLF domains directly regulates latrophilin’s ability to bind to teneurins but not other ligands (O’Sullivan et al., 2012, 2014; Boucard et al., 2014; Meza-Aguilar and Boucard, 2014). There is some disagreement over which domains of the teneurins are involved in latrophilin binding. The initial study by Silva et al. (2011) found that Nb2a neuroblastoma cells over-expressing a C-terminal splice variant of teneurin-2 (which contains TCAP-2), named “Lasso,” heterophilically co-localized with cells over-expressing LPHN-1. In agreement with this, a truncated version of teneurin-2 which does not contain the C-terminal toxin-like domain was unable to bind to the LPHN-1 or 3 LEC domains (Li et al., 2018). More recent modelling of the trimeric teneurin-latrophilin-FLRT *trans*-synaptic complex by X-ray crystallography (del Toro et al., 2020) and cryo-EM (Li et al., 2020) suggest that the LPHN-2 and 3 LEC domains bind to the face of the teneurin-2 Barrel domain which is opposite to the TCAP-containing toxin-like region, such that the LEC and toxin-like regions are arranged in parallel but are separated by the Barrel domain. In the model by Li et al. (2018),

the teneurin-2 toxin-like region was located approximately 6 nm away from the latrophilin-2 LEC binding surface. If the toxin-like region is in fact unnecessary for direct binding to latrophilin while associated with the full-length teneurin, perhaps cleavage at one of the accessible prohormone convertase sites allows for subsequent binding of a soluble C-terminal fragment to another domain within the latrophilin extracellular region. The teneurin-latrophilin *trans*-synaptic pairing via the YD-Barrel/LEC interaction would therefore ensure that any cleaved C-terminal fragment is in close proximity for diffusion to its putative receptive domain within the latrophilin extracellular region, and would explain evidence of downstream G-protein signalling upon treatment of cells over-expressing latrophilin with either Lasso or TCAPs (Silva et al., 2011; Vysokov et al., 2018; Husić et al., 2019). In agreement with this, Lasso triggers an increase in cytosolic calcium in cells over-expressing LPHN-1 and in pre-synaptic nerve terminals of hippocampal cells, which increased the rate of neurotransmitter exocytosis in a manner similar to α -latrotoxin (Silva et al., 2011; Vysokov et al., 2018).

Taken together these data suggest that, like α -latrotoxin, Lasso signals through $G_{q/11}$, and this agonist activity has been implicated in axonal pathfinding in the developing hippocampus (review: Ushkaryov et al., 2019). Similarly, latrophilins may act as receptors for free soluble TCAPs. Human embryonic kidney 293 (HEK 293) cells over-expressing LPHN-1 demonstrate significantly higher co-localization with fluorescently tagged recombinant TCAP-1 compared to wild-type cells, as well as greater cytoskeletal remodelling in response to TCAP-1 (Husić et al., 2019). Given latrophilin’s homology to the CRF-Rs, we posit that the latrophilin HBD is responsible for TCAP binding. Cells transfected with a mutated LPHN-1 construct that does not contain the HBD showed minimal co-localization with TCAP-1, and TCAP-1 co-immunoprecipitated with isolated HBD constructs *in vitro* (Husić et al., 2019). Like α -latrotoxin and Lasso, TCAP-1 may utilize the $G_{q/11}$ signalling pathway. However, since TCAP-1 has also been shown to modulate intracellular cAMP, so $G_{i/o}$ and G_s could also be involved (Qian et al., 2004; Wang et al., 2005). Given that there are 4 isoforms of TCAP in vertebrates and 3 of LPHN, and numerous splice variants and some interspecies variation within these genes, there are many possible combinations of TCAP-latrophilin interactions which could account for TCAP’s diverse actions.

EVOLUTION OF CELL ADHESION VIA THE TENEURIN/TENEURIN C-TERMINAL ASSOCIATED PEPTIDES-LATROPHILIN COMPLEX

The teneurins and TCAPs are evolutionarily ancient and conserved across metazoans. The teneurin genes likely evolved through the horizontal gene transfer (HGT) of a polymorphic proteinaceous toxin (PPT) gene from an aquatic prokaryote to a choanoflagellate, which is a unicellular ancestor to metazoans (Tucker et al., 2012; Zhang et al., 2012). Functionally, the

ancestral teneurin gene may have assisted choanoflagellates in food acquisition, given the adhesive properties of the teneurin extracellular domains (Tucker et al., 2012; Tucker, 2018). Moreover, the presence of 4 teneurin genes in vertebrates supports the “2R” hypothesis, which postulates that 2 genome duplication events occurred during the course of vertebrate evolution (Ohno, 1970; see review: Lovejoy et al., 2006). Like much of the C-terminal region of teneurin, TCAP appears to have a prokaryotic origin and possibly represents an inactive form of the toxin payload from a PPT (Chand et al., 2013). TCAP also shares homology with (but evolutionarily predates) the CRFs, calcitonins and Secretin family peptides, and has approximately 20% sequence similarity with α -latrotoxin (Lovejoy et al., 2006; Michalec et al., 2020). Thus, the ancestral toxin-like gene acquired by HGT could have given rise to all of these peptides. We postulate that in early metazoans, CRF-like and TCAP-like genes worked antagonistically as a rudimentary stress and metabolism control system. This is supported by findings in the chordate species, vase tunicate (*Ciona intestinalis*), where CRF/diuretic hormone-like peptide and TCAP oppositely modulated feeding behaviours (D'Aquila et al., 2017).

The latrophilins are similarly omnipresent in the metazoans, indicating that like the teneurins, they were acquired early in evolutionary history. Upon discovery, latrophilins were initially classified as Secretin family GPCRs due to their possession of an HBD, but they have since been re-classified as members of the Adhesion family (Leliana et al., 1997). Evolutionarily, the Adhesion family of GPCRs are among the oldest GPCRs, even appearing in unicellular fungi, though the extracellular adhesive domains associated with latrophilins such as the LEC, OLF and HBD evolved later (Krishnan et al., 2012; Schöneberg and Prömel, 2019). The latrophilin OLF domain is found only in the vertebrate lineage, and while some modern invertebrates possess LEC and HBD, they are poorly conserved, so it remains uncertain if early metazoan latrophilins would be capable of *trans*-cellular interactions with teneurins on their own, and instead may rely on interactions through a complex with other adhesion proteins (Woelfle et al., 2015; Schöneberg and Prömel, 2019). Interestingly, the Adhesion GPCRs precede the Secretin GPCRs, and comparably, TCAP is a predecessor to the peptide family that

binds to Secretin GPCRs (Lovejoy et al., 2006; Nordström et al., 2009). Thus, the ancestral teneurin/TCAP and latrophilins genes could have given rise to many of the peptide signalling systems present in modern organisms.

Given the evolutionarily ancient history of the teneurins, TCAPs, and latrophilins, there is a high probability that this protein system is functional in a number of tissues across the metazoans. Since early organisms possessing these genes did not have complex nervous systems, there were likely some other evolutionary advantages independent from the described modern role in neuronal cell adhesion. The adhesive properties of both teneurins and latrophilins could assist in development of non-neuronal tissues that require precise organization and structure. Furthermore, the conserved energy regulatory actions of TCAP would be particularly advantageous in tissues that have high energy demands, such as those involved in locomotion.

CONCLUSION

The teneurin-latrophilin *trans*-synaptic pair represents an evolutionarily ancient mechanism for cell adhesion that has been co-opted for neuronal wiring among the vertebrates. At the molecular level, the most recent modelling suggest that the TCAP region does not directly bind to latrophilin while still affiliated with the full-length teneurin protein, but soluble TCAP either cleaved from teneurin or separately transcribed may have a functional role in latrophilin signalling through interaction with the hormone binding domain (Husić et al., 2019; del Toro et al., 2020; Li et al., 2020). There is a clear functionality for soluble TCAP in modulating neuronal contacting in culture, which offers a likely cellular-level explanation for its ability to modulates stress- and anxiety-related behaviours *in vivo*.

AUTHOR CONTRIBUTIONS

TD wrote the drafts of the manuscript. DL oversaw the completion of the final version. Both authors contributed to the article and approved the submitted version.

REFERENCES

- Al Chawaf, A., St. Amant, K., Belsham, D., and Lovejoy, D. A. (2007a). Regulation of neurite growth in immortalized mouse hypothalamic neurons and rat hippocampal primary cultures by teneurin C-terminal associated peptide-1. *Neuroscience* 144, 1241–1254. doi: 10.1016/j.neuroscience.2006.09.062
- Al Chawaf, A., Xu, K., Tan, L., Vaccarino, F. J., Lovejoy, D. A., and Rotzinger, S. (2007b). Cotricotropin-releasing factor (CRF)-induced behaviours are modulated by intravenous administration of teneurin C-terminal associated peptide-1 (TCAP-1). *Peptides* 28, 1406–1415. doi: 10.1016/j.peptides.2007.05.014
- Baumgartner, S., Martin, D., Hagios, C., and Chiquet-Ehrismann, R. (1994). Tenm, a *Drosophila* gene related to tenascin is a new pair-rule gene. *EMBO J.* 13, 3728–3740. doi: 10.1002/j.1460-2075.1994.tb06682.x
- Baumgartner, S., and Wides, R. (2019). Discovery of Teneurins. *Front. Neurosci.* 13:230. doi: 10.3389/fnins.2019.00230
- Berns, D. S., DeNardo, L. A., Pederick, D. T., and Luo, L. (2018). Teneurin-3 controls topographic circuit assembly in the hippocampus. *Nature* 554, 328–333. doi: 10.1038/nature25463
- Bjarnadóttir, T. K., Fredriksson, R., and Schiöth, H. B. (2007). The *Adhesion* GPCRs: a unique family of G protein-coupled receptors with important roles in both central and peripheral tissues. *Cell. Mol. Life Sci.* 64, 2104–2119. doi: 10.1007/s00018-007-7067-1
- Boucard, A. A., Maxeiner, S., and Südhof, T. C. (2014). Latrophilins function as heterophilic cell-adhesion molecules by binding to teneurins: regulation by alternative splicing. *J. Biol. Chem.* 289, 389–402. doi: 10.1074/jbc.M113.504779
- Busby, J. N., Panjikar, S., Landsberg, M. J., Hurst, M. R., and Lott, J. S. (2013). The BC component of ABC toxins is an RHS-repeat-containing protein encapsulation device. *Nature* 501, 547–550. doi: 10.1038/nature12465
- Chand, D., Cassati, C. A., de Lannoy, L., Song, L., Kollara, A., Barsyte-Lovejoy, D., et al. (2013). C-terminal processing of the teneurin proteins: independent actions of a teneurin C-terminal associated peptide in hippocampal cells. *Mol. Cell. Neurosci.* 52, 38–50. doi: 10.1016/j.mcn.2012.09.006

- Chand, D., Song, L., de Lannoy, L., Barsyte-Lovejoy, D., Ackloo, S., Boutros, P. C., et al. (2012). C-terminal region of teneurin-1 co-localizes with dystroglycan and modulates cytoskeletal organization through an extracellular signal-regulated kinase-dependent stathmin- and filamin A-mediated mechanism in hippocampal cells. *Neuroscience* 219, 255–270. doi: 10.1016/j.neuroscience.2012.05.069
- D'Aquila, A. L., Hsieh, A. H.-R., Hsieh, A. H.-M., De Almeida, R., Lovejoy, S. R., and Lovejoy, D. A. (2017). Expression and actions of corticotropin-releasing factor/diuretic hormone-like peptide (CDLP) and teneurin C-terminal associated peptide (TCAP) in the vase tunicate, *Ciona intestinalis*: Antagonism of the feeding response. *Gen. Comp. Endocrinol.* 246, 105–115. doi: 10.1016/j.ygcen.2016.06.015
- Davletov, B. A., Meunier, F. A., Ashton, A. C., Matsushita, H., Hirst, W. D., and Lelanova, V. G. (1998). Vesicle exocytosis stimulated by alpha-latrotoxin is mediated by latrophilin and requires both external and stored Ca^{2+} . *EMBO J.* 17, 3909–3920.
- del Toro, D., Carrasquero-Ordaz, M. A., Chu, A., Ruff, T., Shahin, M., Jackson, V. A., et al. (2020). Structural basis of teneurin-latrophilin interaction in repulsive guidance of migrating neurons. *Cell* 180, 323–339.e19. doi: 10.1016/j.cell.2019.12.014
- Frontali, N., Ceccarelli, B., Gorio, A., Mauro, A., Siekevitz, P., Tzeng, M. C., et al. (1976). Purification from black widow spider venom of a protein factor causing the depletion of synaptic vesicles at neuromuscular junctions. *J. Cell Biol.* 68, 462–479. doi: 10.1083/jcb.68.3.462
- Hogg, D. W., Chen, Y., D'Aquila, A. L., Xu, M., Husic, M., Tan, L. A., et al. (2018). A novel role of the corticotropin-releasing hormone (CRH) regulating peptide, teneurin-1 C-terminal associated peptide (TCAP-1), on glucose uptake into the brain. *J. Neuroendocrinol.* 30:e12579. doi: 10.1111/jne.12579
- Holz, G. G., and Habener, J. F. (1998). Black widow spider α -latrotoxin: a presynaptic neurotoxin that shares structural homology with the glucagon-like peptide-1 family of insulin secretagogic hormones. *Comp. Biochem. Phys. B* 121, 177–184. doi: 10.1016/s0305-0491(98)10088-3
- Husić, M., Barsyte-Lovejoy, D., and Lovejoy, D. A. (2019). Teneurin C-terminal associated peptide (TCAP)-1 and latrophilin interaction in HEK293 cells: evidence for modulation of intracellular adhesion. *Front. Endocrinol.* 10:22. doi: 10.3389/fendo.2019.00022
- Jackson, V. A., Meijer, D. H., Carrasquero, M., van Bezouwen, L. S., Lowe, E. D., Kleanthous, C., et al. (2018). Structures of Teneurin adhesion receptors reveal an ancient fold for cell-cell interaction. *Nat Commun.* 9:1079. doi: 10.1038/s41467-018-03460-0
- Krasnoperov, V. G., Bittner, M. A., Beavis, R., Kuang, Y., Salnikow, K. V., Chepurny, O. G., et al. (1997). Alpha-latrotoxin stimulates exocytosis by the interaction with a neuronal G-protein-coupled receptor. *Neuron* 18, 925–937. doi: 10.1016/s0896-6273(00)80332-3
- Krasnoperov, V. G., Bittner, M. A., Holz, R. W., Chepurny, O., and Petrenko, A. G. (1999). Structural requirements for alpha-latrotoxin binding and alpha-latrotoxin-stimulated secretion. A study with calcium-independent receptor of alpha-latrotoxin (CIRL) deletion mutants. *J. Biol. Chem.* 274, 3590–3596. doi: 10.1074/jbc.274.6.3590
- Krishnan, A., Almén, M. S., Fredriksson, R., and Schiöth, H. B. (2012). The origin of GPCRs: identification of mammalian like Rhodopsin, Adhesion, Glutamate, and Frizzled GPCRs in fungi. *PLoS One* 7:e29817. doi: 10.1371/journal.pone.0029817
- Lelanova, V. G., Davletov, B. A., Sterling, A., Atiqur Rahman, M., Grishin, E. V., Totty, N. F., et al. (1997). α -latrotoxin receptor, latrophilin, is a novel member of the secretin family of G protein-coupled receptors. *J. Biol. Chem.* 272, 21504–21508. doi: 10.1074/jbc.272.34.21504
- Li, J., Shalev-Benami, M., Sando, R., Jiang, X., Kibrom, A., Wang, J., et al. (2018). Structural basis for teneurin function in circuit-wiring: a toxin motif at the synapse. *Cell* 173, 735–748. doi: 10.1016/j.cell.2018.03.036
- Li, J., Xie, Y., Cornelius, S., Jiang, X., Sando, R., Kordon, S. P., et al. (2020). Alternative splicing controls teneurin-latrophilin interaction and synapse specificity by a shape-shifting mechanism. *Nat Commun.* 11:2140. doi: 10.1038/s41467-020-16029-7
- Lovejoy, D. A., Al Chawaf, A., and Alia Cadinouche, M. Z. (2006). Teneurin C-terminal associated peptides: An enigmatic family of neuropeptides with structural similarity to the corticotropin releasing factor and calcitonin families of peptides. *Gen. Comp. Endocrinol.* 148, 299–305. doi: 10.1016/j.ygcen.2006.01.012
- Meza-Aguilar, D. G., and Boucard, A. A. (2014). Latrophilins updated. *Biomol. Concepts* 5, 457–478. doi: 10.1515/bmc-2014-0032
- Michalec, O. M., Chang, B. S. W., Lovejoy, N. R., and Lovejoy, D. A. (2020). Corticotropin-releasing factor: an ancient peptide family related to the secretin peptide superfamily. *Front. Endocrinol.* 11:529. doi: 10.3389/fendo.2020.00529
- Mosca, T. J. (2015). On the Teneurin track: a new synaptic organization molecule emerges. *Front Cell Neurosci.* 9:204. doi: 10.3389/fncel.2015.00204
- Müller, A., Winkler, J., Fiedler, F., Sastradihardja, T., Binder, C., Schnabel, R., et al. (2015). Oriented cell division in the *C. elegans* embryo is coordinated by G-protein signaling dependent on the Adhesion GPCR LAT-1. *PLoS Genet.* 11:e1005624. doi: 10.1371/journal.pgen.1005624
- Nazarko, O., Kibrom, A., Winkler, J., Leon, K., Stoveken, H., Salzman, G., et al. (2018). A comprehensive mutagenesis screen of the Adhesion GPCR Latrophilin-1/ADGRL1. *iScience* 3, 264–278. doi: 10.1016/j.isci.2018.04.019
- Nordström, K. J., Lagerström, M. C., Walleir, L. M., Fredriksson, R., and Schiöth, H. B. (2009). The Secretin GPCRs descended from the family of adhesion GPCRs. *Mol. Biol. Evol.* 26, 71–84. doi: 10.1093/molbev/msn228
- Ohno, S. (1970). *Evolution by Gene Duplication*. Berlin: Springer. doi: 10.1007/978-3-642-86659-3
- O'Sullivan, M. L., de Wit, J., Savas, J. N., Comoletti, D., Otto-Hitt, S., Yates, J. R., et al. (2012). Postsynaptic FLRT proteins are endogenous ligands for the black widow spider venom receptor Latrophilin and regulate excitatory synapse development. *Neuron* 73, 903–910. doi: 10.1016/j.neuron.2012.01.018
- O'Sullivan, M. L., Martini, F., von Daake, S., Comoletti, D., and Ghosh, A. (2014). LPHN3, a presynaptic adhesion-GPCR implicated in ADHD, regulates the strength of neocortical layer 2/3 synaptic input to layer 5. *Neural Dev.* 9:7. doi: 10.1186/1749-8104-9-7
- Qian, X., Barsyte-Lovejoy, D., Wang, L., Chewpoy, B., Gautam, N., Al Chawaf, A., et al. (2004). Cloning and characterization of teneurin C-terminus associated peptide (TCAP)-3 from the hypothalamus of an adult rainbow trout (*Oncorhynchus mykiss*). *Gen. Comp. Endocrinol.* 137, 205–216. doi: 10.1016/j.ygcen.2004.02.007
- Rahman, M. A., Ashton, A. C., Meunier, F., Davletov, B. A., Dolly, J. O., and Ushkaryov, Y. A. (1999). Norepinephrine exocytosis stimulated by alpha-latrotoxin requires both external and stored calcium, and is mediated by latrophilin, G proteins and phospholipase C. *Philos. Trans. R. Soc. Lond. B* 354, 379–386. doi: 10.1098/rstb.1999.0390
- Röthe, J., Thor, R., Winkler, J., Knierim, A. B., Binder, C., Huth, S., et al. (2019). Involvement of the adhesion GPCRs latrophilins in the regulation of insulin release. *Cell Rep.* 26, 1537–1584. doi: 10.1016/j.celrep.2019.01.040
- Schöneberg, T., and Prömel, S. (2019). Latrophilins and Teneurins in invertebrates: No love for each other? *Front. Neurosci.* 13:154. doi: 10.3389/fnins.2019.00154
- Seidah, N. G., and Chrétien, M. (1997). Eukaryotic protein processing: endoproteolysis of precursor proteins. *Curr. Opin. Biotechnol.* 8, 602–607. doi: 10.1016/s0958-1669(97)80036-5
- Silva, J. P., Lelanova, V. G., Ermolyuk, Y. S., Vysokov, N., Hitchen, P. G., Berninghausen, O., et al. (2011). Latrophilin 1 and its endogenous ligand Lasso/teneurin-2 form a high-affinity transsynaptic receptor pair with signaling capabilities. *Proc. Natl. Acad. Sci. U.S.A.* 108, 12113–12118. doi: 10.1073/pnas.1019434108
- Silva, J. P., and Ushkaryov, Y. A. (2010). The latrophilins, “split-personality” receptors. *Adv. Exp. Med. Biol.* 706, 59–75. doi: 10.1007/978-1-4419-7913-1_5
- Tan, L. A., Al Chawaf, A., Vaccarino, F. J., Boutros, P. C., and Lovejoy, D. A. (2011). Teneurin C-terminal associated peptide (TCAP)-1 modulates dendritic morphology in hippocampal neurons and decreases anxiety-like behaviours in rats. *Physiol. Behav.* 104, 199–204. doi: 10.1016/j.physbeh.2011.03.015
- Tan, L. A., Xu, K., Vaccarino, F. J., Lovejoy, D. A., and Rotzinger, S. (2009). Teneurin C-terminal associated peptide (TCAP)-1 attenuates corticotropin-releasing factor (CRF)-induced c-Fos expression in the limbic system and modulates anxiety behaviour in male Wistar rats. *Behav. Brain Res.* 201, 198–206. doi: 10.1016/j.bbr.2009.02.013
- Trubiani, G., Al Chawaf, A., Belsham, D. D., Barsyte-Lovejoy, D., and Lovejoy, D. A. (2007). Teneurin carboxy (C)-terminal associated peptide-1 inhibits alkalosis-associated necrotic neuronal death by stimulating superoxide dismutase and catalase activity in immortalized mouse hypothalamic cells. *Brain Res.* 1176, 27–36. doi: 10.1016/j.brainres.2007.07.087

- Tucker, R. P. (2018). Teneurins: domain architecture, evolutionary origins and patterns of expression. *Front. Neurosci.* 12:938. doi: 10.3389/fnins.2018.00938
- Tucker, R. P., Beckmann, J., Leachman, N. T., Schöler, J., and Chiquet-Ehrismann, R. (2012). Phylogenetic analysis of the teneurins: conserved features and premetazoan ancestry. *Mol. Biol. Evol.* 29, 1019–1029.
- Ushkaryov, Y. A., Lelianova, V., and Vysokov, N. V. (2019). Catching Latrophilin with Lasso: a universal mechanism for axonal attraction and synapse formation. *Front. Neurosci.* 13:257. doi: 10.3389/fnins.2019.00257
- Ushkaryov, Y. A., Rohou, A., and Sugita, S. (2008). Alpha-Latrotoxin and its receptors. *Handb. Exp. Pharmacol.* 184, 171–206. doi: 10.1007/978-3-540-74805-2_7
- Vysokov, N. V., Silva, J.-P., Lelianova, V. G., Suckling, J., Cassidy, J., Blackburn, J. K., et al. (2018). Proteolytically released Lasso/teneurin-2 induces axonal attraction by interacting with latrophilin-1 on axonal growth cones. *eLife* 7:e37935. doi: 10.7554/eLife.37935
- Wang, L., Rotzinger, S., Barsyte-Lovejoy, D., Qian, X., Elias, C. F., Bittencourt, J. C., et al. (2005). Teneurin proteins possess a carboxy terminal corticotropin-releasing factor-like sequence that modulates emotionality and neuronal growth. *Mol. Brain Res.* 133, 253–265.
- Woelfle, R., D'Aquila, A. D., Pavlovic, T., Husić, M., and Lovejoy, D. A. (2015). Ancient interaction between the teneurin C-terminal associated peptides (TCAP) and Latrophilin ligand-receptor coupling: a role in behaviour. *Front. Neurosci.* 9:146. doi: 10.3389/fnins.2015.00146
- Young, T. R., and Leamey, C. A. (2009). Teneurins: important regulators of neural circuitry. *Int. J. Biochem. Cell Biol.* 41, 990–993.
- Zhang, D., de Souza, R. F., Anantharaman, V., Iyer, L. M., and Aravind, L. (2012). Polymorphic toxin systems: comprehensive characterization of trafficking modes, processing, mechanisms of action, immunity and ecology using comparative genomics. *Biol. Direct* 25:18.
- Zhou, X. H., Brandau, O., Feng, K., Oohashi, T., Ninomiya, Y., Rauch, U., et al. (2003). The murine *Ten-m/Odz* genes show distinct but overlapping expression patterns during development and in adult brain. *Gene Expr. Patterns* 3, 397–405.

Conflict of Interest: The authors declare that the research was conducted in the absence of any commercial or financial relationships that could be construed as a potential conflict of interest.

Publisher's Note: All claims expressed in this article are solely those of the authors and do not necessarily represent those of their affiliated organizations, or those of the publisher, the editors and the reviewers. Any product that may be evaluated in this article, or claim that may be made by its manufacturer, is not guaranteed or endorsed by the publisher.

Copyright © 2022 Dodsworth and Lovejoy. This is an open-access article distributed under the terms of the Creative Commons Attribution License (CC BY). The use, distribution or reproduction in other forums is permitted, provided the original author(s) and the copyright owner(s) are credited and that the original publication in this journal is cited, in accordance with accepted academic practice. No use, distribution or reproduction is permitted which does not comply with these terms.



Spatiotemporal Control of Neuronal Remodeling by Cell Adhesion Molecules: Insights From *Drosophila*

Hagar Meltzer^{1,2*} and Oren Schuldiner^{1,2*}

¹ Department of Molecular Cell Biology, Weizmann Institute of Science, Rehovot, Israel, ² Department of Molecular Neuroscience, Weizmann Institute of Science, Rehovot, Israel

OPEN ACCESS

Edited by:

Zsolt Lele,
Institute of Experimental Medicine,
Hungary

Reviewed by:

Heather Brohier,
Case Western Reserve University,
United States

*Correspondence:

Hagar Meltzer
hagar.meltzer@weizmann.ac.il
Oren Schuldiner
oren.schuldiner@weizmann.ac.il

Specialty section:

This article was submitted to
Neurodevelopment,
a section of the journal
Frontiers in Neuroscience

Received: 16 March 2022

Accepted: 22 April 2022

Published: 12 May 2022

Citation:

Meltzer H and Schuldiner O
(2022) Spatiotemporal Control
of Neuronal Remodeling by Cell
Adhesion Molecules: Insights From
Drosophila.
Front. Neurosci. 16:897706.
doi: 10.3389/fnins.2022.897706

Developmental neuronal remodeling is required for shaping the precise connectivity of the mature nervous system. Remodeling involves pruning of exuberant neural connections, often followed by regrowth of adult-specific ones, as a strategy to refine neural circuits. Errors in remodeling are associated with neurodevelopmental disorders such as schizophrenia and autism. Despite its fundamental nature, our understanding of the mechanisms governing neuronal remodeling is far from complete. Specifically, how precise spatiotemporal control of remodeling and rewiring is achieved is largely unknown. In recent years, cell adhesion molecules (CAMs), and other cell surface and secreted proteins of various families, have been implicated in processes of neurite pruning and wiring specificity during circuit reassembly. Here, we review some of the known as well as speculated roles of CAMs in these processes, highlighting recent advances in uncovering spatiotemporal aspects of regulation. Our focus is on the fruit fly *Drosophila*, which is emerging as a powerful model in the field, due to the extensive, well-characterized and stereotypic remodeling events occurring throughout its nervous system during metamorphosis, combined with the wide and constantly growing toolkit to identify CAM binding and resulting cellular interactions *in vivo*. We believe that its many advantages pose *Drosophila* as a leading candidate for future breakthroughs in the field of neuronal remodeling in general, and spatiotemporal control by CAMs specifically.

Keywords: pruning, cell adhesion molecules, *Drosophila*, neuronal remodeling, wiring and pruning, IgSF

INTRODUCTION

Following their initial establishment, developing neural circuits are further refined by a combination of degenerative and regenerative events. Collectively known as developmental neuronal remodeling, such processes are essential for shaping the connectivity of functional circuits, and represent a conserved strategy occurring throughout the animal kingdom and across the peripheral and central nervous systems. Remodeling varies in scale, from retraction of single synapses, up to degeneration of long stretches of axons or dendrites, often with remarkable spatiotemporal precision. Regressive steps are generally followed by progressive ones including stabilization and even reformation of new, adult-specific connections (Luo and O'Leary, 2005; Riccomagno and Kolodkin, 2015; Schuldiner and Yaron, 2015; Yaniv and Schuldiner, 2016). Defects in the normal progression of remodeling have been implicated in various neurodevelopmental and neuropsychiatric conditions, such as schizophrenia, autism spectrum disorder and Alzheimer's disease (Cocchi et al., 2016; Hong et al., 2016; Sekar et al., 2016; Thomas et al., 2016).

Despite constant progress, the molecular mechanisms underlying remodeling, and specifically its spatiotemporal control, remain poorly understood.

In recent years, it is becoming increasingly evident that neuronal remodeling is not solely governed by intrinsic genetic programs and cell-autonomous mechanisms (reviewed in Riccomagno and Kolodkin, 2015; Schuldiner and Yaron, 2015; Rumpf et al., 2019), but is also highly dependent on interactions with the environment – whether other neurons, non-neuronal cells or the extracellular matrix (Meltzer and Schuldiner, 2020). Moreover, recent studies have highlighted the importance of orchestrated circuit remodeling, in which different neuronal types in a given network simultaneously remodel in an interdependent manner (Mayseless et al., 2018; Lee and Doe, 2021). Due to their location on plasma membranes, cell adhesion molecules (CAMs) are prime candidates to mediate cell–cell interactions during coordinated circuit assembly and remodeling. Indeed, during initial steps of circuit formation, such as axon pathfinding and fasciculation, the role of CAMs, and other cell surface and secreted proteins (CSSPs), is relatively established (e.g., Dickson, 2002; Pollerberg et al., 2013). However, much less is known about the function of CAMs in regulating the spatiotemporal precision of developmental remodeling. Arguably, circuit reassembly during remodeling, occurring at late developmental stages, in larger neurons and for specific neuronal components, provides an excellent opportunity to deduce about similar mechanisms of initial circuit formation, which is less experimentally accessible at least in part due to its spatiotemporally “dense” nature.

Here, we explore recent advances in uncovering how CAMs and other CSSPs shape neuronal remodeling – including both neurite pruning and subsequent regrowth – in the fruit fly, *Drosophila melanogaster* (notably, for the sake of simplicity, the term “CAMs” is loosely used hereafter, as in some cases it refers to CSSPs of families generally known to be associated with adhesion, even when an adhesive role was not directly established). Of course, focusing on *Drosophila* does not underestimate the significant contributions of research in mammalian models, mostly to understanding the roles of CAMs in synapse retraction/stabilization (reviewed in Duncan et al., 2021). However, we believe that *Drosophila* holds major advantages that position it as an ideal model for substantial progress in the field. First, as a holometabolous insect, its entire nervous system is dramatically and stereotypically reorganized during metamorphosis. Indeed, many of its central and peripheral circuits undergo remodeling, and these are often well-characterized in terms of anatomy, development, and function (Yu and Schuldiner, 2014; Yaniv and Schuldiner, 2016). Second, and more importantly, *Drosophila* offers a particularly wide, and continuously expanding, arsenal of cutting-edge tools and techniques. Most pronounced is the ability to genetically access and perturb almost every neuronal type, but more recent advances in genomic tools, and in delineating protein interaction networks (“interactomes”; e.g., Ozkan et al., 2013), combined with the virtually complete EM-based connectome data of the fly brain (Scheffer et al., 2020), are now providing solid ground for delving into the

mechanisms underlying neuronal remodeling and (re)wiring at up to subcellular resolution. Finally, relevant genes and pathways are largely conserved, and many important mammalian neuronal CSSPs have orthologs, or were even originally discovered, in *Drosophila*. Furthermore, neurodevelopmental processes, such as the molecular mechanisms of axon guidance and target selection, as well as neural organizational principles, such as the logical flow in the olfactory system, show striking similarity between flies and mammals (Komiyama and Luo, 2006; Reichert, 2009; Gonda et al., 2020; Li F. et al., 2020; Malin and Desplan, 2021). Thus, insights and principles obtained in *Drosophila* are likely to be relevant to similar processes in higher organisms.

TRANSCRIPTION OF CELL ADHESION MOLECULES IS HIGHLY DYNAMIC DURING DEVELOPMENT

Cell adhesion molecules that are required in specific locations at distinct time-windows could potentially have different or even deleterious effects if expressed in ectopic locations or developmental stages. Thus, precise CAM expression, in the right place and time, must be tightly regulated. Recent advances in high-throughput RNA-sequencing technologies provided the opportunity to map the transcriptional profiles of developing neurons (Alyagor et al., 2018; McLaughlin et al., 2021; Ozel et al., 2021; Xie et al., 2021; Janssens et al., 2022), thus revealing the temporally dynamic expression of CAMs and other CSSPs.

The *Drosophila* mushroom body (MB) is a well-characterized circuit in the fly brain that is comprised of three types of intrinsic neurons, known as Kenyon cells (KCs), which are sequentially born from the same neuroblasts. The first-born KCs – called γ -KCs – undergo stereotypic remodeling during metamorphosis, in which they prune their dendrites completely, and their bifurcated axons up to their branchpoint. Later during the pupal stage, γ -KCs regrow their dendrites, and their axons to form adult-specific projections (Lee et al., 1999; Yaniv and Schuldiner, 2016; **Figure 1**). γ -KCs were recently sequenced at unprecedented temporal resolution, including every 3 hours during early pupal development (Alyagor et al., 2018). This γ -KC transcriptional atlas revealed the extremely dynamic nature of gene expression in general, and CAMs/CSSPs specifically, along development. In fact, the transcriptional landscape of adult γ -KCs resembles the landscape of other adult neurons more than that of γ -KCs during pupal development. A follow-up study, which focused on the genetic program of γ -axon regrowth, highlighted the dynamic expression of Immunoglobulin Superfamily (IgSF) proteins (Bornstein et al., 2021). Moreover, IgSFs were enriched among genes whose expression changed upon inhibition of regrowth. Among IgSFs, the expression of proteins of the Defective in proboscis extension response (Dpr) family was especially striking, as 16 out of the 21 family members are expressed in γ -KCs in temporally dynamic patterns. Dpr12, for example, is downregulated at the onset of metamorphosis (prior to pruning) but is later gradually upregulated, in a timeframe suitable for γ axon regrowth. Indeed, while Dpr12 was found to be redundant for axon pruning, it is critical for the subsequent

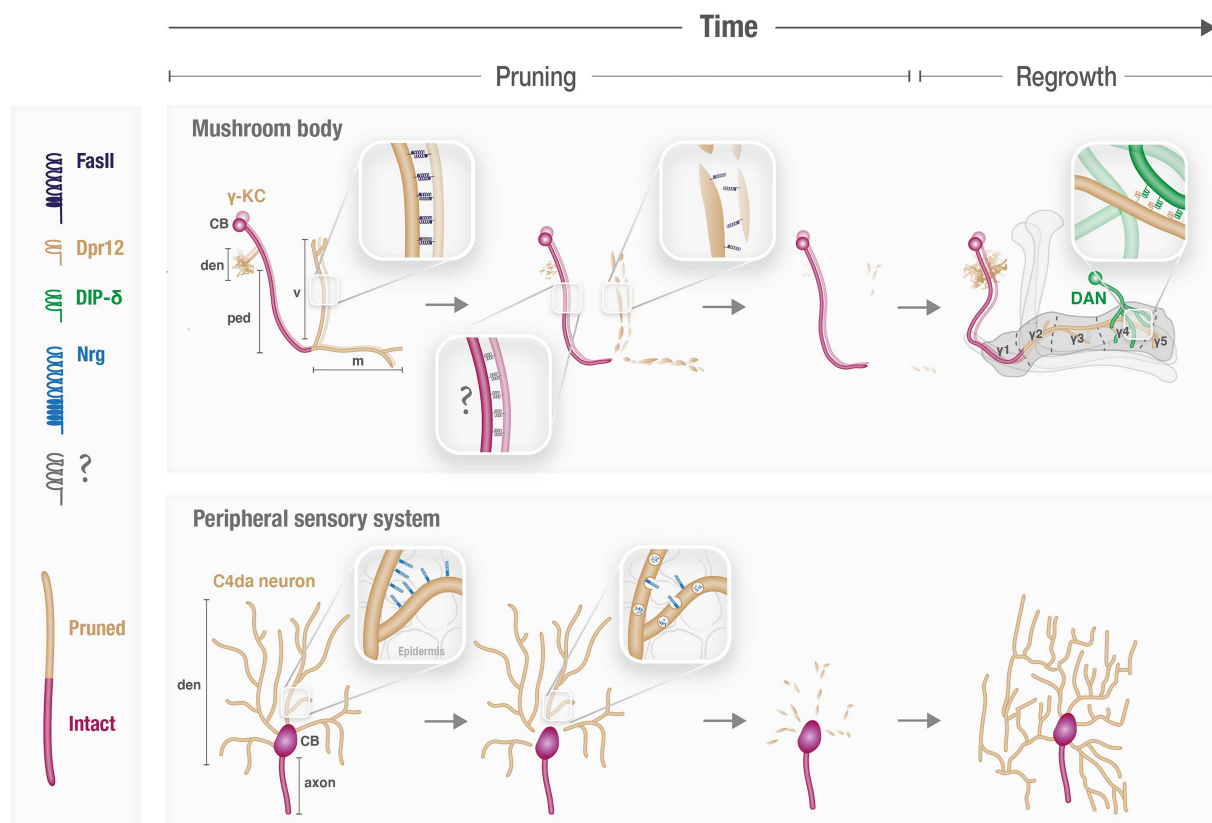


FIGURE 1 | Cell adhesion molecules participate in spatiotemporal control of neuronal remodeling. Schematic illustration of the known and speculated roles of CAMs during pruning and regrowth of the γ -Kenyon cells (KCs) in the mushroom body (MB) and peripheral sensory Class 4 (C4) da neurons. CB, cell body; den, dendrites; ped, axon peduncle; v and m, vertical and medial axonal branches, respectively.

phase of γ -KC remodeling – in which axons regrow to occupy the full extent of the γ -lobe (Bornstein et al., 2021). Thus, this study demonstrates how temporally resolved transcriptional datasets can be translated to analyses of protein function (see also later). Interestingly, several other Dprs are upregulated in time points that precede γ -axon pruning (Alyagor et al., 2018), suggesting members of the Dpr family play yet undiscovered roles in the pruning process, and not only during axon regrowth.

Other studies focused on revealing the transcriptomes of developing neurons in the *Drosophila* olfactory sensory circuit. In this system, olfactory sensory neurons (OSNs) expressing the same odorant receptor converge onto one of ~50 discrete glomeruli in the antennal lobe – a structure analogous to the mammalian olfactory bulb – where they synapse with a single class of projection neurons in each glomerulus (PNs, which correlate to mammalian mitral cells and relay sensory information to higher brain centers). It was previously shown that embryonic-born PNs participate in both the larval and adult olfactory circuits, in which they innervate different glomeruli. Developmental studies indicate that during metamorphosis, PNs undergo local pruning of their dendritic and axonal terminal branches, followed by re-extension of adult projections. In contrast, larval-born PNs, which constitute the majority of PN types, only participate in the adult circuitry and do not remodel

(Jefferis et al., 2002; Marin et al., 2005). CAMs of different families were shown to play key roles in determining wiring specificity in antennal lobe, by confining and segregating PN dendritic fields within specific glomeruli, as well as dictating PN-ORN synaptic matching (Hong and Luo, 2014). Recently, single-cell RNA sequencing of PNs was performed at four developmental stages (early/mid/late pupae and adult; Xie et al., 2021). Among the genes that were differentially expressed in all stages, CSSPs and transcription factors were the two most over-represented groups of proteins. CSSPs included many molecules that were previously implicated in neural wiring, such as Dprs, Dscam and Fasciclins. Interestingly, in the early pupal stage, PNs formed two distinct clusters, with the smaller cluster representing embryonically born PNs. Thus, the fact that these neurons undergo remodeling indeed reflects in significant transcriptomic changes, but how this correlates with CSSP expression is yet to be analyzed. Another recent study, which profiled the single-cell transcriptome of developing OSNs (McLaughlin et al., 2021), also revealed over-representation of CSSPs. Comparison of the PN/OSN datasets highlighted CSSPs that are broadly expressed in both, while others that are enriched in either OSNs or PNs. Uncovering PN/OSN ligand/receptor candidates should promote understanding not only of how their precise matching is achieved, but also of how OSNs facilitate refinement of PN

dendrites following their glomeruli occupation, as was recently demonstrated by time-lapse imaging (Li et al., 2021).

Taken together, genomic and genetic studies in developing fly neurons imply that the full spectrum of functions played by CAMs/CSSPs during neural circuit pruning and (re)wiring are just beginning to be unraveled.

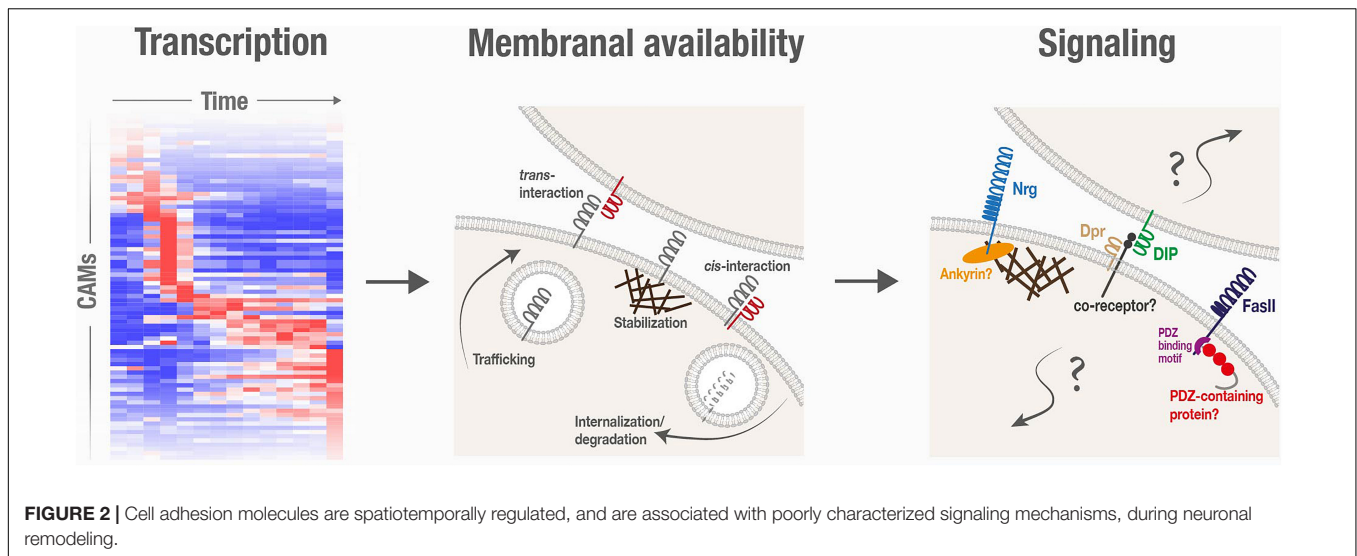
THE MEMBRANAL AVAILABILITY OF CELL ADHESION MOLECULES IS SPATIOTEMPORALLY REGULATED DURING REMODELING

Following transcription, the abundance and binding availability of CAMs on plasma membranes can be further regulated *via* cellular processes that affect delivery to the membrane (such as trafficking and exocytosis), stabilization within the membrane (such as interactions with the cytoskeleton) and, finally, removal from the membrane (such as endocytosis and degradation; **Figure 2**). Here we will describe some regulated alterations in membranal CAM expression that were shown to underlie spatiotemporal specificity of neurite pruning and circuit reformation.

Reducing the membranal abundance of CAMs is a key step in the remodeling of *Drosophila* sensory dendritic arborization (da) neurons, which extend highly branched dendrites along the body wall. Proper dendritic coverage during the initial elaboration of da dendrites requires self-avoidance and tiling mechanisms which are both mediated by CAMs (including Dscam and integrins; Matthews et al., 2007; Han et al., 2012; Kim et al., 2012). During metamorphosis, da neurons of two classes (I and IV) prune their larval dendritic arbors by local fragmentation, while their axons remain intact, and later regrow adult-specific dendritic arbors (Yu and Schuldiner, 2014; **Figure 1**). Downregulation of Neuroglian (Nrg), the sole homolog of L1-type CAMs in *Drosophila*, was found to be required for dendrite pruning of class IV da neurons (Zhang et al., 2014; **Figure 1**). Nrg downregulation occurs *via* endocytosis, as evident by its redistribution from the plasma membrane to endosomal compartments at the onset of pruning. Accordingly, overexpression of Nrg within da neurons is sufficient to inhibit their pruning, while its loss leads to precocious pruning (i.e., at an earlier time point). This indicates that the temporal specificity of dendrite pruning is dictated, at least in part, by precise timing of Nrg internalization. Interestingly, while Nrg is expressed, and internalized to endosomes, in both axons and dendrites, its loss selectively affects dendrites, and does not “force” ectopic pruning of axons. Therefore, the mechanism underlying compartment-specific pruning, and whether and how it relates to Nrg, remains unclear. Perhaps Nrg downregulation renders da neurons more susceptible to pruning by reducing their adhesion – most likely to the epidermis – and another, Nrg-independent mechanism protects axons from a similar fate. Since its identification, many additional regulators of Nrg endocytosis-mediated pruning have been uncovered, including members of the secretory pathway, protein trafficking, and endo-lysosomal degradation (Wang et al.,

2017, 2018; Zong et al., 2018; Kramer et al., 2019; Rui et al., 2020). However, while this machinery must be tightly regulated in time to ensure stereotypic pruning of da dendrites, how this is achieved is unclear. Notably, the binding partner of Nrg in this context, and the potential cellular interactions it mediates, remain to be identified. It is thus possible that spatiotemporal cues for pruning are contributed by the interacting cells, such as epidermal cells, which are known to engulf pruned debris, or glia, shown to be tightly associated with da dendrites near their proximal severing sites (Han et al., 2011). Interestingly, Nrg-mediated interactions were also shown to be required for synaptic stability in the developing fly neuromuscular junction (NMJ), as Nrg loss results in increased synapse pruning (Enneking et al., 2013). Furthermore, Nrg was implicated in the remodeling of the *Drosophila* Giant Fiber (GF) circuitry, which exhibits pruning of extraneous axonal branches during the pupal stage (Borgen et al., 2017). In this system, Nrg was shown to be retrogradely transported from GF terminals in an Amyloid Precursor Protein-like (APPL)-dependent manner (Kudumala et al., 2017; Penserga et al., 2019). APPL mutants exhibit pruning defects of GF transient branches, thus implying a potential role for Nrg in GF pruning, although this was not directly tested. Interestingly, mammalian L1-type CAMs, including NrCAM and CHL1, were implicated in adolescent spine pruning in mouse genetic models. However, unlike with *Drosophila* Nrg, NrCAM/CHL1 absence actually results in increased spine density (i.e., decreased pruning), as their interactions induce intracellular signals that eventually lead to spine collapse (Demyanenko et al., 2014; Mohan et al., 2019a,b). The underlying cause of these seemingly opposite outcomes, perhaps stemming from differences in the balance between adhesive and signaling functions, is yet to be resolved.

Downregulation of membranal CAM levels is also crucial during MB remodeling, in which γ axons must be defasciculated at the onset of metamorphosis to prune (Bornstein et al., 2015; **Figure 1**). This destabilization is achieved *via* c-Jun N-terminal Kinase (JNK)-mediated reduction in the membranal levels of the IgSF CAM Fascilin II (FasII), the ortholog of the mammalian neural cell adhesion molecule (NCAM). While trafficking was ruled out as the major regulator of FasII membranal levels, whether FasII downregulation also occurs *via* endocytosis, or by an alternative destabilizing mechanism, is unknown. Mutating JNK, or overexpressing FasII, is sufficient to inhibit pruning of γ axons, but not dendrites. Moreover, overexpressing other CAMs has a similar effect, suggesting that increased axo-axonal adhesion, in general, prevents normal progression of pruning. Manipulations of JNK or FasII are the first case of selective regulation of axon vs. dendrite pruning. Interestingly, endogenous FasII is indeed only expressed in γ axons and excluded from dendrites and cell bodies, which could, in theory, account for the observed phenotype of JNK mutants. However, even strong transgenic FasII overexpression, which was also localized to dendrites, did not inhibit dendrite pruning (Bornstein et al., 2015). Thus, the differential subcellular distribution of endogenous FasII within γ -KCs cannot alone account for the axon-specific pruning defect, and the full mechanism underlying its different effects on dendrites and



axons remains undetermined. One option is that it stems from anatomical constraints, since γ dendrites are not tightly fasciculated as the axons. However, one cannot rule out the contribution of additional factors, such as potential involvement of other cell populations (neurons or glia) that occupy the axonal but not dendritic area, or vice versa. Notably, the fact that γ -axon pruning accurately stops at the axonal branchpoint and does not extend into the axonal peduncle (**Figure 1**) also remains unexplained. The involvement of neighboring cells, and/or another CAM type that maintains its membranal expression in the peduncle, are interesting directions for future investigation.

Another mechanism for plasma-membrane stabilization could be *via trans*-interactions with neighboring cells. The MB circuitry includes, in addition to KCs, input neurons (mostly PNs), output neurons (MBONs), and modulatory neurons that are mostly dopaminergic (DANs). MBONs and DANs innervate the KC lobes in a compartmentalized fashion thus dividing the MB lobes to discrete and functionally relevant sub-axonal zones (Tanaka et al., 2008; Aso et al., 2014; **Figure 1**). Finer examination of the Dpr12 regrowth phenotype (see previous section) revealed a specific lack of the γ 4/5 zones. Dprs form an elaborate network of interactions – presumed to be adhesive in nature – with Dpr interacting proteins (DIPs; Carrillo et al., 2015; Cosmanescu et al., 2018). Indeed, Dpr12 was found to interact with DIP- δ , expressed in a sub-population of DANs (Bornstein et al., 2021), to mediate γ 4/5 zone formation. GFP-fusion proteins indicate that both DIP- δ and Dpr12 are localized to the γ 4/5 zones. Remarkably, misexpressing DIP- δ in DANs that target the γ 3 zone leads to ectopic localization of Dpr12 in the γ 3 zone within γ -KCs. Conversely, loss of DIP- δ resulted in diffuse Dpr12 mislocalization (Bornstein et al., 2021). This suggests that the subcellular membranal localization of Dpr12 along the γ -KC axon is instructed and/or stabilized by its transneuronal interactions with DIP- δ in neighboring DANs. Similar mechanisms for differential subcellular distribution along

the membrane might also be employed by other CAMs and in other neurodevelopmental contexts.

Finally, once on the plasma membrane, binding availability is another potential layer for regulation. Interestingly, the growing body of transcriptomics and proteomics datasets of developing neurons highlight cases in which known CAMs and their interacting proteins are expressed within the same neurons. For example, in the γ -KCs, cognate Dpr/DIP pairs are expressed in overlapping temporal patterns (Bornstein et al., 2021), suggesting that they co-exist on the same membrane. Co-expression, and potentially consequent binding in *cis*, might inhibit *trans* interactions with adjacent cells, a phenomenon known as *cis*-inhibition. Alternatively, *cis* binding can induce an intracellular signaling response, i.e., *cis*-activation. *Cis*-interactions were reported for several CSSPs, including Notch and its receptors, Ephrins/Eph receptors and Semaphorins/Plexins (del Alamo et al., 2011; Nandagopal et al., 2019; Rozbesky et al., 2020; Cecchini and Cornelison, 2021), and are important for developmental processes such as tissue patterning. Whether *cis*-interactions occur and play a role in neuronal remodeling is currently unknown and warrants further investigations.

SIGNALING PATHWAYS ASSOCIATED WITH CELL ADHESION MOLECULES DURING REMODELING ARE INCOMPLETELY UNDERSTOOD

A major unresolved question in the context of CAMs in neuronal remodeling is how does signaling fit into the picture? Beyond their roles in forming and stabilizing cell–cell adhesive structures, CAMs often propagate signal transduction, regulating crucial cellular responses such as cytoskeletal dynamics, cell polarity, and transcription activation (e.g., Cavallaro and Dejana, 2011). Various findings strongly imply that CAM-triggered signaling events are also central to neuronal remodeling in *Drosophila*, but their precise nature is mostly obscure (**Figure 2**).

Fascilin II downregulation was shown to be required for pruning of γ -KCs, but the mechanism by which JNK negatively regulates its membranal stability/residence is unclear. Interestingly, the c-terminal PDZ binding sequence of FasII – known to mediate interactions with cytoplasmic PDZ-containing scaffold proteins – was found to be crucial for the JNK-FasII regulation (Bornstein et al., 2015). While it was shown that JNK is unlikely to directly phosphorylate FasII, it is possible that it phosphorylates the PDZ-containing protein, but its identity remains to be revealed. NCAM, the mammalian ortholog of FasII, was shown to be important for pruning of excess perisomatic synapses during postnatal development of the prefrontal cortex. In this case, the suggested mechanism involves a complex interplay with Ephrins/Eph receptors and signaling by Rho-associated protein kinase (Brenneman et al., 2013; Sullivan et al., 2016). It remains to be determined if similar molecular players in *Drosophila* participate in FasII-mediated signaling during MB axon pruning.

Cell adhesion molecule-associated signaling seems to also be important in later steps of MB remodeling, during axon regrowth and circuit reformation. If Dpr12/DIP- δ interactions are adhesive in nature, why do axons stop in their absence? Furthermore, in replacement experiments, while the DIP- α -Dpr6/10 interaction was sufficient to compensate for the absence of Dpr12-DIP- δ , replacing their interaction by the adhesive interactions of FasII was not (Bornstein et al., 2021). This suggests that matching pairs of the Dpr/DIP network, regardless of their specific identity, exert their function *via* signaling mechanisms that are beyond mere adhesion. Since Dpr/DIPs are either GPI-anchored or contain small intracellular domains (Cheng et al., 2019a), it is likely that co-receptors are involved in mediating downstream signaling, but the identity of these, at the moment, is a complete mystery. Elucidating the mechanisms of Dpr/DIP interactions can potentially also shed light on interactions mediated by their mammalian orthologs – the five members of the IgLON family (Cheng et al., 2019b), which are also implicated in neurodevelopment, and are associated with neuropsychiatric disorders (Karis et al., 2018; Fearnley et al., 2021).

Similarly, within the developing fly NMJ, loss of Nrg results in increased synapse retraction that cannot be compensated by overexpression of FasII (which has known roles in synapse stabilization; Packard et al., 2003), implying specific Nrg-mediated signaling. In this case, the Ankyrin-binding domain of Nrg is crucial for its function in synaptic stability, suggesting a spectrin/cytoskeleton-related mechanism (Enneking et al., 2013; Weber et al., 2019). Notably, recruitment of Ankyrins to the cytoplasmic domains of L1-type CAMs as a mechanism to stabilize synapses is conserved in mammals (Duncan et al., 2021). A similar mechanism might also be associated with the function of Nrg in pruning of da dendrites. In general, while disassembly of the cytoskeleton is well-established as an early step of pruning in both invertebrate and vertebrate neurons (Watts et al., 2003; Brill et al., 2016; Rumpf et al., 2019), the significance of CAM-cytoskeleton associations in this context are yet to be fully elucidated.

Modified assays for *in vivo* proximity-labeling were recently applied in *Drosophila* pupae for cell-surface proteomic profiling of developing PNs (Li J. et al., 2020). Similar assays could be

employed in developing flies to reveal novel binding partners of specific proteins, by directly fusing the biotinylating enzyme to the endogenous protein of interest. Such assays, combined with the availability of multiple binary systems to simultaneously perturb and/or visualize distinct cell populations, should facilitate future identification and functional analysis of co-receptors and downstream effectors of signaling pathways associated with CAMs during remodeling.

DISCUSSION

Despite the fundamental significance of neuronal remodeling for the proper formation of mature neural circuits, our understanding of the mechanisms that regulate it is limited. Developments in the *Drosophila* toolkit facilitate gradual unraveling of the roles played by CAMs and other CSSPs during distinct remodeling processes, and highlight their potential contributions to timely execution, spatial precision and wiring specificity. Naturally, many open questions remain to be resolved before we can reach a comprehensive understanding of the various functions of CAMs during developmental remodeling.

A fascinating aspect in the field, which is only beginning to be unraveled, is the concurrent remodeling of different neuronal types within the same circuit. While CAMs are excellent candidates to coordinate such processes, their functions in this context are largely unknown. In the *Drosophila* MB, γ -KCs and the GABAergic anterior paired lateral (APL) neuron were shown to undergo developmental remodeling in the same timeframe. Moreover, cell-autonomous inhibition of γ -KC pruning disrupts APL pruning. This coordination relies on γ -KC activity, and Calcium/Calmodulin signaling within the APL neuron. Interestingly, artificially increasing γ -KC-to-APL adhesion by ectopically expressing FasII is sufficient to inhibit pruning of both neuronal types (Mayseless et al., 2018). Whether and how CAMs provide the spatiotemporal cues triggering orchestrated remodeling of neuronal circuits, and the regulatory interplay between CAM expression and neuronal activity in this specific context, are yet to be resolved. *Drosophila* is an ideal model to address such issues, due to its well-characterized circuits and the genetic handle to almost all cell types.

Another aspect that may revolutionize our understanding of neural network assembly is deciphering “adhesion codes” that underlie synaptic (re)wiring of complex and stereotypic circuits. In the MB, Dpr12 and DIP- δ mediate formation of the γ 4/5 axonal zones during γ -KC regrowth (Bornstein et al., 2021), but they are just one pair out the many “Dpr-ome” members that are dynamically expressed in developing γ -KCs (Alyagor et al., 2018; Bornstein et al., 2021), while many DIPs are differentially expressed in DANs and MBONs (Croset et al., 2018; Aso et al., 2019). Thus, it is tempting to speculate that other Dpr/DIP combinations instruct the formation the remaining MB axonal zones, by encoding the match between DANs, MBONs, and KCs. Dpr/DIPs were demonstrated to mediate synaptic specificity in targeting of motoneurons to muscle fibers in the developing NMJ, for specific layer targeting in the visual system, and for positioning of OSNs to specific glomeruli in the olfactory system (e.g., Barish et al., 2018; Xu et al., 2018; Ashley et al., 2019;

Menon et al., 2019). It therefore seems that similar molecular principles are employed for targeting of neurites to specific cell types/layers/structures during circuit assembly, and for specifying sub-axonal compartmentalization during circuit reassembly. Thus, studying the signaling mechanisms of Dpr/DIPs during MB circuit reassembly – occurring late in development in a genetically and visually accessible environment – provides an opportunity to also understand their function during initial circuit assembly in other neuronal systems. Moreover, Due to extensive biochemical and structural work (Cosmanescu et al., 2018; Sergeeva et al., 2020), the Dpr/DIP families also hold the promise to dissect how affinity variations between binding partners translate into their function during distinct steps of remodeling. Redundancy seems to be a complicating factor, as many of the Dpr/DIPs, as well as other IgSF CAMs (such as Beat/Sides; Li et al., 2017), can bind multiple partners. Circuit (re)formation in various *Drosophila* neuropils offers an excellent system to overcome redundancy because of the full connectome data, available single cell transcriptomic datasets, and, in the era of CRISPR, genetic ability to perturb the function of multiple genes within a single cell. The zoned structure of the MB is especially intriguing as it can be correlated with layered structures in mammals such as the cerebellum (Li F. et al., 2020).

Due to its awesome genetic power and the wide array of biochemical and imaging techniques, we strongly anticipate breakthroughs in our undertesting of the roles of CAMs in spatiotemporal control of remodeling to arise from *Drosophila*. These are likely to transform our approach to similar mechanisms of neuronal remodeling and (re)wiring in other systems and organisms, in both physiological and pathological contexts.

AUTHOR CONTRIBUTIONS

HM and OS wrote the manuscript. Both authors contributed to the article and approved the submitted version.

FUNDING

Research in our lab was funded by the Israel Science Foundation (#1890/21), DFG (FOR2705 and D83915Z), Minerva Stiftung (#714145), Volkswagen Stiftung (Lower Saxony-Israel collaboration #76251-10-10/19 ZN3459), and ERC AdvGrant (101054886 NeuRemodelBehavior).

REFERENCES

- Alyagor, I., Berkun, V., Keren-Shaul, H., Marmor-Kollet, N., David, E., Mayseless, O., et al. (2018). Combining Developmental and Perturbation-Seq Uncovers Transcriptional Modules Orchestrating Neuronal Remodeling. *Dev. Cell* 47:e36. doi: 10.1016/j.devcel.2018.09.013
- Ashley, J., Sorrentino, V., Lobb-Rabe, M., Nagarkar-Jaiswal, S., Tan, L., Xu, S., et al. (2019). Transsynaptic interactions between IgSF proteins DIP-alpha and Dpr10 are required for motor neuron targeting specificity. *Elife* 8:e42690. doi: 10.7554/eLife.42690
- Aso, Y., Hattori, D., Yu, Y., Johnston, R. M., Iyer, N. A., Ngo, T. T., et al. (2014). The neuronal architecture of the mushroom body provides a logic for associative learning. *Elife* 3:e04577. doi: 10.7554/eLife.04577
- Aso, Y., Ray, R. P., Long, X., Bushey, D., Cichewicz, K., Ngo, T. T., et al. (2019). Nitric oxide acts as a cotransmitter in a subset of dopaminergic neurons to diversify memory dynamics. *Elife* 8:e49257. doi: 10.7554/eLife.49257
- Barish, S., Nuss, S., Strunilin, I., Bao, S., Mukherjee, S., Jones, C. D., et al. (2018). Combinations of DIPs and Dprs control organization of olfactory receptor neuron terminals in *Drosophila*. *PLoS Genet.* 14:e1007560. doi: 10.1371/journal.pgen.1007560
- Borgen, M., Rowland, K., Boerner, J., Lloyd, B., Khan, A., and Murphey, R. (2017). Axon Termination, Pruning, and Synaptogenesis in the Giant Fiber System of *Drosophila melanogaster* Is Promoted by Highwire. *Genetics* 205, 1229–1245. doi: 10.1534/genetics.116.197343
- Bornstein, B., Meltzer, H., Adler, R., Alyagor, I., Berkun, V., Cummings, G., et al. (2021). Transneuronal Dpr12/DIP-delta interactions facilitate compartmentalized dopaminergic innervation of *Drosophila* mushroom body axons. *EMBO J.* 40:e105763. doi: 10.15252/embj.2020105763
- Bornstein, B., Zahavi, E. E., Gelley, S., Zoosman, M., Yaniv, S. P., Fuchs, O., et al. (2015). Developmental Axon Pruning Requires Destabilization of Cell Adhesion by JNK Signaling. *Neuron* 88, 926–940. doi: 10.1016/j.neuron.2015.10.023
- Brenneman, L. H., Zhang, X., Guan, H., Triplett, J. W., Brown, A., Demyanenko, G. P., et al. (2013). Polysialylated NCAM and ephrinA/EphA regulate synaptic development of GABAergic interneurons in prefrontal cortex. *Cereb. Cortex* 23, 162–177. doi: 10.1093/cercor/bhr392
- Brill, M. S., Kleele, T., Ruschkies, L., Wang, M., Marahori, N. A., Reuter, M. S., et al. (2016). Branch-Specific Microtubule Destabilization Mediates Axon Branch Loss during Neuromuscular Synapse Elimination. *Neuron* 92, 845–856. doi: 10.1016/j.neuron.2016.09.049
- Carrillo, R. A., Ozkan, E., Menon, K. P., Nagarkar-Jaiswal, S., Lee, P. T., Jeon, M., et al. (2015). Control of Synaptic Connectivity by a Network of *Drosophila* IgSF Cell Surface Proteins. *Cell* 163, 1770–1782. doi: 10.1016/j.cell.2015.1.022
- Cavallaro, U., and Dejana, E. (2011). Adhesion molecule signalling: not always a sticky business. *Nat. Rev. Mol. Cell Biol.* 12, 189–197. doi: 10.1038/nrm3068
- Cecchini, A., and Cornelison, D. D. W. (2021). Eph/Ephrin-Based Protein Complexes: the Importance of cis Interactions in Guiding Cellular Processes. *Front. Mol. Biosci.* 8:809364. doi: 10.3389/fmolb.2021.809364
- Cheng, S., Ashley, J., Kurlito, J. D., Lobb-Rabe, M., Park, Y. J., Carrillo, R. A., et al. (2019a). Molecular basis of synaptic specificity by immunoglobulin superfamily receptors in *Drosophila*. *Elife* 8:e41028. doi: 10.7554/eLife.41028
- Cheng, S., Park, Y., Kurlito, J. D., Jeon, M., Zinn, K., Thornton, J. W., et al. (2019b). Family of neural wiring receptors in bilaterians defined by phylogenetic, biochemical, and structural evidence. *Proc. Natl. Acad. Sci. U.S.A.* 116, 9837–9842. doi: 10.1073/pnas.1818631116
- Cocchi, E., Drago, A., and Serretti, A. (2016). Hippocampal Pruning as a New Theory of Schizophrenia Etiopathogenesis. *Mol. Neurobiol.* 53, 2065–2081. doi: 10.1007/s12035-015-9174-6
- Cosmanescu, F., Katsamba, P. S., Sergeeva, A. P., Ahlsen, G., Patel, S. D., Brewer, J. J., et al. (2018). Neuron-Subtype-Specific Expression, Interaction Affinities, and Specificity Determinants of DIP/Dpr Cell Recognition Proteins. *Neuron* 100, 1385.e6–1400.e6. doi: 10.1016/j.neuron.2018.10.046
- Croset, V., Treiber, C. D., and Waddell, S. (2018). Cellular diversity in the *Drosophila* midbrain revealed by single-cell transcriptomics. *Elife* 7:e34550. doi: 10.7554/eLife.34550
- del Alamo, D., Rouault, H., and Schweisguth, F. (2011). Mechanism and significance of cis-inhibition in Notch signalling. *Curr. Biol.* 21, R40–R47. doi: 10.1016/j.cub.2010.10.034
- Demyanenko, G. P., Mohan, V., Zhang, X., Brenneman, L. H., Dharbal, K. E., Tran, T. S., et al. (2014). Neural cell adhesion molecule NrCAM regulates Semaphorin 3F-induced dendritic spine remodeling. *J. Neurosci.* 34, 11274–11287. doi: 10.1523/JNEUROSCI.1774-14.2014

- Dickson, B. J. (2002). Molecular mechanisms of axon guidance. *Science* 298, 1959–1964. doi: 10.1126/science.1072165
- Duncan, B. W., Murphy, K. E., and Maness, P. F. (2021). Molecular Mechanisms of L1 and NCAM Adhesion Molecules in Synaptic Pruning, Plasticity, and Stabilization. *Front. Cell Dev. Biol.* 9:625340. doi: 10.3389/fcell.2021.625340
- Enneking, E. M., Kudumala, S. R., Moreno, E., Stephan, R., Boerner, J., Godenschwege, T. A., et al. (2013). Transsynaptic coordination of synaptic growth, function, and stability by the L1-type CAM Neuroglian. *PLoS Biol.* 11:e1001537. doi: 10.1371/journal.pbio.1001537
- Fearnley, S., Raja, R., and Cloutier, J. F. (2021). Spatiotemporal expression of IgLON family members in the developing mouse nervous system. *Sci. Rep.* 11:19536. doi: 10.1038/s41598-021-97768-5
- Gonda, Y., Namba, T., and Hanashima, C. (2020). Beyond Axon Guidance: roles of Slit-Robo Signaling in Neocortical Formation. *Front. Cell Dev. Biol.* 8:607415. doi: 10.3389/fcell.2020.607415
- Han, C., Jan, L. Y., and Jan, Y. N. (2011). Enhancer-driven membrane markers for analysis of nonautonomous mechanisms reveal neuron-glia interactions in *Drosophila*. *Proc. Natl. Acad. Sci. U.S.A.* 108, 9673–9678. doi: 10.1073/pnas.1106386108
- Han, C., Wang, D., Soba, P., Zhu, S., Lin, X., Jan, L. Y., et al. (2012). Integrins regulate repulsion-mediated dendritic patterning of *drosophila* sensory neurons by restricting dendrites in a 2D space. *Neuron* 73, 64–78. doi: 10.1016/j.neuron.2011.10.036
- Hong, S., Beja-Glasser, V. F., Nfonoyim, B. M., Frouin, A., Li, S., Ramakrishnan, S., et al. (2016). Complement and microglia mediate early synapse loss in Alzheimer mouse models. *Science* 352, 712–716. doi: 10.1126/science.aad8373
- Hong, W., and Luo, L. (2014). Genetic control of wiring specificity in the fly olfactory system. *Genetics* 196, 17–29. doi: 10.1534/genetics.113.154336
- Janssens, J., Aibar, S., Taskiran, I. I., Ismail, J. N., Gomez, A. E., Aughey, G., et al. (2022). Decoding gene regulation in the fly brain. *Nature* 601, 630–636. doi: 10.1038/s41586-021-04262-z
- Jefferis, G. S., Marin, E. C., Watts, R. J., and Luo, L. (2002). Development of neuronal connectivity in *Drosophila* antennal lobes and mushroom bodies. *Curr. Opin. Neurobiol.* 12, 80–86. doi: 10.1016/s0959-4388(02)00293-3
- Karis, K., Eskla, K. L., Kaare, M., Taht, K., Tuusov, J., Visnapuu, T., et al. (2018). Altered Expression Profile of IgLON Family of Neural Cell Adhesion Molecules in the Dorsolateral Prefrontal Cortex of Schizophrenic Patients. *Front. Mol. Neurosci.* 11:8. doi: 10.3389/fnmol.2018.00008
- Kim, M. E., Shrestha, B. R., Blazewski, R., Mason, C. A., and Grueber, W. B. (2012). Integrins establish dendrite-substrate relationships that promote dendritic self-avoidance and patterning in *drosophila* sensory neurons. *Neuron* 73, 79–91. doi: 10.1016/j.neuron.2011.10.033
- Komiyama, T., and Luo, L. (2006). Development of wiring specificity in the olfactory system. *Curr. Opin. Neurobiol.* 16, 67–73. doi: 10.1016/j.conb.2005.12.002
- Kramer, R., Rode, S., and Rumpf, S. (2019). Rab11 is required for neurite pruning and developmental membrane protein degradation in *Drosophila* sensory neurons. *Dev. Biol.* 451, 68–78. doi: 10.1016/j.ydbio.2019.03.003
- Kudumala, S. R., Penserga, T., Borner, J., Slipchuk, O., Kakad, P., Lee, L. H., et al. (2017). Lissencephaly-1 dependent axonal retrograde transport of L1-type CAM Neuroglian in the adult *drosophila* central nervous system. *PLoS One* 12:e0183605. doi: 10.1371/journal.pone.0183605
- Lee, K., and Doe, C. Q. (2021). A locomotor neural circuit persists and functions similarly in larvae and adult *Drosophila*. *Elife* 10:e69767. doi: 10.7554/eLife.69767
- Lee, T., Lee, A., and Luo, L. (1999). Development of the *Drosophila* mushroom bodies: sequential generation of three distinct types of neurons from a neuroblast. *Development* 126, 4065–4076. doi: 10.1242/dev.126.18.4065
- Li, F., Lindsey, J. W., Marin, E. C., Otto, N., Dreher, M., Dempsey, G., et al. (2020). The connectome of the adult *Drosophila* mushroom body provides insights into function. *Elife* 9:e62576. doi: 10.7554/eLife.62576
- Li, J., Han, S., Li, H., Udeshi, N. D., Svinkina, T., Mani, D. R., et al. (2020). Cell-Surface Proteomic Profiling in the Fly Brain Uncovers Wiring Regulators. *Cell* 180, 373.e–386.e. doi: 10.1016/j.cell.2019.12.029
- Li, H., Watson, A., Olechwie, A., Anaya, M., Sorooshyari, S. K., Harnett, D. P., et al. (2017). Deconstruction of the beaten Path-Sidestep interaction network provides insights into neuromuscular system development. *Elife* 6:e28111. doi: 10.7554/eLife.28111
- Li, T., Fu, T. M., Wong, K. K. L., Li, H., Xie, Q., Luginbuhl, D. J., et al. (2021). Cellular bases of olfactory circuit assembly revealed by systematic time-lapse imaging. *Cell* 184, 5107.e–5121.e. doi: 10.1016/j.cell.2021.08.030
- Luo, L., and O'Leary, D. D. (2005). Axon retraction and degeneration in development and disease. *Annu. Rev. Neurosci.* 28, 127–156. doi: 10.1146/annurev.neuro.28.061604.135632
- Malin, J., and Desplan, C. (2021). Neural specification, targeting, and circuit formation during visual system assembly. *Proc. Natl. Acad. Sci. U.S.A.* 118:e2101823118. doi: 10.1073/pnas.2101823118
- Marin, E. C., Watts, R. J., Tanaka, N. K., Ito, K., and Luo, L. (2005). Developmentally programmed remodeling of the *Drosophila* olfactory circuit. *Development* 132, 725–737. doi: 10.1242/dev.01614
- Matthews, B. J., Kim, M. E., Flanagan, J. J., Hattori, D., Clemens, J. C., Zipursky, S. L., et al. (2007). Dendrite self-avoidance is controlled by Dscam. *Cell* 129, 593–604. doi: 10.1016/j.cell.2007.04.013
- Mayseless, O., Berns, D. S., Yu, X. M., Riemensperger, T., Fiala, A., and Schuldiner, O. (2018). Developmental Coordination during Olfactory Circuit Remodeling in *Drosophila*. *Neuron* 99, 1204.e–1215.e. doi: 10.1016/j.neuron.2018.07.050
- McLaughlin, C. N., Brbic, M., Xie, Q., Li, T., Horns, F., Kolluru, S. S., et al. (2021). Single-cell transcriptomes of developing and adult olfactory receptor neurons in *Drosophila*. *Elife* 10:e63856. doi: 10.7554/eLife.63856
- Meltzer, H., and Schuldiner, O. (2020). With a little help from my friends: how intercellular communication shapes neuronal remodeling. *Curr. Opin. Neurobiol.* 63, 23–30. doi: 10.1016/j.conb.2020.01.018
- Menon, K. P., Kulkarni, V., Takemura, S. Y., Anaya, M., and Zinn, K. (2019). Interactions between Dpr11 and DIP-gamma control selection of amacrine neurons in *Drosophila* color vision circuits. *Elife* 8:e48935. doi: 10.7554/eLife.48935
- Mohan, V., Sullivan, C. S., Guo, J., Wade, S. D., Majumder, S., Agarwal, A., et al. (2019a). Temporal Regulation of Dendritic Spines Through NrCAM-Semaphorin3F Receptor Signaling in Developing Cortical Pyramidal Neurons. *Cereb. Cortex* 29, 963–977. doi: 10.1093/cercor/bhy004
- Mohan, V., Wade, S. D., Sullivan, C. S., Kasten, M. R., Sweetman, C., Stewart, R., et al. (2019b). Close Homolog of L1 Regulates Dendritic Spine Density in the Mouse Cerebral Cortex Through Semaphorin 3B. *J. Neurosci.* 39, 6233–6250. doi: 10.1523/JNEUROSCI.2984-18.2019
- Nandagopal, N., Santat, L. A., and Elowitz, M. B. (2019). Cis-activation in the Notch signaling pathway. *Elife* 8:e37880. doi: 10.7554/eLife.37880
- Ozel, M. N., Simon, F., Jafari, S., Holguera, I., Chen, Y. C., Benhra, N., et al. (2021). Neuronal diversity and convergence in a visual system developmental atlas. *Nature* 589, 88–95. doi: 10.1038/s41586-020-2879-3
- Ozkan, E., Carrillo, R. A., Eastman, C. L., Weiszmam, R., Waghray, D., Johnson, K. G., et al. (2013). An extracellular interactome of immunoglobulin and LRR proteins reveals receptor-ligand networks. *Cell* 154, 228–239. doi: 10.1016/j.cell.2013.06.006
- Packard, M., Mathew, D., and Budnik, V. (2003). FAST remodeling of synapses in *Drosophila*. *Curr. Opin. Neurobiol.* 13, 527–534. doi: 10.1016/j.conb.2003.09.008
- Penserga, T., Kudumala, S. R., Poulos, R., and Godenschwege, T. A. (2019). A Role for *Drosophila* Amyloid Precursor Protein in Retrograde Trafficking of L1-Type Cell Adhesion Molecule Neuroglian. *Front. Cell Neurosci.* 13:322. doi: 10.3389/fncel.2019.00322
- Pollerberg, G. E., Thelen, K., Theiss, M. O., and Hochlehnert, B. C. (2013). The role of cell adhesion molecules for navigating axons: density matters. *Mech. Dev.* 130, 359–372. doi: 10.1016/j.mod.2012.11.002
- Reichert, H. (2009). Evolutionary conservation of mechanisms for neural regionalization, proliferation and interconnection in brain development. *Biol. Lett.* 5, 112–116. doi: 10.1098/rsbl.2008.0337
- Riccomagno, M. M., and Kolodkin, A. L. (2015). Sculpting neural circuits by axon and dendrite pruning. *Annu. Rev. Cell Dev. Biol.* 31, 779–805. doi: 10.1146/annurev-cellbio-100913-013038
- Rozbesky, D., Verhagen, M. G., Karia, D., Nagy, G. N., Alvarez, L., Robinson, R. A., et al. (2020). Structural basis of semaphorin-plexin cis interaction. *EMBO J.* 39:e102926. doi: 10.15252/embj.2019102926

- Rui, M., Bu, S., Chew, L. Y., Wang, Q., and Yu, F. (2020). The membrane protein Raw regulates dendrite pruning via the secretory pathway. *Development* 147:e37880. doi: 10.1242/dev.191155
- Rumpf, S., Wolterhoff, N., and Herzmann, S. (2019). Functions of Microtubule Disassembly during Neurite Pruning. *Trends Cell Biol.* 29, 291–297. doi: 10.1016/j.tcb.2019.01.002
- Scheffer, L. K., Xu, C. S., Januszewski, M., Lu, Z., Takemura, S. Y., Hayworth, K. J., et al. (2020). A connectome and analysis of the adult *Drosophila* central brain. *Elife* 9:e57443. doi: 10.7554/eLife.57443
- Schuldiner, O., and Yaron, A. (2015). Mechanisms of developmental neurite pruning. *Cell. Mol. Life Sci.* 72, 101–119. doi: 10.1007/s00018-014-1729-6
- Sekar, A., Bialas, A. R., de Rivera, H., Davis, A., Hammond, T. R., Kamitaki, N., et al. (2016). Schizophrenia risk from complex variation of complement component 4. *Nature* 530, 177–183. doi: 10.1038/nature16549
- Sergeeva, A. P., Katsamba, P. S., Cosmanescu, F., Brewer, J. J., Ahlsen, G., Manneppalli, S., et al. (2020). DIP/Dpr interactions and the evolutionary design of specificity in protein families. *Nat. Commun.* 11:2125. doi: 10.1038/s41467-020-15981-8
- Sullivan, C. S., Kumper, M., Temple, B. S., and Maness, P. F. (2016). The Neural Cell Adhesion Molecule (NCAM) Promotes Clustering and Activation of EphA3 Receptors in GABAergic Interneurons to Induce Ras Homolog Gene Family, Member A (RhoA)/Rho-associated protein kinase (ROCK)-mediated Growth Cone Collapse. *J. Biol. Chem.* 291, 26262–26272. doi: 10.1074/jbc.M116.760017
- Tanaka, N. K., Tanimoto, H., and Ito, K. (2008). Neuronal assemblies of the *Drosophila* mushroom body. *J. Comp. Neurol.* 508, 711–755. doi: 10.1002/cne.21692
- Thomas, M. S., Davis, R., Karmiloff-Smith, A., Knowland, V. C., and Charman, T. (2016). The over-pruning hypothesis of autism. *Dev. Sci.* 19, 284–305. doi: 10.1111/desc.12303
- Wang, Q., Wang, Y., and Yu, F. (2018). Yif1 associates with Yip1 on Golgi and regulates dendrite pruning in sensory neurons during *Drosophila* metamorphosis. *Development* 145:dev164475. doi: 10.1242/dev.164475
- Wang, Y., Zhang, H., Shi, M., Liou, Y. C., Lu, L., and Yu, F. (2017). Sec71 functions as a GEF for the small GTPase Arf1 to govern dendrite pruning of *Drosophila* sensory neurons. *Development* 144, 1851–1862. doi: 10.1242/dev.146175
- Watts, R. J., Hoopfer, E. D., and Luo, L. (2003). Axon pruning during *Drosophila* metamorphosis: evidence for local degeneration and requirement of the ubiquitin-proteasome system. *Neuron* 38, 871–885. doi: 10.1016/s0896-6273(03)00295-2
- Weber, T., Stephan, R., Moreno, E., and Pielage, J. (2019). The Ankyrin Repeat Domain Controls Presynaptic Localization of *Drosophila* Ankyrin2 and Is Essential for Synaptic Stability. *Front. Cell Dev. Biol.* 7:148. doi: 10.3389/fcell.2019.00148
- Xie, Q., Brbic, M., Horns, F., Kolluru, S. S., Jones, R. C., Li, J., et al. (2021). Temporal evolution of single-cell transcriptomes of *Drosophila* olfactory projection neurons. *Elife* 10:e63450. doi: 10.7554/eLife.63450
- Xu, S., Xiao, Q., Cosmanescu, F., Sergeeva, A. P., Yoo, J., Lin, Y., et al. (2018). Interactions between the Ig-Superfamily Proteins DIP-alpha and Dpr6/10 Regulate Assembly of Neural Circuits. *Neuron* 100, 1369.e–1384.e. doi: 10.1016/j.neuron.2018.11.001
- Yaniv, S. P., and Schuldiner, O. (2016). A fly's view of neuronal remodeling. *Wiley Interdiscip. Rev. Dev. Biol.* 5, 618–635. doi: 10.1002/wdev.241
- Yu, F., and Schuldiner, O. (2014). Axon and dendrite pruning in *Drosophila*. *Curr. Opin. Neurobiol.* 27, 192–198. doi: 10.1016/j.conb.2014.04.005
- Zhang, H., Wang, Y., Wong, J. J., Lim, K. L., Liou, Y. C., Wang, H., et al. (2014). Endocytic pathways downregulate the L1-type cell adhesion molecule neuroglian to promote dendrite pruning in *Drosophila*. *Dev. Cell* 30, 463–478. doi: 10.1016/j.devcel.2014.06.014
- Zong, W., Wang, Y., Tang, Q., Zhang, H., and Yu, F. (2018). Prd1 associates with the clathrin adaptor alpha-Adaptin and the kinesin-3 Imac/Unc-104 to govern dendrite pruning in *Drosophila*. *PLoS Biol.* 16:e2004506. doi: 10.1371/journal.pbio.2004506

Conflict of Interest: The authors declare that the research was conducted in the absence of any commercial or financial relationships that could be construed as a potential conflict of interest.

Publisher's Note: All claims expressed in this article are solely those of the authors and do not necessarily represent those of their affiliated organizations, or those of the publisher, the editors and the reviewers. Any product that may be evaluated in this article, or claim that may be made by its manufacturer, is not guaranteed or endorsed by the publisher.

Copyright © 2022 Meltzer and Schuldiner. This is an open-access article distributed under the terms of the Creative Commons Attribution License (CC BY). The use, distribution or reproduction in other forums is permitted, provided the original author(s) and the copyright owner(s) are credited and that the original publication in this journal is cited, in accordance with accepted academic practice. No use, distribution or reproduction is permitted which does not comply with these terms.



Endoglycan Regulates Purkinje Cell Migration by Balancing Cell-Cell Adhesion

Thomas Baeriswyl, Martina Schaettin, Simone Leoni, Alexandre Dumoulin and Esther T. Stoeckli*

Department of Molecular Life Sciences and Neuroscience Center Zurich, University of Zurich, Zurich, Switzerland

OPEN ACCESS

Edited by:

Robert Hindges,
King's College London,
United Kingdom

Reviewed by:

Fekrije Selimi,
Collège de France, France
Annalisa Buffo,
University of Turin, Italy

*Correspondence:

Esther T. Stoeckli
esther.stoeckli@mls.uzh.ch

Specialty section:

This article was submitted to
Neurodevelopment,
a section of the journal
Frontiers in Neuroscience

Received: 12 March 2022

Accepted: 20 May 2022

Published: 20 June 2022

Citation:

Baeriswyl T, Schaettin M, Leoni S,
Dumoulin A and Stoeckli ET (2022)
Endoglycan Regulates Purkinje Cell
Migration by Balancing Cell-Cell
Adhesion.
Front. Neurosci. 16:894962.
doi: 10.3389/fnins.2022.894962

The importance of cell adhesion molecules for the development of the nervous system has been recognized many decades ago. Functional *in vitro* and *in vivo* studies demonstrated a role of cell adhesion molecules in cell migration, axon growth and guidance, as well as synaptogenesis. Clearly, cell adhesion molecules have to be more than static glue making cells stick together. During axon guidance, cell adhesion molecules have been shown to act as pathway selectors but also as a means to prevent axons going astray by bundling or fasciculating axons. We identified Endoglycan as a negative regulator of cell-cell adhesion during commissural axon guidance across the midline. The presence of Endoglycan allowed commissural growth cones to smoothly navigate the floor-plate area. In the absence of Endoglycan, axons failed to exit the floor plate and turn rostrally. These observations are in line with the idea of Endoglycan acting as a lubricant, as its presence was important, but it did not matter whether Endoglycan was provided by the growth cone or the floor-plate cells. Here, we expand on these observations by demonstrating a role of Endoglycan during cell migration. In the developing cerebellum, Endoglycan was expressed by Purkinje cells during their migration from the ventricular zone to the periphery. In the absence of Endoglycan, Purkinje cells failed to migrate and, as a consequence, cerebellar morphology was strongly affected. Cerebellar folds failed to form and grow, consistent with earlier observations on a role of Purkinje cells as Shh deliverers to trigger granule cell proliferation.

Keywords: cerebellum development, neural circuit development, chicken embryo, sialomucins, cell adhesion, Purkinje cells

INTRODUCTION

In the cerebellum, like in other parts of the nervous system, cells proliferate in specific zones, from where they migrate to their final destinations. Once they have reached their final position, neurons start to extend processes, axons and dendrites, to connect to their targets and form synapses, and thus, establish neural circuits. The cerebellum has two proliferative zones, the ventricular zone, where most cell types have their origin, and the external granular cell layer, where the granule cells are born (Butts et al., 2014; Leto et al., 2016; Beckinghausen and Sillitoe, 2019). Cells migrate either radially or tangentially from their place of birth to their final destination. For radial migration, they

are supported by radial glia fibers. Migrating cells interact with the processes of radial glia cells to find their way toward the periphery, away from the ventricular zone (Rahimi-Balaei et al., 2018). For tangential migration, the signals that guide migrating cells have not been identified. In analogy to axon guidance, where the growth cone rather than the cell body needs to navigate through the three-dimensional tissue, the idea is that specific guidance cues, recognized by surface receptors on the migrating cell, will allow for navigation to the final position. An early hypothesis suggested that proteases would allow a growth cone to ease its way through the pre-existing tissue held together by cell adhesion molecules (Krystosek and Seeds, 1981a; Seeds et al., 1997). Therefore, proteolytic support for cells migrating through the tissue might also be necessary. Indeed, granule cells *in vitro* were shown to exhibit protease activity (Krystosek and Seeds, 1981b). Although the image of a larva eating its way through food may not be an appropriate analogy to a growth cone navigating or a cell migrating through neural tissue, there is still a need to regulate adhesive strength between the migrating cell and the environment to allow advance.

The neural cell adhesion molecule NCAM was the first cell-cell adhesion molecule to be identified in the nervous system (Edelman, 1983). Interestingly, it had a regulatory mechanism for adhesive strength built in. The post-translational modification with poly-sialic acid added to some NCAM isoforms was found to lower not only the adhesion between NCAM molecules but also to interfere with the interactions of other cell adhesion molecules of the immunoglobulin superfamily, such as NgCAM (Rutishauser and Landmesser, 1996; Kiss and Rougon, 1997).

Recently, we identified a related mechanism for the regulation of adhesive strength between growth cones and their intermediate target during axon guidance (Baeriswyl et al., 2021). Commissural growth cones and the floor plate, their intermediate target, both express Endoglycan, a molecule that is heavily glycosylated in its extracellular part. Unlike NCAM, Endoglycan is not suggested to act as a receptor or ligand, but rather as lubricant, allowing growth cones to advance through the three-dimensional tissue. This may be different in the hematopoietic system, where Endoglycan was suggested to be a ligand for L-Selectin (Fieger et al., 2003).

Endoglycan, also known as Podocalyxin-like-2, belongs to the CD34 family of sialomucins, which also comprises CD34 and Podocalyxin (Sasseti et al., 2000; Furness and McNagny, 2006; Nielsen and McNagny, 2008). Sialomucins are single-pass transmembrane proteins with a bulky extracellular domain that is negatively charged due to its extensive N- and O-glycosylation.

Our studies demonstrated that during axon guidance, Endoglycan could either be provided by the growth cone or by the floor plate, but it was necessary to lower the adhesion between the migrating growth cone and the floor-plate cells during midline crossing (Baeriswyl et al., 2021). In the absence of Endoglycan, the excessive adhesive strength prevented the smooth passage of growth cones. As a result, floor-plate cells were “torn out” of the floor plate and dislocated into the commissure beneath the floor plate. In an *ex vivo* preparation for live imaging of commissural axon navigation (Dumoulin et al., 2021), the growth speed was decreased due to too much

adhesion, most likely contributing to the pathfinding errors observed at the floor-plate exit site (Baeriswyl et al., 2021). Too much Endoglycan also perturbed the correct navigation of the floor-plate area by commissural axons, in agreement with the idea that adhesive strength needs to be set within a certain range.

Interestingly, a recent study not only confirmed the role of Endoglycan as an anti-adhesion molecule, but also went one step further in showing that the level of Endoglycan expression on the cell surface was under the control of ADAM10, an α -secretase capable of shedding proteins from the cell surface (Hsia et al., 2021).

Here, we extend our previous studies and demonstrate that Endoglycan is not only acting as a negative regulator of adhesion for navigating growth cones at their intermediate target but that Endoglycan also supports cell migration. Removing Endoglycan from Purkinje cells prevented their radial migration during cerebellum development. Because Purkinje cells did not reach their final position, they failed to provide Shh, the proliferation-inducing signal, to granule cell precursors. As a consequence the number of granule cells was reduced, which in turn reduced the size of the cerebellar lobes (De Luca et al., 2016).

MATERIALS AND METHODS

Preparation of Digoxigenin-Labeled RNA Probes and *in situ* Hybridization

For *in vitro* transcription 1 μ g of the linearized and purified plasmid encoding Endoglycan (EndoORF: 1028-1546pb, Endo3'UTR: 3150-3743bp, and 5070-5754bp; numbers are derived from the human sequence), were used to prepare DIG-(digoxigenin)-labeled *in situ* probes as described earlier (Mauti et al., 2006). The same fragments were used to prepare dsRNA (Pekarik et al., 2003).

Ex ovo RNAi

All experiments including animals were carried out according to the guidelines and regulations of the Cantonal authorities (Veterinäramt des Kanton Zürich). To analyze the *in vivo* function of Endoglycan in the developing cerebellum *ex ovo* cultures of chicken embryos were prepared (Baeriswyl and Stoeckli, 2008). Injections and electroporations were performed at E8 (HH34). To have direct access to the embryo a small hole of 3–4 mm diameter was cut into the extraembryonic membranes above the eye. For positioning and stabilization of the head during injection and subsequent electroporation, we used a hook prepared from a spatula. Approximately 1 μ l of the nucleic acid mixture, consisting of a plasmid encoding EGFP under the control of the β -actin promoter (100 ng/ μ l), dsRNA derived from the ORF of *Endoglycan* (500 ng/ μ l), and 0.04% (vol/vol) Trypan Blue (Invitrogen) dissolved in sterile PBS, were injected into the cerebellum using a borosilicate glass capillary with a tip diameter of 5 μ m (World Precision Instruments). Before electroporation, a few drops of sterile PBS were added to the embryo. For the electroporation, a platelet electrode of 7 mm diameter

(Tweezertrodes Model #520, BTX Instrument Division, Harvard Apparatus) was placed parallel to the head of the embryo. Six pulses of 40 V and 99 ms duration were applied using a square wave electroporator (ECM830, BTX).

Efficiency and specificity of Endoglycan downregulation with the long dsRNA derived from *Endoglycan*, which was used here, was verified and quantified in detail in our previously published study on the role of Endoglycan in commissural axon guidance in the spinal cord (Figure 2 and Supplementary Figure 3 in Baeriswyl et al., 2021). In short, we used two different non-overlapping sequences from the 3'-UTR and one sequence from the ORF of *Endoglycan* to produce long dsRNA. The phenotypes resulting from electroporation of the three different dsRNAs did not differ. Silencing other CD34 family members did not interfere with commissural axon guidance. The *Endoglycan* mRNA levels in the electroporated area were markedly reduced, reaching about 80% of the theoretical maximum given that about 50% of the cells were transfected.

Tissue Preparation and Analysis

The embryos were sacrificed for the analysis of the cerebellum 4 days after electroporation. The whole brain was removed and analyzed for EGFP expression using a fluorescence stereomicroscope (Olympus SZX12). The brain tissue was fixed for 2 h at room temperature in 4% PFA in PBS. After fixation, the brain tissue was rinsed in PBS and transferred to 25% sucrose in 0.1M sodium phosphate buffer, pH 7.4, for cryoprotection. In this study, 30 μ m-thick sagittal cryostat sections were used for analysis. For the preparation of cryostat sections, the brains were embedded with O.C.T Tissue-Tek (Sakura) in Peel-a-Way disposable embedding molds (Polysciences), frozen in isopentane on dry ice and cut on a cryocut (CM1850, Leica Microsystems). The sections were collected on SuperFrostPlus microscope slides (Menzel-Glaeser).

Immunohistochemistry

Cryostat sections were rinsed in PBS at 37°C for 3 min followed by 3 min in cold water. Subsequently the sections were incubated in 20 mM lysine in 0.1 M sodium phosphate (pH 7.4) for 30 min at room temperature before being rinsed in PBS three times for 10 min. The tissue was permeabilized with 0.1% Triton in PBS for 30 min at room temperature and then washed again three times with PBS for 10 min. To prevent unspecific binding of the antibody the tissue was blocked with 10% fetal calf serum (FCS) in PBS for 1 h. Goat anti-GFP (1:400; Rockland), rabbit anti-Calbindin D-28K (CB38a; Swant), mouse anti-Pax6 (2 μ g/ml; Developmental Studies Hybridoma Bank) were dissolved in 10% FCS/PBS and incubated overnight at 4°C. After three washes in PBS, 10% FCS in PBS was applied again for 1 h, followed by the incubation with donkey anti-rabbit IgG-Cy3 (1:250; Molecular Probes), donkey anti-goat IgG-Alexa488 (1:250; Molecular Probes/Invitrogen) and goat anti-mouse IgG-Cy3 (1:250; Jackson ImmunoResearch) dissolved in 10% FCS in PBS for 90 min at room temperature. The tissue was rinsed 5 times in PBS for 12 min and then mounted in Celvol (Celanese). The staining of cryostat sections was analyzed with an upright microscope equipped with fluorescence optics (Olympus BX51).

Analysis of Cell Proliferation and Cell Death

To assess cell proliferation in the developing cerebellum, we used BrdU incorporation. Embryos were injected and electroporated at HH34 with dsRNA derived from *Endoglycan* and the *EGFP* plasmid or with the *EGFP* plasmid alone. After 1 (HH35) or 4 days (HH38) 200 μ l 50 mM BrdU in H₂O were pipetted onto the chorioallantois. After 3 h the embryos were sacrificed, the brains were dissected and prepared for cryostat sections as described above. For visualization of the incorporated BrdU, the sections were incubated in 50% formamide in 2xSSC for 1–2 h at 65°C, rinsed twice in 2xSSC for 15 min followed by incubation in 2 N HCl for 30 min at 37°C. Sections were rinsed in 0.1 M borate buffer (pH 8.5) for 10 min at room temperature, followed by PBS (six changes). BrdU was detected with mouse anti-BrdU (Sigma; 1:200) using the protocol detailed above. Sections were counterstained with DAPI (5 μ g/ml in PBS) for 20 min at room temperature.

Apoptosis was analyzed as described previously (Baeriswyl and Stoeckli, 2008). In brief, to detect apoptotic cells, the ApoAlert DNA Fragmentation Assay Kit (Clontech, Mountain View, CA) was used according to the manufacturer's instructions. The fragmented, fluorescein-labeled DNA was visualized with an alkaline phosphatase-conjugated sheep anti-FITC antibody (1:1,000 dissolved in 10% fetal calf serum/PBS; Roche). As a positive control, sections were treated with DNase I (300 U/ml; Roche) for 10 min at room temperature.

Quantification

All measurements, including Calbindin fluorescence intensities, real and outer cerebellar circumference, EGL thickness, and number of BrdU positive cells were performed with the analySIS Five software from Soft Imaging System. Embryos injected and electroporated with dsRNA derived from *Endoglycan* were compared with control-treated embryos, injected and electroporated with the *EGFP* plasmid only, and untreated controls. For statistical analyses, one-way ANOVA with Tukey's multiple comparisons test (GraphPad software) was used. Values are given as mean \pm SEM. 1 asterisk: $P < 0.05$. 2 asterisks: $P < 0.01$. 3 asterisks: $P < 0.001$.

RESULTS

Endoglycan Is Expressed Widely in the Developing Cerebellum

The analysis of *Endoglycan* expression in the developing chicken cerebellum revealed *Endoglycan* mRNA distribution in a dynamic pattern (Figure 1). At early stages (HH34; Figure 1A), *Endoglycan* mRNA was found throughout the cerebellar anlage. *Endoglycan* expression was maintained in migrating Purkinje cells until they reached their final destination in the periphery of the cerebellar folds (HH42; Figure 1E). Expression in granule cells was restricted to the inner granular cell layer and was maintained also at the latest stages before hatching that we tested (HH43; Figure 1F). In addition to granule cells, also

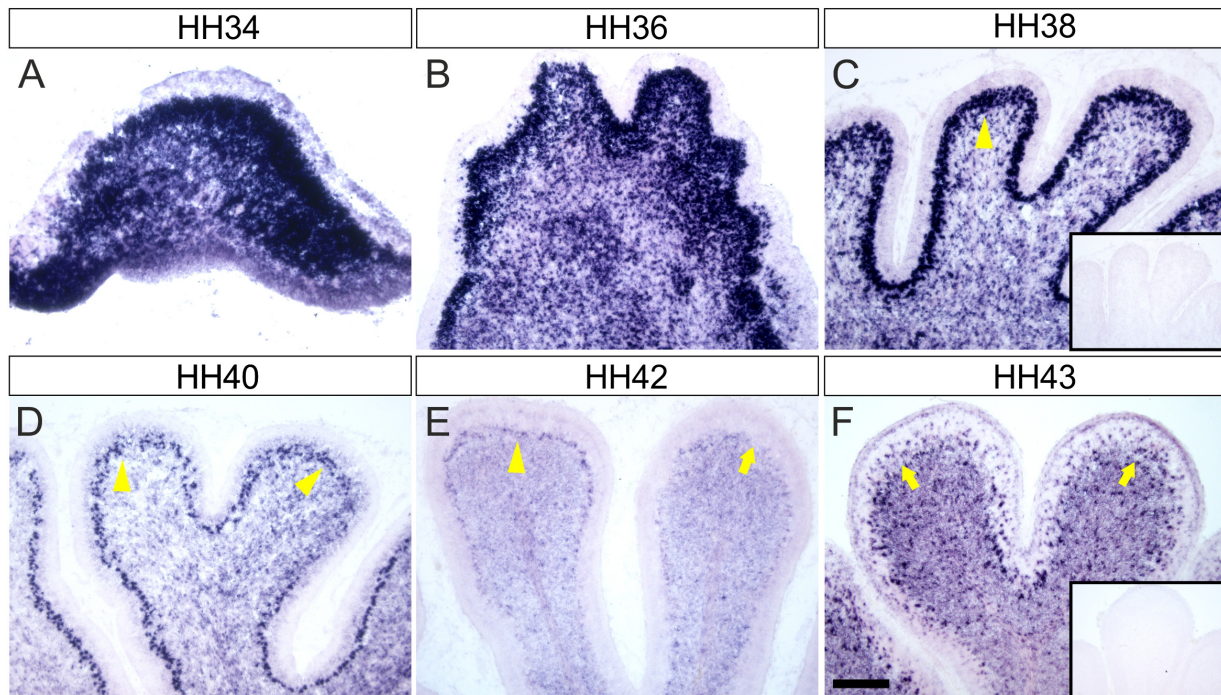


FIGURE 1 | Endoglycan is expressed in different cell types during cerebellar development. **(A)** Endoglycan mRNA was detected already at early stages of cerebellum development, when cells born in the ventricular zone start migrating radially toward the periphery of the cerebellar anlage at HH34/E8 (Hamburger and Hamilton stage 34; Hamburger and Hamilton, 1951). Endoglycan is found scattered throughout the cerebellar tissue at HH36/E10 **(B)** and HH38/E12 **(C)**. At both stages, Endoglycan is expressed also in Purkinje cells. The Purkinje cell layer is labeled with yellow arrowheads. By HH40/E14 **(D)**, Purkinje cells have completed their migration and are about to align to a single cell layer. The single cell layer is perfectly formed at HH42/E16 **(E)**. At this stage, the intensity of the Endoglycan mRNA signal is strongly reduced in some lobes (arrow). By HH43/E17 **(F)**, Purkinje cells appear to express little, if any *Endoglycan* mRNA. However, as at earlier stages, Endoglycan is still found in the inner granule cell layer and now also in interneurons of the molecular layer. Inserts show adjacent sections hybridized with the sense probe as negative control. Bar, 200 μ m.

interneurons in the molecular layer express *Endoglycan* mRNA until late stages.

Expression in Purkinje cells was confirmed by co-localization of the *in situ* signal for *Endoglycan* mRNA with the Purkinje cell marker Calbindin (**Figures 2A–F**). At HH38, Purkinje cells have migrated to the periphery of the folds but are not yet aligned to a single cell layer (**Figures 2D–F**).

Ex ovo RNAi Allows for Specific Knockdown of Endoglycan in the Developing Cerebellum

In ovo RNAi is an efficient method developed for silencing of candidate genes in the developing spinal cord (Pekarik et al., 2003; Wilson and Stoeckli, 2011; Andermatt et al., 2014). However, because the cerebellum starts developing in the chicken embryo only after 1 week (HH34, E8), it is not the method of choice to knockdown candidate genes in the developing brain. The embryo has already grown considerably and the head is not readily accessible through the window in the eggshell. For this reason, we developed *ex ovo* RNAi. In order to have access to the embryo for manipulations of the brain, the embryo is transferred with egg yolk and albumen to a domed plastic dish (Baeriswyl and Stoeckli, 2008). We have successfully used this method before

to demonstrate a role of Contactin-2/Axonin-1 in parallel fiber development (Baeriswyl and Stoeckli, 2008).

Endoglycan Is Required for Purkinje Cell Migration

Purkinje cells are born in the ventricular zone of the cerebellar anlage (Butts et al., 2014; Fleming and Chiang, 2015; Leto et al., 2016). From there, they migrate radially toward the cerebellar surface to form the distinct Purkinje cell layer (**Figure 3A**). At HH 38, Purkinje cells have migrated toward the periphery of the lobes. They are not yet aligned to a single cell layer, but very few, if any, Purkinje cells were still migrating in the cerebellum of untreated control chicken embryos (**Figures 3B,C**). The same was true in control-treated embryos injected with the EGFP-expression plasmid only (**Figures 3D–F**). In contrast, large numbers of Purkinje cells were still found in the center of the lobes in sections taken from HH38 embryos treated with dsRNA derived from *Endoglycan* (**Figures 3G–I**). In addition, the gross morphology of the cerebellum was severely altered. The lobes failed to grow and some of them failed to separate. Overall, the size of the cerebellum was significantly reduced. To quantify the failure to migrate, we compared the Calbindin-positive area of the cerebellum between the different groups.

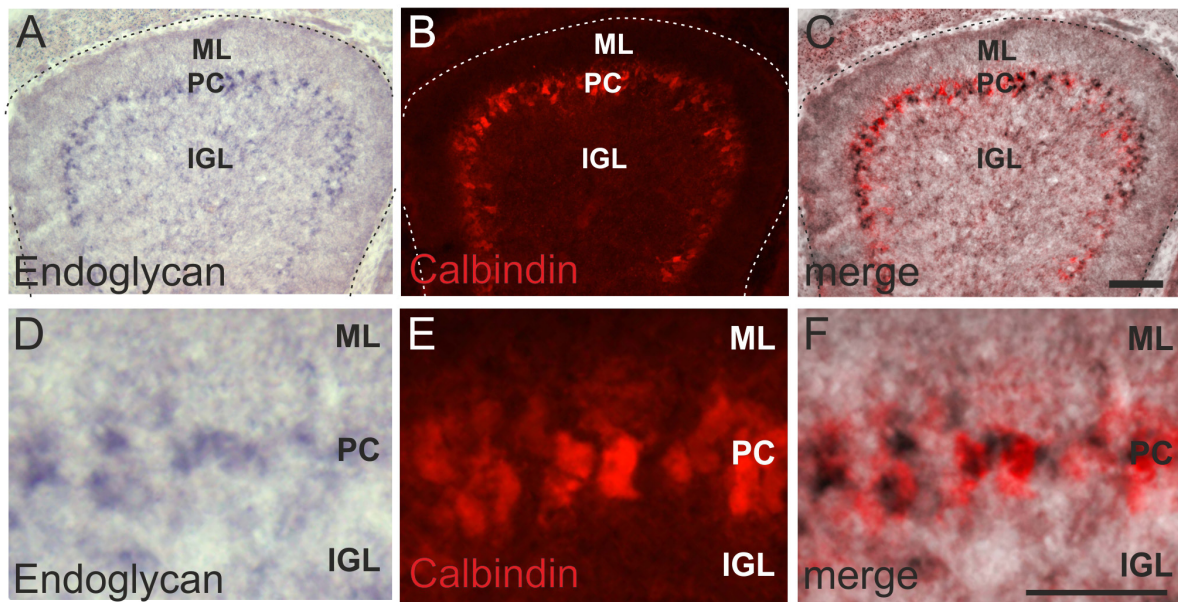


FIGURE 2 | Endoglycan is expressed in Purkinje cells. The distribution of Endoglycan mRNA during cerebellar development clearly suggested expression in Purkinje cells (A). However, we verified this by combining the *in situ* hybridization with Calbindin staining, a marker for Purkinje cells (B). Merged images shown in (C). Higher magnification clearly reveals the overlap between *in situ* hybridization signal and Calbindin staining (D–F). ML, molecular layer; PC, Purkinje cell layer; IGL, Inner granule cell layer. Bar, 100 μ m in (A–C), 50 μ m in (D–F).

There was no difference between the untreated and the control-treated, GFP-expressing embryos. The Calbindin-positive area of the cerebellum was about 7 times bigger in the sections taken from embryos electroporated with dsEndoglycan (Figures 3J,M). We quantified the size of the cerebellum in two different ways. When we measured the perimeter of the parasagittal sections, we found a significant reduction in the absence of Endoglycan (Figures 3K,N). And similarly, when we quantified foliation by dividing the circumference by the perimeter of the cerebellum, we again found a significant reduction in the experimental group (Figures 3L,O). Taken together, these *in vivo* results demonstrate a role of Endoglycan in Purkinje cell migration.

Aberrant Migration of Purkinje Cells Reduces Granule Cell Proliferation

We hypothesized that aberrant Purkinje cell migration and failure to establish the Purkinje cell layer in the periphery of the cerebellar folds prevented cerebellar growth and the formation of the lobes. Purkinje cells are suggested to regulate the proliferation of granule cells (Dahmane and Ruiz i Altaba, 1999; Wallace, 1999; Wechsler-Reya and Scott, 1999; Lewis et al., 2004). It was demonstrated that Shh (Sonic hedgehog) released by Purkinje cells affected proliferation of granule cells in the outer EGL (external granule cell layer). In turn, reduced proliferation of granule cells was shown to result in changes of cerebellar morphology similar to the ones we observed after downregulation of Endoglycan (Lewis et al., 2004; De Luca et al., 2016; Figure 3). A reduced rate of granule cell proliferation was indeed what we found in embryos after silencing *Endoglycan*. When we used Pax6 as a marker for granule cells, we found

a thinner EGL in experimental embryos compared to control-treated and untreated embryos (Figures 4A–D). This decrease in EGL width was due to a reduced proliferation rate of granule cells rather than apoptosis (Figure 4). When we compared BrdU-positive cells in the EGL, we found no difference between untreated (Figure 4E) and control-treated embryos (Figure 4F). However, there were only about half as many proliferating granule cells in the EGL of embryos after electroporation of dsEndoglycan (Figures 4G,H). Apoptosis did not contribute to the decrease in granule cell number, as we did not find any cell death in the cerebellum of control or experimental embryos at these stages (Figures 4I–K). In contrast to granule cells, the proliferation rate of Purkinje cells and other cells born in the ventricular zone at HH35 did not differ between control embryos and embryos lacking Endoglycan (Figure 5). These results are consistent with a lack of Shh provided by Purkinje cells as a reason for the decrease in granule cell proliferation.

Taken together, our *in vivo* experiments demonstrate that Purkinje cell migration in the developing cerebellum requires Endoglycan. In its absence, Purkinje cells fail to reach their target positions in the periphery. The observed stunted growth of the cerebellum and the failure to develop the lobes properly could be explained due to a lack of Shh-induced proliferation of granule cell precursors.

DISCUSSION

In summary, our results demonstrate a vital role for Endoglycan in Purkinje cell migration in the developing cerebellum. In

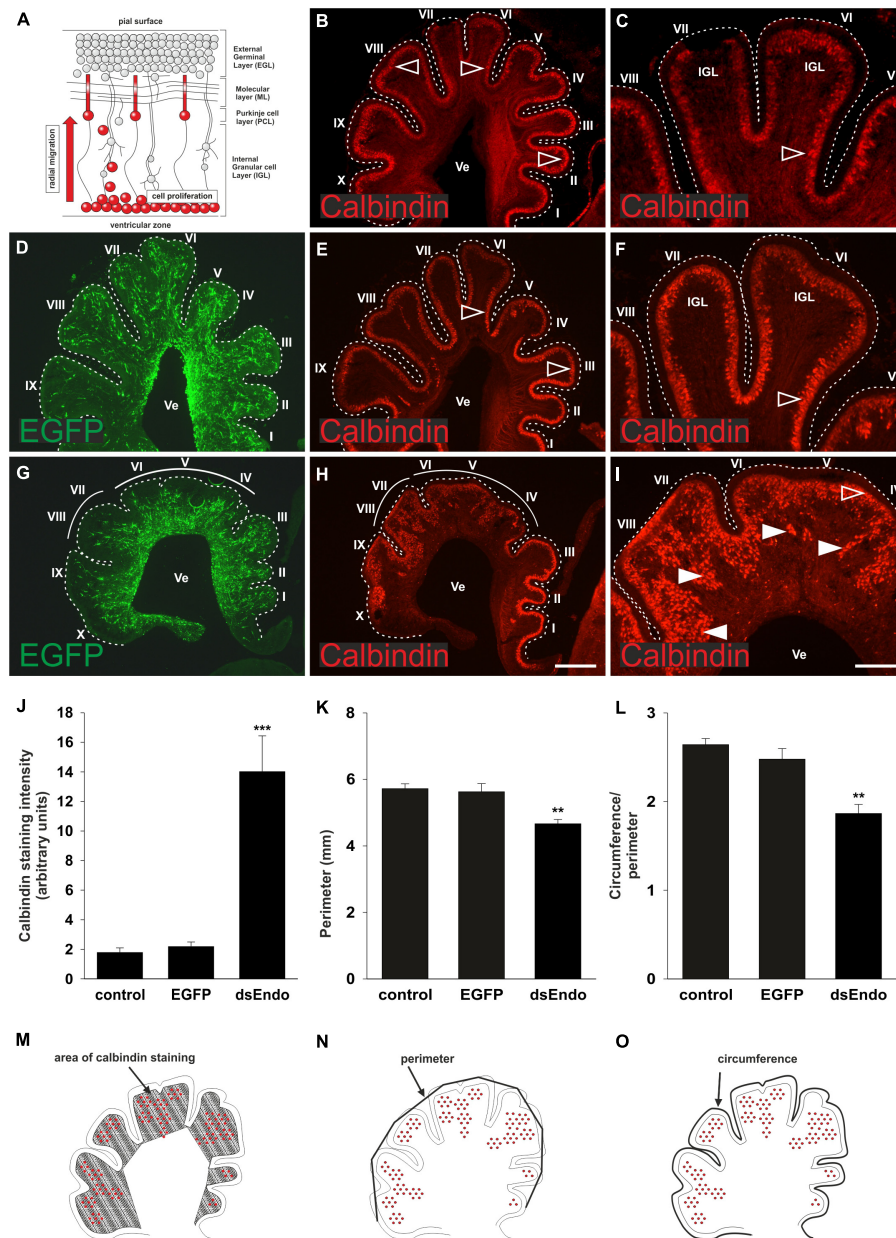


FIGURE 3 | Endoglycan is required for Purkinje cell migration. Purkinje cells are born in the ventricular zone and migrate radially toward the periphery of the cerebellum, while granule cells proliferate in the external germinal layer (EGL; **A**). In the cerebellum of untreated chicken embryos sacrificed at HH38, Purkinje cells have reached the periphery of the developing folds (**B**). Higher magnification of lobes VI and VII reveals that cells have reached their destination but have not yet finished the alignment to a single cell layer (**C**). The developmental trajectory and the distribution of Purkinje cells is not different in control-treated embryos sacrificed at HH38. Control-treated embryos were injected and electroporated *ex vivo* at HH34 with the EGFP-expressing plasmid alone (**D–F**). In embryos injected and electroporated with the EGFP plasmid and dsRNA derived from Endoglycan (dsEndo), the cerebellum failed to develop the characteristic lobes. They were much shorter and failed to segregate properly (**G–I**). There was a striking failure of Purkinje cells to migrate toward the periphery. Arrowheads indicated clusters of Purkinje cells that failed to migrate and reach the periphery of the cerebellum. Open arrowheads indicated the correct location of Purkinje cells. For quantification, we measured the Calbindin-positive areas as a proportion of the area of the lobes in parasagittal sections (**J,M**). There was no difference between the distribution of Purkinje cells, measured as Calbindin-positive pixels between non-treated and control-treated embryos (1.88 and 2.29, respectively). However, the area of the folds containing Purkinje cells was drastically increased, despite the fact that the area of the lobes was strongly reduced (14.05; *** $p = 0.0008$ for dsEndo vs. EGFP, *** $p = 0.0004$ for dsEndo vs. non-treated control). The circumference of parasagittal sections of the cerebellum (**K**), as outlined in (**N**) was significantly smaller for the sections taken from embryos injected and electroporated with dsEndoglycan (4.67 compared to 5.72 for untreated and 5.63 for EGFP controls; ** $p = 0.0043$ for dsEndo vs. EGFP controls, ** $p = 0.0013$ for dsEndo vs. non-treated controls). Finally, to have a relative measure for the lack of lobe separation, we divided the outer circumference (as shown in **N**) and divided the value by the circumference of the same parasagittal sections when the length of the folds was included (**L,O**). Values were 2.64 for untreated controls, 2.48 for EGFP expressing controls, 1.87 for dsEndo group. ** $p = 0.0026$ for dsEndo vs. EGFP, *** $p = 0.0002$ for dsEndo vs. non-treated controls. Lobes are labeled by Roman numbers. IGL, inner granule cell layer; Ve ventricle. One-way ANOVA with Tukey's multiple comparisons test used for statistical analysis.

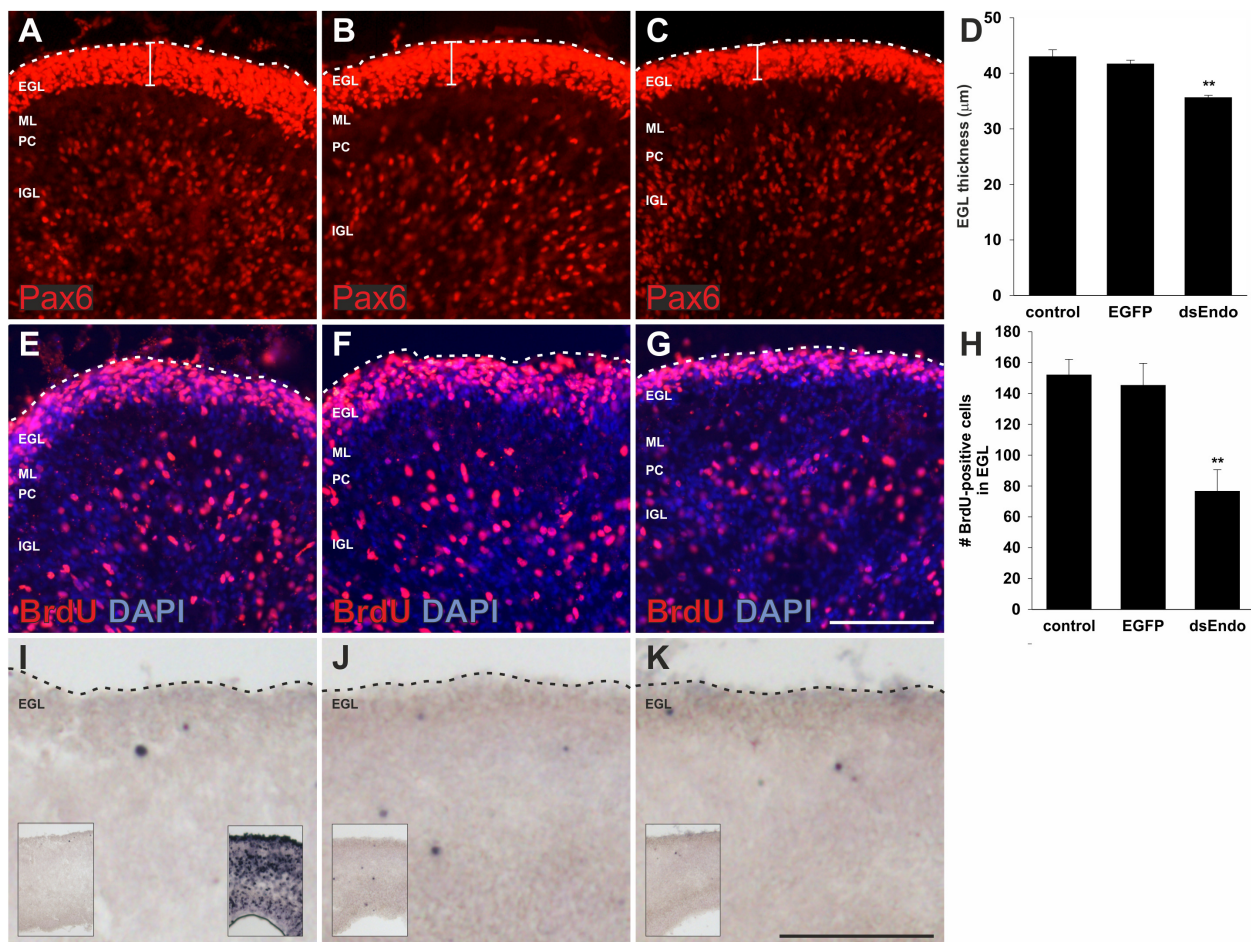


FIGURE 4 | The external germinal layer is reduced due to a reduction in granule cell proliferation after silencing Endoglycan. The width of the external germinal layer (EGL) was measured in sections taken from embryos sacrificed at HH35, 1 day after *ex ovo* electroporation (**A–D**). Pax6 stains proliferating granule cells in the EGL of untreated control embryos (**A**), control-treated, EGFP-expressing embryos (**B**), and in embryos injected and electroporated with dsEndoglycan (dsEndo; **C**). The thickness of the EGL was significantly reduced in embryos lacking Endoglycan (**D**). Thickness of the EGL was determined as 43 μm in non-treated and 41.7 μm in control-treated brains, compared to only 35.6 μm width in the dsEndo group (** $p = 0.0023$ for dsEndo vs. non-treated, and ** $p = 0.0096$ for dsEndo vs. EGFP-expressing controls). The decrease in granule cell proliferation was confirmed by staining for BrdU. The number of BrdU-positive cells was significantly lower in dsEndo-treated embryos (**G,H**; 76.6), compared to untreated (**E**; 152) and control-treated embryos (**F**; 145.5). ** $p = 0.0021$ dsEndo vs. untreated, ** $p = 0.0085$ dsEndo vs. EGFP-expressing controls. We also compared apoptosis in the cerebellum of untreated (**I**), control-treated (**J**), and dsEndo-treated (**K**) embryos. We found no contribution of cell death to the number of granule cells, as we did not see apoptosis at this stage of development. The inserts in (**I–K**) show lower magnification overviews. The insert in the right corner of (**I**) shows a positive control, where DNA fragmentation was induced with DNase treatment. One-way ANOVA with Tukey's multiple comparisons test used for statistical analysis. EGL, external germinal layer; ML, molecular layer; PC, Purkinje cell layer; IGL, inner granule cell layer. Bar, 100 μm.

agreement with the results of our *in vivo* studies in the developing spinal cord (Baeriswyl et al., 2021), the observed phenotype is consistent with the hypothesis that Endoglycan is an essential regulator of cell-cell contacts by modulating the strength of adhesion between cells. This model is supported by observations *in vitro* (Baeriswyl et al., 2021). In analogy to our findings in the developing spinal cord (Baeriswyl et al., 2021) we suggest a role of Endoglycan as a regulator of adhesive strength also in the cerebellum. In the absence of Endoglycan, the adhesion between precursor cells in the cerebellar anlage is too strong for Purkinje cells to migrate properly. This failure to migrate results indirectly in a reduced proliferation rate of granule cell

precursors. Because Purkinje cells get stuck in the center of the folds along their migratory path, they fail to deliver Shh to the external granule cell layer, where granule cell precursors are located during proliferation. Reduced granule cell proliferation in the absence of sufficient Shh was previously demonstrated to result in very similar cerebellar phenotypes, with merged folds and reduced size (Dahmane and Ruiz i Altaba, 1999; Wallace, 1999; Wechsler-Reya and Scott, 1999; Lewis et al., 2004; De Luca et al., 2016).

We have not analyzed whether the migration of interneuron precursors giving rise to stellate and basked cells would be perturbed as well in the absence of Endoglycan. Because these

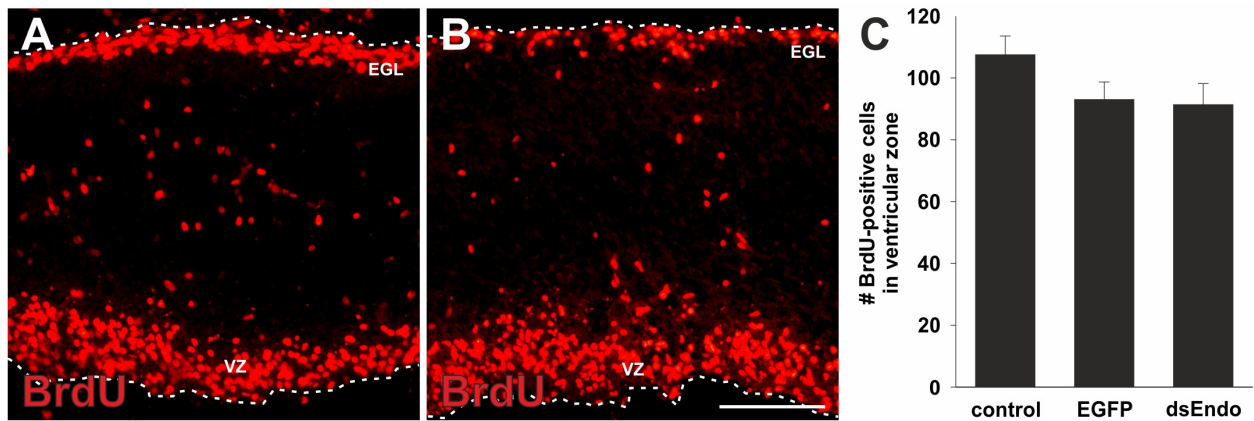


FIGURE 5 | The lack of proliferation in the absence of Endoglycan is specific for granule cells. To rule out a general effect of Endoglycan on cell proliferation, we also quantified the number of BrdU-positive cells in the ventricular zone (VZ). At HH35, there are many BrdU-positive cells in the external granule cell layer (EGL), but also in the ventricular zone. We found no significant difference in the number of proliferating cells in sections taken from controls (**A**) compared to embryos lacking Endoglycan (dsEndo; **B**, $p = 0.1978$ and 0.9873). Bar: 100 μ m. (**C**) We counted an average of 107.5 ± 6.1 cells in untreated embryos ($n = 7$), 93.0 ± 5.7 cells in control-treated, EGFP-expressing embryos ($n = 3$), and 91.3 ± 6.9 cells in dsEndo-treated embryos ($n = 5$). One-way ANOVA with Tukey's multiple comparisons test used for statistical analysis.

cells migrate over a longer period of time and not as a “wave,” a reduced migration rate would be very difficult to detect. Therefore, we focused on the analysis of Purkinje cells. However, we do not suggest a cell-autonomous effect of Endoglycan in Purkinje cells. Our results shown here are comparable to our previous findings in the spinal cord, where the level but not the source of Endoglycan mattered for the navigation of commissural growth cones at the ventral midline, the floor plate (Baeriswyl et al., 2021).

The fine-tuning of adhesive strength for migrating cells or extending neurites is an important aspect of neural circuit formation. Not only growth cones, but also cells need to reach distant destinations. In the cerebellum, in contrast to the cortex, cells are also born in the periphery, not only in the ventricular zone (Sotelo, 2011; Hashimoto and Hibi, 2012; Butts et al., 2014; Marzban et al., 2015; Leto et al., 2016). Granule cell precursors migrate tangentially from the rhombic lip to form the external granular layer, where they respond to Shh, a proliferative signal for granule cell precursors. Once they cease to proliferate and mature, they start to extend processes parallel to the cerebellar surface. At a slightly later stage, they form a third process, this time parallel to the Bergman glia fibers. Mature granule cells then slide along the glial fibers toward the center of the lobes by crossing the developing Purkinje cell layer to form the internal granule cell layer.

Purkinje cells have to migrate in the opposite direction during their radial migration from the ventricular zone. The appropriate localization of Purkinje cells appears to be essential for cerebellar function (Fleming and Chiang, 2015). Purkinje cells integrate the afferent information received directly from climbing fibers, or indirectly from mossy fibers, relayed by granule cells. The spontaneous mouse mutants *reeler* and *scrambler* demonstrate the importance of Purkinje cell location for cerebellar function, as the abnormal behavior of these mice

due to aberrant motor control was linked to aberrant positioning of Purkinje cells (Goldowitz et al., 1997; Miyata et al., 2010). However, the cerebellum does much more than motor control and motor learning. Non-motor functions of the cerebellum, that is, its contribution to cognition and language, have been widely recognized by now (Schmahmann, 1991; Strick et al., 2009; Buckner, 2013). Therefore, it comes as no surprise that changes in cerebellar structure and function have been linked to many neurodevelopmental disorders, such as attention deficit-hyperactivity disorder (ADHD) or autism spectrum disorders (ASD) (Courchesne et al., 2005; Fatemi et al., 2012; Stoodley, 2016). Aberrant Purkinje cell localization has been identified as one of the recurrent findings in autistic patients (Wang et al., 2014; Thabault et al., 2022).

Despite of the importance of Purkinje cell migration for cerebellar development and function, its molecular basis is still poorly understood (Hatten, 1999; Sotelo, 2004; Rahimi-Balaei et al., 2018). In contrast, to granule cells, where a number of cell adhesion molecules contributing to cell migration or neurite extension have been identified, much less is known about Purkinje cells. Astrotactin was shown to slow down migration of granule cells in an N-Cadherin-dependent manner (Fishell and Hatten, 1991; Horn et al., 2018). Similarly, an effect of NB3/Cntn6 (Sakurai et al., 2009), Cadherin-2 (Rieger et al., 2009), NrCAM and NgCAM on granule cell migration was found in knockout mice (Sakurai et al., 2001), but Purkinje cell migration was not disturbed in any of these lines. Cell adhesion molecules of the Distactin family have been shown to affect parallel fiber development (Baeriswyl and Stoeckli, 2008; Stoeckli, 2010) but there are no reports on differences in Purkinje cell migration.

Aberrant positioning of Purkinje cells and similar cerebellar morphologies as the one described in this study were found in *reeler* and *scrambler* mice (Goffinet et al., 1984; Goldowitz et al., 1997; Goldowitz and Hamre, 1998). In these mice, the expression

of Reelin by granule cells, or the expression and function of the receptors in Purkinje cells are perturbed and result in a failure of Purkinje cells to reach their target layer. In addition, defects in Purkinje cell migration have been shown in the absence of α N-Catenin (Park et al., 2002).

Most interesting in the context of our findings is a report by Sergaki and Ibáñez (2017) where GFR α 1 was shown to affect Purkinje cell migration by counteracting NCAM. According to their observations, homophilic NCAM interactions negatively regulate migration. Migration can be enhanced by either modifying NCAM with poly-sialic acid (PSA) or by direct interaction with GFR α 1. Poly-sialic acid is well known as a regulator of cell adhesion, not only for homophilic NCAM-NCAM interactions but also for heterophilic interactions of NCAM (Rutishauser et al., 1988; Brusés and Rutishauser, 2001; Burgess et al., 2008).

The expression of PSA-NCAM compared to non-PSA-NCAM is temporally regulated during development. Similarly, we found expression of Endoglycan during Purkinje cell migration, in line with an effect of Endoglycan as a negative regulator of cell-cell adhesion or “lubricant”. Interestingly, Endoglycan function could be controlled by ADAM10, which was shown to shed Endoglycan from the cell surface (Hsia et al., 2021).

Thus, it is still unknown which of the large number of cell adhesion molecules are required for the migration of Purkinje cells to their final position. However, our results are comparable to the effect of Endoglycan in commissural axon guidance, where Endoglycan was shown to negatively regulate adhesive strength (Baeriswyl et al., 2021). The same mechanism appears to allow for the migration of Purkinje cells to their final position.

REFERENCES

- Andermatt, I., Wilson, N., and Stoeckli, E. T. (2014). In ovo electroporation of miRNA-based-plasmids to investigate gene function in the developing neural tube. *Methods Mol. Biol.* 1101, 353–368. doi: 10.1007/978-1-62703-721-1_17
- Baeriswyl, T., Dumoulin, A., Schaettin, M., Tsapara, G., Niederkofler, V., Helbling, D., et al. (2021). Endoglycan plays a role in axon guidance by modulating cell adhesion. *Elife* 10:e64767. doi: 10.7554/eLife.64767
- Baeriswyl, T., and Stoeckli, E. T. (2008). Axonin-1/TAG-1 is required for pathfinding of granule cell axons in the developing cerebellum. *Neural Dev.* 3:7. doi: 10.1186/1749-8104-3-7
- Beckinghausen, J., and Sillitoe, R. V. (2019). Insights into cerebellar development and connectivity. *Neurosci. Lett.* 688, 2–13. doi: 10.1016/j.neulet.2018.05.013
- Brusés, J. L., and Rutishauser, U. (2001). Roles, regulation, and mechanism of polysialic acid function during neural development. *Biochimie* 83, 635–643. doi: 10.1016/s0300-9084(01)01293-7
- Buckner, R. L. (2013). The cerebellum and cognitive function: 25 years of insight from anatomy and neuroimaging. *Neuron* 80, 807–815. doi: 10.1016/j.neuron.2013.10.044
- Burgess, A., Wainwright, S. R., Shihabuddin, L. S., Rutishauser, U., Seki, T., and Aubert, I. (2008). Polysialic acid regulates the clustering, migration, and neuronal differentiation of progenitor cells in the adult hippocampus. *Dev. Neurobiol.* 68, 1580–1590. doi: 10.1002/dneu.20681
- Butts, T., Green, M. J., and Wingate, R. J. T. (2014). Development of the cerebellum: simple steps to make a ‘little brain.’. *Dev.* 141, 4031–4041. doi: 10.1242/dev.106559
- Courchesne, E., Redcay, E., Morgan, J. T., and Kennedy, D. P. (2005). Autism at the beginning: microstructural and growth abnormalities underlying the cognitive and behavioral phenotype of autism. *Dev. Psychopathol.* 17, 577–597. doi: 10.1017/S0954579405050285
- Dahmane, N., and Ruiz i Altaba, A. (1999). Sonic hedgehog regulates the growth and patterning of the cerebellum. *Development* 126, 3089–3100. doi: 10.1242/dev.126.14.3089
- De Luca, A., Cerrato, V., Fucà, E., Parmigiani, E., Buffo, A., and Leto, K. (2016). Sonic hedgehog patterning during cerebellar development. *Cell. Mol. Life Sci.* 73, 291–303. doi: 10.1007/s00018-015-2065-1
- Dumoulin, A., Zúñiga, N. R., and Stoeckli, E. T. (2021). Axon guidance at the spinal cord midline—A live imaging perspective. *J. Comp. Neurol.* 529, 2517–2538. doi: 10.1002/cne.25107
- Edelman, G. M. (1983). Cell adhesion molecules. *Science* 219, 450–457.
- Fatemi, S. H., Aldinger, K. A., Ashwood, P., Bauman, M. L., Blaha, C. D., Blatt, G. J., et al. (2012). Consensus paper: pathological role of the cerebellum in Autism. *Cerebellum* 11, 777–807. doi: 10.1007/s12311-012-0355-9
- Fieger, C. B., Sassetti, C. M., and Rosen, S. D. (2003). Endoglycan, a member of the CD34 family, functions as an L-selectin ligand through modification with tyrosine sulfation and sialyl Lewis x. *J. Biol. Chem.* 278, 27390–27398. doi: 10.1074/jbc.M304204200
- Fishell, G., and Hatten, M. E. (1991). Astrotactin provides a receptor system for CNS neuronal migration. *Development* 113, 755–765.
- Fleming, J., and Chiang, C. (2015). The Purkinje neuron: a central orchestrator of cerebellar neurogenesis. *Neurogenesis* 2:e1025940. doi: 10.1080/23262133.2015.1025940
- Furness, S. G. B., and McNagny, K. (2006). Beyond mere markers: functions for CD34 family of sialomucins in hematopoiesis. *Immunol. Res.* 34, 13–32. doi: 10.1385/IR:34:1:13

DATA AVAILABILITY STATEMENT

The original contributions presented in this study are included in the article/supplementary material, further inquiries can be directed to the corresponding author.

ETHICS STATEMENT

The animal study was reviewed and approved by the Cantonal Veterinary Office, Canton of Zürich.

AUTHOR CONTRIBUTIONS

TB, MS, and SL carried out experiments. AD and ES wrote the manuscript. All authors contributed to the article and approved the submitted version.

FUNDING

This research was funded by grants from the Swiss National Science Foundation (310030_185247 and 31003A_146676) to ES, and the University Research Priority Program AdaBD (Adaptive Brain Circuits in Development and Learning).

ACKNOWLEDGMENTS

We thank Tiziana Flego and Beat Kunz for excellent technical support.

- Goffinet, A. M., So, K. F., Yamamoto, M., Edwards, M., and Caviness, V. S. (1984). Architectonic and hodological organization of the cerebellum in reeler mutant mice. *Dev. Brain Res.* 16, 263–276. doi: 10.1016/0165-3806(84)90031-2
- Goldowitz, D., Gushing, R. C., Laywell, E., D'Arcangelo, G., Sheldon, M., Sweet, H. O., et al. (1997). Cerebellar disorganization characteristic of reeler in scrambler mutant mice despite presence of reelin. *J. Neurosci.* 17, 8767–8777. doi: 10.1523/JNEUROSCI.17-22-08767.1997
- Goldowitz, D., and Hamre, K. (1998). The cells and molecules that make a cerebellum. *Trends Neurosci.* 21, 375–382. doi: 10.1016/s0166-2236(98)01313-7
- Hamburger, V., and Hamilton, H. L. (1951). A series of normal stages in the development of the chick embryo. *J. Morphol.* 88, 49–92.
- Hashimoto, M., and Hibi, M. (2012). Development and evolution of cerebellar neural circuits. *Dev. Growth Differ.* 54, 373–389. doi: 10.1111/j.1440-169X.2012.01348.x
- Hatten, M. E. (1999). Central nervous system neuronal migration. *Annu. Rev. Neurosci.* 22, 511–539.
- Horn, Z., Behesti, H., and Hatten, M. E. (2018). N-cadherin provides a cis and trans ligand for astrotactin that functions in glial-guided neuronal migration. *Proc. Natl. Acad. Sci. U. S. A.* 115, 10556–10563. doi: 10.1073/pnas.1811100115
- Hsia, H. E., Tüshaus, J., Feng, X., Hofmann, L. I., Wefers, B., Marciano, D. K., et al. (2021). Endoglycan (PODXL2) is proteolytically processed by ADAM10 (a disintegrin and metalloprotease 10) and controls neurite branching in primary neurons. *FASEB J.* 35:e21813. doi: 10.1096/fj.202100475R
- Kiss, J. Z., and Rougon, G. (1997). Cell biology of polysialic acid. *Curr. Opin. Neurobiol.* 7, 640–646. doi: 10.1016/s0959-4388(97)80083-9
- Krystosek, A., and Seeds, N. W. (1981a). Plasminogen activator release at the neuronal growth cone. *Science* 213, 1532–1534. doi: 10.1126/science.7197054
- Krystosek, A., and Seeds, N. W. (1981b). Plasminogen activator secretion by granule neurons in cultures of developing cerebellum. *Proc. Natl. Acad. Sci. U. S. A.* 78, 7810–7814. doi: 10.1073/pnas.78.12.7810
- Leto, K., Arancillo, M., Becker, E. B. E., Buffo, A., Chiang, C., Ding, B., et al. (2016). Consensus paper: cerebellar development. *Cerebellum* 15, 789–828. doi: 10.1007/s12311-015-0724-2
- Lewis, P. M., Gritli-Linde, A., Smeyne, R., Kottmann, A., and McMahon, A. P. (2004). Sonic hedgehog signaling is required for expansion of granule neuron precursors and patterning of the mouse cerebellum. *Dev. Biol.* 270, 393–410. doi: 10.1016/j.ydbio.2004.03.007
- Marzban, H., Del Bigio, M. R., Alizadeh, J., Ghavami, S., Zachariah, R. M., and Rastegar, M. (2015). Cellular commitment in the developing cerebellum. *Front. Cell. Neurosci.* 8:450. doi: 10.3389/fncel.2014.00450
- Mauti, O., Sadhu, R., Gemayel, J., Gesemann, M., and Stoeckli, E. T. (2006). Expression patterns of plexins and neuropilins are consistent with cooperative and separate functions during neural development. *BMC Dev. Biol.* 6:32. doi: 10.1186/1471-213X-6-32
- Miyata, T., Ono, Y., Okamoto, M., Masaoka, M., Sakakibara, A., Kawaguchi, A., et al. (2010). Migration, early axonogenesis, and Reelin-dependent layer-forming behavior of early/posterior-born Purkinje cells in the developing mouse lateral cerebellum. *Neural Dev.* 5:23. doi: 10.1186/1749-8104-5-23
- Nielsen, J. S., and McNagny, K. M. (2008). Erratum: novel functions of the CD34 family. *J. Cell Sci.* 121, 3683–3692. doi: 10.1242/jcs.037507
- Park, C., Falls, W., Finger, J. H., Longo-Guess, C. M., and Ackerman, S. L. (2002). Deletion in Catna2, encoding α N-catenin, causes cerebellar and hippocampal lamination defects and impaired startle modulation. *Nat. Genet.* 31, 279–284. doi: 10.1038/ng908
- Pekarik, V., Bourikas, D., Miglino, N., Joset, P., Preiswerk, S., and Stoeckli, E. T. (2003). Screening for gene function in chicken embryo using RNAi and electroporation. *Nat. Biotechnol.* 21, 93–96. doi: 10.1038/nbt770
- Rahimi-Balaei, M., Bergen, H., Kong, J., and Marzban, H. (2018). Neuronal migration during development of the cerebellum. *Front. Cell. Neurosci.* 12:484. doi: 10.3389/fncel.2018.00484
- Rieger, S., Senghaas, N., Walch, A., and Köster, R. W. (2009). Cadherin-2 controls directional chain migration of cerebellar granule neurons. *PLoS Biol.* 7:1000240. doi: 10.1371/journal.pbio.1000240
- Rutishauser, U., Acheson, A., Hall, A. K., Mann, D. M., and Sunshine, J. (1988). The neural cell adhesion molecule (NCAM) as a regulator of cell-cell interactions. *Science* 240, 53–57. doi: 10.1126/science.3281256
- Rutishauser, U., and Landmesser, L. (1996). Polysialic acid in the vertebrate nervous system: a promoter of plasticity in cell-cell interactions. *Trends Neurosci.* 19, 422–427. doi: 10.1016/0166-2236(96)10041-2
- Sakurai, K., Toyoshima, M., Ueda, H., Matsubara, K., Takeda, Y., Karagogeos, D., et al. (2009). Contribution of the neural cell recognition molecule NB-3 to synapse formation between parallel fibers and Purkinje cells in mouse. *Dev. Neurobiol.* 69, 811–824. doi: 10.1002/dneu.20742
- Sakurai, T., Lustig, M., Babiarz, J., Furley, A. J. W., Tait, S., Brophy, P. J., et al. (2001). Overlapping functions of the cell adhesion molecules Nr-CAM and L1 in cerebellar granule cell development. *J. Cell Biol.* 154, 1259–1273. doi: 10.1083/jcb.200104122
- Sassetti, C., Van Zante, A., and Rosen, S. D. (2000). Identification of endoglycan, a member of the CD34/podocalyxin family of sialomucins. *J. Biol. Chem.* 275, 9001–9010. doi: 10.1074/jbc.275.12.9001
- Schmahmann, J. D. (1991). An emerging concept: the cerebellar contribution to higher function. *Arch. Neurol.* 48, 1178–1187. doi: 10.1001/archneur.1991.00530230086029
- Seeds, N. W., Siconolfi, L. B., and Haffke, S. P. (1997). Neuronal extracellular proteases facilitate cell migration, axonal growth, and pathfinding. *Cell Tissue Res.* 290, 367–370. doi: 10.1007/s004410050942
- Sergaki, M. C., and Ibáñez, C. F. (2017). GFR α 1 regulates purkinje cell migration by counteracting NCAM function. *Cell Rep.* 18, 367–379. doi: 10.1016/j.celrep.2016.12.039
- Sotelo, C. (2004). Cellular and genetic regulation of the development of the cerebellar system. *Prog. Neurobiol.* 72, 295–339. doi: 10.1016/j.pneurobio.2004.03.004
- Sotelo, C. (2011). Camillo Golgi and Santiago Ramon y Cajal: the anatomical organization of the cortex of the cerebellum. Can the neuron doctrine still support our actual knowledge on the cerebellar structural arrangement? *Brain Res. Rev.* 66, 16–34. doi: 10.1016/j.brainresrev.2010.05.004
- Stoeckli, E. T. (2010). Neural circuit formation in the cerebellum is controlled by cell adhesion molecules of the Contactin family. *Cell Adh. Migr.* 4, 523–526. doi: 10.4161/cam.4.4.12733
- Stoodley, C. J. (2016). The cerebellum and neurodevelopmental disorders. *Cerebellum* 15, 34–37.
- Strick, P. L., Dum, R. P., and Fiez, J. A. (2009). Cerebellum and nonmotor function. *Annu. Rev. Neurosci.* 32, 413–434. doi: 10.1146/annurev.neuro.31.060407.125606
- Thabault, M., Turpin, V., Maisterrena, A., Jaber, M., Egloff, M., and Galvan, L. (2022). Cerebellar and striatal implications in autism spectrum disorders: from clinical observations to animal models. *Int. J. Mol. Sci.* 23:2294. doi: 10.3390/ijms23042294
- Wallace, V. A. (1999). Purkinje-cell-derived Sonic hedgehog regulates granule neuron precursor cell proliferation in the developing mouse cerebellum. *Curr. Biol.* 9, 445–448. doi: 10.1016/s0960-9822(99)80195-x
- Wang, S. S. H., Kloth, A. D., and Badura, A. (2014). The cerebellum, sensitive periods, and autism. *Neuron* 83, 518–532. doi: 10.1016/j.neuron.2014.07.016
- Wechsler-Reya, R. J., and Scott, M. P. (1999). Control of neuronal precursor proliferation in the cerebellum by sonic hedgehog. *Neuron* 22, 103–114. doi: 10.1016/s0896-6273(00)80682-0
- Wilson, N. H., and Stoeckli, E. T. (2011). Cell type specific, traceable gene silencing for functional gene analysis during vertebrate neural development. *Nucleic Acids Res.* 39:e133. doi: 10.1093/nar/gkr628

Conflict of Interest: The authors declare that the research was conducted in the absence of any commercial or financial relationships that could be construed as a potential conflict of interest.

Publisher's Note: All claims expressed in this article are solely those of the authors and do not necessarily represent those of their affiliated organizations, or those of the publisher, the editors and the reviewers. Any product that may be evaluated in this article, or claim that may be made by its manufacturer, is not guaranteed or endorsed by the publisher.

Copyright © 2022 Baeriswyl, Schaettin, Leoni, Dumoulin and Stoeckli. This is an open-access article distributed under the terms of the Creative Commons Attribution License (CC BY). The use, distribution or reproduction in other forums is permitted, provided the original author(s) and the copyright owner(s) are credited and that the original publication in this journal is cited, in accordance with accepted academic practice. No use, distribution or reproduction is permitted which does not comply with these terms.



OPEN ACCESS

EDITED BY

Zsolt Lele,
Institute of Experimental Medicine,
Hungary

REVIEWED BY

Fekrije Selimi,
Collège de France, France
Silvia Bassani,
Institute of Neuroscience (CNR), Italy

*CORRESPONDENCE

Csaba Földy
foldy@hifo.uzh.ch

SPECIALTY SECTION

This article was submitted to
Neurodevelopment,
a section of the journal
Frontiers in Neuroscience

RECEIVED 02 March 2022

ACCEPTED 26 July 2022

PUBLISHED 01 September 2022

CITATION

Luo W, Cruz-Ochoa NA, Seng C,
Egger M, Lukacsovich D, Lukacsovich T
and Földy C (2022) *Pcdh11x* controls
target specification of mossy fiber
sprouting.
Front. Neurosci. 16:888362.
doi: 10.3389/fnins.2022.888362

COPYRIGHT

© 2022 Luo, Cruz-Ochoa, Seng, Egger,
Lukacsovich, Lukacsovich and Földy.
This is an open-access article
distributed under the terms of the
[Creative Commons Attribution License](#)
(CC BY). The use, distribution or
reproduction in other forums is
permitted, provided the original
author(s) and the copyright owner(s)
are credited and that the original
publication in this journal is cited, in
accordance with accepted academic
practice. No use, distribution or
reproduction is permitted which does
not comply with these terms.

Pcdh11x controls target specification of mossy fiber sprouting

Wenshu Luo, Natalia Andrea Cruz-Ochoa, Charlotte Seng,
Matteo Egger, David Lukacsovich, Tamás Lukacsovich and
Csaba Földy*

Laboratory of Neural Connectivity, Brain Research Institute, Faculties of Medicine and Science,
University of Zürich, Zurich, Switzerland

Circuit formation is a defining characteristic of the developing brain. However, multiple lines of evidence suggest that circuit formation can also take place in adults, the mechanisms of which remain poorly understood. Here, we investigated the epilepsy-associated mossy fiber (MF) sprouting in the adult hippocampus and asked which cell surface molecules define its target specificity. Using single-cell RNAseq data, we found lack and expression of *Pcdh11x* in non-sprouting and sprouting neurons respectively. Subsequently, we used CRISPR/Cas9 genome editing to disrupt the *Pcdh11x* gene and characterized its consequences on sprouting. Although MF sprouting still developed, its target specificity was altered. New synapses were frequently formed on granule cell somata in addition to dendrites. Our findings shed light onto a key molecular determinant of target specificity in MF sprouting and contribute to understanding the molecular mechanism of adult brain rewiring.

KEYWORDS

granule cell, axonal rewiring, mossy fiber sprouting, cell adhesion molecule, synaptic adhesion molecule, protocadherin, *Pcdh11x*, target specificity

Introduction

Mossy fiber (MF) sprouting in the hippocampal dentate gyrus represents a non-developmental form of circuit formation in the adult brain (for review, see Seng et al., 2022). MF sprouting has been extensively studied in the context of temporal lobe epilepsies (Noebels et al., 2012) and is inducible by mechanical (Laurberg and Zimmer, 1981; Zimmer and Gähwiler, 1987), electrical (Sutula et al., 1988), chemical (Tauck and Nadler, 1985), and genetic approaches (Luo et al., 2021). During MF sprouting, granule cells (GCs) grow new axonal branches into the inner molecular layer (IML) of dentate gyrus and form synapses mostly on proximal dendrites of GCs (Laurberg and Zimmer, 1981; Wenzel et al., 2000; Cavazos et al., 2003; Frotscher et al., 2006; Luo et al., 2021), but potentially also on interneurons as observed in chronically epileptic rats (Frotscher et al., 2006). This new circuit is formed on top of the developmentally established

MF circuit, which extends into CA3 (Hainmueller and Bartos, 2020). As any neuronal wiring, MF sprouting is thought to require molecular programs for axon growth, target specification, and synapse formation (Godale and Danzer, 2018; Koyama and Ikegaya, 2018; Luo et al., 2021). Such processes generally involve synaptic cell-surface receptors and cell-adhesion molecules (Missaire and Hindges, 2015; de Wit and Ghosh, 2016; Sanes and Zipursky, 2020; Südhof, 2021), which hereafter we collectively refer to as CAMs, for short.

The role of different CAMs during developmental MF wiring is relatively well understood. Netrin and slit signaling control axon guidance toward CA3 (Muramatsu et al., 2010). Plexin and semaphorin signaling establish layer specificity within CA3 (Chen et al., 2000; Suto et al., 2007; Tawarayama et al., 2010). Other CAMs regulate MF target specificity and/or synapse function to CA3 pyramidal cells (NCAM, Cdh9, Gpr158) (Cremer et al., 1998; Williams et al., 2011; Basu et al., 2017; Condomitti et al., 2018), interneurons (Kirrel3, Igsf8) (Martin et al., 2015; Apóstolo et al., 2020), or possibly to both (Pcdh19) (Hoshina et al., 2021). Finally, semaphorin-neuropilin-plexin (Bagri et al., 2003) and ephrin (Xu and Henkemeyer, 2009; Liu et al., 2018) signaling control MF pruning. By contrast, CAM signaling in MF sprouting is much less understood. While abundance changes in multiple CAMs have been reported in models of temporal lobe epilepsy or directly in sprouting fibers, their involvement in sprouting remains elusive (see section “Discussion”). Recently, we studied transcriptomic mechanisms of MF sprouting and identified a transcriptomic regulator, Id2, whose sole overexpression in GCs induced MF sprouting (Luo et al., 2021). While Id2-induced MF sprouting alone was insufficient to provoke pathological network activity seen in epilepsy, further lessening its potential as a clinical target (Buckmaster, 2014), MF sprouting remains a robust model for studying circuit formation in the adult brain.

Here, we used single-cell RNA-seq data generated using the intrahippocampal kainic acid- (KA) injection model to study CAMs in MF sprouting. We used the KA, but not Id2, model because MF sprouting develops significantly faster by KA (within weeks) than by Id2 (requires months) (Luo et al., 2021). Thus, functional testing, which here we aimed for, is more attainable in the KA model. We focused on differentially expressed CAMs, and identified three candidate genes—*Fat3*, *Cntn4* and *Pcdh11x*—which were upregulated after sprouting. We targeted these genes by CRISPR/Cas9 guide RNAs (gRNAs) to disrupt their genomic sequences in GCs *in vivo*, and confirmed mutation/deletions in *Pcdh11x*, likely rendering this gene null mutant in most cells. After GC-specific *Pcdh11x* KO, KA still induced MF sprouting, but new synapses frequently and atypically formed on GC somata.

Materials and methods

Animals

All animal protocols and husbandry practices were approved by the Veterinary Office of Zurich Kanton. The University of Zurich animal facilities comply with all appropriate standards (cages, space per animal, temperature, light, humidity, food, and water) and cages were enriched with materials that allow the animals to exert their natural behavior. The following lines were used in this study: Calb1-Cre: B6;129S-Calb1^{TM2.1^(cre)Hze}/J, JAX:028532 and H11-LSL-Cas9: B6;129-Igs2tm1(CAG-cas9*)Mmw/J, JAX:026816. The animals used in this study were obtained by mating the homozygous Calb1-Cre mice with heterozygous H11-LSL-Cas9 mice. In each experiment, the control and non-control animals were littermates.

List of CAMs

An extended set of 421 CAMs was used for gene expression analysis. We used a previously published list of 406 CAMs (Földy et al., 2016), to which *Nptxr*, *Sema3a*, *Sema3c*, *Sema3d*, *Sema3g*, *Sema4a*, *Sema4b*, *Sema4c*, *Sema4f*, *Sema5a*, *Sema5b*, *Sema6a*, *Sema6b*, *Sema6c*, *Slit1*, *Slit2*, *Slit3* were added, whereas *Ptpn2* and *Ptpn5* were removed as non-receptor type protein tyrosine phosphatases.

Design of guide RNAs

To design guide RNAs (gRNAs), we prioritized to (i) target early coding regions that are shared by all transcript variants of a gene in order to maximize the probability of introducing functionally disabling mutations and/or deletions, (ii) minimize the possibility of unwanted off-target effects, and (iii) maximize editing efficacy at the intended target site. For each targeted gene (i.e., *Fat3*, *Cntn4*, and *Pcdh11x*), two gRNAs (19–21 bp long) were designed targeting possible target sites on exons 1–3, followed by a 3 bp long NGG PAM sequence on the 3' end (see **Supplementary Figure 1A** for specific sequences). Each gRNAs were evaluated by “CRISPR-Cas9 gRNA checker” (Integrated DNA technologies, Inc.), resulting in two scores: (1) “on-target score” that indicates the predicted editing performance of gRNA at the intended target site (higher value indicates better performance) and (2) “off-target score” that indicates potential off-target effects and N (number) nucleotide mismatch hits during genome screening (in a range from 0 to 100, higher value indicates lower off-target risk). *Fat3*-gRNA1: on-target score 66, off-target score 36 (high off-target risk), 0 mismatch only on *Fat3*, no potential off-target sites were identified with

1 or 2 mismatches. *Fat3*-gRNA2: on-target score 36 (low on-target performance), off-target score 82, 0 mismatch hit only on *Fat3*, no potential off-target sites with 1 mismatch, one 2 mismatch off-target site were found in a non-coding region (chr5: + 18040716). *Cntn4*-gRNA1: on-target score 40 (low on-target performance), off-target score 86, 0 mismatch hit only on *Cntn4*, no potential off-target sites with 1 mismatch, one 2 mismatch off-target site were found in a non-coding region (chr6: + 8683610). *Cntn4*-gRNA2: on-target score 8 (low on-target performance), off-target score 58, 0 mismatch hit only on *Cntn4*, no potential off-target sites with 1 or 2 mismatches. *Pcdh11x*-gRNA1: on-target score 56, off-target score 85, 0 mismatch only on *Pcdh11x*, no potential off-target sites with 1 or 2 mismatches. *Pcdh11x*-gRNA2: on-target score 53, off-target score 72, 0 mismatch hit only on *Pcdh11x*, no potential off-target sites with 1 or 2 mismatches. Note that the gRNAs on-target performance was subsequently tested and validated in cell cultures before *in vivo* experiments (see below).

Plasmids and viruses

For *in vivo* genomic targeting of CAMs, gRNAs were designed and cloned into pBSK-U6 backbone (pBSK-U6-gRNAs). The plasmids were purified and used for evaluation of knockout efficiency in cell culture. After evaluation, the same gRNAs were cloned into Cre-dependent tRFP expression vector and packaged into adeno-associated virus (AAV) serotype DJ/8. For *Fat3* targeting, a viral mixture (2.2×10^{13} vg/ml) of vWL51.AAVDJ8/2-[hU6-gRNA1(mFat3)]rev-hSyn1-dlox-TurboRFP(rev)-dlox-WPRE-hGHp(A) and vWL52.AAVDJ8/2-[hU6-gRNA2(mFat3)]rev-hSyn1-dlox-TurboRFP(rev)-dlox-WPRE-hGHp(A) were used. For *Cntn4* targeting, a viral mixture (1.7×10^{13} vg/ml) of vWL44.AAVDJ8/2-[hU6-gRNA1(mCNTN4)]rev-hSyn1-TurboRFP(rev)-WPRE-hGHp(A) and vWL45.AAVDJ8/2-[hU6-gRNA2(mCntn4)]rev-hSyn1-TurboRFP(rev)-WPRE-hGHp(A) were used. For *Pcdh11x* targeting, a viral mixture (1.7×10^{13} vg/ml) of vWL46.AAVDJ8/2-[hU6-gRNA1(mPcdh11x)]rev-hSyn1-TurboRFP(rev)-WPRE-hGHp(A) and vWL47.AAVDJ8/2-[hU6-gRNA2(mPcdh11x)]rev-hSyn1-TurboRFP(rev)-WPRE-hGHp(A) were used. All viral vectors were produced by the Viral Vector Facility (VVF) of the Neuroscience Center Zurich (ZNZ).

Validation of CAM targeting guide RNAs in cell culture

The mixture of gRNA expressing vectors (0.4 μ g of pBSK-U6-gRNA1 and 0.4 μ g of pBSK-U6-gRNA2) were transfected into Neuro-2a cells expressing doxycycline-inducible CRISPR Cas9 nuclease from Rosa26 locus (GeneCopoeia, SL508)

using Lipofectamine 3000, according to recommendations of the manufacturer (Invitrogen). Forty-eight hours after transfection, doxycycline (1 μ g/ml) was applied to induce stable Cas9 expression. To maintain Cas9 expression, the medium containing doxycycline was renewed every 48 h. Cells were harvested 7 days after transfection and prepared for Sanger sequencing.

Stereotaxic injection

Mice were deeply anesthetized and placed into a stereotactic apparatus. Microinjections were performed at a rate of 100 nl/min using a programmable syringe pump with a 35-gauge beveled NanoFil needle (World Precision Instruments, United States). For *in vivo* CAM targeting, 500 nl of the above mentioned viruses were injected into the ventral dentate gyrus (−3.4 mm anterior/posterior, 2.9 mm middle/lateral, −3.3 mm ventral/dorsal to bregma). To induce MF sprouting, 70 nl of KA (5 mM) was injected into the same position 4 weeks later or into gRNA non-injected animals.

In vitro electrophysiology

Brain slice preparation, recording solutions, whole-cell patch-clamp recording, and measurement of biophysical properties were as previously described (Luo et al., 2021). In short, neurons were visualized by infrared differential interference contrast optics in an upright microscope (Olympus; BX-51WI) using Hamamatsu Orca-Flash 4.0 CMOS camera and recorded using borosilicate glass pipettes with filament (Harvard Apparatus; GC150F-10; o.d. 1.5 mm; i.d. 0.86 mm; 10-cm length). Recordings were made using MultiClamp700B amplifier (Molecular Devices), signals were filtered at 10 kHz (Bessel filter) and digitized (50 kHz) with a Digidata1440A and pClamp10 (Molecular Devices). Spontaneous events were recorded in voltage clamp mode at −60 mV for 5 min, in presence of Gabazine (10 μ M), or APV (10 μ M) and NBQX (5 μ M). The data analysis was performed using Python, R, Clampfit (Molecular Devices), and MiniAnalysis. For subsequent *post hoc* visualization, cells were filled with biocytin (Sigma-Aldrich, 2%) during recording. For all electrophysiological experiments, the experimenter was blind to the recording condition.

Histology

Sample preparation

Animals were deeply anesthetized and transcardially perfused first with 3 ml 0.9% saline solution followed by 3 ml 0.1% Na₂S in 0.1 M PB solution, and then by 4%

paraformaldehyde (PFA) in 0.1 M PB (1ml/1g bodyweight). Brains were immersed into 4% PFA in 0.1 M PB overnight at 4°C and then sectioned the next day using a vibratome, or further transferred into 30% sucrose in 0.1 M PB and stored at 4°C until sectioning using a frozen tissue sliding microtome. Fixed brains were cut into 50 or 80 μ m thick horizontal sections.

Immunohistochemistry

Slices were first permeabilized and blocked in incubating medium (0.1 M PB containing 5% normal goat serum and 0.2% Triton) for 1 hour at room temperature, and then incubated overnight with primary antibodies at 4°C. Primary antibodies used: rabbit monoclonal anti-SLC30A3 (ZnT3; ThermoFisher, PA5-77769, 1:600), guinea pig polyclonal ZnT3 antiserum (Synaptic system, #197004, 1:500), rabbit polyclonal PCDH11X antibody (aa987-1117, LS-C673568, LifeSpan BioSciences, 1:500). Next day, slices were rinsed in 0.1 M PB and incubated with secondary antibodies overnight at 4°C. Secondary antibodies used: goat anti-rabbit IgG (H + L) cross-adsorbed, Alexa Fluor 488 (Invitrogen, A-11008, 1:500), anti-guinea pig IgG (H + L) highly cross-adsorbed secondary antibody, Alexa Fluor 568 (Invitrogen, A-11075, 1:500). Sections were rinsed in 0.1 M PB (some sections were subsequently stained with DAPI for nuclear staining) and mounted in Vectashield (Vector Laboratories) for analysis.

Timm's staining

Sections were rinsed in 0.1 M PB and post-fixed in 2.5% glutaraldehyde in 0.1 M PB solution for 10 min. Then, sections were rinsed in 0.1 M PB and immersed in Timm's reaction solutions, a 12:6:2 mixture of 20% gum arabic, hydroquinone, and citric acid trisodium citrate buffer, with 100 μ l of 17% silver nitrate solution. The reaction was carried out for 20–30 min at 29°C, then slices were washed thoroughly in 0.1 M PB. After dehydration steps, the sections were mounted using DPX mounting medium and imaged using a Leica wide-field microscope.

Morphological reconstruction

Biocytin-filled cell-containing brain slices were fixed 4% PFA in 0.1 M PB overnight at 4°C. Next day, DAB staining (Vectastain ABC KIT, Vector Laboratories) was performed, and sections were dehydrated and mounted in DPX mounting medium (Electron Microscopy Science, United Kingdom). Cells were reconstructed using Neurolucida (MicroBrightField, Inc., United States).

Image analysis and quantification

Fluorescent images were acquired using Leica Stellaris 5 confocal microscope. Image analyses and quantification were performed in Fiji (version 2.0.0-rc-68/1.52h).

Quantification of PCDH11X immunostaining in wild-type animals after kainic acid injection

Tile-scan confocal images (1,024 \times 1,024 pixels, zoom 0.75) were obtained using 20x immersion lens (0.75 NA). The mean gray value of PCDH11X immunostaining signals were measured in hilus, granule cell layer (GCL), inner molecular layer (IML), and middle/outer molecular layer (MML/OML). In addition, the mean gray value of PCDH11X immunostaining signal was measured in an area (that is below CA3 and outside hilus) that appeared to be PCDH11X negative in all conditions, to be used as baseline. Then, GCL, IML, and MML/OML signal intensities were normalized by subtracting this baseline signal intensity. In this manner, two images per animal were analyzed, the average values of which are shown in figure(s). As controls, normalized mean gray values from sections collected from ipsi- and contralateral hippocampus of saline injected animals (6 or 10 days after saline) and from the contralateral hippocampus of KA injected animals (6 or 10 days after KA) were averaged and used.

Quantification of PCDH11X immunostaining after *Pcdh11x*^{Control+KA} and *Pcdh11x*^{KO+KA}

To confirm the location of injections and sufficient delivery of gRNAs into GCs, we included a turboRFP (tRFP) sequence in gRNA expression vectors. As intended, the tRFP signal broadly labeled GCs. However, we also found that the tRFP signal was strong and cross-bleed into the GFP channel to be used for detection of PCDH11X signals. This effect was most prominent in GCL where GC somata were strongly labeled with tRFP. To alleviate this problem, we exposed sections to light for several hours to bleach the tRFP signal and stained them for PCDH11X only afterward. While this treatment lowered the tRFP intensity, it did not completely eliminate the tRFP signal from the GFP channel. We then quantified PCDH11X signal intensity with and without normalization for the tRFP signal seen in the GFP channel. For quantification, tile-scan confocal images (1,024 \times 1,024 pixels, zoom 0.75) were obtained using 20x immersion lens (0.75 NA). To obtain tRFP-normalized values, we used the same approach as described above (see *Quantification of PCDH11X immunostaining in wild-type animals after KA injection*). To obtain tRFP-normalized values, we first measured signal intensity in the GFP channel in hilus, GCL, IML, MML, and OML separately in sections from *Pcdh11x*^{Control} and *Pcdh11x*^{KO} animals. We chose to do this in KA-non-injected samples, because in these the tRFP signal in the GFP channel was similar to those in KA-injected samples, but the PCDH11X signal was expected to be the lowest. Then, these values were averaged between *Pcdh11x*^{Control} and *Pcdh11x*^{KO} in each region separately (i.e. hilus, GCL, IML, MML/OML), to be used as baselines. Subsequently, these baseline values

were subtracted from PCDH11X signal intensities measured in each area (i.e., hilus, GCL, IML, MML/OML) from KA-injected *Pcdh11x*^{Control+KA} and *Pcdh11x*^{KO+KA} animals. In this manner, two images per animal were analyzed, the average values of which are shown in figure(s). Independently of the approach used (i.e., tRFP-normalization or tRFP-non-normalization), PCDH11X signal intensities were significantly lower in GCL and IML of *Pcdh11x*^{KO+KA} samples compared to *Pcdh11x*^{Control+KA} samples.

Quantification of Timm's staining intensity

Bright-field images were acquired using a THUNDER (Leica) wide-field microscope using 40x lens (0.95 NA). Using Fiji, the mean gray value of Timm signals were measured in both GCL and IML, from which the GCL/IML ratio of gray values was calculated. The average value from 4 sections per animal was shown in the plot.

Quantification of ZnT3-positive puncta surrounding GC somata

Single panel confocal images (1,024 × 1,024 pixels) were obtained using 63× oil lens (1.4 NA). ZnT3 + signals on 95–170 GC somata from at least 2 images were quantified per animal. The percentage of GC somata surrounded by different numbers of ZnT3 + puncta was calculated based on the surrounding ZnT3 + puncta numbers per soma and total number of somata analyzed.

Immuno-electron microscopy

After fixation, brains were cut into 80 μm thick sections using a vibratome. For better penetration of the antibodies, single sections were frozen/thawed in liquid nitrogen using sucrose as cryoprotectant with the following concentration steps 10, 20, 30, 20, 10% and washed several times in 0.1 M PB. Then, the sections were treated with 0.5% NaBH₄ to bind free aldehyde groups for 15 min, followed by 5 min treatment with 3% H₂O₂ and 10% Methanol in 0.1 M PB to reduce endogenous peroxidase. After thoroughly washing in 0.1 M PB, the sections were blocked for 1 h at room temperature in 5% normal goat serum in 0.1 M PB and then incubated in rabbit monoclonal anti-SLC30A3 (ZnT3; ThermoFisher, PA5-77769, 1:600) at 4°C overnight. Next day, sections were incubated in biotinylated anti-rabbit solution (1:100, Vector Laboratories) at 4°C overnight. Next day, sections were developed with a standard avidin-biotin peroxidase kit (1:500; Vectastain) and postfixed in 1% OsO₄ followed by 3 × 5 min washing in 0.1 M PB. After washing, sections were dehydrated and embedded in durcupan

(Sigma-Aldrich) and re-sectioned. Finally, 60 nm ultra-thin sections were contrasted with 3% Lead citrate (Leica) and imaged using a FEI Tecnai G2 Spirit transmission electron microscope or Apreo VS (Thermo Fisher Scientific) scanning electron microscope. 3D rendering was performed with Fiji/ImageJ.

Statistical analyses

Statistical analyses were performed using Prism 9. All values represent mean ± standard error of the mean (SEM). The significance of differences was assessed using Welch's *t*-test, Mann–Whitney *U* test, one-way ANOVA, or two-way ANOVA, whichever is applicable (noted in text and/or figure legends). Data distribution normality was tested by Shapiro–Wilk Test. For normal distributions, Welch's *t*-test was performed. For non-normal distributions, non-parametric Mann–Whitney *U* test were performed. Significant main effects or interactions were followed up with *post hoc* testing using the original FDR method of Benjamini and Hochberg. The threshold for significance was *p* = 0.05 or FDR = 0.05, with a precise *p* value stated in each case. Non-significance is indicated with 'ns'. All tests were two-sided. Data analyses and quantifications were done blindly with respect to treatment.

Results

CAM expression changes during mossy fiber sprouting

To begin, we further analyzed our previously published single-cell transcriptomic data set consisting of control GCs as well as GCs 1 and 14 days after unilateral hippocampal KA injection (Figure 1A) (Luo et al., 2021; GSE 161619). Based on an extended list of 421 CAMs (see Földy et al., 2016 and section “Materials and methods”), we considered differentially expressed genes (fold change > 2 and FDR < 0.05) between the control and KA data sets (Figure 1B). This analysis revealed significant enrichment of *Fat3*, *Pcdh11x* in KA GCs, both 1 and 14 days after KA injection. *Fat3*, an atypical cadherin, has been implicated in the development of neuronal morphology (Deans et al., 2011; Krol et al., 2016). *Pcdh11x*, a delta1-type protocadherin, has been implicated in homophilic *trans* cell-cell interactions (Harrison et al., 2020; Pancho et al., 2020), dendritic branching (Wu et al., 2015), and neuronal stem cell differentiation and proliferation (Zhang et al., 2014). We shortlisted these molecules for further analysis. Although *Cntn4* was significantly enriched only in 14-day KA GCs after MF sprouting has developed, we also shortlisted this gene, because it has been linked to circuit formation

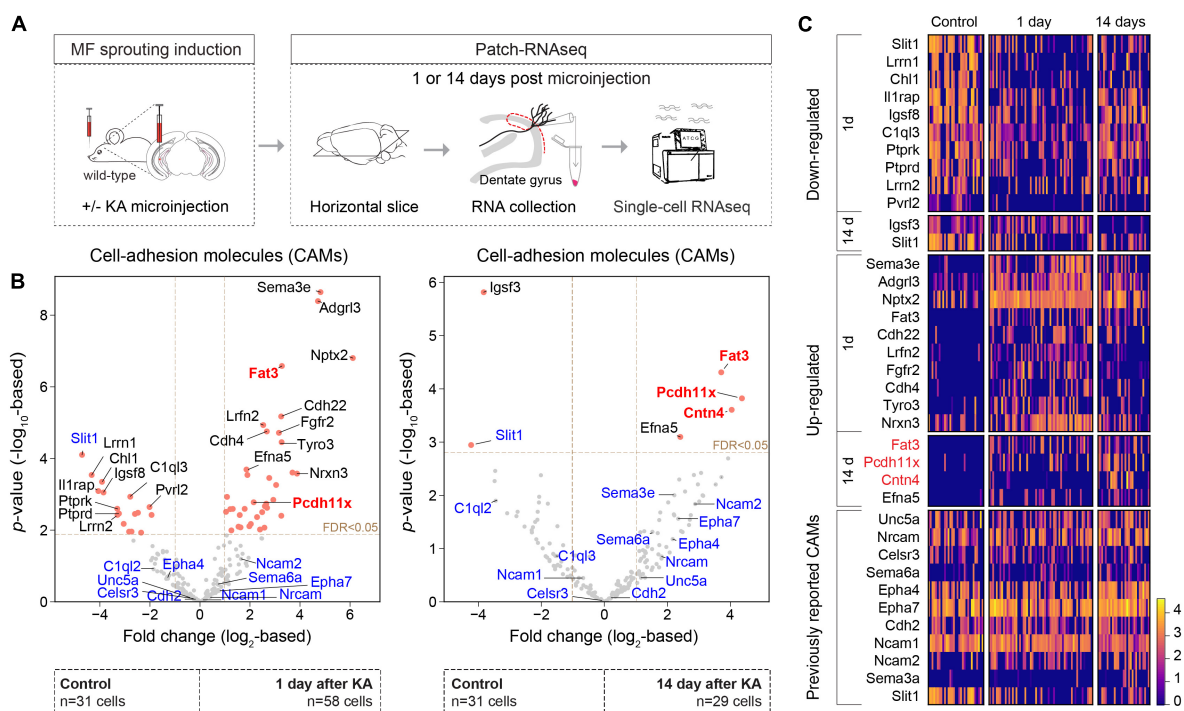


FIGURE 1

CAM expression changes during MF sprouting. (A) Experimental design and schedules used for generating the single-cell RNAseq dataset (Luo et al., 2021; GSE 161619). (B) Volcano plots show differentially expressed CAMs in GC 1 (left panel) and 14 days (right panel) after intrahippocampal KA injection compared to controls. Red points denote differentially expressed genes (FDR < 0.05 and fold change > 2). Gene names highlighted with blue were previously reported in epilepsy and/or MF sprouting models (see section “Discussion”). Gene names highlighted with red were shortlisted for further analysis in this study. (C) Heat map of top 10 differentially expressed genes and genes/molecules previously reported in epilepsy and/or MF sprouting models. Scale bar shows log2-normalized gene expression level.

(Oguro-Ando et al., 2017), target specification (Osterhout et al., 2015), synaptic plasticity (Oguro-Ando et al., 2021), neurodevelopmental disorders (Baig et al., 2017; Oguro-Ando et al., 2017), and Alzheimer's disease (Carrasquillo et al., 2009). In addition, we looked for CAMs, whose abundance change has been reported in different temporal lobe epilepsy models or in MF sprouting (see section “Discussion,” Figure 1C). However, with the exception of *Slit1* (previously reported to be up-regulated in hippocampal tissue, but down-regulated in KA GCs), their expression did not significantly change in our single-cell data (Figures 1B,C).

Genomic targeting of CAMs in adult granule cells

To study the role of *Fat3*, *Pcdh11x*, and *Cntn4* in MF sprouting, we aimed to introduce loss-of-function deletions and/or mutations in their genomic sequences. To achieve this goal, we designed two CRISPR/Cas9 guide RNAs (gRNAs) targeting each gene, to be delivered into GCs in the adult brain (Figure 2A and Supplementary Figure 1A, and section “Materials and methods”). To identify the transfected area

and neurons that expressed the gRNA, we also included a Cre-dependent turboRFP (tRFP) reporter into the gRNA-expressing AAV vectors. This *in vivo* gene editing approach minimized unwanted effects during development, ensured cell type-specificity and—since *Fat3*, *Pcdh11x*, and *Cntn4* transcripts were virtually absent from control GCs (Figure 1C)—that loss-of-function effects would manifest themselves only after KA injections.

First, we tested gRNAs targeting each gene in cell cultures and confirmed their efficacy in introducing genomic mutations (Supplementary Figure 1). Second, to achieve GC-specific gene manipulations, we separately delivered the pairs of gRNAs into the dentate gyrus of 2 months old *Calb1^{Cre/+};H1^{LSL-Cas9/+}* mice, in which GCs expressed Cas9. Four weeks later, we confirmed broad presence of the tRFP reporter in the dentate gyrus and prepared lysates for target gene specific PCR amplification. Genomic sequence analysis revealed multiple mutations or large deletions (>200 basepair) in *Pcdh11x*, likely rendering this gene null mutant (KO) in most neurons (Figure 2B and Supplementary Figure 1). By contrast, *Fat3* and *Cntn4* sequences did not display deleterious effects. To further test these two genes, we sequenced 24 single clones from the PCR product of each. This analysis revealed insertions/deletions

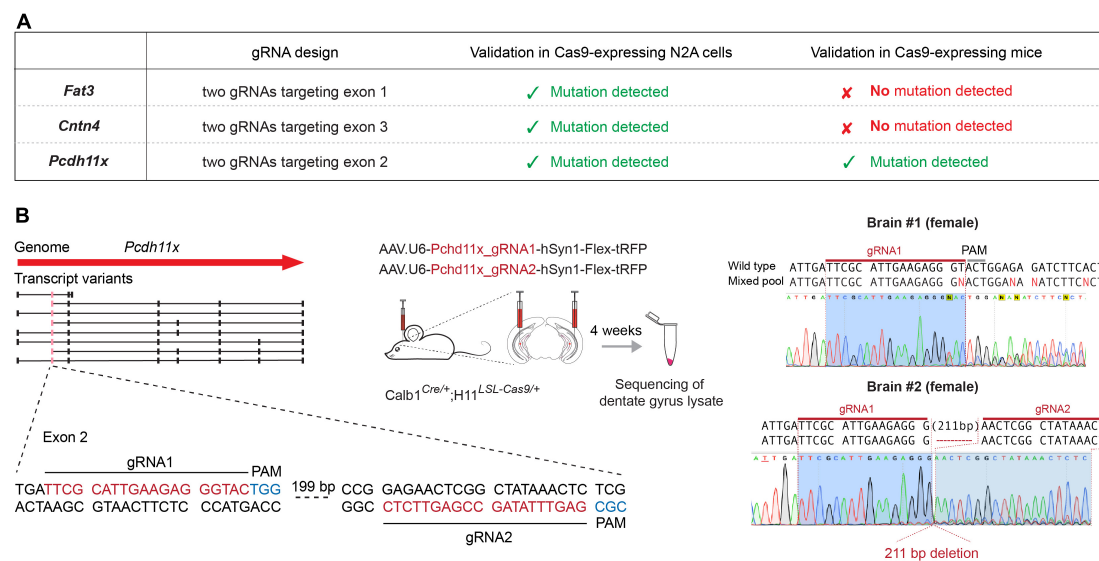


FIGURE 2

Genomic targeting of CAMs in adult GCs. (A) Schematic representation of the genome targeting approach for *Fat3*, *Cntn4*, and *Pcdh11x*. Table shows targeted exons and the presence or absence of mutations during cell culture (Cas9-expressing N2A cells) and *in vivo* (Cas9-expressing mice) validation. (B) *In vivo* genomic targeting of *Pcdh11x*. Left panel shows specific gRNA design and experimental schedule. Right panel shows sequence maps of detected mutations and/or deletions in dentate gyrus lysates prepared from two different mice.

only in 1/24 of *Fat3* and 2/24 of *Cntn4* clones, further confirming their inefficient targeting *in vivo* (Supplementary Figure 1). Variations in the *in vivo* targeting efficiency of different genes were not completely unexpected, however, based on these results we could proceed further only with *Pcdh11x*.

PCDH11X protein levels in the dentate gyrus

To investigate the role of *Pcdh11x* in MF sprouting, we first aimed to establish the extent of PCDH11X protein expression (we refer to protein form with capitalized gene name) in the dentate gyrus of wild-type animals, including if cell types other than GCs expressed this protein. Using PCDH11X antibody, we immunostained sections 6–10 days after saline- and KA-injections (Figures 3A,B and Supplementary Figure 2). We presumed that *Pcdh11x* mRNA seen 1 day after KA (Figure 1) would be translated and detectable by this time. In addition, 6–10 days after KA likely represents a critical period for establishing MF target specificity, since most growing axons would still advance toward IML during this phase (MF sprouting starts ~2–3 days after KA and becomes largely established ~14 days after KA) (Luo et al., 2021).

In controls, some cells in the hilus, GCL and dentate molecular layers appeared to be PCDH11X positive and a weak punctate, possibly background signal, could be observed in all dentate layers (Figure 3B and Supplementary Figure 2). About 6–10 after KA, less hilar but more GCL cells were

PCDH11X positive, and a prominent punctate PCDH11X signal became apparent in GCL and IML (Figures 3B,C). In part, the emergence of this signal was due to PCDH11X located in the somato-dendritic domain of GCs (Figure 3B). In addition, PCDH11X appeared to localize in zinc transporter-3 (ZnT3, a frequently used MF marker) positive MF boutons in IML and GCL (Figure 3B, inserts in lower right panels). These results thus revealed KA-induced PCDH11X enrichment in areas relevant for MF sprouting and during a phase likely critical for target specification. However, the question whether PCDH11X enrichment originated only from GCs or possibly also from other cells expressing this protein remained open. To answer this question, we used the above described Cas9 system to evaluate if genetic *Pcdh11x* KO in GCs occluded KA-induced PCDH11X enrichment.

We injected *Pcdh11x* targeting gRNA- and tRFP-containing AAVs into the ventral dentate gyrus of *Calb1*^{Cre/+} (*Pcdh11x*^{Control}, lacking Cas9 expression) or *Calb1*^{Cre/+};H11^{LSL-Cas9/+} mice (*Pcdh11x*^{KO}). Four weeks later, we injected KA into the left dentate gyrus to induce *Pcdh11x* upregulation and MF sprouting, and then two weeks later, we prepared 50 μ m thick horizontal sections for histological analysis (Figure 3D). Using the tRFP reporter, we localized the transfected area and quantified the ratio of tRFP + and DAPI + cells in GCL, which revealed > 90% transfection efficacy both conditions (*Pcdh11x*^{Control}+KA: 92.4 \pm 0.97%, n = 3; *Pcdh11x*^{KO}+KA: 92.82 \pm 0.49%, n = 3) showing that our manipulations broadly impacted GCs. Using immunostaining, we then examined PCDH11X protein expression 14 days

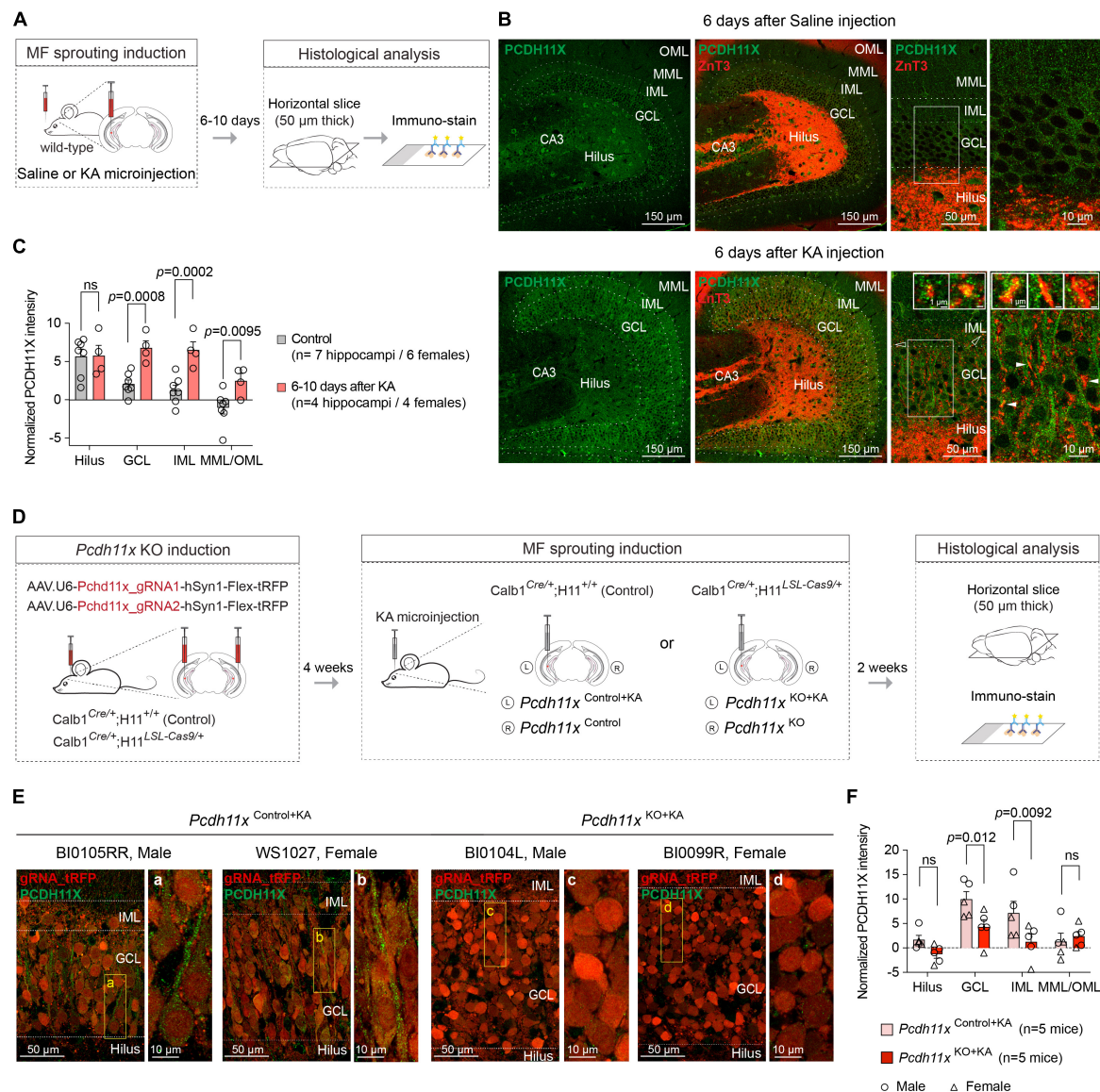


FIGURE 3

PCDH11X protein expression in the dentate gyrus. **(A)** Schematic representation of the experimental design. **(B)** Confocal images show PCDH11X and ZnT3 immunostaining in the dentate gyrus 6 days after saline (upper row) and KA injection (lower row). From left to right, PCDH11X immunostaining, PCDH11X and ZnT3 immunostaining, higher magnification images of the PCDH11X and ZnT3 immunostaining, and finally higher magnification images of the regions highlighted with white frames in the previous panels are shown. In the lower right panels, inserts show PCDH11X localization in ZnT3 + MF boutons in IML (empty arrowheads) and in GCL (white arrowheads). **(C)** Quantification of the PCDH11X signal in controls and 6–10 days after KA (two-way ANOVA, F_{Layer} (3,27) = 17, $p < 0.0001$; $F_{\text{Treatment}}$ (1,9) = 14, $p = 0.0051$; $F_{\text{Layer} \times \text{Treatment}}$ (3,27) = 5.1, $p = 0.0066$; post hoc analyses: control vs KA, hilus: ns, $p = 0.94$; GCL: $p = 0.0008$; IML: $p = 0.0002$; MML/OML: $p = 0.0095$). **(D)** Schematic representation of the experimental design in Cas9-expressing and -non-expressing mice. **(E)** Confocal images show PCDH11X immunostaining in the dentate gyrus of Pcdh11x^{Control+KA} and Pcdh11x^{KO+KA} mice 14 days after KA. Areas highlighted with boxes are shown in higher magnification in panels (a–d). **(F)** Quantification of tRFP-normalized PCDH11X levels in dentate gyrus of Pcdh11x^{Control+KA} and Pcdh11x^{KO+KA} mice [two-way ANOVA, F_{Layer} (3,24) = 19, $p < 0.0001$; F_{KO} (1,8) = 3.7, $p = 0.091$; $F_{\text{Layer} \times \text{KO}}$ (3,24) = 5.5, $p = 0.0049$; post hoc analyses: Pcdh11x^{Control+KA} vs Pcdh11x^{KO+KA}, hilus: ns, $p = 0.17$; GCL: $p = 0.012$; IML: $p = 0.0092$; MML/OML: $p = 0.62$] (for tRFP-non-normalized values see [Supplementary Figure 2](#)).

after KA injection. We found that the punctate and in some cells somato-dendritic PCDH11X labeling was present in Pcdh11x^{Control+KA} (following the same pattern as in wild-type animals 6 days after KA), but largely absent from Pcdh11x^{KO+KA}

samples ([Figure 3B](#)). However, in both Pcdh11x^{Control+KA} and Pcdh11x^{KO+KA} samples, we also noticed that the tRFP signal used for cell labeling (intended to be visible only in RFP channel) was intense and visible in the GFP channel used

for PCDH11X detection. This effect was most prominent in GCL where GC somata are located. To address this issue, we quantified PCDH11X signals with and without normalization to tRFP seen in the GFP channel (see section “Materials and methods”). Independently of the normalization approach used, PCDH11X signal intensity was significantly lower in GCL and IML in *Pcdh11x*^{KO+KA} compared to *Pcdh11x*^{Control+KA} samples (tRFP-normalized, *Pcdh11x*^{Control+KA}: hilus: 1.7 ± 0.88 , GCL: 9.97 ± 1.57 , IML: 7.17 ± 2.39 , MML/OML: 1.33 ± 1.68 , $n = 5$; *Pcdh11x*^{KO+KA}: hilus: -1.28 ± 0.81 , GCL: 4.30 ± 1.49 , IML: 1.27 ± 1.57 , MML/OML: 2.40 ± 0.98 , $n = 5$, **Figures 3E,F**) (for tRFP-non-normalized data, see **Supplementary Figure 2B,C**).

Together, these results suggested that the KA-induced *Pcdh11x* mRNA upregulation (**Figures 1B,C**) lead to an increased PCDH11X protein expression in the dentate gyrus, and this PCDH11X enrichment was GC-dependent. In addition, related to *Pcdh11x* KO but irrespective of PCDH11X labeling, an increased GCL dispersion in the *Pcdh11x*^{KO+KA} dentate gyrus become apparent (see **Figure 3E** and below).

Impact of *Pcdh11x* KO on mossy fiber sprouting

To study the KA-induced phenotypes in *Pcdh11x* KO, we employed the same experimental approach as described above (**Figure 3D**). First, we analyzed GCL dispersion, which is although mechanistically independent from MF sprouting (Haas et al., 2002; Heinrich et al., 2006; Duveau et al., 2011), a known phenotype of KA injections in the dentate gyrus. While KA-induced GCL dispersion developed both in *Pcdh11x*^{Control+KA} and *Pcdh11x*^{KO+KA}, it was more pronounced in KOs (GCL width: non-injected, $66 \pm 1.8 \mu\text{m}$, *Pcdh11x*^{Control+KA}, $109 \pm 6.2 \mu\text{m}$, *Pcdh11x*^{KO+KA}, $138 \pm 5.9 \mu\text{m}$; one-way ANOVA, *Pcdh11x*^{Control+KA} vs *Pcdh11x*^{KO+KA}, $p = 0.0031$; GCL area: non-injected, $0.097 \pm 0.005 \text{ mm}^2$, *Pcdh11x*^{Control+KA}, $0.16 \pm 0.013 \text{ mm}^2$, *Pcdh11x*^{KO+KA}, $0.21 \pm 0.011 \text{ mm}^2$, **Figures 4A,B**).

Next, we examined the impact of *Pcdh11x* KO on MF sprouting. To visualize MF sprouting, we utilized two MF labeling approaches: Timm's staining and ZnT3 immunostaining (**Figure 4C**) (Luo et al., 2021). Using Timm's staining, we observed dense signal in IML of *Pcdh11x*^{Control+KA}, which is the typical targeting zone of MF sprouting. By contrast, the Timm's signal became more diffuse overall but also denser in GCL of *Pcdh11x*^{KO+KA}, highlighting a pattern atypical for MF sprouting. To quantify these observations, we measured the signal intensity ratio between GCL and IML, which was significantly higher in KOs than in controls (GCL/IML signal ratio: *Pcdh11x*^{KO+KA}, 0.93 ± 0.046 , $n = 6$ mice; *Pcdh11x*^{Control+KA}, 0.71 ± 0.04 , $n = 6$ mice; Welch's t -test, $p = 0.0054$) (**Figures 4D,E**). ZnT3 immunostaining confirmed this pattern. A large number of ZnT3 + puncta were present

in the IML of both *Pcdh11x*^{Control+KA} and *Pcdh11x*^{KO+KA}, but become significantly enriched in the GCL of *Pcdh11x*^{KO+KA} compared to *Pcdh11x*^{Control+KA} (**Figure 4F**), suggesting that MF sprouting target specification was altered in KOs.

To further study this phenotype, we first considered the possibility that the apparent change in target specificity appeared as a consequence of increased GCL dispersion in KOs. According to this scenario, sprouting MF axons in KOs populated the same spatial area as in controls, but the broader GC dispersion created an altered context. To test this possibility, we quantified ZnT3 + puncta density in the inner (proximal to hilus) and outer (proximal to IML) half of GCL, and in IML. We hypothesized that ZnT3 + puncta density would not change in the inner half of GCL if the effect was due to increased GCL dispersion, because the inner half of GCL in KOs remained before the GCL/IML border seen in controls. However, ZnT3 + puncta density was significantly increased both in the inner and outer half of GCL in KOs compared to controls, whereas that in IML was similar in both conditions (*Pcdh11x*^{Control+KA}: GCL inner: $1.4 \pm 0.26 \times 10^4$ puncta/mm², GCL outer: $1.0 \pm 0.13 \times 10^4$ puncta/mm², IML: $3.4 \pm 0.58 \times 10^4$ puncta/mm², $n = 5$ mice; *Pcdh11x*^{KO+KA}: GCL inner: $2.6 \pm 0.27 \times 10^4$ puncta/mm², GCL outer: $2.2 \pm 0.21 \times 10^4$ puncta/mm², IML: $3.8 \pm 0.31 \times 10^4$ puncta/mm², $n = 6$ mice) (**Figure 4G**), suggesting that target specificity in KOs has changed independently of GCL dispersion. Consequently, the total (as measured in the inner and outer half of GCL, and IML) ZnT3 + puncta density (*Pcdh11x*^{Control+KA}: $1.8 \pm 0.25 \times 10^4$ puncta/mm², $n = 5$ mice; *Pcdh11x*^{KO+KA}: $2.8 \pm 0.17 \times 10^4$ puncta/mm², $n = 6$ mice) and the GCL/IML ZnT3 + puncta density ratio increased in KOs (*Pcdh11x*^{Control+KA}: 0.39 ± 0.044 , $n = 5$ mice; *Pcdh11x*^{KO+KA}: 0.66 ± 0.043 , $n = 6$ mice) (**Figure 4G**).

To gain further insights into the target specification of MF sprouting, we quantified the number of ZnT3 + puncta surrounding GC somata as a proxy for potential synapses. In *Pcdh11x*^{Control+KA}, we found that ~50% of GCs somata were lacking adjacent ZnT3 + puncta. By contrast, in *Pcdh11x*^{KO+KA}, only ~20% of GCs somata were lacking adjacent ZnT3 + puncta while the rest were surrounded with more ZnT3 + puncta than those in controls (**Figure 4H**).

Electrophysiological characterization of *Pcdh11x* KO GCs

Next, following the same injection schedule as above, we made patch-clamp recordings from *Pcdh11x*^{Control+KA} and *Pcdh11x*^{KO+KA} GCs. As additional controls, we also included GCs from *Pcdh11x*^{Control} and *Pcdh11x*^{KO} (six weeks after gRNA injection), neither of which received KA (**Figure 5A**). The resting membrane potential (RMP), input resistance (R), and capacitance (C) of cells reflected consequences of

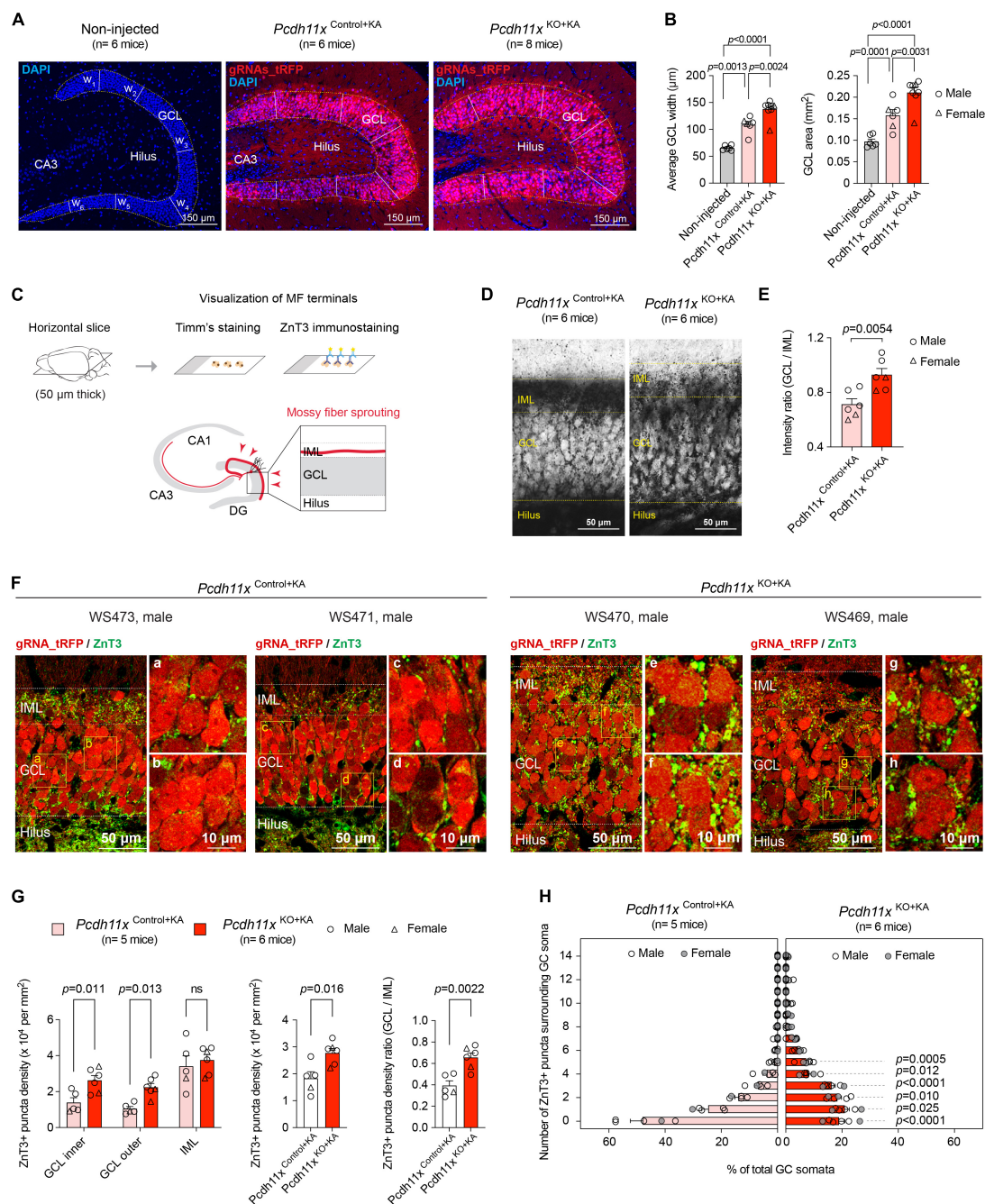


FIGURE 4

Impact of *Pcdh11x* KO on MF sprouting. **(A)** Confocal images show DAPI immunostaining and virally-delivered trFP signal in the dentate gyrus of non-injected control, *Pcdh11x* Control+KA, and *Pcdh11x* KO+KA mice. In each sample, the width of GCL was determined as the average of six width measurement (w_1 to w_6) based on DAPI staining. **(B)** Left plot shows quantification of average GCL width in non-injected, *Pcdh11x* Control+KA, and *Pcdh11x* KO+KA samples. The transected area was localized based on the trFP signal. Right plot shows quantification of GCL area (quantified as the circumference of DAPI staining) in non-injected, *Pcdh11x* Control+KA, and *Pcdh11x* KO+KA samples. Each data point represents one animal (one-way ANOVA tests, $F(2,17) = 29$, $p < 0.0001$; p -values of the post hoc analyses are indicated in the figure). **(C)** Experimental design for visualizing MF boutons by Timm's staining and ZnT3 immunostaining. **(D)** Timm's staining shows stratification of MF boutons in *Pcdh11x* Control+KA and *Pcdh11x* KO+KA mice. **(E)** Quantification of Timm's signal intensity between GCL and IML in *Pcdh11x* Control+KA and *Pcdh11x* KO+KA mice (Welch's t -test). **(F)** ZnT3 staining shows stratification of MF boutons in *Pcdh11x* Control+KA and *Pcdh11x* KO+KA mice. Areas highlighted with boxes are shown in higher magnification in panels (a–h). **(G)** Quantification of ZnT3+ puncta density in the inner and outer half of GCL and in IML (left plot; two-way ANOVA, F_{Layer} (2,18) = 31, $p < 0.0001$; F_{KO} (1,9) = 7.8, $p = 0.021$; $F_{\text{Layer} \times KO}$ (2,18) = 1.9, $p = 0.18$; post hoc analyses: *Pcdh11x* Control+KA vs *Pcdh11x* KO+KA, GCL inner: $p = 0.01$; GCL outer: $p = 0.013$; IML: ns, $p = 0.46$), in GCL and IML together (middle plot; Welch's t -test, $p = 0.016$), and the GCL/IML ratio of ZnT3+ puncta density (right plot; Welch's t -test, $p = 0.0022$). **(H)** Distribution of GC somata (in %) that are surrounded by 0, 1, 2, ..., 14 ZnT3+ boutons in *Pcdh11x* Control+KA and *Pcdh11x* KO+KA mice (two-way ANOVA, $F_{\# \text{ of puncta}}$ (14,126) = 141, $p < 0.0001$; F_{KO} (1,9) = 2.8, $p = 0.13$; $F_{\# \text{ of puncta} \times KO}$ (14,126) = 26, $p < 0.0001$; p -values of the post hoc analysis are indicated in the figure; p -values are > 0.05 for 6 or more puncta).

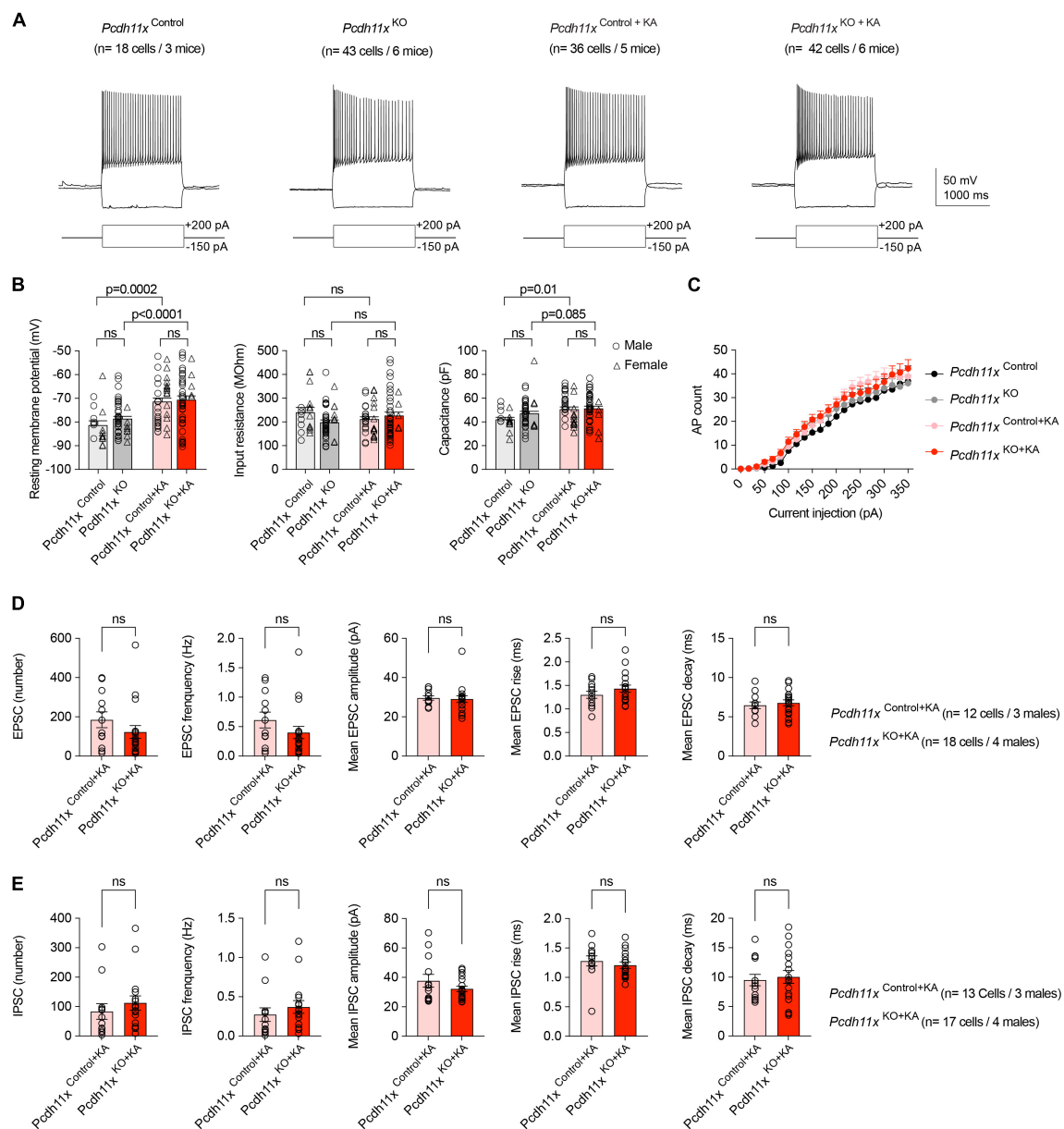


FIGURE 5

Electrophysiological characterization of *Pcdh11x*^{Control+KA} and *Pcdh11x*^{KO+KA} GCs. (A) Example electrophysiological traces show responses to 1.5 s long current pulse injections in *Pcdh11x*^{Control}, *Pcdh11x*^{KO}, *Pcdh11x*^{Control+KA}, and *Pcdh11x*^{KO+KA} GCs. (B) Quantification of resting membrane potential, input resistance, and capacitance (two-way ANOVA tests; resting membrane potential: $F_{KA\ treatment} (1,135) = 30$, $p < 0.0001$; $F_{KO} (1, 135) = 1.1$, $p = 0.30$; $F_{KA\ treatment \times KO} (1,135) = 0.35$, $p = 0.56$; input resistance: $F_{KA\ treatment} (1,135) = 0.0009$, $p = 0.98$; $F_{KO} (1, 135) = 0.92$, $p = 0.33$; $F_{KA\ treatment \times KO} (1,135) = 4.3$, $p = 0.04$; capacitance: $F_{KA\ treatment} (1,135) = 9.8$, $p = 0.0022$; $F_{KO} (1, 135) = 1.8$, $p = 0.18$; $F_{KA\ treatment \times KO} (1,135) = 1.1$, $p = 0.30$; p -values of *post hoc* analyses are indicated in the figure; data points represent single cells). (C) Quantification of steady-state current injection-evoked action potential (AP) counts. (D) Quantification of EPSC parameters recorded from *Pcdh11x*^{Control+KA} and *Pcdh11x*^{KO+KA} GCs (Mann-Whitney U test; data points represent single cells recorded from males). (E) Quantification of IPSC parameters recorded from *Pcdh11x*^{Control+KA} and *Pcdh11x*^{KO+KA} GCs (Mann-Whitney U test; data points represent single cells recorded from males).

KA, but not gRNA treatment (for *Pcdh11x*^{Control}, $n = 18$ cells/*Pcdh11x*^{KO}, $n = 43$ cells/*Pcdh11x*^{Control+KA}, $n = 36$ cells/*Pcdh11x*^{KO+KA}, $n = 42$ cells, respectively; RMP (mV): $-81 \pm 1.80/-79 \pm 1.0/-71 \pm 1.6/-71 \pm 1.7$; R

(MOhm): $240 \pm 20/198 \pm 10/211 \pm 11/226 \pm 14$; C (pF): $42 \pm 1.8/47 \pm 1.8/51 \pm 2.0/52 \pm 1.8$) (Figure 5B). In addition, we analyzed action potential firing threshold, amplitude, and attenuation, none of which showed difference between

the different conditions (not shown). Further, steady-state current injection-evoked action potential (AP) counts did not differ between the groups (Figure 5C). These results established that *Pcdh11x* KO had no effect on the intrinsic electrophysiological properties of GCs. Next, we analyzed spontaneous glutamatergic EPSCs (in presence of 10 μ M Gabazine) and GABAergic IPSCs (in presence of 10 μ M APV and 5 μ M NBQX) in *Pcdh11x*^{Control+KA} and *Pcdh11x*^{KO+KA} GCs. We hypothesized that somatic boutons in *Pcdh11x* KOs may elicit larger and/or faster synaptic events, because they were closer to the recording pipette. However, neither the number and frequency of recorded EPSCs and IPSCs, nor their amplitudes, rise and decay times revealed significant differences between the two groups (Figures 5D,E). This could be because synaptic events evoked by sprouted synapses were not sufficiently represented in our recordings (e.g., they were not spontaneously activated or possibly represented silent synapses), or the recordings did not have sufficient resolution for differences, or both.

Morphological characterization of *Pcdh11x* KO GCs

To study the morphology of individual GCs, we filled cells with biocytin during the patch-clamp recordings and reconstructed them afterwards. A limitation of this approach, however, is that the recovery of axons (e.g. in CA3 or sprouted fibers in IML) is limited in brain slice preparation. First, we analyzed dendritic morphology (Figure 6A), because the overexpression and knockdown of *Pcdh11x* was previously reported to reduce and increase dendritic complexity in developing neurons, respectively (Wu et al., 2015). However, neither the total dendritic length, total dendritic branch count, number of primary and secondary dendrites, nor Sholl analysis showed a difference between *Pcdh11x*^{Control}, *Pcdh11x*^{KO}, *Pcdh11x*^{Control+KA}, and *Pcdh11x*^{KO+KA} GCs (Figures 6B,C). Second, whenever possible, we reconstructed axons from GCs. As expected, GCs in the KA-non-injected control groups (*Pcdh11x*^{Control} and *Pcdh11x*^{KO} GCs) lacked axons in GCL or IML. By comparison, GCs in both KA-injected groups (*Pcdh11x*^{Control+KA} and *Pcdh11x*^{KO+KA} GCs) displayed MF sprouting, i.e., axons were detectable in GCL and to some extent in IML (Figure 6D and Supplementary Figure 3). While insights into target specification by this analysis were limited, it confirmed the presence of *Pcdh11x*^{KO+KA} GC axons in GCL.

Immuno-electron microscopy characterization of sprouted *Pcdh11x* KO GC synapses

Thus far, our histological analyses revealed differences in target specificity between *Pcdh11x* controls and KOs after

MF sprouting, but our electrophysiological and morphological analyses could not further substantiate this. Importantly, the question whether ZnT3 + and Timm + boutons in GCL formed synapses remained open. To answer this question, we prepared horizontal sections from the ventral dentate gyrus, immunostained them with ZnT3 antibody and used immuno-electron microscopy (Figure 7 and Supplementary Figure 4). In *Pcdh11x*^{Control+KA}, we only found dendritic synapses, an expected outcome after KA treatment (Supplementary Figure 4). By contrast, in *Pcdh11x*^{KO+KA}, electron microscopy revealed an abundance of ZnT3 + synapses on GC somata (7G,F,M,N and Supplementary Figure 4). The synapses contained one or multiple release sites and many vesicles. In some cases, ZnT3 + boutons formed synapses both on soma and neighboring dendrites in GCL (Figure 7H) or only on dendrites (Figures 7I,J and Supplementary Figure 4). Such dendrites in GCL may have belonged to GCs whose soma was proximal to hilus or interneurons (Frotscher et al., 2006).

Discussion

Hippocampal MF sprouting is a striking example of circuit formation in the adult brain (Seng et al., 2022). Previously, we studied the induction mechanisms of MF sprouting (Luo et al., 2021). Here, we investigated the question of target specificity.

Associated with MF sprouting, CAM expression and/or abundance changes have been previously described in different models, such as pilocarpine (PC) or kainate (KA) induced status epilepticus and intrahippocampal electrical stimulation (IES). Arguably, the most striking phenotype was achieved by the knockdown of *Unc5a*, which prevented PC-induced recurrent MF sprouting in hippocampal slice cultures (Muramatsu et al., 2010), directly implicating this molecule in axon guidance. Others reported up-regulation of *Nrcam*, *Slit1*, *Celsr3*, *Sema6a*, *Epha4*, and *Epha7* transcripts in whole hippocampal tissue (PC model) (Hansen et al., 2014), increased protein abundance of N-cadherin (Cdh2) (PC model) (Shan et al., 2002) and NCAM (encoded by *Ncam1* or *Ncam2*) (KA model) (Niquet et al., 1993) in sprouted MF synapses, and transient down-regulation of *Sema3a* (IES model) (Holtmaat et al., 2003). In addition, C1q-like-s were characterized in MF sprouting. Typically, C1QL1 and C1QL3 are secreted from MF synapses and form a complex with presynaptic NRXN3 to facilitate trans-synaptic recruitment of kainate-sensitive glutamate receptors (KARs) in CA3 cells (Matsuda et al., 2016). While MF sprouting still developed in the double *C1ql2/C1ql3* knock-out mice, KARs were not recruited to sprouted synapses (PC model; Matsuda et al., 2016), showing a shared feature between naive and sprouted MF synapses.

Together, these findings illuminated a complex landscape behind MF sprouting. As a caveat, most observations were made in tissue-level samples and/or after seizures, limiting delineation of cell types in which CAM abundance has

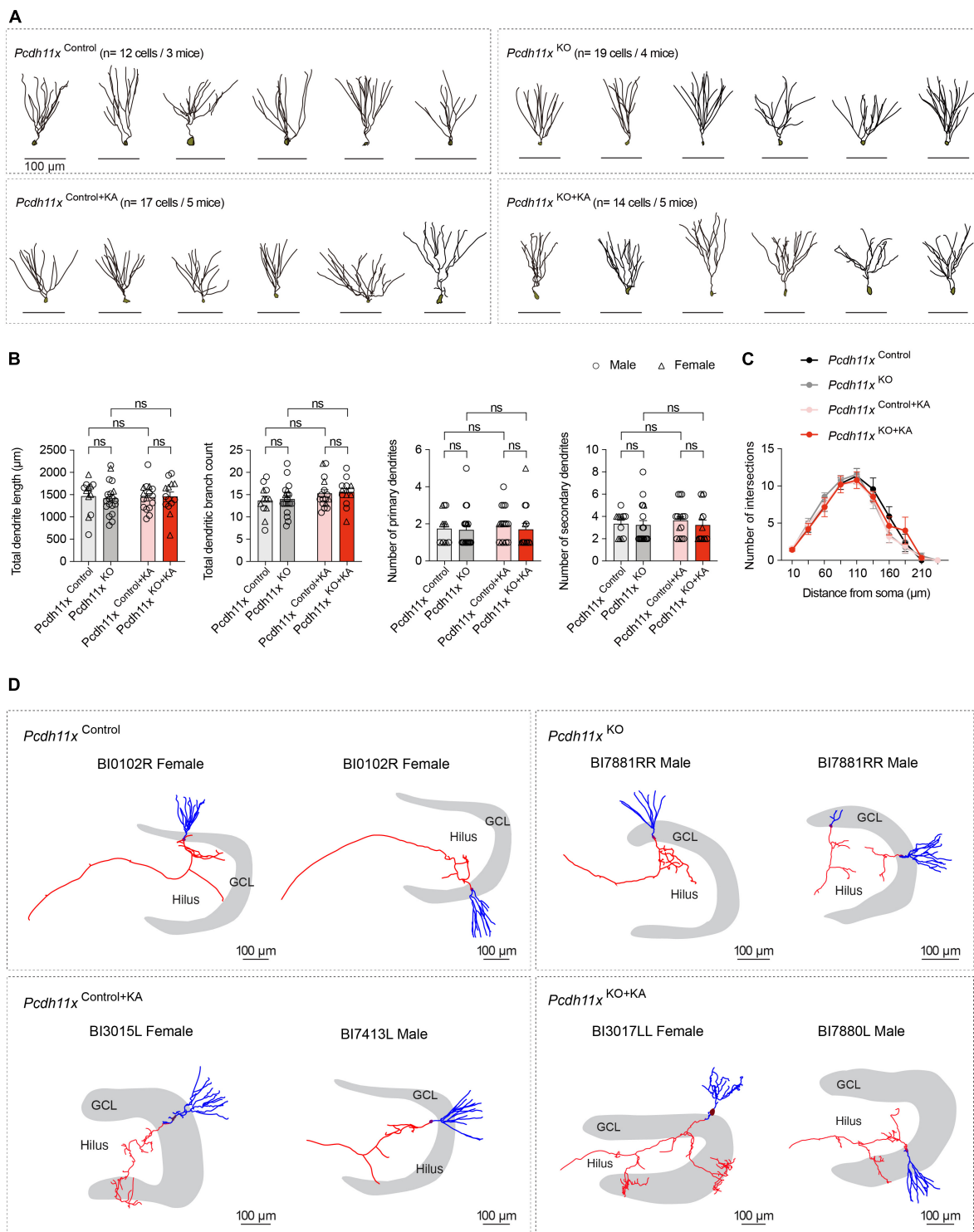


FIGURE 6

Morphological characterization of *Pcdh11x*^{Control+KA} and *Pcdh11x*^{KO+KA} GCs. (A) Morphological reconstruction of dendrites from *Pcdh11x*^{Control}, *Pcdh11x*^{KO}, *Pcdh11x*^{Control+KA}, and *Pcdh11x*^{KO+KA} GCs. (B) Quantification of dendritic parameters, such as total dendrite length, total dendritic branch count, number of primary dendrites, and number of secondary dendrites (two-way ANOVA test; data points represent single cells). (C) Sholl analysis of dendritic complexity. None of the comparisons had significance $p < 0.05$ (two-way ANOVA test). (D) Morphological reconstruction of axons from *Pcdh11x*^{Control}, *Pcdh11x*^{KO}, *Pcdh11x*^{Control+KA}, and *Pcdh11x*^{KO+KA} GCs. Axons and dendrites are shown in red and blue respectively. For further examples, see [Supplementary Figure 3](#).

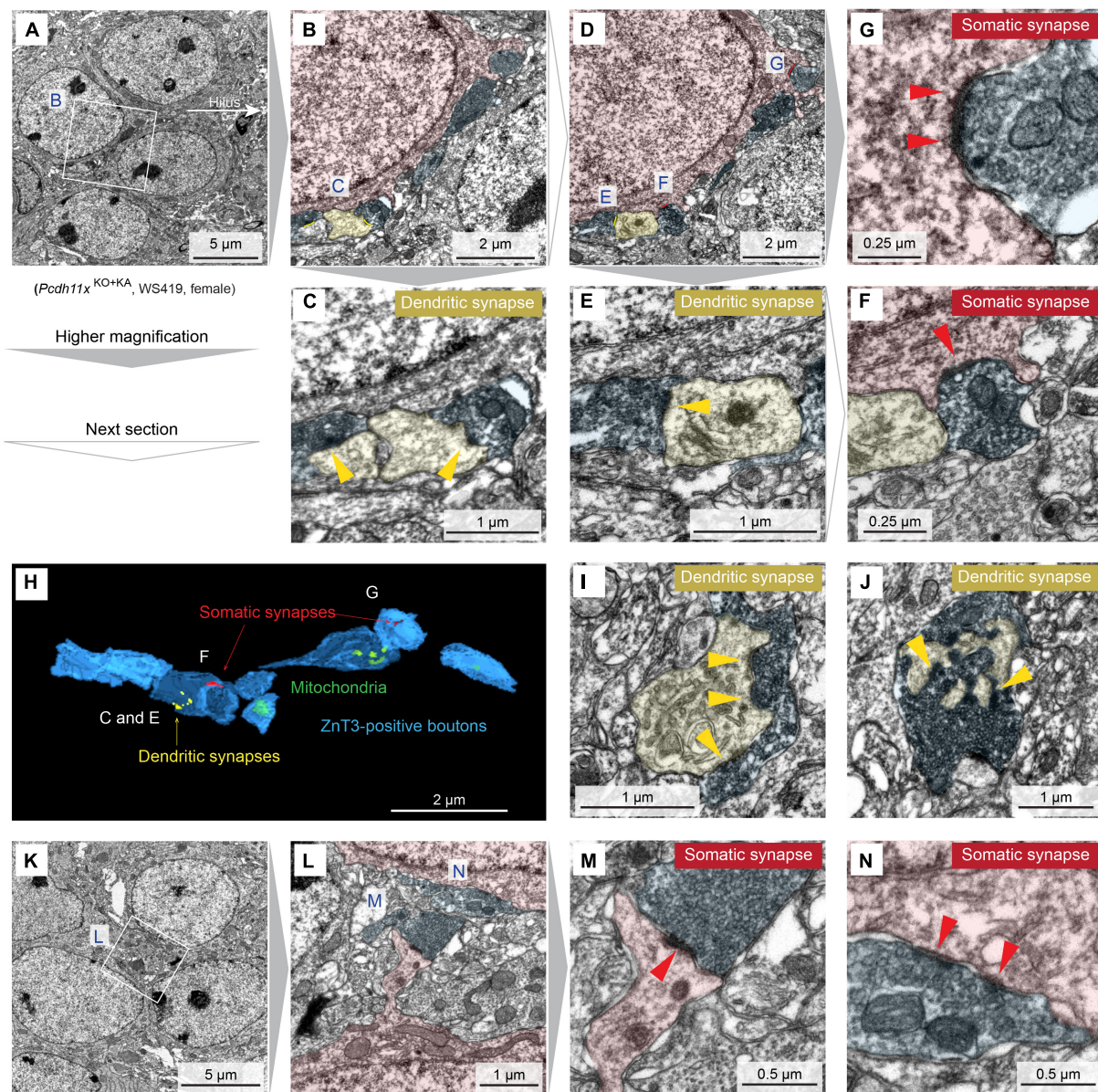
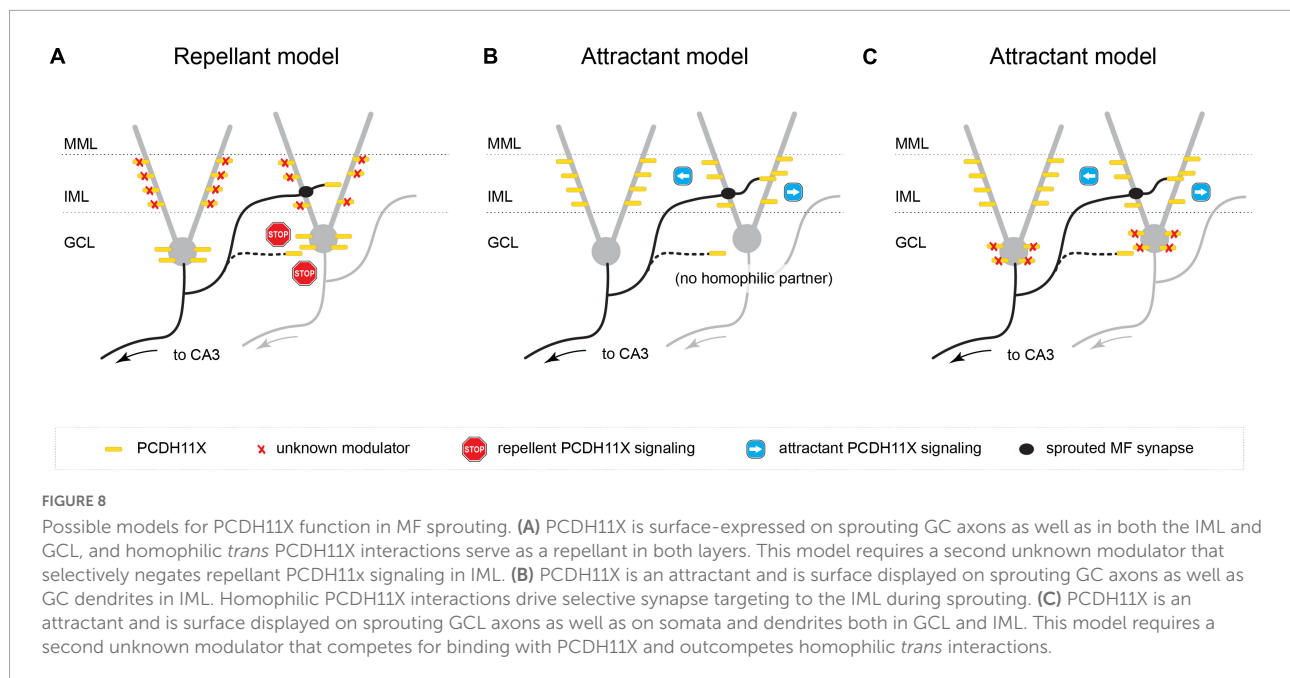


FIGURE 7

Immuno-electron microscopy characterization of *Pcdh11x*^{KO+KA} GC synapses. (A) Transmission electron microscopy image of four GC somata in GCL. In white box, ZnT3 + boutons are visible next to GC soma. (B) Magnification of the white box in panel A. GC soma, dendrite, and presynaptic ZnT3 + boutons are pseudo-colored in red, yellow, and blue, respectively. (C) Magnification of the area labeled with C in panel B shows synapses on boutons (yellow arrowheads). (D) Image shows the next section of what is shown in panel (B). (E–G) Magnification of the areas labeled with E, G, and F in panel (D) show somatic, somatic and dendritic, and dendritic synapses, respectively (yellow and red arrowheads). In the lower right part of panel (F), a dendritic synapse is also visible. However, the presynaptic compartment is lacking ZnT3 and thus MF identity of this synapse could not be confirmed. (H) 3D reconstruction of ZnT3 + boutons and synapses shown in panels (A–F). (I, J) Images show additional dendritic synapses with multiple release sites (yellow arrowheads) from the same animal. (K) Image shows five GC somata in GCL. (L) Magnification of the area shown in panel (K). (M, N) Magnification of the areas labeled with M and N in panel (L) show somatic synapses with one and multiple release sites, respectively (red arrowheads).

changed and causal dependencies (e.g., if CAM changes were required for sprouting or induced by seizures). We alleviated these limitations by specifically studying non-sprouting and sprouting GCs (1 and 14 days after KA), sampled before the expected onset of status epilepticus (typically 14–28 days

after KA) (Tanaka et al., 1992; Ben-Ari and Cossart, 2000). Our results did not reveal significant transcriptomic changes in the above listed molecules, with the one exception of *Slit1*. However, in contrast to up-regulation at the tissue level (Hansen et al., 2014), we found down-regulation of



Slit1 in KA GCs (Figure 1). It is possible that (i) previously reported molecules did not change in GCs (but in other cell types), (ii) their expression changed in GCs but at other time points as in our study, (iii) they were induced by status epilepticus, (iv) they manifested themselves only at protein level (e.g., N-cadherin, NCAM), or (v) they were model specific. Thus, we focused on differentially expressed CAMs that were upregulated in our single GC data set, and shortlisted *Fat3*, *Pcdh11x*, and *Cntn4* for a CRISPR/Cas9-based *in vivo* screen. Sequence analysis revealed loss-of-function deletions in *Pcdh11x*, but not in *Fat3* or *Cntn4*, which were not considered further in this study.

With regard to *Pcdh11x*, we showed upregulation of *Pcdh11x* mRNA and enrichment of PCDH11X protein in *Pcdh11x* non-deficient control GCs during MF sprouting. Furthermore, using a CRISPR/Cas9-based strategy *in vivo*, we showed that while MF sprouting still developed in *Pcdh11x* KO (*Pcdh11x*^{KO+KA}), (i) GC dispersion was increased, (ii) sprouted synapses frequently formed on GC somata in addition to dendrites, and (iii) ~50% more ZnT3 + puncta were detectable in GCL compared to *Pcdh11x* non-deficient controls (Figures 1–4, 7 and Supplementary Figure 4).

Pcdh11x was previously implicated in dendritic branching in developing neurons (Wu et al., 2015) and in the differentiation and proliferation of neural stem cells (Zhang et al., 2014). However, it is unlikely that these functions contributed to the phenotypes. First, dendritic branching was not different between *Pcdh11x*^{Control+KA} and *Pcdh11x*^{KO+KA} GCs (Figure 6), and second, although the adult dentate gyrus retains a neurogenic niche producing GCs, the use of *Calb1*^{Cre/+} line and adeno associated virus (AAV) ensured that *Pcdh11x* mutations

occurred only in mature GCs but not in neural stem cells (Brandt et al., 2003).

Alternatively, *Pcdh11x* also has been implicated in homophilic *trans* cell-cell interactions (Harrison et al., 2020; Pancho et al., 2020). In a first potential hypothesis, PCDH11X is surface-expressed on sprouting GC axons (ZnT3 + MF boutons) as well as in both the IML and GCL, and homophilic *trans* PCDH11X interactions serve as a repellant or inhibit synapse targeting in both layers. This model is consistent with the phenotype we observed in the *Pcdh11x* KO, where KA-induced sprouting occurs not only in the IML (as seen in controls) but in the GCL as well—presumably, according to this model, due to a release of PCDH11X-mediated inhibition of synapse targeting in the GCL. However, in order to achieve the IML-specific targeting seen in KA-treated wildtypes, this model requires that either (a) PCDH11X is exclusively expressed in GCL, which our immunostaining data shows not to be the case, or (b) a second unknown modulator selectively negates repellant PCDH11X signaling or releases inhibition of synapse targeting in the IML (Figure 8A).

A second, simpler model assumes that PCDH11X is a strong attractive signal and is surface displayed on sprouting GC axons as well as GC proximal dendrites in the IML; by virtue of specific expression in the IML (as opposed to the GCL), homophilic PCDH11X interactions drive selective synapse targeting to the IML during sprouting. In apparent contradiction to the model, we observed PCDH11X immunostaining in both the IML and GCL, including somatic and proximal dendritic compartments of GCs; however, the antibody we used targeted the intracellular domain of PCDH11X and could conceivably label intracellularly-retained molecules instead of

surface-displayed PCDH11X in the soma, therefore preserving the possibility of this second hypothesis. Assuming this model, we explain the targeting of sprouted MF synapses onto both GC somata and dendrites of *Pcdh11x*^{KO+KA} as follows: in the absence of a strong attractive signal that condenses or concentrates synapse targeting to the IML, synapses will form indiscriminately, in both the GCL and IML (Figure 8B).

Finally, a third model posits that PCDH11X—similarly to the second model—is an attractive cue. However, unlike the second model, it assumes that PCDH11X is expressed in both the GCL and/or GC cell bodies as well as in the IML and/or GC proximal dendrites, since we cannot rule out the possibility that the antibody used in our immunostaining experiments does indeed label surface-displayed PCDH11X molecules at the soma. Instead, it invokes a modulatory or repellant signal specific to the GCL, such as an unidentified CAM that competes for binding with PCDH11X (e.g., via repellant, heterophilic interactions that outcompete homophilic *trans* interactions) (Figure 8C).

While not in our focus, the lack of an attractant, homophilic *trans* PCDH11X interaction may also explain the increased GCL dispersion seen in *Pcdh11x* KOs. Although both GC dispersion and MF sprouting were induced by KA, they are mechanistically independent. GC dispersion is due to impaired Reelin secretion by Cajal-Retzius cells (Haas et al., 2002; Heinrich et al., 2006; Duveau et al., 2011), whereas MF sprouting is a GC autonomous process (Luo et al., 2021). It is plausible that *trans* binding of PCDH11Xs displayed on neighboring neurons/dendrites after KA could serve as a structural break before further dispersion in controls, but not in KOs.

Together, our results revealed that PCDH11X controls synapse targeting during MF sprouting. With regard to implications for epilepsy, partial *Pcdh11x* duplication (as part of a broader Xq13-q21 duplication) was reported in one patient with recurrent seizures (Linhares et al., 2016). Based on the association of other protocadherins with epilepsy, such as *Pcdh19* (Dibbens et al., 2008; also see Hoshina et al., 2021) and *Pcdh7* (Lal et al., 2015), authors of the partial *Pcdh11x* duplication study hypothesized that the *Pcdh11x* mutation may be relevant for the seizures of this patient (Linhares et al., 2016). Our results provide additional insights showing altered connectivity in *Pcdh11x* KO. However, a more thorough testing of a link between *Pcdh11x* mutations and seizures, including conditions under which somatic synapses become activated in the brain, is beyond the scope of our study. Further, it is also clear that other CAMs may be involved in MF sprouting which our study did not cover. As such, the roles of SLIT1, FAT3, and CNTN4, if any, remain to be determined. More broadly, delineating which signals control target cell type selectivity (among GCs and different GABAergic

interneuron types) as postsynaptic targets remain a major challenge. MF sprouting is a robust model to study these questions. Potentially, at least some of the mechanisms will be generalizable beyond MF sprouting, and applicable in other cell types in which to facilitate circuit repair in brain disorders and after injuries.

Data availability statement

The original contributions presented in this study are included in the article/Supplementary material, further inquiries can be directed to the corresponding author.

Ethics statement

The animal study was reviewed and approved by Veterinary Office of Zurich Kanton.

Author contributions

WL and CF designed research and wrote the manuscript. WL, NC-O, CS, ME, DL, and TL performed research and analyzed data. All authors contributed to the article and approved the submitted version.

Funding

This study received funding from the Swiss National Science Foundation (310030_188506), the Novartis Stiftung für Medizinisch-biologische Forschung (20A022), the Dr. Eric Slack-Gyr-Stiftung, and University Research Priority Program AdaBD (Adaptive Brain Circuits in Development and Learning) of University of Zurich. None of the funders were involved in the study design, collection, analysis, interpretation of data, the writing of this article or the decision to submit it for publication.

Acknowledgments

We thank Rita Bopp and José María Mateos Melero for electron microscopy imaging, and Jean-Charles Paterna and Melanie Rauch (Viral Vector Facility, University of Zürich/ETH Zürich) for discussions and virus production.

Conflict of interest

The authors declare that the research was conducted in the absence of any commercial or financial relationships that could be construed as a potential conflict of interest.

Publisher's note

All claims expressed in this article are solely those of the authors and do not necessarily represent those of their affiliated

organizations, or those of the publisher, the editors and the reviewers. Any product that may be evaluated in this article, or claim that may be made by its manufacturer, is not guaranteed or endorsed by the publisher.

Supplementary material

The Supplementary Material for this article can be found online at: <https://www.frontiersin.org/articles/10.3389/fnins.2022.888362/full#supplementary-material>

References

- Apóstolo, N., Smukowski, S. N., Vanderlinden, J., Condomitti, G., Rybak, V., Ten Bos, J., et al. (2020). Synapse type-specific proteomic dissection identifies IgSF8 as a hippocampal CA3 microcircuit organizer. *Nat. Commun.* 11:5171. doi: 10.1038/s41467-020-18956-x
- Bagri, A., Cheng, H. J., Yaron, A., Pleasure, S. J., and Tessier-Lavigne, M. (2003). Stereotyped pruning of long hippocampal axon branches triggered by retraction inducers of the semaphorin family. *Cell* 113, 285–299. doi: 10.1016/s0092-8674(03)00267-8
- Baig, D. N., Yanagawa, T., and Tabuchi, K. (2017). Distortion of the normal function of synaptic cell adhesion molecules by genetic variants as a risk for autism spectrum disorders. *Brain Res. Bull.* 129, 82–90. doi: 10.1016/j.brainresbull.2016.10.006
- Basu, R., Duan, X., Taylor, M. R., Martin, E. A., Muralidhar, S., Wang, Y., et al. (2017). Heterophilic Type II Cadherins Are Required for High-Magnitude Synaptic Potentiation in the Hippocampus. *Neuron* 96, 160–176.e8. doi: 10.1016/j.neuron.2017.09.009
- Ben-Ari, Y., and Cossart, R. (2000). Kainate, a double agent that generates seizures: Two decades of progress. *Trends Neurosci.* 23, 580–587. doi: 10.1016/s0166-2236(00)01659-3
- Brandt, M. D., Jessberger, S., Steiner, B., Kronenberg, G., Reuter, K., Bick-Sander, A., et al. (2003). Transient calretinin expression defines early postmitotic step of neuronal differentiation in adult hippocampal neurogenesis of mice. *Mol. Cell Neurosci.* 24, 603–613. doi: 10.1016/s1044-7431(03)00207-0
- Buckmaster, P. S. (2014). Does mossy fiber sprouting give rise to the epileptic state? *Adv. Exp. Med. Biol.* 813, 161–168. doi: 10.1007/978-94-017-8914-1_13
- Carrasquillo, M. M., Zou, F., Pankratz, V. S., Wilcox, S. L., Ma, L., Walker, L. P., et al. (2009). Genetic variation in PCDH11X is associated with susceptibility to late-onset Alzheimer's disease. *Nat. Genet.* 41, 192–198. doi: 10.1038/ng.305
- Cavazos, J. E., Zhang, P., Qazi, R., and Sutula, T. P. (2003). Ultrastructural features of sprouted mossy fiber synapses in kindled and kainic acid-treated rats. *J. Comp. Neurol.* 458, 272–292. doi: 10.1002/cne.10581
- Chen, H., Bagri, A., Zupicich, J. A., Zou, Y., Stoeckli, E., Pleasure, S. J., et al. (2000). Neuropilin-2 regulates the development of selective cranial and sensory nerves and hippocampal mossy fiber projections. *Neuron* 25, 43–56. doi: 10.1016/s0896-6273(00)80870-3
- Condomitti, G., Wierda, K. D., Schroeder, A., Rubio, S. E., Vennekens, K. M., Orlandi, C., et al. (2018). An Input-Specific Orphan Receptor GPR158-HSPG Interaction Organizes Hippocampal Mossy Fiber-CA3 Synapses. *Neuron* 100, 201–215.e9. doi: 10.1016/j.neuron.2018.08.038
- Cremer, H., Chazal, G., Carleton, A., Goridis, C., Vincent, J. D., and Lledo, P. M. (1998). Long-term but not short-term plasticity at mossy fiber synapses is impaired in neural cell adhesion molecule-deficient mice. *Proc. Natl. Acad. Sci. U. S. A.* 95, 13242–13247. doi: 10.1073/pnas.95.22.13242
- de Wit, J., and Ghosh, A. (2016). Specification of synaptic connectivity by cell surface interactions. *Nat. Rev. Neurosci.* 17, 22–35. doi: 10.1038/nrn.2015.3
- Deans, M. R., Krol, A., Abaira, V. E., Copley, C. O., Tucker, A. F., and Goodrich, L. V. (2011). Control of neuronal morphology by the atypical cadherin Fat3. *Neuron* 71, 820–832. doi: 10.1016/j.neuron.2011.06.026
- Dibbens, L. M., Tarpey, P. S., Hynes, K., Bayly, M. A., Scheffer, I. E., Smith, R., et al. (2008). X-linked protocadherin 19 mutations cause female-limited epilepsy and cognitive impairment. *Nat. Genet.* 40, 776–781. doi: 10.1038/ng.149
- Duveau, V., Madhusudan, A., Caleo, M., Knuesel, I., and Fritschy, J. M. (2011). Impaired reelin processing and secretion by Cajal-Retzius cells contributes to granule cell dispersion in a mouse model of temporal lobe epilepsy. *Hippocampus* 21, 935–944. doi: 10.1002/hipo.20793
- Földy, C., Darmanis, S., Aoto, J., Malenka, R. C., Quake, S. R., and Südhof, T. C. (2016). Single-cell RNAseq reveals cell adhesion molecule profiles in electrophysiologically defined neurons. *Proc. Natl. Acad. Sci. U. S. A.* 113, E5222–E5231. doi: 10.1073/pnas.1610155113
- Frotscher, M., Jonas, P., and Sloviter, R. S. (2006). Synapses formed by normal and abnormal hippocampal mossy fibers. *Cell Tissue Res.* 326, 361–367.
- Godale, C. M., and Danzer, S. C. (2018). Signaling pathways and cellular mechanisms regulating mossy fiber sprouting in the development of epilepsy. *Front. Neurol.* 9:298. doi: 10.3389/fneur.2018.00298
- Haas, C. A., Dudeck, O., Kirsch, M., Huszka, C., Kann, G., Pollak, S., et al. (2002). Role for reelin in the development of granule cell dispersion in temporal lobe epilepsy. *J. Neurosci.* 22, 5797–5802. doi: 10.1523/JNEUROSCI.22-14-05797.2002
- Hainmueller, T., and Bartos, M. (2020). Dentate gyrus circuits for encoding, retrieval and discrimination of episodic memories. *Nat. Rev. Neurosci.* 21, 153–168. doi: 10.1038/s41583-019-0260-z
- Hansen, K. F., Sakamoto, K., Pelz, C., Impey, S., and Obrietan, K. (2014). Profiling status epilepticus-induced changes in hippocampal RNA expression using high-throughput RNA sequencing. *Sci. Rep.* 4:6930. doi: 10.1038/srep06930
- Harrison, O. J., Brasch, J., Katsamba, P. S., Ahlsen, G., Noble, A. J., Dan, H., et al. (2020). Family-wide Structural and Biophysical Analysis of Binding Interactions among Non-clustered δ -Protocadherins. *Cell Rep.* 30, 2655–2671.e7. doi: 10.1016/j.celrep.2020.02.003
- Heinrich, C., Nitta, N., Flubacher, A., Müller, M., Fahrner, A., Kirsch, M., et al. (2006). Reelin deficiency and displacement of mature neurons, but not neurogenesis, underlie the formation of granule cell dispersion in the epileptic hippocampus. *J. Neurosci.* 26, 4701–4713. doi: 10.1523/JNEUROSCI.5516-05.2006
- Holtmaat, A. J., Gorter, J. A., de Wit, J., Tolner, E. A., Spijker, S., Giger, R. J., et al. (2003). Transient downregulation of Sema3A mRNA in a rat model for temporal lobe epilepsy. A novel molecular event potentially contributing to mossy fiber sprouting. *Exp. Neurol.* 182, 142–150. doi: 10.1016/s0014-4886(03)00035-9
- Hoshina, N., Johnson-Venkatesh, E. M., Hoshina, M., and Umemori, H. (2021). Female-specific synaptic dysfunction and cognitive impairment in a mouse model of PCDH19 disorder. *Science* 372:eaz3893. doi: 10.1126/science.eaz3893
- Koyama, R., and Ikegaya, Y. (2018). The Molecular and cellular mechanisms of axon guidance in mossy fiber sprouting. *Front. Neurol.* 9:382. doi: 10.3389/fneur.2018.00382
- Krol, A., Henle, S. J., and Goodrich, L. V. (2016). Fat3 and Ena/VASP proteins influence the emergence of asymmetric cell morphology in the developing retina. *Development* 143, 2172–2182. doi: 10.1242/dev.133678
- Lal, D., Ruppert, A. K., Trucks, H., Schulz, H., de Kovel, C. G., Kasteleijn-Nolst Trenité, D., et al. (2015). Burden analysis of rare microdeletions suggests a strong

impact of neurodevelopmental genes in genetic generalised epilepsies. *PLoS Genet.* 11:e1005226. doi: 10.1371/journal.pgen.1005226

Laurberg, S., and Zimmer, J. (1981). Lesion-induced sprouting of hippocampal mossy fiber collaterals to the fascia dentata in developing and adult rats. *J. Comp. Neurol.* 200, 433–459. doi: 10.1002/cne.902000310

Linhares, N. D., Valadares, E. R., da Costa, S. S., Arantes, R. R., de Oliveira, L. R., Rosenberg, C., et al. (2016). Inherited Xq13.2-q21.31 duplication in a boy with recurrent seizures and pubertal gynecomastia: Clinical, chromosomal and aCGH characterization. *Meta Gene* 9, 185–190. doi: 10.1016/j.mgene.2016.07.004

Liu, X. D., Zhu, X. N., Halford, M. M., Xu, T. L., Henkemeyer, M., and Xu, N. J. (2018). Retrograde regulation of mossy fiber axon targeting and terminal maturation via postsynaptic Lnx1. *J. Cell Biol.* 217, 4007–4024. doi: 10.1083/jcb.201803105

Luo, W., Egger, M., Domonkos, A., Que, L., Lukacovich, D., Cruz-Ochoa, N. A., et al. (2021). Recurrent rewiring of the adult hippocampal mossy fiber system by a single transcriptional regulator. *Id2. Proc. Natl. Acad. Sci. U. S. A.* 118:e2108239118. doi: 10.1073/pnas.2108239118

Martin, E. A., Muralidhar, S., Wang, Z., Cervantes, D. C., Basu, R., Taylor, M. R., et al. (2015). The intellectual disability gene Kirrel3 regulates target-specific mossy fiber synapse development in the hippocampus. *Elife* 4:e09395. doi: 10.7554/eLife.09395

Matsuda, K., Budisantoso, T., Mitakidis, N., Sugaya, Y., Miura, E., Kakegawa, W., et al. (2016). Transsynaptic Modulation of Kainate Receptor Functions by Clq-like Proteins. *Neuron* 90, 752–767. doi: 10.1016/j.neuron.2016.04.001

Missaire, M., and Hindges, R. (2015). The role of cell adhesion molecules in visual circuit formation: From neurite outgrowth to maps and synaptic specificity. *Dev. Neurobiol.* 75, 569–583. doi: 10.1002/dneu.22267

Muramatsu, R., Nakahara, S., Ichikawa, J., Watanabe, K., Matsuki, N., and Koyama, R. (2010). The ratio of 'deleted in colorectal cancer' to 'uncoordinated-5A' netrin-1 receptors on the growth cone regulates mossy fibre directionality. *Brain* 133, 60–75. doi: 10.1093/brain/awp266

Niquet, J., Jorquera, I., Ben-Ari, Y., and Represa, A. (1993). NCAM immunoreactivity on mossy fibers and reactive astrocytes in the hippocampus of epileptic rats. *Brain Res.* 626, 106–116. doi: 10.1016/0006-8993(93)90569-9

Noebels, J. L., Avoli, M., Rogawski, M. A., Olsen, R. W., and Delgado-Escueta, A. V. (eds) (2012). *Jasper's Basic Mechanisms of the Epilepsies*, (4th Edn). Bethesda, MD: National Center for Biotechnology Information.

Oguro-Ando, A., Bamford, R. A., Sital, W., Sprengers, J. J., Zuko, A., Matsner, J. M., et al. (2021). Cntn4, a risk gene for neuropsychiatric disorders, modulates hippocampal synaptic plasticity and behavior. *Transl. Psychiatry* 11:106. doi: 10.1038/s41398-021-01223-y

Oguro-Ando, A., Zuko, A., Kleijer, K. T. E., and Burbach, J. P. H. (2017). A current view on contactin-4, -5, and -6: Implications in neurodevelopmental disorders. *Mol. Cell Neurosci.* 81, 72–83. doi: 10.1016/j.mcn.2016.12.004

Osterhout, J. A., Stafford, B. K., Nguyen, P. L., Yoshihara, Y., and Huberman, A. D. (2015). Contactin-4 mediates axon-target specificity and functional development of the accessory optic system. *Neuron* 86, 985–999. doi: 10.1016/j.neuron.2015.04.005

Pancho, A., Aerts, T., Mitsogiannis, M. D., and Seuntjens, E. (2020). Protocadherins at the Crossroad of Signaling Pathways. *Front. Mol. Neurosci.* 13:117. doi: 10.3389/fnmol.2020.00117

Sanes, J. R., and Zipursky, S. L. (2020). Synaptic specificity, recognition molecules, and assembly of neural circuits. *Cell* 181, 536–556. doi: 10.1016/j.cell.2020.04.008

Seng, C., Luo, W., and Földy, C. (2022). Circuit formation in the adult brain. *Eur. J. Neurosci.* 56, 4187–4213. doi: 10.1111/ejn.15742

Shan, W., Yoshida, M., Wu, X. R., Huntley, G. W., and Colman, D. R. (2002). Neural (N-) cadherin, a synaptic adhesion molecule, is induced in hippocampal mossy fiber axonal sprouts by seizure. *J. Neurosci. Res.* 69, 292–304. doi: 10.1002/jnr.10305

Südhof, T. C. (2021). The cell biology of synapse formation. *J. Cell Biol.* 220:e202103052. doi: 10.1083/jcb.202103052

Suto, F., Tsuboi, M., Kamiya, H., Mizuno, H., Kiyama, Y., Komai, S., et al. (2007). Interactions between plexin-A2, plexin-A4, and semaphorin 6A control lamina-restricted projection of hippocampal mossy fibers. *Neuron* 53, 535–547. doi: 10.1016/j.neuron.2007.01.028

Sutula, T., He, X. X., Cavazos, J., and Scott, G. (1988). Synaptic reorganization in the hippocampus induced by abnormal functional activity. *Science* 239, 1147–1150. doi: 10.1126/science.2449733

Tanaka, T., Tanaka, S., Fujita, T., Takano, K., Fukuda, H., Sako, K., et al. (1992). Experimental complex partial seizures induced by a microinjection of kainic acid into limbic structures. *Prog. Neurobiol.* 38, 317–334. doi: 10.1016/0301-0082(92)90023-8

Tauk, D. L., and Nadler, J. V. (1985). Evidence of functional mossy fiber sprouting in hippocampal formation of kainic acid-treated rats. *J. Neurosci.* 5, 1016–1022. doi: 10.1523/JNEUROSCI.05-04-01016.1.985

Tawarayama, H., Yoshida, Y., Suto, F., Mitchell, K. J., and Fujisawa, H. (2010). Roles of semaphorin-6B and plexin-A2 in lamina-restricted projection of hippocampal mossy fibers. *J. Neurosci.* 30, 7049–7060. doi: 10.1523/JNEUROSCI.0073-10.2010

Wenzel, H. J., Woolley, C. S., Robbins, C. A., and Schwartzkroin, P. A. (2000). Kainic acid-induced mossy fiber sprouting and synapse formation in the dentate gyrus of rats. *Hippocampus* 10, 244–260. doi: 10.1002/1098-1063(2000)10:3<244::AID-HIPO5>3.0.CO;2-7

Williams, M. E., Wilke, S. A., Daggett, A., Davis, E., Otto, S., Ravi, D., et al. (2011). Cadherin-9 regulates synapse-specific differentiation in the developing hippocampus. *Neuron* 71, 640–655. doi: 10.1016/j.neuron.2011.06.019

Wu, C., Niu, L., Yan, Z., Wang, C., Liu, N., Dai, Y., et al. (2015). Pcdh11x Negatively Regulates Dendritic Branching. *J. Mol. Neurosci.* 56, 822–828. doi: 10.1007/s12031-015-0515-8

Xu, N. J., and Henkemeyer, M. (2009). Ephrin-B3 reverse signaling through Grb4 and cytoskeletal regulators mediates axon pruning. *Nat. Neurosci.* 12, 268–276. doi: 10.1038/nn.2254

Zhang, P., Wu, C., Liu, N., Niu, L., Yan, Z., Feng, Y., et al. (2014). Protocadherin 11 x regulates differentiation and proliferation of neural stem cell in vitro and in vivo. *J. Mol. Neurosci.* 54, 199–210. doi: 10.1007/s12031-014-0275-x

Zimmer, J., and Gähwiler, B. H. (1987). Growth of hippocampal mossy fibers: A lesion and coculture study of organotypic slice cultures. *J. Comp. Neurol.* 264, 1–13. doi: 10.1002/cne.902640102



OPEN ACCESS

EDITED BY

Giorgia Quadrato,
University of Southern California,
United States

REVIEWED BY

Fabienne E. Poulain,
University of South Carolina,
United States
Nael Nadif Kasri,
Radboud University, Netherlands

*CORRESPONDENCE

Zsolt Lele
lele.zsolt@koki.mta.hu

SPECIALTY SECTION

This article was submitted to
Neurodevelopment,
a section of the journal
Frontiers in Neuroscience

RECEIVED 17 June 2022

ACCEPTED 31 August 2022

PUBLISHED 23 September 2022

CITATION

László ZI and Lele Z (2022) Flying
under the radar: CDH2 (N-cadherin),
an important hub molecule in
neurodevelopmental and
neurodegenerative diseases.
Front. Neurosci. 16:972059.
doi: 10.3389/fnins.2022.972059

COPYRIGHT

© 2022 László and Lele. This is an
open-access article distributed under
the terms of the [Creative Commons
Attribution License \(CC BY\)](#). The use,
distribution or reproduction in other
forums is permitted, provided the
original author(s) and the copyright
owner(s) are credited and that the
original publication in this journal is
cited, in accordance with accepted
academic practice. No use, distribution
or reproduction is permitted which
does not comply with these terms.

Flying under the radar: CDH2 (N-cadherin), an important hub molecule in neurodevelopmental and neurodegenerative diseases

Zsófia I. László^{1,2} and Zsolt Lele^{1*}

¹Momentum Laboratory of Molecular Neurobiology, Institute of Experimental Medicine, Budapest, Hungary, ²Division of Cellular and Systems Medicine, School of Medicine, University of Dundee, Dundee, United Kingdom

CDH2 belongs to the classic cadherin family of Ca^{2+} -dependent cell adhesion molecules with a meticulously described dual role in cell adhesion and β -catenin signaling. During CNS development, CDH2 is involved in a wide range of processes including maintenance of neuroepithelial integrity, neural tube closure (neurulation), confinement of radial glia progenitor cells (RGPCs) to the ventricular zone and maintaining their proliferation-differentiation balance, postmitotic neural precursor migration, axon guidance, synaptic development and maintenance. In the past few years, direct and indirect evidence linked CDH2 to various neurological diseases, and in this review, we summarize recent developments regarding CDH2 function and its involvement in pathological alterations of the CNS.

KEYWORDS

N-cadherin, CDH2, adhesion, brain development, neurodegenerative diseases, neurodevelopmental diseases

Introduction

CDH2 is one of the most intensively studied of all the cadherins with thousands of references in PubMed. As a matter of fact, due to this heavy interest, it has become a bit of a bore after all these years, so when someone stands up at a conference introducing CDH2 as his or her subject of study, people tend to yawn, wish stronger for a coffee (or for a stronger coffee) and start reading the abstract of the next talk in the session. Yet somehow, year after year, this protein has been continuously able to surprise us by fulfilling yet another important developmental, physiological, or disease-related function. While aspects of CDH2 function during brain (particularly cortical) development have been studied extensively (Brayshaw and Price, 2016; Martinez-Garay, 2020; de Agustín-Durán et al., 2021), it has been largely overlooked as a potential factor

in various neurodevelopmental and neurodegenerative diseases. In this review, we will summarize previous data regarding CDH2 function in neural development and disease with a particular emphasis on recent additions to the pathophysiological aspect which brought back this old, familiar protein into the limelight.

The role of CDH2 in neural development

Neuroepithelial integrity

Cdh2 expression already appears during neural induction accompanied by a parallel decrease in *Cdh1* (E-cadherin) mRNA levels (Hatta and Takeichi, 1986). General disruption of *Cdh2* in the mouse results in early embryonic (E10) lethality due to cardiac developmental defects (Radice et al., 1997). At this point, the neural tube also displays an abnormally undulated phenotype, but further conclusions regarding its functions in CNS development could not be drawn. In contrast, nonsense mutations in the zebrafish *Cdh2* gene (Jiang et al., 1996; Lele et al., 2002), allow the mutant so-called *parachute* (*pac*), named after the shape of the midbrain cross-section) to develop to a relatively mature stage before becoming lethal (i.e., 48 h post-fertilization, at which point the wild-type zebrafish larvae are hatched and display complex behaviors like swimming and feeding). This is probably due to the combination of quick CNS development and the small size of the embryo which allows a sufficient supply of nutrients from the yolk sac and oxygen *via* simple diffusion into the embryonic tissues. This makes the cardiac function largely irrelevant in this stage of development during which neural induction, patterning, neurulation, and most of the early differentiation processes are already completed. In *pac* mutants, the epithelial structure of the dorsal neural tube gets disrupted in the dorsal part of the midbrain-hindbrain region (Jiang et al., 1996). Similar symptoms also appear in chick embryos after the application of CDH2-function blocking antibodies (Gänzler-Odenthal and Redies, 1998) indicating that CDH2-based adherens junctions also maintain neuroepithelial integrity in Amniotes.

Neurulation and neural crest development

CDH2 is essential for both zebrafish and mouse neurulation despite the fact that neural tube formation follows a different route in these organisms (convergent-extension movements of neural plate cells followed by secondary cavitation vs. direct neural tube formation, respectively). In the zebrafish loss-of-function *Cdh2* mutant *pac^{dr7}*, convergent-extension movements of neural plate cells are disrupted thereby delaying the migration

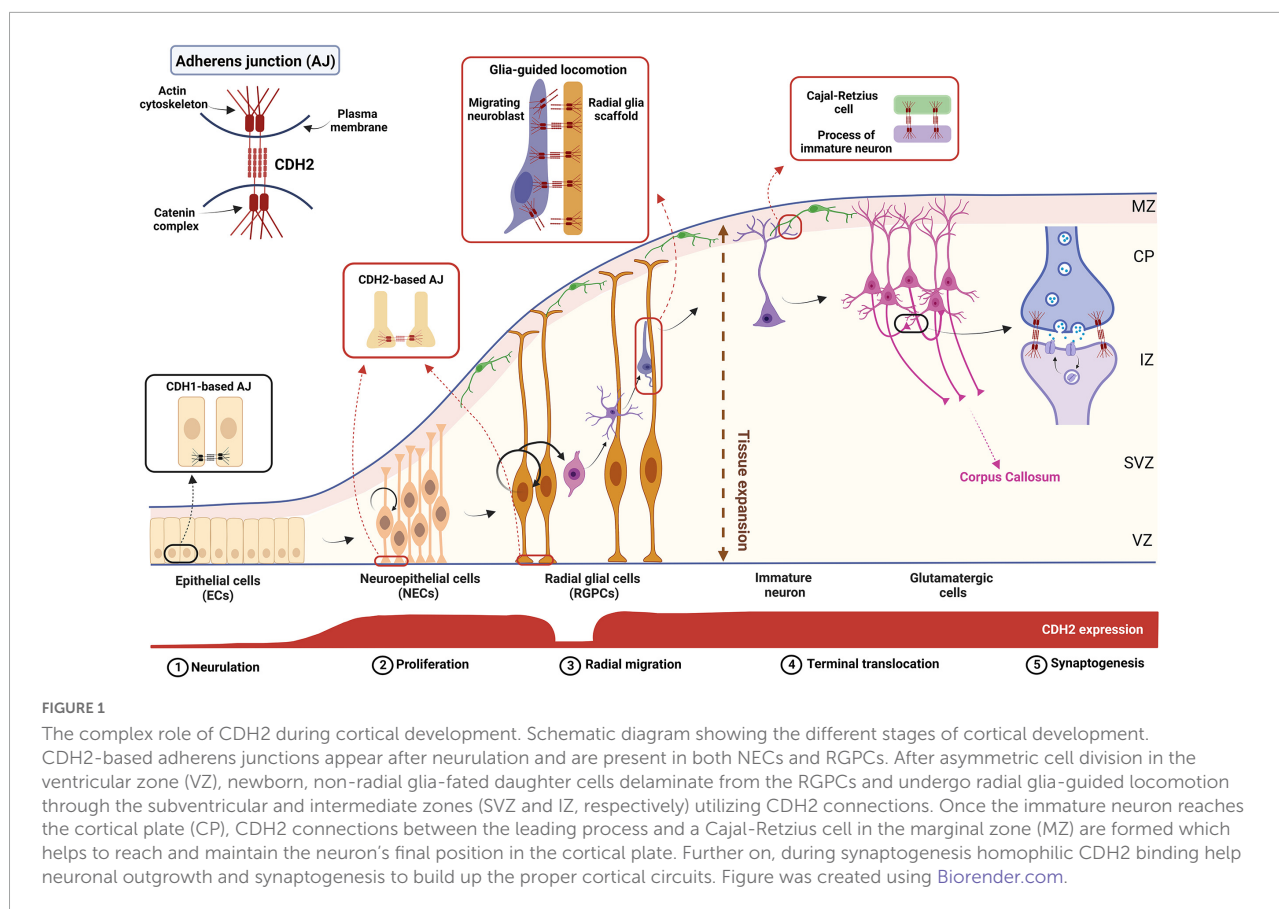
of neural plate cells toward the midline (Lele et al., 2002). As a result, these cells get excluded from the forming neural rod. In the mouse, cardiac rescue of the *Cdh2*^{−/−} animals allows development to proceed further than in the full knockout and in these animals, closure of the anterior neuropore never occurs also indicating a role (albeit a spatially restricted one) for CDH2 in neurulation (Radice et al., 1997; Luo et al., 2001).

Emergence of neural crest (NC) cells from the dorsal neural tube occur simultaneously with neural tube closure. As mentioned above, the closure also requires the presence of CDH2, the main component of adherens junctions keeping neuroepithelial cells to each other (Figure 1). Thus, it is no surprise that escaping the closing neuroepithelium requires a transient decrease of CDH2 expression in NC cells in favor of cadherins with weaker binding ability, CDH6, then CDH7 (Nakagawa and Takeichi, 1995, 1998; Coles et al., 2007; Taneyhill et al., 2007; Park and Gumbiner, 2010; Schiffmacher et al., 2014). Repression of CDH2-mediated adhesion is prompted by BMP4 signal-induced ADAM10 activity (Sela-Donenfeld and Kalcheim, 1999). The C-terminal fragment of CDH2 enters the nucleus and promotes CyclinD transcription and neural crest delamination (Shoval et al., 2006).

Despite the transient decrease of CDH2 levels, the protein has an important function later in the collective migration of neural crest cells in Anamniotes. CDH2-based connections not only provide adhesive force between migrating cells, but are also actively involved in migration *via* treadmilling (Peglion et al., 2014). In addition, intercellular CDH2-dimerization establishes the cells' polarity by altering the actin cytoskeleton *via* RhoA and Rac1 which in turn enables their directed migration toward attracting signals such as SDF1a/CXCL12 (Theveneau et al., 2010; Taneyhill and Schiffmacher, 2017; Szabó and Mayor, 2018).

Radial glia functions and neuronal differentiation during cortex development

Neuroepithelial cells convert to radial glia progenitor cells (RGPCs) in the mouse pallium around E10, a process hallmarked by the loss of tight junctions and extension and thinning of the basal process (Aaku-Saraste et al., 1996). These cells have a dual function during cortical development: by asymmetric cell division they generate an RGPC-fated and a non-RGPC-fated cell, the latter could become an intermediate progenitor cell (IPC) or a fate-committed neuroblast. In addition, the basal process of RGPCs extends to the basal (pial) surface providing a scaffold for the fate-committed neuroblasts to migrate on (Noctor et al., 2004). In rodents, RGPCs in the dorsal part of the telencephalon (the pallium) generate mostly excitatory neurons, while birth of the inhibitory neurons occurs primarily in the ganglionic eminences and



the preoptic area of the subpallium (Anderson et al., 1997). Loss of *Cdh2* in RGCs interferes with the most important processes during cortical development including proliferation, differentiation and cell migration (Kadowaki et al., 2007; Gil-Sanz et al., 2014; László et al., 2020a). These together manifest in severe lamination defects of the mouse cortex (Kadowaki et al., 2007; Miyamoto et al., 2015) similar to what was found in the zebrafish retina earlier (Erdmann et al., 2003; Malicki et al., 2003; Masai, 2003). CDH2-based adherens junctions are also essential for maintaining the stemness of RGCs via the promotion of β -catenin- and Notch signaling (Zhang J. et al., 2010; Hatakeyama et al., 2014). Loss of *Cdh2* disrupts not only the radial glia scaffold which hinders the radial migration of neuroblasts, but also the apical cell-to-cell contacts between RGCs resulting in their dispersion (Kadowaki et al., 2007; Gil-Sanz et al., 2014; László et al., 2020b). In addition, it also promotes premature differentiation (hence a decrease in the number) of PAX6-positive RGCs into TBR2-positive intermediate progenitor cells (IPCs) and TBR1-positive neurons (Zhang J. et al., 2010). In contrast, *Emx1-Cre*-induced loss of *Cdh2* increases the proliferation of precursors resulting in severe cortical heterotopia (Gil-Sanz et al., 2014). The explanation for this contradiction might lie within the difference in applied methods (shRNA knockdown vs. tissue-specific KO) or in the

timing of the *Cdh2*-loss. The electroporation experiment was carried out at E12.5 while the knockout study used the *Emx1-Cre* which acts quite early in pallial cortical differentiation (E9.5-E10.5) therefore the pro-proliferative effect might be due to the loss of *Cdh2* in neuroepithelial cells. Alternatively, it is feasible that there is a developmental time-specific usage of the intracellular α -catenins. This is supported by the fact that only α E-catenin can be found in the ventricular zone of the early E12 cortex, α N-catenin appears only later and even then, only in the subventricular zone (Uchida et al., 1996; Ajioka and Nakajima, 2005; Stocker and Chenn, 2009). In addition, a hyperplasia, similar to what was found in the *Emx1-Cre*-mediated *Cdh2*^{-/-} embryos, has been only reported in α E-catenin, but not in α N-catenin knockout animals (Park et al., 2002; Lien, 2006; Schmid et al., 2014).

CDH2 is also essential for the proper formation of inhibitory neurons born in the subpallium. Although much less publicized than its role in the development of pallial neurons, it has been demonstrated that CDH2 plays a similar role in the subpallial ventricular zone. Loss of *Cdh2* resulted in severe disorganization of the medial ganglionic eminence (MGE) proliferating zone (Luccardini et al., 2013). The number of phosphohistone 3-positive mitotic progenitor cells decreased which in turn resulted in less interneuron precursors reaching

the cortex. These data resemble the results found in the pallium although the number of intermediate progenitors in the MGE has not been examined (Zhang J. et al., 2010).

Importantly, pathophysiological disruption of classic cadherin-based adherens junctions (i.e., CDH1 and CDH2) between RGCs and their evoked random dispersal to upper layers provokes protective suicidal apoptosis in the embryonic cortex called developmental anoikis (László et al., 2020b). This prevents random migration of proliferating progenitors in the cortex which in turn leads to heterotopia and provides an explanation for the relatively low prevalence of these diseases considering the astronomical number of cell division events. It is important to note that the exact cadherin involved in this process has not been identified yet, hence the possibility of compensatory action from other classic cadherins (i.e., CDH1 or even some type II cadherins) which are expressed in the VZ of the developing neocortex, cannot be excluded (Rasin et al., 2007; Lefkovich et al., 2012). Nevertheless, a previous study examining the loss of CDH1 caused by overexpression of its repressor *Scratched* did not find elevated cell death levels in the embryonic cortex, indicating that the cell death requires the loss of CDH2, or both CDH1 and CDH2 (Itoh et al., 2013).

Role of CDH2 in postmitotic neural precursors

The role played by CDH2 in neuronal precursor migration has been studied in detail both in pallial and subpallial neurogenesis. In the pallium, after asymmetric cell division, the non-radial glia-fated daughter cell needs to downregulate CDH2 in order to lose its cell-cell connections which allows the escape from the ventricular zone adherens junction belt (Figure 1). This downregulation is evoked by the NGN2-activated FOXP2/4 transcriptional repressor (Rouso et al., 2012). Loss of *Cdh2* is also essential for the apical abscission process and consequent dismantling of the primary cilium in the migrating cell (Das and Storey, 2014).

Later during neuroblast migration, however, the presence of CDH2 becomes essential again for the multipolar-bipolar transition occurring at the SVZ prior to glial-guided migration of neuroblasts toward the cortical plate (Franco et al., 2011; Jossin and Cooper, 2011; Gil-Sanz et al., 2013). The following glial-guided locomotion also utilizes CDH2 anchoring at the front and recycling at the back of the migrating cell to promote directed migration (Shikanai et al., 2011). The recycling mechanism involved in this is discussed in detail below as it has significant medical relevance. Finally, cadherin function is also necessary for the last part of radial migration called terminal translocation when the migrating neuron extends a process toward the pial surface and after connecting there, utilizes somal translocation to reach its final destination within the cortical plate (Nadarajah et al., 2001). This is demonstrated

by the postmitotic cell-specific *Dcx* promoter-driven expression of dominant negative CDH2 which resulted in migration arrest just prior to the cortical plate entry (Franco et al., 2011).

In the subpallium, CDH2 also plays a substantial role in the migration of postmitotic interneuron (IN) precursors to the cortical plate. CDH2-mediated migration of precursors is 7-times faster on CDH2-coated when compared to laminin-coated surface. This is due to strongly coordinated nuclear and centrosome movements which are disrupted in *Cdh2*^{−/−} precursors (Luccardini et al., 2015). Loss of *Cdh2* in postmitotic cells of the MGE results in delayed migration due to randomized localization of the centrosome within the cell. In turn, this leads to the loss of both the leading process and the polarized phenotype of migratory interneuron precursors in general (Luccardini et al., 2013). Unlike in the proliferating progenitor cells, postmitotic knockout of *Cdh2* does not affect proliferation and cell death rates in the ganglionic eminences (László et al., 2020a). Tangential migration of the affected cells, however is delayed and due to this, some of the precursors reach the pallium too late and cannot enter the cortical plate. Consequently, they are eliminated by the developmental apoptosis process which occurs at the end of the first postnatal week (Southwell et al., 2012; Wong et al., 2018). Remarkably, however, this effect was cell-type specific. The adult somatosensory cortex of *Dlx5/6Cre:Ncad^{fl/fl}* mice showed a strong reduction in CALB2 (calretinin)- and/or SST (somatostatin)-positive interneurons while the number of parvalbumin-positive INs did not change (László et al., 2020a). The molecular mechanism behind this cell-type-specific requirement of CDH2 is currently unclear, although it must be mentioned here that expression of both *Cdh2* and *Calb2* are highly regulated by the Aristaless (*ARX*) transcriptional repressor, an important factor in interneuron differentiation (Kitamura et al., 2002; Friocourt et al., 2008; Quillé et al., 2011).

The reelin signaling pathway and the mechanism of CDH2 action in pallial cortical migration

Reelin is a secreted glycoprotein produced by Cajal-Retzius cells which forms a decreasing gradient in the pial-ventricular direction within the embryonic cortex (Soriano and Del Río, 2005; Sekine et al., 2011). Spontaneous recessive mutation of its gene produces the mouse mutant *Reeler* which is characterized by inverted cortical lamination (D'Arcangelo et al., 1995; Ogawa et al., 1995). Neuroblasts undergoing their final stage of migration to the cortical plane *via* terminal translocation are expressing the receptors of Reelin, the very low-density lipoprotein receptor (VLDLR) and the apolipoprotein receptor E2 (ApoER2; Lane-Donovan and Herz, 2017; Dlugosz and Nimpf, 2018). Loss of these receptors produces a similar inverse cortical phenotype found in the

Reeler mutant (Trommsdorff et al., 1999; Hack et al., 2007). Receptor activation initiates the phosphorylation of Disabled-1 (DAB1) which in turn causes the stabilization of the cytoskeletal protein, cofilin, and the recruitment of integrins to the leading process of the migrating cell. This promotes the establishment of homophilic CDH2 connections between Cajal-Retzius cell and the migrating glutamatergic cell which is essential for terminal translocation the induction of neurite arborization and synaptogenesis (Franco et al., 2011; Gil-Sanz et al., 2013; Matsunaga et al., 2017; Jossin, 2020). For further details of Reelin signaling and function during brain development, the reader is referred to a recently published excellent review (Jossin, 2020).

Regulation of membrane-bound CDH2 protein levels

As we have seen the level of membrane-bound CDH2 is of fundamental importance for cell-cell adhesion during cortical development. Levels of CDH2 must be decreased during neural crest cell exit from the closing neural tube. During neurogenesis, the non-radial glia-fated daughter cell also must decrease their CDH2 levels in order to escape from the ventricular zone. Consequentially, active regulation of CDH2 protein levels represents a possibility to control cell migration. This decrease, however, is transient, as both radial glia-directed migration and the terminal translocation step require the presence of the protein. This tight control of CDH2 protein levels at the cell surface is carried out by two distinct mechanisms: endosomal recycling and proteolytic cleavage.

Endosomal recycling is carried out *via* different Rab-GTPases providing spatial and temporal regulation of CDH2 levels during different phases of radial migration. During glia-guided locomotion, the accumulation of the protein in the migrating precursor cell identifies the leading process which maintains a proper attachment to the radial glia scaffold. In contrast, CDH2 is endocytosed at the posterior end of the cell and these two parallel processes create a treadmilling effect moving the cell along the scaffold. Stable and dynamic locomotion of the cells is ensured by the coordinated action of endocytic vesicle-associated Rab-GTPases such as Rab5, Rab7, Rab11, and Rab23 (Kawauchi et al., 2010; Shikanai et al., 2011; Hor and Goh, 2018). CDH2 is internalized through clathrin- and dynamin-mediated Rab5-dependent endocytosis which could be followed by lysosomal degradation or Rab11-dependent recycling to the plasma membrane (Kawauchi et al., 2010; Shieh et al., 2011). At the final phase of radial migration, called terminal translocation, CDH2 is internalized by a Rab7-dependent pathway which allows the leading process to detach from the radial fiber and form connections to the Cajal-Retzius cells in the marginal zone (MZ, Chai et al., 2009; Kawauchi et al., 2010). This phenomenon is induced by the large extracellular

glycoprotein, Reelin as discussed above (Jossin and Cooper, 2011; Matsunaga et al., 2017).

Proteolytic cleavage of CDH2 is also an important way of regulating its cell surface levels which is carried out sequentially by ADAM10 (A Disintegrin and metalloproteinase domain-containing protein 10) and Presenilin 1 (PSEN1) acting as α - and γ -secretases, respectively (Baki et al., 2001; Marambaud et al., 2003). ADAM10 is a member of the α -disintegrin-and-metalloprotease family sometimes also referred to as MADM or Kuzbanian Protein Homolog after the name of the *Drosophila* mutant. Loss of ADAM10 results in embryonic lethality with some features resembling *Cdh2*^{-/-} embryos, including E9.5 embryonic lethality with defective somite, heart and vascular development and CNS abnormalities (Hartmann et al., 2002). Radial glia-specific disruption of *Adam10* results in perinatal lethality due to vascular hemorrhages in the brain. Importantly, The CTF1 generation of CDH2 was severely reduced in the KO animals. The affected mice also feature disrupted cortical lamination and decreased subpallium size, particularly the caudal ganglionic eminence (Jorissen et al., 2010). In addition, proliferation levels were also decreased during later stages (from E15 onward) of cortical development. Despite the shared features and fate of *Adam10*^{-/-} embryos to *Cdh2*^{-/-} animals, only two other ADAM10 targets, NOTCH and APP (Amyloid precursor protein) were analyzed in this study.

As discussed above, metalloproteases like ADAM10 directly regulate the level of CDH2 at the cell surface (Marambaud et al., 2003; Reiss et al., 2005). Interestingly, extracellular cleavage of CDH2 is also prevented by loss-of *Rab14*. This is due to the trapping of ADAM10 in an endocytic compartment thereby decreasing its levels in the cell membrane. As a result, CDH2-shedding is impaired, and its levels are increased on the cell surface inhibiting cell migration. Accordingly, this effect of *Rab14*-loss could be reverted by siRNA knockdown of CDH2 levels (Linford et al., 2012). It is important to emphasize that the migration assay was carried out on A549 lung carcinoma (i.e., epithelial) cells. Whether a similar effect is also induced in neurons is yet to be seen. Furthermore, ADAM10-mediated shedding liberates secondary messenger molecules from the intracellular complex leading to gene-expression changes (i.e., β -catenin) and cytoskeletal reorganization (*via* p120catenin). Finally, it is essential to note that knock-in mice expressing a cleavage-resistant form of CDH2 did have any early neural development changes indicating that ADAM10-mediated cleavage is not important during these processes (Asada-Utsugi et al., 2021).

CDH2 in neurite outgrowth, axon specification and guidance

Neurite outgrowth is one of the earliest and most thoroughly studied developmental processes to be promoted by CDH2

(Neugebauer et al., 1988; Tomaselli et al., 1988; Bixby and Zhang, 1990; Riehl et al., 1996). The role of CDH2 in axonal and dendritic development, however, already begins at the polarization of the postmitotic cell after asymmetric division (Pollaro et al., 2011). CDH2 concentration in the postmitotic cell promotes centrosome recruitment and the site of first neurite formation *via* PI3K signaling (Gärtner et al., 2012). It has been demonstrated that in the mouse embryonic cortex, NUMB, and NUMBL, two factors inherited asymmetrically by the progenitor but not the postmitotic cell, are co-localized in the apical extension with cadherin-based adherens junctions and help to maintain the apicobasal polarity of the RGPC-fated daughter cell. Coincidentally, disruption of *Numb* and *Numbl* results in the loss of cadherin connections and consequentially polarity in the progenitor cell (Rasin et al., 2007). As we discussed earlier, CDH2-based connections to radial glia fibers during glia-guided locomotion are essential for proper neuronal migration. Even as the postmitotic neuron migrates, however, dendrite vs. axon polarity is already being established in the cell in a CDH2-dependent manner. Recently, Kaibuchi and colleagues demonstrated that axon specification occurs at the opposite side of RGPC-neuron cadherin connections. Disruption of cadherin-based AJs also causes the loss of polarity and axon specification *via* interference with Rho and Rac1 kinase functions (Xu et al., 2015).

CDH2-dependence of axon guidance and targeting has been studied extensively. Without getting into too much detail, CDH2 has been demonstrated to be involved in these processes from *Drosophila* to mammals (Matsunaga et al., 1988; Riehl et al., 1996; Clandinin and Zipursky, 2002; Lele et al., 2002; Treubert-Zimmermann et al., 2002; Hirano and Takeichi, 2012; Sakai et al., 2012; Jontes, 2018; Yamagata et al., 2018; Sanes and Zipursky, 2020). In this respect, the interaction of CDH2 with the SLIT-ROBO signaling is of particular importance. Interestingly this pathway has been implicated previously in a set of developmental processes (e.g., progenitor proliferation and differentiation, interneuron migration, dendrite development, midline crossing of axons) very similar to those also requiring CDH2 function (Plump et al., 2002; Whitford et al., 2002; Andrews et al., 2007; Plachez et al., 2008; Borrell et al., 2012). Yet detailed interaction between CDH2 and SLIT-ROBO signaling has only been described in detail for axon guidance. In summary, activation of ROBO *via* its repulsive guidance cue partner SLIT recruits the Abelson kinase (ABL) which in turn binds the β -catenin-CDH2 complex *via* the linker molecule CABLES. ABL then phosphorylates and frees β -catenin from the adhesion complex which enters the nucleus and promotes the transcription of its targets. Consequently, this process also results in the weakening of CDH2-mediated adhesion and actin cytoskeleton rearrangement, two important steps in growth cone steering (Rhee et al., 2002, 2007). It is very tempting to propose that closer examination of CDH2-SLIT-ROBO interaction in the other, above-mentioned

neurodevelopmental processes could yield important results and help to understand their molecular nature.

CDH2 in synaptogenesis, synapse maintenance and synaptic function

Considering the reversibility of CDH2-based cell-cell interactions, it is not surprising that this molecule also plays a critical role during synaptogenesis and synaptic plasticity. Synapse formation starts in mid-gestation in humans and perinatally in rodents. It is a strictly regulated process influenced by different autocrine and paracrine signals which lead to the formation of the morphologically distinct pre- and postsynaptic regions divided by the synaptic cleft (Li et al., 2010; Budday et al., 2015). The synaptic regions of the two neurons are attached *via* bridge-like adhesion proteins between the two sides. The first, albeit indirect indication that CDH2 is expressed in the synapse was published in 1996 showing synaptic localization of α N-catenin which preferentially binds to CDH2 (Uchida et al., 1996). Later, several studies provided direct evidence using immunohistochemistry and confocal, as well as electron microscopy demonstrating that CDH2 protein appears in both the pre- and postsynaptic membrane. Its distribution is random at first within the synaptic region but as the synapse matures, the CDH2 dimers are gradually restricted to focal points within the synapses (Togashi et al., 2002; Elste and Benson, 2006; Yam et al., 2013).

Cytoskeletal structure and activity-dependent actin reorganization are key elements of both synapse formation and synaptic transmission. Adhesion complexes are usually tightly embedded in the plasma membrane and also hold a strong connection to the cytoskeleton *via* their intracellular part which binds several secondary catenin proteins in a multimolecular complex which creates a multifunctional protein hub (reviewed in Mège and Ishiyama, 2017). CDH2-based junctions, synaptic morphology and synaptic function form a mutually interdependent feedback loop where stronger synaptic activity strengthens synaptic adhesion and spine morphology and vice versa, strong synaptic adhesion leads to maturation of dendritic spines and elevated synaptic transmission (Tanaka et al., 2000; Togashi et al., 2002; Okamura et al., 2004; Bozdagi et al., 2010; Mendez et al., 2010). Importantly, the promotion of synaptic adhesion stabilizes the actin cytoskeleton of the dendritic spine, while loss of adhesion triggers destabilizing cytoskeletal changes. Using live-cell imaging and computer simulations, researchers demonstrated that ablation of CDH2 leads to spine shrinkage which highly depends on the reorganization of its actin cytoskeleton (Mysore et al., 2007; Chazeau et al., 2015). Accordingly, Mendez et al. (2010) showed that long-term potentiation promoted CDH2 cluster formation in stimulated spines. In contrast, utilizing an extracellular domain-lacking mutant CDH2 (Δ 390-Ncad)

caused not only the spine shrinkage but also a decrease in the size of its postsynaptic density (PSD) and consequently, LTP formation.

These transsynaptic CDH2-CDH2 interactions provide not only mechanical support but also evoke both synaptogenesis and synaptic maturation which can help to highlight the functional site of synaptic transmission. To initiate this process, the localization of CDH2 in the axonal growth cone or the developing spine is crucial (Basu et al., 2015). Any disruption of CDH2 or its associated molecules in the adhesion complex leads to spine ablation and reduction in key synaptic proteins such as synaptophysin or PSD95 (Togashi et al., 2002; Elia et al., 2006). Similarly, asymmetric expression of CDH2 in the pre- and postsynaptic cells results in synapse elimination and axon retraction (Pielarski et al., 2013). It has been shown that phospholipase D1 (PLD1) promotes dendritic spine development and increased synaptic adhesion and strength by elevating CDH2 levels in the cell membrane. This occurs *via* inhibition of the ADAM10 metalloprotease, which normally cleaves the extracellular domain of CDH2 (Luo et al., 2017). In addition, a year later the same laboratory found that the protein kinase D1 (PDK1) can phosphorylate the intracellular loop of CDH2 thereby promoting its membrane localization (Cen et al., 2018). Accordingly, disruption of PDK1-CDH2 interaction leads to reduced synapse numbers and impaired LTP formation (Cen et al., 2018). Finally, they demonstrated that these processes are all connected and part of the same pathway. PLD1 activates PDK1 which then regulates CDH2 and promotes spine morphogenesis (Li et al., 2019). In another study, Yamagata and colleagues found that other adhesion proteins such as the presynaptic neuroligin1 β require intercellular CDH2 dimerization to initiate proper postsynaptic differentiation (Yamagata et al., 2018).

Surprisingly, *in vitro* neuronal differentiation of embryonic stem cells from homozygous CDH2 knock-out blastocyst or conditional ablation of CDH2 from excitatory synapses (Bozdagi et al., 2010) did not replicate the aberrant synapse morphology described before but showed altered AMPA-mediated miniature EPSCs and reduced high-frequency stimulation-evoked vesicular release (Jüngling et al., 2006). The authors also found slower vesicular refill and turnover which in turn led to alterations in short-term plasticity. Further investigations revealed that homophilic CDH2 binding enhances vesicular endocytosis in a release-activity-dependent manner thereby coordinating and balancing the two processes in cooperation with Neuroligin1 (Stan et al., 2010; Van Stegen et al., 2017). In addition, this strong adhesion also maintains receptor recycling and stabilization at the postsynaptic region which also highlights its transsynaptic functions. It has been shown, that the GluA2 subunit of postsynaptic AMPA receptors directly interacts with CDH2 extracellular domain in both *cis* (i.e., CDH2 within the same cell) and *trans* (i.e., CDH2 in the presynaptic cell) manner. This heterophilic binding helps the

lateral diffusion of AMPA receptors, which determines the efficacy of excitatory postsynaptic potential and strengthens synaptic morphology (Saglietti et al., 2007). In another study, researchers demonstrated that the interaction of CDH2 and GluA2 leads to cytoskeletal changes by the activation of the actin-binding protein, cofilin. This data also revealed that electrophysiological changes determine the postsynaptic morphology and receptor availability in a CDH2-dependent manner (Zhou et al., 2011). Altogether, these precise molecular changes unravel the task of CDH2 in regulating the activity of the whole network which affects memory formation and behavior (Schrack et al., 2007; Asada-Utsugi et al., 2021).

CDH2 and neuronal cell death

There is one more cellular process that can be linked to CDH2, and that is cell death. In physiological conditions, proper cell-to-cell adhesion perpetuates downstream pro-survival pathways and maintains cell growth and health. *In vitro* evidence demonstrates that CDH2-based adherens junctions stabilize the expression of several anti-apoptotic molecules, such as BCL-2 or support anti-apoptotic pathways mediated by Erk1/2 MAP kinase (Tran et al., 2002; Lelièvre et al., 2012). During certain pathophysiological conditions like fibrosis or metastasis, epithelial cells undergo an epithelial-mesenchymal transition (EMT) which is accompanied by decreased CDH1 and elevated CDH2 expression. CDH2-mediated intercellular connections not only promote the cytoskeletal transition to a migratory phenotype but also act as pro-survival factors (Ko et al., 2012; Geletu et al., 2022). Loss of cell to extracellular matrix adhesion during EMT triggers a specific type of programmed cell death pathway called anoikis to prevent anchorage-independent cell proliferation (Paoli et al., 2013). Some of the metastatic cells, however, can develop an anoikis-resistant phenotype which is a key step to successful cancer metastasis. Interestingly, an identical but physiological process also takes place during cortical development. The establishment of cortical layering highly depends on the asymmetric proliferation of radial glial progenitor cells. Following cell division, the non-radial glia-fated cell delaminates by downregulating its connection to the neighboring cells at the apical and to the ECM at the pial surface while also changing its morphology in preparation for radial migration (Taverna et al., 2014). The molecular mechanism of this process strongly resembles that of classic EMT. Yet despite becoming anchorage-independent, these cells can survive (Singh and Solecki, 2015) which means that there is no anoikis-like protective mechanism during this process, or if there is, the non-radial glia-fated daughter cell can somehow escape it. On the other hand, the daughter cell that becomes a proliferative RGPC remains anchored and preserves its apico-basal polarity. Needless to say, that free migration of RGPCs would present an increased risk for brain malformations

such as various forms of heterotopias. The frequency of these diseases, however, is fairly low despite the millions of cell divisions during cortex development, indicating the presence of a protective anoikis-like cell death mechanism. Indeed, it has been recently demonstrated, that the ablation of cadherin-based adherens junctions by molecular methods and certain chemotoxic (ethanol) insults during cortical development both led to intrinsic, caspase3-mediated cell death (László et al., 2020b).

To further support the protective function of adherens junctions, elevated cell death has been described after the ablation of various other components of the AJ and the actin cytoskeleton. Due to spatial constraints, the reader is referred to a recently published excellent review on this topic (Veeraval et al., 2020).

The role of CDH2 in neuropsychiatric diseases

Based on the overwhelming evidence from various loss-of-function models, CDH2 is unambiguously one of the most important cell adhesion molecules during brain development with important roles in neurulation, neuronal proliferation, differentiation and migration, axon guidance, synaptogenesis and synaptic maintenance. Despite this, *Cdh2* has not been directly linked genetically to any human neurodevelopmental disorders until recently. Below, we summarize various neurological diseases linked to *Cdh2* in the last 10 years and provide details of the underlying molecular mechanisms where it is available (Figure 2). We only discuss diseases due to direct mutations of the *Cdh2* gene or mutations which cause defective regulation of the protein. Other diseases which have only a second-degree connection to CDH2 such as those affecting the various molecules of the actin cytoskeleton (with one exception) or tubulinopathies will not be included due to space constraints.

ACOG-syndrome

In 2019, Accogli et al. reported *de novo* heterozygous pathogenic *Cdh2* variants in 9 individuals. The six different missense mutations affected the extracellular domain of the protein, while the two distal frameshift mutations were found in the cytoplasmic region. Patients had various symptom combinations including global developmental delay, intellectual disability, axonal pathfinding defects, cardiac, ocular, and genital malformations. In order to summarize this wide spectrum of symptoms the collective term ACOG syndrome was created (agenesis of corpus callosum, axon pathfinding, cardiac, ocular, and genital defects; Accogli et al., 2019; Kanjee et al., 2022). These symptoms correlate well with some features of loss-of-CDH2 function models in mice (Riehl et al., 1996; Redies, 1997;

Kadowaki et al., 2007; Oliver et al., 2013; Piprek et al., 2019) and other vertebrates (Gänzler-Odenthal and Redies, 1998; Lele et al., 2002; Masai et al., 2003; Rebman et al., 2016). Of the various mutations, those that are located on the extracellular part of CDH2 all resulted in weaker adhesion than created by the wild-type protein. In particular, Asp353Asn mutation affects one of the Ca^{2+} -binding sites important for trans dimerization and consequently cell-to-cell adhesion (Vendome et al., 2014). The rest of the extracellular domain mutations probably also provide weaker adhesion due to the not perfect sterical alignment of the extracellular cadherin domains during cis and trans dimerization. The frameshift mutations affecting the intracellular part of the molecule obviously prevent proper binding of p120 and/or β -catenin to CDH2 thereby interfering with its interaction with the actin cytoskeleton.

Attention deficit and hyperactivity disorder (ADHD), Obsessive compulsory disorder (OCD), Tourette syndrome (TS), Autism spectrum disorder (ASD).

These diseases have often been shown to express comorbidity, so they will be discussed together.

Attention deficit and hyperactivity disorder

Very recently, Halperin and colleagues reported the first familial *Cdh2* mutation connected to attention-deficit hyperactivity disorder (ADHD). Three siblings of the subject were diagnosed with ADHD in early childhood, two of them are non-identical twins who were born prematurely. Performing whole-genome sequencing, researchers found a single homozygous variant in the locus of c.355 C > T; p.H150Y in *Cdh2* gene, affecting the first full transcript variant. This mutation results in a single amino acid change in a non-organized loop structure between the first extracellular domain of the protein and the pro-domain. This region is indispensable for further protease modification by proteolytic enzymes such as the *FURIN* protease (Halperin et al., 2021). The mutant tyrosine changes the conformation of the binding site, therefore, inhibiting the maturation of the protein. Generating a unique animal model which has this new familial mutation, they found that transgenic animals replicate the human ADHD behavioral phenotype. Moreover, further immunohistochemical analysis revealed that familial *Cdh2* mutation decreases the size of the presynaptic vesicle cluster and changes the excitability of the neurons in the prefrontal cortex and hippocampus. Importantly, this change was cell-type-specific, affecting the dopaminergic neurons in the VTA which project to higher cognitive areas, highlighting the importance of CDH2 function during the previously ignored midbrain development and connectivity. The reduced tyrosine hydroxylase expression and consequent dopamine level drop in the ventral midbrain and prefrontal cortex indicates a compromised reward mechanism which could


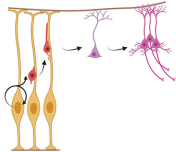
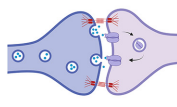
Developmental stage	Molecular link	Disease	Symptoms	Reference
Neurulation/Neural crest/ Stem cell proliferation 	heterozygous <i>Cdh2</i> mutations - missense (p.D353N; p.D597N; p.D597Y; p.N601T; p.C613W; p.D627G; p.Y676C) - frameshift mutations (p.L855Vfs*4; p.L856Ffs*5)	ACOG syndrome	global developmental delay, intellectual disability, axonal pathfinding defects, agenesis of corpus callosum, cardiac, ocular, and genital malformations	Accogli et al. 2019 Kanjee et al. 2022
	CDK5/p35 - CDH2	Miller-Dieker syndrome (MDLS)	lissencephaly, microcephaly, intellectual disability, craniofacial malformation	Kwon et al. 2000
Neuronal migration 	RAB18 - CDH2	Warburg Micro Syndrome (WARBM)	microcephaly, corpus callosum abnormalities, mental retardation, optic atrophy and hypogenitalism	Wu et al. 2016
	mHTT - Rab11- CDH2	Huntington disease (HD)	progressive chorea, motor dysfunction and dementia	Barnat et al. 2016 Barnat et al. 2020
	FilaminA - CDH2	Periventricular heterotopia (PVH)	neuronal migration defects, mild intellectual disability, epilepsy	Ferland et al. 2009
Synaptic physiology 	homozygous <i>Cdh2</i> variant (p.H150Y)	Attention deficit-hyperactivity disorder (ADHD)	impaired brain activity, cognitive and attention deficit, dopamine secretion imbalance	Halperin et al. 2021
	<i>Cdh2</i> missense variants (p.A118T; p.V298I; p.N706S; p.N845S)	Tourette syndrome and Obsessive-compulsive disorder (OCD)	impairment of the mesolimbic circuit simple and complex motor tics, obsession, compulsive behaviour	Moya et al. 2013 McGregor et al. 2016
	Reelin - ApoER2/Vldlr - Dab - CDH2 Presenilin (PSEN1) - CDH2	Alzheimer disease (AD)	extracellular A β deposits, intracellular tau protein tangles, synapse loss, dementia, behavioural changes	Uemura et al. 2003 Andreyeva et al. 2012 Ando et al. 2011 Choi et al. 2020

FIGURE 2

CDH2-linked neurodevelopmental and neurodegenerative diseases. The schematic drawings in the figure represent the different developmental processes associated with *CDH2* function and the associated diseases based on the genetic or direct molecular link. Image was created using Biorender.com.

explain the increased attention-seeking behavior of the affected children (Halperin et al., 2021).

Obsessive compulsory disorder

In 2009 Dodman et al. (2010) carried out a genome-wide association study with fine mapping of the Chromosome 7 region involved in dogs phenotyped for signs of canine compulsory disorder CCD. The most significantly associated single nucleotide polymorphism (SNP) was located within the *Cdh2* gene. In addition, targeted exon sequencing analyses found SNPs within *Cdh2* linked to both increased and reduced risk to develop OCD (McGregor et al., 2015) strongly indicating the involvement of *CDH2* in the disease.

Tourette-syndrome

There are two whole exome sequencing studies involving TS patients which identified variants within the *Cdh2* gene (Moya et al., 2013; Nazaryan et al., 2015). The first study could not establish enough evidence for an association between the mutations and TS but concluded that *CDH2* and cadherins in general are interesting genes to study in the future as plausible contributors to TS and OCD (Moya et al., 2013). The second

study could not find the SNP in their cohort described in the previous study but combining their data with other studies concluded that the variant described previously, albeit extremely rare, is indeed associated with both TS and OCD (Nazaryan et al., 2015). Furthermore, they also described a single nucleotide variant which occurred in a patient with combined symptoms of TS, OCD, ASD and ADHD. It is important to note, however, that both studies have used a relatively small cohort ($N = 219$ and $N = 320$), but these results justify further larger-scale GWA studies in this direction.

Autism spectrum disorder

In a recent study, Liu and colleagues reanalyzed two previous large-scale literature studies involving ASD and OCD research data to identify novel target genes for future GWA studies (Liu et al., 2019). For the genes being predicted for both diseases, a protein-protein interaction literature search was also carried out. The co-occurrence rate for genes linked to both diseases was found to be 6.4% and 8.3% meaning 43 and 47 genes, respectively. Most importantly, for our purposes at least, *Cdh2* was identified as a strongly linked gene in one of the datasets. Interestingly, the *ApoE* gene, previously implicated in ASD and sporadic Alzheimer's disease (AD; Won et al., 2013) was also identified in both datasets as a candidate gene. In fact,

ApoE mutations could interfere with both developmental and synaptic CDH2 functions. First, APOE can significantly inhibit the binding of Reelin to its receptors, VLDLR and APOER2 (D'Arcangelo et al., 1999). This could impair Reelin-dependent, CDH2-mediated terminal translocation of migrating neuron precursors to the cortical plate. Synaptic functions of both Reelin and CDH2 are probably also very important since the appearance of ASD symptoms coincides with the synaptic development stage. ASD manifestation is primarily mediated by the synaptic roles of *ApoE* interfering with NMDA and AMPA receptor function. It is conceivable, however, that similarly to development, Reelin signaling disturbed by *ApoE* mutation contributes to the disease symptoms. This is supported by the importance of CDH2 in AMPAR trafficking (Nuriya and Hukanir, 2006; Saglietti et al., 2007; Zhou et al., 2011) and the fact synaptic effects of *ApoE* mutations are transmitted via PI3K-Akt signaling pathways which is also essential in mediating the neural stem cell maintenance function of CDH2 during cortical development (Zhang Y. et al., 2010; Zhang et al., 2013).

In this regard, it is also interesting to note that *Cdh8*, *Cdh9*, *Cdh10* and *Cdh11*, four types of classic cadherins which are also expressed in the developing cortex, have also been linked to ASD recently indicating a potential, functional redundancy with *Cdh2* (Wang et al., 2009; Pagnamenta et al., 2011; Lefkovic et al., 2012). In addition, CDH13, a unique GPI-anchor-bound cell surface cadherin has been demonstrated to be a very important genetic factor in both ADHD and autism indicating that genetic redundancy and possibly molecular interactions between these proteins should be examined more closely in the future (Rivero et al., 2015).

Peter's anomaly (PA)

PA is a disease that is characterized by the failure of separation of the iris and the cornea (type 1) or the cornea and the lens (type 2) during eye development. Besides these, in about 70% of the patients who have bilateral manifestation additional symptoms including abnormalities in craniofacial and genito-urinary development, brachydactyly and short stature are also present (Bhandari et al., 2011). More importantly, a recent study identified a *de novo* heterozygous splicing variant of *Cdh2* in patients which would result in a truncated variant of the protein terminating translation at the first EC domain. Significantly, all 4 affected patients also displayed agenesis of the corpus callosum and cognitive delay which could be due to disturbance of axon guidance and synaptic maintenance, respectively, processes CDH2 is essential for (Reis et al., 2020).

Next, we discuss several diseases which are indirectly caused by CDH2 malfunction due to mutations in other proteins regulating its availability or function.

Warburg Micro syndrome

Warburg Micro syndrome (WARBM) is a recessive autosomal developmental disorder, characterized by microcephaly, corpus callosum abnormalities, intellectual disability, optic atrophy and hypogenitalism (Morris-Rosendahl et al., 2010). Based on genetic screening, WARBM is classified into four different types: type 1 is caused by the inactivating mutation of *Rab3gap1* gene coding for a catalytic subunit of a GTPase-activating protein, (41% of the cases); type 2 is associated with the mutation in *Rab3gap2* gene (7% of the cases), type 3 mutation affects the *Rab18* gene (5%) and the loss-of-function mutation in the GTPase-activating protein TBC1D20 is responsible for the type 4 (Morris-Rosendahl et al., 2010; Handley et al., 2013; Liegel et al., 2013). All these mutations are affecting various members of the RAB-mediated intracellular transport pathways. Interestingly, however, these diseases share common symptoms with the *Cdh2* mutation linked ACOG syndrome described above which points to the direction that the inadequate vesicular turnover of CDH2 might also be responsible for WARBM. In fact, Wu and colleagues using a combination of *in vivo* and *in vitro* models showed direct evidence that the loss-of-function mutation in *Rab18* gene increases the lysosomal degradation of CDH2, which leads to its decreased membrane presence and caused migration defect and neurite growth (Wu et al., 2016). Furthermore, mouse *Cdh2* loss-of-function experiments resulted in premature differentiation of neuronal progenitors which led to decreased number of neurons in the cortex which might also contribute to the observed microcephaly in WARBM (Zhang J. et al., 2010; Wu et al., 2016; Khalesi et al., 2021).

Miller-Dieker syndrome

Miller-Dieker lissencephaly syndrome (MDLS) is characterized by a combination of classic lissencephalic features (e.g., pachygyria) with microcephaly, intellectual disability, craniofacial malformation and seizures. It is caused by heterozygous deletion of chromosome 17p13.3 including the *Pafah1b1* (more commonly known as *Lis1*) gene which is responsible for the lissencephalic features and the *Ywhae8* gene (14.3.3e) gene the product of which interacts with proteins like CDC25A and CDC25B involved in the proper execution of mitosis. Mice with a heterozygous inactive allele of *Pafah1b1* have severe cortical and cerebellar lamination defects due to defective neuron migration (Hirotsune et al., 1998; Gambello et al., 2003). This is carried out through the regulation of dynein function via NUDEL and CDK5/p35 (Niethammer et al., 2000; Sasaki et al., 2000). Interestingly, in the same year, CDK5/p35 has also been established as the regulator of CDH2-mediated adhesion between cortical neurons (Kwon et al., 2000). Despite this, and the *in vivo* evidence pointing to CDH2 as the main

regulator of cortical stemness *via* the β -catenin pathway, *Cdh2* could not be linked genetically to MDLS before (Zhang J. et al., 2010; Zhang et al., 2013). Recently, however, Ladewig and colleagues (Iefremova et al., 2017) using a cortical organoid model grown from MDLS patients have demonstrated that alterations in the architecture of the cortical neurogenic niche due to disruption of the tubulin cytoskeleton also results in defective CDH2 - AKT - β -catenin signaling. This in turn, evokes an increased premature cell cycle exit and differentiation of cortical progenitors which is one of the main factors causing microcephaly.

Recently, an interesting paper examined the HIC1 (Hipermethylyated in cancer 1) tumor suppressor protein which is also associated with MDS (Ray and Chang, 2020). Just like *Pafah1b1*, the *Hic1* gene is also included in the chromosomal deletion responsible for MDS (Carter et al., 2000). Ray and colleagues used the *Xenopus* as a neural crest model animal to study the effect of *Hic* knockdown. They found that *Hic1*-loss caused defective craniofacial development which was due to the abnormal migration of neural crest cells. Furthermore, they established that *Hic1* regulates the expression of Cadherins 1, 2 and 11 *via* Wnt signaling. The role of CDH2 in the collective migration of the neural crest has been detailed above and these data when combined present a strong argument for the involvement of CDH2 both in the neural and craniofacial aspects of the Miller-Dieker syndrome.

Periventricular nodular heterotopia (PVH)

We have to make one exception in this review despite the fact, that no direct genetic evidence implicates CDH2 involvement in this disease. Cortical malformations are a large group of neurodevelopmental diseases with a wide range of symptomatic appearances (Juric-sekhar and Hevner, 2019). Nevertheless, most of these are caused by the defective function of two extremely important processes during cortical development, namely progenitor proliferation and neuron precursor migration. Here, we focus on periventricular heterotopia which occurs when a large number of neurons and proliferative progenitors fail to migrate normally and accumulate close to the ventricle. Furthermore, disruption of the apical adherens junction barrier sometimes allows this cell mass to intrude into the ventricle. Notably, a very similar process takes place in *Cdh2*^{-/-} mutants (Gil-Sanz et al., 2014). Initial genetic studies identified that mutations in *FilaminA* (*Flna*) and *Arfgef2* genes are associated with the disease. FLNA is an actin regulatory protein promoting branching at the leading edge of migrating cells (Gorlin et al., 1990; Flanagan et al., 2001). It has been also shown to be required for cell-to-cell contact formation during heart and vessel development (Feng et al., 2006). It is an X-chromosome-linked gene and its mutation

causes PVH in heterozygous females but lethality in hemizygous males (Hart et al., 2006). Interestingly, postmortem examination of PVH patients led to the conclusion that the cells forming the nodules are composed of late-born neurons (Ferland et al., 2009). In addition, they also described strong denudation of the ventricular wall a feature phenocopied in mice in which CDH2 function was disrupted perinatally (Oliver et al., 2013). These similarities make it very tempting to speculate that loss-of *Flna* which disrupts the actin-based cytoskeleton eventually also leads to CDH2-based adherens junction disruption producing intraventricular heterotopia.

CDH2 and its connection to neurodegenerative diseases

Dementia and neurodegenerative diseases

With increasing life expectancy all around the world but particularly in developed countries, dementia presents an extremely large social and economic burden on society. In 2018, approximately 9 million people, representing about 7% of the population aged over 60 are living with dementia in EU member states, up from 5.9 million in 2000, and this number is projected to increase to around 14 million in 2040 (OECD/EU (2018). according to the recent report, Health at a Glance: Europe 2018: State of Health in the EU Cycle, OECD Publishing, Paris. https://doi.org/10.1787/health_glance_eur-2018-en).

Alzheimer's disease

Alzheimer's disease is the most common form of frontotemporal dementia characterized by severe neurodegeneration and cortical atrophy. In 2019, Alzheimer's Disease International estimated that there were over 50 million people living with dementia globally, a figure set to increase to 152 million by 2050, and the current annual cost of dementia is estimated at US \$1trillion, a figure set to double by 2030. Alzheimer's Disease International (2019). Synaptic loss is one of the earliest features of AD which correlates well with its symptomatic progression. Generally, it is caused by the extracellular deposition of the toxic amyloid- β and the intracellular accumulation of phosphorylated tau protein tangles resulting in the disruption of neuronal circuits in the prefrontal cortex, hippocampus and at later stages in other brain areas as well (Deture and Dickson, 2019). Synaptic loss, however, can occur independently of amyloidosis *via* enhanced microglial phagocytosis of synaptic structures (Rajendran and Paolicelli, 2018; Subramanian et al., 2020). Below we comprise some of the

data which indicates potential involvement of CDH2 in the etiology of AD.

CDH2, presenilin and the early-onset familial Alzheimer's disease

Familial Alzheimer's disease (FAD) consists only 5% of the total AD cases worldwide. Mutations responsible for FAD occur in 3 genes: amyloid precursor protein (APP), presenilin 1 and 2 (PSEN1 and 2, respectively). All three proteins have their specific synaptic function, including but not limited to neuronal outgrowth, vesicular cycle and release, lysosomal homeostasis and autophagy (Elder et al., 1996; Hung and Livesey, 2018; Padmanabhan et al., 2021).

PSEN1 is the proteolytic subunit of the γ -secretase complex which cleaves transmembrane proteins by initiating a wide range of indispensable biochemical processes and pathways. However, this complex also cleaves the transmembrane domain of the APP protein which produces the toxic and accumulative form of the amyloid- β -peptide (A β 1-42) forming the characteristic plaque depositions in Alzheimer's disease (Takasugi et al., 2003; Watanabe et al., 2021). Besides its plasma membrane localization, PSEN1 is also present in the endoplasmic reticulum, where it is responsible for post-translational endoproteolytic processing by cleaving the N- or C-terminal fragments (NTF or CTF, respectively) of various proteins (Wolfe, 2019). Not surprisingly, the loss of PSEN1 function leads to irreversible malfunctions. PSEN1 knock-out mice die perinatally (Shen et al., 1997) while conditional ablation of the gene in proliferating neuronal progenitors disrupts both neurogenesis and cell proliferation (Kim and Shen, 2008). Human mutations in PSEN1 gene, however, do not replicate the phenotype of the knockout models, moreover, they can rescue the full knock-out lethality (Qian et al., 1998). Currently, more than 350 PSEN1 human mutations are known which affect the enzymatic function of the protein¹, and most of them lead to neuronal cell death and cytotoxicity (Edwards-Lee et al., 2006; Lazarov et al., 2006).

In 1999, Georgakopoulos and colleagues showed for the first time, that PSEN1 can form an intracellular macromolecular complex with cadherins and catenins which maintains cell-to-cell connections and neurite outgrowth. This was also confirmed by electron microscope using rat cornea samples where PSEN1 and CDH2 co-localized in synaptic junctions (Georgakopoulos et al., 1999). Furthermore, utilizing recent developments in super-resolution microscopy, namely Stimulated Emission Depletion (STED) and Single-Molecule Localization Microscopy (SMLM), it has been demonstrated at an even greater resolution that the whole γ -secretase complex

is in close proximity to the CDH2-based macromolecular hub (Escamilla-Ayala et al., 2020). It has also been described that exclusively PSEN1, and not PSEN2 regulates CDH2 levels by cleaving the cytoplasmic part of the protein (Jang et al., 2011) and thereby also altering the vesicular trafficking of CDH2 from the ER to the plasma membrane (Uemura et al., 2003). This precise regulation might work as an ultimate pro-survival signal, as loss of homophilic CDH2-binding due to *Psen1* mutation and/or malfunction leads to synapse loss and cell death. Further substantiates this notion that C-terminal cleavage of CDH2 by PSEN1/ γ -secretase complex produces a truncated CTF which in turn alters AMPA-mediated synaptic transmission and amplifies the effect of toxic A β -induced synapse damage (Priller et al., 2007; Jang et al., 2011; Andreyeva et al., 2012). Beyond the toxic A β accumulation in the AD brain, truncated CDH2 C-terminal fragments also form aggregates in human AD patients (Andreyeva et al., 2012). Interestingly, performing a high-throughput genome-wide analysis revealed a rare autosomal copy number (488kb) polymorphism in the *Cdh2* gene in FAD patients reinforcing the idea that PSEN1/CDH2 signaling is an important part of AD synaptic pathogenesis (Hooli et al., 2014).

Sporadic Alzheimer's disease, ApoE, Reelin and CDH2

Sporadic or late-onset AD (LOAD) cases are the most common forms of the disease which usually appear after the age of 60. There are several risk genes which increase the likelihood of developing LOAD, the most important of them is the lipid carrier protein *Apolipoprotein E* (*ApoE*). The *ApoE* gene has 3 slightly different alleles in humans *ApoE*₂, *ApoE*₃ and *ApoE*₄. The last one has a strong correlation with developing LOAD (Husain et al., 2021) while *ApoE*₃ is neutral and *ApoE*₂ has a positive anti-LOAD effect. All APOE protein variants are ligands for both the low- (LDLR) and the very low-density lipoprotein receptors (VLDLR) as well as ApoE receptors (reviewed in Bock and May, 2016). These receptors are mostly localized in the postsynaptic density and interact with glutamatergic receptors, as well as adhesion and scaffold proteins. This means that Reelin and APOE proteins share a signaling pathway (or at least the receptors) in the synapse. In addition, APOE4 also influences vesicular turnover and receptor recycling leading to altered Reelin and glutamate signaling (Lane-Donovan and Herz, 2017). Interestingly, Reelin also interacts with APP by regulating its localization at the plasma membrane and promotes dendritic arbor development (Hoe et al., 2009). This and other results highlight that Reelin signaling can be neuroprotective in AD at the early stages. Increased levels of Reelin in human AD CSF appear at the early stages of the disease which might be the result of disrupted ApoER signaling or a compensatory mechanism to protect

¹ <https://www.alzforum.org/mutations/>

synapses (Sáez-Valero et al., 2003; Botella-López et al., 2006; Lopez-Font et al., 2019). In contrast, at later stages increasing the amount of Reelin depositions also correlates well with reduced memory formation in aged wild-type rodents indicating a potential dual function for the protein in AD. This phenomenon is greatly enhanced both in AD mouse model and human LOAD cases, where Reelin deposits are co-localized with A β plaques, fibrillary tangles and correlate with cognitive deficits showing a distinct spatial and temporal function of Reelin in AD pathogenesis (Knuesel et al., 2009; Ramsden et al., 2022).

Considering the cooperation between Reelin signaling and CDH2 through the small GTPase RAP1, it is quite tempting to suggest that CDH2-based synaptic junctions are affected in LOAD. Accordingly, the deposition of A β plaques decreases the surface level of CDH2 *via* phosphorylation of Tau and p38 MAPK signaling (Ando et al., 2011). Furthermore, by measuring CDH2 degradation product levels in brain homogenates and CSF from human AD patients Choi et al. (2020) showed that its C-terminal fragment is accumulated in the brain parenchyma. In parallel, NTF levels are also elevated in both human and rodent CSF. Based on this, we dare to hypothesize that CDH2 is a significant downstream effector of the Reelin-ApoER2/VLDLR-DAB pathway not only during development but also in the adult brain. Moreover, the abovementioned evidence suggests that Alzheimer's disease-related ApoE-mutations can disrupt neural function at least partly by interfering with CDH2-dependent synaptic plasticity.

Huntington disease

Huntington disease (HD) is an autosomal fatal neurodegenerative disorder which manifests in progressive chorea, motor disfunction and dementia caused by the CAG expansion repeat of the *huntingtin* gene (HTT). 36 or more CAG repeats change the structure of the mutated HTT (mHTT) protein which will develop soluble monomers and oligomers, then gather as mHTT fibrils eventually causing large inclusions along the cells. This leads to cellular toxicity and cell death of the striatal neurons which also spreads to other brain areas (Gallardo-Orihuela et al., 2019; Tabrizi et al., 2020). Although the disease is usually diagnosed in mid-age, more and more evidence support the notion that HD is a developmental disease and mHTT presence already affects perinatal brain development and wiring. The first indication of its developmental function was when Zeitlin and colleagues demonstrated that full elimination of the *Htt* gene causes early embryonic lethality and elevated levels of cell death (Zeitlin et al., 1995). Loss of *Htt* during cortical development resulted in a decrease of progenitor and an increase in postmitotic cell numbers indicating a premature cell cycle exit (Molina-Calavita et al., 2014). Later, a knock-in model expressing an HTT protein with an increased

poly Q region (Q111) featured delayed cell cycle exit supporting this notion (Molero et al., 2016). Moreover, researchers also found subpallial periventricular heterotopias and misplaced cells in this model (Arteaga-bracho et al., 2016). These results highlight the fact that HTT protein is an important molecular player during brain development, which CDH2 is also involved in. Recently, the first direct functional connection between HTT and CDH2 during cortical development was provided by Barnat et al. (2017). Generating dorsal telencephalon-specific loss-of *Htt* restricted to postmitotic cells, they showed that HTT is indispensable for normal multipolar/bipolar transition during radial migration in the embryonic cortex. Moreover, they also found that HTT affects CDH2 localization through regulation of its Rab11-dependent endosomal trafficking. The reintroduction of Rab11 in animals expressing mHTT proteins could prevent the migration deficit and the mislocalization of CDH2. This interesting connection between HTT and CDH2 was also supported by another study examining the cortical development of 13 weeks old human fetuses carrying polyQ HTT mutation. CDH2-based adherens junction complexes were disrupted at the bottom of the ventricular zone, which leads to abnormal polarization, cell production and fate commitment (Barnat et al., 2020). Very recently, a study analyzing postmortem human tissue from patients with Huntington disease revealed that the abovementioned developmental malformations affected the adult brain, in fact, as changes were still recognizable in adulthood. Examining 8 individuals, they found periventricular heterotopias all along the ventricles, which might be a clear representation of CDH2 function loss *via* mHTT in HD patients (Hickman et al., 2021). Since CDH2 has multiple functions during brain development, it is not surprising that mHTT influences synaptic physiology by altering CDH2-based synaptic junctions. Previously, we highlighted the functional importance of the fine balance between ADAM10 metalloprotease and CDH2 expression levels, which is also completely altered in HD. It has been shown that mHTT triggers the postsynaptic accumulation of ADAM10 which in turn leads to the sequestration and cleavage of CDH2. Furthermore, pharmacological inhibition of ADAM10 could prevent the proteolysis of CDH2 and improve the electrophysiological properties of striatal neurons (Vezzoli et al., 2019). Therefore, just like ADAM10, CDH2 could also be an interesting therapeutics target for slowing or halting the disease in the early phase.

Huntington disease, CDH2, and the hydrocephaly connection

In hydrocephaly (HC) the ventricles of the brain are abnormally enlarged (megaloventriculi) and filled with cerebrospinal fluid. HC can occur due to genetic causes (congenital HC; (Abdelhamed et al., 2018; Furey et al., 2018;

Roy et al., 2019) or as a secondary symptom due to external factors like intraventricular hemorrhages or various tumors (acquired HC) (Kahle et al., 2016; Castaneyra-Ruiz et al., 2018). The elevated pressure caused by the fluid build-up in the brain can cause serious damage to the surrounding brain tissue, particularly in the ependymal cell lining of the ventricles which are important in promoting CSF circulation. Blockage within the CSF draining system or conditions disrupting cilia structure or coordinated cilia movements also results in hydrocephaly which in turn, leads to the loss of the ependymal lining (denudation) of the ventricle walls (Tissir et al., 2010; Abdelhamed et al., 2018). Ependymal cells are derived from radial glia progenitor cells (Spassky, 2005), and consequently, they also do not have tight junction connections. Instead, they are held together exclusively by AJs and gap junctions (Del Bigio, 1995). As described beforehand, CDH2 is an integral part of AJs in the developing CNS so it was not surprising, when it was found that the neurogenic SVZ niche was disrupted in the hydrocephaly model *Hyh* mutant. Causality between the two phenomena was established when later experiments demonstrated that loss-of CDH2-based adherens junctions dispersed ependymal cells of the mouse brain resulting in ventricular wall denudation and hydrocephaly (Gate et al., 2012; Oliver et al., 2013; Guerra et al., 2015). Coincidentally, loss of AJs also precedes ependymal denudation in human fetuses with spina bifida aperta (Sival et al., 2011) which correlates well with the fact that mouse loss-of-function model of CDH2 also has partial neurulation defects (Luo et al., 2001). Moreover, congenital hydrocephalus caused by loss of the *Htt* gene in a mouse model was also associated with corpus callosum defects (Dietrich et al., 2009) in which CDH2 is also heavily involved (see above). The explanation for these events can be found in the normal function of the HTT protein which is to regulate the ciliogenesis of ependymal cells (Keryer et al., 2011). As a consequence, late-onset Huntington disease patients have been misdiagnosed before as normal pressure hydrocephalus (Caserta and Sullivan, 2009; Dennhardt and Ledoux, 2010). Interestingly, there is a form of congenital HC in which intraventricular pressure remains normal called idiopathic normal pressure hydrocephalus (iNPH) also characterized by gait disturbance and dementia. Due to similar symptoms and decreased CSF A β 1 – 42 levels, iNPH can be mistakenly diagnosed as Alzheimer's disease (Picascia et al., 2015; Schirinzi et al., 2015).

From the evidence discussed above and in previous parts of this review indicating the involvement of CDH2 in both Alzheimer's disease and Huntington disease, we dare to hypothesize that CDH2 might be a common pathological factor during the development of these diseases.

In summary, CDH2-loss-dependent ventricular wall denudation leads to CSF circulation defects, and vice

versa, CSF circulation defects can result in ventricular wall denudation creating a positive feedback phenomenon that leads to HC. Either way, CDH2 is right in the middle of this process.

Future considerations

In this review, we summarized recent developments which furthered our understanding of the function of CDH2 in neural development and disease. For years, people working on this protein have wondered how it was possible that CDH2 did not have any direct evidence linking it to any neural diseases. Well, accumulating results of the last few years have put this protein into an entirely new perspective and undoubtedly, the coming years will provide even more novel aspects regarding CDH2 function. Certainly, one of the most interesting question is how one gene could be involved in so many diseases. Well, the most likely answer lies in the occurrence of somatic mutations affecting different areas of the brain at various developmental stages. Therefore, the clarification of whether inherited or somatic mutations are behind a given disease, is essential. And if somatic mutations are responsible then establishing at what stages and which areas are affected will be of utmost importance. In some NDs the overwhelming percentage of the cases are caused by sporadic somatic mutations (e.g., Alzheimer's disease) therefore further large-scale sequencing efforts will have to be carried out in the future which will help to reveal the genetic and molecular interactions behind these diseases. The next important task concerns the regulation of CDH2 levels. Is there a functional reason behind the choice of endocytic vs. shedding method of regulation, or are these complementary or alternative to each other in different cell types or biological processes? Finally, a very interesting and potentially clinically relevant issue is whether shed extracellular CDH2 fragments in the CSF could serve as detectable disease markers in various implicated diseases affecting the CNS.

Although this review focuses on CDH2, the research perspectives section should not ignore the question of potential functional redundancy and possible heterodimerization between CDH2 and other classic cadherins. There are a lot of other classic cadherins which are also expressed strongly in the developing mammalian CNS (Ranscht and Dours-Zimmermann, 1991; Bekirov et al., 2002; Takahashi and Osumi, 2008; Mayer et al., 2010; Lefkovic et al., 2012) some of which have been linked previously to diseases causing various forms of intellectual disability (for review see Redies et al., 2012; Hawi et al., 2018). With the continuous advancement of the CRISPR/Cas9 technique, researchers finally have a straightforward and relatively cheap tool to investigate the question of redundancy among various classic cadherins by

creating double or when it is possible, various combinations of multiple mutations. Undoubtedly this will help to further the efforts of our common goal in developmental neuroscience: understanding the formation of the human brain.

Author contributions

ZIL and ZL planned and equally provided an intellectual contribution during manuscript preparation including conceiving the idea, collecting information, and writing the manuscript. Both authors approved it for publication.

Funding

ZIL holds a Lady Edith Wolfson Junior Non-Clinical Fellowship from The MND Association (Laszlo/Oct21/977-799). Support has been provided by the National Research, Development and Innovation Fund of Hungary under the 'Frontline' - Research Excellence Program KKP_19 (KKP 129961) and the National Program in Brain Sciences (2017-1.2.1-NKP-2017-00002) funding scheme.

References

- Aaku-Saraste, E., Hellwig, A., and Huttner, W. B. (1996). Loss of occludin and functional tight junctions, but Not ZO-1, during neural tube closure-remodeling of the neuroepithelium prior to neurogenesis. *Dev. Biol.* 180, 664–679. doi: 10.1006/dbio.1996.0336
- Abdelhamed, Z., Vuong, S. M., Hill, L., Shula, C., Timms, A., Beier, D., et al. (2018). A mutation in *Cdc39* causes neonatal hydrocephalus with abnormal motile cilia development in mice. *Development* 145:dev154500. doi: 10.1242/dev.154500
- Accogli, A., Calabretta, S., St-Onge, J., Boudrahmed-Addour, N., Dionne-Laporte, A., Joset, P., et al. (2019). De Novo pathogenic variants in N-cadherin Cause a syndromic neurodevelopmental disorder with corpus callosum, axon, cardiac, ocular, and genital defects. *Am. J. Hum. Genet.* 105, 854–868. doi: 10.1016/j.ajhg.2019.09.005
- Ajioka, I., and Nakajima, K. (2005). Switching of α -catenin from α E-catenin in the cortical ventricular zone to α N-catenin II in the intermediate zone. *Dev. Brain Res.* 160, 106–111. doi: 10.1016/j.devbrainres.2005.08.004
- Alzheimer's Disease International (2019). *World Alzheimer Report 2019: Attitudes to Dementia*. London: Alzheimer's Disease International.
- Anderson, S. A., Eisenstat, D. D., Shi, L., and Rubenstein, J. L. R. (1997). Interneuron migration from basal forebrain to neocortex: dependence on *Dlx* genes. *Science* 278, 474–476. doi: 10.1126/science.278.5337.474
- Ando, K., Uemura, K., Kuzuya, A., Maesako, M., Asada-Utsugi, M., Kubota, M., et al. (2011). N-cadherin regulates p38 MAPK signaling via association with JNK-associated leucine zipper protein: implications for neurodegeneration in Alzheimer disease. *J. Biol. Chem.* 286, 7619–7628. doi: 10.1074/jbc.M110.158477
- Andrews, W. D., Barber, M., and Parnavelas, J. G. (2007). Slit-Robo interactions during cortical development. *J. Anat.* 211, 188–198. doi: 10.1111/j.1469-7580.2007.00750.x
- Andreyeva, A., Nieweg, K., Horstmann, K., Klapper, S., Müller-Schiffmann, A., Korth, C., et al. (2012). C-terminal fragment of N-cadherin accelerates synapse destabilization by amyloid- β . *Brain* 135, 2140–2154. doi: 10.1093/brain/awt120
- Arteaga-bracho, E. E., Gulinello, M., Winchester, M. L., Pichamoorthy, N., Gokhan, S., Mehler, M. F., et al. (2016). Neurobiology of disease postnatal and adult consequences of loss of huntingtin during development : implications for Huntington 's disease. *Neurobiol. Dis.* 96, 144–155. doi: 10.1016/j.nbd.2016.09.006
- Asada-Utsugi, M., Uemura, K., Kubota, M., Noda, Y., Tashiro, Y., Uemura, T. M., et al. (2021). Mice with cleavage-resistant N-cadherin exhibit synapse anomaly in the hippocampus and outperformance in spatial learning tasks. *Mol. Brain* 14, 1–16. doi: 10.1186/s13041-021-00738-1
- Baki, L., Marambaud, P., Efthimiopoulos, S., Georgakopoulos, A., Wen, P., Cui, W., et al. (2001). Presenilin-1 binds cytoplasmic epithelial cadherin, inhibits cadherin/p120 association, and regulates stability and function of the cadherin/catenin adhesion complex. *Proc. Natl. Acad. Sci. U.S.A.* 98, 2381–2386. doi: 10.1073/pnas.041603398
- Barnat, M., Capizzi, M., Aparicio, E., Boluda, S., Wennagel, D., Kacher, R., et al. (2020). Huntington's disease alters human neurodevelopment. *Science* 3338:eaax3338. doi: 10.1126/science.aax3338
- Barnat, M., Le Fric, J., Benstaali, C., and Humbert, S. (2017). Huntingtin-Mediated multipolar-bipolar transition of newborn cortical neurons is critical for their postnatal neuronal morphology. *Neuron* 93, 99–114. doi: 10.1016/j.neuron.2016.11.035
- Basu, R., Taylor, M. R., and Williams, M. E. (2015). The classic cadherins in synaptic specificity. *Cell Adhes. Migr.* 9, 193–201. doi: 10.1080/19336918.2014.1000072
- Bekirov, I. H., Needleman, L. A., Zhang, W., and Benson, D. L. (2002). Identification and localization of multiple classic cadherins in developing rat limbic system. *Neuroscience* 115, 213–227. doi: 10.1016/S0306-4522(02)00375-5
- Bhandari, R., Ferri, S., Whittaker, B., Liu, M., and Lazzaro, D. R. (2011). Peters anomaly: review of the literature. *Cornea* 30, 939–944. doi: 10.1097/ICO.0b013e31820156a9
- Bixby, J. L., and Zhang, R. (1990). Purified N-cadherin is a potent substrate for the rapid induction of neurite outgrowth. *J. Cell Biol.* 110, 1253–1260. doi: 10.1083/jcb.110.4.1253

Acknowledgments

The authors would like to thank all the members of the Momentum Molecular Neurobiology Laboratory of the Institute of Experimental Medicine, in particular to István Katona for his continuous support.

Conflict of interest

The authors declare that the research was conducted in the absence of any commercial or financial relationships that could be construed as a potential conflict of interest.

Publisher's note

All claims expressed in this article are solely those of the authors and do not necessarily represent those of their affiliated organizations, or those of the publisher, the editors and the reviewers. Any product that may be evaluated in this article, or claim that may be made by its manufacturer, is not guaranteed or endorsed by the publisher.

- Bock, H. H., and May, P. (2016). Canonical and Non-canonical reelin signaling. *Front. Cell. Neurosci.* 10:166. doi: 10.3389/fncel.2016.00166
- Borrell, V., Cárdenas, A., Ciceri, G., Galcerán, J., Flames, N., Pla, R., et al. (2012). Slit/Robo signaling modulates the proliferation of central nervous system progenitors. *Neuron* 76, 338–352. doi: 10.1016/j.neuron.2012.08.003
- Botella-López, A., Burgaya, F., Gavín, R., García-Ayllón, M. S., Gómez-Tortosa, E., Peña-Casanova, J., et al. (2006). Reelin expression and glycosylation patterns are altered in Alzheimer's disease. *Proc. Natl. Acad. Sci. U.S.A.* 103, 5573–5578. doi: 10.1073/pnas.0601279103
- Bozdagi, O., Wang, X., Nikitczuk, J. S., Anderson, T. R., Bloss, E. B., Radice, G. L., et al. (2010). Persistence of coordinated long-term potentiation and dendritic spine enlargement at mature hippocampal CA1 synapses requires N-cadherin. *J. Neurosci.* 30, 9984–9989. doi: 10.1523/JNEUROSCI.1223-10.2010
- Brayshaw, L. L., and Price, S. R. (2016). "Cadherins in neural development," in *The Cadherin Superfamily*, eds S Hirano, S T. Suzuki (Tokyo: Springer Japan), 315–1340. doi: 10.1007/978-4-431-56033-3_12
- Budday, S., Steinmann, P., and Kuhl, E. (2015). Physical biology of human brain development. *Front. Cell. Neurosci.* 9:257. doi: 10.3389/fncel.2015.00257
- Carter, M. G., Johns, M. A., Zeng, X., Zhou, L., Zink, M. C., Mankowski, J. L., et al. (2000). Mice deficient in the candidate tumor suppressor gene *Hic1* exhibit developmental defects of structures affected in the Miller-Dieker syndrome. *Hum. Mol. Genet.* 9, 413–419. doi: 10.1093/hmg/9.3.413
- Caserta, M. T., and Sullivan, E. (2009). Late-onset huntington's disease masquerading as normal pressure hydrocephalus. *J. Neuropsychiatry Clin. Neurosci.* 21, 97–98. doi: 10.1176/jnp.2009.21.1.97
- Castaneya-Ruiz, L., Morales, D. M., McAllister, J. P., Brody, S. L., Isaacs, A. M., Strahle, J. M., et al. (2018). Blood exposure causes ventricular zone disruption and glial activation in vitro. *J. Neuropathol. Exp. Neurol.* 77, 803–813. doi: 10.1093/jnen/nly058
- Cen, C., Luo, L., Da Li, W. Q., Li, G., Tian, N. X., Zheng, G., et al. (2018). PKD1 promotes functional synapse formation coordinated with N-cadherin in hippocampus. *J. Neurosci.* 38, 183–199. doi: 10.1523/JNEUROSCI.1640-17.2017
- Chai, X., Förster, E., Zhao, S., Bock, H. H., and Frotscher, M. (2009). Reelin stabilizes the actin cytoskeleton of neuronal processes by inducing n-cofilin phosphorylation at serine. *J. Neurosci.* 29, 288–299. doi: 10.1523/JNEUROSCI.2934-08.2009
- Chazeau, A., Garcia, M., Czöndör, K., Perrais, D., Tessier, B., Giannone, G., et al. (2015). Mechanical coupling between transsynaptic N-cadherin adhesions and actin flow stabilizes dendritic spines. *Mol. Biol. Cell* 26, 859–873. doi: 10.1091/mbc.E14-06-1086
- Choi, J. Y., Cho, S. J., Park, J. H., Yun, S. M., Jo, C., Kim, E. J., et al. (2020). Elevated cerebrospinal fluid and plasma N-Cadherin in Alzheimer disease. *J. Neuropathol. Exp. Neurol.* 79, 484–492. doi: 10.1093/jnen/nlaa019
- Clandinin, T. R., and Zipursky, S. L. (2002). Making connections in the fly visual system. *Neuron* 35, 827–841. doi: 10.1016/S0896-6273(02)00876-0
- Coles, E. G., Taneyhill, L. A., and Bronner-Fraser, M. (2007). A critical role for Cadherin6B in regulating avian neural crest emigration. *Dev. Biol.* 312, 533–544. doi: 10.1016/j.ydbio.2007.09.056
- D'Arcangelo, G., Homayouni, R., Keshvara, L., Rice, D. S., Sheldon, M., and Curran, T. (1999). Reelin is a ligand for lipoprotein receptors. *Neuron* 24, 471–479. doi: 10.1016/S0896-6273(00)80860-0
- D'Arcangelo, G., Miao, G., Chen, S.-C., Scares, H. D., Morgan, J. I., and Curran, T. (1995). A protein related to extracellular matrix proteins deleted in the mouse mutant *reeler*. *Nature* 374, 719–723. doi: 10.1038/374719a0
- Das, R. M., and Storey, K. G. (2014). Apical abscission alters cell polarity and dismantles the primary cilium during neurogenesis. *Science* 343, 200–204. doi: 10.1126/science.1247521
- de Agustín-Durán, D., Mateos-White, I., Fabra-Beser, J., and Gil-Sanz, C. (2021). Stick around: cell–cell adhesion molecules during neocortical development. *Cells* 10:118. doi: 10.3390/cells10010118
- Del Bigio, M. R. (1995). The ependyma: a protective barrier between brain and cerebrospinal fluid. *Glia* 14, 1–13. doi: 10.1002/glia.440140102
- Dennhardt, J., and Ledoux, M. S. (2010). Huntington disease in a nonagenarian mistakenly diagnosed as normal pressure hydrocephalus. *J. Clin. Neurosci.* 17, 1066–1067. doi: 10.1016/j.jocn.2009.11.011
- Deture, M. A., and Dickson, D. W. (2019). The neuropathological diagnosis of Alzheimer's disease. *Mol. Neurodegener.* 14, 1–18. doi: 10.1186/s13024-019-0333-5
- Dietrich, P., Shanmugasundaram, R., Shuyu, E., and Dragatsis, I. (2009). Congenital hydrocephalus associated with abnormal subcommissural organ in mice lacking huntingtin in *Wnt1* cell lineages. *Hum. Mol. Genet.* 18, 142–150. doi: 10.1093/hmg/ddn324
- Đlugosz, P., and Nimpf, J. (2018). The reelin receptors apolipoprotein e receptor 2 (ApoER2) and VLDL receptor. *Int. J. Mol. Sci.* 19, 1–22. doi: 10.3390/ijms19103090
- Dodman, N. H., Karlsson, E. K., Moon-Fanelli, A., Galdzicka, M., Perloski, M., Shuster, L., et al. (2010). A canine chromosome 7 locus confers compulsive disorder susceptibility. *Mol. Psychiatry* 15, 8–10. doi: 10.1038/mp.2009.111
- Edwards-Lee, T., Wen, J., Bell, J., Hardy, J., Chung, J., and Momeni, P. (2006). A presenilin-1 mutation (T245P) in transmembrane domain 6 causes early onset Alzheimer's disease. *Neurosci. Lett.* 398, 251–252. doi: 10.1016/j.neulet.2006.01.006
- Elder, G. A., Tezapsidis, N., Carter, J., Shioi, J., Bouras, C., Li, H. C., et al. (1996). Identification and neuron specific expression of the S182/presenilin 1 protein in human and rodent brains. *J. Neurosci. Res.* 45, 308–320. doi: 10.1002/(sici)1097-4547(19960801)45:3<308::aid-jnr13<3.0.co;2-\\#
- Elia, L. P., Yamamoto, M., Zang, K., and Reichardt, L. F. (2006). P120 catenin regulates dendritic spine and synapse development through rho-family GTPases and cadherins. *Neuron* 51, 43–56. doi: 10.1016/j.neuron.2006.05.018
- Elste, A. M., and Benson, D. L. (2006). Structural basis for developmentally regulated changes in cadherin function at synapses. *J. Comp. Neurol.* 495, 324–335. doi: 10.1002/cne.20876
- Erdmann, B., Kirsch, F.-P., Rathjen, F. G., and Moré, M. I. (2003). N-Cadherin is essential for retinal lamination in the zebrafish. *Dev. Dyn.* 226, 570–577. doi: 10.1002/dvdy.10266
- Escamilla-Ayala, A. A., Sannerud, R., Mondin, M., Poersch, K., Vermeire, W., Paparelli, L., et al. (2020). Super-resolution microscopy reveals majorly mono- and dimeric presenilin1/γ-secretase at the cell surface. *Elife* 9:e56679. doi: 10.7554/eLife.56679
- Feng, Y., Chen, M. H., Moskowitz, I. P., Mendonza, A. M., Vidali, L., Nakamura, F., et al. (2006). Filamin A (FLNA) is required for cell–cell contact in vascular development and cardiac morphogenesis. *Proc. Natl. Acad. Sci. U.S.A.* 103, 19836–19841. doi: 10.1073/pnas.0609628104
- Ferland, R. J., Batiz, L. F., Neal, J., Lian, G., Bundock, E., Lu, J., et al. (2009). Disruption of neural progenitors along the ventricular and subventricular zones in periventricular heterotopia. *Hum. Mol. Genet.* 18, 497–516. doi: 10.1093/hmg/ddn377
- Flanagan, L. A., Chou, J., Falet, H., Neujahr, R., Hartwig, J. H., and Stossel, T. P. (2001). Filamin A, the Arp2/3 complex, and the morphology and function of cortical actin filaments in human melanoma cells. *J. Cell Biol.* 155, 511–518. doi: 10.1083/jcb.200105148
- Franco, S. J., Martinez-Garay, I., Gil-Sanz, C., Harkins-Perry, S. R., and Müller, U. (2011). Reelin regulates cadherin function via Dab1/Rap1 to control neuronal migration and lamination in the neocortex. *Neuron* 69, 482–497. doi: 10.1016/j.neuron.2011.01.003
- Friocourt, G., Kanatani, S., Tabata, H., Yozu, M., Takahashi, T., Antypa, M., et al. (2008). Cell-autonomous roles of ARX in cell proliferation and neuronal migration during corticogenesis. *J. Neurosci.* 28, 5794–5805. doi: 10.1523/JNEUROSCI.1067-08.2008
- Furey, C. G., Choi, J., Jin, S. C., Zeng, X., Timberlake, A. T., Nelson-Williams, C., et al. (2018). De Novo mutation in genes regulating neural stem cell fate in human congenital hydrocephalus. *Neuron* 99, 302.e4–314.e4. doi: 10.1016/j.neuron.2018.06.019
- Gallardo-Orihuela, A., Hervás-Corpión, I., Hierro-Bujalance, C., Sanchez-Sotano, D., Jiménez-Gómez, G., Mora-López, F., et al. (2019). Transcriptional correlates of the pathological phenotype in a Huntington's disease mouse model. *Sci. Rep.* 9:18696. doi: 10.1038/s41598-019-5177-9
- Gambello, M. J., Darling, D. L., Yingling, J., Tanaka, T., Gleeson, J. G., and Wynshaw-Boris, A. (2003). Multiple dose-dependent effects of *lisl* on cerebral cortical development. *J. Neurosci.* 23, 1719–1729. doi: 10.1523/JNEUROSCI.23-05-01719.2003
- Gänzler-Odenthal, S. I. I., and Redies, C. (1998). Blocking N-Cadherin function disrupts the epithelial structure of differentiating neural tissue in the embryonic chicken brain. *J. Neurosci.* 18, 5415–5425. doi: 10.1523/JNEUROSCI.18-14-05415.1998
- Gärtner, A., Fornasiero, E. F., Munck, S., Vennekens, K., Seuntjens, E., Huttner, W. B., et al. (2012). N-cadherin specifies first asymmetry in developing neurons. *EMBO J.* 31, 1893–1903. doi: 10.1038/emboj.2012.41
- Gate, D., Rodriguez, J., Kim, G., Breunig, J. J., Town, T., Danielpour, M., et al. (2012). Rapid genetic targeting of pial surface neural progenitors and immature neurons by neonatal electroporation. *Neural Dev.* 27:26. doi: 10.1186/1749-8104-27-26

- Geletu, M., Adan, H., Niit, M., Arulananandam, R., Carefoot, E., Hoskin, V., et al. (2022). Erratum: modulation of Akt vs Stat3 activity by the focal adhesion kinase in non-neoplastic mouse fibroblasts (Experimental Cell Research (2021) 404(1), (S0014482721001336), (10.1016/j.yexcr.2021.112601)). *Exp. Cell Res.* 411:112731. doi: 10.1016/j.yexcr.2021.112731
- Georgakopoulos, A., Marambaud, P., Efthimiopoulos, S., Shioi, J., Cui, W., Li, H. C., et al. (1999). Presenilin-1 forms complexes with the cadherin/catenin cell-cell adhesion system and is recruited to intercellular and synaptic contacts. *Mol. Cell* 4, 893–902. doi: 10.1016/S1097-2765(00)80219-1
- Gil-Sanz, C., Franco, S. J., Martinez-Garay, I., Espinosa, A., Harkins-Perry, S., and Müller, U. (2013). Cajal-Retzius cells instruct neuronal migration by coincidence signaling between secreted and contact-dependent guidance cues. *Neuron* 79, 461–477. doi: 10.1016/j.neuron.2013.06.040
- Gil-Sanz, C., Landeira, B., Ramos, C., Costa, M. R., and Muller, U. (2014). Proliferative defects and formation of a double cortex in mice lacking Mlt4 and Cdh2 in the dorsal telencephalon. *J. Neurosci.* 34, 10475–10487. doi: 10.1523/JNEUROSCI.1793-14.2014
- Gorlin, J. B., Yamin, R., Egan, S., Stewart, M., Stossel, T. P., Kwiatkowski, D. J., et al. (1990). Human endothelial actin-binding protein (ABP-280, nonmuscle filamin): a molecular leaf spring. *J. Cell Biol.* 111, 1089–1105. doi: 10.1083/jcb.111.3.1089
- Guerra, M. M., Henzi, R., Orloff, A., Lichtin, N., Vio, K., Jiménez, A. J., et al. (2015). Cell junction pathology of neural stem cells is associated with ventricular zone disruption, hydrocephalus, and abnormal neurogenesis. *J. Neuropathol. Exp. Neurol.* 74, 653–671. doi: 10.1097/NEN.0000000000000203
- Hack, I., Hellwig, S., Junghans, D., Brunne, B., Bock, H. H., Zhao, S., et al. (2007). Divergent roles of ApoER2 and Vldlr in the migration of cortical neurons. *Development* 134, 3883–3891. doi: 10.1242/dev.005447
- Halperin, D., Stavsky, A., Kadir, R., Drabkin, M., Wormser, O., Yogeve, Y., et al. (2021). CDH2 mutation affecting N-cadherin function causes attention-deficit hyperactivity disorder in humans and mice. *Nat. Commun.* 12:6187. doi: 10.1038/s41467-021-26426-1
- Handley, M. T., Morris-Rosendahl, D. J., Brown, S., Macdonald, F., Hardy, C., Bem, D., et al. (2013). Mutation spectrum in RAB3GAP1, RAB3GAP2, and RAB18 and genotype-phenotype correlations in warburg micro syndrome and martsolf syndrome. *Hum. Mutat.* 34, 686–696. doi: 10.1002/humu.22296
- Hart, A. W., Morgan, J. E., Schneider, J., West, K., McKie, L., Bhattacharya, S., et al. (2006). Cardiac malformations and midline skeletal defects in mice lacking filamin A. *Hum. Mol. Genet.* 15, 2457–2467. doi: 10.1093/hmg/ddl168
- Hartmann, D., De Strooper, B., Serneels, L., Craessaerts, K., Herreman, A., Annaert, W., et al. (2002). The disintegrin/metalloprotease ADAM 10 is essential for Notch signalling but not for α -secretase activity in fibroblasts. *Hum. Mol. Genet.* 11, 2615–2624. doi: 10.1093/hmg/11.21.2615
- Hatakeyama, J., Wakamatsu, Y., Nagafuchi, A., Kageyama, R., Shigemoto, R., and Shimamura, K. (2014). Cadherin-based adhesions in the apical endfoot are required for active Notch signaling to control neurogenesis in vertebrates. *Development* 141, 1671–1682. doi: 10.1242/dev.102988
- Hatta, K., and Takeichi, M. (1986). Expression of N-cadherin adhesion molecules associated with early morphogenetic events in chick development. *Nature* 320, 447–449. doi: 10.1038/320447a0
- Hawi, Z., Tong, J., Dark, C., Yates, H., Johnson, B., and Bellgrove, M. A. (2018). The role of cadherin genes in five major psychiatric disorders: a literature update. *Am. J. Med. Genet. Part B Neuropsychiatr. Genet.* 177, 168–180. doi: 10.1002/ajmg.b.32592
- Hickman, R. A., Faust, P. L., Rosenblum, M. K., Marder, K., Mehler, M. F., and Vonsattel, J. P. (2021). Developmental malformations in Huntington disease: neuropathologic evidence of focal neuronal migration defects in a subset of adult brains. *Acta Neuropathol.* 141, 399–413. doi: 10.1007/s00401-021-02269-4
- Hirano, S., and Takeichi, M. (2012). Cadherins in brain morphogenesis and wiring. *Physiol. Rev.* 92, 597–634. doi: 10.1152/physrev.00014.2011
- Hirosune, S., Fleck, M. W., Gambello, M. J., Bix, G. J., Chen, A., Clark, G. D., et al. (1998). Graded reduction of Pafah1b1 (Lis1) activity results in neuronal migration defects and early embryonic lethality. *Nat. Genet.* 19, 333–339. doi: 10.1038/1221
- Hoe, H. S., Kea, J. L., Carney, R. S. E., Lee, J., Markova, A., Lee, J. Y., et al. (2009). Interaction of reelin with amyloid precursor protein promotes neurite outgrowth. *J. Neurosci.* 29, 7459–7473. doi: 10.1523/JNEUROSCI.4872-08.2009
- Hooli, B. V., Kovacs-Vajna, Z. M., Mullin, K., Blumenthal, M. A., Mattheisen, M., Zhang, C., et al. (2014). Rare autosomal copy number variations in early-onset familial Alzheimer's disease. *Mol. Psychiatry* 19, 676–681. doi: 10.1038/mp.2013.77
- Hor, C. H. H., and Goh, E. L. K. (2018). Rab23 regulates radial migration of projection neurons via N-cadherin. *Cereb. Cortex* 28, 1516–1531. doi: 10.1093/cercor/bhy018
- Hung, C. O. Y., and Livesey, F. J. (2018). Altered γ -Secretase Processing of APP disrupts lysosome and autophagosome function in monogenic Alzheimer's disease. *Cell Rep.* 25, 3647.e2–3660.e2. doi: 10.1016/j.celrep.2018.11.095
- Husain, M. A., Laurent, B., and Plourde, M. (2021). APOE and Alzheimer's disease: from lipid transport to physiopathology and therapeutics. *Front. Neurosci.* 15:630502. doi: 10.3389/fnins.2021.630502
- Iefremova, V., Manikakis, G., Krefft, O., Jabali, A., Weynans, K., Wilkens, R., et al. (2017). An organoid-based model of cortical development identifies non-cell-autonomous defects in wnt signaling contributing to miller-dieker syndrome. *Cell Rep.* 19, 50–59. doi: 10.1016/j.celrep.2017.03.047
- Itoh, Y., Moriyama, Y., Hasegawa, T., Endo, T. A., Toyoda, T., and Gotoh, Y. (2013). Scratch regulates neuronal migration onset via an epithelial-mesenchymal transition-like mechanism. *Nat. Neurosci.* 16, 416–425. doi: 10.1038/nn.3336
- Jang, C., Choi, J., Na, Y., Jang, B., Wasco, W., Buxbaum, J. D., et al. (2011). Calsenilin regulates presenilin 1/ γ -secretase-mediated N-cadherin ϵ -cleavage and β -catenin signaling. *FASEB J.* 25, 4174–4183. doi: 10.1096/fj.11-185926
- Jiang, Y. J., Brand, M., Heisenberg, C. P., Beuchle, D., Furutani-Seiki, M., Kelsh, R. N., et al. (1996). Mutations affecting neurogenesis and brain morphology in the zebrafish, *Danio rerio*. *Development* 123, 205–216. doi: 10.1242/dev.123.1.205
- Jontes, J. D. (2018). The cadherin superfamily in neural circuit assembly. *Cold Spring Harb. Perspect. Biol.* 10:a029306. doi: 10.1101/cshperspect.a029306
- Jorissen, E., Prox, J., Bernreuther, C., Weber, S., Schwanbeck, R., Serneels, L., et al. (2010). The disintegrin/metalloproteinase ADAM10 is essential for the establishment of the brain cortex. *J. Neurosci.* 30, 4833–4844. doi: 10.1523/JNEUROSCI.5221-09.2010
- Jossin, Y. (2020). Reelin functions, mechanisms of action and signaling pathways during brain development and maturation. *Biomolecules* 10:964. doi: 10.3390/biom10060964
- Jossin, Y., and Cooper, J. A. (2011). Reelin, Rap1 and N-cadherin orient the migration of multipolar neurons in the developing neocortex. *Nat. Neurosci.* 14, 697–703. doi: 10.1038/nn.2816
- Jüngling, K., Eulenburg, V., Moore, R., Kemler, R., Lessmann, V., and Gottmann, K. (2006). N-cadherin transsynaptically regulates short-term plasticity at glutamatergic synapses in embryonic stem cell-derived neurons. *J. Neurosci.* 26, 6968–6978. doi: 10.1523/JNEUROSCI.1013-06.2006
- Juric-sekhar, G., and Hevner, R. F. (2019). Malformations of cerebral cortex development: molecules and mechanisms. *Annu. Rev. Pathol.* 14, 293–318. doi: 10.1146/annurev-pathmechdis-012418-012927
- Kadowaki, M., Nakamura, S., Machon, O., Krauss, S., Radice, G. L., and Takeichi, M. (2007). N-cadherin mediates cortical organization in the mouse brain. *Dev. Biol.* 304, 22–33. doi: 10.1016/j.ydbio.2006.12.014
- Kahle, K. T., Kulkarni, A. V., Jr., Limbrick, D. D., and Warf, B. C. (2016). Hydrocephalus in children. *Lancet* 387, 788–799. doi: 10.1016/S0140-6736(15)60694-8
- Kaneej, M., Yuce Kahraman, C., Ercoskun, P., Tatar, A., and Kahraman, M. (2022). A Novel nonsense variant in the CDH2 gene associated with ACOGS: a case report. *Am. J. Med. Genet. Part A* 188, 2815–2818. doi: 10.1002/ajmg.a.62861
- Kawauchi, T., Sekine, K., Shikanai, M., Chihama, K., Tomita, K., Kubo, K. I., et al. (2010). Rab GTPases-dependent endocytic pathways regulate neuronal migration and maturation through N-cadherin trafficking. *Neuron* 67, 588–602. doi: 10.1016/j.neuron.2010.07.007
- Keryer, G., Pineda, J. R., Liot, G., Kim, J., Dietrich, P., Benstaali, C., et al. (2011). Ciliogenesis is regulated by a huntingtin-HAP1-PCMI pathway and is altered in Huntington disease. *J. Clin. Invest.* 121, 4372–4382. doi: 10.1172/JCI57552
- Khalesi, R., Razmara, E., Asgaritarghi, G., Tavasoli, A. R., Riazalhosseini, Y., Auld, D., et al. (2021). Novel manifestations of Warburg micro syndrome type 1 caused by a new splicing variant of RAB3GAP1: a case report. *BMC Neurol.* 21:180. doi: 10.1186/s12883-021-02204-w
- Kim, W., and Shen, J. (2008). Presenilins are required for maintenance of neural stem cells in the developing brain. *Mol. Neurodegener.* 3:2. doi: 10.1186/1750-1326-3-2
- Kitamura, K., Yanazawa, M., Sugiyama, N., Miura, H., Iizuka-Kogo, A., Kusaka, M., et al. (2002). Mutation of ARX causes abnormal development of forebrain and testes in mice and X-linked lissencephaly with abnormal genitalia in humans. *Nat. Genet.* 32, 359–369. doi: 10.1038/ng1009
- Knuesel, I., Nyffeler, M., Mormède, C., Muhia, M., Meyer, U., Pietropaolo, S., et al. (2009). Age-related accumulation of Reelin in amyloid-like deposits. *Neurobiol. Aging* 30, 697–716. doi: 10.1016/j.neurobiolaging.2007.08.011
- Ko, H., Kim, S., Jin, C. H., Lee, E., Ham, S., Yook, J. I., et al. (2012). Protein kinase casein kinase 2-mediated upregulation of N-cadherin confers anoikis resistance on

- esophageal carcinoma cells. *Mol. Cancer Res.* 10, 1032–1038. doi: 10.1158/1541-7786.MCR-12-0261
- Kwon, Y. T., Gupta, A., Zhou, Y., Nikolic, M., and Tsai, L. (2000). Regulation of N-cadherin-mediated adhesion by the p35–Cdk5 kinase. *Curr. Biol.* 10, 363–372. doi: 10.1016/S0960-9822(00)00411-5
- Lane-Donovan, C., and Herz, J. (2017). ApoE, ApoE receptors, and the synapse in Alzheimer's disease. *Trends Endocrinol. Metab.* 28, 273–284. doi: 10.1016/j.tem.2016.12.001
- László, Z. I., Bercsényi, K., Mayer, M., Lefkovich, K., Szabó, G., Katona, I., et al. (2020a). N-cadherin (Cdh2) maintains migration and postmitotic survival of cortical interneuron precursors in a cell-type-specific manner. *Cereb. Cortex* 30, 1318–1329. doi: 10.1093/cercor/bhz168
- László, Z. I., Lele, Z., Zöldi, M., Miczán, V., Mógör, F., Simon, G. M., et al. (2020b). ABHD4-dependent developmental anoikis safeguards the embryonic brain. *Nat. Commun.* 11:4363. doi: 10.1038/s41467-020-18175-4
- Lazarov, O., Peterson, L. D., Peterson, D. A., and Sisodia, S. S. (2006). Expression of a familial Alzheimer's disease-linked presenilin-1 variant enhances perforant pathway lesion-induced neuronal loss in the entorhinal cortex. *J. Neurosci.* 26, 429–434. doi: 10.1523/JNEUROSCI.3961-05.2006
- Lefkovich, K., Mayer, M., Bercsényi, K., Szabó, G., and Lele, Z. (2012). Comparative analysis of type II classic cadherin mRNA distribution patterns in the developing and adult mouse somatosensory cortex and hippocampus suggests significant functional redundancy. *J. Comp. Neurol.* 520, 1387–1405. doi: 10.1002/cne.22801
- Lele, Z., Folchert, A., Concha, M., Rauch, G.-J., Geisler, R., Rosa, F., et al. (2002). Parachute/N-Cadherin is required for morphogenesis and maintained integrity of the zebrafish neural tube. *Development* 129, 3281–3294. doi: 10.1242/dev.129.14.3281
- Lelièvre, E. C., Plestant, C., Boscher, C., Wolff, E., Mège, R.-M., and Birbes, H. (2012). N-Cadherin mediates neuronal cell survival through bim down-regulation. *PLoS One* 7:e33206. doi: 10.1371/journal.pone.0033206
- Li, M., Cui, Z., Niu, Y., Liu, B., Fan, W., Yu, D., et al. (2010). Synaptogenesis in the developing mouse visual cortex. *Brain Res. Bull.* 81, 107–113. doi: 10.1016/j.brainresbull.2009.08.028
- Li, W. Q., Luo, L., Hu, Z. W., Lyu, T. J., Cen, C., and Wang, Y. (2019). PLD1 promotes dendritic spine morphogenesis via activating PKD1. *Mol. Cell. Neurosci.* 99:103394. doi: 10.1016/j.mcn.2019.103394
- Liegel, R. P., Handley, M. T., Ronchetti, A., Brown, S., Langemeyer, L., Linford, A., et al. (2013). Loss-of-function mutations in TBC1D20 cause cataracts and male infertility in blind sterile mice and warburg micro syndrome in humans. *Am. J. Hum. Genet.* 93, 1001–1014. doi: 10.1016/j.ajhg.2013.10.011
- Lien, W.-H. (2006). E-Catenin controls cerebral cortical size by regulating the hedgehog signaling pathway. *Science* 311, 1609–1612. doi: 10.1126/science.1121449
- Linford, A., Yoshimura, S., Bastos, R. N., Langemeyer, L., Gerondopoulos, A., Rigden, D. J., et al. (2012). Rab14 and its exchange factor FAM116 link endocytic recycling and adherens junction stability in migrating cells. *Dev. Cell* 22, 952–966. doi: 10.1016/j.devcel.2012.04.010
- Liu, D., Cao, H., Kural, K. C., Fang, Q., and Zhang, F. (2019). Integrative analysis of shared genetic pathogenesis by autism spectrum disorder and obsessive-compulsive disorder. *Biosci. Rep.* 39:BSR20191942. doi: 10.1042/BSR20191942
- Lopez-Font, I., Iborra-Lazaro, G., Sánchez-Valle, R., Molinuevo, J. L., Cuchillo-Ibanez, I., and Sáez-Valero, J. (2019). CSF-ApoER2 fragments as a read-out of reelin signaling: distinct patterns in sporadic and autosomal-dominant Alzheimer disease. *Clin. Chim. Acta* 490, 6–11. doi: 10.1016/j.cca.2018.12.012
- Luccardini, C., Hennekinne, L., Viou, L., Yanagida, M., Murakami, F., Kessaris, N., et al. (2013). N-Cadherin sustains motility and polarity of future cortical interneurons during tangential migration. *J. Neurosci.* 33, 18149–18160. doi: 10.1523/JNEUROSCI.0593-13.2013
- Luccardini, C., Leclech, C., Viou, L., Rio, J.-P., and Métin, C. (2015). Cortical interneurons migrating on a pure substrate of N-cadherin exhibit fast synchronous centrosomal and nuclear movements and reduced ciliogenesis. *Front. Cell. Neurosci.* 9:286. doi: 10.3389/fncel.2015.00286
- Luo, L., Da Li, G., and Wang, Y. (2017). PLD1 promotes dendritic spine development by inhibiting ADAM10-mediated N-cadherin cleavage. *Sci. Rep.* 7:6035. doi: 10.1038/s41598-017-06121-2
- Luo, Y., Ferreira-Cornwell, M. C., Baldwin, H. S., Kostetskii, I., Lenox, J. M., Lieberman, M., et al. (2001). Rescuing the N-cadherin knockout by cardiac-specific expression of N- or E-cadherin. *Development* 128, 459–469. doi: 10.1242/dev.128.4.459
- Malicki, J., Jo, H., and Pujic, Z. (2003). Zebrafish N-cadherin, encoded by the glass onion locus, plays an essential role in retinal patterning. *Dev. Biol.* 259, 95–108. doi: 10.1016/S0012-1606(03)00181-7
- Marambaud, P., Wen, P. H., Dutt, A., Shioi, J., Takashima, A., Siman, R., et al. (2003). A CBP binding transcriptional repressor produced by the PS1/ε-cleavage of N-Cadherin is inhibited by PS1 FAD mutations. *Cell* 114, 635–645. doi: 10.1016/j.cell.2003.08.008
- Martinez-Garay, I. (2020). Molecular mechanisms of cadherin function during cortical migration. *Front. Cell Dev. Biol.* 8:588152. doi: 10.3389/fcell.2020.588152
- Masai, I. (2003). N-cadherin mediates retinal lamination, maintenance of forebrain compartments and patterning of retinal neurites. *Development* 130, 2479–2494. doi: 10.1242/dev.00465
- Masai, I., Lele, Z., Yamaguchi, M., Komori, A., Nakata, A., Nishiwaki, Y., et al. (2003). N-cadherin mediates retinal lamination, maintenance of forebrain compartments and patterning of retinal neurites. *Development* 130, 2479–2494.
- Matsunaga, M., Hatta, K., and Takeichi, M. (1988). Role of N-cadherin cell adhesion molecules in the histogenesis of neural retina. *Neuron* 1, 289–295. doi: 10.1016/0896-6273(88)90077-3
- Matsunaga, Y., Noda, M., Murakawa, H., Hayashi, K., Nagasaka, A., Inoue, S., et al. (2017). Reelin transiently promotes N-cadherin-dependent neuronal adhesion during mouse cortical development. *Proc. Natl. Acad. Sci. U.S.A.* 114, 2048–2053. doi: 10.1073/pnas.1615215114
- Mayer, M., Bercsényi, K., Géczi, K., Szabó, G., and Lele, Z. (2010). Expression of two type II cadherins, Cdh12 and Cdh22 in the developing and adult mouse brain. *Gene Expr. Patterns* 10, 351–360. doi: 10.1016/j.gep.2010.08.002
- McGregor, N. W., Lochner, C., Stein, D. J., and Hemmings, S. M. J. (2015). Polymorphisms within the neuronal cadherin (CDH2) gene are associated with obsessive-compulsive disorder (OCD) in a South African cohort. *Metab. Brain Dis.* 31, 191–196. doi: 10.1007/s11011-015-9693-x
- Mège, R. M., and Ishiyama, N. (2017). Integration of cadherin adhesion and cytoskeleton at adherens junctions. *Cold Spring Harb. Perspect. Biol.* 9:a028738. doi: 10.1101/cshperspect.a028738
- Mendez, P., De Roo, M., Poglia, L., Klausner, P., and Muller, D. (2010). N-cadherin mediates plasticity-induced long-term spine stabilization. *J. Cell Biol.* 189, 589–600. doi: 10.1083/jcb.201003007
- Miyamoto, Y., Sakane, F., and Hashimoto, K. (2015). N-cadherin-based adherens junction regulates the maintenance, proliferation, and differentiation of neural progenitor cells during development. *Cell Adh. Migr.* 9, 183–192. doi: 10.1080/19336918.2015.1005466
- Molero, A. E., Arteaga-bracho, E. E., Chen, C. H., and Gulinello, M. (2016). Selective expression of mutant huntingtin during development recapitulates characteristic features of Huntington's disease. *Proc. Natl. Acad. Sci. U.S.A.* 113, 5736–5741. doi: 10.1073/pnas.1603871113
- Molina-Calavita, M., Barnat, M., Elias, S., Aparicio, E., Piel, M., and Humbert, S. (2014). Mutant huntingtin affects cortical progenitor cell division and development of the mouse neocortex. *J. Neurosci.* 34, 10034–10040. doi: 10.1523/JNEUROSCI.0715-14.2014
- Morris-Rosendahl, D. J., Segel, R., Born, A. P., Conrad, C., Loeys, B., Brooks, S. S., et al. (2010). New RAB3GAP1 mutations in patients with warburg micro syndrome from different ethnic backgrounds and a possible founder effect in the Danish. *Eur. J. Hum. Genet.* 18, 1100–1106. doi: 10.1038/ejhg.2010.79
- Moya, P. R., Dodman, N. H., Timpano, K. R., Rubenstein, L. M., Rana, Z., Fried, R. L., et al. (2013). Rare missense neuronal cadherin gene (CDH2) variants in specific obsessive-compulsive disorder and Tourette disorder phenotypes. *Eur. J. Hum. Genet.* 21, 850–854. doi: 10.1038/ejhg.2012.245
- Mysore, S. P., Tai, C. Y., and Schuman, E. M. (2007). Effects of N-cadherin disruption on spine morphological dynamics. *Front. Cell. Neurosci.* 1:1. doi: 10.3389/neuro.03.001.2007
- Nadarajah, B., Brunstrom, J. E., Grutzendler, J., Wong, R. O. L., and Pearlman, A. L. (2001). Two modes of radial migration in early development of the cerebral cortex. *Nat. Neurosci.* 4, 143–150. doi: 10.1038/83967
- Nakagawa, S., and Takeichi, M. (1995). Neural crest cell-cell adhesion controlled by sequential and subpopulation-specific expression of novel cadherins. *Development* 121, 1321–1332. doi: 10.1242/dev.121.5.1321
- Nakagawa, S., and Takeichi, M. (1998). Neural crest emigration from the neural tube depends on regulated cadherin expression. *Development* 125, 2963–2971.
- Nazaryan, L., Bertelsen, B., Padmanabhuni, S. S., Debes, N. M., LuCamp, Have, C. T., et al. (2015). Association study between CDH2 and Gilles de la

Tourette syndrome in a Danish cohort. *Psychiatry Res.* 228, 974–975. doi: 10.1016/j.psychres.2015.05.010

Neugebauer, K. M., Tomaselli, K. J., Lilien, J., and Reichardt, L. F. (1988). N-cadherin, NCAM, and integrins promote retinal neurite outgrowth on astrocytes in vitro. *J. Cell Biol.* 107, 1177–1187. doi: 10.1083/jcb.107.3.1177

Niethammer, M., Smith, D. S., Ayala, R., Peng, J., Ko, J., Lee, M., et al. (2000). NUDEL is a novel Cdk5 substrate that associates with LIS1 and cytoplasmic dynein. *Neuron* 28, 697–711. doi: 10.1016/S0896-6273(00)00147-1

Noctor, S. C., Martinez-Cerdeño, V., Ivic, L., and Kriegstein, A. R. (2004). Cortical neurons arise in symmetric and asymmetric division zones and migrate through specific phases. *Nat. Neurosci.* 7, 136–144. doi: 10.1038/nn1172

Nuriya, M., and Hagan, R. L. (2006). Regulation of AMPA receptor trafficking by N-cadherin. *J. Neurochem.* 97, 652–661. doi: 10.1111/j.1471-4159.2006.03740.x

OECD/EU (2018). *Health at a Glance: Europe 2018: State of Health in the EU Cycle*. Paris: OECD Publishing. doi: 10.1787/health_glance_eur-2018-en

Ogawa, M., Miyata, T., Nakajima, K., Yagyu, K., Seike, M., Ikenaka, K., et al. (1995). The reeler gene-associated antigen on calyx-retzius neurons is a crucial molecule for laminar organization of cortical neurons. *Neuron* 14, 899–912. doi: 10.1016/0896-6273(95)90329-1

Okamura, K., Tanaka, H., Yagita, Y., Saeki, Y., Taguchi, A., Hiraoka, Y., et al. (2004). Cadherin activity is required for activity-induced spine remodeling. *J. Cell Biol.* 167, 961–972. doi: 10.1083/jcb.200406030

Oliver, C., González, C. A., Alvial, G., Flores, C. A., Rodríguez, E. M., and Bätz, L. F. (2013). Disruption of CDH2/N-cadherin-based adherens junctions leads to apoptosis of ependymal cells and denudation of brain ventricular walls. *J. Neuropathol. Exp. Neurol.* 72, 846–860. doi: 10.1097/NEN.0b013e3182a2d5fe

Padmanabhan, P., Kneynsberg, A., and Götz, J. (2021). Super-resolution microscopy: a closer look at synaptic dysfunction in Alzheimer disease. *Nat. Rev. Neurosci.* 22, 723–740. doi: 10.1038/s41583-021-00531-y

Pagnamenta, A. T., Khan, H., Walker, S., Gerrelli, D., Wing, K., Bonaglia, M. C., et al. (2011). Rare familial 16q21 microdeletions under a linkage peak implicate cadherin 8 (CDH8) in susceptibility to autism and learning disability. *J. Med. Genet.* 48, 48–54. doi: 10.1136/jmg.2010.079426

Paoli, P., Giannoni, E., and Chiarugi, P. (2013). Anoikis molecular pathways and its role in cancer progression. *Biochim. Biophys. Acta Mol. Cell Res.* 1833, 3481–3498. doi: 10.1016/j.bbmr.2013.06.026

Park, C., Falls, W., Finger, J. H., Longo-Guess, C. M., and Ackerman, S. L. (2002). Deletion in *Catna2*, encoding α -catenin, causes cerebellar and hippocampal lamination defects and impaired startle modulation. *Nat. Genet.* 31, 279–284. doi: 10.1038/ng908

Park, K. S., and Gumbiner, B. M. (2010). Cadherin 6B induces BMP signaling and de-epithelialization during the epithelial mesenchymal transition of the neural crest. *Development* 137, 2691–2701. doi: 10.1242/dev.050096

Peglion, F., Llense, F., and Etienne-Manneville, S. (2014). Adherens junction treadmill during collective migration. *Nat. Cell Biol.* 16, 639–651. doi: 10.1038/ncb2985

Picascia, M., Zangaglia, R., Bernini, S., Minafra, B., Sinforiani, E., and Pacchetti, C. (2015). A review of cognitive impairment and differential diagnosis in idiopathic normal pressure hydrocephalus. *Funct. Neurol.* 30, 217–228. doi: 10.11138/fneur/2015.30.4.217

Pielarski, K. N., van Stegen, B., Andreyeva, A., Nieweg, K., Jüngling, K., Redies, C., et al. (2013). Asymmetric N-cadherin expression results in synapse dysfunction. Synapse elimination, and axon retraction in cultured mouse neurons. *PLoS One* 8:e54105. doi: 10.1371/journal.pone.0054105

Piprek, R. P., Kolasa, M., Podkowa, D., Kloc, M., and Kubiak, J. Z. (2019). N-cadherin is critical for the survival of germ cells, the formation of steroidogenic cells, and the architecture of developing mouse gonads. *Cells* 8:1610. doi: 10.3390/cells8121610

Plachez, C., Andrews, W., Liapi, A., Knoell, B., Drescher, U., Mankoo, B., et al. (2008). Robos are required for the correct targeting of retinal ganglion cell axons in the visual pathway of the brain. *Mol. Cell. Neurosci.* 37, 719–730. doi: 10.1016/j.mcn.2007.12.017

Plump, A. S., Erskine, L., Sabatier, C., Brose, K., Epstein, C. J., Goodman, C. S., et al. (2002). Slit1 and Slit2 cooperate to prevent premature midline crossing of retinal axons in the mouse visual system. *Neuron* 33, 219–232. doi: 10.1016/S0896-6273(01)00586-4

Pollarolo, G., Schulz, J. G., Munck, S., and Dotti, C. G. (2011). Cytokinesis remnants define first neuronal asymmetry in vivo. *Nat. Neurosci.* 14, 1525–1534. doi: 10.1038/nn.2976

Priller, C., Dewachter, I., Vassallo, N., Paluch, S., Pace, C., Kretschmar, H. A., et al. (2007). Mutant presenilin 1 alters synaptic transmission in

cultured hippocampal neurons. *J. Biol. Chem.* 282, 1119–1127. doi: 10.1074/jbc.M605066200

Qian, S., Jiang, P., Guan, X. M., Singh, G., Trumbauer, M. E., Yu, H., et al. (1998). Mutant human presenilin 1 protects presenilin 1 null mouse against embryonic lethality and elevates A β 1-42/43 expression. *Neuron* 20, 611–617. doi: 10.1016/S0896-6273(00)80999-X

Quillé, M. L., Carat, S., Quémener-Redon, S., Hirschaud, E., Baron, D., Benech, C., et al. (2011). High-throughput analysis of promoter occupancy reveals new targets for Arx, a gene mutated in mental retardation and interneuronopathies. *PLoS One* 6:e25181. doi: 10.1371/journal.pone.0025181

Radice, G. L., Rayburn, H., Matsunami, H., Knudsen, K. A., Takeichi, M., and Hynes, R. O. (1997). Developmental defects in mouse embryos lacking N-cadherin. *Dev. Biol.* 181, 64–78. doi: 10.1006/dbio.1996.8443

Rajendran, L., and Paolicelli, R. C. (2018). Microglia-mediated synapse loss in Alzheimer's disease. *J. Neurosci.* 38, 2911–2919. doi: 10.1523/JNEUROSCI.1136-17.2017

Ramsden, C. E., Keyes, G. S., Calzada, E., Horowitz, M. S., Zamora, D., Jahanipour, J., et al. (2022). Lipid peroxidation induced ApoE receptor-ligand disruption as a unifying hypothesis underlying sporadic Alzheimer's disease in humans. *J. Alzheimers Dis.* 87, 1251–1290. doi: 10.3233/JAD-220071

Ranscht, B., and Dours-Zimmermann, M. T. (1991). T-cadherin, a novel cadherin cell adhesion molecule in the nervous system lacks the conserved cytoplasmic region. *Neuron* 7, 391–402. doi: 10.1016/0896-6273(91)90291-7

Rasin, M.-R., Gazula, V.-R., Breunig, J. J., Kwan, K. Y., Johnson, M. B., Liu-Chen, S., et al. (2007). Numb and Numbl are required for maintenance of cadherin-based adhesion and polarity of neural progenitors. *Nat. Neurosci.* 10, 819–827. doi: 10.1038/nn1924

Ray, H., and Chang, C. (2020). The transcription factor Hypermethylated in Cancer 1 (Hic1) regulates neural crest migration via interaction with Wnt signaling. *Dev. Biol.* 463, 169–181. doi: 10.1016/j.ydbio.2020.05.012

Rebman, J. K., Kirchoff, K. E., and Walsh, G. S. (2016). Cadherin-2 is required cell autonomously for collective migration of facial branchiomotor neurons. *PLoS One* 11:e0164433. doi: 10.1371/journal.pone.0164433

Redies, C. (1997). Cadherins and the formation of neural circuitry in the vertebrate CNS. *Cell Tissue Res.* 290, 405–413. doi: 10.1007/s004410050947

Redies, C., Hertel, N., and Hübner, C. A. (2012). Cadherins and neuropsychiatric disorders. *Brain Res.* 1470, 130–144. doi: 10.1016/j.brainres.2012.06.020

Reis, L. M., Houssin, N. S., Zamora, C., Abdul-Rahman, O., Kalish, J. M., Zackai, E. H., et al. (2020). Novel variants in CDH2 are associated with a new syndrome including Peters anomaly. *Clin. Genet.* 97, 502–508. doi: 10.1111/cge.13660

Reiss, K., Maretzky, T., Ludwig, A., Tousseyn, T., De Strooper, B., Hartmann, D., et al. (2005). ADAM10 cleavage of N-cadherin and regulation of cell-cell adhesion and β -catenin nuclear signalling. *EMBO J.* 24, 742–752. doi: 10.1038/sj.emboj.7600548

Rhee, J., Buchan, T., Zukerberg, L., Lilien, J., and Balsamo, J. (2007). Cables links Robo-bound Abl kinase to N-cadherin-bound β -catenin to mediate Slit-induced modulation of adhesion and transcription. *Nat. Cell Biol.* 9, 883–892. doi: 10.1038/ncb1614

Rhee, J., Mahfooz, N. S., Arregui, C., Lilien, J., Balsamo, J., and VanBerkum, M. F. A. (2002). Activation of the repulsive receptor roundabout inhibits N-cadherin-mediated cell adhesion. *Nat. Cell Biol.* 4, 798–805. doi: 10.1038/ncb858

Riehl, R., Johnson, K., Bradley, R., Grunwald, G. B., Corneli, E., Lilienbaum, A., et al. (1996). Cadherin function is required for axon outgrowth in retinal ganglion cells in vivo. *Neuron* 17, 837–848. doi: 10.1016/S0896-6273(00)80216-0

Rivero, O., Seltzer, M. M., Sich, S., Popp, S., Bacmeister, L., Amendola, E., et al. (2015). Cadherin-13, a risk gene for ADHD and comorbid disorders, impacts GABAergic function in hippocampus and cognition. *Transl. Psychiatry* 5:e655. doi: 10.1038/tp.2015.152

Roussou, D. L., Pearson, C. A., Gaber, Z. B., Miquelajaregui, A., Li, S., Portera-Cailliau, C., et al. (2012). Foxp-Mediated suppression of N-cadherin regulates neuroepithelial character and progenitor maintenance in the CNS. *Neuron* 74, 314–330. doi: 10.1016/j.neuron.2012.02.024

Roy, A., Murphy, R. M., Deng, M., MacDonald, J. W., Bammler, T. K., Aldinger, K. A., et al. (2019). PI3K-Yap activity drives cortical gyrification and hydrocephalus in mice. *Elife* 8:e45961. doi: 10.7554/eLife.45961

Sáez-Valero, J., Costell, M., Sjögren, M., Andreasen, N., Blennow, K., and Luque, J. M. (2003). Altered levels of cerebrospinal fluid reelin in frontotemporal dementia and Alzheimer's disease. *J. Neurosci. Res.* 72, 132–136. doi: 10.1002/jnr.10554

- Saglietti, L., Dequidt, C., Kamieniarz, K., Rousset, M. C., Valnegri, P., Thoumine, O., et al. (2007). Extracellular interactions between GluR2 and N-Cadherin in spine regulation. *Neuron* 54, 461–477. doi: 10.1016/j.neuron.2007.04.012
- Sakai, N., Insolera, R., Sillitoe, R. V., Shi, S. H., and Kaprielian, Z. (2012). Axon sorting within the spinal cord marginal zone via Robo-mediated inhibition of N-cadherin controls spinocerebellar tract formation. *J. Neurosci.* 32, 15377–15387. doi: 10.1523/JNEUROSCI.2225-12.2012
- Sanes, J. R., and Zipursky, S. L. (2020). Synaptic specificity, recognition molecules, and assembly of neural circuits. *Cell* 181, 536–556. doi: 10.1016/j.cell.2020.04.008
- Sasaki, S., Shionoya, A., Ishida, M., Gambello, M. J., Yingling, J., Wynshaw-Boris, A., et al. (2000). A LIS1/NUDEL/Cytoplasmic dynein heavy chain complex in the developing and adult nervous system. *Neuron* 28, 681–696. doi: 10.1016/S0896-6273(00)00146-X
- Schiffmacher, A. T., Padmanabhan, R., Jhingory, S., and Taneyhill, L. A. (2014). Cadherin-6B is proteolytically processed during epithelial-to-mesenchymal transitions of the cranial neural crest. *Mol. Biol. Cell* 25, 41–54. doi: 10.1091/mbc.E13-08-0459
- Schirinzi, T., Sancesario, G. M., Ialongo, C., Imbriani, P., Madeo, G., Toniolo, S., et al. (2015). A clinical and biochemical analysis in the differential diagnosis of idiopathic normal pressure hydrocephalus. *Front. Neurol.* 6:86. doi: 10.3389/fneur.2015.00086
- Schmid, M.-T., Weinandy, F., Wilsch-Bräuninger, M., Huttner, W. B., Cappello, S., and Götz, M. (2014). The role of α -E-catenin in cerebral cortex development: radial glia specific effect on neuronal migration. *Front. Cell. Neurosci.* 8:215. doi: 10.3389/fncel.2014.00215
- Schrack, C., Fischer, A., Srivastava, D. P., Tronson, N. C., Penzes, P., and Radulovic, J. (2007). N-Cadherin regulates cytoskeletally associated IQGAP1/ERK signaling and memory formation. *Neuron* 55, 786–798. doi: 10.1016/j.neuron.2007.07.034
- Sekine, K., Honda, T., Kawauchi, T., Kubo, K., and Nakajima, K. (2011). The outermost region of the developing cortical plate is crucial for both the switch of the radial migration mode and the *dab1*-dependent “inside-out” lamination in the neocortex. *J. Neurosci.* 31, 9426–9439. doi: 10.1523/JNEUROSCI.0650-11.2011
- Sela-Donenfeld, D., and Kalcheim, C. (1999). Regulation of the onset of neural crest migration by coordinated activity of BMP4 and Noggin in the dorsal neural tube. *Development* 126, 4749–4762. doi: 10.1242/dev.126.21.4749
- Shen, J., Bronson, R. T., Chen, D. F., Xia, W., Selkoe, D. J., and Tonegawa, S. (1997). Skeletal and CNS defects in presenilin-1-deficient mice. *Cell* 89, 629–639. doi: 10.1016/S0092-8674(00)80244-5
- Shieh, J. C., Schaar, B. T., Srinivasan, K., Brodsky, F. M., and McConnell, S. K. (2011). Endocytosis regulates cell soma translocation and the distribution of adhesion proteins in migrating neurons. *PLoS One* 6:e17802. doi: 10.1371/journal.pone.0017802
- Shikanai, M., Nakajima, K., and Kawauchi, T. (2011). N-Cadherin regulates radial glial fiber-dependent migration of cortical locomoting neurons. *Commun. Integr. Biol.* 4, 326–330. doi: 10.4161/cib.4.3.14886
- Shoval, I., Ludwig, A., and Kalcheim, C. (2006). Antagonistic roles of full-length N-cadherin and its soluble BMP cleavage product in neural crest delamination. *Development* 134, 491–501. doi: 10.1242/dev.02742
- Singh, S., and Solecik, D. J. (2015). Polarity transitions during neurogenesis and germinal zone exit in the developing central nervous system. *Front. Cell. Neurosci.* 9:62. doi: 10.3389/fncel.2015.00062
- Sival, D. A., Guerra, M., Den Dunnen, W. F. A., Bätz, L. F., Alvial, G., Castañeyra-Perdomo, A., et al. (2011). Neuroependymal denudation is in progress in full-term human foetal spina bifida aperta. *Brain Pathol.* 21, 163–179. doi: 10.1111/j.1750-3639.2010.00432.x
- Soriano, E., and Del Rio, J. A. (2005). The cells of cajal-retzius: still a mystery one century after. *Neuron* 46, 389–394. doi: 10.1016/j.neuron.2005.04.019
- Southwell, D. G., Paredes, M. F., Galvao, R. P., Jones, D. L., Froemke, R. C., Sebe, J. Y., et al. (2012). Intrinsically determined cell death of developing cortical interneurons. *Nature* 491, 109–113. doi: 10.1038/nature11523
- Spassky, N. (2005). Adult ependymal cells are postmitotic and are derived from radial glial cells during embryogenesis. *J. Neurosci.* 25, 10–18. doi: 10.1523/JNEUROSCI.1108-04.2005
- Stan, A., Pielski, K. N., Brigadski, T., Wittenmayer, N., Fedorchenko, O., Gohla, A., et al. (2010). Essential cooperation of N-cadherin and neuroligin-1 in the transsynaptic control of vesicle accumulation. *Proc. Natl. Acad. Sci. U.S.A.* 107, 11116–11121. doi: 10.1073/pnas.0914233107
- Stocker, A. M., and Chenn, A. (2009). Focal reduction of α E-catenin causes premature differentiation and reduction of β -catenin signaling during cortical development. *Dev. Biol.* 328, 66–77. doi: 10.1016/j.ydbio.2009.01.010
- Subramanian, J., Savage, J. C., and Tremblay, M. È. (2020). Synaptic loss in Alzheimer's disease: mechanistic insights provided by two-photon in vivo imaging of transgenic mouse models. *Front. Cell. Neurosci.* 14:592607. doi: 10.3389/fncel.2020.592607
- Szabó, A., and Mayor, R. (2018). Mechanisms of neural crest migration. *Annu. Rev. Genet.* 52, 43–63. doi: 10.1146/annurev-genet-120417-031559
- Tabrizi, S. J., Flower, M. D., Ross, C. A., and Wild, E. J. (2020). Huntington disease: new insights into molecular pathogenesis and therapeutic opportunities. *Nat. Rev. Neurol.* 16, 529–546. doi: 10.1038/s41582-020-0389-4
- Takahashi, M., and Osumi, N. (2008). Expression study of cadherin7 and cadherin20 in the embryonic and adult rat central nervous system. *BMC Dev. Biol.* 8:87. doi: 10.1186/1471-213X-8-87
- Takasugi, N., Tomita, T., Hayashi, I., Tsuruoka, M., Niimura, M., Takahashi, Y., et al. (2003). The role of presenilin cofactors in the γ -secretase complex. *Nature* 422, 438–441. doi: 10.1038/nature01506
- Tanaka, H., Shan, W., Phillips, G. R., Arndt, K., Bozdagi, O., Shapiro, L., et al. (2000). Molecular modification of N-cadherin response to synaptic activity. *Neuron* 25, 93–107. doi: 10.1016/S0896-6273(00)80874-0
- Taneyhill, L. A., and Schiffmacher, A. T. (2017). Should I stay or should I go? Cadherin function and regulation in the neural crest. *Genesis* 55:e23028. doi: 10.1002/dvg.23028
- Taneyhill, L. A., Coles, E. G., and Bronner-Fraser, M. (2007). Snail2 directly represses cadherin6B during epithelial-to-mesenchymal transitions of the neural crest. *Development* 134, 1481–1490. doi: 10.1242/dev.02834
- Taverna, E., Götz, M., and Huttner, W. B. (2014). The cell biology of neurogenesis: toward an understanding of the development and evolution of the neocortex. *Annu. Rev. Cell Dev. Biol.* 30, 465–502. doi: 10.1146/annurev-cellbio-101011-155801
- Theveneau, E., Marchant, L., Kuriyama, S., Gull, M., Moepps, B., Parsons, M., et al. (2019). Collective chemotaxis requires contact-dependent cell polarity. *Dev. Cell* 19, 39–53. doi: 10.1016/j.devcel.2010.06.012
- Tissir, F., Qu, Y., Montcouquiol, M., Zhou, L., Komatsu, K., Shi, D., et al. (2010). Lack of cadherins Celsr2 and Celsr3 impairs ependymal ciliogenesis, leading to fatal hydrocephalus. *Nat. Neurosci.* 13, 700–707. doi: 10.1038/nn.2555
- Togashi, H., Abe, K., Mizoguchi, A., Takaoka, K., Chisaka, O., and Takeichi, M. (2002). Cadherin regulates dendritic spine morphogenesis. *Neuron* 35, 77–89. doi: 10.1016/S0896-6273(02)00748-1
- Tomaselli, K. J., Neugebauer, K. M., Bixby, J. L., Lilien, J., and Reichard, L. F. (1988). N-cadherin and integrins: two receptor systems that mediate neuronal process outgrowth on astrocyte surfaces. *Neuron* 1, 33–43. doi: 10.1016/0896-6273(88)90207-3
- Tran, N. L., Adams, D. G., Vaillancourt, R. R., and Heimark, R. L. (2002). Signal transduction from N-cadherin increases Bcl-2. Regulation of the phosphatidylinositol 3-kinase/Akt pathway by homophilic adhesion and actin cytoskeletal organization. *J. Biol. Chem.* 277, 32905–32914. doi: 10.1074/jbc.M200300200
- Treubert-Zimmermann, U., Heyers, D., and Redies, C. (2002). Targeting axons to specific fiber tracts in vivo by altering cadherin expression. *J. Neurosci.* 22, 7617–7626. doi: 10.1523/jneurosci.22-17-07617.2002
- Trommsdorff, M., Gotthardt, M., Hiesberger, T., Shelton, J., Stockinger, W., Nimpf, J., et al. (1999). Reeler/disabled-like disruption of neuronal migration in knockout mice lacking the VLDL receptor and ApoE receptor 2. *Cell* 97, 689–701. doi: 10.1016/S0092-8674(00)80782-5
- Uchida, N., Honjo, Y., Johnson, K. R., Wheelock, M. J., and Takeichi, M. (1996). The catenin/cadherin adhesion system is localized in synaptic junctions bordering transmitter release zones. *J. Cell Biol.* 135, 767–779. doi: 10.1083/jcb.135.3.767
- Uemura, K., Kitagawa, N., Kohno, R., Kuzuya, A., Kageyama, T., Chonabayashi, K., et al. (2003). Presenilin 1 is involved in maturation and trafficking of N-cadherin to the plasma membrane. *J. Neurosci. Res.* 74, 184–191. doi: 10.1002/jnr.10753
- Van Stegen, B., Dagar, S., and Gottmann, K. (2017). Release activity-dependent control of vesicle endocytosis by the synaptic adhesion molecule N-cadherin. *Sci. Rep.* 7:40865. doi: 10.1038/srep40865
- Veeraval, L., O'Leary, C. J., and Cooper, H. M. (2020). Adherens junctions: guardians of cortical development. *Front. Cell Dev. Biol.* 8:6. doi: 10.3389/fcell.2020.00006
- Vendome, J., Felsovalyi, K., Song, H., Yang, Z., Jin, X., Brasch, J., et al. (2014). Structural and energetic determinants of adhesive binding specificity in type I cadherins. *Proc. Natl. Acad. Sci. U.S.A.* 111, E4175–E4184. doi: 10.1073/pnas.1416737111

- Vezzoli, E., Caron, I., Talpo, F., Besusso, D., Conforti, P., Battaglia, E., et al. (2019). Inhibiting pathologically active ADAM10 rescues synaptic and cognitive decline in Huntington's disease. *J. Clin. Invest.* 129, 2390–2403. doi: 10.1172/JCI120616
- Wang, K., Zhang, H., Ma, D., Bucan, M., Glessner, J. T., Abrahams, B. S., et al. (2009). Common genetic variants on 5p14.1 associate with autism spectrum disorders. *Nature* 459, 528–533. doi: 10.1038/nature07999
- Watanabe, H., Imaizumi, K., Cai, T., Zhou, Z., Tomita, T., and Okano, H. (2021). Flexible and accurate substrate processing with distinct presenilin/ γ -secretases in human cortical neurons. *eNeuro* 8:ENEURO.0500-20.2021. doi: 10.1523/ENEURO.0500-20.2021
- Whitford, K. L., Marillat, V., Stein, E., Goodman, C. S., Tessier-Lavigne, M., Chédotal, A., et al. (2002). Regulation of cortical dendrite development by slit-robo interactions. *Neuron* 33, 47–61. doi: 10.1016/S0896-6273(01)00566-9
- Wolfe, M. S. (2019). Structure and function of the γ -secretase complex. *Biochemistry* 58, 2953–2966. doi: 10.1021/acs.biochem.9b00401
- Won, H., Mah, W., and Kim, E. (2013). Autism spectrum disorder causes, mechanisms, and treatments: focus on neuronal synapses. *Front. Mol. Neurosci.* 6:19. doi: 10.3389/fnmol.2013.00019
- Wong, F. K., Bercsenyi, K., Sreenivasan, V., Portalés, A., Fernández-Otero, M., and Marín, O. (2018). Pyramidal cell regulation of interneuron survival sculpts cortical networks. *Nature* 557, 668–673. doi: 10.1038/s41586-018-0139-6
- Wu, Q., Sun, X., Yue, W., Lu, T., Ruan, Y., Chen, T., et al. (2016). RAB18, a protein associated with Warburg Micro syndrome, controls neuronal migration in the developing cerebral cortex. *Mol. Brain* 9:19. doi: 10.1186/s13041-016-0198-2
- Xu, C., Funahashi, Y., Watanabe, T., Takano, T., Nakamuta, S., Namba, T., et al. (2015). Radial glial cell-neuron interaction directs axon formation at the opposite side of the neuron from the contact site. *J. Neurosci.* 35, 14517–14532. doi: 10.1523/JNEUROSCI.1266-15.2015
- Yam, P. T., Pincus, Z., Gupta, G. D., Bashkurov, M., Charron, F., Pelletier, L., et al. (2013). N-cadherin relocates from the periphery to the center of the synapse after transient synaptic stimulation in hippocampal neurons. *PLoS One* 8:e79679. doi: 10.1371/journal.pone.0079679
- Yamagata, M., Duan, X., and Sanes, J. R. (2018). Cadherins interact with synaptic organizers to promote synaptic differentiation. *Front. Mol. Neurosci.* 11:142. doi: 10.3389/fnmol.2018.00142
- Zeitlin, S., Liu, J., Chapman, D. L., Papaioannou, V. E., and Efstratiadis, A. (1995). Increased apoptosis and early embryonic lethality in mice nullizygous for the Huntington's disease gene homologue. *Nat. Genet.* 11, 155–163. doi: 10.1038/ng1095-155
- Zhang, J., Shemezis, J. R., McQuinn, E. R., Wang, J., Sverdllov, M., and Chenn, A. (2013). AKT activation by N-cadherin regulates beta-catenin signaling and neuronal differentiation during cortical development. *Neural Dev.* 8:7. doi: 10.1186/1749-8104-8-7
- Zhang, J., Woodhead, G. J., Swaminathan, S. K., Noles, S. R., McQuinn, E. R., Pisarek, A. J., et al. (2010). Cortical neural precursors inhibit their own differentiation via N-Cadherin maintenance of β -catenin signaling. *Dev. Cell* 18, 472–479. doi: 10.1016/j.devcel.2009.12.025
- Zhang, Y., Niu, B., Yu, D., Cheng, X., Liu, B., and Deng, J. (2010). Radial glial cells and the lamination of the cerebellar cortex. *Brain Struct. Funct.* 215, 115–122. doi: 10.1007/s00429-010-0278-5
- Zhou, Z., Hu, J., Passafaro, M., Xie, W., and Jia, Z. (2011). GluA2 (GluR2) regulates metabotropic glutamate receptor-dependent long-term depression through N-cadherin-dependent and cofilin-mediated actin reorganization. *J. Neurosci.* 31, 819–833. doi: 10.1523/JNEUROSCI.3869-10.2011



OPEN ACCESS

EDITED BY

Zsolt Lele,
Institute of Experimental
Medicine, Hungary

REVIEWED BY

Hidenori Tabata,
Aichi Human Service Center, Japan
Emilie Pacary,
INSERM U1215 Neurocentre
Magendie, France

*CORRESPONDENCE

Eve Seuntjens
eve.seuntjens@kuleuven.be
Anna Pancho
anna.pancho@unibas.ch

†PRESENT ADDRESS

Anna Pancho,
Developmental Genetics, Department
of Biomedicine, University of Basel,
Basel, Switzerland

SPECIALTY SECTION

This article was submitted to
Neurodevelopment,
a section of the journal
Frontiers in Neuroscience

RECEIVED 01 March 2022

ACCEPTED 20 September 2022

PUBLISHED 25 October 2022

CITATION

Pancho A, Mitsogiannis MD, Aerts T,
Dalla Vecchia M, Ebert LK, Geenen L,
Noterdaeme L, Vanlaer R, Stulens A,
Hulpiau P, Staes K, Van Roy F,
Dedecker P, Schermer B and
Seuntjens E (2022) Modifying PCDH19
levels affects cortical interneuron
migration. *Front. Neurosci.* 16:887478.
doi: 10.3389/fnins.2022.887478

COPYRIGHT

© 2022 Pancho, Mitsogiannis, Aerts,
Dalla Vecchia, Ebert, Geenen,
Noterdaeme, Vanlaer, Stulens, Hulpiau,
Staes, Van Roy, Dedecker, Schermer
and Seuntjens. This is an open-access
article distributed under the terms of
the [Creative Commons Attribution
License \(CC BY\)](#). The use, distribution
or reproduction in other forums is
permitted, provided the original
author(s) and the copyright owner(s)
are credited and that the original
publication in this journal is cited, in
accordance with accepted academic
practice. No use, distribution or
reproduction is permitted which does
not comply with these terms.

Modifying PCDH19 levels affects cortical interneuron migration

Anna Pancho^{1*†}, Manuela D. Mitsogiannis¹, Tania Aerts¹,
Marco Dalla Vecchia^{2,3,4}, Lena K. Ebert^{5,6}, Lieve Geenen^{1,7},
Lut Noterdaeme¹, Ria Vanlaer¹, Anne Stulens¹, Paco Hulpiau^{8,9},
Katrien Staes⁸, Frans Van Roy⁸, Peter Dedecker²,
Bernhard Schermer^{5,6} and Eve Seuntjens^{1*}

¹Developmental Neurobiology Group, Animal Physiology and Neurobiology Division, Department of Biology, KU Leuven, Leuven, Belgium, ²Laboratory for NanoBiology, Department of Chemistry, KU Leuven, Leuven, Belgium, ³Molecular Signaling and Cell Death Unit, Department of Biomedical Molecular Biology, Ghent University, Ghent, Belgium, ⁴VIB Center for Inflammation Research, Ghent, Belgium, ⁵Department II of Internal Medicine and Center for Molecular Medicine Cologne, Faculty of Medicine and University Hospital Cologne, University of Cologne, Cologne, Germany, ⁶Cologne Cluster of Excellence on Cellular Stress Responses in Ageing-Associated Diseases (CECAD), University of Cologne, Cologne, Germany, ⁷Laboratory of Neuroplasticity and Neuroproteomics, Animal Physiology and Neurobiology Division, Department of Biology, Katholieke Universiteit Leuven, Leuven, Belgium, ⁸Department of Biomedical Molecular Biology, Ghent University, Inflammation Research Center, VIB, Cancer Research Institute Ghent (CRIG), Ghent, Belgium, ⁹Bioinformatics Knowledge Center (BiKC), Howest University of Applied Sciences, Bruges, Belgium

PCDH19 is a transmembrane protein and member of the protocadherin family. It is encoded by the X-chromosome and more than 200 mutations have been linked to the neurodevelopmental PCDH-clustering epilepsy (PCDH19-CE) syndrome. A disturbed cell-cell contact that arises when random X-inactivation creates mosaic absence of PCDH19 has been proposed to cause the syndrome. Several studies have shown roles for PCDH19 in neuronal proliferation, migration, and synapse function, yet most of them have focused on cortical and hippocampal neurons. As epilepsy can also be caused by impaired interneuron migration, we studied the role of PCDH19 in cortical interneurons during embryogenesis. We show that cortical interneuron migration is affected by altering PCDH19 dosage by means of overexpression in brain slices and medial ganglionic eminence (MGE) explants. We also detect subtle defects when PCDH19 expression was reduced in MGE explants, suggesting that the dosage of PCDH19 is important for proper interneuron migration. We confirm this finding *in vivo* by showing a mild reduction in interneuron migration in heterozygote, but not in homozygote PCDH19 knockout animals. In addition, we provide evidence that subdomains of PCDH19 have a different impact on cell survival and interneuron migration. Intriguingly, we also observed domain-dependent differences in migration of the non-targeted cell population in explants, demonstrating a non-cell-autonomous effect of PCDH19 dosage changes. Overall, our findings suggest new roles for the extracellular and cytoplasmic domains of PCDH19 and support that cortical interneuron migration is dependent on balanced PCDH19 dosage.

KEYWORDS

interneuron, medial ganglionic eminence, PCDH19-CE, neuronal migration, brain development, neurodevelopmental disorder

Introduction

The developing cerebral cortex generates excitatory glutamatergic pyramidal neurons, which project and signal to different regions of the brain. These cells also make local microcircuits with GABAergic interneurons, which provide inhibitory input into these assemblies. The balance between excitation and inhibition needs to be perfectly controlled for the brain to function properly. Unlike the pyramidal neurons that are formed within the cortex and migrate radially to the cortical plate, interneurons originally derive from the medial and caudal ganglionic eminences (MGE and CGE resp.) during embryonic development (Marín, 2013). From there, they migrate tangentially to the cortex, guided by different extrinsic cues that are either repulsive or attractive (Marín et al., 2010). Besides extrinsic cues, neurons also make use of membrane-bound factors to read their environment while migrating (van den Berghe et al., 2014). Defects in the migration of these cells to the cortex lead to a disturbed balance between excitation and inhibition that can ultimately result in severe early-onset epilepsy (van den Berghe et al., 2013).

PCDH19 is the second most prevalent gene linked to early infantile epileptic encephalopathy (EIEE) and causes EIEE9 (OMIM #300088) (Dibbens et al., 2008; Jamal et al., 2010; Depienne et al., 2011; Duszyc et al., 2015), a disorder first described by Juberg and Hellman (1971). Recently, this disorder has been renamed to PCDH19-Clustering Epilepsy (CE) (Gecz and Thomas, 2020). Patients with PCDH19-CE suffer from epilepsy already early after birth. In addition to suffering from epileptic seizures, 75 percent of these patients also present with variable cognitive impairment (Cappelletti et al., 2015), and psychiatric comorbidities, such as hyperactivity, obsessive-compulsive behavior, and autism, have been most frequently reported (Kolc et al., 2019).

The pattern of inheritance of this disorder is very peculiar. *PCDH19* is coded by the X-chromosome, yet only females have the disorder, whereas carrier fathers do not have seizures. The discovery of several mosaic male patients suffering from the disease (Depienne et al., 2009; Terracciano et al., 2016; Thiffault et al., 2016; Kolc et al., 2019) showed that the co-existence of cells expressing the wild-type *PCDH19* and cells without *PCDH19* has a detrimental impact on brain function (Depienne et al., 2009; Kolc et al., 2019). This situation occurs naturally in females after random inactivation of the X chromosome, or in males that have a somatic mutation during early development and become mosaic for *PCDH19*. Depienne et al. postulated that the mosaicism might lead to impaired cell-cell communication or “cellular interference” (Depienne et al., 2012).

Mice heterozygous for *PCDH19* showed relatively minor abnormalities in the brain, yet a striking homotypic clustering

of the *PCDH19* KO and WT cells within the forebrain correlated with impaired network activity (Pederick et al., 2016, 2018). Lamination of the cortex was not affected and included the presence of cortical interneurons in normal numbers (Galindo-Riera et al., 2021). Nevertheless, minor changes have been observed when studying the behavior of these mice, and *PCDH19* has been implicated in mossy fiber synapse formation, supporting the idea that *PCDH19* has an important role in establishment and plasticity of micro-circuitry (Galindo-Riera et al., 2021; Hoshina et al., 2021).

PCDH19 is a member of the non-clustered 82-type protocadherins, has 6 cadherin repeats in the extracellular part, and a cytoplasmic tail containing two conserved domains (CM1 and CM2) (Wolverton and Lalande, 2001; Vanhalst et al., 2005; Hulpiau and van Roy, 2009; Kim et al., 2011). It has only limited adhesive capacity through homophilic interactions but becomes strongly adhesive upon interaction with Cdh2 (N-Cadherin) (Biswas et al., 2010; Emond et al., 2011). In zebrafish, *PCDH19* knockdown disturbs the convergent movement of cells during the formation of the neural tube, indicating a role in early neural cell migration (Emond et al., 2009). The cytoplasmic domain of *PCDH19* interacts with the WAVE regulatory complex through the so-called WIRS motif (Chen et al., 2014). This interaction is of particular importance since the WAVE regulatory complex controls cytoskeletal remodeling (essential during cell migration), and WAVE complex components, such as CYFIP2, are linked to neurodevelopmental disorders (Takenawa and Miki, 2001; Tai et al., 2010; Abekhouk and Bardoni, 2014; Chen et al., 2014). This cytoplasmic interaction with the WAVE regulatory complex is shared with several other *PCDH*s, such as the related *PCDH17*, which plays a role in collective axon extension (Hayashi et al., 2014). The cytoplasmic domain of *PCDH19* is proteolytically cleaved off upon neural activation in hippocampal neurons, and relocates to the nucleus to stimulate gene transcription of immediate early genes (Gerosa et al., 2022). Whether such cleavage takes place during embryogenesis has not been shown.

While other studies have assessed *PCDH19* migration in hippocampal neurons (Bassani et al., 2018) or in *in vitro* studies in neurospheres derived from cortical neurons (Pederick et al., 2016), to our knowledge, the role of *PCDH19* has not been assessed in cortical interneuron migration before.

Here, we tested the hypothesis that *PCDH19* is important for cortical interneuron migration. We found that *PCDH19* is expressed dynamically during embryogenesis in the regions generating cortical interneurons, as well as in interneurons invading the cortex. By mimicking the *PCDH19* dosage imbalance between cells in *ex vivo* assays, we found that a loss of *PCDH19* is less detrimental to migration compared to overdosing. In explants, dosage changes of particular *PCDH19* subdomains non-autonomously affected migration of non-targeted cells. In addition, we revealed cell-autonomous

domain-specific roles of the PCDH19 protein in migration and apoptosis, and confirmed an *in vivo* role for PCDH19 in interneuron migration.

Materials and methods

Animals

All animal experiments were conducted in compliance with the European union and Belgian laws in accordance with the guidelines of the Ethical Committee Animal Experimentation of the KU Leuven (P267/2015). Mice were maintained on CD1 Swiss genetic background. The CD1 mice were crossed with transgenic *Dlx5/6cre-IRES-eGFP* mice strain, which labels telencephalic interneurons green (*Dlx5/6-Cre-IRES-eGFP*) (Stenman et al., 2003). The mice were kept in a 14/10-h light-dark cycle in a humidity- and temperature-controlled pathogen free animal unit. Timed matings were performed to obtain pregnant female mice, and a plug check was done every day early in the morning to confirm mating. The vaginal plug day was considered as E0.5.*Dlx5/6-Cre-IRES-eGFP* positive embryos were verified under a fluorescence binocular microscope (SteREO Discovery.V8; Zeiss; Oberkochen; Germany). Dissection of mouse brains was done in cold phosphate-buffered saline (PBS) and fixation in 4% w/v paraformaldehyde (PFA)/PBS for 16–24 h at 4°C. After fixation, samples were washed two times in PBS and then placed into a storage buffer (0.01% w/v thimerosal/PBS) to preserve the brains. In addition, mouse tail biopsy samples (~5 mm) were also collected for DNA extraction and genotyping of the embryos.

Cre genotyping

PCR reaction was done with a GoTAQ Polymerase (Promega). The used forward and reverse primer sequences are shown in [Supplementary Table S1](#). Initial denaturation was performed at 94°C for 4 min. Cycling was done for 35 cycles with a denaturation at 94°C for 30 s, primer annealing at 58°C for 30 s and elongation at 72°C for 30 s. The final elongation was done for 7 min at 72°C and then cooled down to 4°C. The PCR product was visualized on a 1% agarose gel.

Cloning of PCDH19 tagged overexpression constructs

PCDH19 FL, ECDTM, ICD, and ICDΔNLS constructs were obtained from a plasmid containing the full-length murine sequence (PCDH19FL) and cloned into a second plasmid containing the green fluorescent protein (eGFP) behind a

cytomegalovirus promoter. Primer sequences to generate the PCR products are shown in [Supplementary Table S2](#).

PCDH19ICDeGFP and PCDH19ICDΔNLS-eGFP were generated using tail PCR, and PCDH19FL-eGFP and PCDH19ECDTM-eGFP were generated using dovetail PCR. Finally, all PCDH19-eGFP constructs were recloned into a pCAGGS plasmid, expressing IRES-TdTomato.

Generation of PCDH19-V5 and PCDH19 KO mice

All the primers used to generate the PCDH19-V5 and PCDH19 KO mouse lines were ordered from IDT. These mouse lines were created in the lab of Bernhard Schermer.

Single-guide RNA generation

In order to generate the single-guide RNA (sgRNA), a PCR reaction was done. The PCR was done with the Q5 High-Fidelity Polymerase (NEB). The used forward and reverse primer sequences are shown in [Supplementary Table S3](#). As a PCR template, the pSpCas9 (BB)-2APuro (Px459) V 2.0 (Addgene62988) was used. Initial denaturation was performed at 98°C for 30 s. Cycling was done for 30 cycles with a denaturation at 98°C for 10 s, primer annealing at 60°C for 30 s, and elongation at 72°C for 10 s. The final elongation was done for 2 min at 72°C and then cooled down to 10°C.

Gel extraction

A 1% gel was done to extract the PCR product. To visualize the PCR reaction, 2 μl loading dye was added to the reaction. The complete PCR product was loaded onto the gel. The electrophoresis was done for 30 min at 90 V. The gel-extracted band had a size of 120 bp. Gel extraction was performed using the Qiagen gel extraction kit according to the manufacturer's instructions. Elution was performed in a 30 μl elution buffer. After elution the concentration was measured using the Nanodrop. In order to verify the extraction, 2 μl of the extracted DNA was loaded into a 1% gel.

In vitro transcription

The HiScribe T7 High-Yield RNA Synthesis Kit (NEBE2040S) was used to transcribe the DNA into RNA. The reaction was set for short transcripts (<0.3 kb). A reaction of 20 μl was set up where the final concentration of the reaction buffer was 0.75X. About 11 μl was used of the template gel-extracted DNA. About 1.5 μl was used from the T7 RNA polymerase mix. The transcription was performed for 16 h overnight at 37°C. To verify if the transcription was successful,

2 μ l of the obtained unpurified RNA was loaded on a 2% agarose gel.

RNA purification

For the purification, the RNeasy kit (Qiagen) was used. About 700 μ l of QIAzol lysis reagent was added to the sample to homogenize. The homogenate was incubated at room temperature for 5 min. After chloroform extraction, samples were loaded on the RNeasy mini column in a 2-ml collection tube. The samples were eluted in 30–50 μ l RNase free water. Concentration of the eluted RNA was measured on a 1:10 diluted sample and verified on a 2% gel.

Generation of mouse lines via electroporation of zygotes

Mouse generation was done according to Tröder et al. (2018). For the PCDH19-V5 mouse line, 4- μ M sgRNA, 4- μ M Cas9protein, and 10- μ M ssODN were used. sgRNA was made as described above and the repair template ordered from IDT (sequences in Supplementary Table S3). For the PCDH19 KO mouse line, 4 μ M of SpCas9 WT protein was complexed with a mix of 4 different guide RNAs (2 μ M each), targeting a large deletion. Guide RNAs were ordered via IDT as crRNA (IDT, Alt-RTM crRNA) (sequences in Supplementary Table S3) and used together with the tracrRNA (IDT, 1072532).

Genotyping

A small ear biopsy was collected at weaning and used as well for identification of the mouse. Ear biopsy was deposited into a sterile Eppendorf tube and incubated with a 200 μ l lysis buffer [1-M Tris-HCl (pH = 8.5), 0.5-M EDTA (pH = 8), 10% sodium dodecyl sulfate (SDS), and 5-M NaCl], containing 1:100 Proteinase K (10 μ g/ μ l in 40% glycerol/nuclease free water) at 56°C overnight.

Pcdh19-V5 and KO Genotyping

PCR reaction was done with a GoTAQ Polymerase. The used forward and reverse primer sequences are shown in Supplementary Table S4. Initial denaturation was performed at 94°C for 3 min. Cycling was done for 34 cycles with a denaturation at 94°C for 30 s, primer annealing at 60°C for 30 s, and elongation at 72°C for 1 min. The final elongation was done for 10 min at 72°C and then cooled down to 10°C. The PCR product was visualized on a 2% agarose gel. Primers are in Supplementary Table S4.

In situ hybridization

A 560 base pair fragment of the mouse *PCDH19* gene exon1 was cloned into a pJET1.2 vector. *In vitro* transcription was done using 1 μ g as a template of the linearized plasmid, using the T7 DIG RNA labeling kit (Roche, Sigma-Aldrich). Purification of the RNA was done using the Micro Bio-Spin™ P30 gel columns (Bio-rad) according to the manufacturer's instructions, and RNA concentration was measured using the SimpliNano spectrometer (Biochrom). All the ISH were done on 6- μ m paraffin sections using an automated platform (Ventana Discovery, Roche). About 200 ng of dioxigenin labeled probe was diluted in RiboHybe (Roche) and vortexed prior to use. After deparaffination *via* heat, slides underwent pre-treatment with a citrate buffer (pH = 6.) at 95°C and with proteinase K at 37°C for 4 min. The probe in the aforementioned amount was added per slide, and denaturation was performed at 80°C. Next, hybridization was performed for 6 h at 65°C. Several washes had occurred before the anti-DIG antibody conjugated to alkaline phosphatase was added at the concentration of 1:1,000, followed by an incubation of 8 h with the substrate (BlueMap Detection Kit, Roche). Slides were manually dehydrated in a graded ethanol dilution and mounted with Eukitt (Sigma). Brightfield images were acquired using a LeicaDM6 B microscope connected to a digital CMOS camera (DMC2900, Leica) with the LAS Xsoftware suite (Leica). Further processing was done with Fiji and GIMP or Photoshop.

Hybridization chain reaction

This protocol is an adaptation of the HCR3.0 protocol described in Choi et al. (2018). We refer to buffer compositions described in this protocol, and used the method described in Elagöz et al. (2022) for probe design. To ensure the probe could distinguish WT from KO, we used the ~1,000 bp PCDH19 sequence that was deleted in the PCDH19 KO mice as input for the probe generator. Off-target probes were identified using BlastN and were excluded from the probe set. DNA oligo pools from the designed probes were ordered from Integrated DNA Technologies (IDT), dissolved in UltraPure™ DNase/RNase-Free Distilled Water (Invitrogen) and stored at –20°C. HCR B2 amplifier labeled with Alexa Fluor® 647 was ordered from Molecular Instruments. Components of all used buffers and solutions as well as the sequences for the DNA probe sets are listed in Supplementary Tables S5–S9.

Before starting the protocol, vibratome sections were placed in a 24-well plate (maximum, three sections per well). First, tissues were permeabilized with 600 μ l of a permeabilization buffer (1% DMSO, 1% Triton-X in autoclaved PBS) for 2 h at 37°C in a humidified surrounding in the dark. Next, a permeabilization buffer was replaced with a 600 μ l pre-warmed

TABLE 1 Probe wash steps for the HCRv3 protocol.

Step	Solution	Timing
1	25% 5X SSCT/75% probe wash buffer pre-warmed at 37°C	15 min
2	50% 5X SSCT/50% probe wash buffer pre-warmed at 37°C	15 min
3	75% 5X SSCT/25% probe wash buffer pre-warmed at 37°C	15 min
4	100% 5X SSCT pre-warmed at 37°C	15 min
5	100% 5X SSCT at RT	5 min

probe hybridization buffer, and tissue was incubated for 1 h at 37°C in a humidified surrounding in the dark. In the meantime, HCR probes were thawed on ice, spun, and a 12 nmol DNA probe was diluted in a 200 µl pre-warmed probe hybridization buffer (probe solution) per well or glass slide. After incubation, the probe hybridization buffer was replaced by 200 µl of probe solution. Tissue was incubated for 18 h at 37°C in a humidified surrounding in the dark.

The next day, excess probes were washed from the tissue in several wash steps (600 µl of each wash solution, see Table 1) at 37°C in a humidified surrounding in the dark.

To amplify the probe, the last wash solution was replaced by a 600 µl amplification buffer, and tissue was incubated for at least 30 min at RT in a humidified surrounding in the dark. Next, 9 pmol of both amplification hairpins (H1 and H2) per well or glass slide was pipetted into pcr-tubes, heated at 95°C for 90 s, immediately put on ice for 5 min, and incubated at RT for 30 min in the dark. Next, the hairpins were individually dissolved in the amplification buffer (100 µl per 9 pmol hairpin) before they were combined and mixed well (hairpin solution). The amplification buffer was replaced with 200 µl hairpin solution. Tissue was incubated for 16 h at RT in a humidified surrounding in the dark.

The following day excess hairpins were removed by washing tissue three times with 600 µl of 5X SSCT for 10 min. Next, sections were stained with DAPI and mounted.

A control condition in a well was included in which probe solution was replaced by a 300 µl probe hybridization buffer, and hairpin solution was replaced by a 300 µl amplification buffer. Thus, these sections were not treated with probes and hairpins to control for autofluorescence of the tissue.

Protein isolation and western blotting

Depending on the experiment, MGE, LGE and CGE was dissected out of 10 embryos at stage E13.5 and pooled per brain region (Figure 1J) or individual whole telencephalon (Figures 1E,I), ventral telencephalon (Figure 1J) or entire brain (Supplementary Figure 1F) were isolated. For protein isolation and quantification, the tissue lysates were homogenized in a

100 µl/sample ASBA buffer [1% Triton-X-100, 0.1% SDS, 1-mM EDTA, 50-mM NaCl, 20-mM Trizma base (pH = 7.5)] and 4 µl/sample cocktail protease inhibitor solution (Roche). The homogenization was performed mechanically with a drill for 5-x-10 s/sample and kept on ice. Afterwards, the brain samples were centrifuged for 5 min at 13,000 rpm at 4°C. Supernatants were collected, and the Qubit Protein Assay Kit (Invitrogen) was used to determine protein concentration of the brain lysates.

About 15 µg of the protein lysates was loaded on a precasted 4–12% Criterion XT Bis-Tris 26 well-gel of Biorad and blotted on a PVDF membrane using the Trans Turbo Blot from BioRad (7 min). Next, the membranes were dehydrated in Tris-saline for 5 min and incubated with a blocking buffer for the following 2 h. All the washing and incubation steps occurred at room temperature (RT) and placed on the shaker. After the 2-h incubation, the membrane was incubated with the PCDH19 primary antibody (Bethyl A304-468A) diluted 1/1,000 and left overnight to incubate. The next day, blots were rinsed 3 x 5 min with Tris-saline and incubated with the secondary antibody solution with HRP-labeled antibodies (GAR:Goat Anti-Rabbit) 1/10,000 in the blocking buffer for 30 min. Next, membranes were rinsed with Tris-saline (2 x 5 min) and incubated with Tris-Stock (1 x 5 min). After the Tris-Stock incubation, the Clarity western ECL substrate kit (BioRad) was used to reveal the blots. Imaging of the membranes occurred with the imaging system (BioRad).

The membranes were stripped using a Restore western blot stripping buffer of Thermo Scientific. Next, the membrane was rinsed again with Tris-saline (3 x 5 min) and incubated with the blocking buffer for 2 h. The membranes were incubated overnight with GAPDH 1/1,000 (GAPDH Millipore cat nr: MAB374) in the blocking buffer. The next day, a HRP-labeled antibody (Goat Anti-Mouse) 1/25,000 solution was added and, afterwards, imaged with the BioRad imaging system.

Organotrophic slice electroporation

One day before the actual experiment, Millicell Cell Culture inserts with a pore size of 0.4 µm were coated with poly-L-Lysin (Sigma) and Laminin (Sigma). Coated inserts were placed in PBS into a 6-well plate overnight at 37°C in the cell culture incubator. On the next day, coating solution was removed, and inserts were placed on top of a slice culture medium. Dlx5/6-Cre-IRES-eGFP E13.5 brains were dissected in ice-cold L15++ (a Leibovitz's L15 medium, supplemented with glucose and Hepes). Subsequently, the dissected brains were embedded in 4% low-melting point agarose in L15++. Polymerization was obtained after 1 h on ice. Next, coronal slices of 300 µm were obtained with the vibratome and collected in L15++ media.

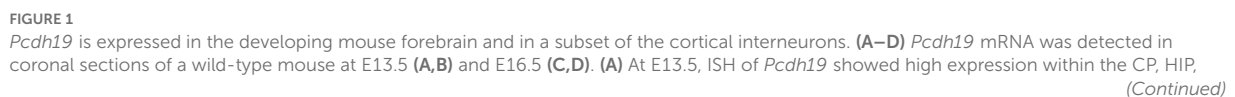


FIGURE 1 (Continued)

and, to a lower extent, in the SVZ within the NCTX. In the VT, *Pcdh19* was detected in the GEs within the LGE, MZ, and in the LCS. Sparse expression is detected within the VZ in the VT. **(B)** More caudal expression is also detected within the CGE, TH, and HYP at E13.4. **(C)** At E16.5, mRNA becomes more confined to the CP within the NCTX. **(D)** Scanty expression can still be detected in the SVZ and LCS. **(E)** Caudal expression is found within the limbic system in the TH, the AM (LA, BLA, cortical AM), and the HYP. **(F)** Quantification of PCDH19 protein in lysates of telencephalon collected at different embryonic stages showed a significant increase in the production of PCDH19 at late embryonic and early postnatal stages. **(F–I)** HCR for PCDH19 at E13.5, dots represent RNA molecules. **(F)** PCDH19 was expressed at high levels in the NCTX cortical plate, and at lower levels in the (S)VZ, and is nearly absent from the IZ. **(G)** PCDH19 was expressed at low levels in the (S)VZ and nearly absent from the mantle zone. **(H,I)** Zooms on migrating interneurons showed some expressed PCDH19 stronger (white arrowheads), whereas others were negative. Interneurons migrating in the cortical plate mostly had a low-level expression of PCDH19. **(J)** Western blot and relative quantification of E13.5 mouse VT, TEL, and the distinct GE regions show PCDH19 protein production at the expected molecular weight of nearly 126 kDa in all the lanes. Total protein was assessed with the housekeeping gene mGAPDH. AM, amygdala; BLA, basolateral amygdala; CGE, caudal ganglionic eminence; CP, cortical plate; E, embryonic day; HIP, hippocampus; HYP, hypothalamus; ICD, intracellular domain; IZ, intermediate zone; LA, lateral amygdala; LCS, lateral cortical stream; LGE, lateral ganglionic eminence; MZ, mantle zone; MGE, medial ganglionic eminence; mGAPDH, murine glyceraldehyde 3-phosphate dehydrogenase; NCTX, neocortex; P, postnatal day; SVZ, subventricular zone; TEL, telencephalon; TH, thalamus; VT, ventral telencephalon; VZ, ventricular zone.

Settings of the vibratome were the following: speed was less than 15, frequency was set at 60, and the amplitude at 0.6. Sectioned slices were placed on top of a membrane and placed on top of an agarose bed, previously prepared into the square well of a Petri dish square platinum electrode (CUY701P20E, Nepagene). Injection was performed under a binocular (Leica) into the MGE. For OE Plasmids, we injected at a concentration of 2 µg/µl. To generate the LOF, clustered regularly interspaced short palindromic repeats (CRISPR-Cas9) components were pre complexed to ribonucleoprotein (RNP) in an Opti-Mem medium for at least 20 min at room temperature injected at the amount of 380 ng for the guide ribonucleic acid (RNA) and 300 ng for the Cas9 protein. All LOF compounds were mixed with pCAGGS plasmid at a concentration of 1 µg/µl in order to trace the electroporated cells. To visualize the injection site, Fast Green was used at an amount of 1 µl per 33 µl. For the negative electrode, an agarose cylinder of 1% was attached to the cover square of platinum plate electrode (CUY701P20L, Nepagene). Electroporation was performed using the following settings: 5 pulses, 150V with a pulse length duration of 5 ms using 100-ms intervals. A BTX electroporator (ECM830, Harvard Apparatus) was used. Subsequently, after electroporation, electroporated sliced were placed on top of the coated inserts and placed on ice. Three slices with the same condition were placed on top of an insert. After all the inserts were covered with slices, the slices were cultivated in the cell culture incubator. After 2 days *in vitro* (div), 500 µl of the used slice culture media was removed and refreshed with new slice culture media. After 3 div slices were fixed in 4% PFA for at least 2 h, stained with DAPI and mounted on microscope slides with Mowiol and imaged with the confocal microscope (Olympus). Analysis was performed using ImageJ software, total amount of TdT positive cells was quantified within every slide side, and the proportion or cells reaching the cortex compared to the total amount was calculated.

Statistical significance was determined using a Kruskal Wallis multicomparison test with Dunn's *post hoc* test.

MGE explants in Matrigel culture

At E13.5 *Dlx5/6-Cre-IRES-eGFP* embryos were dissected from the mother in L15++ media. Embryos were kept on ice, while the skin and meninges were removed. Subsequently, the neocortex (NCTX) was open up from the top, superficially, in order to expose the GEs. Injection into the MGE was performed using approximately 10 injection sites per MGE. The same injection mixtures and amount of OE plasmids and CRISPR-Cas9 components as used for the slice electroporation (slice EP) were used. Subsequently, after injection in both MGEs, electroporation was performed using the following settings, 5 pulses, 50 V with a pulse length duration of 50 ms using 1-s intervals. Electrodes (CUY650P5 tweezer electrodes) connected to a BTX electroporator (Harvard Apparatus) were placed on each side of the embryonic head at the position of the ears. After electroporation embryos were kept at 4°C for 3 h in L15++. Meanwhile, the matrigel was thawed in ice. Matrigel was diluted in a 1:1 ratio with complete neuro basal media. After the incubation period, MGE was dissected from the embryos, and each MGE was cut into small pieces. Subsequently, these pieces were embedded carefully into the neurobasal media-diluted matrigel and placed as matrigel drops containing the piece into 35-mm glass bottom imaging (Ibidi) dishes. Once placed into the dish, the Matrigel containing explant was allowed to polymerize at 37°C. After polymerization, the explant was surrounded with complete neurobasal media and cultured in the cell culture incubator for 2 days. After 2 div explants were fixed with 4% PFA and imaged with the confocal microscope (Olympus). Stacks were projected with the Image J software, and analysis of migration from the explant was performed

using Cell Profiler software (McQuin et al., 2018; Stirling et al., 2021). Statistical significance was determined using the Mann–Whitney U Test for the sample size of 2 and with the Kruskal–Wallis non-parametric test and the Dunn's *post hoc* test for bigger sample sizes.

Cell profiler analysis migration from the explant

The following cell profiler pipeline for analysis with the following modules was used. The z-projected image of the explant and the red fluorescence channel for the positive TdT cells were used as starting images for the images module. Metadata was extracted from the image file. The explant brightfield image and the TdT cell image were defined with names and types. We used “identify primary objects” as modules to detect the explant and the TdT neurons. The explant was defined with the Cell profiler as one primary object. All the TdT neurons cell bodies were identified as primary objects; the result was verified. Once all objects were identified, we used the two-module mask objects and relate objects. In the relate object module, the explant was set as a parent object and the neuron cell bodies as child objects. Using this module, distance between the parent object and all child objects was measured. Distances were obtained in pixels. Transforming of pixels into μm was achieved using the conversion factor stored in the .oib file using Image J. Finally, Graph Pad Prism 8.3.0 was used to determine the statistical significance.

MGE explant morphological analysis

Morphological analysis of MGE explant-derived neurons was performed using the SNT ImageJ plugin (Longair et al., 2011; Arshadi et al., 2021). A minimum of 4 explants obtained from at least two experimental replicates were analyzed per treatment group. Means per experimental group were compared with the Kruskal–Wallis non-parametric test and the Dunn's *post hoc* test for a sample size bigger than 2 and with the Mann–Whitney U test for the comparison between two samples. Polarity analysis was compared across experimental conditions using two-way repeated measures ANOVA with Holm–Sidak *post hoc* comparison. Neuronal category frequencies were compared between neuronal morphology and experimental groups using two-way repeated measures ANOVA with Holm–Sidak *post hoc* comparison.

Cell culture and transfection

N2A cells were grown in DMEM high glucose supplemented with 2-mM L-glutamine, 1% penicillin/streptomycin, and 10%

fetal bovine serum albumine (Neuro2A media). For confocal microscopy, we used glass bottom dishes (Ibidi) and pre coated them with geltrex at least 3 h prior seeding; for the rest of applications, we used 6-well plates. One day prior, transfection cells were seeded to a density of 5×10^5 (a 6-well plate) and 5×10^4 (Ibidi dish) and left to adhere. On the day of the transfection, the cells were checked for adherence and confluency under the microscope. Transfection was performed using Lipofectamine 3000 (Thermo Fisher Scientific). Briefly, Lipofectamine 3000 reagent was diluted in Opti-Mem using the higher amount suggested by the manufacturer for 6-well or 24-well (Ibidi dish) and vortexed and spun down. About 5 μg of plasmid DNA was diluted in Opti-MEM, and, subsequently, the 2 μl of P3000 reagent per 1 μg DNA was added to generate the master mix. The mastermix was spun down and mixed 1:1 with the prior diluted lipofectamine in Opti-Mem. The mixture was spun down and incubated for 30 min at room temperature. After the incubation, mixture was added to one well/dish drop by drop, and the cells were given an easy shake to mix the reagent better into their media. The cells were incubated at 37 °C in an incubator. Transfection efficiency was controlled after 24 and 48 h under a fluorescent microscope.

GFP Pulldown

About 500 μg of protein per condition was used to start the pull down. The Miltenyi μM ACSGFP isolation kit (130-091-125) was used. About 50 μg GFP beads were incubated with lysate, containing 500 μg protein for 1 h in the cold room with overhead shaking. A μMACS column and magnet were placed in the cold room. About 200 μl of an ice cold lysis buffer containing the proteinase inhibitor cocktail was used to preclear the columns. Whole lysate containing the beads was loaded on the magnetic column. Beads were washed two times with a wash buffer 1 [50 mM Tris (pH = 7.5), 150-mM NaCl, 5% glycerol, and 0.05% Triton-X100]. Then, the beads were washed three times with wash buffer 2 [50-mM Tris (pH = 7.5), 150-mM NaCl]. Elution was conducted *via* adding 20 μl of a 95°C pre-heated elution buffer to the column and incubated at room temperature for 5 min. Subsequently, 50 μl was further eluted through the column, and analysis was done by Western Blot.

For western blot detection after the GFP pull down, proteins were heat denatured in a mixture of sample-reducing agent 10 \times (NOVEX, NP0009), and loading dye LDS Sample Buffer 4 \times (NOVEX, NP0007) was as well added to the protein. All amounts were calculated for a volume of 20 μl and boiled at 70°C for 10 min. Separation was performed on a precast NuPAGE 4–12% Bis-Tris gel [Invitrogen, (WG1403BX10) with NuPAGE MOPS SDS Running Buffer (NP0001) and immune blotted to a nitrocellulose membrane (Transfer Pack, Midi format, 0.2- μm nitrocellulose, Bio-Rad, 170-4159) using a Trans Blot Turbo system (Bio-Rad)]. Standard protein detection was

performed using mouse anti-GFP antibody -HRP (1:5,000; Biorad), rabbit anti-PCDH19 (1:500 Millipore). After 2-h blocking in 5% w/v non-fat dry milk/TBST (a blocking buffer) at RT, o/n incubation at 4°C in a primary antibody diluted in the blocking buffer, and washing in TBST, transfer membranes were incubated during 45 min in HRP-conjugated anti-rabbit secondary antibodies (Bio-Rad) diluted 1:10,000 in a WB buffer. Protein bands were visualized with a ChemiDoc MP imaging system (Bio-Rad) after incubation in ECL substrate (Thermo Fisher Scientific).

Flow cytometric analysis

To perform our apoptosis analyses, we trypsinated the Neuro2A cells and stopped the enzyme with media-containing serum. In addition, we kept all the washes to not lose dead cells. After centrifugation, the supernatant was discarded, and cell pellets were resuspended in PBS and transferred into micro centrifuge tubes. In order to have a positive control for early and late apoptosis, the untransfected cell condition was used. Half of the cells were killed intentionally for 15 min at 75°C. These cells were then mixed with the rest of untransfected cells in equal parts and spun down. Once the positive apoptosis control was made, all the cell suspensions were spun down and resuspended into a 100 µl Annexin V-binding buffer (BD Biosciences). Annexin V (V450, 560506 BDBiosciences) and 7-aminoactinomycin D (7AAD) (559925 BD Biosciences) were added to analyze for early and late apoptosis, excluding the single-stain controls. The single-stain controls were the positive apoptosis control either incubated with Annexin V or 7AAD. Incubation was performed for 15 min at room temperature in the dark. After the incubation, an Annexin V-binding buffer was added, and cells were passed through tubes with a 35-mm strainer (VWR) and analyzed with the SH800 Cell Sorter (Sony).

Image acquisition

N2A cells images were acquired using the 60X magnification with oil immersion of the confocal microscope (an Olympus FV1000 microscope) and taking fluorescent z-stacks with a depth of 1–2 µm, a speed of 4 µs/pix and a pixel size of at least 1024 × 1024 pixels. Whole z-depth of the DAPI-channel was covered.

Quantification of the nuclear-cytoplasmic ratio

For nuclear-cytoplasmic distribution calculations, a single z-slice was manually selected from the provided z-stack in order to have the most central view of the cell through the nucleus and to

have the highest number of cells in focus. These images were split in individual channels [DAPI (blue), GFP (green) and TexRed (red)]. Images were segmented and analyzed using Cell Profiler using a custom-made pipeline. Briefly, the cells were segmented by identifying individual nuclei through the DAPI channel using a global Otsu threshold method. Cells edges were identified using a propagation algorithm using the fluorescence channel that would best describe the totality of the cell, leading to a one-to-one correspondence between each nucleus and the respective cell. Nuclear areas were defined by the DAPI stain and the cytoplasmic areas were obtained by subtracting the nuclear areas to the identified total cell areas. Shrinking of 1 pixel of nuclei was used to better define the cytoplasmic areas. After segmentation, the average fluorescence intensity was calculated for each cell in both the nucleus and cytoplasm-identified objects. Image analysis with CellProfiler 2.2.0 and R Studio 3.6.1 was conducted by Marco Dalla Vecchia. Images with cells in a clearly dying state or with many saturated pixels were discarded from the analysis.

Quantification of the GFP-TdT ratio

Z max projection was made of the explant images. The area of the explant was defined by the Dlx5/6-Cre-IRES-eGFP IN in the GFP channel. The same area was applied to the TdT channel, and the threshold was adjusted before measurement. Intensity measurements were performed with Fiji is just ImageJ and statistical analysis performed with Graph Pad Prism 8.3.

Results

Pcdh19 mRNA and PCDH19 protein are produced in the ganglionic eminences during embryonic mouse brain development

Different studies have shown that *Pcdh19* is expressed in the developing mouse cortex and hippocampus within pyramidal neurons (Kim et al., 2007; Fujitani et al., 2017; Pederick et al., 2018; Gerosa et al., 2022). Only a few groups have investigated *Pcdh19* expression in inhibitory neurons (Bassani et al., 2018; Serratto et al., 2020; Galindo-Riera et al., 2021). We hypothesized that proper migration of inhibitory neurons to the cortex could be affected in PCDH19-CE. To address this question, we first assessed *Pcdh19* expression in developing cortical interneurons neurons by means of *in situ hybridization* (ISH). GABAergic cortical interneuron migration occurs from E12-E19 in the developing mouse brain from the ganglionic eminence to the NCTX (Guo and Anton, 2014). We, therefore, studied *Pcdh19* mRNA at E13.5 and E16.5 in the ganglionic eminence and NCTX in mouse embryonic brain slices (Figures 1A–D). At E13.5, *Pcdh19* is clearly expressed in the cortical plate and the

ventricular zone within the NCTX, and in the mantle zone (MZ), the dorsal lateral ganglionic eminence (LGE) ventricular zone (VZ), and the lateral cortical stream (LCS) of the ventral telencephalon. Caudally, *Pcdh19* mRNA could be detected throughout the CGE, thalamus (TH), and hypothalamus (HYP) (Figure 1B). At E16.5, *Pcdh19* expression became less prominent in the cortical plate (CP) than at E13.5 (Figure 1C) but appeared more restricted, which could be the prospective layer 5, where *Pcdh19* expression has been described postnatally (Galindo-Riera et al., 2021) (Figure 1C). In the ventral telencephalon, it was still visible within the LCS. Caudally, expression was high in the limbic system within the TH, amygdala (AM) and HYP (Figure 1D). To investigate the temporal dynamics of protein production of PCDH19, we performed western blot (WB) on lysates of whole telencephalon at E13.5, 15.5, 17.5, and P7 and quantified the relative amount of PCDH19 at each stage (Figure 1E, Supplementary Figure 1A for WB). This analysis showed a significant increase in PCDH19 production at late embryonic stages and at P7, in line with the described roles of PCDH19 at the synapse. To further explore the expression of *Pcdh19* in embryonic cortical interneurons, we made use of the *Dlx5/6-Cre-IRES-eGFP* mouse line that labels migrating cortical interneurons during embryogenesis (Stenman et al., 2003). We focused our analysis on E13.5, given many assays in this manuscript use this time point, and interneuron migration is easy to visualize at this stage. We revealed *Pcdh19* expression by hybridization chain reaction, which enables co-localization and semi-quantitative evaluation of expression *in situ*. The HCR signal appears dotted, and each dot represents at least one mRNA molecule. The number of dots can be used as a proxy for the expression level. This analysis confirmed the colorimetric ISH data shown in Figures 1A,B, and indicated that some, but not all interneurons migrating through the cortex, expressed *Pcdh19* (Figures 1F,H, Supplementary Figure 1F). *Pcdh19* was also expressed in the ventricular zone of the MGE, while it was nearly absent from the mantle zone (Figure 1G). The marginal zone stream of interneurons tends to express *Pcdh19* at a low level in most cells (Figure 1I, Supplementary Figure 1G). We complemented this analysis with a study at the protein level, performing WB on lysates from the whole ventral telencephalon, telencephalon and distinct parts of the ganglionic eminence at E13.5. A strong band around 126 kDa, which is the predicted MW of PCDH19, indicated that PCDH19 was produced in the MGE, CGE, and LGE (Figure 1J). Taken together, these results show that PCDH19 was present in the main regions that generate cortical inhibitory neurons at the assessed time points, and in variable levels in individual interneurons migrating in the cortex.

To complement our analysis of endogenous PCDH19 production, we generated two mouse lines: a C-terminus-tagged PCDH19-V5 mouse line, which would allow detection of PCDH19 with higher sensitivity, as the V5 antibody has been verified in more studies; a PCDH19 KO mouse line,

which served as a negative control for the HCR analysis (Supplementary Figures 1B,C). The PCDH19 KO mouse line was designed to have a large deletion of 1,186 bp in the first exon 1. This deletion leads to a frameshift from AA176 onwards and a truncation of the protein at AA189. We could not observe any HCR signal nor any protein production in this knockout model (Supplementary Figures 1C,D), also not on any other height, ruling out alternative start exons that might generate a residual intracellular domain. Western Blot analysis of brain lysates showed the production of PCDH19-V5 with a stronger band around 126 kDa at E13.5, E14.5, and postnatal Day (P)7 (Supplementary Figure 1E). The multiple bands at the full-length size could represent different known PCDH19 mouse isoforms (Hunt et al., 2018) or post translational modifications. In the embryonic and P7 samples, but not in the adult brain, an additional band was detected at 50 kDa, the predicted MW of the PCDH19 intracellular domain. This fragment might have been generated by enzymatic cleavage, similar to some other PCDHs, as has been shown recently (Pancho et al., 2020; Gerosa et al., 2022). Besides a weak band around 70 kDa, no bands were observed in the wild-type control, showing the specificity of the V5 antibody. Our data thus suggested that, in the developing brain, PCDH19 appeared in different forms, including a cleaved version.

Distinct subdomains target PCDH19 to different subcellular localizations

Cleavage of the ICD of transmembrane proteins is often followed by nuclear translocation, driven by a nuclear localization signal. We used distinct prediction tools to search for nuclear localization signals within the PCDH19 sequence (Figure 2A). Three NLS sequences of the longest PCDH19 isoform (Q80TF3) were predicted, yet scored differently in the prediction program NLStradamus (Supplementary Figure 2A) (Nguyen Ba et al., 2009).

To further study the subcellular localization of distinct PCDH19 subdomains, we generated C-terminally tagged overexpression constructs of subdomains of PCDH19 in bicistronic TdTomato expression plasmids (pCAGGS-PCDH19-eGFP-IRES-TdTomato): a full-length version: PCDH19FL; extracellular and transmembrane domains: PCDH19ECDTM, an intracellular domain: PCDH19ICD and intracellular domains without a predicted nuclear localization signal (NLS): PCDH19ICDΔNLS (Figure 2B). PCDH19ICDΔNLS was lacking the predicted NLS with the highest score and analysis with NLStradamus showed loss of most nuclear localization activity (Supplementary Figure 2A). The constructs were validated by expressing them in Neuro 2a cells (Supplementary Figure 2C). Western Blot analysis indicated a proper production of the GFP-tagged

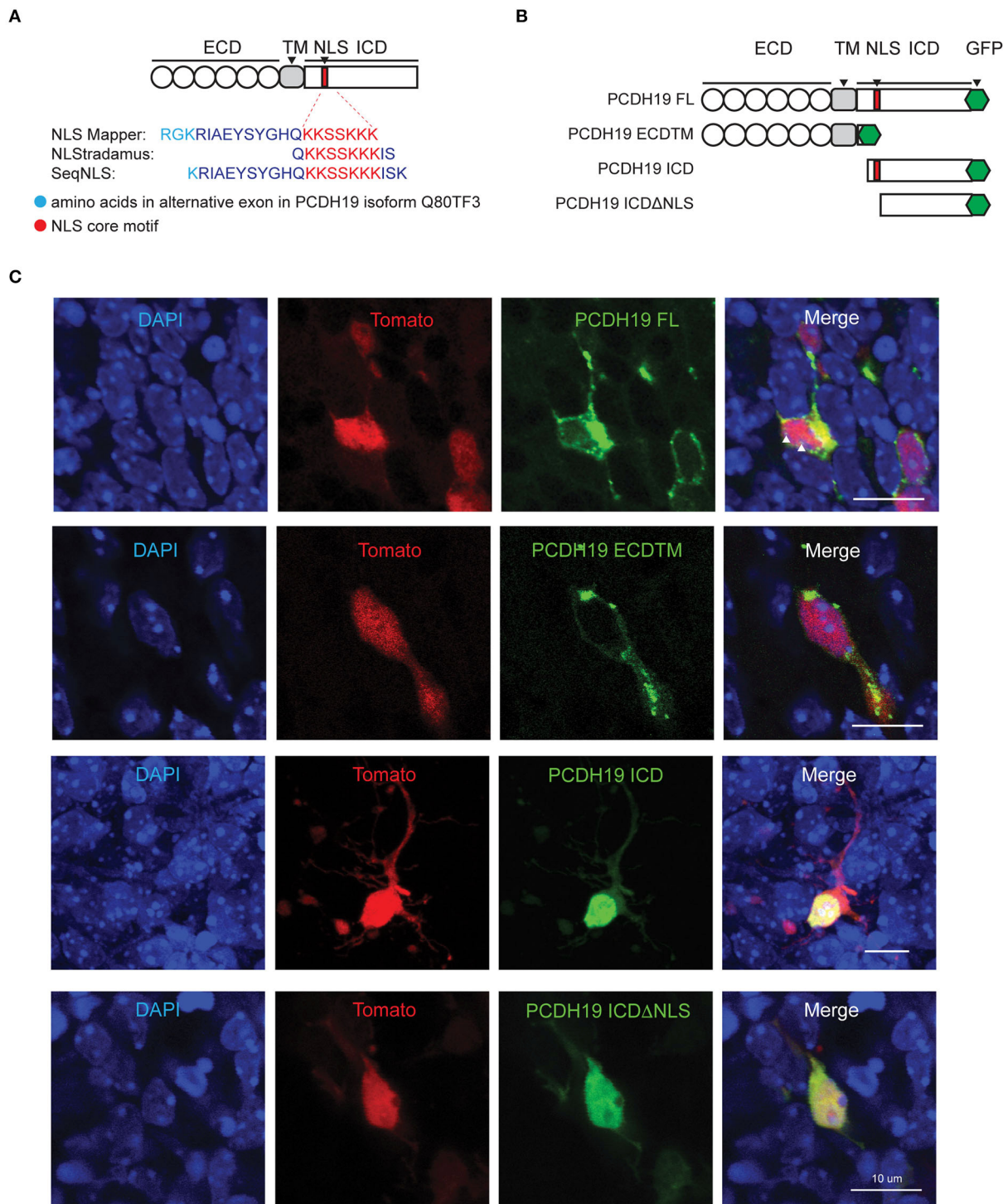


FIGURE 2
PCDH19 subdomain constructs target expression to different subcellular locations. **(A)** NLS prediction within the mouse PCDH19 amino acid sequence with three different programs. Cyan represents the alternate exon and red the consensus sequence. **(B)** Full-length PCDH19 and overexpression subdomain constructs were produced C-terminally tagged with a GFP tag and inserted into a bicistronic plasmid containing TdTomato. **(C)** PCDH19 subdomain expression in slice EP neurons 72 h after electroporation. Separate fluorescence channels, as well as the overlay, show a similar subcellular localization to the Neuro2A cells. White arrowheads in PCDH19 FL indicate a GFP signal in the nucleoli.

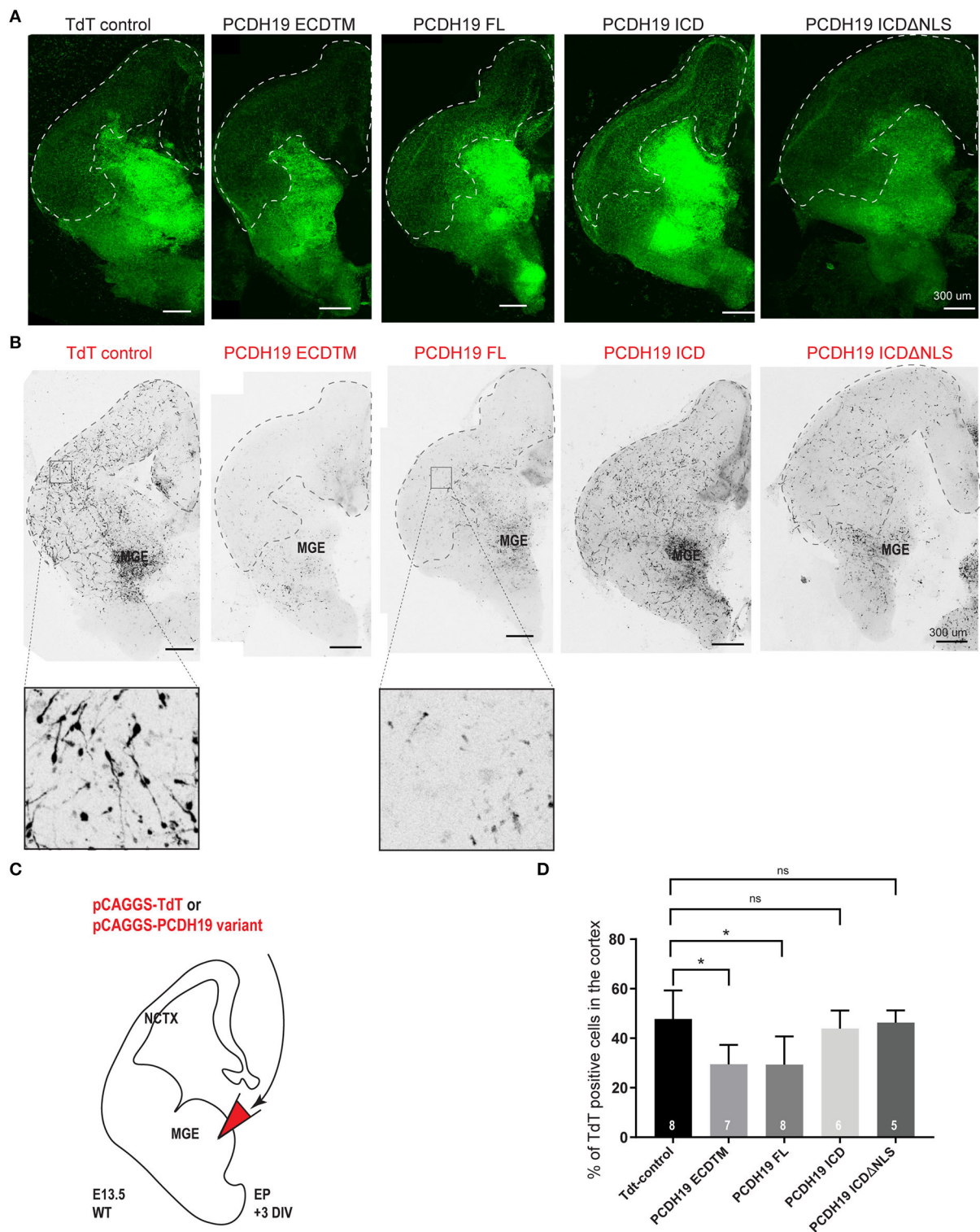


FIGURE 3
PCDH19 extracellular domain misexpression significantly decreases cortical IN migration. **(A)** 72-h post electroporation taken Z-stack example images of brain slices of TdT control and various PCDH19 overexpression constructs for the Dlx5/6-CRE-IRES-eGFP fluorescence, including the dotted line marking the cortical field. **(B)** Z-stack example images of the brain slices shown in A of TdT control and diverse PCDH19 overexpression constructs for the electroporated neurons (Tomato fluorescence); the dotted line shows the cortical field. **(C)** A schematic of the
(Continued)

FIGURE 3 (Continued)

ex vivo brain slice electroporation setup to study the overdose of PCDH19 on cortical IN migration from MGE-derived IN. Analysis of 72-h post electroporation in Dlx5/6-CRE-IRES-eGFP brain slices electroporated with bicistronic plasmids co-expressing a PCDH19 subdomain and TdTomato or only TdTomato in the empty bicistronic plasmid that was used as control. **(D)** After 72 h in culture, IN migration to the cortical field was determined by measuring the intensity of the TdT⁺ neurons within the cortical field divided by the intensity of the TdT⁺ neurons spread over the whole brain slice. Upon PCDH19 ECD TM misexpression, significant reduction in cortical IN migration to the cortical field could be measured [the Kruskal–Wallis multicomparison test with the Dunn's *post hoc* test, * $p = 0.0312$ (PCDH19 ECDTM) and * $p = 0.0122$ (PCDH19 FL)]. N number of replicates is indicated within the bars.

domain mutants (Supplementary Figure 2B). PCDH19 FL overexpression resulted in accumulation of tagged PCDH19 around the nuclear membrane. Overexpression of PCDH19ECDTM resulted in accumulation of PCDH19 at the membrane of the cell. PCDH19ICD localized to the nucleus, while PCDH19ICD Δ NLS could be found distributed over the whole cell and less prominent in the nucleus. Therefore, removing the NLS in this construct seems to inhibit nuclear translocation at least partially. Indeed, when we quantified the nuclear-cytoplasmic ratio (Supplementary Figure 2D), we found that PCDH19ICD localized preferentially in the nucleus, while this preference was lost upon removal of the NLS. To investigate whether overexpression in the developing mouse forebrain yields similar results, we performed slice electroporation and visualized subcellular distribution of GFP-tagged PCDH19. A similar subcellular distribution could be observed: PCDH19ECDTM was mainly found at the membrane. PCDH19FL was at the membrane, strongly again surrounding the nucleus but could also be identified in the nucleoli. PCDH19ICD localized to the nucleus while PCDH19ICD Δ NLS was distributed all over the cell (Figure 2C). Taken together, our data show that PCDH19ICD translocated to the nucleus, probably using the predicted NLS. In addition, these constructs now allowed us to study the role of PCDH19 at the membrane and distinguish it from a potential role in the nucleus in different mosaic overexpression paradigms.

Cortical interneuron migration is decreased by gain-of-function of *Pcdh19*

As PCDH19-CE only affects women that display cellular mosaicism of PCDH19, the imbalance in PCDH19 dosage at cell-cell contact sites might be a driver of the phenotype. We decided to model this mosaic imbalance by altering PCDH19 levels in some cells only by electroporation. In order to follow up the survival and quality of the slices, we used Dlx5/6-Cre-IRES-eGFP organotypic brain slices in which proper interneuron migration of non-targeted cells was a proxy for healthy slices. A PCDH19 subdomain-expressing plasmid or the empty TdTomato control plasmid was electroporated in the MGE. This allowed us to study the effect of overdosing distinct domains of PCDH19 on the migrational

behavior of MGE cortical IN after 3 days in organotypic culture (Figures 3A–C). Representative images of organotypic brain slices for the endogenous fluorescence Dlx5/6ireseGFP (Figure 3A) and the electroporated fluorescence TdTomato (Figure 3B) after 3DIV are shown for all conditions, and the cortical field is depicted by the dotted line (Figures 3A,B). Quantification of the percentage of TdT positive neurons within the cortical field compared to the whole brain slice showed significantly reduced cortical IN migration for PCDH19ECDTM and PCDH19FL compared to the control condition (Figure 3D, Kruskal–Wallis test with the Dunn's *post hoc* test). Stunted neuronal morphology could be observed after PCDH19FL (Figure 3B) as well as after PCDH19 ECDTM overexpression, suggesting that increasing the PCDH19 extracellular amount could affect cell morphology or survival. In contrast, increasing the dosage of the intracellular domain of PCDH19 did not impact IN migration nor morphology. As we hypothesized that an imbalance in PCDH19 dosage between migrating interneurons and their environment would influence migration, one could argue that non-targeted migrating interneurons might be affected as well when neighboring, co-migrating interneurons would express an excessive amount of PCDH19. We therefore investigated the migration of all eGFP-labeled neurons, and although we saw a reduction, this effect was not significant (Supplementary Figure 3, Kruskal–Wallis test), potentially because only a fraction of interneurons was targeted. Our data thus indicated that overdosing in especially the extracellular part of PCDH19 hampered tangential migration of interneurons to the neocortex.

Pcdh19 gain-of-function affects migration distance and affects neuronal processes

To further study the effect of excess PCDH19 on neuronal migration and morphology, we investigated PCDH19 overexpressing neurons in cultured MGE explants. Interneurons generated from these explants migrate out over the course of hours, during which they detach from the explant and make plenty short-term contacts with migrating cells in their vicinity. Besides revealing the impact of PCDH19 gain-of-function on individual cells and their migration capacity, this

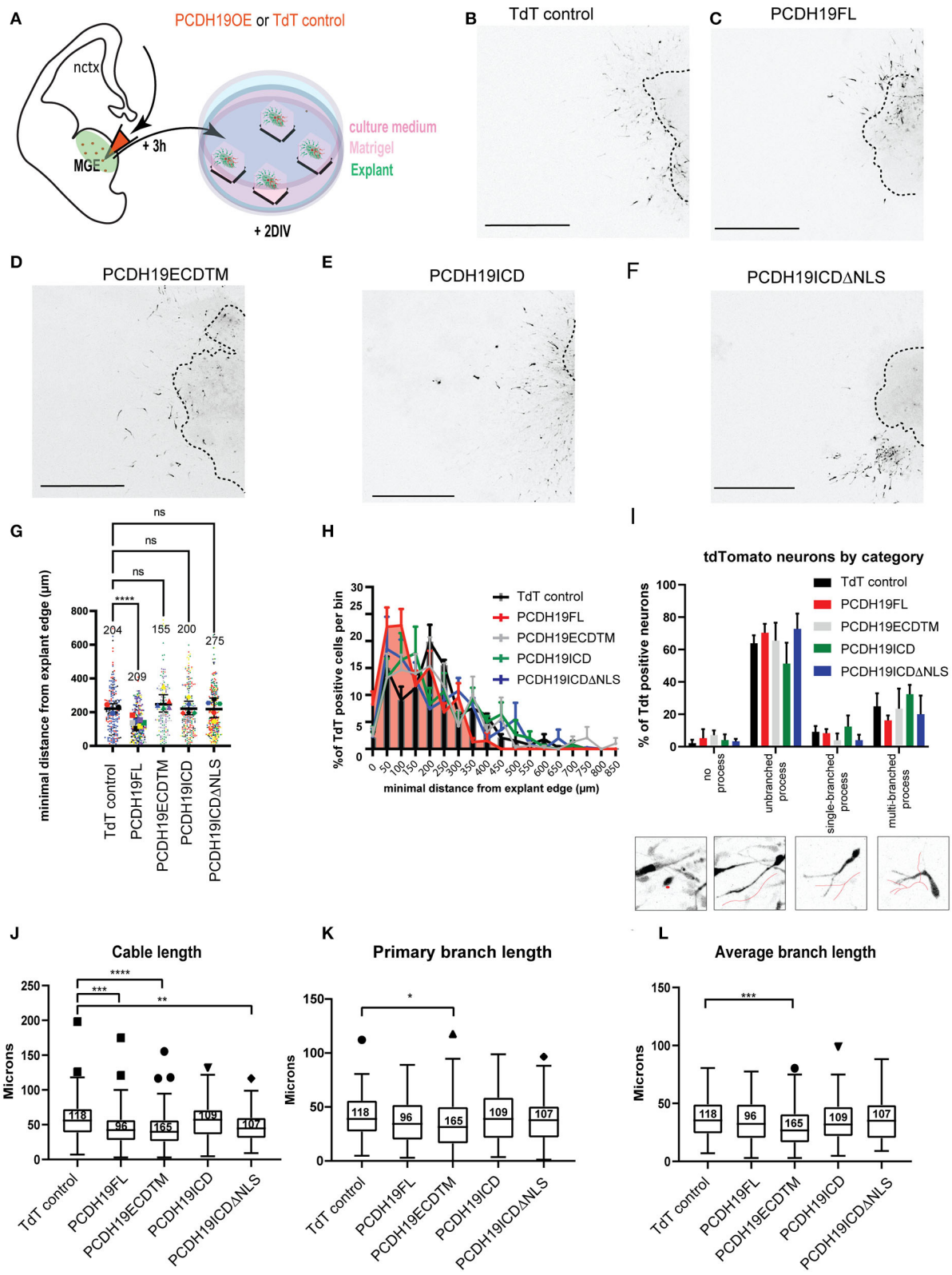


FIGURE 4
Effects of overexpressing PCDH19 subdomains on MGE cell migration and morphology. **(A)** A schematic of the *ex vivo* MGE explant electroporation setup to investigate the effect of PCDH19 overexpression in MGE-derived IN. Total minimum migration distance ‘d’ was
(Continued)

FIGURE 4 (Continued)

assessed after 48 h of electroporation in *Dlx5/6*-CRE-IRES-eGFP MGE explants with a PCDH19 construct or the empty TdTomato plasmid. (B–F) Example images of electroporated and cultured explants 48 h post electroporation of the TdTomato control plasmid (B) and PCDH19 constructs (C–F). (G) A dot plot depicting TdTomato⁺ IN-related minimal distance from the explant edge. Each dot represents one electroporated neuron in the respective condition; colors of the dots relate to different explants. Significantly shorter distance from the explant edge could be measured between PCDH19 FL and TdT control (the Kruskal–Wallis non-parametric test and the Dunn's *post hoc* test, **** $p < 0.0001$). (H) Quantification of TdTomato neurons per bin normalized against the total amount of TdT neurons per bin showed non-significant difference per bin (the mixed model ANOVA test). (I) A bar chart showing the percentages of INs that were classified into 4 different categories (insets depicting the diverse neuron morphology categories) from different electroporated explants calculated on the total amount of INs per category within each experimental group. Nonsignificant differences could be identified within the experimental groups per category (two-way repeated measures ANOVA with Holm–Sidak *post hoc* comparison). (J–L) Boxplots depicting TdTomato⁺ neuron-associated cable length (J), primary branch length (K), and average branch length (L) measurements in TdT control and PCDH19 constructs-electroporated MGE explants. Significant differences could be measured in the neuron cable length between PCDH19 FL and TdT control (**** $p < 0.0001$), PCDH19 ECDTM, and TdTcontrol (**** $p < 0.0001$) and PCDH19ICDΔNLS and TdT control (* $p = 0.0026$) (the Kruskal–Wallis non-parametric test and the Dunn's *post hoc* test). The primary branch length (the Kruskal–Wallis non parametric test and the Dunn's *post hoc* test, * $p = 0.0118$) and the average branch length (the Kruskal–Wallis non parametric test and the Dunn's *post hoc* test, *** $p = 0.0003$) were significantly shorter in PCDH19 ECDTM compared to TdT control. DIV, days in vitro; scale bar: 500 μm .

assay can also uncover disturbed cell-cell adhesion. E13.5 *Dlx5/6*-Cre-IRES-eGFP MGE explants were electroporated with the different PCDH19 subdomain expressing and control constructs, allowing the detection of electroporated (GFP + TdT +) vs. non-electroporated (GFP + TdT–) cells (Figure 4A). Next, we measured the total migration distance after 2DIV. Example images are shown for explant per experimental condition (Figures 4B–F). Statistical analysis with the Kruskal–Wallis non-parametric test and the Dunn's *post hoc* test showed a significant reduction in the spread of PCDH19FL-expressing INs compared to the TdT control condition ($p < 0.0001$) (Figure 4G). Binned distribution analysis indicated that PCDH19FL-overexpressing IN distribution is closer to the explant than the rest of the conditions; nevertheless, no particular bin-specific means were found to be significantly changed (mixed-model ANOVA) (Figure 4H).

Similarly, as in the brain slice, we asked whether we would see a non-cell autonomous effect and, therefore, also analyzed non-targeted eGFP-positive neurons (Supplementary Figure 4). Also here, statistical analysis with the Kruskal–Wallis non-parametric test and the Dunn's *post hoc* test displayed a significant reduction in the spread of eGFP + TdT – neurons in the PCDH19FL condition ($p < 0.0001$) compared to the TdT control, and, unexpectedly, a significantly larger spread of the eGFP + TdT – neurons in the PCDH19ICD condition ($p < 0.0001$) (Supplementary Figure 4F). Statistical analysis per bin was also not significant for the non-cell autonomous effect of PCDH19 overexpression (Supplementary Figure 4G).

To further address the previous observation of the stunted neuronal morphology in the brain slices, we wondered whether upon overexpression of the different subdomains neuronal morphology was affected. Each neuron was assessed depending on the morphology of the leading process into “no process”, “unbranched process”, “single-branch process”, and into “multi-branch process”, and then the percentage of total neurons per experimental condition per explant was calculated per phenotype (Figure 4I). Most neurons had an

unbranched process (50–70%), which fits to the previous observed morphology in the explant assay (Mitsogiannis et al., 2021). Overexpression of PCDH19FL compared to the control TdT-control did not result in any significant observation. Since total migration distance was reduced upon PCDH19FL overexpression, we also decided to look into the topological morphological characteristics of the neuronal processes. Assessment of the total cable length, a measure for neurite outgrowth, resulted in significant differences for PCDH19FL, PCDH19ECDTM, as well as PCDH19ICDΔNLS, compared to the control condition (Figure 4J), the Kruskal–Wallis non-parametric test, and the Dunn's *post hoc* test). Primary branch length and average branch length were only significantly affected upon overexpression of PCDH19ECDTM compared to the control condition (Figures 4K,L, the Kruskal–Wallis non parametric test, and the Dunn's *post hoc* test). Thus, the observed reduced migration distance upon PCDH19FL overexpression cannot be explained only by an affected neuronal morphology.

Overexpressing the extracellular part of PCDH19 increases apoptosis

The observed impact on cortical IN migration and total migration distance could not be explained by aberrant cell morphology of the electroporated neurons only. Therefore, we sought to investigate whether cell survival was affected. First, we tested our hypothesis in the Neuro2A neuronal cell line. After 48 h of transfection with the PCDH19 or control constructs, apoptosis was measured using flow cytometry. AnnexinV was used to detect early apoptotic cells and 7AAD to detect late apoptotic cells within transfected and untransfected cells after overexpression. Flow cytometry example plots show transfected cells (TdT +) and early apoptotic cells (Figure 5A, the upper row) and late apoptotic cells (Figure 5A, the bottom row). Quantification of targeted cells results in more early and late

apoptotic cells upon PCDH19FL overexpression compared to the control condition (Figure 5B, the left panel, Welch ANOVA, and the Dunnett's *post hoc* test) and in more late apoptotic cells upon PCDH19ECDTM and PCDH19FL compared to the control condition (Figure 5B, the right panel, Welch ANOVA, and the Dunnett's *post hoc* test). Quantification of early and late apoptotic cells in the untargeted cells resulted in non-significant differences, suggesting that the cells were not suffering because of the procedure, or that apoptosis was also induced by a non-cell-autonomous effect (Figure 5C, left and right panels). Therefore, the observed effect is specific for the PCDH19 overexpressing cell population, but only when the extracellular domain is present.

Next, we wondered whether we could address apoptosis in a more physiological model like the MGE explant. More cells can be targeted than in the slice electroporation with this approach, and, also, cellular resolution is better achieved with the assay than with the slice electroporation. We approximated the cell number of targeted cells *via* the TdT signal, again using the background of the *Dlx5/6-Cre-IRES-eGFP* mouse line. We reasoned that, if overexpression would affect cell viability and survival, we might lose more targeted cells and, hence, TdT expression, whereas overall GFP expression should stay constant. We measured the ratio between the TdT+ and GFP+ signals, whereby we normalized measurements by the explant area as shapes were diverse between measured conditions, and repeated the experiment several times to account for differences in electroporation efficiencies between experiments (Figure 5D). Our data consistently showed significantly lower ratios for PCDH19ECDTM and PCDH19FL compared to the control condition (Figure 5E, the Kruskal–Wallis non parametric test, and the Dunn's *post hoc* test), which could indicate that overexpression of these plasmids triggers neuronal loss. Taken together, our data suggest that an additional explanation for the observed impact on cortical interneuron migration could rely on increased neuronal cell death.

***Pcdh19* loss-of-function affects migration distance and polarity of MGE-derived interneurons yet does not affect neuronal processes**

Another way to model mosaic imbalance in PCDH19 dosage at cell-cell contact sites is to deplete PCDH19 levels in some cells only. We applied a CRISPR RNP electroporation approach to downregulate PCDH19. Two guides targeting Exon 1 were designed (P1, P2) (Supplementary Figure 5A) and validated *in vitro* on a PCDH19FLeGFPiresTdT construct expressed in Neuro2A cells. Both guides were able to significantly reduce the percentage of GFP-positive cells on the total number of transfected cells (Supplementary Figures 5B,C).

To address migration characteristics at the cellular level, we again used MGE tissue derived from *Dlx5/6-Cre-IRES-eGFP* mice. Embryonic brains were injected and electroporated with ribonuclear particles containing a guide targeting *Pcdh19* and Cas9 protein (referred to as PCDH19KO RNPs) or Cas9 protein alone (control), and a TdT-expressing plasmid in the MGE at E13.5. Subsequently, MGE pieces were cultured in Matrigel for 2 days (DIV) (Figure 6A). At 2 DIV, total migration distance was measured from the edge to the neuronal soma (Figure 6B). Figures 6C,D show representative examples of TdT-labeled neurons for each condition images. Migration distance was measured for more than 200 neurons in the PCDH19KO and control condition. Statistical comparison with the Mann–Whitney U test resulted in a slight significant decrease ($p < 0.05$) of total migration distance upon loss of function of *Pcdh19* (Figure 6E). Binned distribution analysis of the migration distance suggested that, in the PCDH19KO condition, more neurons are distributed closer to the explant; however, no bin-specific means were found to significantly differ (Multiple Mann–Whitney tests with FDR for multiple corrections) (Figure 6F). Also, for this analysis, we addressed the non-cell autonomous effect of the PCDH19KO condition on eGFP+TdT– neurons and detected a significant decrease ($p < 0.001$) compared to the control condition (the Mann–Whitney U test) (Supplementary Figure 6). We further investigated whether the direction of migration could be affected in the PCDH19KO-electroporated neurons. To this aim, we classified the leading neurite direction, showing away from the explant, toward the explant or when the direction could not be specified in both categories, parallel to the radial migration. The total amount of neurons within these three classifications was counted in 4 explants for each experimental condition. Statistical analysis indicated that more leading neurites were pointed toward the explant in the PCDH19KO condition (two-way repeated measures ANOVA with Holm–Sidak *post hoc* comparison, $p < 0.05$) (Figure 6G). Overall, about 70% of the counted neurons pointed their main neurite away from the explant in both conditions. During interneuron migration, extension of the leading process is followed by branching as the neuron senses the environment, and, eventually, nucleokinesis. Microtubule and actin cytoskeleton remodeling events govern these dynamic processes (Bellion et al., 2005; Métin et al., 2006; Guo and Anton, 2014). A second reason for hampered migration could be disturbed by branch elongation and secondary branch formation. Hence, we measured primary branch length (Figure 6H), average branch length (Figure 6I), and cable length (Figure 6J) for more than 200 neurons in each condition, yielding no difference between the conditions.

In addition, we also assessed cell survival in a similar manner as described above (Figure 5D). Reducing the level of PCDH19 did not affect cell survival; we observed a lower number of targeted cells only in the control condition; however, this difference remained

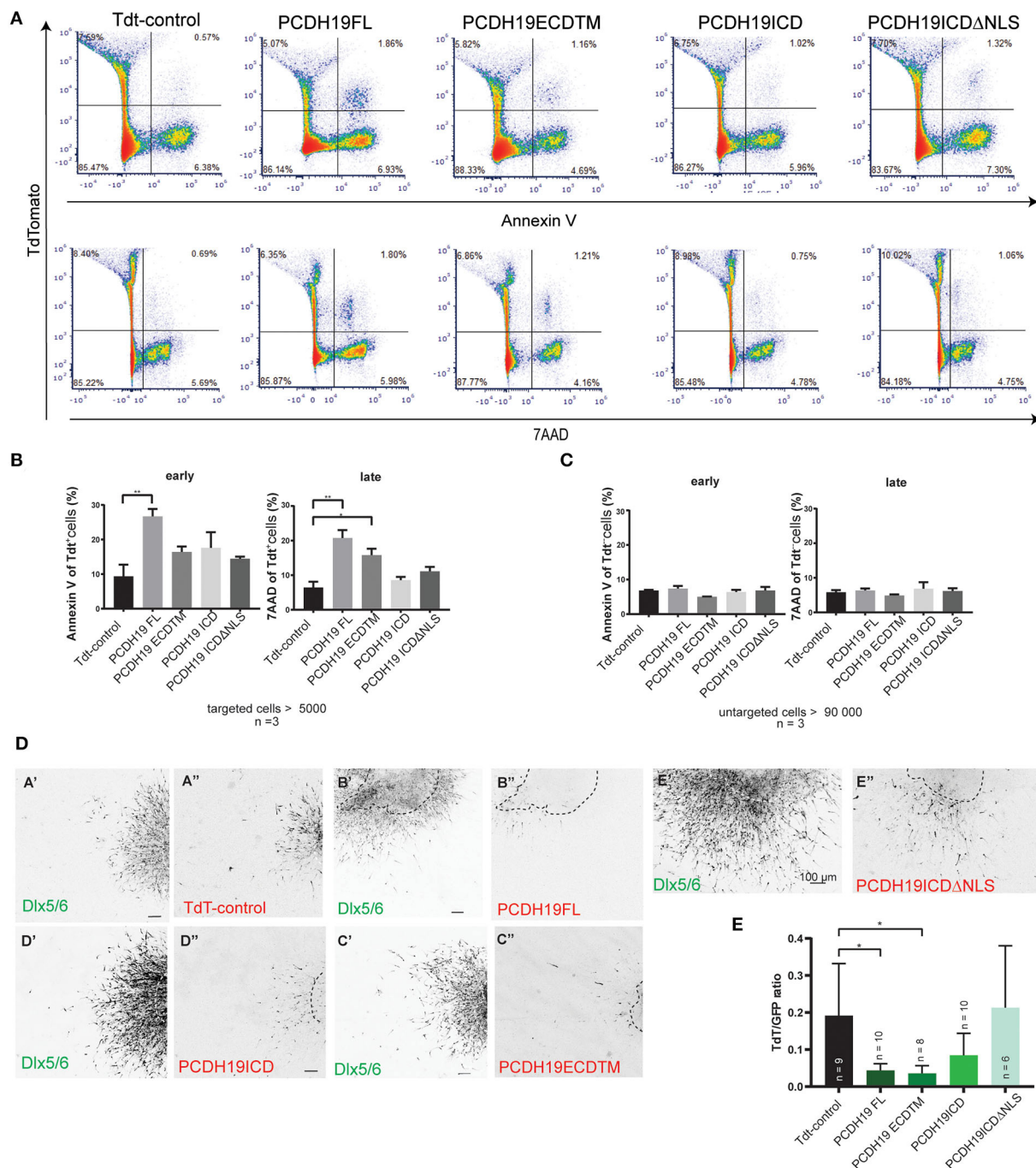


FIGURE 5

PCDH19 ECD overexpression increases apoptosis in Neuro 2A-transfected cells and might induce apoptosis in MGE electroporated INs. **(A)** Examples of flow cytometry pseudo color plots after 48 h of transfection of control and PCDH19 constructs. Early apoptotic detection is shown by AnnexinV fluorescence [(A), the upper row], and late apoptotic detection is shown by 7AAD fluorescence [(A), the lower row]. **(B)** Quantification of early apoptotic targeted cells indicated significant increase in PCDH19 FL compared to Tdt control (the right panel, Welch ANOVA, and the Dunnet's *post hoc* test, $**p = 0.0025$). Similarly, quantification of late apoptotic cells yielded significant increases in PCDH19 FL, PCDH19 ECD TM compared to Tdt control [the left panel, Welch ANOVA, and the Dunnet's *post hoc* test, $**p = 0.0038$ (PCDH19 FL) $*p = 0.0112$ (PCDH19 ECDTM)]. **(C)** Untargeted cells showed no significant differences in early nor in late apoptotic cells. **(D)** Explant examples of the control plasmid and the diverse PCDH19 constructs depicted in the GFP channel (Dlx 5/6) and in the red channel (TdT, PCDH19-eGFP-IRES-TdT constructs). Areas and shapes differ within the different experimental conditions; the original explant boundary is indicated by the dotted line. **(E)** Quantification of TdTomato intensity (a proxy for amount of targeted cells) relative to the GFP signal (Dlx5/6 INs) and normalized to the size of an explant. Significant less TdTomato-expressing cells are found upon overexpression of PCDH19 FL and PCDH19 ECDTM [the Kruskal–Wallis non parametric test and the Dunn's *post hoc* test, $*p = 0.0229$ (PCDH19 FL) and $*p = 0.0219$ (PCDH19 ECDTM)].

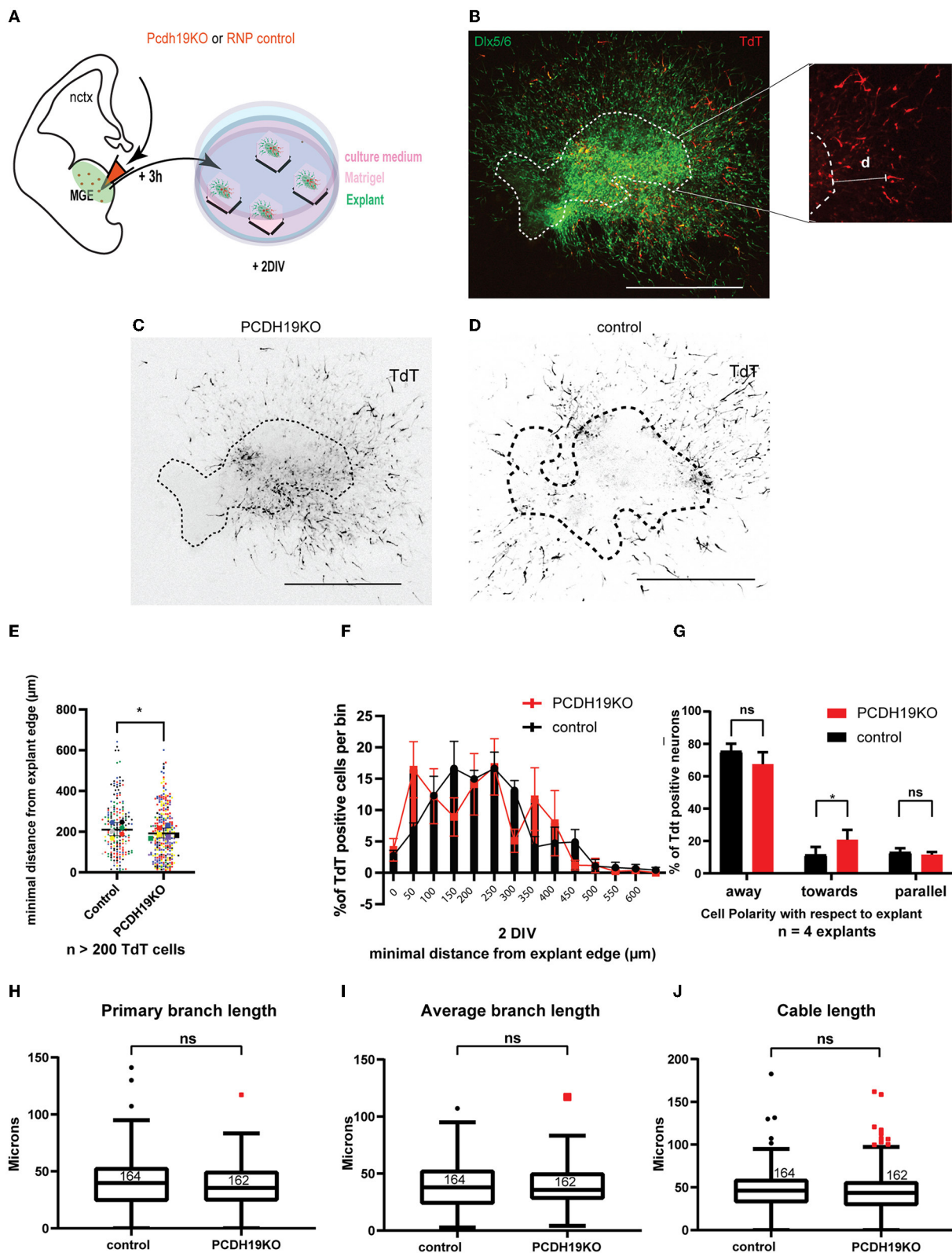


FIGURE 6
Subtle effect of PCDH19 loss on the total minimum migration distance of MGE explants-derived INs might arise from disturbed migration polarity. **(A)** A schematic of the ex vivo MGE explant electroporation setup to investigate the effect of PCDH19 KO in MGE-derived IN. **(B)** Total
(Continued)

FIGURE 6 (Continued)

minimum migration distance “d” was assessed after 48 h of electroporation in Dlx5/6-CRE-IRES-eGFP MGE explants with PCDH19KO RNPs co-electroporated with tdTomato. Minimum distance capacity was analyzed in electroporated neurons (red) measuring ‘d’ in MGE-derived IN (green). (C,D) Representative images of electroporated and cultured explants 48 h post electroporation of PCDH19KO RNP (C) and control Cas9 (D). (E) A dot plot depicting tdTomato⁺ IN-related minimal distance from the explant edge. Each dot represents one electroporated neuron in the respective condition; colors of the dots relate to different explants. Significantly shorter distance from the explant edge could be measured between PCDH19KO and control (the Mann–Whitney *U* test, **p* < 0.05). (F) Quantification of TdTomato neurons per bin normalized against the total amount of TdT neurons per bin showed non-significant difference per bin (the Mann–Whitney *U* test, followed by multiple false discovery rate corrections). (G) Polarity with respect to the explant of more than 120 TdTomato neurons was assessed in 4 explants, showing significantly more neurons migrating toward the explant in the PCDH19KO experimental condition. (Two-way repeated measures ANOVA with Holm–Sidak *post hoc* comparison, **p* < 0.05). (H–J) Boxplots depicting TdTomato⁺ neuron-associated primary branch length (H), average branch length (I), and cable length (J) measurements in control and PCDH19KO conditions. No significant differences could be detected in these morphology-associated aspects. DIV, days *in vitro*; IN, interneuron; RNP, ribonucleotide protein; ns, not significant; scale bar: 500 μm.

statistically non-significant (the Mann–Whitney *U* test) (Supplementary Figure 7).

Collectively, these results indicated that, similar to PCDH19 overexpression, loss of PCDH19 in MGE-derived IN mildly reduced the total migration distance in MGE explants, which might be explained in part by a disturbed migration polarity. However, the cell-cell variation in the effectiveness of the knockout, as well as the potential off-target effects, was difficult to measure in this explant model.

Mild reduction in cortical interneuron migration in an *in vivo* model of PCDH19-CE

To further study the impact of PCDH19 imbalance and its impact on cortical interneuron migration, we modeled the mosaic loss by crossing the PCDH19 knockout mouse line heterozygotes with Dlx5/6-Cre-IRES-eGFP mice in order to obtain control (PCDH19^{+/+}; Dlx5/6-Cre-IRES-eGFP), heterozygotes (PCDH19^{+/-}; Dlx5/6-Cre-IRES-eGFP), and PCDH19 KO (PCDH19^{-/-}; Dlx5/6-Cre-IRES-eGFP) mice in which VT-derived interneurons would be eGFP labeled. We studied the proportion of labeled cells in the cortex at E13.5 as a proxy for cell migration, similar to the analysis performed on the slices (Figure 7A). In doing so, we found that, at this early stage, we could detect a mild but significant reduction in migration in the heterozygote mice, but not in the homozygous KOs [Figure 7B, (**p* = 0.0135, the Kruskal–Wallis test, and the Dunn’s *post hoc* test)]. These data suggest that, also, *in vivo*, creating an imbalance in the dosages of PCDH19 in interneurons and neurons hampers the overall interneuron migration to the cortex.

Discussion

This paper investigated the hypothesis that the early-onset epilepsy in females bearing a loss-of-function mutation on one allele of the *PCDH19* gene might be linked to a developmental

failure of pallial interneurons to properly migrate to the pallium. Our study shows presence of *PCDH19* expression in the developing forebrain, including those regions generating pallial interneurons, and, in particular, demonstrated a temporally and spatially dynamic pattern. At the level of individual interneurons, we could detect variation in expression levels between cells, suggesting that different cell types might depend on PCDH19 to a different extent. This observation was done at the RNA level, so at this point, it is still unknown whether this translates to effectively variable amounts of PCDH19 at the membrane level. The level of PCDH19 differs between cells, regions, and time points, which suggests that expression of this gene is tightly regulated. Specific types of interneurons might thus be depending on PCDH19 at different stages of their development. This corroborates the findings that PCDH19 has been implicated in neurogenesis (Cooper et al., 2015; Fujitani et al., 2017; Homan et al., 2018; Lv et al., 2019), neural sorting (Pederick et al., 2018), and synaptogenesis and function (Bassani et al., 2018; Serratto et al., 2020; Hoshina et al., 2021; Mincheva-Tasheva et al., 2021). Our study focused on a, hitherto, less well-studied role in neural migration, taking the role of PCDH19 subdomains into account.

We could not detect an increase in neuronal migration in our loss of function studies in contrast to the previous *in vitro* observation for cortical PCDH19KO neurons (Pederick et al., 2016). This discrepancy might arise from the diversity of the assays, from the cell type investigated, as well as from the context of the experiment. Our analysis measured the total migration distance of PCDH19KO cortical interneurons that were still mixed with PCDH19 WT cortical interneurons, while Pederick et al. (2016) made their observation using full KO neurospheres. Our binning analysis together with the polarity assessment detected neurons migrating toward the explant, suggesting a disturbed migration polarity. Along the same line, ectopic positioning and orientation of PCDH19 loss of function hippocampal neurons have been detected in rats (Bassani et al., 2018). In human iPSC progenitors, PCDH19 is found in a polarized manner at the apical membrane, suggesting a role in polarity (Compagnucci et al., 2015). Whether PCDH19 loss affects neuronal polarity and if these

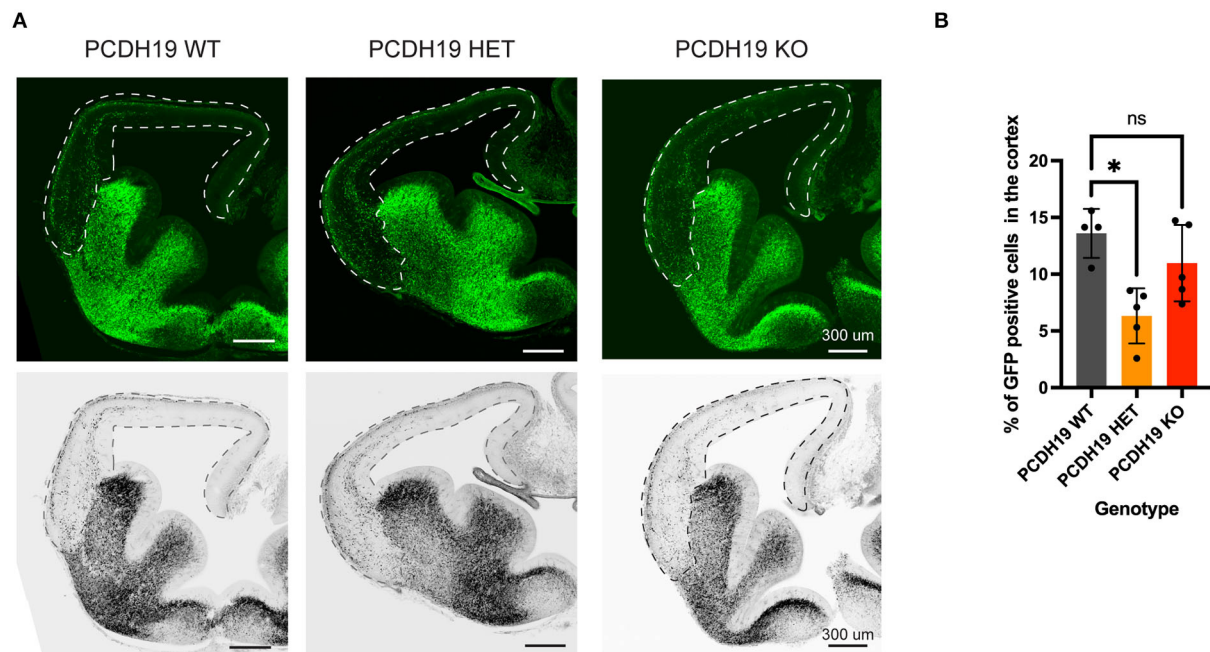


FIGURE 7
Cortical interneuron migration upon loss of PCDH19 *in vivo*. **(A)** Representative brain slices for the PCDH19 WT mouse, the PCDH19 HET mouse, and the PCDH19 KO mouse; the dotted line represents the area that was measured. **(B)** Quantification of GFP positive cells in the measured area shows average of GFP-positive cells percentage in the cortex per mouse genotype. Less migration to the cortex could be detected in the PCDH19 HET mouse compared to the control PCDH19 WT (* $p = 0.0135$), the Kruskal–Wallis test, and the Dunn's *post hoc* test.

could contribute to the phenotype of PCDH19-CE remains to be investigated.

Our data suggest that, in the developing mouse brain, PCDH19 is proteolytically processed, and the cytoplasmic fragment accumulates in the nucleus. Protein processing has been described for classical Cadherins (Marambaud et al., 2002; Maretzky et al., 2005; Reiss et al., 2005; Symowicz et al., 2007; Jang et al., 2011; Conant et al., 2017) and, for other Protocadherins, such as PCDH12 (Bouillot et al., 2011) and the clustered α - and γ -PCDHs (Junghans et al., 2005; Reiss et al., 2006; Buchanan et al., 2010). The released cytoplasmic fragment of Cadherins is bound by CREB-binding protein and diverged to the proteasome, suggesting that processing serves a role to remove the adhesive contact. The cytoplasmic fragment of PCDH γ C3 that is released travels to the nucleus and might exert a role there (Haas et al., 2005). Recently, PCDH19 has been shown to be proteolytically processed in an activity-dependent manner in rat hippocampal cells and human iPSC-derived neurons, further confirming our findings (Gerosa et al., 2022). Upon overexpression of full-length PCDH19 in Neuro2A cells, the majority of the protein appeared in the cytoplasm and on the membrane, and not in the nucleus. This might suggest that either the necessary processing machinery is not present in Neuro2A cells, and/or additional conditions need to be fulfilled to elicit cleavage. In our *ex vivo* slice electroporation neurons, we did detect a signal in the nucleoli; a similar localization was obtained

in hippocampal neurons for PCDH19FL, and the cytoplasmic fragment of PCDH19 also localized to the nucleus in this study (Pham et al., 2017). Our data indicate that proteolytic processing is also happening *in vivo*, during the embryonic period, which suggests that it might play a more general role, beyond the synaptic role suggested by activity-dependent processing in mature neuronal cultures.

We applied different overexpression and knockout paradigms to mimic the mosaic imbalance of the disease condition during embryonic forebrain development, and found that, in general, having an excessive amount of PCDH19 (or facing absence of PCDH19 on neighboring cells) leads to defects in migration. This seemed to originate from the extracellular domain, as overexpression of the intracellular domain had no such effect, and was, at least, partly caused by enhanced apoptosis or reduced cell survival. We, therefore, hypothesize that having an excessive level of unbound PCDH19 at the membrane might trigger an apoptotic response.

A similar concept has been described for dependence receptors (Fombonne et al., 2012; Genevois et al., 2013; Causeret et al., 2016). These are a group of membrane proteins that need to be bound by a ligand in order for the cell to survive, or, conversely, when unbound, will trigger an apoptotic response (Mehlen and Bredeisen, 2004). It remains to be investigated whether PCDH19 fulfills the criteria of a dependence receptor; whether it can be cleaved

by caspases and initiate apoptosis, or whether it acts indirectly by stabilizing a known dependence receptor at the membrane. Interesting is the finding that PCDH19 interacts with Protein Tyrosine Phosphatase Non-Receptor Type 13 (PTPN13), a protein that prevents apoptosis when bound to NGFR, a known dependence receptor (Emond et al., 2020). Stabilization of a dependence receptor also fits with the observation that a truncated PCDH19-ECD, which is unlikely to exert any cytoplasmic interactions, can trigger apoptosis upon overexpression as well.

Other protocadherins have been linked to apoptosis in a different manner. Deletion of the whole γ -PCDH-cluster leads to a very particular loss of interneurons, namely, cortical interneurons (Carriere et al., 2020; Mancía Leon et al., 2020). Along the same line, removing PCDH γ C4 from cortical or cerebellar interneurons results in significant losses in interneuron cell number, caused by apoptosis, suggesting that this isoform sustains interneuron survival (Garrett et al., 2019; Mancía Leon et al., 2020). Although these functions seem to be contradictory to the idea of dependence receptors, they do link PCDHs to the process of apoptosis. We also refer to our recent review, describing the importance of PCDH dosage control for neuronal survival in the brain (Pancho et al., 2020).

The fact that different PCDH19 domains induce opposite migration behaviors non-cell-autonomously is more difficult to explain. On the other hand, it indicates that cell-cell interactions occurring in these explants might be differentially affected by extracellular or intracellular PCDH19 domains. The PCDH19 intracellular domain, which is translocated to the nucleus, might exert a nuclear role and change gene expression of immediate early genes (IEGs) as shown recently in hippocampal neurons (Gerosa et al., 2022). These IEGs perhaps initiate a gene expression cascade that results in the secretion of a factor that stimulates cell migration. The reduced migration of non-targeted cells upon overexpression of PCDH19FL but not PCDH19 ECD might be caused by a potential binding partner at the cytoplasmic domain, such as Cdh2 (N-Cad), which is a known a PCDH19-binding partner (Emond et al., 2011). During neurulation, both PCDH19 and Cdh2 need to be present to obtain directional and coherent migration of cells (Biswas et al., 2010). Cdh2 has been shown to be important for interneuron migration speed, polarity, and postnatal survival (Luccardini et al., 2013, 2015; László et al., 2020). Further research is needed to validate whether PCDH19FL overexpression increases the expression of Cdh2 at the surface and thus non-cell-autonomously might influence migration. For the moment, these remain speculations that need further experimental investigation; however, the influence of PCDH19-interacting partners is not to be neglected.

Although we found a decrease in interneurons populating the PCDH19 heterozygous cortex at a very early time point,

other mouse models of the disorder could not demonstrate a significant cell loss in cortical interneurons at P20 or pyramidal neurons or a thinning of cortical layers at P10 (Galindo-Riera et al., 2021). In these models, wild-type and PCDH19 knockout cells reorganize themselves into columns of cells with similar genotypes, resulting in a decrease of imbalanced cell-cell contacts (Pederick et al., 2018). Combined with the cell-specific pattern of expression, a potentially hazardous imbalance situation might be avoided. On the other hand, the PCDH19 mosaicism might only delay the migration of interneurons, and the situation might be normalized at young postnatal stages.

Future studies on the endogenous interaction partners of PCDH19 in the developing brain will hopefully aid in revealing the pathways involved in the dynamic action of this protein in neurogenesis, neural survival, differentiation, migration, and synaptic function and plasticity.

Data availability statement

The original contributions presented in the study are included in the article/Supplementary material, further inquiries can be directed to the corresponding author

Ethics statement

The animal study was reviewed and approved by ECD Ethical Committee on Animal Experimentation, KU Leuven, Leuven, Belgium. The generation of the PCDH19-V5 tagged mouse and the PCDH19 KO mouse were done in accordance with European, national and institutional guidelines and approved by the State Office of North Rhine-Westphalia, Department of Nature, Environment and Consumer Protection (LANUV NRW, Germany; animal study protocol AZ 84-02.04.2014.A372).

Author contributions

ES and AP conceived the research project and designed the experiments. AP performed all the experiments unless other mentioned and analyzed experimental results and data. MM helped in all MGE explant and brain slice electroporation experiments. TA designed the sgRNA P1 and P2 and helped in experiments. MD performed the analysis of the nucleo-cytoplasmic localization under supervision of PD. LE generated the sgRNA and ssODN and performed the experiments to generate the PCDH19-V5-tagged mouse and PCDH19 KO mouse under supervision of BS. PH did the NLS prediction. LE and KS supervised by BS and FV respectively, produced plasmid constructs for the subcloning of PCDH19-eGFP constructs. RV, LN, and LG provided technical support

in genotyping and WB. AP and ES wrote the manuscript. All the authors contributed to the article and approved the submitted version.

Funding

This work was supported by funding of the FWO (G0B5916N) and the KU Leuven 1051 (C14/16/049). BS was supported by the German Research Foundation (SCHE1562/8-1 and SFB1403, project No. 414786233). MD was supported by funding of the FWO (1S39418N).

Acknowledgments

We would like to thank Evelien Herinckx for her essential work and assistance in the husbandry and care of all laboratory animals used for this study. Furthermore, they would like to thank Isabel Martinez Garay for thoroughly proofreading the manuscript and all the members of the ES and Arckens labs for critical discussions.

References

- Abekhouk, S., and Bardoni, B. (2014). CYFIP family proteins between autism and intellectual disability: links with Fragile X syndrome. *Front. Cell Neurosci.* 8, 81. doi: 10.3389/fncel.2014.00081
- Arshadi, C., Günther, U., Eddison, M., Harrington, K. I. S., and Ferreira, T. A. (2021). SNT: a unifying toolbox for quantification of neuronal anatomy. *Nat Methods* 18, 374–377. doi: 10.1038/s41592-021-01105-7
- Bassani, S., Cwetsch, A. W., Gerosa, L., Serratto, G. M., Folci, A., Hall, I. F., et al. (2018). The female epilepsy protein PCDH19 is a new GABAAR-binding partner that regulates GABAergic transmission as well as migration and morphological maturation of hippocampal neurons. *Hum. Molec. Genet.* 27, 1027–1038. doi: 10.1093/hmg/ddy019
- Bellion, A., Baudoin, J.-P., Alvarez, C., Bornens, M., and Métin, C. (2005). Nucleokinesis in Tangentially Migrating Neurons Comprises Two Alternating Phases: Forward Migration of the Golgi/Centrosome Associated with Centrosome Splitting and Myosin Contraction at the Rear. *J. Neurosci.* 25, 5691–5699. doi: 10.1523/JNEUROSCI.1030-05.2005
- Biswas, S., Emond, M. R., and Jontes, J. D. (2010). Protocadherin-19 and N-cadherin interact to control cell movements during anterior neurulation. *J. Cell Biol.* 191, 1029–1041. doi: 10.1083/jcb.201007008
- Bouillot, S., Tillet, E., Carmona, G., Prandini, M.-H., Gauchez, A.-S., Hoffmann, P., et al. (2011). Protocadherin-12 cleavage is a regulated process mediated by ADAM10 protein: evidence of shedding up-regulation in pre-eclampsia. *J. Biol. Chem.* 286, 15195–15204. doi: 10.1074/jbc.M111.230045
- Buchanan, S. M., Schalm, S. S., and Maniatis, T. (2010). "Proteolytic processing of protocadherin proteins requires endocytosis," in *Proceedings of the National Academy of Sciences of the United States of America*. vol. 107, p. 17774–17779. doi: 10.1073/pnas.1013105107
- Cappelletti, S., Specchio, N., Moavero, R., Terracciano, A., Trivisano, M., Pontrelli, G., et al. (2015). Cognitive development in females with PCDH19 gene-related epilepsy. *Epilepsy Behav. EandB* 42, 36–40. doi: 10.1016/j.yebeh.2014.10.019
- Carriere, C. H., Wang, W. X., Sing, A. D., Fekete, A., Jones, B. E., Yee, Y., et al. (2020). The gamma-Protocadherins regulate the survival of GABAergic interneurons during developmental cell death. *J. Neurosci.* 40, 8652–8668. doi: 10.1523/JNEUROSCI.1636-20.2020
- Causseret, F., Sumia, I., and Pierani, A. (2016). Kremen1 and Dickkopf1 control cell survival in a Wnt-independent manner. *Cell Death Differ.* 23, 323–332. doi: 10.1038/cdd.2015.100
- Chen, B., Brinkmann, K., Chen, Z., Pak, C. W., Liao, Y., Shi, S., et al. (2014). The WAVE regulatory complex links diverse receptors to the actin cytoskeleton. *Cell* 156, 195–207. doi: 10.1016/j.cell.2013.11.048
- Choi, H. M. T., Schwarzkopf, M., Fornace, M. E., Acharya, A., Artavanis, G., Stegmaier, J., et al. (2018). Third-generation in situ hybridization chain reaction: multiplexed, quantitative, sensitive, versatile, robust. *Development* 145, dev165753. doi: 10.1242/dev.165753
- Compagnucci, C., Petrini, S., Higurashi, N., Trivisano, M., Specchio, N., Hirose, S., et al. (2015). Characterizing PCDH19 in human induced pluripotent stem cells (iPSCs) and iPSC-derived developing neurons: emerging role of a protein involved in controlling polarity during neurogenesis. *Oncotarget* 6, 26804–26813. doi: 10.18632/oncotarget.5757
- Conant, K., Daniele, S., Bozzelli, P. L., Abdi, T., Edwards, A., Szklarczyk, A., et al. (2017). Matrix metalloproteinase activity stimulates N-cadherin shedding and the soluble N-cadherin ectodomain promotes classical microglial activation. *J. Neuroinflamm.* 14, 56. doi: 10.1186/s12974-017-0827-4
- Cooper, S. R., Emond, M. R., Duy, P. Q., Liebau, B. G., Wolman, M. A., and Jontes, J. D. (2015). Protocadherins control the modular assembly of neuronal columns in the zebrafish optic tectum. *J. Cell Biol.* 211, 807–814. doi: 10.1083/jcb.201507108
- Depienne, C., Bouteiller, D., Keren, B., Cheuret, E., Poirier, K., Trouillard, O., et al. (2009). Sporadic infantile epileptic encephalopathy caused by mutations in PCDH19 resembles Dravet syndrome but mainly affects females. *PLoS Genet.* 5, e1000381. doi: 10.1371/annotation/314060d5-06da-46e0-b9e4-57194e8ece3a
- Depienne, C., Gourfinkel-An, I., Baulac, S., and LeGuern, E. (2012). "Genes in infantile epileptic encephalopathies," in *Jasper's Basic Mechanisms of the Epilepsies*, eds. J. L. Noebels, M. Avoli, M. A. Rogawski, R. W. Olsen, and A. V. Delgado-Escueta (Bethesda (MD): National Center for Biotechnology Information (US)). Available online at: <http://www.ncbi.nlm.nih.gov/books/NBK98182/> (accessed May 26, 2019).
- Depienne, C., Trouillard, O., Bouteiller, D., Gourfinkel-An, I., Poirier, K., Rivier, F., et al. (2011). Mutations and deletions in PCDH19 account for

Conflict of interest

The authors declare that the research was conducted in the absence of any commercial or financial relationships that could be construed as a potential conflict of interest.

Publisher's note

All claims expressed in this article are solely those of the authors and do not necessarily represent those of their affiliated organizations, or those of the publisher, the editors and the reviewers. Any product that may be evaluated in this article, or claim that may be made by its manufacturer, is not guaranteed or endorsed by the publisher.

Supplementary material

The Supplementary Material for this article can be found online at: <https://www.frontiersin.org/articles/10.3389/fnins.2022.887478/full#supplementary-material>

various familial or isolated epilepsies in females. *Hum. Mutat.* 32, E1959–1975. doi: 10.1002/humu.21373

Dibbens, L. M., Tarpey, P. S., Hynes, K., Bayly, M. A., Scheffer, I. E., Smith, R., et al. (2008). X-linked protocadherin 19 mutations cause female-limited epilepsy and cognitive impairment. *Nat. Genet.* 40, 776–781. doi: 10.1038/ng.149

Duszyk, K., Terczynska, I., and Hoffman-Zacharska, D. (2015). Epilepsy and mental retardation restricted to females: X-linked epileptic infantile encephalopathy of unusual inheritance. *J. Appl. Genet.* 56, 49–56. doi: 10.1007/s13353-014-0243-8

Elagoz, A. M., Styfals, R., Maccuro, S., Masin, L., Moons, L., and Seuntjens, E. (2022). Optimization of Whole Mount RNA Multiplexed in situ Hybridization Chain Reaction With Immunohistochemistry, Clearing and Imaging to Visualize Octopus Embryonic Neurogenesis. *Front. Physiol.* 13, 882413. doi: 10.3389/fphys.2022.882413

Emond, M. R., Biswas, S., Blevins, C. J., and Jontes, J. D. (2011). A complex of Protocadherin-19 and N-cadherin mediates a novel mechanism of cell adhesion. *J. Cell Biol.* 195, 1115–1121. doi: 10.1083/jcb.201108115

Emond, M. R., Biswas, S., and Jontes, J. D. (2009). Protocadherin-19 is essential for early steps in brain morphogenesis. *Dev. Biol.* 334, 72–83. doi: 10.1016/j.ydbio.2009.07.008

Emond, M. R., Biswas, S., Morrow, M. L., and Jontes, J. D. (2020). Proximity-dependent proteomics reveals extensive interactions of Protocadherin-19 with regulators of Rho GTPases and the microtubule cytoskeleton. *Neuroscience.* 452, 26–36. doi: 10.1016/2020.09.11.293589

Fombonne, J., Bissey, P.-A., Guix, C., Sadoul, R., Thibert, C., and Mehlen, P. (2012). Patched dependence receptor triggers apoptosis through ubiquitination of caspase-9. *Proc. Natl. Acad. Sci. U S A.* 109, 10510–10515. doi: 10.1073/pnas.120094109

Fujitani, M., Zhang, S., Fujiki, R., Fujihara, Y., and Yamashita, T. (2017). A chromosome 16p13.11 microduplication causes hyperactivity through dysregulation of miR-484/protocadherin-19 signaling. *Molec. Psychiat.* 22, 364–374. doi: 10.1038/mp.2016.106

Galindo-Riera, N., Newbold, S. A., Sledziowska, M., Llinares-Benadero, C., Griffiths, J., Mire, E., et al. (2021). Cellular and behavioral characterization of Pcdh19 mutant mice: subtle molecular changes, increased exploratory behavior and an impact of social environment. *eNeuro* 8, ENEURO.0510-20.2021. doi: 10.1523/ENEURO.0510-20.2021

Garrett, A. M., Bosch, P. J., Steffen, D. M., Fuller, L. C., Marcucci, C. G., Koch, A. A., et al. (2019). CRISPR/Cas9 interrogation of the mouse Pcdhg gene cluster reveals a crucial isoform-specific role for Pcdhg4. *PLoS Genet.* 15, e1008554. doi: 10.1371/journal.pgen.1008554

Gecz, J., and Thomas, P. Q. (2020). Disentangling the paradox of the PCDH19 clustering epilepsy, a disorder of cellular mosaics. *Curr. Opin. Genet. Develop.* 65, 169–175. doi: 10.1016/j.gde.2020.06.012

Genevois, A.-L., Ichim, G., Coissieux, M.-M., Lambert, M.-P., Lavial, F., Goldschneider, D., et al. (2013). Dependence receptor TrkC is a putative colon cancer tumor suppressor. *Proc. Natl. Acad. Sci. U S A.* 110, 3017–3022. doi: 10.1073/pnas.1212331110

Gerosa, L., Mazzoleni, S., Rusconi, F., Longaretti, A., Lewerissa, E., Pelucchi, S., et al. (2022). The epilepsy-associated protein PCDH19 undergoes NMDA receptor-dependent proteolytic cleavage and regulates the expression of immediate-early genes. *Cell Rep.* 39, 110857. doi: 10.1016/j.celrep.2022.110857

Guo, J., and Anton, E. S. (2014). Decision making during interneuron migration in the developing cerebral cortex. *Trends Cell Biol.* 24, 342–351. doi: 10.1016/j.tcb.2013.12.001

Haas, I. G., Frank, M., Véron, N., and Kemler, R. (2005). Presenilin-dependent Processing and Nuclear Function of γ -Protocadherins. *J. Biol. Chem.* 280, 9313–9319. doi: 10.1074/jbc.M412909200

Hayashi, S., Inoue, Y., Kiyonari, H., Abe, T., Misaki, K., Moriguchi, H., et al. (2014). Protocadherin-17 mediates collective axon extension by recruiting actin regulator complexes to interaxonal contacts. *Developmental Cell.* 30, 673–687. doi: 10.1016/j.devcel.2014.07.015

Homan, C. C., Pederson, S., To, T.-H., Tan, C., Piltz, S., Corbett, M. A., et al. (2018). PCDH19 regulation of neural progenitor cell differentiation suggests asynchrony of neurogenesis as a mechanism contributing to PCDH19 Girls Clustering Epilepsy. *Neurobiol. Dis.* 116, 106–119. doi: 10.1016/j.nbd.2018.05.004

Hoshina, N., Johnson-Venkatesh, E. M., Hoshina, M., and Umemori, H. (2021). Female-specific synaptic dysfunction and cognitive impairment in a mouse model of PCDH19 disorder. *Science* 372, eaaz3893. doi: 10.1126/science.aaz3893

Hulpiau, P., and van Roy, F. (2009). Molecular evolution of the cadherin superfamily. *Int. J. Biochem. Cell Biol.* 41, 349–369. doi: 10.1016/j.biocel.2008.09.027

Hunt, S. E., McLaren, W., Gil, L., Thormann, A., Schuilenburg, H., Sheppard, D., et al. (2018). Ensembl variation resources. *Database* 2018. doi: 10.1093/database/bay119

Jamal, S. M., Basran, R. K., Newton, S., Wang, Z., and Milunsky, J. M. (2010). Novel de novo PCDH19 mutations in three unrelated females with epilepsy female restricted mental retardation syndrome. *Am. J. Med. Genet. Part A* 152A, 2475–2481. doi: 10.1002/ajmg.a.33611

Jang, C., Choi, J.-K., Na, Y.-J., Jang, B., Wasco, W., Buxbaum, J. D., et al. (2011). Calsenilin regulates presenilin 1/ γ -secretase-mediated N-cadherin ϵ -cleavage and β -catenin signaling. *FASEB J.* 25, 4174–4183. doi: 10.1096/fj.11-185926

Juberg, R. C., and Hellman, C. D. (1971). A new familial form of convulsive disorder and mental retardation limited to females. *J. Pediatr.* 79, 726–732. doi: 10.1016/S0022-3476(71)80382-7

Junghans, D., Haas, I. G., and Kemler, R. (2005). Mammalian cadherins and protocadherins: about cell death, synapses and processing. *Curr. Opin. Cell Biol.* 17, 446–452. doi: 10.1016/j.ccb.2005.08.008

Kim, S.-Y., Chung, H. S., Sun, W., and Kim, H. (2007). Spatiotemporal expression pattern of non-clustered protocadherin family members in the developing rat brain. *Neuroscience* 147, 996–1021. doi: 10.1016/j.neuroscience.2007.03.052

Kim, S.-Y., Yasuda, S., Tanaka, H., Yamagata, K., and Kim, H. (2011). Non-clustered protocadherin. *Cell Adhesion Migr.* 5, 97–105. doi: 10.4161/cam.5.2.14374

Kolc, K. L., Sadleir, L. G., Scheffer, I. E., Ivancevic, A., Roberts, R., Pham, D. H., et al. (2019). A systematic review and meta-analysis of 271 PCDH19-variant individuals identifies psychiatric comorbidities, and association of seizure onset and disease severity. *Molec. Psychiat.* 24, 241–251. doi: 10.1038/s41380-018-0066-9

László, Z. I., Bercsényi, K., Mayer, M., Lefkovich, K., Szabó, G., Katona, I., et al. (2019). N-cadherin (Cdh2) maintains migration and postmitotic survival of cortical interneuron precursors in a cell-type-specific manner. *Cerebral Cortex* 30, 1318–1329. doi: 10.1093/cercor/bhz168

Longair, M. H., Baker, D. A., and Armstrong, J. D. (2011). Simple Neurite Tracer: open source software for reconstruction, visualization and analysis of neuronal processes. *Bioinformatics* 27, 2453–2454. doi: 10.1093/bioinformatics/btr390

Luccardini, C., Hennekinne, L., Viou, L., Yanagida, M., Murakami, F., Kessaris, N., et al. (2013). N-cadherin sustains motility and polarity of future cortical interneurons during tangential migration. *J. Neurosci.* 33, 18149–18160. doi: 10.1523/JNEUROSCI.0593-13.2013

Luccardini, C., Leclech, C., Viou, L., Rio, J.-P., and Métin, C. (2015). Cortical interneurons migrating on a pure substrate of N-cadherin exhibit fast synchronous centrosomal and nuclear movements and reduced ciliogenesis. *Front. Cell. Neurosci.* 9, 286. doi: 10.3389/fncel.2015.00286

Lv, X., Ren, S.-Q., Zhang, X.-J., Shen, Z., Ghosh, T., Xianyu, A., et al. (2019). TBR2 coordinates neurogenesis expansion and precise microcircuit organization via Protocadherin 19 in the mammalian cortex. *Nat. Commun.* 10, 1–15. doi: 10.1038/s41467-019-11854-x

Mancia Leon, W. R., Spatazza, J., Rakela, B., Chatterjee, A., Pande, V., Maniatis, T., et al. (2020). Clustered gamma-protocadherins regulate cortical interneuron programmed cell death. *Elife* 9, e55374. doi: 10.7554/eLife.55374

Marambaud, P., Shioi, J., Serban, G., Georgakopoulos, A., Sarner, S., Nagy, V., et al. (2002). A presenilin-1/gamma-secretase cleavage releases the E-cadherin intracellular domain and regulates disassembly of adherens junctions. *EMBO J.* 21, 1948–1956. doi: 10.1093/emboj/21.8.1948

Maretzky, T., Reiss, K., Ludwig, A., Buchholz, J., Scholz, F., Proksch, E., et al. (2005). ADAM10 mediates E-cadherin shedding and regulates epithelial cell-cell adhesion, migration, and β -catenin translocation. *Proc. Nat. Acad. Sci.* 102, 9182–9187. doi: 10.1073/pnas.0500918102

Marín, O. (2013). Cellular and molecular mechanisms controlling the migration of neocortical interneurons. *Eur. J. Neurosci.* 38, 2019–2029. doi: 10.1111/ejn.12225

Marín, O., Valiente, M., Ge, X., and Tsai, L.-H. (2010). Guiding neuronal cell migrations. *Cold Spring Harbor Perspec. Biol.* 2, a001834. doi: 10.1101/cshperspect.a001834

McQuinn, C., Goodman, A., Chernyshev, V., Kamentsky, L., Cimini, B. A., Karhohs, K. W., et al. (2018). CellProfiler 3.0: Next-generation image processing for biology. *PLoS Biol.* 16, e2005970. doi: 10.1371/journal.pbio.2005970

Mehlen, P., and Bredesen, D. E. (2004). The dependence receptor hypothesis. *Apoptosis* 9, 37–49. doi: 10.1023/B:APPT.0000012120.66221.b2

Métin, C., Baudoin, J.-P., Rakić, S., and Parnavelas, J. G. (2006). Cell and molecular mechanisms involved in the migration of cortical interneurons. *Eur. J. Neurosci.* 23, 894–900. doi: 10.1111/j.1460-9568.2006.04630.x

Mincheva-Tasheva, S., Nieto Guil, A. F., Homan, C. C., Gecz, J., and Thomas, P. Q. (2021). Disrupted Excitatory Synaptic Contacts and Altered Neuronal Network

Activity Underpins the Neurological Phenotype in PCDH19-Clustering Epilepsy (PCDH19-CE). *Mol. Neurobiol.* 58, 2005–2018. doi: 10.1007/s12035-020-02242-4

Mitsogiannis, M. D., Pancho, A., Aerts, T., Sachse, S. M., Vanlaer, R., Noterdaeme, L., et al. (2021). Subtle Roles of Down Syndrome Cell Adhesion Molecules in Embryonic Forebrain Development and Neuronal Migration. *Front. Cell Develop. Biol.* 8, 624181. doi: 10.3389/fcell.2020.624181

Nguyen Ba, A. N., Pogoutse, A., Provart, N., and Moses, A. M. (2009). NLStradamus: a simple Hidden Markov Model for nuclear localization signal prediction. *BMC Bioinform.* 10, 202. doi: 10.1186/1471-2105-10-202

Pancho, A., Aerts, T., Mitsogiannis, M. D., and Seuntjens, E. (2020). Protocadherins at the crossroad of signaling pathways. *Front. Mol. Neurosci.* 13, 117. doi: 10.3389/fnmol.2020.00117

Pederick, D. T., Homan, C. C., Jaehne, E. J., Piltz, S. G., Haines, B. P., Baune, B. T., et al. (2016). Pcdh19 loss-of-function increases neuronal migration in vitro but is dispensable for brain development in mice. *Sci. Rep.* 6, 26765. doi: 10.1038/srep26765

Pederick, D. T., Richards, K. L., Piltz, S. G., Kumar, R., Mincheva-Tasheva, S., Mandelstam, S. A., et al. (2018). Abnormal cell sorting underlies the unique x-linked inheritance of PCDH19 Epilepsy. *Neuron* 97, 59–66.e5. doi: 10.1016/j.neuron.2017.12.005

Pham, D. H., Tan, C. C., Homan, C. C., Kolc, K. L., Corbett, M. A., McAninch, D., et al. (2017). Protocadherin 19 (PCDH19) interacts with paraspeckle protein NONO to co-regulate gene expression with estrogen receptor alpha (ERα). *Hum. Molec. Genet.* 26, 2042–2052. doi: 10.1093/hmg/ddx094

Reiss, K., Maretzky, T., Haas, I. G., Schulte, M., Ludwig, A., Frank, M., et al. (2006). Regulated ADAM10-dependent ectodomain shedding of gamma-protocadherin C3 modulates cell-cell adhesion. *J. Biol. Chem.* 281, 21735–21744. doi: 10.1074/jbc.M602663200

Reiss, K., Maretzky, T., Ludwig, A., Tousseyn, T., de Strooper, B., Hartmann, D., et al. (2005). ADAM10 cleavage of N-cadherin and regulation of cell-cell adhesion and beta-catenin nuclear signalling. *EMBO J.* 24, 742–752. doi: 10.1038/sj.emboj.7600548

Serratto, G. M., Pizzi, E., Murru, L., Mazzoleni, S., Pelucchi, S., Marcello, E., et al. (2020). The epilepsy-related protein PCDH19 regulates tonic inhibition, GABAAR kinetics, and the intrinsic excitability of hippocampal neurons. *Mol. Neurobiol.* 57, 5336–5351. doi: 10.1007/s12035-020-02099-7

Stenman, J., Toresson, H., and Campbell, K. (2003). Identification of two distinct progenitor populations in the lateral ganglionic eminence:

implications for striatal and olfactory bulb neurogenesis. *J. Neurosci.* 23, 167–174. doi: 10.1523/JNEUROSCI.23-01-00167.2003

Stirling, D. R., Swain-Bowden, M. J., Lucas, A. M., Carpenter, A. E., Cimini, B. A., and Goodman, A. (2021). CellProfiler 4: improvements in speed, utility and usability. *BMC Bioinform.* 22, 433. doi: 10.1186/s12859-021-04344-9

Symowicz, J., Adley, B. P., Gleason, K. J., Johnson, J. J., Ghosh, S., Fishman, D. A., et al. (2007). Engagement of collagen-binding integrins promotes matrix metalloproteinase-9-dependent E-cadherin ectodomain shedding in ovarian carcinoma cells. *Cancer Res.* 67, 2030–2039. doi: 10.1158/0008-5472.CAN-06-2808

Tai, K., Kubota, M., Shiono, K., Tokutsu, H., and Suzuki, S. T. (2010). Adhesion properties and retinofugal expression of chicken protocadherin-19. *Brain Res.* 1344, 13–24. doi: 10.1016/j.brainres.2010.04.065

Takenawa, T., and Miki, H. (2001). WASP and WAVE family proteins: key molecules for rapid rearrangement of cortical actin filaments and cell movement. *J. Cell Sci.* 114, 1801–1809. doi: 10.1242/jcs.114.10.1801

Terracciano, A., Trivisano, M., Cusmai, R., De Palma, L., Fusco, L., Compagnucci, C., et al. (2016). PCDH19-related epilepsy in two mosaic male patients. *Epilepsia* 57, e51–55. doi: 10.1111/epi.13295

Thiffault, I., Farrow, E., Smith, L., Lowry, J., Zellmer, L., Black, B., et al. (2016). PCDH19-related epileptic encephalopathy in a male mosaic for a truncating variant. *Am. J. Med. Genet. Part A* 170, 1585–1589. doi: 10.1002/ajmg.a.37617

Tröder, S. E., Ebert, L. K., Butt, L., Assenmacher, S., Schermer, B., and Zevnik, B. (2018). An optimized electroporation approach for efficient CRISPR/Cas9 genome editing in murine zygotes. *PLoS ONE* 13, e0196891. doi: 10.1371/journal.pone.0196891

van den Berghe, V., Stappers, E., and Seuntjens, E. (2014). How cell-autonomous is neuronal migration in the forebrain? Molecular cross-talk at the cell membrane. *Neuroscientist* 20, 571–575. doi: 10.1177/1073858414539396

van den Berghe, V., Stappers, E., Vandesande, B., Dimidschstein, J., Kroes, R., Francis, A., et al. (2013). Directed migration of cortical interneurons depends on the cell-autonomous action of Sip1. *Neuron* 77, 70–82. doi: 10.1016/j.neuron.2012.11.009

Vanhalst, K., Kools, P., Staes, K., van Roy, F., and Redies, C. (2005). δ-Protocadherins: a gene family expressed differentially in the mouse brain. *Cell. Molec. Life Sci. CMLS* 62, 1247–1259. doi: 10.1007/s00018-005-5021-7

Wolverton, T., and Lalande, M. (2001). Identification and characterization of three members of a novel subclass of protocadherins. *Genomics* 76, 66–72. doi: 10.1006/geno.2001.6592



OPEN ACCESS

EDITED BY

Eric Boué-Grabot,
UMR 5293 Institut des Maladies
Neurodégénératives (IMN), France

REVIEWED BY

Timothy Mosca,
Thomas Jefferson University,
United States
Olivier Thoumine,
Centre National de la Recherche
Scientifique (CNRS), France
Richard P. Tucker,
University of California, Davis,
United States

*CORRESPONDENCE

Robert Hindges
robert.hindges@kcl.ac.uk

SPECIALTY SECTION

This article was submitted to
Neurodevelopment,
a section of the journal
Frontiers in Neuroscience

RECEIVED 07 April 2022

ACCEPTED 07 October 2022

PUBLISHED 03 November 2022

CITATION

Cheung A, Schachermayer G,
Biehler A, Wallis A, Missaire M and
Hindges R (2022) Teneurin paralogues
are able to localise synaptic sites
driven by the intracellular domain and
have the potential to form
cis-heterodimers.
Front. Neurosci. 16:915149.
doi: 10.3389/fnins.2022.915149

COPYRIGHT

© 2022 Cheung, Schachermayer,
Biehler, Wallis, Missaire and Hindges.
This is an open-access article
distributed under the terms of the
[Creative Commons Attribution License](#)
(CC BY). The use, distribution or
reproduction in other forums is
permitted, provided the original
author(s) and the copyright owner(s)
are credited and that the original
publication in this journal is cited, in
accordance with accepted academic
practice. No use, distribution or
reproduction is permitted which does
not comply with these terms.

Teneurin paralogues are able to localise synaptic sites driven by the intracellular domain and have the potential to form *cis*-heterodimers

Angela Cheung¹, Greta Schachermayer¹, Aude Biehler¹,
Amber Wallis¹, Mégane Missaire¹ and Robert Hindges^{1,2*}

¹Centre for Developmental Neurobiology, King's College London, London, United Kingdom,

²MRC Centre for Neurodevelopmental Disorders, King's College London, London, United Kingdom

Synaptic specificity during neurodevelopment is driven by combinatorial interactions between select cell adhesion molecules expressed at the synaptic membrane. These protein–protein interactions are important for instructing the correct connectivity and functionality of the nervous system. Teneurins are one family of synaptic adhesion molecules, highly conserved and widely expressed across interconnected areas during development. These type-II transmembrane glycoproteins are involved in regulating key neurodevelopmental processes during the establishment of neural connectivity. While four teneurin paralogues are found in vertebrates, their subcellular distribution within neurons and interaction between these different paralogues remains largely unexplored. Here we show, through fluorescently tagging teneurin paralogues, that true to their function as synaptic adhesion molecules, all four paralogues are found in a punctate manner and partially localised to synapses when overexpressed in neurons *in vitro*. Interestingly, each paralogue is differentially distributed across different pre- and post-synaptic sites. In organotypic cultures, Tenm3 is similarly localised to dendritic spines in CA1 neurons, particularly to spine attachment points. Furthermore, we show that the intracellular domain of teneurin plays an important role for synaptic localisation. Finally, while previous studies have shown that the extracellular domain of teneurins allows for active dimer formation and transsynaptic interactions, we find that all paralogues are able to form the full complement of homodimers and *cis*-heterodimers. This suggests that the combinatorial power to generate distinct molecular teneurin complexes underlying synaptic specificity is even higher than previously thought. The emerging link between teneurin with cancers and neurological disorders only serves to emphasise the importance of further elucidating the molecular mechanisms of teneurin function and their relation to human health and disease.

KEYWORDS

teneurin, synapse, protein interaction, cell adhesion molecule, dendritic spine

Introduction

The formation of precise synaptic connections between neurons during development is a fundamental process which ultimately dictates the correct functionality of the nervous system. Much research has been done on trying to unravel these complex mechanisms and pathways, focusing on different aspects including molecular, structural or activity-related processes. Protein interactions at the synaptic membrane play a pivotal role in driving synaptic specificity, for example, through cell adhesion molecules interacting in a combinatorial manner to generate diverse cellular interactions. While many cell adhesion molecules are implicated in this process, the teneurin family of type II transmembrane glycoproteins have been shown to be key mediators of intercellular signalling during development in both vertebrates and invertebrates.

Also known as Tenm/Odz, the teneurins were originally discovered in the early 1990s in *Drosophila* as tenascin-like molecule accessory (tena) and tenascin-like molecule major (tenm) (Baumgartner and Chiquet-Ehrismann, 1993; Baumgartner et al., 1994; Levine et al., 1994). Subsequent studies showed they are highly expressed across both the developing and adult nervous systems, particularly in interconnected regions (Oohashi et al., 1999; Cheung et al., 2019), reflecting a significant role in mediating basic neurodevelopmental processes, such as cell migration, axonal guidance, and synaptic partner matching (Drabikowski et al., 2005; Leamey et al., 2008; Hong et al., 2012; Berns et al., 2018; Del Toro et al., 2020; Pederick et al., 2021). While only one teneurin gene has been identified in most invertebrates, insects have two paralogues (Tucker et al., 2012) and four teneurin paralogues are present in vertebrates (Mosca, 2015). There is a high degree of conservation between paralogues, with 58–70% sequence identity between human teneurin-1 to -4 alone (Jackson et al., 2018).

Structurally, the teneurins are large proteins of around 300 kDa with a small N-terminal intracellular domain, a single span transmembrane domain, and a large C-terminal extracellular region (Rubin et al., 1999; Tucker and Chiquet-Ehrismann, 2006; Jackson et al., 2018; Li et al., 2018). While the small ~45 kDa intracellular domain is less conserved than the extracellular region (Minet et al., 1999; Nunes et al., 2005), it nevertheless shows up to 70% sequence similarity between orthologues (Scholer et al., 2015). Shared features of the intracellular domain include an EF-hand-like Ca^{2+} binding site and polyproline-rich regions that can interact with SH3 domain-containing proteins, hypothesised to mediate interactions with the cytoskeleton (Nunes et al., 2005; Tucker and Chiquet-Ehrismann, 2006). Similarly, the C-terminal extracellular region is also composed of a number of domains, including epidermal growth factor (EGF)-like repeats, a cysteine-rich domain, a TTR (transthyretin-related) domain, a FN (fibronectin)-plug domain, five NHL (NCL-1, HT2A, and Lin-41) repeats, a YD

(tyrosine-aspartate)-repeat domain, an internal linker domain, an ABD (antibiotic-binding domain-like) domain, the Tox-GHH domain, and a teneurin C-terminal associated peptide region (Qian et al., 2004; Wang et al., 2005; Jackson et al., 2018; Li et al., 2018; Cheung et al., 2019). The EGF-like repeats allow for the dimerisation of teneurin monomers in *cis* to form active dimers (Feng et al., 2002; Beckmann et al., 2013), while the NHL domains allow for transsynaptic interactions, either with teneurin itself, or with other cell adhesion molecules such as latrophilins (Boucard et al., 2014). The teneurin C-terminal associated peptide region, or TCAP, may be cleaved and released as a bioactive peptide and has even been shown to be able to interact with other protein receptors such as the latrophilins (Qian et al., 2004; Wang et al., 2005; Al Chawaf et al., 2007; Lovejoy et al., 2009; Woelfle et al., 2015).

In *cis*, active teneurin dimers can form as a result of both homophilic and heterophilic interactions between teneurin monomers. Electron microscope analysis showed that homophilic interactions are able to occur between the extracellular domains of all teneurins to form homodimers, while co-transfection experiments of cells with two different extracellular domains suggest teneurin heterodimers can also form (Feng et al., 2002). In *trans*, interactions can occur between teneurin proteins homophilically, or heterophilically with other protein families. Separate *in vitro* studies have shown that cell transfection expression constructs for with either *tenm2* or *tenm3* promotes homophilic cell-cell adhesion (Rubin et al., 2002; Beckmann et al., 2013; Berns et al., 2018), while *in vivo*, work in *Drosophila* show that the two teneurin paralogues, Ten-a and Ten-m, both contribute to synaptic specificity by interacting homo- and heterophilically in *trans* between select pairs of pre- and postsynaptic partners in the olfactory bulb and neuromuscular junction (Hong et al., 2012; Mosca et al., 2012; Mosca, 2015). Surprisingly, the *trans*-homophilic interactions between Tenm3 in promoting cell aggregation was dependent on the alternatively spliced isoform expressed (Berns et al., 2018). More recently, *trans*-synaptic heterophilic interactions between mammalian teneurins and latrophilins have been shown to be important in shaping synapse formation and neural connectivity (Boucard et al., 2014; Vysokov et al., 2016; Sando et al., 2019; Pederick et al., 2021).

Indeed, the disruption of teneurin function using *in vivo* models highlight the importance of teneurins during synaptic partner matching and the establishment of functional connectivity. For instance, the knockdown of *tenm3* in zebrafish leads to defects in retinal ganglion cell (RGC) and amacrine cell connectivity in the retina affecting, as a consequence, the functional development of a specific visual feature, orientation selectivity (Antinucci et al., 2013). Furthermore, studies in mouse have shown that the loss of Tenm2 and Tenm3 significantly affects the mapping of ipsilateral retinal projections to the superior colliculus (Leamey et al., 2007;

Young et al., 2013). In addition to these studies focusing on the visual system, teneurins, together with their heterophilic interaction partners latrophilins, have been shown to regulate topographic circuit assembly between the CA1 region of the mouse hippocampus and the subiculum (Berns et al., 2018; Pederick et al., 2021). As such, with such an integral role in neurodevelopment and the establishment of connectivity in the brain, it is not surprising that mutations in all four human genes have also been linked to neurodevelopmental disorders (Mosca, 2015).

Although teneurins have been shown to play a significant role in regulating different aspects of neurodevelopment, much about their synaptic localisation, mechanism of action and role in synapse formation remains to be explored. The synthesis of synaptic proteins in neurons can occur in the soma, with proteins subsequently transported to synaptic sites, or alternatively, the mRNA is transported along axons and dendrites and locally translated in the vicinity of synaptic structures (Steward and Levy, 1982; Sutton and Schuman, 2006; Doyle and Kiebler, 2011; Donlin-Asp et al., 2021). However, it is so far not clear if teneurins undergo local translation or are transported in protein form to their site of action. Furthermore, despite the available data on *trans*-interactions, little is known about the extent of forming heterodimers in *cis* through their EGF domains, and thus increasing the molecular repertoire to control synaptic specificity. Here, we show the differential subcellular localisation of teneurin paralogues and further examine structural factors affecting its distribution in neurons. Furthermore, we show that all teneurin paralogues are able to interact with each other in *cis* and that there is a full complement of interactions. Our results set an important basis for future studies to shine light on the molecular diversity of synaptic protein complexes underlying synapse formation, specificity and function.

Materials and methods

Cortical neuronal culture and transfection

Dissociated neurons were generated from cortices of embryonic day 18 Sprague-Dawley rats of either sex. Dissected cortices were treated with 5 mg/ml trypsin (Thermo Fisher Scientific, UK) for 5 min at 37°C and triturated with fire-polished Pasteur pipettes. Neurons were plated at 80,000 viable cells/ml directly onto poly-L-lysine (100 µg/ml; Sigma-Aldrich, UK) coated sterile borosilicate glass coverslips for confocal imaging (18-mm diameter; Marienfeld, Germany). Cultures were maintained in Neurobasal A[®] medium supplemented with 2% B27 supplement, 2% foetal bovine serum, 1% glutamax (all Thermo Fisher Scientific, UK) and 1% penicillin/streptomycin (Sigma-Aldrich, UK), at

37°C in a humidified incubator with 5% CO₂. After 3 days *in vitro* (DIV) the medium was exchanged for serum-free media. At 7 DIV neurons were transfected with expression plasmids expressing EGFP, membrane-EGFP, LRRTM2-myc and EGFP/tagRFP-tagged full length mouse teneurin paralogues (tenm1_EGFP/tagRFP, tenm2_EGFP/tagRFP, tenm3_EGFP/tagRFP, tenm4_EGFP/tagRFP, tenm3ΔECD_EGFP, and tenm3ΔICD_EGFP) under the control of a CAG promoter using Lipofectamine 2000 transfection reagent (2-h incubation; Thermo Fisher Scientific, UK). After transfection neurons were maintained in serum-free medium until fixation with 4% paraformaldehyde (15 min; Sigma-Aldrich, UK) at 17 DIV.

Organotypic hippocampal cultures

Organotypic hippocampal slices were acquired from CD1 mice sacrificed at postnatal day 7. Only schedule 1 procedures performed by a competent individual were used in these studies, which are exempt under the Animals Scientific Procedures Act 1986. After decapitation, the brains were removed and placed in a petri dish with ice-cold dissecting solution containing 23 mM D-glucose (Sigma-Aldrich, UK) in Gey's balanced salt solution (GBSS, Sigma-Aldrich, UK). The hippocampi were dissected and placed on the Teflon stage of a tissue cutter, and coronal slices of 400 µm were cut and separated from each other by addition of dissecting solution and gentle mixing in a falcon tube. Well defined and undamaged slices were selected under the microscope and transferred onto sterile, porous (0.4 µm) Millicell-CM membranes (Merck Millipore) in six well tissue culture plates at a density of 4 slices per membrane. The slices were incubated at 35.5°C, 5% CO₂ in 1.2 ml slice culture medium containing 49% Minimum essential medium (Thermo Fisher Scientific, UK), 25% Earle's balanced salt solution (EBSS, Gibco), 25% heat inactivated horse serum (Thermo Fisher Scientific, UK), 1% B27 supplement and 35.4 mM D-glucose. At 1 DIV and every two days thereafter a full media change was done.

DNA bullets and biolistic transfection

To make DNA bullets for biolistic transfection with a gene gun, 0.015 g of 1.6 µm gold microcarriers (Bio-Rad) were mixed with 100 µl spermidine (0.05 M, Alfa Aesar) and sonicated for 3 s. A total of 35 µg of *tenm3* expression vector and 10 µg of membrane-bound GFP expression vector, or 25 µg of membrane-bound GFP expression vector only, were added to the gold solution and vortexed. Then 100 µl of 1 M calcium chloride was added drop-wise to each of the gold-DNA solutions whilst vortexing. The gold microcarriers were left to precipitate for 10 min at room temperature and then centrifuged for

15 s. The supernatant was removed and 1 ml 100% ethanol added to the gold microcarriers, vortexed and centrifuged four times. Finally, 3 ml of 100% ethanol was added to the gold microcarriers and the gold-DNA solutions were vortexed and sonicated again for 3 s. The gold-DNA solutions were injected into 70 cm of tubing, which was previously rinsed with 100% ethanol and dried with nitrogen gas at 3–4 LPM flow for 20 min in a tubing prep station (Bio-Rad). The gold microcarriers were left to settle in the tube for 4 min before the ethanol was removed carefully and the tubing rotated by 180° and left for 4 s. Nitrogen was then passed through the tubing at 5 psi, 3 LPM whilst spinning for 5 min, the tubing cut using a clean razor blade and the DNA bullets stored at 4°C in tubes with silica gel. Organotypic slices from postnatal day 7 mice were transfected at 1 DIV. A Helios gene gun system (Bio-Rad) was used to shoot organotypic hippocampal slices with a helium pressure of ~140 PSI (~9.5 Bar). After transfection the slices were placed back into the incubator and gene expression and cell survival checked after 24 and 48 h.

Immunofluorescence

Fixed cultures were washed in PBS before permeabilisation with 0.1% Triton X-100 in PBS (PBST) for 5 min. Cells were then washed again in PBS before non-specific antibody-binding sites were blocked by incubation in 5% goat serum (Sigma-Aldrich, UK) in PBST for 60 min at RT before incubation with appropriate dilutions of primary antibodies in PBST, 5% goat serum overnight at 4°C. Primary antibodies were used at the following concentrations: rabbit anti-synapsin I (1:500; Merck Millipore), mouse anti-bassoon (1:500; Abcam), mouse anti-shank2 (1:500; Neuromab), rabbit anti-vGLUT1 (1:500; GeneTex), rabbit anti-vGAT (1:250; GeneTex), mouse anti-PSD-95 (1:250; Thermo Fisher Scientific, UK), mouse anti-gephyrin (1:500; Synaptic Systems), chicken anti-GFP (1:500, Abcam), mouse anti-myc (1:200, Abcam), and rabbit anti-tagRFP (1:500, Invitrogen). Cells were washed three times in PBS before incubation with secondary antibodies in PBST for 2 h at RT, counterstained with Hoechst (Thermo Fisher Scientific, UK) and washed four times in PBS. Secondary antibodies were used at the following concentrations: Alexa Fluor goat anti-chicken 488, Alexa Fluor goat anti-mouse 488, Alexa Fluor goat anti-rabbit 568 and Alexa Fluor goat anti-mouse 568 (all used at 1:500; Thermo Fisher Scientific, UK). Cells were mounted using Fluoromount-G mounting medium (Thermo Fisher Scientific, UK).

Confocal microscopy

Cultures were imaged on a Nikon A1R inverted confocal microscope (Nikon instruments, Melville, NY, USA) using a

60× Plan Fluor oil immersion objective (numerical aperture of 1.4). Excitation wavelengths of 405, 488, 561, or 640 nm were used. Images were acquired using NIS-Elements imaging software and were processed in image processing package FIJI (Schindelin et al., 2012).

The imaging of dendritic spines in organotypic slices was carried out using a Nikon A1R inverted confocal microscope with a 40× water immersion objective (NA 1.15) and 408-, 488, and 561 nm excitation wavelengths. Images were taken at 1× zoom for whole neuron morphology and 3× zoom for spine morphology and synaptic puncta (1× zoom = 0.31 μm/pixel, 3× zoom = 0.10 μm/pixel) and as a z-stack with 0.3 μm steps. Images were acquired using the NIS-Elements software and image stacks were exported as raw 16-bit ND2 files.

HEK293 and neuro-2a cell culture

The human embryonic kidney cell line HEK293, and immortalised mouse neuroblastoma cell line Neuro-2a (N2a) was maintained in Dulbecco's Modified Eagle's Medium (DMEM, Thermo Fisher Scientific, UK) supplemented with 10% foetal bovine serum (Thermo Fisher Scientific, UK) and 1% penicillin/streptomycin (Sigma-Aldrich, UK), at 37°C in a humidified incubator with 5% CO₂. Expression plasmids expressing EGFP-only and EGFP- or tagRFP-tagged teneurin paralogues (full length teneurin constructs or *tenm3_ΔEGF-EGFP*) were transfected into HEK293 or N2a cells using Lipofectamine 2000 transfection reagent and Opti-MEM reduced serum medium (3-h incubation; Thermo Fisher Scientific, UK). After transfection, HEK293 or N2a cells were maintained in complete media before fixation with 4% paraformaldehyde (15 min; Sigma-Aldrich, UK) and immunostaining or co-immunoprecipitation studies.

Puncta analysis and statistical analysis

Puncta colocalisation analysis was carried out on images in FIJI using the Puncta Analyzer plugin developed and described (Ippolito and Eroglu, 2010). Puncta sizes below 0.1 μm and above 10 μm were excluded from the analysis. Plots were based on the mean of at least 12 cells per condition pooled from a minimum of three independent experiments. Data were plotted using GraphPad Prism data analysis software (GraphPad Software Inc., San Diego, CA, USA) and the appropriate statistical test (one-way ANOVA with Dunnett's multiple comparison *post hoc* test) applied to the means.

Co-immunoprecipitation and Western blot analysis

Expression vectors containing EGFP-tagged teneurin paralogues were co-transfected with tagRFP/Myc-tagged teneurin paralogues into Neuro2A cells with Lipofectamine 2000, the cell lysates collected after 2 DIV and immunoprecipitated with GFP-Trap agarose beads (ChromoTek, Germany). An EGFP-only vector was used as the bait control and co-transfected with the prey tagRFP/Myc-tagged teneurin paralogues. The precipitated products were separated using SDS-PAGE gel electrophoresis, transferred onto PVDF membrane and blocked for 1 h with 5% milk powder in TBS-Tween 20 (TBST) blocking solution before incubating overnight with primary antibody in blocking solution at 4°C. After primary incubation, blots were washed three times in TBST before incubation with secondary antibody in blocking solution for 2 h at RT. Blots were washed another three times in TBST before developed using Novex ECL chemiluminescent substrate reagent kit (Thermo Fisher Scientific, UK) and visualised on the Odyssey Fc imaging system (LI-COR Biosciences, UK). Blots were chemically stripped and re-probed with different antibodies. Antibodies were used at the following concentrations: Primaries mouse anti-myc tag (1:1,000; Cell Signaling) and chicken anti-GFP (1:5,000; Abcam), and secondaries goat anti-mouse IgG HRP conjugate (1:5,000; Abcam) and goat anti-chicken IgY HRP conjugate (1:5,000; Abcam).

Results

Teneurins do not evenly distribute along the membrane but are partially localised to puncta at synaptic sites

To investigate the subcellular localisation pattern of all four teneurin paralogues in neurons *in vitro*, we used dissociated primary neuronal cultures. Due to a lack of reliable antibodies for all teneurins, we transfected neurons with expression constructs for EGFP-tagged mouse teneurins at 7 DIV and analysed the cultures at 17 DIV, when synaptic connections are formed and matured. Teneurin insertion into the membrane in HEK293 cells was unaffected by the EGFP-tag ([Supplementary Figure 1](#)). In dissociated neurons, all four teneurins were found to form discrete puncta along both dendrites and axons, instead of being evenly distributed along the membranes as seen in HEK cells ([Figure 1A](#)). To assess a possible co-localisation of the detected teneurin puncta with the presence of synapses, we used specific antibodies against the general marker synapsin I. We found that all four teneurins partially co-localise with synapsin I ([Figure 1B](#)), with no significant difference in the proportion

between Tenm1 (21%), Tenm2 (22%) Tenm3 (21%), and Tenm4 (24%) ([Figure 1C](#), $n = 14-16$). The values are generally slightly lower than for our controls assessing synapsin I co-localisation with other bona fide synaptic proteins bassoon (56%), shank 2 (38%) or LRRTM2 (65%) ([Figure 1D](#)), however we find good co-localisation of LRRTM2 with teneurins as seen in one example for Tenm3 ([Supplementary Figure 2](#)). Rotation of one image channel by 90° and assessing its puncta co-localisation with the synapsin I puncta as a control showed values consistently below 4% (example shown in [Supplementary Figure 3](#)).

Teneurins are differentially distributed across inhibitory and excitatory pre- and postsynaptic sites

To further investigate the distribution of teneurin paralogues, we assessed teneurin co-localisation with specific types of synapses. To distinguish between excitatory and inhibitory synapses and their pre- and postsynaptic components, we used an immunocytochemistry approach using antibodies against the vesicular glutamate transporter vGLUT ([Figure 2A](#)) and the vesicular GABA transporter vGAT ([Figure 2B](#)), as well as postsynaptic density protein 95 (PSD-95, [Figure 2C](#)) and gephyrin ([Figure 2D](#)), respectively. Overall, we found that all four teneurin paralogues partially co-localise with all these markers in various proportions ([Figures 2A'-D'](#)).

For presynaptic compartments, our results show that roughly 13% of teneurin clusters were also positive for vGLUT [Tenm1 (11%), Tenm2 (14%), Tenm3 (15%), and Tenm4 (15%), $n = 14-15$] and there was no significant difference in the distribution of teneurin paralogues across excitatory presynaptic sites ([Figure 2A'](#)). Similarly, around 15% of teneurin clusters were also positive for vGAT [Tenm1 (16%), Tenm2 (15%), Tenm3 (15%), and Tenm4 (15%), $n = 12-17$], again with no significant difference observed between the presence of different teneurin paralogues at inhibitory presynaptic termini ([Figure 2B'](#)). Similar to the presynaptic compartments, we found all teneurins to be present in both excitatory and inhibitory postsynaptic compartments. Co-localisation with excitatory postsynaptic PSD-95 was detected in Tenm1 (16%), Tenm2 (17%), Tenm3 (24%), and Tenm4 (23%) ([Figure 2C'](#), $n = 16-17$). Finally, the localisation of teneurin paralogues to inhibitory postsynaptic sites, as labelled by gephyrin, was the lowest out of all the synaptic sites with just over 9% of teneurin clusters also gephyrin positive (Tenm1 (9%), Tenm2 (9%), Tenm3 (7%), and Tenm4 (11%) and no significant difference observed between paralogues ([Figure 2D'](#), $n = 14-17$). From these experiments we conclude that, despite the rather low percentages, teneurins are generally able to localise to pre- and postsynaptic compartments, both in excitatory and inhibitory cells.

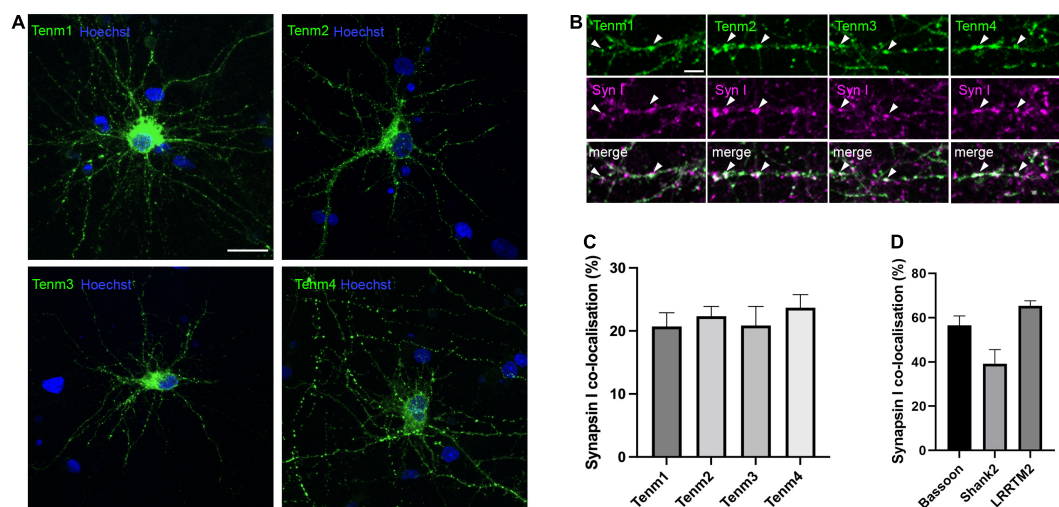


FIGURE 1

Teneurins form discrete puncta, some of which are localised to synaptic sites. (A) EGFP-tagged teneurin paralogues overexpressed in rat cortical cultures are unevenly distributed across the membrane. (B) Synapsin I immunostaining in dissociated cortical cells overexpressing EGFP-tagged teneurin show partial co-localisation of teneurin puncta with synapsin I (two examples marked with arrow heads for each teneurin member). (C) Similar levels of partial co-localisation are observed between all four teneurin paralogues with synapsin I. (D) Synapsin I co-localisation for bona fide synaptic proteins bassoon (56%), shank (38%), and LRRTM2 (65%). Data represents mean \pm SE based on samples with at least 14 cells/condition pooled from a least three different experiments. One-way ANOVA with Dunnett's multiple comparison test was performed between all paralogues ($p < 0.05$). Scale bar, 20 μ m (A), 5 μ m (B).

Teneurin 3 is localised to spine heads and spine attachment points in CA1 neurons

Tenm3 is expressed in CA1 neurons of the hippocampus in a strong proximal-to-distal gradient along the CA1 region of the hippocampus (Berns et al., 2018). To further explore the subcellular localisation pattern of Tenm3 in CA1 neurons we biolistically co-transfected organotypic mouse hippocampal slice cultures with expression vectors for myc-tagged Tenm3 and membrane-GFP, allowing the subcellular detection of Tenm3 as well as visualisation of the overall cell morphology (Figures 3A,B). Our general analysis showed that Tenm3 is localised to dendritic spines in CA1 neurons with a total proportion similar to our *in vitro* assessment before (19.87% for both apical and basal spines combined, Supplementary Figure 4). Furthermore, we found strong differences in Tenm3 signal in spines within a few micrometres of each other along the same dendrite; some showed high levels of Tenm3 while neighbouring spines had barely detectable levels (Figures 3C,C'). Interestingly, Tenm3 was detected not only in the spine head, but also inside the dendritic shaft below the spines, referred to as the spine base or spine attachment points (SAPs; Supplementary Figure 5). In basal and apical dendrites where we found Tenm3 signals in the spine head, we also detected a clear signal in the SAPs in 71.95 and 93.02% of the cases, respectively (Figure 3D). There is a positive correlation between the Tenm3 signal detected in the spine head and the

one in the SAPs (Figure 3E, $r = 0.237$, $p < 0.0001$ and $r = 0.192$, $p = 0.0075$ for basal and apical spines, respectively). However, we noted that there is a considerable number of Tenm3-negative spine heads that nevertheless showed strong Tenm3 signal at the SAPs (basal: 46.41%; apical: 56.33%, Figure 3D), pointing towards a possible involvement for Tenm3 in processes occurring at the shaft, including dendritic spine organisation.

The intracellular domain of Tenm3 facilitates protein localisation to synaptic puncta

Based on our findings showing that Teneurins, when expressed in neurons, do not simply distribute evenly in the membrane, but appear in part in discrete puncta overlapping synaptic locations, we wondered how this specific localisation is achieved. Teneurins are large proteins with well-defined domains responsible for mediating a variety of interactions, but which domain, if any, is responsible for driving its synaptic localisation? To address this question, we created two different deletion mutants of our *tenm3* expression construct leading to different Tenm3 proteins: one lacking the extracellular domain (*tenm3* Δ ECD) and one lacking the intracellular domain (*tenm3* Δ ICD). In both constructs an EGFP-tag replaced the truncated domain to allow detection, while the original short transmembrane domain was kept present. We then assessed both mutants

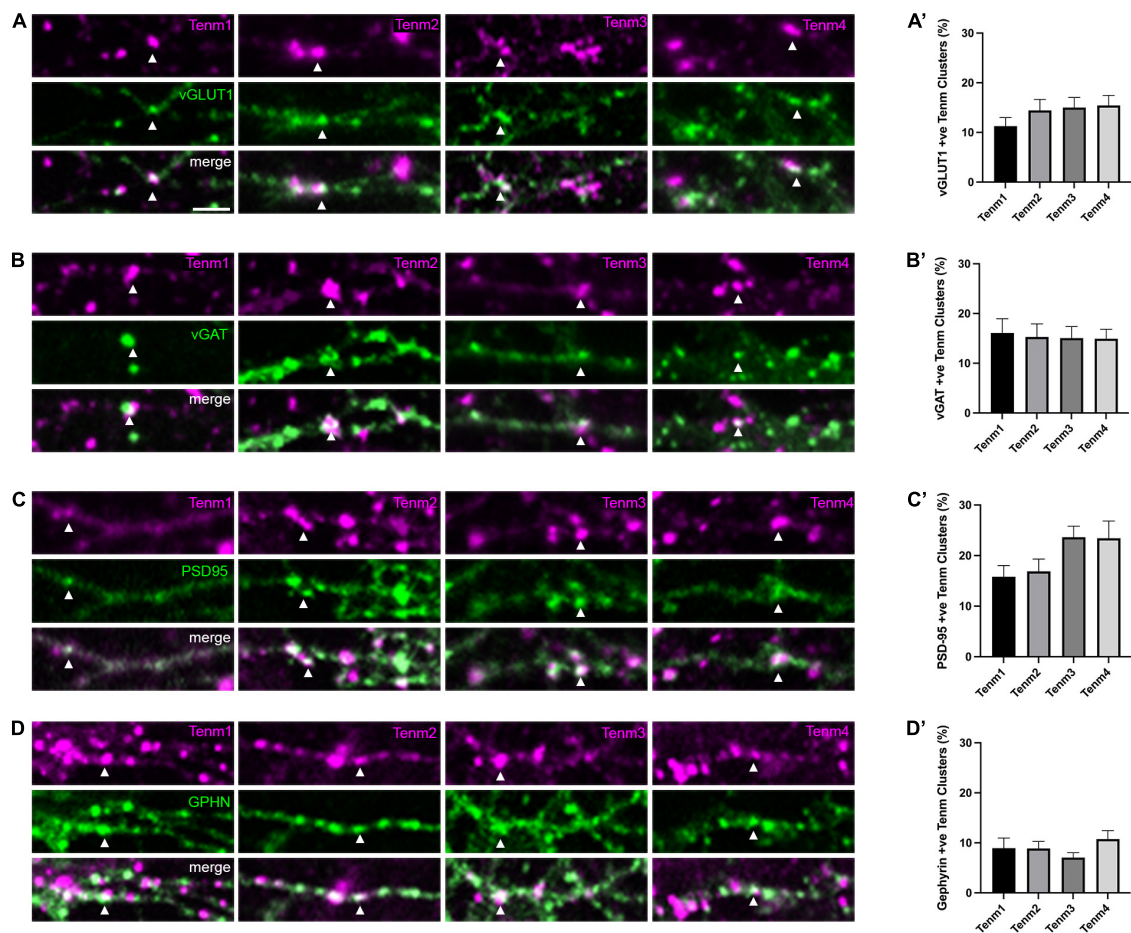


FIGURE 2

Teneurin distribution across different synaptic sites. Immunocytochemistry detection of (A) vGLUT1, (B) vGAT, (C) PSD95, and (D) Gephyrin in dissociated neurons transfected with EGFP-tagged teneurin paralogues. In each panel, one example colocalisation is indicated by the arrowhead. Graphs on the right show quantification of colocalisation. (A'–D') Levels of teneurin colocalisation with vGLUT1, vGAT, and PSD-95 are similar (10–20%), while co-localisation with Gephyrin is slightly lower (below 10%). Data represents mean \pm SE based on samples with at least 12 cells/condition pooled from a least three different experiments. One-way ANOVA with Dunnett's multiple comparison test was performed between all paralogues ($p < 0.05$). Scale bar, 5 μ m (all panels).

for (a) the general formation of discrete puncta and (b) the overlap of Tenm3 puncta with the synaptic marker synapsin I. After confirming that our deletion constructs are expressing efficiently and that the proteins are inserted into the membrane using N2a cells (Supplementary Figure 6) we transfected these different variants into dissociated rat cortical neurons. Surprisingly, we found that both variants, Tenm3 Δ ECD and Tenm3 Δ ICD, are still forming distinct puncta along neurites similar to full length Tenm3 (Figures 4A–C).

We then investigated further if these puncta co-localise to synaptic structures at comparable levels to the full-length protein or if the deletion of either the extra- or intracellular domain alter these values. Interestingly, we found that the intracellular domain alone (Tenm3_ Δ ECD) showed a 36% increase in co-localisation with synapsin I, while deletion of the

intracellular domain resulted in a 32% reduction compared to the proportion for the full-length protein (Figure 4D). These results indicate that the Tenm3 intracellular domain plays an important role for synaptic localisation.

All teneurin paralogues can form heterodimers with each other in *cis*

Teneurins act as *cis*-dimers and interact either homophilically or heterophilically in *trans* (Antinucci et al., 2013; Berns et al., 2018; Sando et al., 2019). It is generally established that these *cis*-dimers are generated through the assembly of two identical molecules of the same teneurin paralogue. However, there is only limited information on the ability of different full-length teneurin paralogues to form

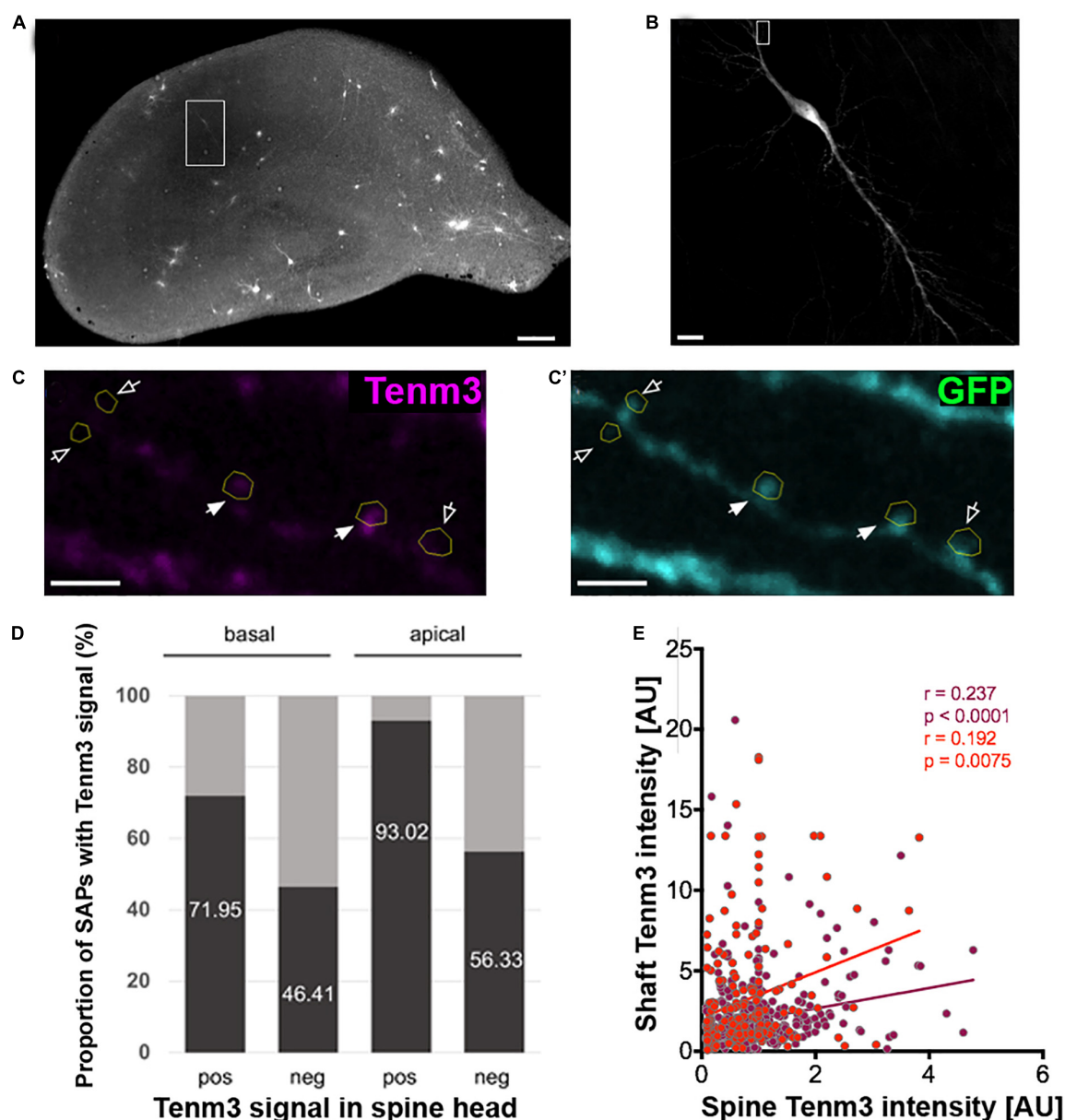


FIGURE 3

Tenm3 is localised to SAPs in CA1 neurons. (A) Organotypic hippocampal slice biolistically transfected with Tenm3 and GFP. White square indicates a positively transfected CA1 neuron. (B) Magnified view of transfected CA1 neuron. (C,C') Representative images showing the expression of Tenm3 and GFP in a basal dendritic segment of the CA1 neuron from panel (B). Dendritic spines are indicated by yellow ROIs. Note the different Tenm3 levels in neighbouring spines, with some spines expressing Tenm3 (filled arrows) and some devoid of Tenm3 expression (empty arrows). (D) Proportion of SAPs with high and low Tenm3 signal below basal and apical Tenm3-positive and -negative spines. (E) Correlation of SAP- and spine-Tenm3 intensity in basal (purple) and apical (red) dendrites. r , non-parametric Spearman correlation coefficient. SAP: Spine Attachment Point. Scale bar, 200 μ m (A), 20 μ m (B), and 10 μ m (C).

cis-heterodimers (Feng et al., 2002). To investigate this in more detail we used a co-immunoprecipitation approach.

We generated EGFP-tagged versions of each teneurin paralogue as baits and tested if they were able to pull-down any of the other paralogue tagged with a myc-tag (prey, Figure 5A). We expressed both bait and prey proteins in N2a cells and used GFP-Trap beads for our pull downs and subsequent

Western blot analysis. To detect the prey proteins, we used specific antibodies against the myc epitope. Both full-length protein bands and some proteolytic fragments can be detected. Interestingly, we found that all four teneurin paralogue (Tenm1 to Tenm4) used as bait were able to pull down all prey teneurin paralogue (Figures 5B–E). A Tenm3 variant with the EGF-like repeats removed did not result in the pull-down of any

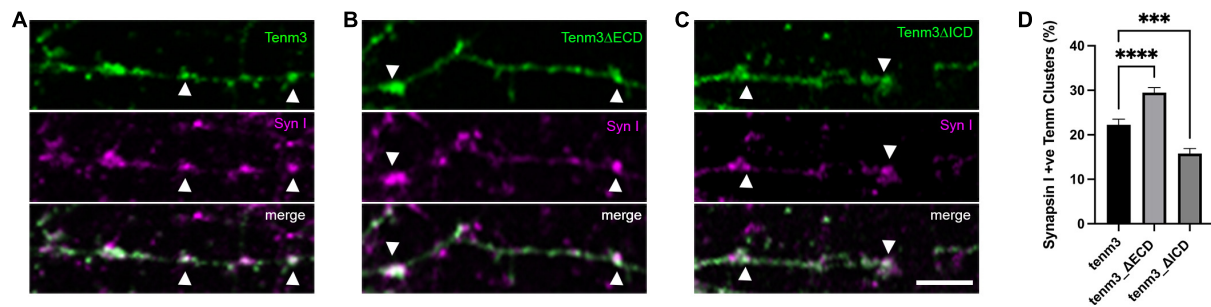


FIGURE 4

The intracellular domain of Tenm3 drives protein localisation to the synapse. Synapsin I immunostaining in dissociated cortical cells overexpressing (A) full-length, (B) ECD-deleted (Tenm3ΔECD), and (C) ICD-deleted (Tenm3ΔICD) variants of EGFP-tagged Tenm3 showing punctate expression for all cases. Arrow heads show two example for co-localisation in each panel. (D) Quantification of co-localisation with Tenm3ΔECD showing significantly higher ($****p < 0.0001$), and Tenm3ΔICD significantly lower ($***p = 0.0004$), co-localisation with synapsin I. Data represents mean \pm SE based on samples with at least 37 cells/condition pooled from at least three different experiments. One-way ANOVA with Dunnett's multiple comparison test was performed between all conditions ($p < 0.05$). Scale bar, 5 μ m.

teneurin paralogue (data not shown). These results show, at least in an *in vitro* setting, that all teneurin paralogues are able to form heterodimers with each other and thus present different molecular *cis*-complexes for possible *trans*-interaction partners.

Teneurin paralogues can be expressed in the same cell and are able to localise to different synaptic sites

To investigate the possibility of different teneurin paralogues being expressed in the same neuron *in vivo*, we used a combination of transgenic bacterial artificial chromosome (BAC) zebrafish lines to label teneurin-expressing cells (Cheung et al., 2019). Our results show indeed the presence of double labelled cells, for example, for Tenm2 and Tenm3 found in the retina (Figure 6). However, co-expression in the same neuron does not necessarily confirm co-localisation at synapses. We therefore co-expressed different fluorescently tagged teneurin paralogues in dissociated rat cortical neurons and assessed co-localisation using immunocytochemistry. Interestingly, we find that although most of the puncta along the neurites overlap between the different pairs of teneurin homologues (Supplementary Figure 7), we clearly find sites where only one or the other paralogue is localised (Figure 7). This suggests a possible mechanism to form different protein complexes and thus increases the molecular diversity at individual synapses.

Discussion

Since their initial discovery in *Drosophila*, many studies have contributed to show the importance of teneurins in conferring neural connectivity and synaptic specificity across different species. While recent progress has been made in resolving the

protein structure of teneurins, this has been focused on the large extracellular domain while the intracellular domain is still unresolved (Li et al., 2018; Jackson et al., 2019). Furthermore, other more basic biological characteristics of these proteins, for example, the *cis*-complex formation or localisation to different types of synapses, had so far not been systematically assessed. Here, we sought to answer some of these unanswered questions about teneurin biology by exploring the prevalence of teneurin at different synaptic sites, investigate factors driving its synaptic localisation, and further delve into the interchangeable interaction between different teneurin paralogues.

Using dissociated neurons and organotypic slice cultures, we found that while membrane-GFP on its own does not tend to cluster (Supplementary Figure 2C), all teneurins partially localise to individual puncta along axons and dendrites, overlapping well with synaptic markers. This is consistent with their important role during the formation of neural circuitry and specific synaptic interactions. The teneurin paralogues in *Drosophila*, Ten-m and Ten-a, are found localised to presynaptic, and mostly postsynaptic sites, respectively, and play a key role in neuromuscular synapse organisation (Mosca et al., 2012). In vertebrate cells, however, the pattern of teneurin presence across synapses was less clear. Previous data showed that Lasso, a splice variant of Tenm2, was localised mainly on dendrites in cultured neurons *in vitro* (Silva et al., 2011). Our findings on the synaptic localisation profile of all four teneurin paralogues in cultured neurons and comparison to other synaptic proteins strives to close this gap. Synaptic localisation was comparable between teneurin paralogues, with roughly a fifth (22%) of all teneurin protein puncta co-localising with the general presynaptic marker synapsin I. This apparently low proportion of co-localisation is however in line with our own and other previously published results for the synaptic proteins bassoon and shank2, which also show only a partial co-localisation with synapsin I (tom Dieck et al., 1998). Even the

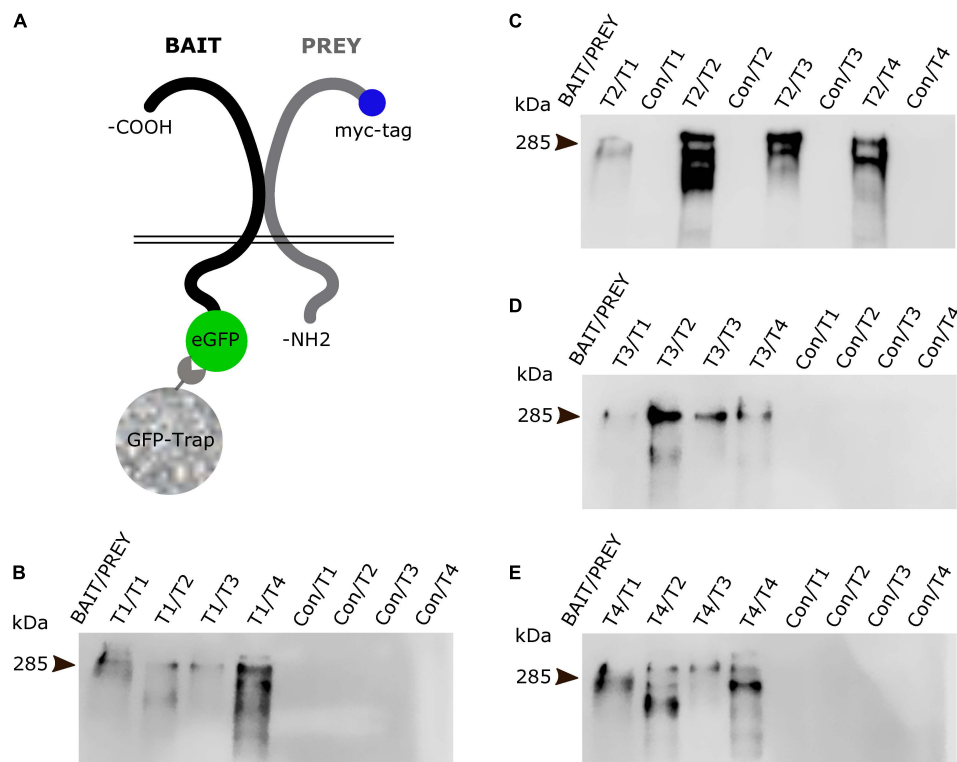


FIGURE 5

All teneurin paralogs can form heterodimers *in cis*. (A) Co-immunoprecipitation strategy with EGFP-tagged teneurin bait construct after co-transfection with tagRFP-tagged prey constructs in N2a cells. EGFP only expressing construct was used as control bait. Blots were probed for myc-tag which is only present on the prey constructs. (B–E) Bait teneurin paralogs were able to interact and specifically pull down itself and all other paralogs. Representative anti-myc-tag (prey) blots from (B) Tenm1, (C) Tenm2, (D) Tenm3 and, (E) Tenm4 pulldowns reveal presence of prey protein only in lanes with teneurin bait (Bait/Prey) but not with control bait (Con/Prey).

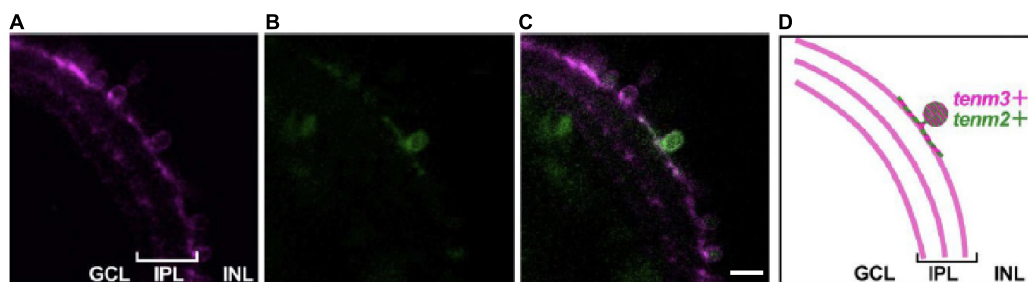


FIGURE 6

Teneurins are expressed together in the same cell *in vivo*. Tg (*tenm3:Gal4*; *UAS:RFP*) zebrafish embryos were injected with a *tenm2:citrine* BAC construct to mosaically label Tenm2-positive cells (citrine signal, B) in the background of all Tenm3-positive cells (RFP signal, A). (C) Merged image to show a small-field amacrine cell expressing both Tenm2 and Tenm3. (D) Schematic of the images showing the Tenm3- (tenm3+) and Tenm2 double-positive (tenm2+) amacrine cell. Scale bar, 10 μ m.

leucine-rich transmembrane protein LRRTM2, a key regulator and inducer of excitatory synapse development, is not fully co-localised with synapsin I when overexpressed in neurons, despite its potential to induce synapse formation (de Wit et al., 2009). Interestingly, we detected very good co-localisation of LRRTM2 and Tenm3. The fact that the majority (~70%) of teneurin puncta did not co-localise with synapsin I is not

completely unexpected, considering data for other synaptic cell adhesion molecules, such as cadherin 9 and α N-catenin, for example, which also form puncta along neurites and are enriched at synapses, but do not overlap perfectly with synaptic markers (Uchida et al., 1996; Williams et al., 2011). It is possible that this is either an effect from the overexpression strategy or that teneurins in general have additional roles along neurons,

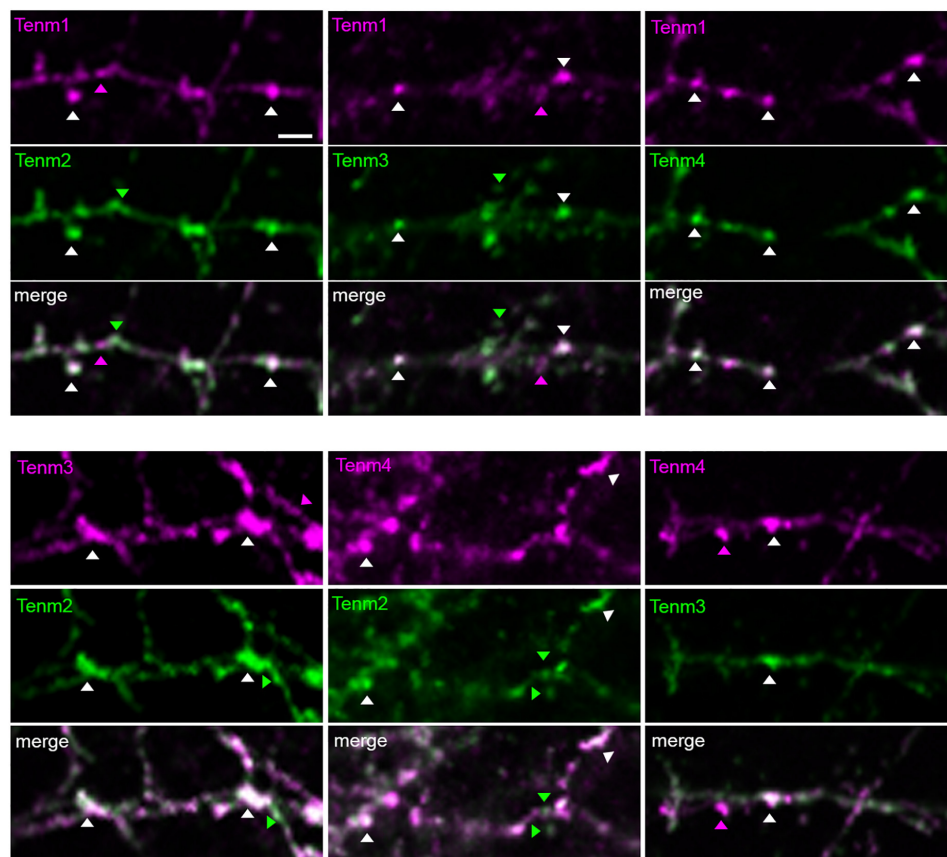


FIGURE 7

Different teneurin paralogs show overlapping localisation when expressed together in dissociated neurons. EGFP- and tagRFP-tagged teneurin paralogs co-transfected in primary neuronal cultures show partial co-localisation of puncta. Arrow heads show examples of puncta from individual paralogs and co-localisations. Scale bar, 20 μ m.

independent of the synaptic function. Further studies will be needed to ascertain the reasons behind this incomplete co-localisation.

The distribution of teneurin paralogs across different types of synapses showed that the localisation of teneurin to presynaptic puncta, whether this be excitatory or inhibitory, was similar (between 13 and 15% of puncta) and there was no significant difference between them. While the proportion of each teneurin paralogue at different sites is slightly lower than that of synapsin I, as expected, the combined total of teneurin puncta at excitatory and inhibitory presynaptic sites (28%) is, interestingly, a bit higher than the total observed colocalised with general presynaptic synapsin I. Similarly, while the overlap of teneurin is lowest with inhibitory postsynaptic sites (9%), paralogue localisation to excitatory postsynaptic sites is higher. The double-labelling of hippocampal sections for Tenm3 and synaptic markers in a recent study also shows that Tenm3 is more likely to be co-localised with excitatory synaptic markers (Zhang et al., 2022). On average, the total (excitatory and inhibitory) combined proportion of teneurin localised

at either presynaptic (28%) or postsynaptic sites (29.5%) is almost equivalent, consistent for proteins that form homophilic complexes across the synaptic cleft.

Indeed, the slight variability in distribution, especially between teneurin either co-localised with synapsin I or combined vGAT and vGLUT, may be due to the natural heterogeneity of transfected neurons. Primary neuronal cultures consist of a heterogeneous population of cells with varying levels of pre-existing endogenous teneurin expression. This could therefore potentially lead to variations in overexpressed protein localisation. The direct epitope tagging of endogenous teneurins in neurons, *via* CRISPR gene editing for example, would circumvent this problem and is a possible alternative (Willems et al., 2020). Additionally, the co-localisation analysis method conducted indiscriminately accounts for all protein clusters, regardless of their localisation to axons or dendrites, and may represent protein clusters that are actively being transported along dendrites and axons. Although this transport is normally restricted to young neurons during the early stages of synapse formation, certain transport vesicles (or dense core

vesicles), transporting the synaptic proteins piccolo and bassoon for instance, can be observed not only transporting to nascent presynapses in young neurons but also in mature synapses (Grabrucker et al., 2009). However, based on time-lapse imaging of transfected neurons, we could not detect any movement of the visible teneurin puncta (data not shown), therefore making this option unlikely.

The punctate and partial distribution of teneurin to synapses is reminiscent of Sema5B, which also only partially colocalises with PSD-95 and synapsin I (O'Connor et al., 2009). In addition to the cadherin-catenin complex, semaphorins have been shown to interact with the cytoskeleton and these interactions may be crucial for the regulation of synaptic connectivity and axon guidance, respectively (Salinas and Price, 2005; Pasterkamp and Giger, 2009; Wang et al., 2012). Teneurins have similarly been shown to be able to interact with the cytoskeleton, which further supports a role for teneurins in contributing to the establishment of synaptic connectivity, possibly through similar mechanisms (Nunes et al., 2005; Zheng et al., 2011; Mosca et al., 2012). It could also be that there are specific sites for local translation (for example, at the SAPs or elsewhere along the neurite) described for other synaptic proteins, which would generate a punctate pattern not necessarily overlapping with synaptic markers. However, currently it is not known if the mRNAs of teneurin paralogues are transported along neurites and would need further work.

We further explored the subcellular localisation of one of the teneurin paralogues, Tenm3. Using organotypic hippocampal slice cultures where the different areas can be directly recognised, we concentrated on neurons in the CA1 region, where Tenm3 is readily expressed. We found that tagged Tenm3 formed distinct puncta, overlapping with dendritic spines. Interestingly, Tenm3 was also found more frequently, and usually with higher relative signal intensity, to the SAPs below the spine neck, than inside the spine heads. This suggests that Tenm3 in the SAPs may potentially serve as a reserve pool for synaptic recruitment to the spine head, as has been observed for other proteins such as the cadherin-associated β -catenin and profilin, a regulator of actin polymerisation (Murase et al., 2002; Ackermann and Matus, 2003). The more abundant levels of Tenm3 at SAPs and their location at the base of spines also suggest a more general role for teneurins in synaptic assembly and organisation. The disruption of teneurins in invertebrates, for example, displays phenotypes consistent with a broad failure of synaptic organisation, such as failed active zone apposition, the disorganisation of synaptic proteins, and failure of pre- and postsynaptic differentiation (Mosca et al., 2012). The ability of teneurins to interact with the cytoskeleton (Nunes et al., 2005; Zheng et al., 2011; Mosca et al., 2012) suggests a role for Tenm3 protein in the SAPs in controlling synapse formation and assembly by arranging a cytoskeletal meshwork to regulate spatial organisation at the synapse.

Although we have demonstrated the localisation of teneurins to synapses, factors driving this localisation are still unknown. Our data shows that truncating full length Tenm3 significantly alters its ability to localise to synaptic sites. While a Tenm3 deletion mutant only containing the intracellular domain (Tenm3 Δ ECD) show an increased co-localisation with synapsin I, the mutant lacking this domain (Tenm3 Δ ICD) was significantly less likely to co-localise with synapsin I. These findings point towards a role of the intracellular domain in harbouring motifs that help bring teneurins to synaptic sites. While a synaptic targeting domain is known in some proteins, such as the short tyrosine-based motif followed by a pair of hydrophobic amino acids required for targeting PSD-95 protein to its postsynaptic localisation (Craven and Bredt, 2000), the potential synaptic localisation signal in the ICD of teneurin is currently unknown and will require further investigation. However, why is the deletion of such a domain not resulting in a complete abolishment of synaptic localisation? One possibility is that the extracellular domain alone is still able to form *cis*- and *trans*-dimers with endogenous, full-length proteins present at synapses and thus generate the GFP signal overlapping with synaptic staining. Future studies should show if the intracellular domains of the other teneurin paralogues also influence synaptic localisation.

Finally, we sought to further explore the possibility for heterodimeric interactions between different teneurin paralogues and what combinations were possible in *cis*. Recent studies utilising cell aggregation assays have shown that the ECD of Tenm4 is capable of interacting with the ECDs of all other teneurins (Hayashi et al., 2020). We show through co-immunoprecipitation experiments that *cis*-heterodimers can indeed form between all full-length teneurin paralogues *in vitro*. A control, where the EGF-like repeats crucial for *cis*-dimerisation were removed, failed to co-precipitate any protein partners in this assay. Although previous studies have demonstrated the possible heterodimerisation of the extracellular domain of different teneurin paralogues in HEK-293 cells (Feng et al., 2002), this is the first time the full *cis*-interaction matrix of all four full-length teneurin paralogues is presented. While further investigation is required over whether such interactions occur also *in vivo*, and under what circumstances, we can envisage a scenario where the precise combination of different teneurin paralogues is required for controlling synapse specificity in neuronal subpopulations. Heterodimer formation is common throughout biology as a simple way to increase functional diversity and the specific combination of proteins found within the synaptic area contributes to the molecular diversity of neuronal connections. However, for this to happen, different teneurin paralogues would have to be expressed in the same neuron. Our experiments in zebrafish showed that this is indeed the case.

Combining this observation with our biochemical findings of detecting Tenm2/Tenm3 *cis*-interactions (as well as others), we speculate that such heterodimers indeed exist and play a role *in vivo*. However, our results based on the presence of different teneurins in dissociated neurons suggest that such *cis*-heterodimers are not necessarily a default mechanism in co-expressing cells. Interestingly, we find some puncta along neurites that seem to contain only one of the two paralogues present (Figure 7 and Supplementary Figure 7). Although this approach does not confirm the presence of teneurin *cis*-heterodimers, it does hint at a possible mechanism to change the molecular composition of individual synapses of a neuron and could be adding to the diversity of specific interactions in *trans*. Future more detailed molecular and biophysical assessment of such complexes and their underlying mechanisms should shine light on this central issue.

As important as the interactions in *cis*, the *trans*-heterophilic interactions of teneurin with the cell-surface protein latrophilin (LPHN) have been well documented in recent years and been shown to be critically involved in regulating synapse specificity (excitatory versus inhibitory), for example, through the alternative splicing of *tenm2* altering the Tenm2/LPHN adhesion complex (Li et al., 2020). It remains to be seen whether teneurin interactions in *trans* with other teneurins (either heterophilic or homophilic) are able to contribute to synaptic specificity in the same way in vertebrates as the orthologues in *Drosophila* (Hong et al., 2012; Mosca et al., 2012). Indeed, recent observations suggest that while teneurins are expressed both pre- and postsynaptically, they possibly function primarily as presynaptic adhesion molecules that interact with other postsynaptic ligands such as LPHNs and may not actually be required for postsynaptic interactions themselves (Zhang et al., 2022). This is because only the pre- but not postsynaptic deletions of Tenm3 and Tenm4 in the medial entorhinal cortex produced impairments in synaptic connectivity in mice (Zhang et al., 2022). Although this seems to contradict the *trans*-synaptic teneurin-teneurin interaction suggested by other studies, Zhang et al. observed this through studying only a subset of synapses, and teneurins may function distinctly in different neuron types, and as discussed earlier, are likely to be involved in other processes such as regulating aspects of synaptic organisation and homeostasis. Through our characterisation of the synaptic localisation of different teneurin paralogues, exploration of factors contributing to its localisation and identification of a novel way in which teneurins may increase molecular diversity through heterodimerisation, we make significant progress in expanding our understanding of this unique and multifaceted protein. In the future, it will be important to further discover in detail the necessary factors that influence the generation of different molecular complexes at the synapse, including teneurins, and thus control the generation of synaptic diversity in the nervous system.

Data availability statement

The original contributions presented in this study are included in the article/Supplementary material, further inquiries can be directed to the corresponding author.

Ethics statement

This animal study was reviewed and approved by the Animal Welfare and Ethical Review Body, King's College London, and Home Office Project Licence PPL70/9036.

Author contributions

RH, AC, and GS contributed to the conception and design of the study and finalised the manuscript. AC and GS performed the main localisation studies. AW performed the deletion construct localisation studies. AB carried out the statistical analysis. MM performed the zebrafish co-expression analysis. AC wrote the first draft of the manuscript. All authors contributed to the article and approved the submitted version.

Funding

This work was funded by a Leverhulme Trust Research Project Grant (RPG-2017-168) and further supported by the Medical Research Council (MR/N026063/1 and MR/W006251/1). Costs for open access publication fees were covered by institutional block grant to King's College London.

Acknowledgments

We thank Maddy Parsons and Juan Burrone for helpful discussions throughout the project, as well as the Burrone Lab and the Eugene Makeyev Lab for providing the PSD95/Gephyrin antibodies and the N2A cell line, respectively. The LRRTM2-myc expression plasmid was a gift from Joris de Wit.

Conflict of interest

The authors declare that the research was conducted in the absence of any commercial or financial relationships that could be construed as a potential conflict of interest.

Publisher's note

All claims expressed in this article are solely those of the authors and do not necessarily represent those of their affiliated organizations, or those of the publisher, the editors and the reviewers. Any product that may be evaluated in this article, or claim that may be made by its manufacturer, is not guaranteed or endorsed by the publisher.

Supplementary material

The Supplementary Material for this article can be found online at: <https://www.frontiersin.org/articles/10.3389/fnins.2022.915149/full#supplementary-material>

SUPPLEMENTARY FIGURE 1

Tagged teneurin constructs are expressed at the cell membrane in HEK293 cells. EGFP-tagged teneurin constructs were transfected into HEK cells and imaged 48 h post transfection. All four EGFP-tagged teneurin paralogues could be found expressed at the membrane. Representative images showing Tenm1_EGFP (A), Tenm2_EGFP (B), Tenm3_EGFP (C), and Tenm4_EGFP (D) expression. Scale bar, 20 μ m.

SUPPLEMENTARY FIGURE 2

Co-localisation between LRRTM2, synapsin I and Tenm3. (A) Immunocytochemistry detection of synapsin I (green) in dissociated cortical cultures transfected with a construct to express LRRTM2 (magenta). (B) Neurons co-transfected with constructs to express LRRTM2 (magenta) and Tenm3 (green). (C) Control cultures transfected with a general construct to express EGFP showing no punctate pattern for EGFP (green) and no specific co-localisation with synapsin I (magenta). Scale bar, 5 μ m.

SUPPLEMENTARY FIGURE 3

Representative image of the co-localisation analysis between bassoon and synapsin I in a dissociated hippocampal neuron. (a) Image of a representative hippocampal neuron stained for bassoon and synapsin I. Scale bar, 10 μ m. (b) Dendritic segment of the neuron shown in panel

(a). Scale bar, 5 μ m. (c) Dendritic segment stained for bassoon. (d) Dendritic segment stained for synapsin I. (e) Colocalisation between bassoon and synapsin I after image analysis. (f) ROIs around bassoon puncta after image analysis. (g) Binary image of synapsin I puncta after image analysis. (h) Control colocalisation between bassoon and synapsin I after 90° rotation of the bassoon image channel (c,f). (i) ROIs around bassoon puncta after image channel was rotated 90°. (j) Binary image of synapsin I puncta after image analysis. (k) Co-localisation between bassoon and synapsin I (black) and synapsin I and bassoon-control (grey), **** $p < 0.0001$. (l) Proportion of bassoon clusters (black) and bassoon-control clusters (grey) co-localised with synapsin I per neuron, ** $p = 0.0079$.

SUPPLEMENTARY FIGURE 4

Histogram of basal (blue) and apical (red) spine Tenm3 intensity, where Tenm3 intensity is determined as the ratio Tenm3/GFP intensity. The dotted black line indicates the threshold, which spines are considered to express Tenm3 (1.531). Signal in spines below this threshold was considered to be background (calculated using the mean ratio of intensity throughout the dendrite versus spine structures). This data indicates that that only a subpopulation of 17.34% of all basal spines and 25.5% of all apical spines are Tenm3-positive. When apical and basal spines are pooled together, the total proportion of Tenm3-positive CA1 spines amounted to 19.87%.

SUPPLEMENTARY FIGURE 5

Tenm3 localisation and analysis in dendritic SAPs of CA1 neurons. Representative image showing expression of Tenm3 (A) and GFP (B) in a basal dendritic segment. A merged image is shown in (C), where for every image three ROIs were traced for analysis: spine ROI, SAP ROI, and background ROI. Scale bar, 1 μ m.

SUPPLEMENTARY FIGURE 6

EGFP-tagged truncated teneurin variants are localised to the cell membrane in N2a cells. EGFP-tagged Tenm3 expression constructs were transfected into N2a cells and imaged 48 h post transfection. Both EGFP-tagged truncated Tenm3 variants could be found expressed at the membrane. Representative images showing Tenm3 Δ ECD_EGFP (A) and Tenm3 Δ ICD_EGFP (B) expression. Scale bar, 20 μ m.

SUPPLEMENTARY FIGURE 7

Different teneurin paralogues show overlapping expression when expressed together in dissociated neurons. EGFP- and tagRFP-tagged teneurin paralogues co-transfected in primary neuronal cultures have similar patterns of expression and can be found in clusters along neurites. Scale bar, 20 μ m.

References

- Ackermann, M., and Matus, A. (2003). Activity-induced targeting of profilin and stabilization of dendritic spine morphology. *Nat. Neurosci.* 6, 1194–1200. doi: 10.1038/nn1135
- Al Chawaf, A., Xu, K., Tan, L., Vaccarino, F. J., Lovejoy, D. A., and Rotzinger, S. (2007). Corticotropin-releasing factor (CRF)-induced behaviors are modulated by intravenous administration of teneurin C-terminal associated peptide-1 (TCAP-1). *Peptides* 28, 1406–1415. doi: 10.1016/j.peptides.2007.05.014
- Antinucci, P., Nikolaou, N., Meyer, M. P., and Hindges, R. (2013). Teneurin-3 specifies morphological and functional connectivity of retinal ganglion cells in the vertebrate visual system. *Cell Rep.* 5, 582–592. doi: 10.1016/j.celrep.2013.09.045
- Baumgartner, S., and Chiquet-Ehrismann, R. (1993). Tena, a *Drosophila* gene related to tenascin, shows selective transcript localization. *Mech. Dev.* 40, 165–176. doi: 10.1016/0925-4773(93)90074-8
- Baumgartner, S., Martin, D., Hagios, C., and Chiquet-Ehrismann, R. (1994). Tenm, a *Drosophila* gene related to tenascin, is a new pair-rule gene. *EMBO J.* 13, 3728–3740. doi: 10.1002/j.1460-2075.1994.tb06682.x
- Beckmann, J., Schubert, R., Chiquet-Ehrismann, R., and Muller, D. J. (2013). Deciphering teneurin domains that facilitate cellular recognition, cell-cell adhesion, and neurite outgrowth using atomic force microscopy-based single-cell force spectroscopy. *Nano Lett.* 13, 2937–2946. doi: 10.1021/nl4013248
- Berns, D. S., DeNardo, L. A., Pederick, D. T., and Luo, L. (2018). Teneurin-3 controls topographic circuit assembly in the hippocampus. *Nature* 554, 328–333. doi: 10.1038/nature25463
- Boucard, A. A., Maxeiner, S., and Sudhof, T. C. (2014). Latrophilins function as heterophilic cell-adhesion molecules by binding to teneurins: Regulation by alternative splicing. *J. Biol. Chem.* 289, 387–402. doi: 10.1074/jbc.M113.504779
- Cheung, A., Trevers, K. E., Reyes-Corral, M., Antinucci, P., and Hindges, R. (2019). Expression and roles of teneurins in zebrafish. *Front. Neurosci.* 13:158. doi: 10.3389/fnins.2019.00158
- Craven, S. E., and Bredt, D. S. (2000). Synaptic targeting of the postsynaptic density protein PSD-95 mediated by a tyrosine-based trafficking signal. *J. Biol. Chem.* 275, 20045–20051. doi: 10.1074/jbc.M910153199
- de Wit, J., Sylwestrak, E., O'Sullivan, M. L., Otto, S., Tiglio, K., Savas, J. N., et al. (2009). LRRTM2 interacts with Neurexin1 and regulates excitatory synapse formation. *Neuron* 64, 799–806. doi: 10.1016/j.neuron.2009.12.019
- Del Toro, D., Carrasquero-Ordaz, M. A., Chu, A., Ruff, T., Shahin, M., Jackson, V. A., et al. (2020). Structural basis of teneurin-latrophilin interaction in repulsive guidance of migrating neurons. *Cell* 180, 323–339.e19. doi: 10.1016/j.cell.2019.12.014
- Donlin-Asp, P. G., Polisseni, C., Klimek, R., Heckel, A., and Schuman, E. M. (2021). Differential regulation of local mRNA dynamics and translation

following long-term potentiation and depression. *Proc. Natl. Acad. Sci. U.S.A.* 118:e2017578118. doi: 10.1073/pnas.2017578118

Doyle, M., and Kiebler, M. A. (2011). Mechanisms of dendritic mRNA transport and its role in synaptic tagging. *EMBO J.* 30, 3540–3552. doi: 10.1038/emboj.2011.278

Drabikowski, K., Trzebiatowska, A., and Chiquet-Ehrismann, R. (2005). ten-1, an essential gene for germ cell development, epidermal morphogenesis, gonad migration, and neuronal pathfinding in *Caenorhabditis elegans*. *Dev. Biol.* 282, 27–38. doi: 10.1016/j.ydbio.2005.02.017

Feng, K., Zhou, X. H., Oohashi, T., Morgelin, M., Lustig, A., Hirakawa, S., et al. (2002). All four members of the ten-m/Odz family of transmembrane proteins form dimers. *J. Biol. Chem.* 277, 26128–26135. doi: 10.1074/jbc.M20372.2200

Grabrucker, A., Vaida, B., Bockmann, J., and Boeckers, T. M. (2009). Synaptogenesis of hippocampal neurons in primary cell culture. *Cell Tissue Res.* 338, 333–341.

Hayashi, C., Suzuki, N., Mabuchi, Y., Kikura, N., Hosoda, Y., de Vega, S., et al. (2020). The extracellular domain of teneurin-4 promotes cell adhesion for oligodendrocyte differentiation. *Biochem. Biophys. Res. Commun.* 523, 171–176. doi: 10.1016/j.bbrc.2019.12.002

Hong, W., Mosca, T. J., and Luo, L. (2012). Teneurins instruct synaptic partner matching in an olfactory map. *Nature* 484, 201–207. doi: 10.1038/nature10926

Ippolito, D. M., and Eroglu, C. (2010). Quantifying synapses: An immunocytochemistry-based assay to quantify synapse number. *J. Vis. Exp.* 45:2270. doi: 10.3791/2270

Jackson, V. A., Busby, J. N., Janssen, B. J. C., Lott, J. S., and Seiradake, E. (2019). Teneurin structures are composed of ancient bacterial protein domains. *Front. Neurosci.* 13:183. doi: 10.3389/fnins.2019.00183

Jackson, V. A., Meijer, D. H., Carrasquero, M., van Bezouwen, L. S., Lowe, E. D., Kleanthous, C., et al. (2018). Structures of teneurin adhesion receptors reveal an ancient fold for cell-cell interaction. *Nat. Commun.* 9:1079. doi: 10.1038/s41467-018-03460-0

Leamey, C. A., Glendinning, K. A., Kreiman, G., Kang, N. D., Wang, K. H., Fassler, R., et al. (2008). Differential gene expression between sensory neocortical areas: Potential roles for Ten_m3 and Bcl6 in patterning visual and somatosensory pathways. *Cereb. Cortex* 18, 53–66. doi: 10.1093/cercor/bh031

Leamey, C. A., Merlin, S., Lattouf, P., Sawatari, A., Zhou, X., Demel, N., et al. (2007). Ten_m3 regulates eye-specific patterning in the mammalian visual pathway and is required for binocular vision. *PLoS Biol.* 5:e241. doi: 10.1371/journal.pbio.0050241

Levine, A., Bashan-Ahrend, A., Budai-Hadrian, O., Gartenberg, D., Menasheerow, S., and Wides, R. (1994). Odd Oz: A novel *Drosophila* pair rule gene. *Cell* 77, 587–598.

Li, J., Shalev-Benami, M., Sando, R., Jiang, X., Kibrom, A., Wang, J., et al. (2018). Structural basis for teneurin function in circuit-wiring: A toxin motif at the synapse. *Cell* 173, 735–748.e15. doi: 10.1016/j.cell.2018.03.036

Li, J., Xie, Y., Cornelius, S., Jiang, X., Sando, R., Kordon, S. P., et al. (2020). Alternative splicing controls teneurin-latrophilin interaction and synapse specificity by a shape-shifting mechanism. *Nat. Commun.* 11:2140. doi: 10.1038/s41467-020-16029-7

Lovejoy, D. A., Rotzinger, S., and Barsyte-Lovejoy, D. (2009). Evolution of complementary peptide systems: Teneurin C-terminal-associated peptides and corticotropin-releasing factor superfamilies. *Ann. N Y Acad. Sci.* 1163, 215–220. doi: 10.1111/j.1749-6632.2008.03629.x

Minet, A. D., Rubin, B. P., Tucker, R. P., Baumgartner, S., and Chiquet-Ehrismann, R. (1999). Teneurin-1, a vertebrate homologue of the *Drosophila* pair-rule gene ten-m, is a neuronal protein with a novel type of heparin-binding domain. *J. Cell Sci.* 112(Pt 12), 2019–2032. doi: 10.1242/jcs.112.12.2019

Mosca, T. J. (2015). On the teneurin track: A new synaptic organization molecule emerges. *Front. Cell. Neurosci.* 9:204. doi: 10.3389/fncel.2015.00204

Mosca, T. J., Hong, W., Dani, V. S., Favaloro, V., and Luo, L. (2012). Trans-synaptic teneurin signalling in neuromuscular synapse organization and target choice. *Nature* 484, 237–241. doi: 10.1038/nature10923

Murase, S., Mosser, E., and Schuman, E. M. (2002). Depolarization drives beta-Catenin into neuronal spines promoting changes in synaptic structure and function. *Neuron* 35, 91–105. doi: 10.1016/s0896-6273(02)00764-x

Nunes, S. M., Ferralli, J., Choi, K., Brown-Luedi, M., Minet, A. D., and Chiquet-Ehrismann, R. (2005). The intracellular domain of teneurin-1 interacts with MBD1

and CAP/ponsin resulting in subcellular codistribution and translocation to the nuclear matrix. *Exp. Cell Res.* 305, 122–132. doi: 10.1016/j.yexcr.2004.12.020

O'Connor, T. P., Cockburn, K., Wang, W., Tapia, L., Currie, E., and Bamji, S. X. (2009). Semaphorin 5B mediates synapse elimination in hippocampal neurons. *Neural Dev.* 4:18. doi: 10.1186/1749-8104-4-18

Oohashi, T., Zhou, X. H., Feng, K., Richter, B., Morgelin, M., Perez, M. T., et al. (1999). Mouse ten-m/Odz is a new family of dimeric type II transmembrane proteins expressed in many tissues. *J. Cell Biol.* 145, 563–577. doi: 10.1083/jcb.145.3.563

Pasterkamp, R. J., and Giger, R. J. (2009). Semaphorin function in neural plasticity and disease. *Curr. Opin. Neurobiol.* 19, 263–274.

Pederick, D. T., Lui, J. H., Gingrich, E. C., Xu, C., Wagner, M. J., Liu, Y., et al. (2021). Reciprocal repulsions instruct the precise assembly of parallel hippocampal networks. *Science* 372, 1068–1073. doi: 10.1126/science.abg1774

Qian, X., Barsyte-Lovejoy, D., Wang, L., Chewpoy, B., Gautam, N., Al Chawaf, A., et al. (2004). Cloning and characterization of teneurin C-terminus associated peptide (TCAP)-3 from the hypothalamus of an adult rainbow trout (*Oncorhynchus mykiss*). *Gen. Comp. Endocrinol.* 137, 205–216. doi: 10.1016/j.ygcen.2004.02.007

Rubin, B. P., Tucker, R. P., Brown-Luedi, M., Martin, D., and Chiquet-Ehrismann, R. (2002). Teneurin 2 is expressed by the neurons of the thalamofugal visual system in situ and promotes homophilic cell-cell adhesion in vitro. *Development* 129, 4697–4705. doi: 10.1242/dev.129.20.4697

Rubin, B. P., Tucker, R. P., Martin, D., and Chiquet-Ehrismann, R. (1999). Teneurins: A novel family of neuronal cell surface proteins in vertebrates, homologous to the *Drosophila* pair-rule gene product Ten-m. *Dev. Biol.* 216, 195–209. doi: 10.1006/dbio.1999.9503

Salinas, P. C., and Price, S. R. (2005). Cadherins and catenins in synapse development. *Curr. Opin. Neurobiol.* 15, 73–80.

Sando, R., Jiang, X., and Sudhof, T. C. (2019). Latrophilin GPCRs direct synapse specificity by coincident binding of FLRTs and teneurins. *Science* 363:eav7969. doi: 10.1126/science.aav7969

Schindelin, J., Arganda-Carreras, I., Frise, E., Kaynig, V., Longair, M., Pietzsch, T., et al. (2012). Fiji: An open-source platform for biological-image analysis. *Nat. Methods* 9, 676–682. doi: 10.1038/nmeth.2019

Scholer, J., Ferralli, J., Thiry, S., and Chiquet-Ehrismann, R. (2015). The intracellular domain of teneurin-1 induces the activity of microphthalmia-associated transcription factor (MITF) by binding to transcriptional repressor HINT1. *J. Biol. Chem.* 290, 8154–8165. doi: 10.1074/jbc.M114.615922

Silva, J. P., Leliana, V. G., Ermolyuk, Y. S., Vysokov, N., Hitchen, P. G., Berninghausen, O., et al. (2011). Latrophilin 1 and its endogenous ligand lasso/teneurin-2 form a high-affinity transsynaptic receptor pair with signaling capabilities. *Proc. Natl. Acad. Sci. U.S.A.* 108, 12113–12118. doi: 10.1073/pnas.1019434108

Steward, O., and Levy, W. B. (1982). Preferential localization of polyribosomes under the base of dendritic spines in granule cells of the dentate gyrus. *J. Neurosci.* 2, 284–291. doi: 10.1523/JNEUROSCI.02-03-00284.1982

Sutton, M. A., and Schuman, E. M. (2006). Dendritic protein synthesis, synaptic plasticity, and memory. *Cell* 127, 49–58.

tom Dieck, S., Sanmarti-Vila, L., Langnaese, K., Richter, K., Kindler, S., Soyke, A., et al. (1998). Bassoon, a novel zinc-finger CAG/glutamine-repeat protein selectively localized at the active zone of presynaptic nerve terminals. *J. Cell Biol.* 142, 499–509. doi: 10.1083/jcb.142.2.499

Tucker, R. P., and Chiquet-Ehrismann, R. (2006). Teneurins: A conserved family of transmembrane proteins involved in intercellular signaling during development. *Dev. Biol.* 290, 237–245. doi: 10.1016/j.ydbio.2005.11.038

Tucker, R. P., Beckmann, J., Leachman, N. T., Scholer, J., and Chiquet-Ehrismann, R. (2012). Phylogenetic analysis of the teneurins: Conserved features and premetazoan ancestry. *Mol. Biol. Evol.* 29, 1019–1029. doi: 10.1093/molbev/msr271

Uchida, N., Honjo, Y., Johnson, K. R., Wheelock, M. J., and Takeichi, M. (1996). The catenin/cadherin adhesion system is localized in synaptic junctions bordering transmitter release zones. *J. Cell Biol.* 135, 767–779. doi: 10.1083/jcb.135.3.767

Vysokov, N. V., Silva, J. P., Leliana, V. G., Ho, C., Djamgoz, M. B., Tonevitsky, A. G., et al. (2016). The mechanism of regulated release of lasso/teneurin-2. *Front. Mol. Neurosci.* 9:59. doi: 10.3389/fnfmol.2016.00059

Wang, L., Rotzinger, S., Al Chawaf, A., Elias, C. F., Barsyte-Lovejoy, D., Qian, X., et al. (2005). Teneurin proteins possess a carboxy terminal sequence with neuromodulatory activity. *Brain Res. Mol. Brain Res.* 133, 253–265. doi: 10.1016/j.molbrainres.2004.10.019

- Wang, Y., He, H., Srivastava, N., Vikarunnessa, S., Chen, Y. B., Jiang, J., et al. (2012). Plexins are GTPase-activating proteins for Rap and are activated by induced dimerization. *Sci. Signal.* 5:ra6.
- Willems, J., de Jong, A. P. H., Scheefhals, N., Mertens, E., Catsburg, L. A. E., Poorthuis, R. B., et al. (2020). ORANGE: A CRISPR/Cas9-based genome editing toolbox for epitope tagging of endogenous proteins in neurons. *PLoS Biol.* 18:e3000665. doi: 10.1371/journal.pbio.3000665
- Williams, M. E., Wilke, S. A., Daggett, A., Davis, E., Otto, S., Ravi, D., et al. (2011). Cadherin-9 regulates synapse-specific differentiation in the developing hippocampus. *Neuron* 71, 640–655. doi: 10.1016/j.neuron.2011.06.019
- Woelfle, R., D'Aquila, A. L., Pavlovic, T., Husic, M., and Lovejoy, D. A. (2015). Ancient interaction between the teneurin C-terminal associated peptides (TCAP) and latrophilin ligand-receptor coupling: A role in behavior. *Front. Neurosci.* 9:146. doi: 10.3389/fnins.2015.00146
- Young, T. R., Bourke, M., Zhou, X., Oohashi, T., Sawatari, A., Fässler, R., et al. (2013). Ten-m2 is required for the generation of binocular visual circuits. *J. Neurosci.* 33, 12490–12509. doi: 10.1523/JNEUROSCI.4708-12.2013
- Zhang, X., Lin, P. Y., Liakath-Ali, K., and Südhof, T. C. (2022). Teneurins assemble into presynaptic nanoclusters that promote synapse formation via postsynaptic non-teneurin ligands. *Nat. Commun.* 13:2297. doi: 10.1038/s41467-022-29751-1
- Zheng, L., Michelson, Y., Freger, V., Avraham, Z., Venken, K. J., Bellen, H. J., et al. (2011). *Drosophila* Ten-m and filamin affect motor neuron growth cone guidance. *PLoS One* 6:e22956. doi: 10.1371/journal.pone.0022956

Frontiers in Neuroscience

Provides a holistic understanding of brain
function from genes to behavior

Part of the most cited neuroscience journal series
which explores the brain - from the new eras
of causation and anatomical neurosciences to
neuroeconomics and neuroenergetics.

Discover the latest Research Topics

[See more →](#)

Frontiers

Avenue du Tribunal-Fédéral 34
1005 Lausanne, Switzerland
frontiersin.org

Contact us

+41 (0)21 510 17 00
frontiersin.org/about/contact

